

AD \_\_\_\_\_

Award Number: DAMD17-99-1-9547

TITLE: Genetic and Epigenetic Mechanisms Underlying Acute and Delayed Neurodegenerative Consequences of Stress and Anticholinesterase Exposure

PRINCIPAL INVESTIGATOR: Hermona Soreq, Ph.D.

CONTRACTING ORGANIZATION: Hebrew University of Jerusalem  
91904 Jerusalem, Israel

REPORT DATE: August 2001

TYPE OF REPORT: Annual

PREPARED FOR: U.S. Army Medical Research and Materiel Command  
Fort Detrick, Maryland 21702-5012

DISTRIBUTION STATEMENT: Approved for Public Release;  
Distribution Unlimited

The views, opinions and/or findings contained in this report are those of the author(s) and should not be construed as an official Department of the Army position, policy or decision unless so designated by other documentation.

20030904 135

# REPORT DOCUMENTATION PAGE

*Form Approved*  
OMB No. 074-0188

Public reporting burden for this collection of information is estimated to average 1 hour per response, including the time for reviewing instructions, searching existing data sources, gathering and maintaining the data needed, and completing and reviewing this collection of information. Send comments regarding this burden estimate or any other aspect of this collection of information, including suggestions for reducing this burden to Washington Headquarters Services, Directorate for Information Operations and Reports, 1215 Jefferson Davis Highway, Suite 1204, Arlington, VA 22202-4302, and to the Office of Management and Budget, Paperwork Reduction Project (0704-0188), Washington, DC 20503

<b>1. AGENCY USE ONLY (Leave blank)</b>	<b>2. REPORT DATE</b> August 2001	<b>3. REPORT TYPE AND DATES COVERED</b> Annual (15 Jul 00 - 14 Jul 01)
---	--------------------------------------	---

<b>4. TITLE AND SUBTITLE</b> Genetic and Epigenetic Mechanisms Underlying Acute and Delayed Neurodegenerative Consequences of Stress and Anticholinesterase Exposure	<b>5. FUNDING NUMBERS</b> DAMD17-99-1-9547
---	---

<b>6. AUTHOR(S)</b> Hermona Soreq, Ph.D.	
---	--

<b>7. PERFORMING ORGANIZATION NAME(S) AND ADDRESS(ES)</b>  Hebrew University of Jerusalem 91904 Jerusalem, Israel  E-Mail: <a href="mailto:soreq@shum.huji.ac.il">soreq@shum.huji.ac.il</a>	<b>8. PERFORMING ORGANIZATION REPORT NUMBER</b>
--	---

<b>9. SPONSORING / MONITORING AGENCY NAME(S) AND ADDRESS(ES)</b>  U.S. Army Medical Research and Materiel Command Fort Detrick, Maryland 21702-5012	<b>10. SPONSORING / MONITORING AGENCY REPORT NUMBER</b>
--	---

<b>11. SUPPLEMENTARY NOTES</b> Report contains color
---

<b>12a. DISTRIBUTION / AVAILABILITY STATEMENT</b> Approved for Public Release; Distribution Unlimited	<b>12b. DISTRIBUTION CODE</b>
--	-------------------------------

<b>13. ABSTRACT (Maximum 200 Words)</b> We have observed the role of the stress-associated acetylcholinesterase variant, AChE-R in several model systems. In AChE transgenic mice, the neuronal overexpression of AChE-R is associated with behavioral impairments. In another animal model, the honey bee, developmental reduction of <i>ache</i> gene expression paralleled their normal, consistent improvement of behavioral functions, and experimental improvement under mild rivastigmine exposure. In the rodent neuromuscular system, we observed AChE-R overexpression under exposure of mice to DFP and in experimental autoimmune myasthenia gravis in rats. This overexpression was associated with impaired muscle structure and myopathy (in mice) and in electromyographic deterioration (in rats). Both effects were preventable by systemic administration of antisense oligonucleotides to block AChE-R production; such treatment also transiently improved the behavioral abnormalities associated with AChE-R overproduction. AChE-R production was also observed in differentiating hematopoietic and sperm cells; in AChE-R transgenic mice, this induced male infertility, and unusual AChE-R distribution was also observed in human sperm samples from the male members of some infertile couples. Finally, AChE-R was found to bind to RACK1, a known binding partner of a protein kinase C variant known to regulate anxiety responses.
---

<b>14. SUBJECT TERMS</b> Neurotoxin	<b>15. NUMBER OF PAGES</b> 296
	<b>16. PRICE CODE</b>

<b>17. SECURITY CLASSIFICATION OF REPORT</b> Unclassified	<b>18. SECURITY CLASSIFICATION OF THIS PAGE</b> Unclassified	<b>19. SECURITY CLASSIFICATION OF ABSTRACT</b> Unclassified	<b>20. LIMITATION OF ABSTRACT</b> Unlimited
--	---	--	--

## Table of Contents

	page
Front cover	1
Standard form (SF) 298	2
Table of contents	3
Introduction	4
Body	
Task 1: Neuronal overexpression of 'readthrough' acetylcholinesterase is associated with antisense-suppressible behavioral impairments	6
Antisense oligonucleotides relieve neuromuscular weakness in experimental autoimmune myasthenia gravis	21
Task 2: Modified testicular expression of stress-associated 'readthrough' acetylcholinesterase predicts male infertility	32
Task 3: Development of AChE variant-specific antibodies for the demonstration of differential expression of variants in hematopoietic cells	40
Changes in neuronal acetylcholinesterase gene expression and division of labor in honey bee colonies	52
Task 5: Complex host cell responses to antisense suppression of <i>ACHE</i> gene expression	58
Synaptogenesis and myopathy under AChE over-expression	65
Task 6: The stress-induced AChE-R variant forms neuronal complexes with PKCBII and RACK1, a protein of the WD family	74
Task 7: Conditionally transgenic mice (preliminary findings)	90
Task 8: Autism, stress and chromosome 7 genes	96
Key research accomplishments	104
Reportable outcomes	105
Conclusions	107
References	108
Appendices	
Letter from Col. J.K. Zadinsky dated 20 July 2001	
Salmon et al., The stress-associated "readthrough" acetylcholinesterase variant . . .	
Brenner et al., Antisense oligonucleotides relieve . . .	
Cohen et al., Neuronal overexpression . . .	
Galyam et al. Complex host cell responses . . .	
Lev-Lehman et al., Synaptogenesis and myopathy . . .	
Mor et al., Modified testicular expression . . .	
Shapira et al., Autism, stress and chromosome 7 genes	
Shapira et al., Changes in neuronal acetylcholinesterase . . .	
Soreq & Glick, 'Readthrough' acetylcholinesterase (AChE-R) . . .	
Soreq & Glick, Novel roles for cholinesterases . . .	
Soreq & Seidman, Acetylcholinesterase – new roles . . .	
Soreq et al., Anti-sense approach . . .	
Soreq et al., Blood-brain barrier modulations . . .	

## Introduction

Transgenic mice that overexpress human AChE-S in central nervous system tissues (Beeri et al., 1995) have now been found to also have elevated levels of murine AChE-R; and an antisense oligonucleotide (AS-ON) (Seidman et al., 1999) depresses synthesis of the murine AChE-R variant and its tissue levels. These two tools have allowed us to demonstrate the importance of AChE-R in several model systems and the utility of the antisense approach for controlling the levels of this variant. In pheochromocytoma (PC12) cells, the levels of AChE-R mRNA and of AChE-R itself were rapidly depressed by treatment with the AS-ON. Extremely low levels of the AS-ON, in the nanomolar range, were effective, and were non-cytotoxic by several criteria (Galyam et al., 2001). Chronic exposure of mice, both control and the transgenic mice, to sub-lethal doses of the organophosphate, DFP, caused proliferation of their neuromuscular junctions, which was prevented by treatment with the AS-ODN (Lev-Lehman et al., 2000). These transgenic mice perform poorly in a test of short-term memory (Beeri et al., 1997). Their performance is markedly, if only temporarily, improved by injection the AS-ON into their brains. The same AS-ON corrects the electrophysiological defects of experimental autoimmune myasthenia gravis in rats and improves their performance in a test of stamina. In these animals, administration of the AS-ON was attempted by *i.v.* injection and orally; surprisingly, both routes of administration were successful.

Creation of novel antibodies selective for the C-terminal peptides that are unique to the S and R variants of AChE (Flores-Flores et al., 2001) enabled us to test their cell-type specific expression patterns. In human umbilical cord stem cells, surface AChE-S is associated with monocytic lineages whereas AChE-R is associated with granulocytes. This suggests that myelopoietic differentiation is accompanied by a shift in AChE pre-mRNA splicing.

An additional model system, a transgenic mouse that overexpresses human AChE-R (Sternfeld et al., 2000) has been useful in exploring the role of this protein in stress-dependent male infertility. The transgenic mice, like stressed normal mice, had characteristically lower sperm counts, lower levels of AChE-R in sperm heads, reduced motility and lower seminal gland weight, emphasizing the importance of the central role of the AChE-R variant in yet another stress-associated function (Mor et al., 2001).

There is good reason to suspect a locus on chromosome 7 as contributing to the occurrence of autism. Accordingly, the frequency of a deletion in the promoter region of the *ACHE* gene was assessed among a population of 616 normal and 190 autistic individuals in the USA (in collaboration with John Gilbert of Duke University). However, perhaps because of the low incidence of the mutation, no significant difference in frequency was noted.

We were able to take advantage of having on sabbatical leave in our laboratory, an expert from the University of Illinois on honey bee behavior. Therefore we were able to use these animals as yet another test system in which to study the effects of AChE and its inhibition by an anti-AChE agent, on learning. Consistent with studies in other model systems, moderate reduction of AChE accompanied behavioral maturation, and mild exposure to metrifonate, a carbamate anti-AChE supported an enhancement of learning (Shapira et al., 2001).

Below are enumerated the work tasks that were undertaken:

- task 1: characterize the sensory, cognitive and neuromotor consequences of a transgenic excess in AChE variants.
- task 2: employ transgenic mouse models with up to 300-fold differences in peripheral AChE levels for demonstration of direct correlation between AChE dosage and protection from stress and chemical warfare agents and to test their responses to pyridostigmine administration.
- task 3: develop RT-PCR tests in peripheral blood cells of model animals, and additional surrogate markers, for follow-up of responses and protection.
- task 4: adapt such tests to use in humans following accidental exposure to agricultural anti-ChEs.
- task 5: employ the transgenic mouse models to test effects of sudden changes in AChE levels at all the above sites and functions.
- task 6: delineate the protein partners through which AChE exerts non-catalytic signals which lead to delayed symptoms.
- task 7: develop tetracycline-inducible animal models in which AChE activity can be induced or antisense-suppressed at will.
- task 8: continue the search for promoter sequence polymorphisms which lead to natural variations in human AChE levels and correlate them with responses to anti-ChEs.
- task 9: expedite transgenic models for production from milk of recombinant human AChE, as a potential scavenger.

Work on task 4 involved the training of a neurologist, Dr. Tatiana Vender of Soroka Hospital (Beersheva), in DNA extraction and PCR amplification and in AChE enzyme assays. The experimentation itself has been awaiting approval of human studies. As this report was being compiled, this approval was granted conditional upon compliance with several requests. The notification of this conditional approval is appended (letter from Col. J.K. Zadinsky, 20 July 2001). Work on task 9 was reported in the previous annual report; and work on task 7 is in progress.

In the pages that follow, progress in tasks 1, 3, 5, 6, 7 and 8 is reported.

## Neuronal overexpression of "readthrough" acetylcholinesterase is associated with antisense-suppressible behavioral impairments (task 1)

Social behavior is a complex phenotype, composed of the individual's general level of activity, cognitive perception and anticipation of the outcome of such behavior (Carlson, 1994). Working and storage memory and the ability to integrate information can also contribute towards social behavior, which is tightly linked to cholinergic neurotransmission. For example, the hypocholinergic features of Alzheimer's disease (AD) patients include aggressive behavior and/or avoidance of novel social challenges (Cummings and Back, 1998), as well as fears of social interactions alleviated by treatment with anticholinesterases (Giacobini, 2000). Surprisingly, anticholinesterases, e.g. tacrine (tetrahydroaminoacridine, Cognex™, Parke-Davis), donepezil (Aricept™, Pfizer), rivastigmine (Exelon™, Novartis) and galantamine (Reminyl™, Janssen), were reported to cause more pronounced improvement in more severely affected patients. To explain the molecular basis of this phenomenon, re-evaluation is needed of the linkage between cholinergic neural pathways, social behavior and acetylcholinesterase (AChE).

Both anticholinesterase exposure and stressful insults, i.e. confined swim, induce in the mammalian brain a rapid *c-fos* elevation that mediates muscarinic responses and subsequent *ACHE* overexpression (Kaufer et al., 1998). A stress-associated switch in alternative splicing (Xie and McCobb, 1998; Kaufer and Soreq, 1999) diverts AChE from the major, "synaptic" AChE-S to the normally rare "readthrough" AChE-R variant (Grisaru et al., 1999). The distinctive non-catalytic activities of these AChE isoforms (Sternfeld et al., 2000), suggest links between AChE-R accumulation and behavioral anticholinesterase responses.

Transgenic (Tg) mice overexpressing human (h) AChE-S in brain neurons are amenable to pursuit of this linkage. These mice present , early-onset loss of learning and memory capacities (Beeri et al., 1995), progressive dendritic depletion (Beeri et al., 1997), stress-related neuropathology (Sternfeld et al., 2000), and modified anxiety responses (Erb et al., 2001). However, their social behavior and psychological stress responses have not yet been addressed.

AChE-S Tg mice constitutively overexpress AChE-R mRNA in their intestinal epithelium. When exposed to an organophosphate anticholinesterase (DFP), they fail to increase further the already overproduced AChE-R, and present extreme DFP sensitivity. Humans with inherited AChE overexpression are likewise hypersensitive to the anticholinesterase pyridostigmine (Shapira et al., 2000). Our working hypothesis postulated that at appropriate levels, AChE-R accumulation in response to stress restores normal cholinergic activity and social behavior. However, under chronic stress, acute anti-AChE treatment or exposure, or in individuals with inherited AChE excess, AChE-R increases to a limit beyond which their cholinergic system cannot further respond and impaired social behavior is a result.

To test this hypothesis, we ascertained whether (a) AChE-S Tg mice display excessive response to a mildly stressful stimulus, a switch in the day/night cycle (Suer et al., 1998), (b) examined AChE-R expression in the brain neurons of AChE-S Tg mice; and (c) studied the social recognition behavior (Thor and Holloway, 1982) of AChE-S Tg mice before and after administration of tacrine or AS3, an antisense oligonucleotide (AS-ON) shown to selectively suppress AChE-R production (Shohami et al., 2000). Our findings demonstrate constitutive

mAChE-R accumulation with inter-animal variability in brain neurons of hAChE-S Tg mice, associated with an exaggerated response to changes in circadian rhythm, and impaired social recognition, which are amenable to effective AS-ON suppression.

#### Materials and Methods

**Animals:** AChE-S Tg mice were obtained in a 100% FVB/N genotype from heterozygous breeding pairs (Beeri et al., 1995). Control, non-Tg FVB/N mice were obtained by littermate breeding. Adult, 8-20 wk old Tg and control male mice were housed 4-5/cage in a 12 hr dark/light cycle with free access to food and water. All experiments were conducted during the first half of the dark phase of a reversed 12 hr dark/light cycle, under dim illumination. Routine locomotor activity in the home cage was measured using a remote motility detector (MFU 2100, Rhema-Labortechnik, Hofheim, Germany) to quantify changes in the electromagnetic field.

**Telemetric measurements:** Battery operated biotelemetric transmitters (model VM-FH, Mini Mitter, Sun River, OR, USA) were implanted in the peritoneal cavity under ether anesthesia 12 days prior to the test. After implantation, mice were housed in separate cages with free access to food and water. Output was monitored by a receiver board (model RA-1010, Mini Mitter) placed under each animal's cage and fed into a peripheral processor (BCM 100) connected to a desktop computer. Locomotor activity after the dark/light shift was measured by detecting changes in signal strength as animals moved about in their cages, so that the number of pulses that were generated by the transmitter was proportional to the distance the animal moved. The cumulative number of pulses generated over the noted periods was recorded (Yirmiya et al., 1997). Recording lasted 24 consecutive hrs, starting at 9:30 am, with the light phase of a 12:12 hr dark / light cycle beginning at 7:00 a.m. To initiate a day/night switch, the dark/light periods were reversed and recording started 72 hr after the switch and lasted 24 hr. Following intraperitoneal injection of AS-ONs (see below), recording proceeded for an additional 3 hr.

**Social exploration tests:** Each mouse was placed in a semicircular, transparent observation box and allowed 15 min for habituation, following which a juvenile male mouse (23-29 days old) was introduced. The time spent by the experimental mouse in social exploration consisted mainly of body and anogenital sniffing, chasing, attacking and crawling over the juvenile. Measurements covered a 4-min period, using a computerized event recorder. Each mouse underwent 2 successive social exploration sessions at the noted inter-session intervals. The first session was considered as baseline. In the second session (test), either the same or a different juvenile was introduced. Social recognition was calculated as percentage of tested out of baseline exploration time recorded for each mouse.

***In situ* hybridization and AChE activity measurements:** Animals were sacrificed by cervical dislocation, and brains were removed and dissected or fixed for *in situ* hybridization. AChE activity was measured in hippocampus, cortex and cerebellum extracts as described (Sternfeld et al., 1998). Protein determination was performed using a detergent-compatible kit (DC, Bio-Rad, München, Germany). Immunoblot detection of specific AChE isoforms was as reported (Shohami et al., 2000).

For *in situ* hybridization, 5  $\mu$ m paraffin sections of brain tissue were prepared after fixation by transcardial perfusion of anaesthetized mice with 4% paraformaldehyde in PBS (pH 7.4). A 50-mer fully 2'-O-methylated 5'-biotinylated AChE-R cRNA probe was applied as described

(Kaufer et al., 1998). Following probe detection with a streptavidin-alkaline phosphatase conjugate (Amersham Pharmacia Biotech Ltd., Little Chalfont, UK) and Fast Red as the reaction substrate (Roche Diagnostics, Mannheim, Germany), micrographs of hippocampal and cortical neurons were subjected to semi-quantitative evaluation of Fast Red staining. Mean signal intensities of light micrographs (taken with a Real-14 color digital camera, CRI, Boston, MA, USA) were analyzed using Image Pro Plus (Media Cybernetics, Silver Spring, MD, USA) image analysis software. The mean intensity of Fast Red labeling was measured in CA3 hippocampal and cortical neurons and corrected for background staining in each picture.

**Immunocytochemistry** of glial fibrillary acidic protein (GFAP) was performed as described (Sternfeld et al., 2000). Briefly, floating, formalin-fixed, 30  $\mu\text{m}$ , coronal cryostat-sections were pretreated with trypsin (type II, Sigma Chemical Co., St. Louis, MO, USA) 0.001% for 1 min. Sections were incubated overnight at 4°C with a mouse anti-glial fibrillary acidic protein (GFAP) antibody (clone GA-5, Sigma-Israel, Rehovot, Israel), diluted 1:500. Then sections were incubated overnight at 4°C with horseradish peroxidase-labeled goat-anti-mouse antibody (Sigma-Israel), diluted 1:100. Color was developed by reaction with diaminobenzidine 0.0125%, nickel ammonium sulfate 0.05% and hydrogen peroxide (0.00125%). The development time of the DAB reaction product was controlled by stopwatch to ensure comparability between experiments. Sections were counterstained with cresyl violet.

Quantitative analysis of the hippocampal stratum lacunosum moleculare (SLM) was performed at the level of posterior 2.5 mm from bregma. Using a 40x objective, consecutive fields of the SLM were visualized with a Nikon microscope and processed using an AnalySIS image analysis system. A total of 35 astrocytes were sampled from each group (control vs. Tg). The variables that were compared were intensity of staining of the soma (arbitrary units from a range of 256 shades of gray), soma size ( $\mu\text{m}^2$ ), and thickness of the largest process of each astrocyte at the process stem ( $\mu\text{m}$ ). Statistical comparisons were made using Student's t-test, with 68 degrees of freedom.

**Considerations for designing antisense tests:** *In vivo* antisense suppression of *de novo* AChE-R synthesis was employed throughout the current study to provide a proof of concept (i.e. demonstrate the causal involvement of the secretory, soluble mAChE-R variant in the excessive locomotor activity and the impaired social recognition of Tg mice). Two types of experiments were performed: (1) intracerebroventricular (*i.c.v.*) AS3 injection of animals subjected to longitudinal social exploration tests (up to one week post-treatment) and (2) *i.c.v.* injection followed by 1-day social exploration test, immunochemical detection and measurement of catalytic activity of brain AChE. Both of these were associated with certain inherent limitations, as is detailed below, yet each test provided evidence to support part of the explored concept.

Intracranial AS-ON injection is inherently more powerful when centrally controlled behavioral parameters are sought; limitations in this case involve the duration of tests (as the animals are all at a post-surgery state) and the requirement to control for the outcome of this surgical procedure in addition to the behavioral test itself. To avoid excessive complications, we refrained from employing double operations (and, therefore, could not use telemetric measurements, which require transmitter implantation, on *i.c.v.*-injected animals).

The experimental controls, as well, were chosen after careful consideration. Each test should involve both Tg and control animals, as well as sham treatment (injection of either saline or

an irrelevant oligonucleotide) and comparison between pre- and post-treatment phenotypes. Whenever possible, animals were self-compared, requiring careful time-of-day comparisons; in other cases, groups of animals with similar pre-treatment behavior patterns were compared to each other with regard to the efficacy of the antisense treatment. Neither of these tests is conclusive by itself, however, their cumulative outcome substantially supported the possibility of employing antisense knockdown in careful behavioral tests.

**Cannula implantation:** Mice under sodium pentobarbital anesthesia (50 mg/Kg, *i.p.*) were placed in a stereotaxic apparatus. Skulls were exposed and a burr hole was drilled. Implantation was with a 26-gauge stainless steel guide cannula (Plastics-One Inc., Roanoke, VA, USA). The tip of the guide cannula was positioned 1 mm above the left lateral ventricle according to the following coordinates: A: -0.4 -0.66\* (bl-3.8), (bl = bregma-lambda); L: 1.5; D: -2.2. The guide cannula was secured to the skull with 3 stainless-steel screws and dental cement, and was closed by a dummy cannula. Mice were housed in individual cages and allowed postoperative recovery of 10-14 days before experiments.

**Preparation of AS-ON:** For *i.c.v.* injection, 2'-O-methyl protected (three-3' nucleotides) oligonucleotides (5  $\mu$ M) targeted against murine AChE (AS3) or BuChE (ASB) mRNA (Shohami et al., 2000) were combined with 13  $\mu$ M of the lipophilic transfection reagent DOTAP (Roche Diagnostics) in PBS and incubated for 15 min at 37°C prior to injection. One  $\mu$ l (25 ng) of this oligonucleotide solution was injected in each treatment.

***I.c.v.* administration of AS-ON:** For intracranial microinjections, solutions were administered through a 33-gauge stainless steel internal cannula (Plastic One Inc.), which was 1 mm longer than the guide cannula. A PE20 tube connected the internal cannula to a microsyringe pump (KD Scientific Instruments, Boulder, CO, USA). Solutions were administered at a constant rate during 1 min, followed by 1 min during which the internal cannula was left within the guide cannula, to avoid spillage from the guide cannula. Correct positioning of the cannula was verified following each experiment by injection of trypan blue through the cannula and testing dye distribution after removal of the brains.

**Statistical analysis:** The results of the *in situ* hybridization experiment were analyzed by a t-test. The results of the circadian shift (Figure 3C) were analyzed by a three-way, repeated measures ANOVA (genotype x day (routine/reversed) x circadian phase (dark/light)). The results of the social recognition test (Figure 4) were analyzed by a three-way, repeated measures ANOVA (genotype x stimulus animal (same or different juvenile) x intersession interval). The results of the experiment on tacrine's effect on social recognition (Figure 5) were analyzed by a three-way ANOVA (genotype x stimulus animal (same or different juvenile) x drug (tacrine/saline)). The results of the effect of AS3 on social recognition (Figure 6B) were analyzed by a two-way, repeated measures ANOVA (pretreatment (short/long explorers) x time (days after injection)). The results of the specificity of AS3 effect (Figure 7) were analyzed by a three-way ANOVA (genotype x drug (AS3/ASB) x time (before/after the treatment)). All ANOVAs were followed by post-hoc tests with the Fisher PLSD procedure.

## Results

**Transgenic mice overexpress host AChE-R:** To explore the specific contribution of variant AChE mRNA transcripts towards neuronal *ACHE* gene expression, Tg mice overexpressing hAChE-S in the nervous system were tested by high resolution *in situ* hybridization using

cRNA probes selective for each of the two major AChE variants. Excessive labeling was observed in hAChE-S Tg mice as compared with controls in which hybridization was performed with the AChE-S selective probe. This was consistent with the expected cumulative contribution of the overexpressed human transgene and the host mouse (m)AChE-S mRNA transcript (Beeri et al., 1995; Beeri et al., 1997). However, hAChE-S Tg mice also displayed variably excessive labeling with the AChE-R cRNA probe, decorating mouse (m)AChE-R mRNA. Figure 1 presents a representative micrograph of mAChE-R mRNA overexpression in the cortex and hippocampus of a Tg as compared to a control mouse. Neuronal mAChE-R mRNA overproduction in these Tg mice was heterogeneous in its extent, yet significantly higher than that in control mice. Analysis of Fast Red staining showed an increase from an average of  $20 \pm 3$  arbitrary intensity units ( $\pm$  standard error of the mean, S.E.M.) in 5 control animals to  $41 \pm 5.5$  in 6 transgenics ( $t(9) = 10.27, p < 0.05$ ). This suggested an inherited predisposition to constitutive AChE-R overproduction in Tg mice. Because AChE-R overproduction is associated with psychological stress, this further called for evaluating its neuroanatomical and behavioral manifestations.

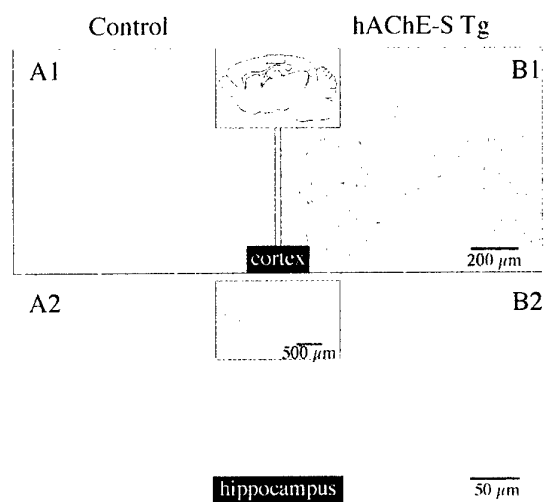


**Figure 1: Intensive neuronal AChE-R mRNA expression in Tg mice** Shown are representative micrographs of *in situ* hybridization in parietal cortex (A<sub>1</sub>, B<sub>1</sub>) and hippocampus (A<sub>2</sub>, B<sub>2</sub>) using an AChE-R cRNA probe and Fast Red detection. Insets: schematic drawing (top) or low-magnification micrograph (bottom) presenting the location of higher magnification micrographs in the cortex and hippocampal CA3 region. Note the intense AChE-R expression in cortical and hippocampal neurons of Tg mice.

**Hypertrophy in hippocampal astrocytes reflects elevated stress in hAChE-S Tg mice:** Immunocytochemical labeling of glial fibrillary acidic protein (GFAP) was used in search of an independent parameter for evaluating the stress-prone state of hAChE-S Tg mice. Hippocampal astrocytes are known from previous studies to be sensitive to various forms of stress (Laping et al., 1994; Sirevaag et al., 1991). This property is manifest in morphological changes, increased size of cell soma and of astrocytic processes collectively called "hypertrophy" and which is accompanied by increased expression of GFAP. The hippocampal SLM is particularly enriched in astrocytes, which appeared to be hypertrophic in hAChE-S Tg mice (Figure 2, B,D) as compared to age-matched controls (Figure 2, A,C). Astrocytes in other regions, such as cortex appeared unchanged (Figure 2, E,F). Figure 2 presents this selective hippocampal change, which is generally considered to reflect the cumulative load of stressful insults in the mammalian brain and is frequently associated with impaired cognitive and behavioral properties (McEwen and Sapolsky, 1995).

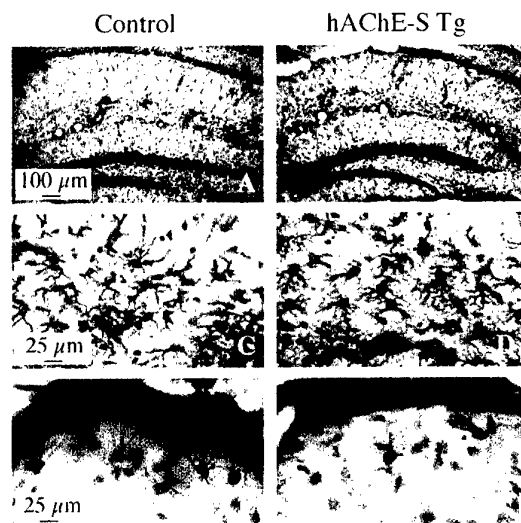


**Figure 2: Intensified GFAP staining in hypertrophic hippocampal astrocytes of hAChE-S Tg mice.** Shown are light microscopy micrographs of GFAP immunocytochemical staining in the brain of control (A,C,E) and Tg (B, D, F) mice. Note the intensified cell body staining in hippocampal (A-D) but not in cortical astrocytes (E,F) and the thickened process extensions in the transgenics' astrocytes.

Intensity of staining of GFAP-like immunoreactivity in the astrocytic soma was significantly higher in Tg mice ( $176.3 \pm 4.0$ , arbitrary units) compared to control mice ( $147.8 \pm 3.5$ ,  $t = 5.3$ ,  $p < 0.0001$ ). Cross-sectional area of the astrocytic soma was significantly increased in Tg ( $45.9 \pm 1.4 \mu\text{m}^2$ ) compared to control mice ( $35.4 \pm 1.5$ ,  $t = 5.16$ ,  $p < 0.0001$ ). The stem thickness of the large astrocytic process was greater in Tg mice ( $1.75 \pm 0.05 \mu\text{m}$ ) compared to control mice ( $1.32 \pm 0.05$ ,  $t = 6.21$ ,  $p < 0.0001$ ). Taken together, these data form a picture of 20-30% hypertrophy in hippocampal astrocytes of hAChE-S Tg mice, consistent with the earlier reports of stress-associated and pathology-associated astrocytic hypertrophy (Laping et al., 1994; Sirevaag et al., 1991).

**AChE overexpression predisposes to hypersensitivity to changed circadian cycle:** Behavioral differences between Tg and control mice were first sought by recording locomotion patterns. Under routine conditions, both genotypes displayed similar home cage activity (Figure 3A). Their circadian rhythms included, as expected, significantly more frequent and pronounced locomotor activity during the dark phase of the circadian cycle ( $F(1,24) = 18.16$ ,  $p < 0.001$ ) (summarized in Figure 3C). Seventy-two hr following reversal of the light/dark phases both genotypes lost most of the circadian rhythm in their locomotor activity, as reported by others (Hillegaart and Ahlenius, 1994), but presented distinctive behavioral patterns (Figure 3B and 3C). After the shift, hAChE-S Tg mice showed a general increase in activity, which was reflected in a significant genotype by day (routine vs. reversed) interaction ( $F(1,24) = 4.68$ ,  $p < 0.05$ ). Post-hoc tests demonstrated in Tg mice significantly increased activity in the reversed cycle (compared with activity in the routine cycle), both during the dark and the light phases ( $p < 0.05$ ). In addition, activity in the dark phase of the reversed cycle, was significantly greater in Tg compared with control mice. These findings indicate that adjustment to the circadian insult was markedly impaired in Tg mice, suggesting that these mice display a genetic predisposition to abnormal responses to changes in the circadian rhythm. The transgenics' intensified activity was found to be suppressed for a short time ( $< 3$  hr) by i.p. administration of AS-ONs targeted to the common domain shared by all AChE mRNA variants (preliminary data, data not shown).

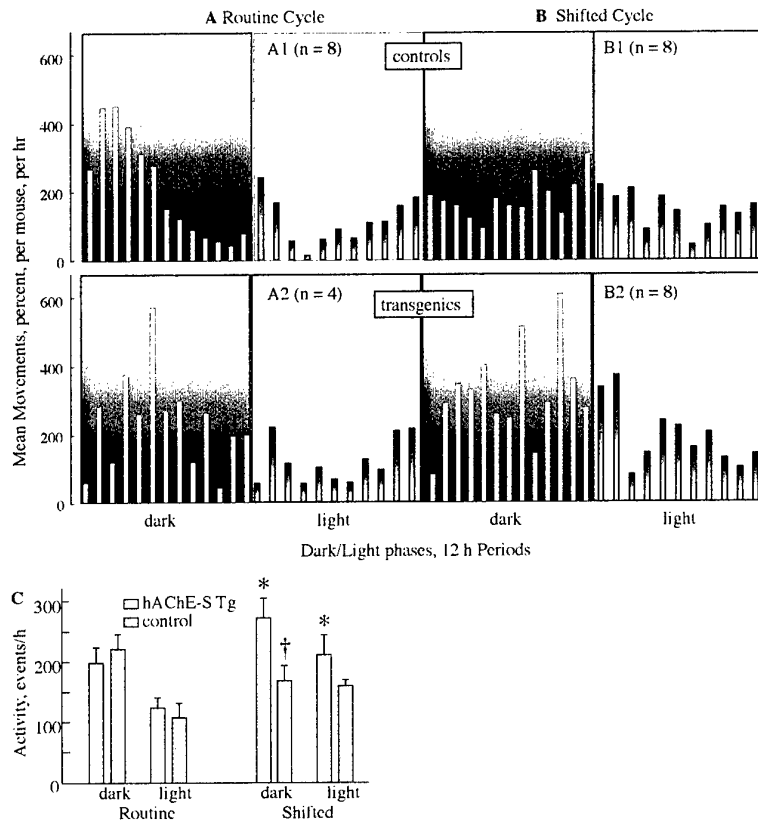


**Figure 3: Spontaneous locomotor activity of control and Tg mice under routine dark/light cycle and following cycle reversal.**

Locomotor activity was detected by biotelemetric-recorded movements for 24 hr and is displayed as percent of the mean movements per mouse per hr. Shaded areas in the figure indicate the dark phases of the light/dark cycle. A, routine cycle; B, shifted cycle; C, summated activity intensification. Shown are values of locomotor activity during the dark and light phases in the daily cycle for Tg and age-matched control mice

under routine and reversed cycles. \*Significantly different from the corresponding group in the routine condition ( $p < 0.05$ ). †Significantly different from Tg mice in the dark phase of the reversed condition.

**Impaired social recognition due to AChE excess:** In the social recognition paradigm, control mice could recognize a previously encountered (“same”) juvenile. This is manifest as a reduction in exploration time in the second exposure of the mice to the same, but not to a different juvenile, provided that the time interval from the end of the first encounter with that juvenile to the beginning of the memory test did not exceed 15 min. As expected, this memory decayed with increased intersession interval. In contrast, Tg mice tended to explore the previously introduced juvenile longer than control mice and did not display social recognition even after a short interval of 5 min (Figure 4). These findings were reflected by a significant statistical interaction between the genotype (control vs. Tg) and the stimulus juvenile (same/different) ( $F(1,76) = 9.93, p < 0.01$ ). In Tg mice, post-hoc analysis revealed significant reduction in exploration time only when Tg mice were tested immediately after the baseline (0 interval) with the same juvenile. These results are consistent with the cholinergic modulation of social recognition behavior (Winslow and Camacho, 1995).

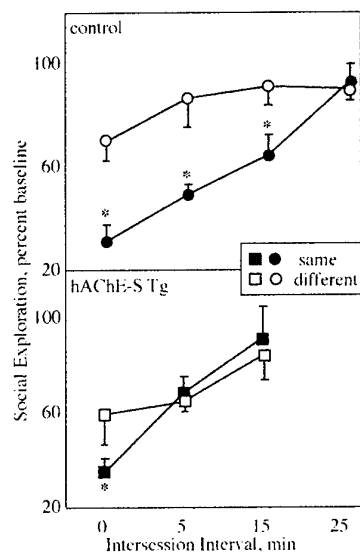


**Figure 4: Working memory deficiency in Tg mice**

Shown is percent of baseline social exploration time for 8-11 wk old Tg and control male mice as a function of the intersession interval. Average baseline exploration time was  $143 \pm 5$  and  $153 \pm 5$  (sec  $\pm$  S.E.M.) for transgenics ( $n = 42$ ) and control mice ( $n = 48$ ), respectively. Asterisks mark significant reductions of exploration time toward the same juvenile ( $p < 0.05$ ), as compared to a different juvenile, i.e. short-term working memory. Increased exploration time of the same juvenile with increasing intersession intervals reflects time-dependent decay in the working memory of control mice. After a 5 min interval, Tg mice displayed no reduction in exploration time toward the same juvenile, indicating that they did not remember the same mouse for even 5 min.

The reversible AChE inhibitor, tacrine, has been clinically used for blocking acetylcholine hydrolysis and extending the impaired memory of Alzheimer's disease patients (Giacobini, 2000). Therefore, we tested the capacity of tacrine (1.5 mg/Kg), injected immediately following a baseline encounter with a juvenile mouse, to improve the social recognition of Tg mice. Injected mice were tested with either the same or a different juvenile following a 10-min interval. As expected from previous reports on the beneficial effects of tacrine on social recognition in rats (Gheusi et al., 1994), injection of Tg mice with tacrine induced a significant improvement in recognition memory, with post-treatment performance similar to that displayed by untreated control mice. In contrast, Tg mice displayed no recognition of the same juvenile when injected with saline, and non-Tg control mice maintained unchanged recognition performance when injected with either tacrine or saline (Figure 5). These findings were reflected by a significant 3-way interaction between the genotype, (control/Tg), the stimulus juvenile (same/different) and the drug (tacrine/saline) ( $F(1,52) = 4.18, p < 0.05$ ). In a similar experiment, in which the injections preceded the social recognition test by 40, rather than 10 min, tacrine had no effect in either Tg or control mice (data not shown). Therefore, tacrine facilitated memory consolidation when administered during the consolidation process, but did not affect acquisition of memory when given in advance.

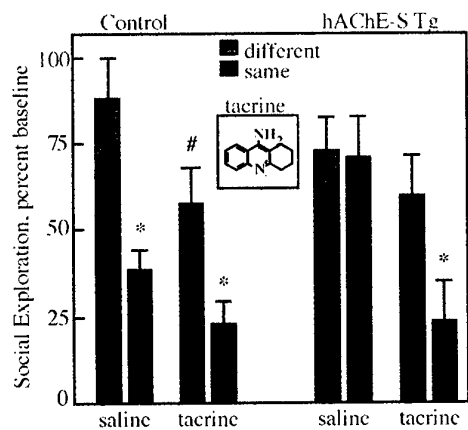


**Figure 5: Tacrine improves working memory of Tg mice.**

Presented is the mean social exploration time  $\pm$  S.E.M. as percentage of baseline time for 29 control and 32 Tg mice (12-15 wk. old, 7-8 mice/group) where either tacrine (1.5 mg/Kg) or saline (10 ml/Kg body weight) was administered intraperitoneally immediately following the baseline exploration period. The intersession interval was 10 min for all groups. Note the post-treatment shortening of explorative time of Tg mice, reflecting improved working memory. Asterisks mark significant

reduction of exploration time toward the same juvenile ( $p < 0.05$ ) as compared to a different juvenile. # marks a significant tacrine-induced reduction of exploration time toward the different juvenile ( $p < 0.05$ ).

**Explorative behavior is inversely correlated with brain AChE activity:** Apart from its improvement of memory, tacrine suppressed the exploration behavior toward a different juvenile in control ( $p < 0.05$ ) but not in Tg mice. Decreased locomotor activity under tacrine treatment was suggested to reflect cholinergic mediation of social exploration behavior (Shannon and Peters, 1990). To further investigate this concept, control mice were divided into 3 equal groups ( $n = 10$ ), presenting short, intermediate or long exploration time of same juveniles. AChE activity was determined in the cortex and hippocampus of each subgroup, 24 hr following social recognition tests of the "same" juvenile (presented 10 min following first exposure). Mice with lower levels of cortical and hippocampal AChE activity spent more interaction time with the "same" juvenile than mice with high AChE activity levels (Table 1), so that their explorative behavior was inversely correlated with cortical and hippocampal AChE activity levels (correlation magnitude,  $r = -0.49$  and  $0.41$ , respectively). Compared to shorter explorers, longer explorer mice exhibited a 29% reduction in cortical AChE activity, corresponding to a >80% increase in social exploration time. The significance of the difference between the shorter and longer explorers was verified by ANOVA ( $F(2,27) = 4.89$ ,  $p < 0.05$ ) and post-hoc tests.

**Table 1: Social exploration behavior and brain AChE activities.<sup>a</sup>**

	exploration time percent of baseline	specific AChE activity nmol ATCh hydrolyzed/min/mg protein	
		hippocampus	cortex
<b>total population</b>	80 ± 4	87 ± 4	90 ± 5
<b>shorter exploration time</b>	57 ± 3	96 ± 6	104 ± 10
<b>intermediate exploration time</b>	78 ± 2	95 ± 6	92 ± 10
<b>longer exploration time</b>	104 ± 3	71 ± 7**	74 ± 8*

<sup>a</sup>Control FVB/N male mouse population ( $n = 30$ ) (3-5 months) was divided into three equal groups ( $n = 10$ ) with short, intermediate and long exploration time of the same juvenile (shown as average ± S.E.M. percent of baseline). Intersession interval was 10 min for all groups. Mice were sacrificed 24 hr after the behavior test and AChE specific activities were measured in hippocampus and cortex extracts. Asterisks mark significantly lower AChE specific activity in control long explorers as compared with short explorers ( $p < 0.01$  for hippocampus and  $p < 0.05$  for cortex; ANOVA followed by post-hoc tests with the Fisher PLSD procedure).

The lack of tacrine effect on the social recognition performance in control mice, and its improvement effect on the social recognition in transgenics, with approximately 50% excess AChE (Sternfeld et al., 2000), presented an apparent contradiction to the inverse correlation between AChE catalytic activity and social exploration. One potential explanation to this complex situation was that the inverse correlation in control mice reflected primarily the levels of the synaptic enzyme AChE-S; in contrast, the massive mAChE-R excess in the Tg brain could cause their impaired social recognition behavior. According to this working hypothesis, selective suppression of AChE-R should improve the social recognition performance. To test this hypothesis, we adopted *i.c.v.* injection of AS3 to prevent *de-novo* mAChE-R production (Shohami et al., 2000). Mice were tested in the social exploration paradigm once before (baseline) and then 1, 3 and 6 days after 2 daily injections of AS3. Figure 6A presents the experimental design of these tests.

**AS3 improvement of social exploration increases in efficacy and duration in animals with severe pre-treatment impairments:** Post-treatment follow-up of social exploration was performed 1, 3 and 6 days following AS3 treatment in animals with short, medium and long pre-treatment social exploration behavior ( $n = 5-6/\text{group}$ ). As expected, there was a significant overall difference between the short and the long groups in exploration time ( $F(1,24) = 10.81, p < 0.05$ ). However, post-hoc tests revealed that these groups differed significantly only during the pre-treatment day ( $p < 0.05$ ), and not after the AS3 treatment (Figure 6B). Furthermore, within the long, but not the short explorers group, social exploration of the “same” juvenile was significantly reduced ( $p < 0.05$ ) one day after the AS3 injection, with progressive increases in social exploration time during the 5 subsequent days. Because of the pre-treatment differences, the severely impaired animals sustained a certain level of improvement even at the sixth post-treatment day (Figure 6B) (i.e., even on this day there was no resumption of the pre-treatment difference between the short and long explorers). This experiment thus demonstrated both the efficacy and the reversibility of the antisense treatment, however with exceedingly long duration, especially in animals with severe pre-treatment impairments and in comparison to the short-term efficacy of tacrine.

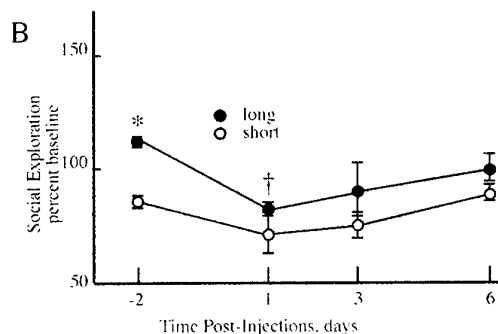
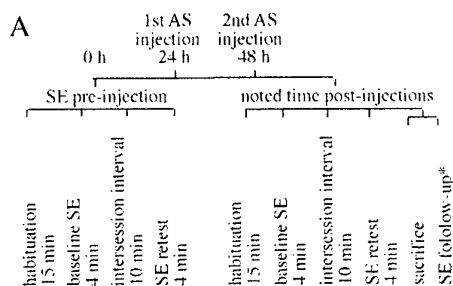


**Figure 6: *I.c.v.* antisense effect on the excessive social exploration behavior of Tg mice.** A. The experimental paradigm. Shown is the order of procedures and tests of the social exploration capacity in cannula-implanted mice following antisense treatment. See Materials and Methods for details. B. Long-term reversibility and correlation of treatment efficacy with the severity of pre-treatment symptoms. Shown are social exploration values, in percent of baseline performance, for cannulated hAChE-S Tg mice with short and long pre-treatment exploration of the “same” juvenile, following *i.c.v.* AS3 treatment ( $n = 5$  mice per group). Note that both the efficacy and the duration of the suppression effect are directly correlated to the severity of pre-treatment symptoms. \*Significantly different from mice with short exploration time, at day  $-2$  ( $p < 0.05$ ). †Significantly different from mice

with long exploration time, at day  $-2$  ( $p < 0.05$ ).

**Antisense AChE-R mRNA suppression selectively reduces brain AChE-R protein:** Tg mice with long pre-treatment explorative behavior displayed a significant improvement in social exploration of the “same” juvenile 24 hr following the second treatment with AS3, but not with the irrelevant AS-ON ASB (Figure 8A) ( $F(1,10) = 33.95, p < 0.001$ ). ASB, targeted to the related enzyme, butyrylcholinesterase, served as a sequence specificity control. Control mice with either long or short pre-treatment social exploration showed no response to either AS3 or ASB (Figure 7A and data not shown).

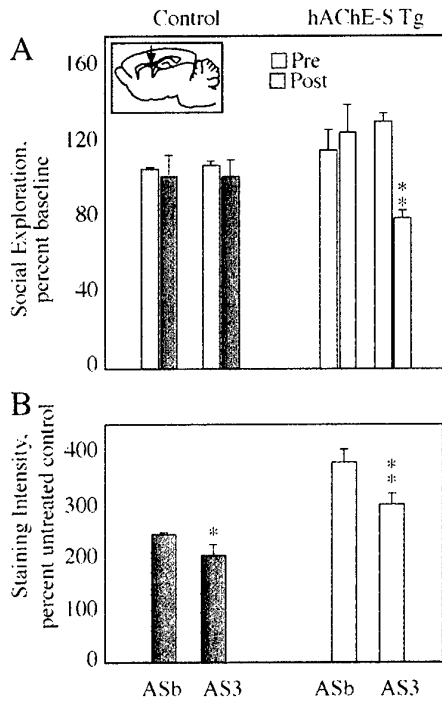


**Figure 7: AS3 decreases brain AChE-R levels and ameliorates social recognition deficits in Tg-mice.** Tg (n = 36) and control (n = 22) cannula-implanted mice, 10-20 wk old, were injected *i.c.v.* with AS-ONs targeted against AChE (AS3) or butyrylcholinesterase (ASB) on 2 consecutive days. Social exploration of the "same" juvenile was tested 24 hr before (pre) and 24 hr after (post) injections. Mice were sacrificed immediately after the last social recognition test and brain homogenates subjected to immunodetection of AChE-R. A. Social exploration behavior. Shown are mean social exploration of the same juvenile (percent of baseline  $\pm$  S.E.M.) before (pre) and 24 hr after (post) AS-ON treatment for long explorer mice (see Table 1). Asterisk marks significant reduction of social exploration time after AS3 treatment ( $p < 0.05$ ). Inset: Location of *i.c.v.* cannula in the brain (arrow). B. Immunodetected AChE-R. Mean  $\pm$  S.E.M. densitometry values for immunodetected AChE-R in cortex extracts of the noted groups post-treatment.

AChE-R levels in uncannulated control mice were considered 100%. Asterisks mark significant reduction of AChE-R levels in AS3 as compared to ASB treated mice (\*\*:  $p < 0.05$ , \*:  $p < 0.1$ ). Note the significant reduction of immunodetected AChE-R and fragments thereof in cortices from both groups treated with AS3 as compared with those treated with the control reagent, ASB.

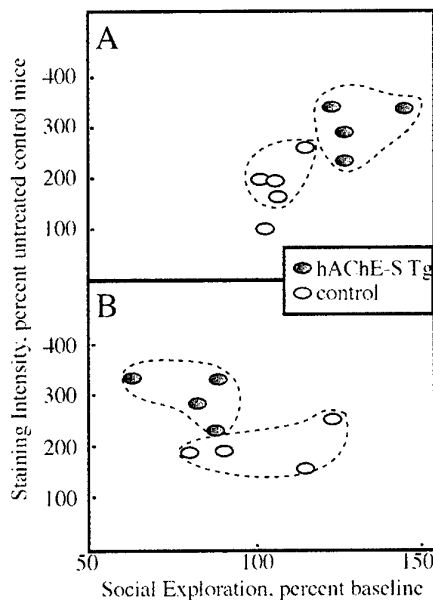


**Figure 8: Decreased AChE-R levels correlate with reduced social exploration time in Tg mice.** Presented are cortical AChE-R levels (immunodetected protein, percent of levels in uncannulated controls) as a function of social exploration for each mouse before (A) and after (B) AS3 treatment. Long-explorer mice, each represented by a dot, were sorted by their genetic backgrounds (control and Tg). Note the exclusive post-treatment shift in the clustered distribution of the Tg long explorers, with excessive mAChE-R levels, as compared with the non-shifted cluster of long-explorer controls.

Catalytic activity measurements performed 24 hr after the last AS-ON injection failed to show differences, perhaps due to the limited number of animals and the variable enzyme levels. However, immunodetected AChE-R protein levels were significantly lower in AS3 treated mice as compared with ASB treated mice, regardless of their genotype or pre-treatment behavior pattern (Fig 7B and data not shown,  $F(1,22) = 19.63$ ,  $p < 0.001$ ). In contrast,

densitometric analysis of immunodetected total AChE protein (detected by an antibody targeted to the N-terminus, common to both isoforms) revealed essentially unchanged signals (data not shown). In further tests for potential association, post-treatment AChE-R levels were plotted as a function of the social exploration values. Data points clustered separately before the AS-ON treatment (Figure 8A), with both AChE-R levels and exploration times of controls clearly different from transgenics. After treatment, long explorer transgenics shifted to short exploration values (Figure 8B). Intriguingly, the explorative behavior of long explorer controls was not affected by the treatment, indicating that the reduction in mAChE-R following AS3 treatment affected only animals that were behaviorally impaired before the treatment. Together, these findings attest to the selectivity of the antisense treatment for treating AChE-R overexpressing animals and its sequence-specificity in reversing the AChE-R induced impairment of behavior.

### Discussion

Combination of behavioral, molecular and biochemical analyses revealed multileveled contributions of cholinergic neurotransmission and *ACHE* gene expression, towards the general activity and social behavior of adult Tg mice over-expressing neuronal AChE. In addition to inherited excess of hAChE-S, these Tg mice display conspicuous yet heterogeneous overexpression of the stress-associated "readthrough" mAChE-R in their cortical and hippocampal neurons. Nevertheless, they present close to normal activity patterns under normal maintenance conditions with minimal external challenges. In contrast, their capacity to adjust to behavioral changes in response to external signals appears to be compromised, suggesting that they suffer genetic predisposition for adverse responses to stressful stimuli (McEwen and Sapolsky, 1995). This should be of particular interest to the Army, as inherited tendency for AChE overproduction was associated with a promoter polymorphism in the *ACHE* gene (Shapria et al., 2000) and because impaired social behavior can be detrimental in the field.

**Behavioral and learning impairments of cholinergic origin:** When subjected to a day/night switch, hAChE-S Tg mice respond with excessive bursts of locomotor activity, particularly during the dark phase, but also during the light phase of the post-shift diurnal cycle. In preliminary experiments, this excessive activity could be transiently suppressed by antisense oligonucleotides, which was especially encouraging in view of the progressively impaired neuromotor functioning in these mice (Andres et al., 1997). Matched controls, unlike transgenics, display, as expected, relatively suppressed locomotor activity during the post-shift dark phase (Murata et al., 1999). When confronted twice with a conspecific young mouse, hAChE-S Tg mice spend significantly longer periods than controls in the social interactions characterizing such confrontations. Similarly, in a new environment, hAChE-S Tg mice displayed increased locomotor activity as compared with controls (Erb et al., 2001). In the social recognition paradigm, they failed to remember a conspecific juvenile, even following a delay interval of only 5 min. This extends previous reports on their spatial learning and memory impairments (Beeri et al., 1995; Beeri et al., 1997) and agrees with previous reports (Perio et al., 1989; Winslow and Camacho, 1995) on the social behavior changes associated with cholinergic impairments.

A clear pattern appears to be emerging regarding acetylcholine function and behavioral deficits, highlighting potentially major effects on behavior, both motor and cognitive. Moreover, some in some cases, suppression of the excess of AChE of the transgenic animals returned many of the behaviors to normal, suggesting that the consequences of toxin exposure

may be similarly reversible in the field. Also, the influences on circadian periodicity and the potential disruptions to behavioral periodicity are striking. This is probably often overlooked in the military arena and is likely to be highly significant due to the 24 h activity status of combat troops.

Several other neurotransmission systems, e.g. vasopressin (Bluthe et al., 1990), are most likely related, as well, with impaired social interactions. In hAChE-S Tg mice, however, this phenotype may be attributed to hypocholinergic functioning due to AChE excess, as is evident from the capacity of the AChE inhibitor tacrine to retrieve their social recognition. Nevertheless, tacrine's effects appeared surprisingly short-lived, consistent with findings of others (Sekiguchi et al., 1991). In contrast, exceedingly low doses of oligonucleotides suppressing AChE-R synthesis exerted considerably longer-term improvement of the social recognition skills of Tg mice. This suggested non-catalytic activities as an alternative explanation (s) for the behavioral and cognitive impairments caused by AChE-R excess (Soreq and Seidman, 2001).

**Circadian switch as a behavioral stressor:** Cholinergic neurotransmission circuits are known to be subject to circadian changes (Carlson, 1994) and control the sensorimotor cortical regions regulating such activity (Fibiger et al., 1991). Therefore, the intensified response of hAChE-S Tg mice to the circadian switch suggested that their hypocholinergic state is the cause. The variable nature of the excessive locomotor activity in the Tg mice indicates an acquired basis for its extent and duration. A potential origin of such heterogeneity could be the variable extent of neuronal mAChE-R mRNA in the sensorimotor cortex and hippocampal neurons. Both psychological (Kaufer et al., 1998) and physical stressors (Shohami et al., 2000) induce neuronal AChE-R overproduction. Exaggerated stress responses, such as the intense locomotor response to the mild stress of a circadian switch, can hence be expected to exacerbate the hypocholinergic state of these already compromised animals,

In social behavior tests, hAChE-S Tg mice display impaired recall processes causing poor recognition when confronted with a conspecific young mouse. Therefore AChE-R overexpression, which is also induced under stress (Kaufer et al., 1998), may be causally involved with the reported suppression of recall processes under stress (Kramer et al., 1991) as well as with the apparent correlation between stress and hippocampal dysfunction (Liberzon et al., 1999). This suggests that excess AChE-R can simultaneously impair recall processes and induce excessive locomotion. Stress-induced effects on learning and memory processes have been reported by others (Kaneto, 1997), but were not correlated with AChE levels. Our current findings of improvement in transgenics' exploration behavior following tacrine injection, which would be expected to augment cholinergic neurotransmission, strongly indicate that their hypocholinergic state was the cause.

**Advantages and limitations of anticholinesterases:** In control mice, with low AChE-R levels, tacrine did not affect the normal social recognition capacity. This suggests that suppression of AChE activity may have distinct effects under normal and stress-induced conditions. Tg mice with higher AChE levels have accommodated themselves to this state, and it may be this accommodation that renders them incapable of facing a challenge by an anticholinesterase. One option is that of a threshold AChE-R activity that would be compatible both with satisfactory memory and normal locomotion. This balance is impaired in the Tg mice and may also be disrupted under inducers of long-term AChE-R

overproduction, e.g. stress or exposure to anticholinesterases (Kaufer and Soreq, 1999). This, in turn, implies that the effect of anticholinesterases would depend on the initial levels of specific AChE variants in the treated mammal. Above the behaviorally-compatible threshold of AChE-R, anticholinesterases would exert behavioral improvement, whereas below it, their effects would be limited, which can explain their differential efficacy in patients with different severity of symptoms.

**Glucocorticoid regulation of cholinergic behavioral patterns:** The separation between general behavior patterns and learning paradigms as those relate to cholinergic transmission may explain why AChE transgenics, so dramatically impaired in their learning capacities, display such subtle deficiencies in their daily behavior. According to this concept, a constitutive hypocholinergic condition would be evident as a failure to learn and remember, however, its behavioral effect will be far less pronounced, unless challenged. This predisposition to drastic responses to external insults is indeed reminiscent of the reported behavior of demented patients. It had been initially attributed to their elevated cortisol levels (Weiner et al., 1997), which matches recent findings in primates (Habib et al., 2000). Indeed, cortisol upregulates *ACHE* gene expression and elevates AChE-R levels (Grisaru et al., 2001), possibly above the required threshold. In addition, both psychological stress and glucocorticoid hormones were reported to impair spatial working memory (de Quervain et al., 1998; Diamond et al., 1996), consistent with such impairments in the hAChE-S Tg mice. The intensive overexpression of mAChE-R in these mice mimics a situation in which the individual capacity for AChE-R overproduction would be tightly correlated both with the severity of the behavioral impairments induced under cholinergic hypofunction and with the capacity of anticholinesterases to affect learning and behavior properties.

**Brain region specificity:**

Working and storage memory and the ability to integrate information are tightly linked not only to cholinergic neurotransmission, but to other neurotransmitters as well. Several studies demonstrate that even mild environmental changes (like a day-to-night switch), are accompanied by increased dopamine and noradrenaline extracellular concentration in the prefrontal cortex, and only to a minor extent in the limbic and striatal areas<sup>40</sup>. This activation is very selective, since molecular studies have shown that thirty minutes of restraint increase Fos protein in dopamine neurons projecting to the cortex but not in those projecting to the n. accumbens. In this respect altered accumbens and cortical extracellular dopamine concentrations during stress are not secondary to motor activation, but instead reflect increased attention to the provocative stimulus or attempts by the intruder to "cope" with the stimulus, and therefore are independent of a specific motor activation<sup>41</sup>.

The ventral hippocampus is an important neuronal "gate" which should be regarded as system modulator of the cortical response to stress. In this respect cholinergic transmission may contribute to the significance of environmental cues. When neonatal ibotenic acid lesions are produced in the ventral hippocampus, repeated intraperitoneal saline injections attenuate dopamine release in the medial prefrontal cortex, while chronic haloperidol augments dopamine release in the same area of lesioned animals compared to controls<sup>42</sup>. This suggests that the ventral hippocampus influences the functioning of midbrain dopamine systems during environmental and pharmacological challenges in different ways<sup>43</sup>.

**Low dose and long duration of efficacy for antisense agents:** The short duration of the behavioral and memory improvements afforded by administration of tacrine parallels the time scale reported for the induction by such inhibitors of a transcriptional activation (Kaufer et al., 1998). Together with a shift in alternative splicing this feedback response causes secondary AChE-R accumulation facilitating the hypocholinergic condition (Coyle et al., 1983). Recent reports demonstrate AChE accumulation in the cerebrospinal fluid of anticholinesterases-treated Alzheimer's disease patients<sup>45</sup>, suggesting that such feedback response occurs also in humans with cholinergic deficiencies<sup>46</sup> and perhaps explaining the gradual increase in anticholinesterase dosage that is necessary to maintain their palliative value in patients.

Unlike tacrine, the temporary antisense suppression of AChE synthesis improves social recognition in Tg mice for up to 6 days. This requires exceedingly low doses (25 ng per daily treatment) of the antisense agent, about 104-fold lower in molar terms than tacrine concentrations. Active site enzyme inhibitors should be administered in stoichiometric ratios with the large numbers of their protein target molecules. Moreover, the action of such inhibitors terminates when they reach their target. In contrast, a single chemically protected antisense molecule can cause the destruction of numerous mRNA transcripts, each capable of producing dozens of protein molecules. Assuming translation rates of approximately half-hour per chain and an average half-life of several hours for each transcript, destruction of each mRNA chain would prevent the production of many protein molecules. Therefore, the cumulative efficacy of antisense agents can exceed that of protein blockers by several orders of magnitude<sup>47,48</sup>. Moreover, the palliative effects of AS-ON destroying AChE-R mRNA should extend long after the AS-ON is destroyed, because AChE-R-induced adverse consequences would occur only above a certain threshold which takes time to accumulate. Therefore, the dose dependent nature of the adverse consequences of AChE-R excess makes it particularly attractive as a target for antisense therapeutics.

We have recently found that AChE-R mRNA, having a long 3' untranslated domain, is significantly more sensitive to antisense destruction than the synaptic transcript (Grisaru et al., 2001; Shohami et al., 2000). AChE-R mRNA transcripts would hence be preferentially destroyed, so that the excess of AChE-R, but not much of the synaptic enzyme, would decrease. This effect may explain the extended duration and increased efficacy of the antisense treatment in modifying behavior and learning exclusively in those mice with disturbed social recognition.

In conclusion, our study provides a tentative explanation for the behavioral impairments under imbalanced cholinergic neurotransmission, attributes much of these impairments to the stress-related effects of the AChE-R variant and suggests the development of antisense approach to selectively ameliorate these effects.

## Antisense oligonucleotides relieve neuromuscular weakness in experimental autoimmune myasthenia gravis (task 1)

Recently, we observed that the irreversible cholinesterase inhibitor diisopropylfluorophosphonate (DFP) induces overexpression of AChE-R, a non-abundant, non-synaptic splicing variant of AChE, in mouse brain and intestine, and muscle (Shapira et al., 2000). Muscles from DFP treated animals treated with DFP displayed exaggerated neurite branching, disorganized wasting fibers and proliferation of neuromuscular junctions (NMJs). EN101, a partially protected 2'-oxymethyl AS-ON preferentially reducing AChE-R mRNA suppressed feedback upregulation of AChE and partially ameliorated DFP-induced NMJ proliferation (Lev-Lehman et al., 2000). These observations demonstrated that cholinergic stress can induce specific overexpression of AChE-R in muscle, and raised the possibility that AChE-R plays a previously unsuspected role in the pathophysiology of additional states associated with cholinergic imbalance.

Myasthenia gravis (MG) is caused by defective neuromuscular transmission mediated by autoantibodies that severely reduce the number of post-synaptic muscle nAChR (Drachman, 1994; Vincent, 1999). MG is characterized by fluctuating muscle weakness that is transiently improved by inhibitors of AChE, the acetylcholine hydrolyzing enzyme (Penn and Rowland, 1995). The diagnostic electrophysiological abnormality characterizing MG is a progressive decrement in the amplitude of compound muscle action potentials (CMAP) evoked by repetitive nerve stimulation. Standard treatment for MG includes immunosuppression and multiple daily doses of peripheral AChE inhibitors such as pyridostigmine (Mestinon™) (Penn and Rowland, 1995). While AChE inhibitors provide effective palliative relief to MG patients, a direct role for AChE in the pathophysiology of MG has not been demonstrated.

Here, we demonstrate overexpression of AChE-R in muscles and peripheral blood of EAMG rats. Moreover, we show that AS-ON-mediated suppression of AChE-R elicits pronounced and long-lasting relief of muscle fatigue in EAMG rats. These data indicate a previously unrecognized role for AChE-R in MG pathology, and raise questions about the long-term consequences of therapeutic AChE inhibitors. Moreover, they suggest that AS-ON targeting AChE may offer a novel mode of therapeutic intervention in neuromuscular diseases with cholinergic involvement.

### Methods

**Human MG patients:** Serum samples from anonymous MG patients were used according to the guidelines of the Hebrew University's Bioethics Committee.

**Materials:** Unless otherwise specified, materials were purchased from Sigma Chemical Co. (St. Louis, MO).

**Animals:** EAMG was induced in female Lewis rats (120-150 g) purchased from the Jackson Laboratory (Bar Harbor, ME), and housed in the Animal Facility at the Hebrew University Faculty of Medicine, in accordance with NIH guidelines. Control FVB/N mice were bred from the FVB/N strain purchased from Harlan Biotech Israel (Rehovot, Israel). Transgenic FVB/N mice overexpressing AChE-R were as described (Sternfeld et al., 2000).

**Oligonucleotides:** HPLC-purified, GLP grade oligodeoxynucleotides (purity >90% as verified by capillary electrophoresis) were purchased from Hybridon, Inc. (Worcester, MA). Lyophilized oligonucleotides were resuspended in sterile double distilled water (24 mg/ml), and stored at -20 °C. The three 3'-terminal residues in all of the employed AS-ON agents were substituted with oxymethyl groups at the 2' position. The primary sequences used in this study were:

rEN101 5'-CTGCAATATTTTCTTGCA \*C\*C\*-3';  
rEN102 5'-GGGAGAGGAGGAGGAAGA \*G\*G\*-3'; and  
inv-rEN102 5'-GGAGAAGGAGGAGGAGAG \*G\*G\*-3'.  
(Asterisks denote 2'-oxymethyl protected residues.)

All of these AS-ONs are complementary or inverse (inv) to the coding sequence of the rat (r) AChE mRNA sequence common to all variants (Legay et al., 1993).

**Antibodies:** Rabbit polyclonal Abs against the C-terminal sequence that is unique to AChE-R were prepared and purified as described (Sternfeld et al., 2000). Goat polyclonal anti-nAChR (C-20, S.C.-1448) Abs were from Santa Cruz Biotechnology (Santa Cruz, CA). Biotinylated donkey anti-rabbit Ab (Chemicon International, Temecula, CA) and biotinylated donkey anti-goat Ab (Jackson ImmunoResearch Laboratories, West Grove, PA) were used as secondary antibodies.

**Induction of EAMG:** The *Torpedo* acetylcholine receptor (tAChR) was purified from *T. californica* electroplax by affinity chromatography on neurotoxin-Sepharose resin, as previously described (Boneva et al., 2000). Rats were immunized with 40 µg of purified tAChR emulsified in CFA supplemented with 1 mg of *M. tuberculosis* H37Ra (Difco, Detroit MI). Subcutaneous injection in the hind footpads was followed by a booster injection of the same amount after 30 d. A third injection was administered to animals that did not develop EAMG after the second injection. Animals were weighed and inspected weekly during the first month, and daily after the booster immunization, for evaluation of muscle weakness. The muscle weakness status of the rats was graded according to: apparently healthy – Without definite weakness (treadmill running time, 23 ± 3 min), Mild – weight loss >10% during a week, accompanied by weak grip or audible complaint with fatigue (4-8 min run on the treadmill). Moderate – hunched posture at rest, head down and forelimb digit flexed, tremulous ambulation (1-3.5 min run on treadmill). Severe – general weakness, no audible complaint or grip (treadmill running time <1 min).

**Anti-AChR Ab determination:** Sera from EAMG animals and MG patients were assayed by direct radioimmunoassay, for <sup>125</sup>I-α-bungarotoxin (BgT) binding to tAChR or rat (r) AChR (Boneva et al., 2000; Wirguin et al., 1994). All the EAMG rats displayed high anti-tAChR and/or anti-rAChR titers, with serum mean ± SEM values of 82.1 ± 16.0 nM for anti-tAChR antibodies and 19.9 ± 1.8 nM for anti-rAChR.

**Quantification of nAChR:** AChR concentration in the gastrocnemius and tibialis muscles was determined using <sup>125</sup>I-α-BgT binding followed by precipitation in saturated ammonium sulfate as described previously (Changeux et al., 1992).

**Electromyography:** Rats were anesthetized by *i.p.* injection of 2.5 mg/Kg pentobarbital, immobilized, and subjected to repetitive sciatic nerve stimulation, using a pair of concentric needle electrodes at 3 Hz. Baseline compound muscle action potential (CMAP) was recorded by a concentric needle electrode placed in the gastrocnemius muscle, following a train of repetitive nerve stimulations at supramaximal intensity. Decrease (percent) in the amplitude of the fifth vs. the first muscle action potential was determined in two sets of repetitive stimulations for each animal. A reduction of 7% or more was considered indicative of neuromuscular transmission dysfunction (Wirguin et al., 1994).

**Drug administrations:** Intravenous injections and blood sampling for anti-nAChR Ab determination, were via the right jugular vein under anesthesia. For oral administration, a special intubation feeding curved needle with a ball end (Stoelting, Wood Dale, IL) was used. Mestionin, administered in a dose of 1 mg/Kg per day, was purchased from Hoffmann La-Roche (Basel, Switzerland).

**Exercise training on treadmill:** To establish a physiological measure of neuromuscular performance in EAMG rats, animals were placed on an electrically powered treadmill (Moran et al., 1996) running at a rate of 25 m/min, a physical effort of moderate intensity, until visibly

fatigued. The time the rats were able to run was recorded before and at the noted times after AS-ON or Mestinin treatment.

**In situ hybridization** was performed with fully 2'-oxymethylated AChE-R-or AChE-S-specific 50-mer cRNA probes complementary to pseudointron 4 or exon 6, respectively, in the *ACHE* gene (Galyam et al., 2001). Detection was with alkaline phosphatase and Fast Red™ substrate (Molecular Probes, Eugene, OR). DAPI (Sigma) staining served to visualize nuclei.

**Immunohistochemistry:** Muscle sections (7 μm) were deparaffinized with xylene and were rehydrated in graded ethanol solutions (100%, 90%, 70%) and PBS. Heat-induced antigen retrieval was performed by microwave treatment (850 W for rapid boil followed by 10 min at reduced intensity) in 0.01 M citrate buffer, pH 6.0. Slides were cooled to room temperature and rinsed in double distilled water. Non-specific binding was blocked by 4% naive donkey serum in PBS with 0.3% Triton X-100 and 0.05% Tween 20 (1 h at room temperature). Primary Ab was diluted (1:100 and 1:30 for rabbit anti-AChE-R and goat anti-nAChR, respectively) in the same buffer and slides were incubated 1 h at room temperature following overnight incubation at 4 °C. Sections were rinsed and incubated with the appropriate biotinylated secondary Ab, diluted in the same blocking buffer 1 h at room temperature and then overnight at 4 °C. Detection was with streptavidin conjugated to alkaline phosphatase (Amersham Life Science, Arlington Heights, IL) and Fast Red substrate; slides were cover-slipped with Immunomount (Shandon Pittsburgh, PA).

**Patient serum analyses:** Blood samples were drawn from 19 MG patients who displayed Ab titers between 1 and 60 pmol/ml serum. Non-denaturing gel electrophoresis was as described (Kaufer et al., 1998), as were catalytic activity measurements of AChE in the serum of patients and experimental animals.

## Results

### AChE-R accumulates in plasma of MG patients and EAMG rats

To search for potential correlations between AChE-R expression and neuromuscular junction dysfunction in humans, we evaluated the levels of AChE-R in plasma collected from MG patients. Serum samples from healthy individuals showed primarily a slow-migrating enzyme which could be effectively inhibited by  $5 \times 10^{-5}$  M of the AChE-specific inhibitor, BW284c51, but not by the butyrylcholinesterase-specific inhibitor iso-OMPA (Fig. 1 and data not shown). Serum from mice subjected to confined swim stress (Shapira et al., 2000), or transgenic mice overexpressing human AChE-R (Sternfeld et al., 2000) displayed higher levels of a similar rapidly migrating AChE isoform than non-stressed controls. This activity, like the slowly migrating enzyme, was blocked by BW284c51, but not iso-OMPA (Fig. 1A and data not shown). This suggested that the rapidly migrating AChE is AChE-R. In 2 of 4 tested MG patients, but not in patients with other diseases, we observed the presence of a similar fast-migrating, catalytically active AChE isoform (Fig. 1A). This suggested that MG patients, like stressed or AChE-R transgenic mice, accumulate excess serum AChE-R. There was no apparent correlation between the intensity of AChE-R staining and the anti-AChR titers in the 12 analyzed patients (data not shown). Also, total AChE activity measurements in the serum of patients or of stressed and non-stressed mice showed no correlation with these AChE-R migration patterns, probably due to differences in released erythrocytic AChE due to hemolysis (Fig. 1B). Thus, immunodetection or activity gel analyses appeared more informative than serum enzyme assay.

### AChE-R accumulates in muscles and serum of EAMG rats

To address the role of AChE-R in changes occurring at the myasthenic neuromuscular junction (NMJ), we induced EAMG in rats and performed *in situ* hybridization with AChE splice-variant selective probes. In triceps muscles of EAMG rats, we observed pronounced punctuated expression of AChE-R mRNA. In contrast, control rats, displayed only weak diffuse labeling

(Fig. 2A). The "synaptic" AChE-S variant displayed similar staining patterns in both control and EAMG rats (data not shown). Following *i.v.* administration of an EN101, an AS-ON preferentially targeting AChE-R mRNA labeling was reduced close to the limit of detection in both control and myasthenic rats (Fig. 2). In contrast, AChE-S mRNA labeling was nominally affected by EN101.

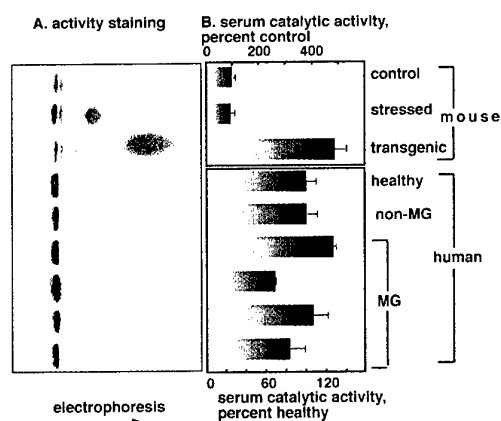


**Fig. 1. A rapidly migrating AChE variant accumulates in the serum of human MG patients.**

Shown is a non-denaturing polyacrylamide gel stained for catalytically active cholinesterases (left) and a bar graph representing the catalytic AChE activities in the serum of these patients and animals (right). Additional lanes depict the catalytically active isoforms in serum from confined-swim stressed mice (lane 1), control mice (lane 2) and AChE-R transgenic mice (lane 3), a healthy human volunteer (lane 4), a patient with an irrelevant metabolic disease (non-MG) (lane 5) and 4 MG patients (lanes 6-9). Note the presence of a rapidly

migrating AChE isoform, parallel to AChE-R in its properties, in the serum of MG patients but not other individuals.

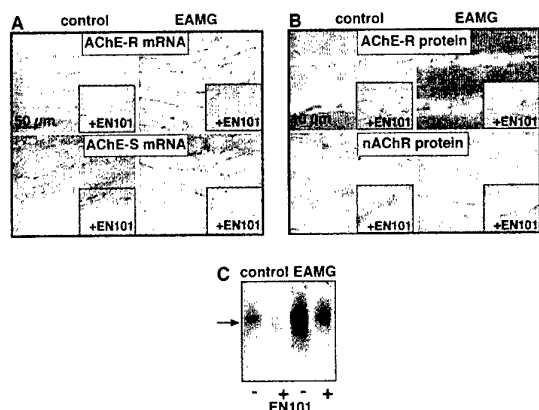


**Fig. 2. EN101 selectively suppresses elevated muscle AChE-R accumulation in EAMG rats.**

**A. Muscle AChE mRNA variants.** Shown are paraffin-embedded sections of triceps muscle from severely ill EAMG or control Lewis rats following *in situ* hybridization with 2'-O-methyl protected cRNA probes specific for AChE-S or -R mRNAs. The white size bar represents 50 µm. Fast Red (red) labeling reflects mRNA presence. DAPI (white) was used to visualize cell nuclei. Note the prominent sub-nuclear accumulation of AChE-R mRNA in preparations from EAMG,

but not control animals. AChE-S mRNA displayed similar focal expression around subnuclear domains in control and EAMG rats. Twenty-four h following treatment with EN101 (250 µg/Kg), AChE-R mRNA was barely detectable in both control and EAMG rats, while AChE-S mRNA levels were not visibly affected (insets).

**B. Inverse intensities of AChE-R and AChR labeling in EAMG.** Shown is immunohistochemical staining observed using polyclonal rabbit antibodies to AChE-R (top) or to nAChR (bottom) and Fast Red. The white size bar represents 10 µm. Immunostaining for AChE-R protein was prominently elevated in EAMG as compared to control rats, and suppressed by EN101 (insets). Consistent with their myasthenic pathology, staining of the nAChR is dramatically reduced in EAMG rats. nAChR was not affected by EN101.

**C. Serum AChE-R labeling.** Serum samples from EAMG and control rats were subjected to non-denaturing polyacrylamide gel electrophoresis and immunolabeling with anti-AChE-R antibodies. Note pronounced enhancement of a band representing AChE-R (arrow) in plasma of EAMG rats and its significant reduction in EN 101-treated control and EAMG animals.

Immunocytochemical staining with a polyclonal antiserum that selectively detects AChE-R (Sternfeld et al., 2000) revealed positive signals in some, but not all muscle fibers of control rats. In contrast, pronounced accumulation of AChE-R in virtually all muscle fibers from EAMG rats indicated increased levels of this protein species (Fig. 2). The disperse cytoplasmic localization of immunodetected AChE-R in EAMG muscle was characteristic of this isoform (Soreq and Seidman, 2001). In contrast, expression of AChE-S was similar in EAMG and control rats (data not shown). Twenty-four h following a single *i.v.* injection of 250  $\mu\text{g}/\text{Kg}$  EN101, AChE-R but not AChE-S was conspicuously reduced in muscles from both control and EAMG rats (Fig. 2). The association between muscle AChE-R accumulation and the EAMG was confirmed by immunohistochemical staining for muscle nAChR protein. In EAMG muscle, marked reduction was observed, as expected in the disease, which is associated with nAChR loss (Fig 4B, bottom). Muscle nAChR loss was confirmed by direct measurement of muscle AChR content, using labeled  $\alpha$ -bungarotoxin. The nAChR content in mild EAMG was reduced by 50% from control and in severe EAMG it was reduced by 70-80% (average,  $n > 10$  in each group).

As AChE-R is a soluble secretory protein, we searched for it in serum from control and EAMG rats. Immunoblot analysis of non-denaturing polyacrylamide gels indeed demonstrated the presence of AChE-R in serum of control and EAMG rats (Fig. 1). However, EAMG rats demonstrated significantly enhanced accumulation of AChE-R in serum as compared with healthy animals. 24 h following a single injection of EN101, both group of animals displayed conspicuously reduced AChE-R signals. (Fig. 1).

#### Antisense oligonucleotides restore normal CMAP in myasthenic rats

To evaluate the severity of muscle pathology in tested animals, we performed electromyography recording from the gastrocnemius muscle. EAMG rats, but never control animals, displayed a characteristic decrement in CMAP in response to repeated stimulation at 3 and 5 Hz (Fig. 3A, inset and data not shown). The baseline decrement, calculated by measuring the decrease from the first to the fifth response, ranged from 7% to 36% (mean =  $13.0\% \pm 2.5\%$ ) as compared to a limited variation around  $4.0\% \pm 0.9\%$  in control animals. To examine whether accumulated AChE-R was causally involved, we treated EAMG rats with rEN101, a partially 2'-oxymethyl protected AS-ON targeted to a region of rAChE mRNA that is common to all 3 variants, but which we found previously to selectively destroyed AChE-R mRNA (Grisaru et al., 2001).

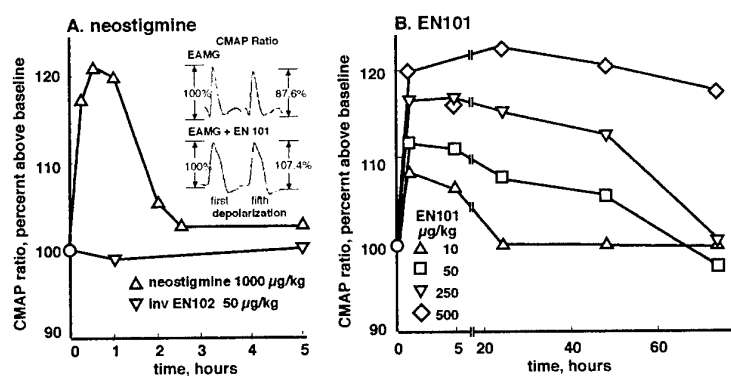


**Fig. 3. EN101 elicits lasting improvement in muscle function of myasthenic rats.**

Compound muscle action potentials (CMAP) were recorded from the gastrocnemius muscle of EAMG rats during repetitive stimulation at 3 Hz and the ratio between the 5<sup>th</sup> and 1<sup>st</sup> peaks determined (inset). Animals

exhibiting a decrement, reflecting the fatigue characteristic of myasthenic muscles (CMAP ratio  $< 90\%$ ), were treated with a single *i.v.* injection (1000  $\mu\text{g}/\text{Kg}$ ) of the AChE inhibitor Prostigmine, increasing concentrations of EN101, or a control AS-ON with the 5'-3' nucleotide sequence of EN102 reversed (INV-EN102). Graphs display percent above baseline of average CMAP ratios (5<sup>th</sup> to 1<sup>st</sup>) measured at the specified times post-injection for at least 6 rats in each

group. The average CMAP ratio of EAMG rats included in the study prior to treatment was  $87 \pm 2.5\%$  of control animals. Inset: CMAP Ratio Improvement. Shown are the 1<sup>st</sup> and 5<sup>th</sup> depolarization peaks in EAMG muscle (top) and in EN101-treated EAMG muscle (bottom; 500  $\mu\text{g}/\text{Kg}$ , 1 h post-treatment). Note the constant size of CMAP peaks under treatment (percent).

A. Prostigmine. Following administration of Prostigmine at a standard therapeutic dose of 1000  $\mu\text{g}/\text{Kg}$  body weight, normal CMAP ratios ( $\geq 100\%$ ) were recorded within 30 min and for up to 2 h. The control AS-ON invEN102 had no effect on muscle responses to stimulation at 3 Hz from EAMG rats, demonstrating sequence-specificity for the AS-ON.

B. EN101. Shown are dose-dependently restored normal CMAPs from 1 h and up to 72 h under 10-500  $\mu\text{g}/\text{Kg}$  EN101. Higher doses conferred longer-lasting relief.

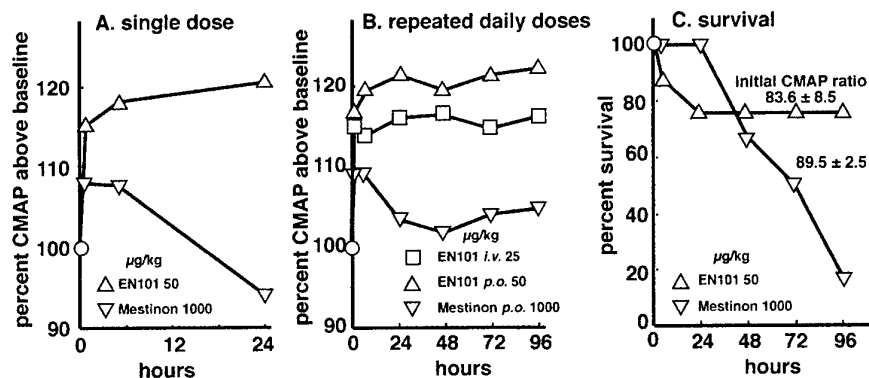


**Fig. 4. Effective oral administration of EN101.**

EAMG rats received EN101 (50  $\mu\text{g}/\text{Kg}$ ) or Mestinson (1000  $\mu\text{g}/\text{Kg}$ ) once daily for up to 4 days via an intubation feeding needle. CMAP ratio was determined 1 and

5 h following the first drug administration and then every 24 h, prior to the administration of the subsequent dose.

A. Single dose. The graph depicts percent CMAP ratios above baseline measured at the noted time points following oral administration of EN101 ( $n=8$ ) or Mestinson ( $n=4$ ). Orally administered Mestinson and EN101 relieved decremental CMAP responses to repetitive stimulation within 1 h. Twenty-four h following administration of Mestinson, CMAP ratios in muscles of treated rats returned to baseline. In contrast, no decrement was detected in rats treated with EN101.

B. Repeated daily doses. The graph depicts the equivalent improvement in muscle function elicited by oral ( $n=8$ ) as compared to *i.v.* ( $n=4$ ) administration of EN101. Note that repeated administration of EN101 conferred stable, long-term alleviation of CMAP decrements. Repeated daily administration of Mestinson at 24 h intervals had no cumulative or long-term effect on CMAP ratios.

C. Survival. The graph depicts the percentage of EAMG rats still alive at specified days following initiation of treatment with repeated oral administrations of Mestinson or EN101. Average CMAP values for each group at the starting day are noted. A greater fraction of animals treated with EN101 survived than those treated with Mestinson at the given doses despite their poorer initial status, as indicated by initial CMAP ratios.

rEN101 effects were compared to those of cholinesterase inhibitors used in the treatment of MG. Intraperitoneally (*i.p.*) administered neostigmine bromide (Prostigmine<sup>TM</sup>, 1000  $\mu\text{g}/\text{Kg}$ , which equals ca. 0.5  $\mu\text{mol}/\text{rat}$ ) rapidly and effectively reversed the myasthenic CMAP decrement in EAMG rats. The effects of cholinesterase blockade were evident starting 30 min after injection and up to 2-3 h post-injection, after which CMAP decrements reverted to baseline (Fig. 3A). A control AS-ON with an inverse sequence to rAChE mRNA, inv-rEN102, showed no effect at 50  $\mu\text{g}/\text{Kg}$ , demonstrating that neither the injection itself nor the presence of an inert AS-ON would alter the CMAP ratio (Fig. 3A). Following *i.v.* injection of EN101 at doses ranging from 50-500  $\mu\text{g}/\text{Kg}$ , i.e. 2 to 20  $\text{nmol}/\text{rat}$ , CMAP ratios changed to normal values within 1 h post-administration (Fig. 3B). CMAP normalization was accompanied by visible improvement in

motor activity associated with increased mobility, upright posture, stronger grip and reduced tremulous ambulation. A second, independent and similarly protected AS-ON, targeting a neighboring sequence in rAChE mRNA (EN102), produced similar rectification of decrements in CMAP in EAMG rats (Table 1), validating the specificity for the target protein. Nevertheless, antisense effects on neuromuscular activity were sequence-dependent, as comparable amounts of inv-rEN102, the control oligonucleotide with inverse sequence, did not improve muscle function (Fig. 3A and Table 1). The duration of CMAP restoration increased with the dose of EN101, from short-term improvement with 10  $\mu\text{g}/\text{Kg}$  up to over 72 h with 500  $\mu\text{g}/\text{Kg}$ . Fifty  $\mu\text{g}/\text{Kg}$  yielded 24 h improvement, and was therefore used for repetitive daily treatments (Fig. 3B).

**Table 1. Summary of responses to treatments<sup>A</sup>**

	Oral <sup>B</sup>					Intravenous <sup>B</sup>			
	EN101 treated healthy	EN101- treated EAMG	EN102- treated EAMG	INV102 -treated EAMG	Mestino n- treated EAMG	EN101 treated healthy	EN101- treated EAMG	EN102- treated EAMG	INV102 -treated EAMG
0 h	101.5±0	83.6±3.	82.3±2.	78.4±5.	89.5±1.	100.5±0	86.7±1.	84.7±5.	88.8±2.
	.9 (4)	0 (8)	0 (4)	5 (4)	0 (6)	.4 (6)	2 (6)	6 (4)	4 (5)
1 h <sup>C</sup>	100.9±1	97.2±2.	85.6±4.	86.3±4.	97.7±1.	102.1±0	100.0±1	103.9±1	89.0±3.
	.7 (4)	0 (8)	4 (3)	5 (4)	1 (6)	.7 (7)	.4 (4)	.3 (4)	0 (5)
5 h	103.0±2	97.4±2.	95.6±2.	86.4±5.	95.8±2.	100.4±1	98.4±2.	98.2±3.	88.6±1.
	.1 (4)	5 (7)	3 (4)	4 (4)	0 (6)	.0 (6)	0 (4)	0 (4)	9 (5)
24 h	101.5±	101.0±1	94.8±2.	81.2±7.	87.2±2.	102.0±0	100.0±0	100.3±1	89.7±1.
	0.7 (4)	.3 (6)	8 (5)	5 (4)	4 (6)	.9 (6)	.0 (4)	.1 (4)	7 (5)

<sup>A</sup>CMAP ratios were determined at the noted times following treatment and the averages  $\pm$  SEM are presented. Each treatment represents similarly, although not simultaneously treated rats, the numbers of which are shown in parentheses.

<sup>B</sup>Drug doses were 50  $\mu\text{g}/\text{Kg}$  for EN101, EN102 or INV102 and 1000  $\mu\text{g}/\text{Kg}$  for Mestimon, for both administration routes.

<sup>C</sup>Note the apparently delayed effect of orally administered EN102 as compared to EN101 or Mestimon.

Since *i.v.* drug administration is of limited value in chronic treatment paradigms, and since oral administration of AS-ONs had been shown to be effective in some applications (Agrawal and Kandimalla, 2000), we explored the activity of orally administered EN101. Fifty  $\mu\text{g}/\text{Kg}$  EN101 was administered via an intubation feeding needle, to EAMG rats, and CMAP recordings were performed 1, 5, and 24 h later. The orally administered EN101 was as active as *i.v.* administered 25  $\mu\text{g}/\text{Kg}$  (Table 1 and Fig. 4A). Orally administered Mestimon (pyridostigmine, 1000  $\mu\text{g}/\text{Kg}$ ) imparted predictable restoration of CMAP for up to several hours, and invEN102 had no effect on CMAP. Under the oral administration route, EN102 appeared slower to affect CMAP than EN101, suggesting sequence-specific differences for this effect (Table 1). Individual variabilities in animal responses to the EN101 treatment may parallel the variable decrement observed in response to calcium channel blockers in EAMG (Wirguin et al., 1994). To compare repeated daily oral and *i.v.* administration routes, we treated EAMG rats with rEN101 once a day for 5 days and performed CMAP recordings prior to each drug treatment.

Neither oral nor *i.v.* repeated administration of EN101 appeared to produce resistance to the therapy, normal electrophysiological activities being recorded over the entire course of treatment (Fig. 4B). Both the efficacy of EN101 treatment and its capacity to reduce the inter-animal variability were comparable to those of Mestinon, with the exceptions that Mestinon's effects were more rapid (data not shown), whereas EN101's effect was considerably longer-lasting. Also, the effect of daily single doses of Mestinon wore off within a day, causing drastic fluctuations in the treated animals' muscle strength (Table 1, Fig. 4B and data not shown). Among the EAMG animals thus treated with single daily administration of Mestinon, 5 out of 6 died within these 5 days. In contrast, 6 out of 8 animals treated by single daily oral administration of EN101, which maintained consistently normal CMAP levels throughout the treatment period, survived the full 5 day period (Fig. 4C). Although inconclusive, this experiment indicated EN101 as suitable for longer treatment evaluation.

### EN101 promotes muscle stamina in EAMG rats

Placed on a treadmill at 25 m/min, control animals ran for  $23.0 \pm 3.0$  min after which time they displayed visible signs of fatigue. Myasthenic animals placed on the treadmill were able to run as short a time as only  $2.3 \pm 0.5$  min before signs of fatigue appeared, depending on the severity of symptoms. We then classified animals as mildly, moderately, or severely affected based on their stamina in the treadmill test and disease signs, and monitored their performance 24 h following administration of 250  $\mu\text{g}/\text{Kg}$  EN101 (Fig. 5). All groups demonstrated improved stamina following injection. Thus, severely sick animals performed, when treated, as well as untreated moderately sick ones, and treated moderately sick animals reached performance levels better than those of untreated mildly sick animals, amounting to 3-fold improved running times of  $6.5 \pm 1.5$  min. EN101 had no significant effect on the running time of control rats (Fig. 5).

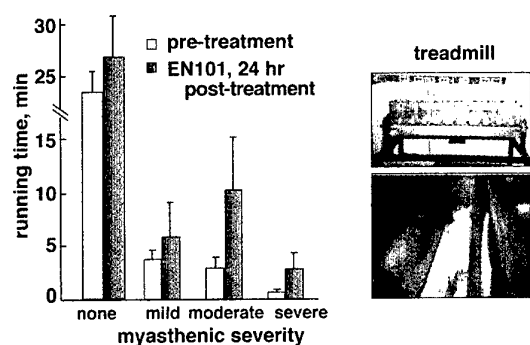


**Fig. 5. EN101 improves stamina in myasthenic rats.**

EAMG rats with varying severity of symptoms (severe  $n=11$ , moderate  $n=4$ , mild  $n=5$ ) and control Lewis rats (none,  $n=7$ ) were prodded to run on an electrically powered treadmill (25 m/min, inset) until visibly fatigued. The time (in min  $\pm$  SEM) each rat was able to run was recorded before, and 24 h following, *i.v.* administration of 250  $\mu\text{g}/\text{Kg}$  EN101. Note that EAMG rats run

considerably less time than controls, and that running time is increased for each group by EN101.

In a yet longer-term treatment regimen, 7 out of 9 EAMG animals under daily EN101 administration presented improved treadmill performance one mo after initiation of treatment, 1 showed no improvement and 1 animal died. In contrast, of 5 similarly sick animals that received daily Mestinon treatment, 3 died, 2 performed worse, and none showed improved performance. Saline injection yielded similar results, 3 dead, 2 worse. Thus, daily EN101 administration appeared effective for long-term treatment, enabling EAMG animals with moderate to severe symptoms to thrive under conditions where untreated or Mestinon-treated animals did not survive.

### Discussion

By targeting an orally delivered AS-ON drug to a long-known MG target, AChE, we achieved rapid, yet long-lasting physiological improvement, associated with reversal of the CMAP

decremental response at 3 Hz nerve stimulation and increased muscle stamina in the treadmill test. The beneficial effect of AS-ON injection on the CMAP response began within 1 h post-treatment and lasted many more hours than the effect of the currently employed anticholinesterases, likely reflecting the mechanistic differences between these two groups of drugs.

Chemical anticholinesterases are stoichiometrically targeted at the large number of AChE molecules present in the NMJ -- density of 3000-5000 molecules/ $\mu\text{m}^2$  (Anglister et al., 1994). In contrast, AChE mRNA chains exist in far lower quantities than their protein products, and are produced only by subsynaptic nuclei -- 1:200 of total muscle nuclei (Rotundo, 1990). Furthermore, AChE-R mRNA is normally the least abundant of the alternative splice variants of AChE mRNA. In addition, AS-ON agents that target the AChE-R mRNA transcripts can operate repeatedly, i.e. one AS-ON is responsible for hydrolysis of many mRNAs. This explains the over 100-fold difference in the molar dose of AS-ON as compared to Prostigmine or Mestinon that is effective in relieving EAMG weakness.

Because of the intrinsic instability of the AChE-R mRNA transcript (Chan et al., 1998), AS-ON agents targeted to the AChE mRNA sequence that is shared by all transcripts, will destroy primarily the longer, less G,C-rich AChE-R mRNA (Grisaru et al., 2001). This provides selectivity towards this normally rare transcript, while protecting most of the synaptic AChE-S variant from the antisense effect. Consequently, neuromuscular functioning is maintained while the disease-associated damaging protein is efficiently removed. The 3' terminal 2'-oxymethyl protection of AS-ON chains increases the hybridization affinity while minimizing toxicity (Galyam et al., 2001). This may further explain the beneficial effect of 2'-oxymethyl protected AS-ON agents following *i.v.* as well as oral administration. In comparison, conventional anticholinesterases would similarly inhibit the catalytic activity of the two variants, but would not remove the blocked enzyme from the system. This may be detrimental for three reasons: first, anticholinesterases induce a robust, multi-tissue feedback response of AChE-R overproduction; second, the overproduced protein apparently possesses additional, non-catalytic activities that are not necessarily blocked by anticholinesterases (reviewed in ref. (Soreq and Seidman, 2001)); third, prolonged exposure may cause tissue damage, as indeed is the case in DFP-exposed muscle. Together, these may explain the apparent absence under AS-ON treatment of adverse effects often associated with chronic anti-cholinesterase exposure. The long-term survival of animals receiving AS-ON by daily oral treatment, as compared with the poor survival of severely diseased animals under the physiologically fluctuating effects of a daily dose of Mestinon, may also reflect these differences.

Chemically protected RNA aptamers, capable of blocking the autoantibodies access to the nAChR, have been developed for the treatment of MG (Lee and Sullenger, 1997), however their reaction with the antibodies is stoichiometric, whereas the AS-ON reaction is catalytic, allowing a considerably lower dosage of the drug. In this context, two surprising properties of EN101 merit special discussion: the rapid onset and the long-lasting effect. The rapid onset of CMAP improvement that is offered by EN101 is most likely due to its easy accessibility to the highly metabolic muscle tissue combined with the instability of its target mRNA. The long-lasting functioning of this AS-ON agent probably reflects the fact that its neuromuscular effect may last after the AS-ON is totally degraded, to cease only when AChE-R accumulation passes a threshold beyond which this protein causes functional damage. This is compatible with the myasthenic symptoms reported in patients with acute anticholinesterase poisoning, which begin several hours after the acute phase (He et al., 1998). Pyridostigmine toxicity, reported in one myasthenic patient and in one healthy control (Cohan et al., 1976), manifested weakness following drug administration, and displayed higher pyridostigmine blood levels than in

myasthenic patients with satisfactory clinical response. This suggests individual differences in the clinical responsiveness to anticholinesterases that may depend on the individual rates of their metabolism.

A polymorphism at the HLA-DQ locus was reported to regulate the susceptibility to EAMG in mice (Raju et al., 1998), and polymorphisms in the  $\beta_2$  adrenergic receptor gene appear to have distinct distributions in human MG patients (Xu et al., 2000), indicating involvement of both immune modulators and general stress responses in the disease process and suggesting that overexpressed AChE-R may contribute to either or both of these levels of response. To this end, the beneficial effect of repeated AS-ON treatment likely reflects long-lasting changes in cytokine balances that contribute to the myasthenic syndrome. The complexity of relevant elements is evident from recently reported animal models that show, for example, that T cell overexpression of IL-10 facilitates EAMG development (Ostlie et al., 2001), whereas genomic disruption of the murine IL-1 $\beta$  gene diminishes the AChR-mediated immune response (Huang et al., 2001), and deficiency in IFN  $\gamma$  receptor limits both EAMG development and the negative feedback cascades that are induced by such development (Zhang et al., 1999). Indeed, injected IL-12, a major inducer of IFN  $\gamma$  production, accelerates and enhances disease in AChR-immunized mice, but not in strain-matched mice with a disrupted IFN  $\gamma$  gene (Sitaraman et al., 2000). The wide span of tissues involved, and the importance of altered cytokine relationships were reflected in the capacity of orally administered AChR fragments to suppress on-going EAMG (Im et al., 1999). Future studies should address the issue of whether AS-ON suppression of systemic AChE-R production affects myasthenic symptoms indirectly by eliminating the hematopoietically active AChE-R (Grisaru et al., 2001) and thus modulating cytokine production.

Apart from its obvious utility, this study, therefore, highlights the previously unperceived involvement of the AChE-R splice variant in MG etiology. Alternative splicing has recently emerged as a primary neuronal stress response, which affects different genes (Ohno et al., 2000; Xie and McCobb, 1998). Our current findings suggest that synaptic muscle nuclei similarly respond to cholinergic stress by alternative splicing of their pre-mRNA products. MG patients are routinely treated by a combination of anticholinesterase, immune and glucocorticoid therapy. Both anticholinesterases and glucocorticoids would enhance AChE gene expression, further increasing the cumulative AChE-R load in treated MG patients. Due to the secretory nature of AChE-R, it also accumulates in the serum. Further studies will be required to test the applicability of AChE-R detection as a surrogate marker for MG; however, the accumulation of serum AChE-R in EAMG rats and human patients gives reason to believe that, unlike blood catalytic AChE activity, immunodetected serum AChE-R may reflect the severity of the disease state.

The pathogenesis of MG and EAMG is primarily related to the destructive effect of anti-AChR antibodies on the NMJ. In addition, neuromuscular weakness associated with cholinergic imbalance is known in patients with congenital myasthenic syndromes (Ohno et al., 2000), where synaptic AChE is the only form missing, as well as following exposure to anticholinesterases, e.g. in Gulf War veterans (reviewed in ref. 20), muscle dystrophy and in amyotrophic lateral sclerosis and post-traumatic stress disorder, among others. As AS-ONs targeted to AChE mRNA provide relief of cholinergic muscle malfunctioning, they should be useful for symptomatically treating these and many other diseases.

The likely existence of a polymorphism that confers AChE overproduction could potentially be assessed using peripheral markers. If this turns out to be the case, it is probable that levels of stress-induced changes could be monitored in the field and prior to deployment to identify those

troops who are most and least at risk. Another observation is the apparent clinical implications these data have on the management of patients with MG. It is likely that the results from these studies will provide opportunities to identify reasons why patients are treatment-resistant, as well as new methods for further alleviating symptoms in patients who do respond.

## **Modified testicular expression of stress-associated “readthrough” acetylcholinesterase predicts male infertility (task 1)**

Reduced male fertility is one of the known consequences of psychological stress (Clarke et al., 1999; Giblin et al., 1988; Negro-Vilar, 1993). The molecular pathways translating stress into depressed male reproductive potency are not yet known, but likely involve stress-hormone-induced alterations in gene expression (Jolly and Morimoto, 1999). Glucocorticoid hormones released by the adrenal gland in response to stress (Sapolsky et al., 2000) are known to exert long lasting effects on gene expression. We previously reported activation of the gene encoding the acetylcholine hydrolyzing enzyme acetylcholinesterase (AChE; EC 3.1.1.7) by forced swim stress and pharmacological inhibitors of AChE in brain (Kaufer et al., 1998), muscle (Lev-Lehman et al., 2000), hematopoietic cells (Grisaru et al., 2000) and intestinal epithelium (Shapira et al., 2000). In all these cases, over-expressed AChE appeared as an otherwise rare splicing variant known as “readthrough” AChE, or AChE-R. Stress-induced overexpression of AChE-R likely involves both glucocorticoid-sensitive (Grisaru et al., 2000) and glucocorticoid-insensitive (Kaufer et al., 1998) components.

The classical function of AChE, acetylcholine hydrolysis (Taylor, 1996), plays a crucial role in cholinergic neurotransmission. AChE was also observed in spermatozoa (Egbunike, 1980; Palmero et al., 1999), where its presence was attributed to cholinergic mechanism(s) involved in sperm motility (Dwivedi and Long, 1989; Young and Laing, 1991). Nevertheless, it has recently been shown that AChE exerts morphogenic and/or developmental activities unrelated to acetylcholine hydrolysis (Grisaru et al., 1999). Furthermore, AChE inhibitors in use as agricultural insecticides were associated with yet unexplained impairments in spermatogenesis and sperm properties (Sarkar et al., 2000; Tielemans et al., 1999). For these reasons, we explored the influence of AChE-R on spermatogenesis and sperm properties.

Male gamete production, spermatogenesis, takes place in the seminiferous tubules of the testes. Progression through this process is accompanied by migration of cells from the tubule periphery towards the central cavity. At the periphery of the tubules are diploid stem cells, spermatogonia, which pass through proliferative mitotic divisions to generate spermatocytes. Spermatocytes give rise to round haploid spermatids through meiosis. Spermatids elongate and differentiate to form spermatozoa that are released to the genital duct system. In the epididymis, spermatozoa acquire motility and fertilization ability (Leonhardt, 1993).

### **Methods**

**Animals and tissue collection:** Male FVB/N mice (2-6 months old) were sacrificed 24 hr following 4 successive daily forced swim sessions as detailed (Kaufer et al., 1998). Control mice, and mice that have a transgene encoding human AChE-R inserted into their genome, were sacrificed with no prior treatment. Serum was prepared from blood samples allowed to clot 1hr at room temperature and overnight at 4°C, followed by centrifugation and supernatant collection. Testes and seminal vesicles were excised and weighed. One testis from each animal was fixed in 4% paraformaldehyde or Bouin’s fixative, the other was kept at -70°C for protein extraction.

**Serum hormone levels:** Serum corticosterone concentrations were determined by radioimmunoassay (ICN Pharmaceuticals, Inc., Costa Mesa, California).

**Sperm Evaluation:** Live, motile sperm were counted manually in isolates prepared from a single cauda epididymis shredded in 1 ml saline. Sperm concentration was measured using

the Improved Neubauer chamber (Heinz Herenz, Hamburg, Germany). For staining with the fluorogenic dye JC-1, epididymal sperm cells were incubated 20 minutes at room temperature in the presence of 3 $\mu$ M JC-1 and 12 $\mu$ M Propidium Iodide (Molecular Probes, Inc., Eugene, Oregon), essentially as detailed (Garner and Thomas, 1999). Samples were centrifuged at 500g for 7min to remove excess dye. A drop of the suspended cells was placed on a coverslip and covered by a second coverslip. Viable motile cells that reached the drop's periphery were subjected to fluorescence microscopy and quantitative evaluation of JC-1 emission at 525nm(green) and 585nm(red). The ratio between red and green fluorescence was considered to reflect mitochondrial membrane potential.

**AChE analysis:** AChE activity assay, 5-20% sucrose gradient and immunoblot analysis were performed essentially as described (Sternfeld et al., 2000) on testes tissue homogenized in 1M NaCl, 0.01M EGTA, 0.01M Tris HCl pH7.4, 1% TritonX100. AChE-R was detected with a polyclonal antibody targeted at the C-terminal peptide of AChE-R (Sternfeld et al., 2000). Band intensities of 2 lanes loaded with protein from individual mice of each group were quantified using Adobe Photoshop 5.0 software.

**In situ hybridization** was performed as detailed elsewhere (Kaufer et al., 1998) on 7 $\mu$ m thick paraformaldehyde-fixed paraffin-embedded sections using 50-mer, biotinylated, 2'-O-methyl cRNA probes targeted to either pseudointron I4 or exon E6 in AChEmRNA transcripts. ELF<sup>TM</sup> (Molecular Probes, Inc., Eugene, Oregon) was used as a fluorogenic alkaline phosphatase substrate.

**Immunohistochemistry:** Detection of the AChE isoforms was performed on 7 $\mu$ m thick paraffin embedded sections with polyclonal antibodies targeted at the C-terminal peptide of synaptic AChE-S (C-16; Santa Cruz Biotechnology, Santa Cruz, California) or of AChE-R (Sternfeld et al., 2000). Biotinylated secondary antibodies were detected with streptavidin-alkaline phosphatase conjugate (Amersham Pharmacia Biotech, Piscataway, New Jersey). Fast Red (Roche Molecular Biochemicals, Mannheim, Germany) was used as a chromogenic substrate. PCNA was detected using a dedicated staining kit (Zymed Laboratories, San Francisco, California); nuclear counterstaining was with hematoxylin (Sigma, St. Louis MI). All immunodetections were performed following heat induced antigen retrieval.

**Confocal analysis:** An MRC-1024 Bio-Rad confocal microscope equipped with an inverted microscope was used to scan the Fast Red precipitate used for immunodetection. Fluorescence was excited at 488nm, and emission was measured with a 580df32 filter. To examine mouse testicular spermia in tissue sections, a confocal plane was scanned every 0.35 $\mu$ m using a 63X/1.4 oil immersion objective and a three-dimensional projection created from all sections. To examine human sperm smears a confocal plane was scanned every 0.30 $\mu$ m using a 40X/1.3 oil immersion objective; three-dimensional projections of the signal were overlaid on a phase contrast image of the cells.

## Results

### **AChE-R is overexpressed in testes from psychologically stressed mice**

To examine the effects of acute stress on AChE expression in the male gonads, we subjected adult male FVB/N mice to 4 successive daily sessions of confined swim (Kaufer et al., 1998). Stressed mice displayed 5-fold elevated serum corticosterone levels (171.0 $\pm$ 62.4 ng/ml serum (Avg $\pm$ SEM); N=4) as compared to naïve mice (31.6 $\pm$ 7.5; N=3; p $\leq$ 0.04, Mann-Whitney). Elevated glucocorticoid levels were accompanied by mildly increased AChE activities in testicular extracts (0.3 $\pm$ 0.03 nmoles substrate/min/mg protein after stress vs 0.1 $\pm$ 0.01

nmoles/min/mg protein in controls). To identify the cell population(s) that respond to stress by increasing *ACHE* gene activity, we employed *in situ* hybridization (Kaufer et al., 1998). A selective 2'-O-methyl biotinylated cRNA probe revealed a circumferential distribution of AChE-R mRNA in testicular tubules from naïve mice (Fig. 1A). In stressed mice 24 hours after the last swim session, AChE-R mRNA signals were notably intensified and extended into all cell layers (Fig. 1B). Immunodetection with an antibody selective for AChE-R (Sternfeld et al., 2000) produced no detectable staining in testes from control mice (Fig. 1C). In contrast, anti-AChE-R antibodies intensively labeled internal cell layers in tubules of stressed mice (Fig. 1D), particularly the innermost stratum containing maturing spermatozoa. Stress therefore induced AChE-R mRNA overproduction in cells undergoing early spermatogenesis and caused accumulation of AChE-R protein at later stages of sperm formation.

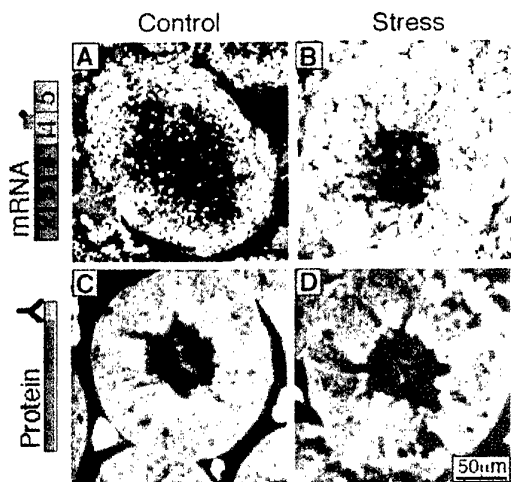


**Fig. 1. Repeated forced swim stress induces testicular AChE-R overexpression**

A,B. *In situ* hybridization was performed on sections of seminiferous testicular tubules from naïve and stressed FVB/N mice. Yellow fluorescence is the product of alkaline phosphatase-mediated hydrolysis of ELF<sup>TM</sup> (Molecular Probes Inc., Eugene, Oregon) and indicates sites of AChE-R mRNA accumulation. Note the intense, dispersed signal in tubules from stressed mice. C,D. Immunohistochemistry with antibodies selective for AChE-R. Signal is orange. Note that in stressed mice AChE-R protein product is localized primarily, but not exclusively,

to the inner cell layer harboring maturing testicular spermatozoa. Schemes present probe location for the hybridization experiment (A,B) and the antibody-targeted domain for the immunostaining (C,D).

### Transgenic mice as a model for chronic testicular overexpression of AChE-R

To establish a model for chronic gonadal overexpression of AChE-R, we exploited mice transgenic for human AChE-R (Sternfeld et al., 2000). Transgenic mice displayed 700-fold excess testicular AChE activity (Fig. 2A). Elevated levels of a 66 KDa immunoreactive band co-migrating with recombinant AChE-R protein was accompanied by unchanged labeling of a slightly faster migrating band (Fig. 2B), potentially reflecting another AChE variant (Soreq and Glick, 2000), different glycosylation patterns (Kronman et al., 2000) or proteolytic cleavage of the AChE protein, which was previously observed the serum of stressed mice (Grisaru et al., 2000). Sucrose gradient centrifugation (5-20%) demonstrated the excess AChE to migrate as a single peak of globular monomeric enzyme, as expected from AChE-R (Fig. 2C). Using *In situ* hybridization, we detected high levels of AChE-R mRNA in the peripheral layers of testicular tubules from transgenic as compared to control FVB/N mice (Fig. 3A,B), similar to that observed following stress (compare to Fig 1B). These are the cell layers harboring both mitotic spermatogonia and post-mitotic spermatocytes. Using anti-AChE-R antibodies, we could not detect protein in sections from control mice (Fig. 3B). In contrast, transgenic mice displayed pronounced deposition of AChE-R in a single peripheral cell layer in 65% of stained tubules (Fig. 3D). The remaining 35% were evenly divided between those with AChE-R deposits in the inner cell layers harboring spermatozoa heads (similar to the stress pattern) and those with labeling within the tubular cavity into which the spermatozoa

tails project (data not shown). Some tubules stained in the periphery were also stained in the inner layer (12%) or the cavity (26%). Thus, AChE-R expression in testes of transgenic mice resembled that of mice subjected to repeated acute stress at the level of the mRNA, but exhibited a more complex pattern of cellular distribution at the level of the protein. In contrast, the expression of the “synaptic” AChE-S splicing variant appeared largely unaffected by either stress or transgenic overexpression of AChE-R (data not shown).

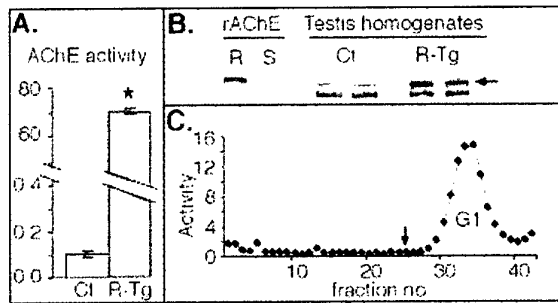


**Fig. 2. Testicular AChE-R overproduction in transgenic mice**

A. Presented are average  $\pm$  SEM specific AChE activity (nmol acetylthiocholine hydrolyzed/min/mg protein) from duplicate measurements performed in testicular homogenates from 3 adult male FVB/N (Cl) or AChE-R-overexpressing transgenic (R-Tg) mice (Sternfeld et al., 2000). Stars

note statistical significance ( $P < 0.05$ , Mann-Whitney).

B. Testicular homogenates were subjected to SDS-polyacrylamide gel electrophoresis and the resultant blots incubated with antibodies directed at the C-terminal peptide unique to AChE-R (Sternfeld et al., 2000) (R). Shown is an immunoblot with each two lanes loaded with homogenates from individual mice of the noted pedigree. Of the two bands observed, the top one (of approximately 66Kd, arrow) co-migrated with recombinant AChE-R produced in transfected phaeochromocytoma PC12 cells (left lane). Recombinant AChE-S (S, second lane from left, Sigma, U.S.A.) remained unlabeled, demonstrating selectivity of the antibody.

C. Presented are AChE activities (nmol acetylthiocholine hydrolyzed/min/mg. protein) in fractions collected following sucrose gradient centrifugation of a testicular homogenate from an AChE-R transgenic mouse. The observed sedimentation coefficient of 4.5-5.0S reflects globular monomers (G1), consistent with the AChE-R isoform. Arrow notes the localization of alkaline phosphatase (6.1S), which served as a sedimentation marker. One of two analyses.

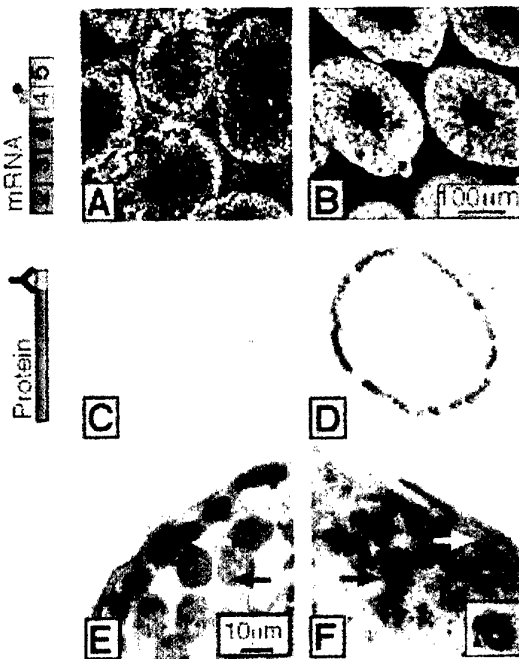


**Fig. 3. AChE-R accumulates in spermatocytes of transgenic mice**

*In situ* hybridization (yellow) and immunohistochemistry (red) of representative tubules from naïve adult FVB/N or AChE-R transgenic mice. Tubuli of transgenic mice display high levels of dispersed AChE-R mRNA (A,B) but restricted localization of AChE-R protein to a single peripheral cell layer (C,D). Antibodies toward proliferating cell nuclear antigen (PCNA) detected mitotic cells undergoing DNA replication in the outermost cell layer containing spermatogonia (E) but not in the next inner layer of meiotic spermatocytes with high levels of AChE-R (F). White arrows indicate spermatogonia; black arrows, spermatocytes. Nuclei were counterstained with hematoxylin. Inset: high magnification image demonstrates focal perinuclear accumulation of AChE-R in spermatocytes.

### Accumulated AChE-R in post-mitotic sperm progenitors imposes a partial block to post-meiotic differentiation

We recently observed that AChE-R promotes expansion of hematopoietic progenitor cells (Grisaru et al., 2000) and terminal differentiation of osteoblasts (Grisaru et al., 1999). We therefore considered the possibility that overproduction of AChE-R may affect the proliferation of male germ cell progenitors. To quantify replicating cells, we stained for proliferating cell nuclear antigen (PCNA). In both naïve FVB/N and AChE-R transgenic mice, PCNA staining was confined to the most peripheral cell layer comprised exclusively of spermatogonia, the proliferative spermatogenic progenitors (Fig. 3E and data not shown). AChE-R was undetectable in this cell layer (Fig 3F), being concentrated in the next inner layer of post-mitotic spermatocytes. In spermatocytes, AChE-R displayed a subcellular disposition that included diffuse cytoplasmic distribution in addition to focal perinuclear sites of accumulation (Fig. 3F, inset). The average number of PCNA labeled cells was identical in transgenic and control mice ( $67.5 \pm 2.8$  vs.  $67.2 \pm 2.0$  cells/normalized tubule perimeter, respectively). In addition, we did not observe any changes in the organization of spermatogonia in testes from transgenic mice (data not shown). In contrast, the number of post-meiotic, differentiating spermatozoa surrounding the tubular cavity was significantly reduced in transgenic as compared to control mice ( $82 \pm 12$  vs.  $97 \pm 15$  cells/normalized tubule perimeter, respectively;  $N=3$ , 8-10 tubules per mouse,  $p < 0.0005$ , Student's t-test).

### Transgenic testicular overproduction of AChE-R is associated with impaired sperm properties

As predicted by the reduced number of spermatozoa in testicular tubules, epididymal sperm counts were also significantly lower in transgenic as compared to control mice (Fig 4). However, the 45% reduction in epididymal sperm cells exceeded the cell loss observed in tubules by 30%, indicating that additional cell loss takes place following the release of spermatozoa from the seminiferous tubules. In addition, motility of surviving sperm appeared compromised in transgenic mice as compared to controls (Fig. 4), suggesting functional impairments. Using JC-1 (Garner and Thomas, 1999) to assess mitochondrial activity of motile transgenic epididymal sperm, we observed hyperpolarization rather than hypopolarization of mitochondrial membranes (data not shown). This observation excluded reduced cellular respiration as a cause for reduced sperm motility, but raised the possibility that mitochondrial hyperpolarization foreshadows apoptotic events that contribute to reduced sperm counts (Matsuyama et al., 2000; Vander Heiden and Thompson, 1999). In addition to sperm properties, seminal gland weight of transgenic mice was also reduced as compared to controls (Fig 4).

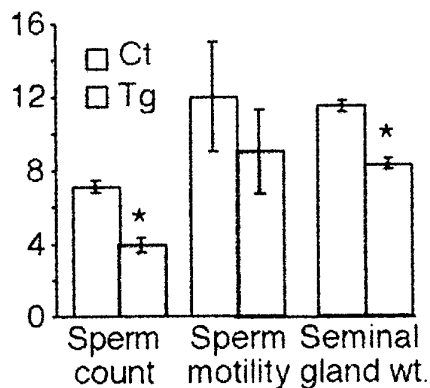


**Fig. 4. Testicular AChE-R overproduction is associated with impaired sperm properties**

Bar Graph represents data from 3-5 adult male FVB/N (Ct) or AChE-R-overexpressing transgenic (Tg) mice. Average  $\pm$  SEM values are shown for sperm counts (cells/epididymis  $\times 10^{-6}$ ), sperm motility (percent motile of total sperm cells), and seminal gland weight (mg/gr body weight). Stars note statistical significance ( $P < 0.05$ , Mann-Whitney).

### AChE-R may serve as a marker of stress-related male infertility

Testicular tubules from stressed mice and a large portion (approx. 60%) of those from transgenic mice displayed accumulation of AChE-R in differentiated spermatozoa residing at the inner cell layer surrounding the cavity. To characterize the expression of AChE-R in mouse spermatozoa, and to explore the relevance of the mouse models to human fertility, we performed confocal microscopy. Anti-AChE-R antibodies failed to label testicular spermatozoa from control mice (Fig. 5A). In contrast, repeated acute stress facilitated strong, punctate, intracellular labeling that was limited to spermatozoa heads (Fig. 5B), with few cells also stained at the neck. Spermatozoa from AChE-R transgenics were either unlabeled (40%), or stained at the neck (35%) or head (25%) (Fig. 5C). We then examined human sperm in air dried smears of ejaculates from apparently fertile donors or from the male partner of couples with unexplained infertility. Normal sperm were stained in both the head and neck regions. In contrast, samples from infertility patients presented large fractions of sperm with intense labeling in the neck region, but no detectable head-associated AChE-R (Fig. 5D). Cumulative analysis by a blind observer of approximately 40 sperm cells from each of 3 individuals in each group demonstrated a significantly decreased proportion ( $p < 0.05$ , Mann Whitney) of head-stained sperm from male partners of infertile couples as compared to sperm-bank donors.

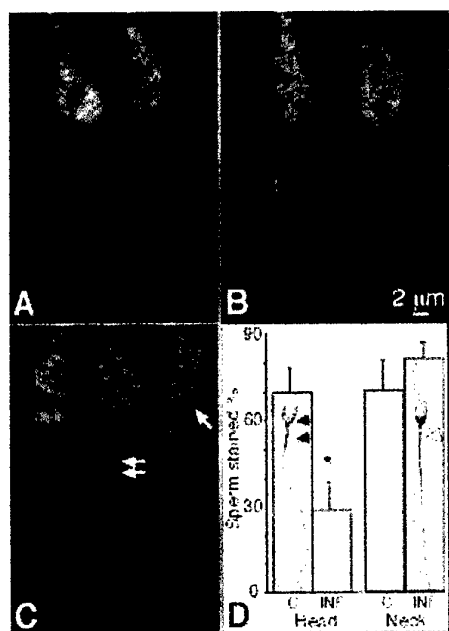


**Fig. 5. AChE-R sperm head staining intensifies in stressed mice and decreases in transgenic mice and in subjects with unexplained infertility**

A-C. Shown are representative compound confocal images of testicular spermatozoa reaching the central space within testicular tubules following immunohistochemical staining with anti-AChE-R antibodies and Fast Red. Note the pronounced labeling in heads of spermatozoa from mice subjected to forced swim stress as compared to those from both naïve FVB/N and transgenic mice. Spermatozoa from transgenic mice were divided among those unstained, and those stained primarily in the tail region, or in the head (white arrows; see text for details). D. Bar Graph shows percentage of sperm labeled by anti-AChE-R antibodies (average  $\pm$  SEM) in the head or neck regions for approximately 40 cells from each of 3 healthy human donors (C) and 3 male partners from infertile couples (INF). Star notes a statistically significant difference between controls and patients ( $p < 0.05$ , Mann Whitney).

Shown in the outside columns are representative compound confocal images of a sperm from a donor (right) or infertility patient (left). Note labeling of the post-acrosomal region of sperm heads and neck in control cells (black arrowheads) as compared with limited sperm head labeling in the patient (white arrowhead).

### Discussion

#### Testicular AChE is subject to stress-induced changes in alternative splicing

Our current findings associate stress with testicular overproduction of AChE-R and suggest that stress insults of varying duration or severity may initiate graded increases in AChE-R in spermatogenic cells (Fig 6). The increase in AChE expression following stress is consistent with the presence of a recently discovered consensus sequence for a putative glucocorticoid response element (GRE) in the upstream promoter region of the human *ACHE* gene locus

(Shapira et al., 2000). AChE overexpression following stress was highly selective as it was observed only for the AChE-R isoform. This suggests active diversion of 3' alternative splicing of AChE mRNA. This pattern of stress-mediated AChE gene expression parallels that observed in other tissues, and strengthens the concept of shifted alternative splicing and the resultant AChE-R protein as universal stress response elements in multiple mammalian organs, including the gonads.

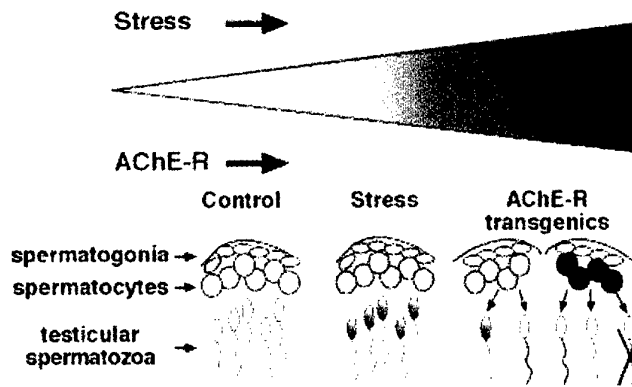


**Fig. 6. Graded increases in AChE-R associated with its altered spermatogenic localization.**

Shown is a schematic representation of seminiferous tubules. Following stress, AChE-R levels increase in spermatocytes and all other spermatogenic cells with the most marked elevation in the head of testicular spermatozoa. A greater or more persistent increase in AChE-R

expression, represented by the transgenic model might be found under intense or prolonged stress. Under such conditions, spermatocytes are stained while AChE-R is either excluded from testicular spermatozoa altogether or localized to the tail, with only a smaller fraction of the spermatids displaying head staining. AChE-R overexpression in spermatocytes could impede spermatogenesis thereby explaining reduced sperm counts in transgenic mice.

### **Massive AChE-R elevation could impair spermatogenesis and sperm function in a non-catalytic manner**

Compared to psychologically-stressed FVB/N mice, transgenic mice exhibiting massive AChE-R overproduction displayed heterogeneity in the cellular and subcellular localization of AChE-R. It is yet unclear whether this difference between stressed and transgenic mice reflects the high levels of overexpression achieved in the transgenic model, or a property resulting from chronic congenital overexpression of the transgenic protein. The greatly elevated expression of AChE-R in transgenic mice was accompanied by decreased sperm counts, sperm motility and seminal gland weight. The decline in post mitotic spermatozoa numbers in AChE-R transgenics suggests that AChE-R excess may impose yet undefined restrictions on spermatogenesis following mitotic cell division. While the reduction in seminal gland weight potentially reflects systemic effects of chronic AChE-R overexpression and its impact on autonomous cholinergic innervation (Prince, 1992), not all the effects should necessarily be attributed to increased cholinesterase activity. The high accumulation of AChE-R in sperm cell progenitors suggests that the primary impact of its transgenic overexpression on spermatogenesis and/or sperm properties results from direct effects of the protein on cellular processes. In this light, non-catalytic, cell signaling capacities now well established for nervous system AChE (Bigbee et al., 2000; Koenigsberger et al., 1997; Sternfeld et al., 1998) may be relevant. Our findings therefore emphasize the need to identify the yet unknown protein partner(s) of AChE-R and its putative signal transduction pathways. The perinuclear localization of AChE-R in spermatocytes resembled the nuclear association of megakaryocytic AChE (Lev-Lehman et al., 1997). In hematopoietic progenitors, AChE regulation is tightly associated with that of CHED, a CDC-related protein kinase (Lapidot Lifson et al., 1992), suggesting potential involvement in cell cycle processes and calling for a search for potential correlation between cyclin regulation during mammalian gametogenesis (Zhang et al., 1999) and AChE-R.

### **AChE-R is potentially involved in the detrimental effects of psychological stress on male fertility**

The transgenic mouse model demonstrates the potentially detrimental effects of high levels of dispersed testicular AChE-R on mammalian sperm maturation and/or properties. Absence of AChE-R from heads of testicular spermatozoa, as was primarily observed in AChE-R transgenic mice, also appeared to be characteristic of sperm from the male partners of human couples with unexplained infertility, but not of sperm from fertile controls. These results support the notion of a role for stress-related changes in AChE expression in impaired sperm quality in humans as well. The differential AChE-R staining patterns observed in the two human groups suggest AChE-R labeling as a possible useful marker for stress-related male infertility, and strengthen the notion that stress-associated overexpression of AChE-R may be a risk factor in fertility disturbances.

### **AChE-R as a molecular target for understanding and resolving various aspects of male infertility**

As anticholinesterases were shown to induce overproduction of AChE-R (see Introduction), our findings may also explain the impaired sperm properties and male infertility associated with exposure to agricultural insecticides or other anti cholinesterase agents (Sarkar et al., 2000; Tielemans et al., 1999). If so, these findings further imply potential modes of intervention, including blockade of AChE feedback overexpression, prevention of the shift in alternative splicing from AChE-S to AChE-R, and selective antisense suppression of AChE-R (Shohami et al., 2000). In the brain, AChE feedback overexpression was shown to be independent of the hypothalamus-pituitary axis (Kaufer et al., 1998). Nevertheless, the recent demonstration of a functional glucocorticoid response element in the extended AChE promoter (Grisaru et al., 2000) suggests a glucocorticoid-mediated component to stress-related AChE overexpression. This could be examined in glucocorticoid-receptor knockout mice (Jolly and Morimoto, 1999; Tronche et al., 1999). AChE-R thus presents a previously unrecognized target for studying, analyzing and treating stress-induced human male infertility.

## Development of AChE variant-specific antibodies for the demonstration of differential expression of variants in hematopoietic cells (task 3)

### A. Development of human antibody fragments directed towards synaptic acetylcholinesterase using a semi-synthetic phage display library

Acetylcholinesterase (AChE) hydrolyzes the neurotransmitter acetylcholine at cholinergic synapses, but also exercises morphogenic activities (Soreq and Seidman, 2001). Three C-terminal variants are generated by alternative splicing of the single *ACHE* gene transcript. "Synaptic" AChE-S constitutes the principal variant protein in brain and muscle, and plays an important role in growth-regulating processes affecting neurons, independently of its catalytic activity (Sternfeld *et al.*, 1998). "Readthrough" AChE-R is a secretory, non-synaptic form of the enzyme that is expressed in embryonic and tumor cells (Karpel *et al.*, 1994), and is induced under psychological and chemical stressors, including therapeutic anticholinesterases (Friedman *et al.*, 1996; Kaufner *et al.*, 1998). In addition, a peptide derived from the unique C-terminal sequence of AChE-R has by itself haematopoietic growth-factor-like activity (Grisaru *et al.*, 2001). "Erythrocytic" AChE-E possesses a C terminus with the potential for phosphoinositide linkage to the external membrane of red blood cells (Futerman *et al.*, 1985).

Alzheimer's disease involves complex changes in acetylcholine-mediated neurotransmission (Coyle *et al.*, 1983). Current therapies include inhibitors of AChE aimed at restoring the cholinergic balance (Schneider, 2001). However, increased AChE activity has been reported in the cerebrospinal fluid of Alzheimer's disease patients treated with inhibitors of the enzyme (Nordberg *et al.*, 1999), which is consistent with AChE-R accumulation in the mouse brain under exposure to commonly used anticholinesterases (Kaufner *et al.*, 1998). Excess AChE accumulation may be detrimental, due to the non-catalytic structural roles of the protein. Indeed, transgenic mice overexpressing AChE-S show late-onset deterioration in cognitive (Beeri *et al.*, 1995, 1997) and neuromotor (Andres *et al.*, 1997) functions reminiscent of Alzheimer's disease. Moreover, accumulation of a yet undefined AChE variant has been observed in amyloid plaques of Alzheimer's patients (Wright *et al.*, 1993), and AChE-amyloid- $\beta$  complexes were reported to be more neurotoxic than  $\beta$ -amyloid peptide alone (Alvarez *et al.*, 1998).

Obtaining monoclonal antibodies directed against the C-terminal region unique to each human AChE variant would be useful for research into the mechanisms by which such variants signal their morphogenic functions, as well as for studying their specific roles in the etiology and drug treatment of Alzheimer's disease, and as surrogate markers for stress and inhibitor exposure.

The phage antibody libraries offer an alternative way to isolate antibodies with many different specificities (Marks *et al.*, 1991; Griffiths *et al.*, 1993; Nissim *et al.*, 1994; Hoogenboom *et al.*, 1999). Selected specific antibodies, phage displayed or secreted from infected bacteria, can be readily used as reagents in immunoblotting, immunohistochemistry, flow cytometric analysis and other applications (Harrison *et al.*, 1996).

We used a library of antibodies encoded by human variable-gene segments rearranged *in vitro*, and displayed on the M13 bacteriophage surface as single-chain Fv (scFv) antibodies (Nissim *et al.*, 1994). Synthetic biotinylated peptides representing the C-terminal sequence unique to human AChE-S were used as targets for selection. Three scFv antibodies were obtained which

are highly specific for the AChE Synaptic Peptide (ASP) and interact with the authentic AChE-S.

## Materials and Methods

### Preparation of biotinylated peptides

Two peptides, ASP:

NH<sub>2</sub>-DTLDEAERQWKAEFHRWSSYMVHWKNQFDHYSKQDRCSDL-COOH, and  
ARP:

NH<sub>2</sub>-GMQGPAGSGWEEGSGSPPGVTPLFSP-COOH,  
were prepared by solid-phase-techniques (Atherton and Sheppard, 1989) with a 4334 peptide synthesizer (Applied Biosystems, Foster City, CA), and biotinylation was performed on the protected peptide before cleavage from the resin. The non-biotinylated ARP and ASP C-ter, the latter representing the C-terminal 23 amino acid residues of ASP, were kindly provided by Dr. M. J. Gait (MRC, UK; Grisaru *et al.*, 2001). Peptides were purified by high-performance liquid chromatography to greater than 90% homogeneity.

### Selection of phage display antibody library

We used a phage display human semi-synthetic library of  $> 10^8$  scFv antibodies (Nissim *et al.*, 1994) for selection. An aliquot of the library (50  $\mu$ l,  $10^{13}$  t.u./ml) was two-fold diluted in PBS, 0.2% BSA (BSA-PBS) (selection buffer) containing 0.1% Tween 20, and then incubated with 4  $\mu$ M biotinylated ASP for 1 h at room temp. In parallel,  $3 \times 10^7$  streptavidin-coated paramagnetic beads (Dynal, Oslo, Norway) were blocked with 1% BSA-PBS, washed with PBS and resuspended in 100  $\mu$ l of selection buffer. Streptavidin beads and phage were mixed and left for 15 min on a rotating wheel at room temp. After 5 washes with selection buffer, 5 washes with PBS, 0.1% Tween 20 (PBS-T), and 5 washes with PBS, the captured phage were eluted by incubating the beads in 40  $\mu$ l 4 M NaCl, 50 mM Tris-HCl, pH 7.5 for 30 min at room temp; the eluates were diluted to 150  $\mu$ l with water. The recovered phage particles were amplified in the *E. coli* amber suppressor strain TG1, and used in a further round of selection after rescue with the helper phage KM13 (Kristensen and Winter, 1998) followed by PEG (20% polyethylene glycol, MW 6000; 2.5 M NaCl) precipitation of the supernatant of the infected bacteria (Harrinson *et al.*, 1996). Before the second round, streptavidin binders were depleted by preadsorption on a streptavidin-coated (10  $\mu$ g/ml) tube. Selection was then repeated as above; to increase the specificity and the stringency of selection, 2 rounds of antigen binding using 2  $\mu$ M ASP-biotin were performed before phage growth in bacteria ("double round").

### Screening and sequencing of clones

Screening of phage binders was done as described with minor variations (Harrinson *et al.*, 1996). Briefly, selected phage were rescued from single ampicillin-resistant colonies of infected *E. coli* TG1 using the helper phage KM13. Bacterial supernatants containing the rescued phage were preincubated with the biotinylated ASP, at the same concentration and conditions as used for the first round of selection, and then added to a streptavidin-coated (10  $\mu$ g/ml) microtiter plate to detect phage binding by ELISA. As negative controls, supernatants preincubated without the biotinylated antigen were used. The diversity of selected clones was determined by PCR amplification using as primers LMB3 (5'-CAGGAAACAGCTATGAC-3') and fd-SEQ1 (5'-GAATTTTCTGTATGAGG-3') and DNA sequencing of scFv inserts with an automated ABI377 sequencer (Applied Biosystems, Foster City, CA). Characterized monoclonal phage were used as reagents after PEG precipitation and quantification of the number of t.u. (Harrinson *et al.*, 1996).

### Induction of soluble scFvs, preparation of periplasmic fraction, and purification of antibody fragments

Once the antiASP 1 scFv antibody was selected, it was further engineered with 6 consecutive C-terminal histidine residues. To this end, a PCR amplified product encoding the scFv antibody was purified and digested with the restriction enzymes *NcoI* and *NotI*. The resultant 750 bp DNA fragment was gel-purified and ligated into the *NcoI* – *NotI* restriction sites of the phagemid vector pHEN1/pTI2 (kindly donated by Dr. I. Tomlinson, MRC, UK) encoding the His6 tail. The ligation product was introduced into the *E.coli* strain TG1 by electroporation. Transformants, picked out from ampicillin-resistant colonies, were checked for antiASP1 scFv amino acid sequence and C-terminal histidine residues deduced after PCR amplification and DNA sequencing. AntiASP 1 phage with the His6 tail were rescued from selected TG1 transformants using the helper phage KM13, concentrated with PEG, and used to infect (non-suppressor) *E. coli* HB2151. Monoclonal His6-tagged scFvs were harvested from the periplasmic fraction of 1 l cultures of infected HB2151 bacteria induced overnight with isopropyl- $\beta$ -D-thiogalactoside at 30 °C (Harrison *et al.*, 1996), and purified over Ni-NTA resin following the protocol provided by the manufacturer (Qiagen). To avoid protein degradation, a protease inhibitor cocktail (Sigma Chemical Co., St. Louis, MO) was added (0.4 mg/ml) to the periplasmic fraction, and the whole protocol was carried out at 4 °C. After eluting from the Ni-NTA resin with 250 mM imidazole, 300 mM NaCl, 50 mM Naphosphate, pH 8.0, the purified antibody fragments were dialyzed overnight against PBS and used immediately or stored at -80 °C with 10% glycerol. The purified scFvs were estimated to be > 90% pure by gel electrophoresis and Coomassie staining. Protein concentration was determined with a protein assay kit (Bio-Rad, Hercules, CA).

### Specificity evaluation of selected antibodies

Specificity of monoclonal phage antibodies was assessed by ELISA, essentially as described by Henderikx *et al.* (1998), using indirectly coated ASP. Briefly, biotinylated BSA was added to a microtiter plate at a concentration of 5  $\mu$ g/ml in PBS, and incubated overnight at 4 °C. After 3 washes with PBS, streptavidin (10  $\mu$ g/ml in PBS, 0.5% gelatin) and 1  $\mu$ g/ml of the biotinylated antigen (ASP, or ARP as negative control) in 3% BSA-PBS were applied in consecutive steps. After coating, 10<sup>11</sup> t.u./ml of the indicated monoclonal phage were added to different wells. Phage binding was then detected with a 1:5000 dilution of horseradish peroxidase/anti-M13-conjugated antibody (Amersham Pharmacia Biotech, Little Chalfont, UK). Phage and secondary antibody were diluted in 3% BSA-PBS. All incubations were for 1 h at room temp, and followed by 3 washes with 0.1% PBS-T and 3 washes with PBS. In the competition experiments, the incubation step with the phage was performed in the presence of the indicated concentrations of human recombinant AChE-S (Sigma) or ARP. For specificity analysis of the soluble antiASP 1 scFv antibody, the same ELISA protocol was carried out, but the concentration of biotinylated ASP or ARP was increased (5  $\mu$ g/ml). In these experiments, the myc tag was exploited for detection of antibody fragments. This peptide tag was originally incorporated into the expression vector of the library subjected to selection to be appended to the scFvs (Nissim *et al.*, 1994). Purified, dialyzed scFv antibodies were added to each coated well at a concentration of 0.35 mg/ml in 3% BSA-PBS. Bound scFvs were detected by adding together 1:500 dilutions of the 9E10 antibody (Santa Cruz Biotechnology, Santa Cruz, CA), which recognizes the c-myc epitope (Munro and Pelham, 1986), and peroxidase-conjugated goat anti-mouse IgG (Jackson ImmunoResearch Laboratories, West Grove, PA) in 3% BSA-PBS. Peroxidase activity was measured with 0.1 mg/ml of 3,3',5,5'-

tetramethylbenzidine containing 0.012% hydrogen peroxide in 0.1 M sodium acetate, pH 6. The reaction was stopped with 1 M H<sub>2</sub>SO<sub>4</sub>, and the resulting absorbance was measured at 450 nm in a microtiter plate reader (Molecular Devices, Sunnyvale, CA).

#### Affinity measurement using the BIAcore technology

The affinity of binding between the antiASP 1 scFv antibody and its epitope was determined using the technique of SPR (BIAcore 3000 System, Uppsala, Sweden) (Roden and Myzka, 1996). The ASP C-ter, human recombinant AChE-S (Sigma) and ARP were immobilized in the different flow cells of a CM5 sensor chip using standard amine coupling procedure (Lofas and Johnsson, 1990). To this end, the ASP C-ter peptide was dissolved to a concentration of 100 µg/ml in 10 mM acetate buffer, pH 4.5, which is below its isoelectric point, to permit preconcentration of the peptide on the biosensor matrix of the BIAcore chip via electrostatic interactions. Immobilization was carried out using a flow of 10 µl/min to obtain 1000 RU. Recombinant AChE-S was diluted to a concentration of 0.87 µM in 10 mM sodium acetate, pH 3.8, and ARP to 100 µg/ml in 10 mM glycine, pH 3.0, for direct immobilization to the chip surface of 2664 RU and 320 RU, respectively. In all cases, the same flow of 10 µl/min was used. The purified scFv antiASP 1 protein was then diluted in 10 mM HEPES, pH 7.4, 150 mM NaCl, 3 mM EDTA and 0.005% (v/v) polysorbate 20, and passed through the different flow cells on the sensor chip at 20 µl/min using concentrations ranging from 125 to 1000 nM. To eliminate the contribution of non-specific binding, the antiASP 1 scFv antibody was passed through a blank flow cell as well. The dissociation constants were calculated using the BIAevaluation software.

## **Results**

### Selection of human phage antibodies to ASP

Two rounds of selection were performed using biotinylated ASP in solution. The conditions of the second round, in which 2 consecutive incubations with antigen were performed before phage amplification in bacteria ("double round"), were designed to enrich the population in specific binders as opposed to phage with growth advantages. A significant decrease in phage titers coming from the second double round demonstrated the stringency of these selection conditions. Whereas in the first simple round, an output phage of  $7.5 \times 10^5$  t.u. was obtained for an input of  $5 \times 10^{12}$  t.u., only  $1.5 \times 10^2$  t.u. were recovered after the second double round for the same input titer. No doubt, the preabsorption on a streptavidin-coated tube to deplete streptavidin binders also contributed to this low yield. Under these conditions, an extraordinarily high frequency (44/96, 46%) of specific anti-ASP monoclonal phage antibodies was found following 2 rounds of selection (Fig. 1). Different clones were then picked out for DNA sequencing, to determine the diversity of the selected antibodies. Three distinct specific clones to ASP were identified, namely antiASP 1, 2 and 3 (Table 1). AntiASP 1 was dominant in the population, representing 4 of the 10 sequenced clones. Moreover, the V<sub>H</sub>-CDR3 sequences of antiASP 1 and 2 are closely related, both including the SRPS motif, attesting to the sequence specificity of their antigen-antibody interactions. Interestingly, antiASP 1, 2 and 3 were not found among the sequenced clones picked out after the first simple round (sequences not shown), indicating their low concentration in the population until this step. Also, the percentage of anti-ASP phage antibodies was much lower in the first round (10/96, 10%) than in the second round, demonstrating efficient enrichment in specific binders owing to double selection before phage growth in bacteria.

**Table 1. V<sub>H</sub>-CDR3 sequences of antibody fragments selected against ASP-biotin<sup>a</sup>**

Antibody designation	Deduced V <sub>H</sub> -CDR3 sequence	Frequency
antiASP 1	SRPSI	4/10
antiASP 2	SRPSH	1/10
antiASP 3	GARFKE	1/10
non-specific	HRAYYS	1/10
non-specific	NSEV	1/10
non-specific	CDMHG	1/10
non-specific	REPVA	1/10

<sup>a</sup>The diversity of selected clones was determined by PCR amplification and DNA sequencing of scFv inserts. After 2 rounds of selection, 3 different specific anti-ASP clones were identified (antiASP 1, 2 and 3) from deduced amino acid sequences of V<sub>H</sub>-CDR3. Moreover, the germline origin of the selected ASP-specific antibodies was determined, according to the nomenclature described in Tomlison *et al.* (1992). The two closely related antibody fragments, antiASP 1 and 2, use DP-24 and DP-3 germline segments, respectively; both belonging to the V<sub>H</sub>1 family. AntiASP 3 uses DP-32 of the V<sub>H</sub>3 family.

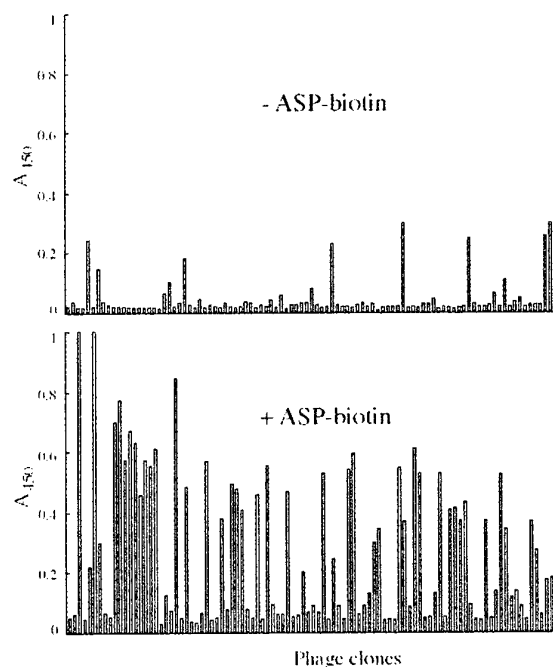


**Fig. 1. Enrichment of anti-ASP phage after two rounds of selection.** Shown are absorption values for culture supernatants of single bacterial clones producing selected phage antibodies. Incubation was with biotinylated ASP, followed by addition to streptavidin coated wells of a microtiter plate. Supernatants preincubated without the biotinylated antigen were used as negative controls. Binding of phage was detected via an anti-M13 peroxidase conjugate as absorption at 450 nm. Phage antibodies were considered specific when A<sub>450</sub> ratios of experimental to controls exceeded 3.

In a parallel search for ARP-specific antibodies, 2 selection attempts were performed against different concentrations (8 and 40  $\mu$ M) of the biotinylated peptide. None of the selected phage antibodies were found to be specific for ARP. In protein blots using a polyclonal rabbit antibody generated against ARP (Sternfeld *et al.*, 2000), we found that the synthetic peptide easily forms self-aggregates of high molecular weight, even in the presence of the dissociating agents sodium dodecyl sulphate and urea (data not shown). The antigenic determinants in ARP would be likely hidden inside of these aggregates, interfering with the antibody selection. ASP therefore appeared to be much more immunogenic than ARP.

### Selected scFv antibodies are highly specific for ASP and do not interact with ARP

To exclude the possibility that the 3 isolated anti-ASP monoclonal phage would also interact with the distinct C-terminal peptide unique for human AChE-R, an ELISA was performed (Fig. 2). The absorbance signal was specific for all phage antibodies, since they reacted strongly with ASP, the antigen used for selection, but not with ARP. AntiASP 1 showed the highest specific signal, as expected for the dominant clone in the population after 2 rounds of selection.

The selected antiASP 1 was engineered with 6 consecutive C-terminal histidine residues, as described in Materials and Methods. AntiASP 1 phage with the embodied histidine residues were used to infect the non-suppressor HB2151 strain of *E. coli*, which was then induced to produce free scFvs (Harrison *et al.*, 1996). The His6-tagged antibody fragments purified over a Ni-NTA resin were highly specific for ASP as judged by ELISA, and did not interact with ARP (Fig. 3). This assay thus reinforced the results obtained for the phage display antibody.

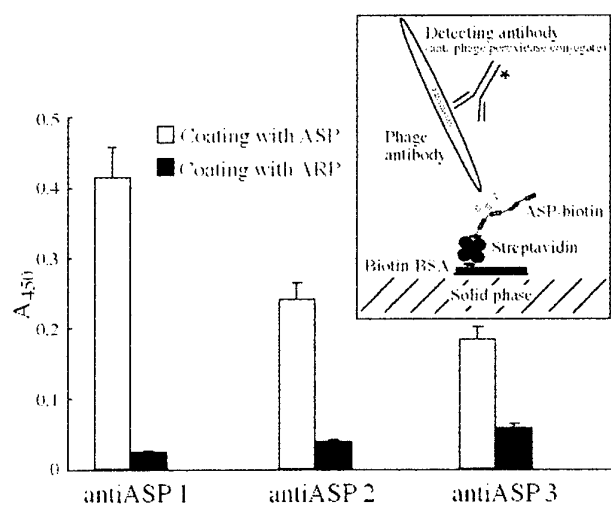


**Fig. 2. Specificity analysis of monoclonal phage antibodies.**

An ELISA was carried out using wells indirectly coated with ASP or ARP, to check the specificity of selected antibodies. For the coating, BSA-biotin, streptavidin and the biotinylated antigen (ASP or ARP) were applied to a microtiter plate in consecutive steps, as described in Materials and Methods. After last wash,  $10^{10}$  t.u. of phage were added to different wells. Detection of bound phage was as in Figure 1. Values reported are average  $\pm$  standard deviation from 4 independent

determinations. Inset: a schematic representation of the ELISA.

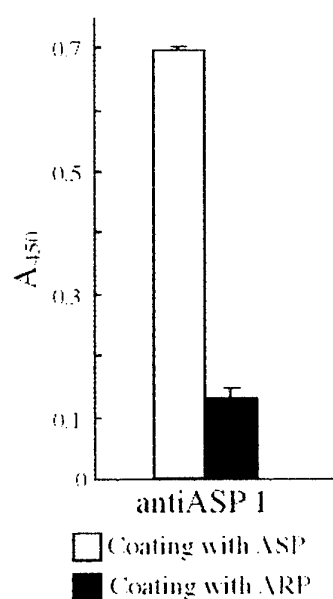


**Fig. 3. Specificity analysis of soluble antiASP 1 scFv antibody.**

The ELISA protocol was carried out as for phage antibodies (Fig. 2), except the last detection step. Thereby, 9E10 and secondary anti-mouse peroxidase antibodies were used to detect the myc-tagged scFvs. Average  $\pm$  standard deviation values are shown for three different measurements.

### AntiASP 1 recognizes authentic AChE-S

To test whether the antiASP 1 monoclonal phage antibody would also be selective for native AChE-S, a competitive ELISA was performed (Fig. 4). The antiASP 1 clone was chosen due to its high occurrence after the last round of selection (Table 1) and because it exhibited the strongest interaction with ASP in ELISA (Fig. 2). Phage were mixed with increasing concentrations of AChE-S or ARP, and then added to different wells of a microtiter plate coated with ASP. The AChE-S protein acted as a competitor diminishing the binding of the antiASP 1 phage to the wells, suggesting that the phage antibody interacted specifically with soluble AChE-S. About 70% of the binding was abolished in the presence of 0.5  $\mu\text{M}$  AChE-S, whereas no effect was observed in the case of soluble ARP (Fig. 4), even when a 8  $\mu\text{M}$  concentration was tested (data not shown).

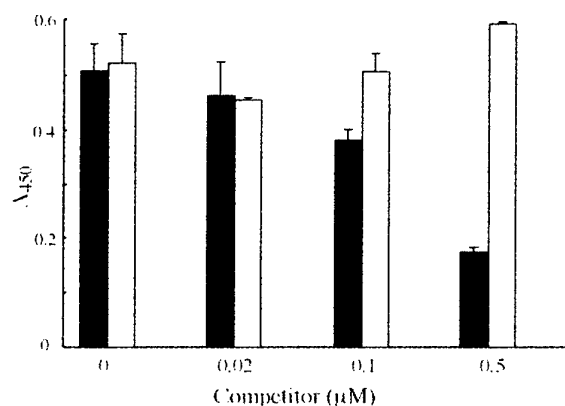


**Fig. 4. AChE-S specific interaction with antiASP 1 analysed by competitive ELISA.** ASP-biotin (100 ng, 19 pmol) was indirectly immobilized as in Figure 2. AntiASP 1 phage suspension (100  $\mu\text{l}$ ;  $10^{11}$  t.u./ml) was added to the ASP-coated wells in the presence of increasing concentrations of either human recombinant AChE-S (black column) or ARP (white column). Average  $\pm$  standard deviation values are shown ( $n = 2$ ).

### AntiASP 1 binds to its antigen with micromolar affinity

The binding affinity of the soluble antiASP 1 scFv antibody was determined using SPR in the BIAcore 3000 system. A peptide with the sequence of the 23 C-terminal residues of AChE-S (ASP C-ter), human recombinant AChE-S and ARP were immobilized in the different flow cells of a CM5 sensor chip. The scFv purified antiASP 1 was passed through the flow cells at several concentrations, and the kinetic constants were determined by the evaluation software of the BIAcore version 1.2. The best fit for the binding curves was obtained using the bivalent analyte model, suggesting that the antibody fragments can partly associate to form a mixture of dimers and monomers (Nissim *et al.*, 1994). The measured affinities of antiASP 1 show dissociation constants at the micromolar range:  $1.6 \times 10^{-6}$  and  $2.0 \times 10^{-6}$  M for ASP C-ter and AChE-S, respectively. No interaction was observed between antiASP 1 and ARP.

The ASP C-ter, unlike ARP, is rich in polar residues, which are often exposed and involved in the interactions between antibodies and antigens (Chothia and Lesk, 1987). In the  $V_{\text{H}}\text{-CDR3}$  of antiASP 1, the replacement of an isoleucine with a histidine residue induces a diminution in the binding signal (Table 1 and Figure 2, antiASP 1 versus 2). This was compatible with electrostatic repulsion, due to the high number of basic residues in ASP C-ter (2 His, 2 Lys, and 1 Arg).

## **Discussion**

During recent years, non-classical AChE functions have been established by several research groups (Layer and Willbold, 1995; Bigbee *et al.*, 2000; Soreq and Seidman, 2001).

Cumulative information attributes some of these alternative activities to the C-terminal variants of the enzyme (Sternfeld *et al.*, 1998, 2000). However, unequivocal evidence for this heterogeneity is still sparse. Therefore, obtaining monoclonal antibodies with the capacity to distinguish among AChE protein isoforms will be of utmost importance to study tissue and cellular distribution of each variant, and to determine whether specific functions may be assigned to specific variants.

Our current findings present one step in a wider effort to develop research tools for studying the distinct properties of AChE variants. Our previous preparation of a polyclonal rabbit antibody against a glutathione transferase fusion protein with ARP (Sternfeld *et al.*, 2000) demonstrated the very low immunogenicity of ARP, which calls for improved methods. To this end, synthetic peptides, which represent the C-terminal sequences unique to human AChE-S and AChE-R, were used as targets for selection from a phage display antibody library. This methodology offers important advantages over the classical hybridoma technology. First, phage display repertoires from variable-genes rearranged *in vitro* enable the isolation of monoclonal antibodies with specificities that have proved difficult by animal immunization and classical technology, for example against highly conserved intracellular proteins (Nissim *et al.*, 1994).

Second, we have assumed that the sequence homology of AChE to nervous system cell adhesion proteins, such as neurotactin, neuroligin, and gliotactin, is the basis of its morphogenic functions (Darboux *et al.*, 1996; Grifman *et al.*, 1998; Grisaru *et al.*, 1999). Interaction of AChE variants with distinct protein partners would, therefore, modify cellular signaling to cause clearly different biological effects (Grisaru *et al.*, 1999). A suitable approach to the identification of these protein partners should be to screen phage display random peptide libraries, since central to this strategy is the observation that peptides isolated by affinity selection from such libraries typically interact with biologically relevant domains of the target protein (Adey and Kay, 1997). The DNA that encodes the selected peptides can be easily sequenced from the appropriate region in the viral genome; this enables a search of sequence homologs to identify potential AChE protein partners. Therefore, the acquired experience with phage repertoires during the selection of monoclonal antibodies will be essential to undertake the next goals of the project. Furthermore, the amino acid V<sub>H</sub>-CDR3 sequences of antibody fragments selected from phage libraries can be readily deduced. The V<sub>H</sub>-CDR3 is the most important region in the recognition between antigen and antibody (Chothia and Lesk, 1987), and can contribute to our understanding of the type of protein interactions in which the AChE C-termini may be involved.

A high frequency (46%) of phage carrying specific anti-ASP scFvs was found after 2 rounds of selection against the biotinylated peptide in solution (Fig. 1). The DNA sequencing of selected phage antibodies allowed identification of 3 different clones, 2 of them with closely related V<sub>H</sub>-CDR3 (Table 1). AntiASP 1 was dominant in the population, representing the 40% of sequenced clones, and showed the strongest specific signal to ASP by ELISA (Fig. 2). Most importantly, antiASP 1 also interacted with the whole AChE-S protein as judged by competitive ELISA and BIAcore analysis (Fig. 4 and SPR results), in accordance with previous work that demonstrated the ability of antibodies selected against peptides from phage display libraries to recognize the native protein (Henderikx *et al.*, 1998; Persic *et al.*, 1999).

The antigenic determinant for antiASP 1 is located within the C-terminal 23 amino acids of ASP, as BIAcore analysis showed interaction between the soluble scFv antibody and the ASP

C-ter. By hybridoma technology, Boschetti *et al.* (1996) obtained monoclonal antibodies against a peptide with the sequence of the 10 C-terminal residues of AChE-S; these antibodies recognized the brain enzyme. All together, these observations demonstrate that the C-terminal sequence of ASP is an efficient and physiologically exposed immunogen, capable of interacting with antibodies also when part of the complete protein. This is an important consideration since the structural properties of ASP are not yet known. Besides surface exposure and accessibility to the large antibody molecule (Thornton *et al.*, 1986), protein regions corresponding to antigenic peptides are thought to possess high mobility. So, based on X-ray crystallographic temperature factors, Tainer *et al.* (1984) showed that anti-peptide antibodies against highly mobile regions react strongly with the native protein, while anti-peptide antibodies from well-ordered regions do not. These authors suggest that molecular mobility could be an essential part not only of the antigenic recognition process but also of protein-protein recognition in general.

The core domain common to all AChE variants possesses a high degree of sequence homology with adhesion proteins but lacks the capacity to form protein interactions by itself. In contrast, their variable C-terminal chains could interact with distinct protein partners. The AChE-S variant includes an exon 6-encoded 40 residue C-terminal extension (ASP), which initiates by a putative amphipathic ring formed by the closest 16 amino acids to the core domain of the protein (Soreq and Glick, 2000). This amphipathic ring may enable the attachment of AChE-S to membranes. On the other hand, our experimental data indicate that the C-terminal 23 amino acid sequence of ASP is highly exposed and mobile, suitable for participation in protein-protein interactions when it is not involved in dimerization of AChE subunits through its cysteine residue.

In conclusion, we have selected human antibody fragments, which are highly specific for the C-terminal sequence unique to human AChE-S. The dissociation constants, calculated by SPR in BIAcore, are  $1.6 \times 10^{-6}$  M for the interaction between ASP C-ter and antiASP 1, and  $2.0 \times 10^{-6}$  M for the interaction between AChE-S and antiASP 1, within the affinity range expected for scFv antibodies selected from phage display libraries (Marks *et al.*, 1991; Griffiths *et al.*, 1993; de Kruif *et al.*, 1995). Antibodies with improved affinities can be obtained by diverse means (Marks *et al.*, 1992; Vaughan *et al.*, 1996; Neri *et al.*, 1997). However, affinity maturation may not be required for *in vivo* biological effects or for other applications. Thereby, antiASP 1 should be useful for a quantitative assay (ELISA or immunoblot-type) for the determination of AChE-S levels in tissues and body fluids, for example during embryonic development and neurogenesis and in syndromes such as Alzheimer's disease, and for studying other processes in which AChE is involved. For these purposes, antiASP 1 can be used as either phage displayed or soluble scFvs, the latter being easy to purify through their His6-tag and detect by their myc-tag. Determination of AChE-S levels in ageing and dementia should be of particular interest.

## **B. Differentially modulated expression of acetylcholinesterase C-terminal variants in hematopoietic cells**

Hematopoiesis is an active and complex process of cell division, commitment and maturation that is regulated by interactive pathways, intimate cell-cell contacts and release of growth factors that are only partially understood. AChE is found in multiple blood cell lineages and has been proposed to exert morphogenic roles unrelated to its well-known involvement in cholinergic neurotransmission. AChE is therefore, an intriguing candidate for both cell-cell interactions and growth factor roles in hematopoietic regulation. The *ACHE* gene, through

alternative splicing, produces 3 C-terminally distinct proteins (Fig. 6): AChE-S, with an amphipathic C-terminus, AChE-E, C-terminally attached to red blood cells through a glycosphosphatidoinositide anchor and AChE-R, with a hydrophilic C-terminus. Recently, the C-terminal sequence that is unique to the AChE-R variant emerged as an independent hematopoietic modulator (Grisaru et al., 2001). To further investigate these properties, selective antibodies have been produced against the C-termini of AChE-S and AChE-R, ASP and ARP respectively. Anti-ARP (Sternfeld et al., 2000) is a rabbit polyclonal antibody while anti-ASP, was selected from a bacteriophage library of monoclonal single-chain antibodies (Flores-Flores et al., in press). Here, we report the use of these two antibodies in flow cytometry to resolve the complex patterns of AChE variants and their C-terminal peptides in human cord blood populations (Fig 7). Anti-ASP primarily displayed surface labeling of hematopoietic lineages, whereas anti-ARP was expressed both in the cytoplasmic and on the surface (Figs. 7, 8). Lymphocytes and granulocytes displayed ARP labeling while monocytes presented ASP (Figs 9, 10), suggesting that hematopoietic differentiation is accompanied by a shift in alternative splicing.

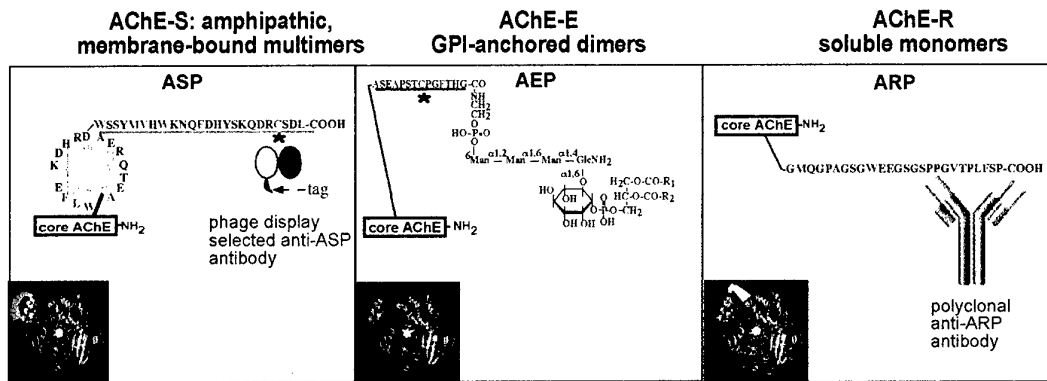


**Fig. 6. The variant C-terminal peptides of human AChE. Shown are the amino acid C-terminal sequences unique to each of the human AChE variants.** The core domain (3-D cartoon) is similar in all 3, but the C-terminus is characteristic of each variant (green, red and yellow flags on the cartoons). Note that both the ASP and AEP but not ARP, include cysteine residues (starred in the peptide sequences), which enable the formation of RBC-associated AChE-E dimers and synapse-associated AChE-S multimers. Note also that ASP, the longest peptide, includes a putative amphipathic ring that may enable its attachment to membranes, and that AEP terminates with a glycosphosphoinositide anchor that can integrate with membrane phospholipids. This leaves ARP as most accessible for proteolytic cleavage. Polyclonal antibodies produced against ARP and a single chain antibody selected from bacteriophage library against ASP enable distinct detection of each of these variants.

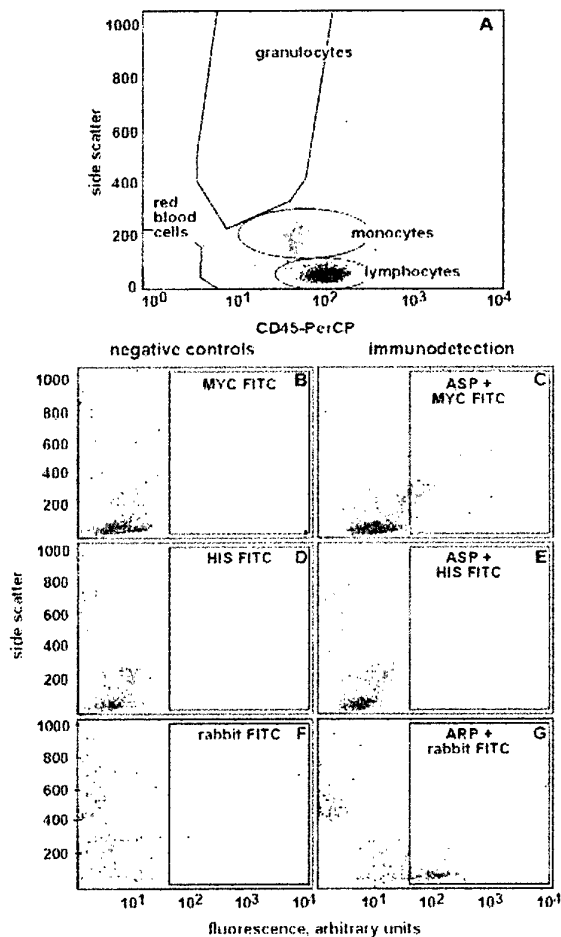


**Fig. 7. Detection of ASP and ARP on the surface of cord blood cell populations.** Cord blood cells were divided into 4 populations depending on their expression of CD45 (A). Red dots, are lymphocytes, green dots, monocytes, yellow dots, granulocytes and blue dots, red blood cells. Expression of surface ASP was detected on these populations using the selected phage anti-ASP antibody, as single chain antibody with a multi-histidine or MYC tag. Surface ARP was detected with the use of a polyclonal rabbit antibody against the C-terminal end of human AChE-R. Two different fluorescent probes, anti-MYC FITC (B and C) and anti-HIS FITC (D and E) were used as secondary labeling to verify the ASP antibody using flow cytometry, while anti-rabbit FITC was used to verify anti-ARP (F and G). Positive cells were defined as those to the right of the black gate. Note that the HIS tag is considerably less efficient than MYC, probably since it is lost during the preparation of the anti-ASP antibody and disappears (E). Therefore, further studies used anti-MYC FITC.

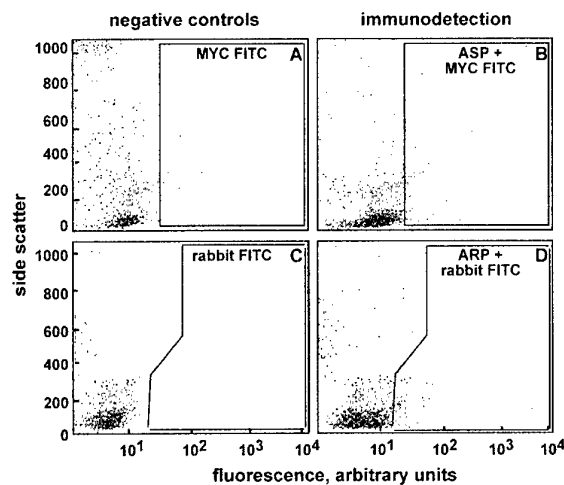


**Fig. 8. Cytoplasmic expression of ASP and ARP in various populations of cord blood cells.** Cord blood cells were divided into four populations, depending on their expression of CD45-PerCP. Red dots are lymphocytes, green dots, monocytes, yellow dots, granulocytes and blue dots, red blood cells, as in Fig. 7. The intensity of fluorescence in the positive cells was weak, less than two log units (B and D), as compared to controls (A and C), likely reflecting a low expression levels of cytoplasmic ASP and ARP in these cells.

This is compatible with the AChE protein being secretory. The cytoplasmic expression of ASP appears to be exclusive to the monocytes (green dots) while ARP seems to be expressed cytoplasmically in lymphocytes and monocytes.

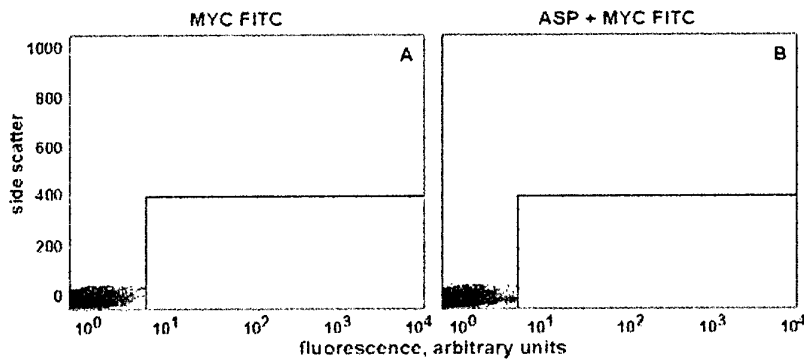


**Fig. 9. Lymphocytes display surface ASP labeling.** Highly CD45-expressing lymphocytes selected as in Fig. 6 were analyzed for their ASP labeling (black box). Illustrated above are dot plot figures of surface labeling with FITC-tagged anti-MYC (negative control, A) and with anti-ASP (immunodetection, B). The abscissa reflects the intensity of fluorescent labeling, with  $10^4$  being the highest observed.

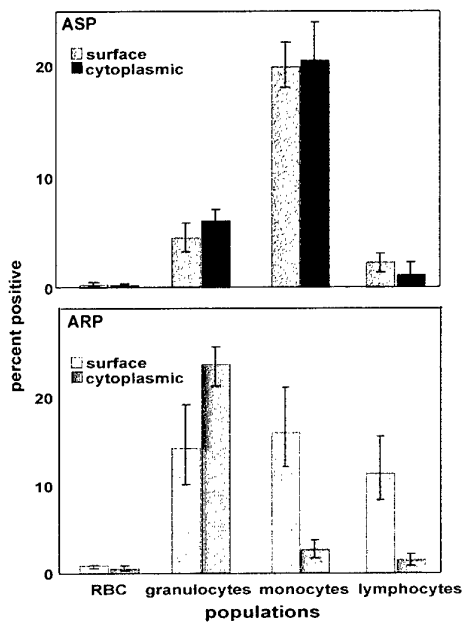


**Fig. 10. Differential ASP and ARP labeling in leukocyte populations.** ASP and ARP expression was quantified by flow cytometry in the cytoplasm and on the surface of cord blood leukocyte populations. Red blood cell labeling was minimal for both antibodies, lymphocytes primarily expressed surface ARP, granulocytes expressed predominantly surface and cytoplasmic ARP, while monocytes expressed surface ARP and were the only population that significantly expressed ASP both on their surface and in their cytoplasm.

## Changes in neuronal acetylcholinesterase gene expression and division of labor in honey bee colonies (task 3)

### Results and Discussion

**Treatment with an AChE inhibitor improves performance in a learning assay.** Cholinergic neurotransmission has been implicated in honey bee olfactory learning (Cano Lozano and Gauthier, 1998; Fresquet et al., 1998; Gauthier et al., 1994), but the influence of AChE modulation is still unclear (Fresquet et al., 1998; Gauthier et al., 1992). We hypothesized that reduced AChE activity in bees enhances performance in a learning assay. We tested this by injecting foragers with the organophosphate AChE inhibitor metrifonate (Oh et al., 1999) (Sigma), and subjecting them to a well-established olfactory associative learning assay (Menzel et al., 1974) (Fig. 1). Metrifonate-treated bees had a significantly higher number of correct responses than saline-treated bees ( $2.48 \pm 0.26$  SE vs.  $1.93 \pm 0.24$ ,  $p < 0.03$ , ANOVA). They also had a faster rate of acquisition, with the biggest treatment effect apparent during the second odor exposure. These results indicate that the cholinergic system plays an important role in olfactory learning in honey bees, consistent with most of the previous studies (not including Fresquet et al., 1998).

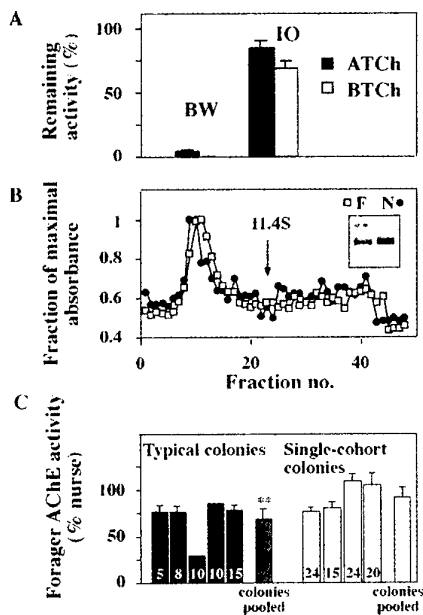


**Fig. 1. Metrifonate improves bee performance on olfactory learning test.** Top. A scheme of the learning assay. Odor exposure (a puff of geraniol-saturated air) was coupled with a reward of 0.5 M sucrose (droplet), which elicits the unconditioned response, the proboscis (arrow) extension reflex (inter-exposure interval: 20 min). A positive response was a complete extension of the proboscis that was observed during odor presentation and before reward presentation. The test began 45 min after injection, an interval which eliminates obvious injection effects (Robinson et al. 1999). Bottom. Mean ( $\pm$  SD) number of bees showing positive responses at each odor exposure. Grand means are based on data from four trials, with bees from 2 different, unrelated, colonies, 37-94 bees/group/trial; 216 metrifonate-injected (1  $\mu$ l, 2 mg/ml in saline; filled squares) and 233 saline-injected (open circles) bees total. Statistical analyses (see text) were conducted on the total number of correct responses/bee.

**Brain acetylcholinesterase is biochemically similar in nurses and foragers.** Honey bee development is marked by a transition from working in the hive to the more complex tasks of foraging outside. To examine whether this transition is associated with a change in AChE that would facilitate cholinergic neurotransmission, we began our comparative analysis of AChE in nurses and foragers with biochemical analyses of brain homogenates. Acetylthiocholine (ATCh) hydrolysis, reflecting AChE activity, was 20-fold higher than butyrylthiocholine (BTCh) hydrolysis, reflecting activity of the closely

related enzyme butyrylcholinesterase (BuChE) (data not shown). ATCh hydrolysis was almost completely abolished by the AChE-specific inhibitor BW284C51, whereas BTCh hydrolysis was only slightly inhibited by the classical BuChE inhibitor iso-OMPA (Fig. 2A). This demonstrates that AChE accounts for about 95% of the total cholinesterase activity in the bee brain and suggests that, similar to the enzyme from *Drosophila melanogaster* (Gnagey et al., 1987), it is responsible for both ATCh and BTCh hydrolysis. There were no differences in these characteristics between nurse and forager bees, identified according to standard behavioral criteria (Wagener-Hulme et al., 1999). The ages of the nurse and forager bees were not known, but since they were from typical colonies we assume that nurses were about 1-2 weeks of age and foragers were about 3-4 weeks of age.

There also were no differences between nurses and foragers in electrophoretic migration and oligomeric assembly for catalytically active brain AChE. Bee AChE migrated as a single band and showed similar electrophoretic mobility to that of recombinant human AChE (Sigma; Fig. 2B and data not shown). Bee AChE also displayed a single peak in sucrose gradient analysis, with a ca. 6S sedimentation coefficient (as was previously described (Belzunces et al., 1988), which most likely corresponds to AChE dimers (Fig. 2B).

**Brain AChE catalytic activity decreases during behavioral development.** Catalytic activity of AChE in brain extracts was 20-65% lower in foragers compared to nurses (Fig. 2C, left). 2-way ANOVA showed that this decrease was significant ( $p < 0.01$ ) and also varied significantly ( $p < 0.05$ ) between bees from different colonies. These results were robust; they were obtained over two different years, from five unrelated typical colonies maintained under field conditions.

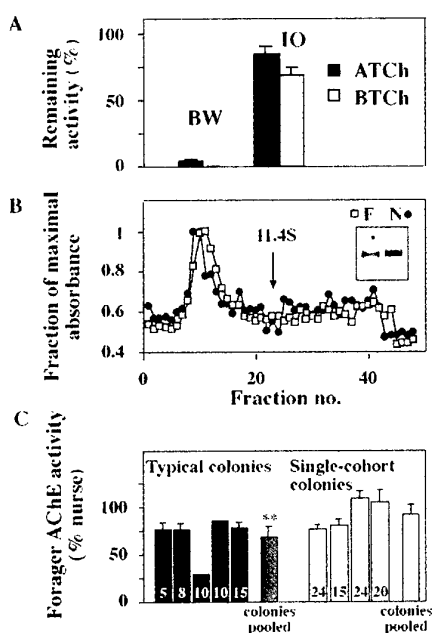


**Fig. 2. Biochemical analyses of AChE from the brains of nurse and forager bees.** **A. Substrate and inhibitor specificities.** Mean ( $\pm$ SE) specific cholinesterase activity in brain homogenates from nurse bees. Homogenates were treated with either the AChE-specific inhibitor BW284C51 (BW) or the BuChE inhibitor iso-OMPA (IO). Rates of acetylthiocholine (ATCh) or butyrylthiocholine (BTCh) hydrolysis were measured colorimetrically (Loewenstein Lichtenstein et al., 1995) (2-3 measurements of one sample, 5 brains/sample) and data normalized to rates without inhibitor. The hydrolysis rate of ATCh was 20-fold higher than BTCh (data not shown). **B. Similar sedimentation and electromobility profiles for nurse and forager AChE.** Extracts representing 10 brains each were subjected to sucrose density centrifugation followed by an ATCh hydrolysis assay (Seidman et al., 1994).

AChE activity was mostly localized to a peak of 6S in both groups, consistent with dimeric enzyme composition. Arrow marks the position of bovine liver catalase. Inset. AChE from nurses and foragers migrates similarly in activity gels. AChE activity staining following gel electrophoresis (Seidman et al., 1995) reveals a single band with similar electromobility in brain homogenates prepared from foragers or nurses (each sample is a 5- $\mu$ l aliquot of brain homogenate representing 10 brains). C. Differences in brain AChE activity levels in foragers and nurses. Left. Mean ( $\pm$  SD) AChE brain activity levels (nmol ATCh hydrolyzed/min/mg total protein) in forager bees from typical colonies, normalized to the mean level for nurse bees from the same colony (number of bees for each colony in bars). Columns without SDs represent colonies where all brains were pooled into one homogenate; dotted bar represents the grand mean across all 5 colonies. 2-way ANOVA (randomized complete block on log-transformed data; SAS, Cary, NC) revealed significant variation between colonies ( $P < 0.05$ ) and between nurses and foragers ( $P < 0.01$ ). Absolute rates of ATCh hydrolysis varied greatly from colony to colony (median: ca. 100 nmol ATCh hydrolyzed/min/mg total protein). Right. Similar results for bees from 4 single-cohort colonies. There were no overall significant differences between nurses and precocious foragers.

According to the basic structure of division of labor in bee colonies, hive work always precedes foraging; foragers are thus both older and more behaviorally advanced than nurses. This means that the changes in AChE may: 1) anticipate or coincide with the transition from hive work to foraging; 2) relate to the acquisition of new tasks once foraging has already begun; and/or 3) relate to chronological aging that is independent of behavioral status. To explore which of these processes are more likely to be associated with the observed changes in AChE, we used "precocious foragers", bees that were induced to develop earlier due to the absence of older individuals (Robinson and Page, 1989). Brain AChE catalytic activity was measured in nurses and precocious foragers that were all 7-10 days of age and were collected from 4 "single-cohort colonies", established with all young bees. ANOVA revealed that there were no significant ( $p > 0.7$ ) differences between nurses and precocious foragers overall (Fig. 2C, right). It thus appears that differences between nurses and foragers in AChE activity do not occur prior to or even immediately following the transition to foraging, leaving both chronological aging and experience-dependent changes as possible causal factors. We speculate that AChE activity in the bee brain is influenced, at least in part, by foraging experience. Foragers from typical colonies presumably had as much as one or two weeks of foraging experience before they were collected and they showed a robust decrease in AChE activity. In contrast, precocious foragers had only one or two days of foraging experience before collection, and perhaps this is not enough to consistently influence AChE. This speculation agrees with the observation that results for single-cohort colonies were more variable than for typical colonies, with precocious foragers from a few colonies showing decreases comparable to those seen in foragers from typical colonies.

**Bee Ache cloned.** To test whether the changes in AChE activity associated with division of labor are caused by transcriptional regulation, we cloned the cDNA sequence encoding the *Apis mellifera* (Am) AChE in order to measure brain mRNA levels. RT-PCR, with partially-degenerate primers designed according to conserved regions of the AChE

protein, yielded two main products, 187 and 245 bp long. The predicted protein encoded by the shorter product (accession no. AF213011) displayed 40% and 35% identity to alpha-esterases of the blowfly, *Lucilia cuprina*, and *D. melanogaster*, respectively (accession no. aaa91812 and aaB01149), enzymes related to AChE which are important for resistance to organophosphates (Newcomb et al., 1996). The protein sequence encoded by the longer product showed high sequence identity with AChEs from various organisms. We obtained a 1715 bp cDNA sequence using the sequence of the longer product by rapid amplification of cDNA edges (5'/3' RACE kit; Boehringer Mannheim) and PCR amplification from a bee brain cDNA library as template. The 492 AA translation-product showed 67.1%, 61% and 39.9% identity to AChE from the beetle *Leptinotarsa decemlineata*, *D. melanogaster* and *H. sapiens*, respectively (Fig. 3). This comparison confirmed the identity of this cDNA as part of the *Ache* gene of the honey bee, *Apis mellifera* (*AmAche*).

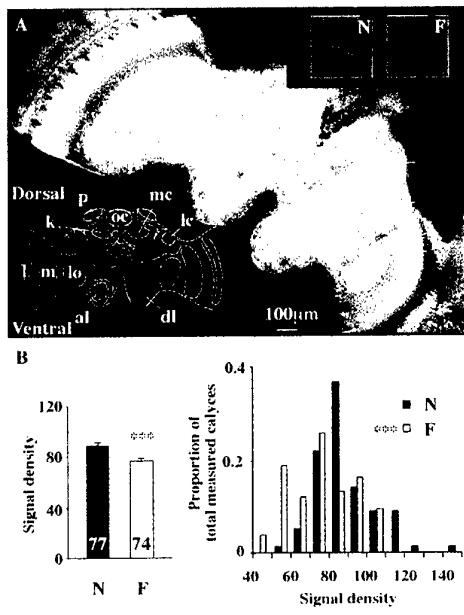


**Fig. 3. AChE Sequence comparison.** Multiple sequence alignment of the translated *AmAChE* partial gene-product with two insect and two vertebrate AChE proteins. Alignment was generated with the PileUp (University of Wisconsin GCG software package) and Boxshade programs. Black and grey shadings represent residues identical or similar, respectively, to a consensus sequence calculated from these sequences (not shown). *Am*, *Apis mellifera* (current report, GeneBank accession no. AF213012); *Ld*, *Leptinotarsa decemlineata* (Swissprot accession number Q27677); *Dm*, *Drosophila melanogaster* (P07140); *Tm*, the electric eel, *Torpedo marmorata* (P07692); *Hs*, *Homo sapiens* (P22303). Asterisks denote the catalytic triad residues.

**AChE brain mRNA levels decrease during behavioral development, especially in the mushroom bodies.** High-resolution *in situ* hybridization (ISH) showed AChE mRNA localization in several brain regions known to be involved with processing of olfactory and visual information, such as the mushroom bodies, the medulla and lamina of the optic lobes, and the area surrounding the antennal lobes (Fig 4A). These results agree with histochemical and immunocytochemical analyses of other components of the cholinergic system (Kreissl and Bicker, 1989). ISH showed especially strong expression in the somata of the Kenyon cells, the intrinsic cells of the mushroom bodies whose projections lie in the surrounding neuropil, the calyces (Fig 4A). These cells receive and integrate olfactory and visual inputs from the antennal and optic lobes and are also involved in learning and memory (de Belle and Heisenberg, 1994; Hammer and Menzel, 1995; Meller and Davis, 1996; Mobbs, 1985). High levels of expression in the mushroom bodies may reflect the fact that the calyx has an extremely high cell density (Ito et al.,

1998). However, quantitative analysis of confocal microscopy images revealed a significantly lower density of mRNA labeling in the Kenyon cells of foragers relative to nurses (Fig. 4B left); such a comparison of the same brain region between different behavioral groups is not subject to the cell density issue. These results indicate that the decreased catalytic activity of AChE in forager bee brains is associated with a decrease in AChE mRNA levels, especially in the mushroom bodies. Differences were especially striking in the centrally located cells (Fig. 4A, insets). Support for this observation comes from an analysis of the distribution of signal densities for all calyces analyzed (Fig. 3B right). Though the distributions for nurses and foragers overlap broadly, they do differ significantly ( $p < 0.001$ , G-test), with an apparent second peak in the low values of signal density for calyces from foragers. Given that sections ( $n = 21$  per behavioral group) were taken randomly with respect to position in the calyx, these results suggest that spatial patterns of AChE expression within the calyces of the mushroom bodies differ between nurses and foragers.

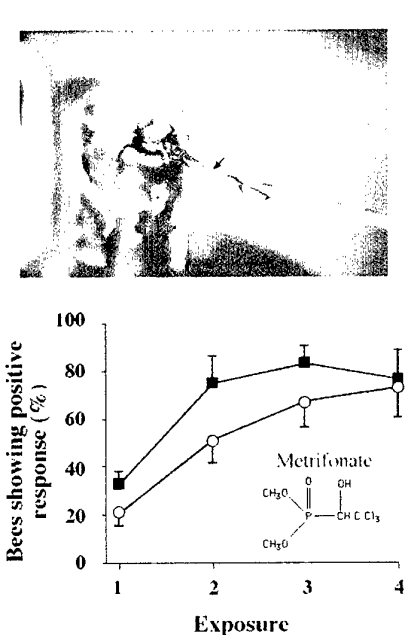


**Fig. 4. AChE brain mRNA levels are lower in foragers than nurses, especially in the mushroom bodies.** A. AChE mRNA labeling in the bee brain. A representative coronal section through the brain of a worker honey bee labeled for AmAChE mRNA, according to a protocol described in [Grifman, 1998 #307] and modified so as to block the relatively high endogenous biotin levels found in the insect brain (Ziegler et al., 1995). Detection of transcripts was achieved using the ELF fluorogenic alkaline phosphatase (AP) substrate (Molecular Probes Inc., Eugene OR) and a fluorescent Zeiss Axioplan microscope (main image). White rectangle delineates the position of a calyx region of a mushroom body shown, magnified, in the top right images. Top right. Representative confocal microscope images ( $N =$  nurse,  $F =$  forager) of calyces from similar brain sections labeled for AmAChE mRNA using the Fast Red AP substrate (Boehringer-Mannheim). Images

were captured with an inverted Olympus microscope equipped with an MRC-1024 Bio-Rad confocal attachment (Hemel Hempstead Herts., UK). Bottom left. Schematic depiction of the bee brain (after (Kreissl and Bicker, 1989) mc and lc, medial and lateral calyces of the mushroom bodies; k, Kenyon cell bodies region; p, pons; oc, one of three ocelli; l, m and lo, lamella, medula and lobula of the optical lobe; al, antennal lobe; dl, dorsal lobe). B. AChE mRNA levels are lower in Kenyon cells of foragers than nurses. Left. Mean  $\pm$  SD signal densities (arbitrary units) of AChE mRNA from calyces (enclosing a population of Kenyon cell bodies) of nurses (N) and foragers (F);  $P < 0.0001$ , t-test. Quantification of confocal images as in [Grisaru et al., 2001]. No significant differences in signal densities between medial and lateral calyces were detected (results not shown). Right. Frequency distribution of signal densities for all analyzed calyces.

Analysis based on 77 calyx sections for nurses and 74 for foragers (2-4 calyces/section, 3 sections/brain, 7 brains/behavioral group).

We have demonstrated differences in AChE mRNA expression in the mushroom bodies of nurses and foragers. This brain structure also shows structural changes during behavioral development that involve an increase in neuropil volume (Withers et al., 1993) and dendritic arborization (Farris et al., 1999). Our results further highlight this brain region as a site for behaviorally related plasticity and suggest cholinergic neurotransmission as a modulator of such processes. In addition, the non-catalytic activities of AChE (Grisaru et al., 1999) may contribute to the structural changes in this region, at least early in adulthood when levels are high.

Changes in neural function that underlie long-term changes in memory are caused in part by transcription-dependent mechanisms (Kaufer et al., 1998). Our results indicate that similar mechanisms may be involved in the long-term changes in neural function that are associated with behavioral development in honey bees. There is only limited evidence for changes in gene expression in the brain that are associated with changes in behavior of animals in their natural environment (Mello et al., 1995; Robinson, 1999). However, this is probably due to the little attention this topic has received. In honey bees, there are only two other known cases of developmental regulation of brain gene expression. There are age-related increases in royal jelly protein-3 mRNA in the brain, the function of which is still unknown (Kucharski et al., 1998) There also are similar increases in brain mRNA levels of *period*, a gene well known for its role in circadian rhythms (Toma et al., 2000). These results, coupled with our findings, suggest that transcription-dependent mechanisms may play diverse roles in naturally occurring behavioral plasticity.

### Complex host cell responses to antisense suppression of *ACHE* gene expression (task 5)

Antisense oligodeoxynucleotides (AS-ODNs) are powerful tools for sequence-dependent suppression of target genes (Agrawal and Kandimalla, 2000; Crooke, 2000). AS-ODNs are presumed to act by facilitating the action of ribonuclease on mRNA-ODN hybrids (Ma et al., 2000; Wu et al., 1999). To exert their effects, AS-ODNs must enter the cell, interact with their target mRNAs long enough for the nuclease to act, and then attach to another mRNA. Much effort has been devoted to understanding the cellular uptake and mechanism of action of AS-ODNs (Beltinger et al., 1995). In contrast, less is known about host cell responses to this process. For example, it is not known whether AS-ODN-treated cells compensate for lost mRNA. This issue is important, since feedback upregulation of a targeted gene may mask antisense effects and encourage the use of excessively high concentrations of ODN.

Another important issue to address relates to the effects of foreign DNA and AS-ODN degradation products such as free nucleotides on cellular physiology. Nucleotides and their analogs modulate cell volume through several independent mechanisms (Galiotta et al., 1992). Under physiological steady-state conditions, cell volume is held constant by a "pump-leak-mechanism". The osmotic pressure arising from impermeable cytoplasmic solutes is balanced by the  $\text{Na}^+/\text{K}^+$  pump, accompanied by the constant expenditure of metabolic energy (Hoffmann, EK 1992). Micromolar or lower adenosine concentrations such as those expected to accumulate by degradation of ODN were shown to activate the A1 adenosine receptor and a  $\text{Cl}^-$  channel in the apical membrane of RCCT-28A endothelial cells (Light et al., 1990; Schwiebert et al., 1992). Extracellular ATP, UTP and related compounds similarly stimulate  $\text{Cl}^-$  secretion and affect cell volume in the nasal epithelium of both normal and cystic fibrosis patients (Knowles et al., 1991). Once they enter the cell, nucleotides affect the nucleocytoplasmic shuttle of proteins and RNA (Gerace, 1995), while non-hydrolyzable GTP analogues inhibit this shuttle (Melchior et al., 1993). Changes in nuclear protein import may affect several levels of cellular metabolism (Gorlich, 1998), but were not yet examined under AS-ODN treatment. These observations predict sequence non-specific cellular responses to AS-ODN treatments. Therefore, both the balance of ion homeostasis and nuclear-cytoplasmic interactions must be considered in AS-ODN studies.

Acetylcholinesterase (AChE) is an appropriate model to investigate host cell responses to AS-ODNs. The single *ACHE* gene produces three 3'-alternatively spliced mRNA transcripts, AChE-S, AChE-E, and AChE-R (Grisaru et al., 1999). AChE is ubiquitously expressed at variable levels in diverse tissues and cell types and undergoes transcript-specific, differentiation-dependent stabilization (Chan et al., 1998). We previously demonstrated that AChE mRNA and protein are overexpressed in rodent brain and muscle following acute pharmacological blockade of catalytic activity (Friedman et al., 1996; Kaufer et al., 1998; Lev-Lehman et al., 2000). However, it was not known whether antisense blockade of AChE synthesis would elicit similar feedback responses. In addition, it was shown that plasmid-encoded AS-cRNA suppressing *ACHE* gene expression alters the growth properties of mouse neuroblastoma cells (Koenigsberger et al., 1997) and rat neuroendocrine PC12 cells (Grifman et al., 1998). These studies suggested complex cellular responses to antisense-mediated AChE deficiencies. Two AS-ODNs targeted to AChE mRNA, AS1 and AS3, suppressed AChE expression in PC12 cells (Grifman and Soreq, 1997), human osteosarcoma Saos-2 cells (Grisaru et al., 1999), and hematopoietic  $\text{CD34}^+$  cells from umbilical cord blood (Grisaru et al., 2000) with corresponding physiological effects. Here, we studied cellular responses of PC12 cells to AChE AS-ODN mediated suppression of AChE activity.

## Materials and methods

**PC12 rat pheochromocytoma cells.** PC12 cells were grown in a fully humidified atmosphere at 37°C and 5% CO<sub>2</sub> in Dulbecco modified Eagle medium (DMEM) containing 8% each fetal calf and horse serum (Tissue culture reagents from Biological Industries, Beth Haemek, Israel). To induce differentiation, 50 ng/ml nerve growth factor (NGF; Alomone, Jerusalem) was added to the medium with 1% FCS and 1% HS. Tissue culture plates or cover slips were coated with 10 µg/ml collagen (type IV, Sigma, St. Louis, MO).

**AS-ODNs.** AS-ODNs targeted to exon 2 of mouse AChE mRNAs (AS1, AS3) have been described previously (Grifman et al., 1997). Oligonucleotides targeted to butyrylcholinesterase mRNA (ASB) served for control (Ehrlich et al., 1994).

AS1: 5'-GGGAGAGGAGGAGGAAGAGG-3'

AS3: 5'-CTGCAATATTTTCTTGACCC-3'

ASB 5'-GACTTTGCTATGCAT-3'

All ODNs were end-capped with either 2'-O-methyl RNA substitutions (Me), or phosphorothioate (PS) modification at their three 3' terminal positions. As lipofectamine was previously shown to be cytotoxic in differentiating PC12 cells (Grifman and Soreq, 1997), AS-ODN was added directly to the culture medium without carrier.

**In situ hybridization** was performed with a fully 2'-O-methylated 50-mer AChE cRNA probe complementary to alternative exon E6 in the AChE gene (Kaufer et al., 1998). As PC12 cells contain endogenous biotin, 5'-DIG-labeled probes were employed. Detection was with alkaline phosphatase and Fast Red<sup>®</sup> substrate (Molecular Probes). Hybridization was as detailed elsewhere (Grisaru et al., 1999). RT-PCR was performed essentially as described (Grifman et al., 1997).

**Confocal microscopy** was carried out using a Bio-Rad MRC-1024 confocal scanhead (Hemel Hempstead Herts., UK) coupled to an inverted Zeiss Axiovert 135 microscope equipped with a plan apochromat 63X/1.4 oil immersion objective. Fast-red was excited at 488nm, and emission was measured through a 580df32 bandpass interference filter (580nm ± 16 nm). The confocal iris was set to 3mm. Sections were scanned every 0.44 µm, corrected for immersion oil/mounting media index of refraction mismatch. The sections were processed in the following way. First, a maximum value projection was created from a set of sections. Intensity based thresholding was used to both isolate the cell from the background, and to identify fast-red precipitates. The threshold was at first selected manually, and later using the automatic object identification capability of Image Pro Plus (version 4.0, Media Cybernetics, Silver Spring, MD). Fast red precipitates were considered to be those objects which contained five or more pixels and exceeded the selected intensity threshold. This threshold was selected such that control cells always showed identical levels of labeling, in order to correct for the variables in preparation (e.g. alkaline phosphatase reaction time, probe efficiency, etc). The total area covered by the fast-red precipitates was then measured. The data were not normalized to cell volume, because the spread in cell volumes was very small.

**Nuclear and cytoplasmic volume** calculations were based on average values of nuclear and cell diameter as measured in the imaged sections. The measured cells and their nuclei were assumed to be spherical and cytoplasmic volume was taken to be cell minus nuclear volume.

## Results

### Peak inhibition of AChE activity at very low concentrations of AS-ODN.

We previously studied AS-ODNs targeted to various regions of AChE mRNA using end-capped 20-mer oligonucleotides in which phosphorothioate (PS) - modified bases were incorporated into the three 3'-terminal positions (Grifman and Soreq, 1997). Two AS-ODNs, AS1 and AS3, targeted to the common exon 2 shared by all AChE mRNA splice variants reduced AChE activity in differentiating PC12 cells by up to 30%. To improve uptake and

stability while reducing toxicity, we prepared 3'-end-capped, 2'-O-methyl (Me)-modified versions of AS1 and AS3 and compared their potency to their PS-modified counterparts. Both PS- and Me- capped AS1 suppressed AChE catalytic activity in nerve-growth factor (NGF)-stimulated PC12 cells to about 50% of controls in a dose and sequence-dependent manner within 48 hrs. AS1-Me displayed significant effects at an extracellular concentration of 0.05 nM, and maximum suppression of AChE activity was observed at 2 nM AS-ODN (Fig. 1A). In contrast, 2nM AS1-PS was required to exert prominent suppression of AChE activity in PC12 cells. Sequence-specificity was shown by the insignificant effects exerted by either PS or Me-protected AS-ODN targeting butyrylcholinesterase (BChE) (Fig. 1, inset). Curiously, increasing the concentrations of AS1 above 2 nM reduced AS-ODN efficacy to the extent that PC12 cells exposed to 1  $\mu$ M AS1, -PS or -Me, displayed only minor loss of AChE activity.

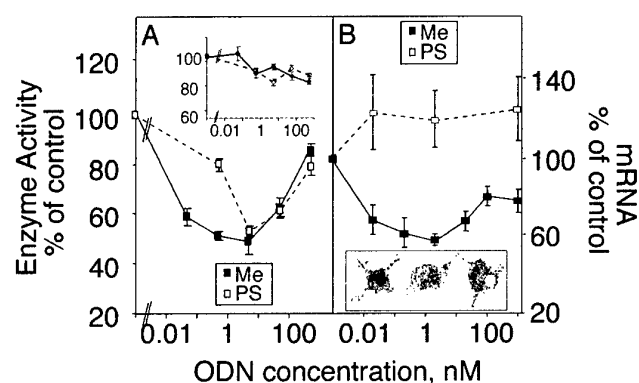


**Fig. 1. 2'-O-Methyl AS-AChE displays a wide effective window at extremely low concentrations.** Varying concentrations of phosphorothioate (PS) and 2'-O-methyl (Me) AS1 or AS3 were added to PC12 cells once daily for 2 days following 24 hr exposure to NGF and cells were analyzed for AChE catalytic activity or mRNA encoding AChE-S. **A:** AChE catalytic activity

was measured using a colorimetric assay and acetylthiocholine as substrate. Results are expressed as percent of activity in control cells  $\pm$  standard error of the mean (SEM) for 5-9 triplicate measurements for each point. Note that 2'-O-methyl modified AS1 elicited significant suppression of AChE at the extremely low concentration of 0.02 nanomolar, while phosphorothioate modification of the same three bases yielded an AS-ODN that exhibited effective suppression of AChE activity only at concentrations above 2 nM. Both oligonucleotides displayed decreasing efficacy at ODN concentrations above 2 nM. The non-relevant control AS-ODN ASB had minimal effects on AChE activity at concentrations up to 100 nM in both the Me and PS modified forms (inset). **B:** *In situ* hybridization with an exon 6-specific AChE cRNA probe was employed to detect AChE-S mRNA in AS3-treated cells. Quantification of AChE-S mRNA levels was by confocal microscopy and computer-assisted image analysis (Methods). Shown are average  $\pm$  SEM of AChE-S mRNA levels as a percentage of that observed in untreated cells. Note that AS3 induced a dose-dependent decrease in AChE-S mRNA levels that was reversed at about 2 nM AS-ODN. ASB had no detectable effect on AChE-S mRNA levels in these cells. Inset depicts cells from the same experiment following cytohistochemical staining for catalytically active AChE. From left to right are representative cells from cultures treated with 0.2, 2, and 1000 micromolar AS3, respectively.

To confirm the observation that increasing concentrations of oligonucleotide neutralize the potency of AS-ODN targeted to AChE mRNA, we used *in situ* hybridization (ISH) to label AChE-S mRNA in cells treated with AS3-Me for 48 hours. Generally, AChE-S mRNA appeared concentrated in one or two cytoplasmic areas close to the nuclear margin, possibly in the Golgi apparatus where AChE would be translated, folded and rendered catalytically active. To quantify ISH signals detecting cytoplasmic AChE mRNA, we applied confocal microscopy and computerized image-analysis. This analysis revealed a "U-shaped" dose-response curve for AS3 that closely paralleled the curve obtained with AS1 using AChE

catalytic activity as the measure of antisense potency (compare Fig 1B to 1A). Dose-dependent increases and decreases in AChE-R mRNA levels were matched by corresponding changes in cell-associated AChE activity as determined by cytohistochemical staining (Fig. 1B, inset). Nevertheless, AChE mRNA appeared more sensitive than AChE protein to the higher AS-ODN concentration. We observed similar dose-dependent effects on RNA and protein in human Saos-2 cells with AS1 (Grisaru et al., 1999 and data not shown). In contrast, ASB-Me did not elicit significant changes in ISH signals. These findings demonstrated effective suppression of AChE expression by two independent AS-ODNs targeted to AChE mRNA, demonstrated the enhanced potency and wide effective window conferred by 2'-O-Me modification of AChE AS-ODNs, and raised the question of why increasing concentrations of AS-ODN fail to elicit reliable suppression of AChE activity in these cells.

### AS-ODN treatment stimulates nuclear accumulation of AChE mRNA

Control PC12 cell never displayed intranuclear staining following ISH. However, at low concentrations of AS3-Me (0.2-2. nM), cells often displayed one or two small intra-nuclear foci of ISH signal (Fig. 2A,B). At higher concentrations of 100-1000 nM AS3-Me, intense nuclear staining of AChE-S mRNA was commonly observed in up to 2 highly-defined focal points. Similar nuclear labeling was also noted in AS-ODN-treated, multinucleated Saos-2 cells where multiple nuclear sites of labeling were observed (Grisaru et al., 1999 and data not shown). These observations suggested a direct association between focal nuclear staining and the number of transcription sites, and hinted at *de novo* accumulation of hn-AChE mRNA in AS-ODN treated cells. To further examine AChE mRNA levels in antisense-treated PC12 cells, we performed reverse transcription and polymerase chain reaction (RT-PCR) on RNA extracted from cultures treated with AS3 for 48 hrs following NGF-stimulated differentiation. RT-PCR revealed both a short mRNA representing mature 3'-spliced AChE-S mRNA, and a longer, unspliced transcript presumably representing heteronuclear (hn) AChE in differentiating PC12 cells (Fig. 2B, inset). Both the long and the short transcript were noted to be about 2-fold higher in cells treated with 100 nM as compared to 10 nM AS3. The nuclear accumulation of AChE mRNA under AS-ODN treatment suggests that the reduced potency of >2 nM AChE AS-ODN in PC12 cells reflects feedback upregulation of the AChE gene in response to highly effective primary antisense effects, and/or to the presence of excess AS-ODN or their degradation products. Moreover, it advances the notion that antisense, like pharmacological, inhibition of AChE below a certain threshold initiates feedback upregulation of AChE expression in multiple cell types. Together, these data point to the need to strike a balance in antisense studies between antisense effects and dose-dependent compensatory host cell responses.

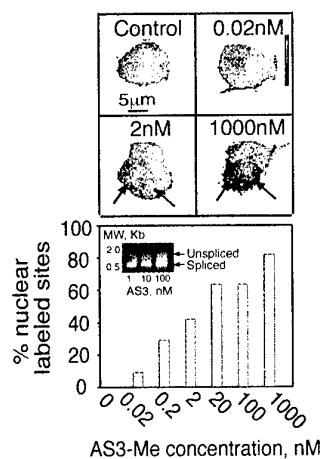


**Fig. 2. Focal nuclear accumulation of AChE mRNA in AS-ODN treated PC12 cells.** Upper panels: Presented are pseudocolored compound confocal images of representative PC12 cells following incubation with 2'-O-methyl RNA-protected AS3 and *in situ* hybridization with a probe detecting AChE-S mRNA. Color coding (upper right corner) correlates with intensity of fast red staining and therefore AChE-S mRNA levels. Note that increasing concentrations of AS3 were associated with the appearance of punctate nuclear staining for AChE-S mRNA (arrows) and reduced antisense efficacy as presented in figure 1. Lower Panels: Graph depicts the percentage of total potential nuclear sites (assuming 2 per cell) labelled by *in situ* hybridization at the noted concentrations of

AS3. Note the prominent concentration dependent increase in the fraction of nuclei labelled for AChE mRNA and the almost universal labeling of nuclei at 1  $\mu$ M AS-ODN. These data indicate feedback transcription and/or stabilization of nascent heteronuclear AChE mRNA under treatment with AS3. Inset presents ethidium bromide stained products of RT-PCR performed on RNA extracted from PC12 cells treated with the noted concentrations of AS3. Note that in addition to product representing mature, spliced AChE-S mRNA, a band of high molecular weight product presumed to represent unspliced hn-AChE mRNA is present; Both bands are intensified above 10 nM AS3, corresponding to the appearance of focal nuclear staining observed by *in situ* hybridization.

### Cellular uptake of AS-ODN

The role of AS-ODN uptake in host cell feedback responses was evaluated using 5'-digoxigenin (DIG)-tagged AS3-Me and the image analysis strategy of ISH. To estimate the sensitivity of the confocal approach, we mixed a 1 nM solution of DIG-tagged AS-ODN into a PC12 cell extract, dried a 50  $\mu$ l drop onto a microscope slide, and performed image analysis (N. Galyam, M.Sc. thesis, Hebrew University of Jerusalem, 1999 and data not shown). In AS-ODN treated PC12 cells, this quantification procedure revealed concentration-dependent increases in intracellular oligonucleotide (Fig. 3A). However, increasing extracellular concentrations between 20 pM and 1  $\mu$ M AS3-Me resulted in exceedingly limited increases in intracellular ODN (approximately 6-fold for the 5000-fold increased external concentration), both for AS1-Me and AS3-Me (Fig. 3A). We calculated 10-100 AS-ODN molecules per 10 pL cell volume under 0.02 nM treatment conditions, close to the external concentration of oligonucleotide. Therefore, 20 pM external concentration of AS3 sufficed to introduce AS3 into PC12 cells at a concentration similar to that of its complementary AChE mRNA (see Discussion). From 0.02 nM, 10-fold increases in external ODN concentration resulted in non-proportional increases in intracellular concentration. Nevertheless, these data indicate that low external concentrations of AS-ODN elicited dose-dependent antisense effects in PC12 cells which are approximately proportional to internal AS-ODN concentration (compare to Fig. 1). At higher concentrations, however, non-specific cellular effects may be result from extracellular effects of oligonucleotides and/or their degradation products.

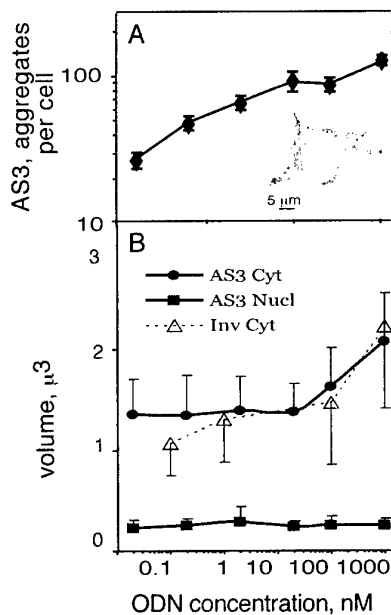


**Fig. 3. AS3 uptake and its effect on cell volume.**

A. Limited AS3 penetrance under increasing concentrations. Differentiated PC12 cells were incubated for 24 hrs with biotinylated AS3, treated with alkaline phosphatase-conjugated streptavidin, and subjected to Fast Red detection. Fast Red signals from 20 cells were quantified as in Fig. 1. Note that large changes in extracellular ODN concentrations result in relatively small changes in intracellular ODN concentration. Inset depicts a representative projection of a single PC12 cell incubated with 1  $\mu$ M ODN.

B. Cytoplasmic but not nuclear volume changes under increasing concentrations of AS3: Total cellular and nuclear volumes of AS-ODN-treated PC12 cells were determined using confocal microscopy as described in Methods. Note that cytoplasmic volume increased in a dose-dependent but sequence independent manner above 10 nM extracellular ODN, while nuclear volume remained

constant over the entire tested range of ODN concentrations

### **Excess AS-ODN mediates sequence-independent increases in cytoplasmic volume**

In search of mechanism(s) controlling the increased AChE gene activity observed at AS-ODN concentrations above 2 nM, we used the confocal microscope to measure cell volume. This analysis revealed >25% increases in cytoplasmic, but not nuclear, volume of PC12 cells exposed to AS-ODN over a range of 10-500 nM (Fig. 3B). The changes in cytoplasmic volume were sequence independent, as they were common to cells treated with either antisense or inverse AChE AS-ODNs. Sustained nuclear volume under these conditions attested to the fact that no apoptotic changes took place. Therefore, increased cytoplasmic volume in this effective range of ODN concentrations may include a host cell response to the extra-and/or intracellular presence of > 2 nM ODNs and/or their degradation products.

### **Discussion**

Several key responses of PC12 cells to the extracellular presence of oligonucleotides were noted when using a wide range of AS-ODN concentrations: 1. Above 50 pM and up to 20 nM AS-ODN, AChE activity was suppressed by up to 50%, with 2'-O-methyl-capped ODN displaying improved activity compared to phosphorothioate-modified oligos; 2. Above 50 nM AS-ODN, AChE activity was refractory to AS-ODN treatment and sequence-dependent increases in nuclear labeling suggestive of transcriptional activation of the target gene. 3. Above 10 nM AS-ODN, cytoplasmic volume increased by >25%, reflecting a sequence-independent host cell response.

### **Nanomolar doses of 2'-O-methyl AS-ODNs suffice to destroy their target mRNA**

AChE mRNA concentrations in differentiating PC12 cells were estimated to be 1-10 molecules per pL, or 1 to 10 pM, assuming approximately  $1 \times 10^8$  cells/ml and 10-100 molecules of a non-abundant target mRNA per cell. Assuming that each AS-ODN chain can inactivate many target molecules, the concentrations of AS1 and AS3 that were used in the present study should be sufficient to destroy all of the AChE mRNA molecules in treated cells, even in neurons, where AChE levels are highest (see Lev-Lehman et al., 2000; Li et al., 1991 for quantitative estimates of AChE mRNA amounts in various cell types). Reversal of the dose response curve at 50% inhibition therefore suggests that this represents the limit of blockade beyond which the AChE feedback loop is activated. 2'-O-methyl end-capped AS-ODN suppressed AChE activity in PC12 cells at 100-fold lower concentrations than the corresponding phosphorothioated ODN. Thus, 2'-O-methyl protection reduced the quantity of ODN needed to suppress AChE expression, in addition to preventing the cytotoxicity associated with phosphorothioate protection (Ehrlich et al., 1994).

### **Micromolar AS-ODN induces AChE mRNA accumulation**

In the micromolar range, sequence-dependent refractoriness to AS-ODN was observed. AS-ODN concentration-dependent decreases and increases in AChE mRNA and enzyme activity suggest that the inefficacy of high levels of oligonucleotide represents a cellular response triggered by changes in cellular AChE concentrations. Changes in AChE gene expression under antisense inhibition may be expected to include enhanced transcription, changes in specific splicing patterns, selective stabilization of certain mRNA transcripts or all of these combined. The intense nuclear labeling of AChE mRNA suggest enhanced transcription and/or nuclear stabilization of nascent transcripts under AS-ODN concentrations greater than 2nM. The cytoplasmic accumulation of AChE mRNA could reflect selective stabilization, similar to that observed in differentiating nerve and muscle (Luo et al., 1999) and hematopoietic cells (Chan et al., 1998). Diversion of default 3' alternative splicing patterns may also be involved, similar to the selective increases in unspliced AChE-R mRNA

observed under stress or exposure to AChE inhibitors (Kaufer et al., 1998). Disproportionate increases in AChE-R would account for the apparent discrepancy between full recovery of AChE activity above 100 nM AS-ODN and the only partial recovery of AChE-S mRNA (Fig. 1).

#### **ODNs may regulate cellular volume:**

In the picomolar-nanomolar range, AS-ODN induced the destruction of its target AChE mRNA. In the presence of increasing extracellular concentrations (>10 nM) of AS-ODN, confocal microscopy revealed sequence-independent changes in cytoplasmic volume. Reports on the cellular effects of low nucleotide concentrations point to the extracellular increase in nucleotide breakdown products of AS-ODNs, in particular increases in adenosine, as a likely cause for these changes (see Galietta et al., 1992, for example). Another important consideration refers to the extent of change in cytoplasmic volume. Because the cytoplasm is crowded with cytoskeletal elements, ribosomes and endoplasmic reticulum, a change of 25-50% may imply a considerably larger change in the volume of the liquid microenvironment where biochemical reactions regulating cellular physiology take place. This would be expected to impose metabolic disequilibrium and could initiate cellular stress responses. As AChE is proving to be a ubiquitous stress response element, this could contribute to the feedback response initiated by reduced intracellular AChE levels. These data therefore caution against the use of unnecessarily high concentrations of AS-ODN and suggest reevaluation of our concepts of the oligonucleotide concentrations previously believed to be physiologically relevant. This conclusion is particularly relevant in light of reported saturation of ODN uptake at concentrations as low as 160 nM (Nakai et al., 1996).

#### **In summary**

Our findings indicate that 2'-O-methyl-protected AChE AS-ODN effectively suppress AChE activity in cell types of different origins in the pM-nM range. These concentrations are much lower than those reported previously for AChE targeted AS-ODN and considerably lower than commonly used concentrations (50 nM-1  $\mu$ M) for AS-ODN targeted to various other mRNAs. Notably, increasing the extracellular AS-ODN above these levels neither elevated their intracellular concentrations proportionally, nor increased their ultimate effectiveness. In the yet higher  $\mu$ M range, the antisense strategy was relatively ineffective, apparently due to feedback activation of AChE gene activity. These findings may explain inconsistencies reported with numerous AS-ODNs. Furthermore, they call for *in vivo* experiments using similarly reduced concentrations of AS-ODNs. Recently, we have successfully utilized low doses of AS3 to suppress overexpressed AChE-R mRNA in brain of head-injured mice (Shohami et al., 2000) and in muscles of anticholinesterase-treated mice (Lev-Lehman et al., 2000) and rats with experimental myasthenia gravis (T. Brenner and H. Soreq, manuscript in preparation). The advantages of greatly reduced AS-ODN concentrations are many, including reduced side-effects, and increased cost-effectiveness.

### Synaptogenesis and myopathy under acetylcholinesterase overexpression (task 5)

Neuromuscular junctions (NMJ) are highly specialized, morphologically distinct, and well-characterized cholinergic synapses (Sanes and Lichtman, 1999). Chronic impairments in NMJ activity induce neuromuscular disorders characterized by deterioration of muscle structure and function. Thus, etiologically diverse insults interfering with acetylcholine-mediated neurotransmission cause a variety of “myasthenic” syndromes presenting muscle weakness and fatigue (Lindstrom, 1998; Donger et al., 1998; Engelhart et al., 1997; Schonbeck et al., 1990; Livneh et al., 1988). The molecular and cellular mechanisms leading from compromised NMJ activity to muscle wasting have not been elucidated. However, it is likely that physiological stress imposed on the nerve and/or muscle under conditions of NMJ dysfunction initiate changes in gene expression. Inhibitors of the acetylcholine-hydrolyzing enzyme, AChE, induce neuromuscular pathologies sharing features with the myasthenic syndromes. Among the delayed effects of anticholinesterase intoxication are degeneration of synaptic folds, terminal nerve branching, enlargement of motor endplates, and disorganization of muscle fibers (Laskowski et al., 1975; Kawabuchi et al., 1976). Cholinesterase inhibitors promoting myopathy include organophosphate poisons such as DFP and paraoxon (the toxic metabolite of the agricultural insecticide parathion), and carbamate drugs like pyridostigmine and neostigmine, used to treat myasthenia gravis (Evoli et al., 1996). The similarities between the neuromuscular impairments resulting from anticholinesterase exposure and that of pathophysiological NMJ dysfunction suggest overlapping and/or convergent pathways involving AChE.

RNA transcribed from the mammalian *ACHE* gene is subject to 3' alternative splicing yielding mRNAs encoding a “synaptic” (S) isoform, a “hematopoietic” (H) isoform, and the stress-related “readthrough” AChE-R derived from the 3'-unspliced transcript (Ben Aziz-Aloya et al., 1993; Massoulie et al., 1993). In addition to their hydrolytic activities, the various AChEs exert sequence-specific morphogenic effects on neurite outgrowth (Layer et al., 1995; Koenigsberger et al., 1997; Sharma et al., 1998; Grifman et al., 1998; Sternfeld et al., 1998) and NMJ structure (Shapira et al., 1994; Seidman et al., 1995). Transgenic mice overexpressing human AChE-S in spinal cord motoneurons displayed progressive neuromotor impairments that were associated with changes in NMJ ultrastructure (Andres et al., 1997, 1998). However, the molecular mechanisms mediating neuromuscular deterioration in these mice was unclear. Elevated intracellular calcium was previously implicated in anticholinesterase-mediated myopathologies (Laskowski et al., 1975). Electromyography (EMG) data revealed exaggerated post-synaptic responses in muscles of transgenic mice that indicated similarly enhanced calcium influx. In rodent brain, we found that both stress and cholinesterase inhibitors induce dramatic calcium-dependent overexpression of AChE-R (Kaufer et al., 1998). We therefore predicted that feedback overexpression of AChE-R would also occur in muscles of both anticholinesterase-treated control and NMJ-stressed AChE transgenic mice. Moreover, we expected that overexpressed AChE would have morphogenic implications for the nerves and/or muscles. To test these hypotheses, we examined AChE expression, motor endplate organization, neurite outgrowth, and muscle integrity in AChE-S transgenic mice and in normal mice treated with DFP with or without co-administration of antisense oligonucleotides to AChE mRNA. Our findings identify the AChE feedback loop as a molecular response common to both physiological NMJ stress and anticholinesterase exposure in muscle. Furthermore, they suggest that induced overexpression of AChE-R contributes to neuromuscular deterioration under diverse conditions leading to disease and demonstrate *in vivo* antisense blockade of the AChE feedback response to NMJ stress.

## Materials and Methods

**Animals and tissue preparations.** FVB/N mice, aged postnatal day (P) 0, 15, 30 and 4 months (M) were sacrificed and their tongues removed into liquid nitrogen for PCR and biochemical analyses. For *in situ* hybridization and silver staining, 2mm<sup>3</sup> cubes of tongue tissue were incubated in 3.7% formaldehyde overnight at room temperature and then paraffin embedded. Sections were cut (5µm) and placed on 3-aminopropyltriethoxysilane treated slides, dried at 37°C overnight and kept at 4°C until use. For cytochemistry, whole diaphragms were fixed for 1hr in 4% paraformaldehyde at 22°C, rinsed twice in phosphate buffered saline (PBS), and stained for catalytically active AChE activity as previously described (Andres et al., 1997).

**Chronic DFP treatment.** Mouse pups were housed with the dam in a light- and temperature-controlled room. Animals were injected subcutaneously once daily with either 1.0 mg/Kg DFP (Aldrich Chemical Co., Milwaukee, WI) dissolved in corn-oil or with corn oil alone during the first 2 postnatal weeks. To minimize central nervous system toxicity, pups were pretreated with 10 mg/Kg (i.p.) atropine sulfate (Sigma Chemical Co., St. Louis, MO) in saline 15 min before injection. At P15, about 4 h after the last injection, pups were sacrificed and their tongues removed.

**DFP/Antisense Experiments.** Adult FVB/N mice were coinjected (i.p.) once daily for 4 consecutive days with DFP alone or together with 5 µg/Kg of an antisense oligonucleotide (AS3; 3'CCA GCT TCT TTT ATA ACG TC) targeted to exon E2 in the mouse acetylcholinesterase gene. AS3 included 2'-O-methyl ribonucleotide substitutions at the three 3'-terminal positions to stabilize it against nucleolytic degradation.

**RT-PCR analysis.** RNA from tongue samples was extracted by RNA Clean (PeqLAB, Heidelberg, Germany) according to manufacturer's instructions. RT-PCR reactions were performed as previously described using a common upstream (+) primer and downstream (-) primers selective for each of the alternative AChE mRNA exons (Fig. 1A):

E3: 1361(+) {5'-CCGGGTCTATGCCTACATCTTTGAA-3'}

E6: 1844(-) {5' CACAGGTCTGAGCAGCGCTCCTGCTTG-CTA-3'}

E5: 240(-) {5'-AAGGAAGAAGAGGAGGGA-CAGGGCTAAG-3'}

I4: 74(-) {5'-TTGCCGCCTTGTGCATTCCT-3'}

To detect *c-Fos* mRNA we used the primer pair 1604(+)/2306(-) (Kaufer et al., 1998). PCR products sampled every third cycle from cycles 24-36 for the AChE and *c-Fos* mRNAs, and from cycles 18-24 for β-actin mRNA were electrophoresed on 1.5% agarose gels and stained with ethidium bromide.

**In situ hybridization.** 2'-O-methylated, 5'-biotinylated cRNA probes were used to selectively decorate alternative mouse (m) AChE mRNAs. Detection was with alkaline phosphatase-conjugated streptavidin and ELF (Molecular Probes).

mI4: (-79) 5'-

AACCCUUGCCGCCUUGUGCAUUCCUGCUCSCCCACUCCAUGCGCCUAC-3'(-29); mE6: (209) 5'-

CCCCUAGUGGGAGGAAGUCGGGGAGGAGUGGACAGGGCCUGGGGGCUCGG-3' (258); mE5: (-249) 5'-

GAGGAGGAAAAGGAAGAAGAGGAGGGACAGGGCUAAGUCCGGCCCCGGGC-3'(-200);

Paraffin embedded tongue sections were deparaffinized and dehydrated in a methanol/PBT (PBS, 0.1% Tween-20) series. Hybridization included preclearing in H<sub>2</sub>O<sub>2</sub> (6% in PBT, 30 min), proteinase treatment, glycine wash and refixation (4% paraformaldehyde, 20 min), all essentially as described elsewhere (Kaufer et al., 1998; Grisaru et al., 1999) except that 1%

SDS was added to the hybridization buffer and to solution 1 and 0.1% Tween-20 was added to solution 2.

**Neurites silver stain:** Paraffin embedded tongue muscle sections were stained for neuronal fibers basically according to Gros-Bielschowsky using silver nitrate (20%, 60 min at 37°C), distilled water washes and incubation in ammonium hydroxide-silver nitrate solution (60 min). Color was developed for 24 to 36 h. For fixation, slides were dipped in sodium thiosulfate (2 sec), washed in water and dehydrated.

## Results

**Chronic cholinesterase blockade and transgenic overexpression of synaptic neuronal AChE promote elevated *c-Fos* and *readthrough* AChE mRNAs in muscle.** Both acute stress and cholinesterase inhibitors were shown to trigger overexpression of AChE-R in rodent brain via a *c-fos*-mediated pathway (Kaufer et al., 1998). To investigate whether the AChE feedback loop is active in muscle, we performed reverse-transcription (RT) PCR on mRNA extracted from tongue of two-week-old (P15) mice injected daily, from birth, with 1 mg/kg DFP. This dose of DFP blocked approximately 80% of muscle AChE activity, but did not elicit overt symptoms of cholinergic poisoning. In parallel, RT-PCR was performed on tongue RNA from transgenic mice overexpressing AChE-S in spinal cord motoneurons. Semi-quantitative analyses performed with primers detecting mouse mRNAs encoding either *c-fos* or AChE-R revealed over 2-fold elevated levels of both transcripts following either chronic inhibition or congenital overexpression of AChE (Fig. 1). In contrast, neither endogenous AChE-S- nor AChE-H- mRNA levels were detectably affected by either DFP or transgenic AChE (Fig. 1 and data not shown).  $\beta$ -actin mRNA displayed similar levels among all groups, indicating equal starting amounts of RNA in all reactions (Fig. 1). These data demonstrated that both chronic overproduction and acute blockade of AChE catalytic activity stimulate selective *de novo* synthesis of AChE-R in muscle.

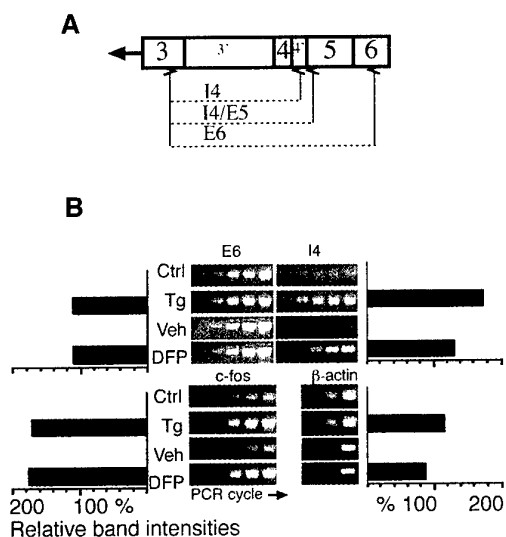


**Fig. 1. Transgenic AChE-S and DFP similarly induce enhanced *c-fos* and AChE-R mRNA production in muscle.**

**A. The mouse AChE gene and alternative splicing products.** Presented is a schematic illustration of coding exons 3, 4, 5 and 6 (shaded boxes) and intron 3 to 4 (white boxes) in the mouse AChE gene. The “synaptic” AChE-S mRNA transcript (E6) results from splicing of exon 4 to 6; the “hematopoietic” AChE-H mRNA transcript (E5) from splicing of exon 4 to 5; *Readthrough* AChE-R mRNA retains intron I4 in a mature unspliced transcript. Arrowheads indicate PCR primer pairs detecting the individual mRNA transcripts.

**B. RT-PCR analyses.** RT-PCR was performed using primers specific for the various alternative AChE mRNAs (Materials and Methods). Presented are PCR products of AChE mRNA derived from tongue muscle of control (Ctrl) or AChE transgenic (Tg) newborn mice or from control mice treated for 2 weeks with either DFP or vehicle (Veh). Note the increased levels of both endogenous mouse and *c-fos* mRNAs in transgenic vs. control mice and in control mice injected with DFP. Neither endogenous AChE-S or the unrelated  $\beta$ -actin mRNAs responded to either transgenic AChE

overexpression or AChE inhibition. Displayed are PCR reactions sampled every third cycle from cycle 24 for AChE and *c-fos*, and from cycle 18 for  $\beta$ -actin. One of 4 experiments for each mRNA, using different RNA preparations is presented. Bar graph represents the relative band intensity for each mRNA in the presented PCR images as determined by densitometric analysis. Quantification was performed at cycle 33 for AChE and *c-fos* mRNAs and at cycle 24 for  $\beta$ -actin mRNA, within the exponential phase of product accumulation.

**Readthrough AChE mRNA accumulates in both muscle and epithelium under cholinesterase blockade and transgenic AChE overexpression.** To determine the localization of induced AChE-R mRNA in tongue, we employed high resolution, fluorescent *in situ* hybridization. Fluorescent hybridization signals obtained using an AChE-S mRNA-specific probe exhibited similar moderate intensities and bandwidth in epithelium of newborn transgenic and control mice (Fig. 2a,b). AChE-H mRNA was also detected at low levels in the epithelium of both control and transgenic mice (not shown). AChE-R mRNA was barely detectable in sections from control mice, consistent with the PCR data. In contrast, pronounced expression of AChE-R mRNA was observed in tongue epithelium of newborn transgenic mice (Fig. 2c,d). With DFP, no significant differences were observed in the expression of AChE-S mRNA in treated- versus vehicle-injected mice (Fig. 2e,f). However, fifteen-day-old DFP-treated, but not their littermate controls, exhibited high levels of AChE-R mRNA across the entire width of the tongue epithelium, extending into the muscle (Fig. 2g,h). In general, hybridization with the AChE-S mRNA probe gave moderate and somewhat punctuated staining, consistent with the localization of this message around junctional nuclei (Jasmin et al., 1993). In contrast, staining with the AChE-R mRNA-specific probe yielded a more diffuse staining pattern, especially following DFP treatment, suggesting extrajunctional synthesis. These data demonstrated that both transgenic overexpression and inhibitor-mediated blockade of AChE promote a specific induction of AChE-R mRNA that takes place in both muscle and epithelium.

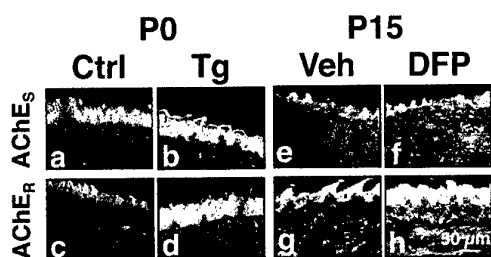


**Fig. 2. Overexpressed transgenic AChE-S and DFP induce accumulation of endogenous AChE-R mRNA in both epithelium and muscle.**

*In situ* hybridization was performed on 7  $\mu$ m sections of tongue from newborn (P0) control (a,c) and AChE transgenic (b,d) mice, or 15-day-old (P15) control mice injected with either vehicle (e,g) or the AChE inhibitor DFP (f,h). Note

enhanced and delocalized fluorescent labeling of AChE-R but not AChE-S mRNA in epithelial cells and muscle fibers from both transgenic and DFP-treated mice as compared to controls.

**Transgenic mice display delocalized overexpression of catalytically active AChE in muscle.** High-salt/detergent extracts of tongue revealed a developmental increase in AChE enzyme activity in control mice ( $12 \pm 2$  nmol substrate hydrolyzed/min/mg protein at P7 versus  $24 \pm 4$  at P15;  $n=8$ ). Two-fold increased levels of catalytically active AChE were observed in tongue homogenates from transgenic over control mice at P7, but only 25% at P15. These findings suggested that adjustments in the feedback response take place over time and/or during development. To localize overexpressed AChE in the tongue, we performed cytohistochemical staining for AChE on sections from one-month-old control and transgenic mice. In control mice, activity staining was pale except for intense, highly localized staining

observed at motor endplates (Fig. 3A,B). In contrast, transgenic mice displayed overall darker staining of the muscle layers, particularly near the submucosal epithelium (Fig. 3C). In transgenic mice, intense staining was observed along muscle fibers, not restricted to endplate regions (Fig. 3D). This staining pattern was reminiscent of AChE-S overexpressed in myotomes of microinjected *Xenopus* embryos (Seidman et al., 1995). The relative contributions of endogenous AChE-R and transgenic AChE-S isoforms to this overexpression pattern were not discernable in this experiment. Nevertheless, AChE-R mRNA displayed pronounced overexpression in epithelium of transgenic mice that contrasted with the accumulation of catalytically active protein that was primarily limited to muscle.

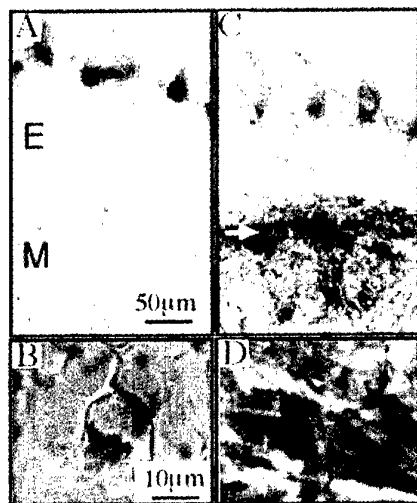


**Fig. 3. AChE-Transgenic mice display pronounced non-junctional enzyme activity in muscle.**

Tongue sections from one-month-old control and transgenic mice were stained for catalytically active AChE. At low magnification, diffuse, light staining of both epithelium (E) and muscle (M) layers was observed in sections from control mice (A). Higher magnification revealed strong AChE activity localized to motor endplates (B). In sections from transgenic mice, minimal levels of AChE are visible in the epithelium (C), while intense staining is evident in the muscle layer, widely distributed along muscle fibers (C, arrow; D).

**Cholinesterase inhibition and overexpressed AChE cause similar muscle pathologies.** We previously reported aberrant NMJ ultrastructure and progressive neuromotor dysfunction among adult AChE transgenic mice. We hypothesized that induced AChE-R contributes to this neuromuscular deterioration. In that case, DFP, as an instigator of the AChE feedback loop would be expected to elicit parallel myopathologies. To determine if the ability of cholinesterase inhibition to promote deterioration of muscle is correlated with overexpressed AChE-R, we studied the gross morphological features of tongue muscle. Muscle fibers from 15-day-old untreated control mice were organized in a linear fashion within parallel bundles. In contrast, muscle fibers from both DFP-treated FVB/N mice and AChE-transgenic mice displayed chaotic disorder (Fig. 4). At higher magnification, severely atrophic, vacuolated muscles could be observed in both experimental systems. Despite these muscle malformations, transgenic pups suckled normally and displayed normal growth in their first weeks, suggesting a fairly large safety margin for non-strenuous muscle activity.

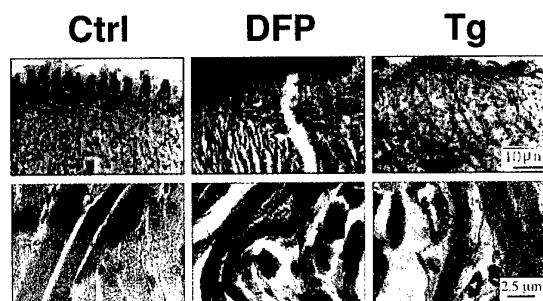


**Fig. 4. Transgenic and DFP-induced AChE excesses associated with muscle pathologies.**

Tongue muscle from P15 untreated control (Ctrl), chronic-DFP-treated control (DFP), or untreated AChE transgenic (Tg) mice was stained with hematoxyllin-eosin and evaluated for gross morphological features. Muscle tissue of control mice displayed a high degree of organization, with fibers closely aligned in regular parallel arrays. In control mice injected

with DFP, muscle fibers were disorganized and severely atrophic. In transgenic mice, muscle fibers were also disorganized and severely atrophic, similar to the DFP-treated control mice.

daily with DFP, and in untreated transgenic mice, the corresponding tissues appeared distorted, with apparently atrophic, disorganized muscle fibers. Upper panels present low magnification photomicrographs that include epithelial and muscle layers. Lower panels display high magnification of the muscle layer alone.

**Both transgenic and anti-AChE insults cause excessive muscle reinnervation.** Neurite-growth promoting activities have been demonstrated for AChE *in vitro*. We therefore hypothesized that overexpressed AChE may exert morphogenic activities on motoneurons. To test this hypothesis, we used Bielschovsky-based silver staining to characterize the distribution of motor axons in tongue muscle from DFP-treated FVB/N and untreated AChE transgenic mice as compared to untreated control mice. Large bundles of neurites (Fig. 5A) were observed in muscles of all three groups in similar numbers, suggesting similar primary nerve input to the tongue in all mice. However, both DFP-injected and AChE transgenic mice displayed 2-fold increases in the number of small (<200  $\mu\text{m}^2$ ), apparently unbundled neurites as compared to both untreated and vehicle-injected controls (Fig. 5B,C). These results indicated axon branching in AChE-R overexpressing muscles, and hinted at a process of denervation-reinnervation in muscles of both DFP-treated and AChE transgenic mice.

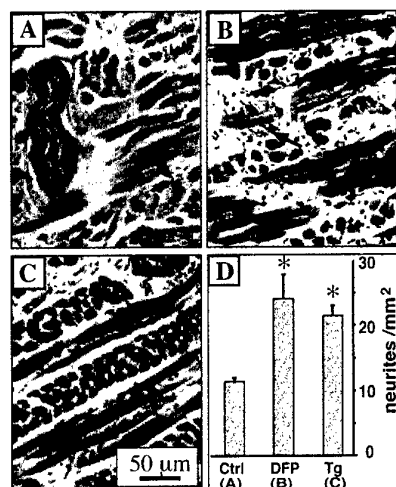


**Fig. 5. Both transgenic AChE and DFP induce neurite sprouting.**

Silver-stained tongue-muscle neurites are shown in parallel sections from (A) 15-day-old control, (B) DFP-injected control, and (C) AChE transgenic mice. Both DFP-treated and transgenic mice displayed numerous small (<200  $\mu\text{m}^2$ ) bundles of neurites as compared with untreated controls (black arrows). Shown are representative photomicrographs in an equivalent location beneath the tongue epithelium. White arrow indicates a representative large (>1000  $\mu\text{m}^2$ ) neurite bundle observed in all groups in similar numbers. Sections from vehicle-injected animals were indistinguishable from untreated controls (not shown). Bar graph represents number of small neurites per  $\text{mm}^2$

(average  $\pm$  SEM) for at least 3 animals from each group. Asterisk indicates statistically significant difference compared to control ( $p < 0.05$ , ANOVA)

**Elevated AChE induces antisense-blocked expansion of motor endplate fields.** The observed increase in small, silver-stained neurites in transgenic and DFP-treated mice suggested that cholinergic insults may be associated with reinnervation processes and the formation of new endplates. To examine this possibility, we counted motor endplates in intact diaphragms from adult control and transgenic mice, and from control mice one month following a course of four daily i.p. injections of DFP (1 mg/kg). In diaphragms from DFP-treated mice, we observed a 2-fold increase over controls in the average number of endplates per  $\text{mm}^2$  as measured along the length of the innervating nerve ( $16.14 \pm 2.44$  vs.  $8.52 \pm 2.42$  ( $\pm$  SEM)) (Fig. 6A,B). In diaphragms from transgenic mice, we observed a 50% increase in the density of motor endplates compared to controls ( $12.61 \pm 0.49$  NMJs/ $\text{mm}^2$ ) (Fig. 6C). Overall, these endplates appeared smaller than endplates from control mice. However, in addition to the many small endplates, we often observed abnormal, elongated endplates in muscles from both DFP-treated and transgenic mice. Two weeks after treatment with DFP, muscles from FVB/N mice displayed AChE activity that was elevated approximately two-fold

above controls ( $10.2 \pm 2.3$  vs.  $6.1 \pm 2.1$  nanomoles substrate hydrolyzed/min/mg tissue;  $N \geq 6$ ). However, co-administration of as little as  $80 \mu\text{g/Kg}$  of a 3'-end-capped, 2'-O-methyl antisense oligonucleotide antisense against AChE (Grisaru et al., 1999) prevented accumulation of catalytically active enzyme by 60% and largely suppressed DFP-induced increases in the number of diaphragm motor endplates Fig. 6D). AS3 alone reduced NMJ densities to values well below those measured in control muscles without dramatically altering AChE activity. Together with data indicating a relative sensitivity of AChE-R mRNA over AChE-S mRNA to AS3-mediated destruction (Grisaru et al., 1999 and manuscript in preparation), these observations suggest that AChE-R represents a minor but physiologically significant component of total muscle AChE in control untreated animals.

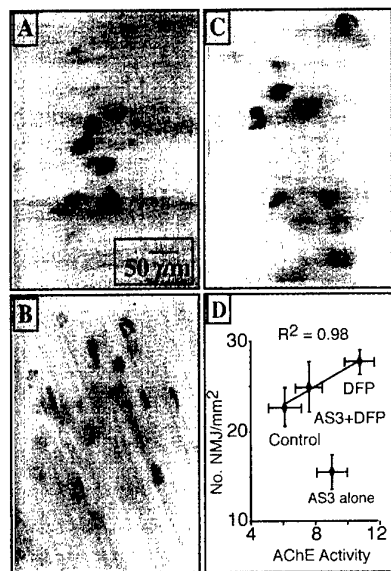


**Fig. 6. Transgenic AChE and DFP promote proliferation of motor endplates.**

Diaphragm motor endplates from 4 month-old control mice (A), control mice one month following repeated treatment with DFP (B) and AChE-transgenic mice (C) were visualized by staining for catalytically active AChE. Both DFP-treated control mice and AChE-transgenic mice displayed an increased number of small synapses as compared to controls. (D) Graph represents the number of synapses (average  $\pm$  SEM;  $n \geq 3$ ) per  $\text{mm}^2$  tissue as a function of AChE catalytic activity (average  $\pm$  SEM;  $n \geq 6$ ) as determined in high salt/detergent extracts by the acetylthiocholine colorimetric assay (Seidman et al., 1995). AChE activity is expressed as nanomoles acetylthiocholine hydrolyzed/min/mg tissue. Note that the NMJ/activity ratio in diaphragms from AS3 treated control mice deviates significantly from that expected given the correlation

established in the DFP+AS3 paradigm.

### Discussion

We observed common molecular and cellular responses in mouse muscle to transgenic overexpression of neuronal AChE and to chronic administration of the potent AChE inhibitor DFP. On the surface, the convergent outcome of these two experimental manipulations appears paradoxical. DFP imposes a rapid, irreversible blockade of the acetylcholine-hydrolyzing activity of AChE, leading to acetylcholine excess and cholinergic excitation (Taylor, 1995; Friedman et al., 1996). In contrast, transgenic overexpression of AChE in motoneurons is predicted to locally elevate acetylcholine-hydrolyzing activity at the NMJ, presumably resulting in an acetylcholine deficit and cholinergic hypoactivity. Yet, in both cases, we observed elevated levels of *c-fos* and AChE-R mRNAs associated with changes in the number and structure of motor endplates, branching of motor axons, and severe myopathologies. These findings suggest that both gain- and loss- of synaptic activity impose a physiological stress on the muscle that is translated into changes in gene expression having long-term implications for neuromuscular function. In transgenic mice, abnormally intense electrophysiological activity suggested that long-term adaptation to overexpressed synaptic AChE promotes enhanced cholinergic activity at some sites (Andres et al., 1997 and unpublished data). In that case, even normal neuromotor activity would elicit cholinergic hyperexcitation and induce expression of AChE-R in muscles of transgenic mice. Nevertheless, AChE overexpression following either stress or anticholinesterase intoxication

carries dire implications for neuromuscular structure and function *in vivo*. These findings in muscle parallel the overexpression of AChE-R observed in rodent brain under stress and anticholinesterase exposure. The profound impact of AChE-R overexpression on the structure and organization of NMJs, advances the notion that overexpressed AChE-R in the central nervous system plays a role in the delayed psychopathologies associated with trauma or anticholinesterase intoxication (Reviewed by Kaufer et al., 1999). It is noteworthy that transgenic mice overexpressing very high levels of AChE-R (Sternfeld et al., 1998) display dramatic 4-fold elevated NMJ densities (unpublished observation).

Until recently, the low-level basal expression of AChE-R precluded characterization of this protein from natural sources. Nonetheless, heterologous expression studies demonstrated AChE-R to be a soluble, secreted, non-synaptic, catalytically active form of the enzyme (Seidman et al., 1995). In microinjected *Xenopus* embryos, expression of AChE-R was restricted to secretory epidermal cells. This is consistent with our observations of induced AChE-R mRNA in tongue epithelium. However, the absence of significant AChE activity in the tongue epithelium suggests that excess AChE-R is excreted from, rather than retained within, this tissue as well. Normally, the accumulation of AChE in mature NMJs is accomplished by focal transcription at subjunctional nuclei combined with restrictions on diffusion of AChE mRNA or protein to non-junctional sites (Jasmin et al., 1993). The diffuse localization of overexpressed AChE-R mRNA and of AChE enzyme in transgenic and DFP treated muscle is consistent with a non-junctional disposition for this enzyme. Moreover, it suggests that transcription of AChE mRNA is activated following DFP in otherwise "quiescent" non-junctional nuclei. Nevertheless, the extent of overexpressed AChE in transgenic mice displayed a downward trend during post-natal development. Our current findings indicate adjustments of the AChE feedback loop and would explain our previous detection of only slightly elevated AChE activity in muscles of adult transgenic mice (Andres et al., 1997).

Increased numbers of small neurites were associated with increased numbers of small, immature endplates in diaphragms of DFP and transgenic mice. This suggests that NMJ stress stimulates compensatory mechanisms designed to increase the number of functional synapses. Intraperitoneal injections of antisense oligonucleotides to AChE mRNA ameliorated both induced AChE overexpression and motor endplate expansion. Since oligonucleotides are not known to cross the blood-brain-barrier unassisted (Seidman et al., 1999), the observation that systemic administration of AS3 effectively blocked DFP-promoted synaptogenesis indicates a prominent role for muscle-derived AChE-R in this phenomenon. Neurite growth promoting functions attributed to the synaptic AChE-S variant were shown to be independent of catalytic activity (Sternfeld et al., 1998). In the current study, repeated DFP treatments were associated with elevated levels of AChE-R mRNA and enhanced neurite branching even though *de novo* synthesized enzyme would be rapidly inactivated by residual inhibitor. This is compatible with the idea that catalytically inactive AChE-R exerts morphogenetic activities on mammalian motoneurons. Moreover, recent studies in our laboratory demonstrate long-term (at least 1 month) overproduction of AChE-R in brain following exposure to DFP (Friedman et al, in preparation). This could help explain the devastating myopathic effects of even a single exposure to this agent (Taylor, 1996). As DFP promotes overexpression of AChE in central neurons, the signal driving changes in neurite structure could originate from either the muscle or the motoneurons themselves. Similarly, the effects of DFP on muscle may reflect its status as a target tissue of neurons overexpressing AChE-R. This latter possibility suggests

further studies into the potential effects of overexpressed neuronal AChE on other target tissues such as adrenal gland and intestine.

A massive and transitory increase in *c-fos* mRNA and Fos protein was reported to occur in rats intoxicated by a single dose of Soman, a highly toxic irreversible inhibitor of cholinesterase (Chollat et al., 1993). In our study, both DFP and transgenic AChE promoted elevated levels of *c-fos* mRNA in muscle. Upregulation of this nuclear transcription factor could be due to muscle necrosis and cell death since chronic elevation of Fos usually accompanies cell injury or apoptosis (Slotkin et al., 1997). However, induction of *c-Fos* was also reported to follow nerve growth factor administration in cholinergic neurons of the adult rat basal forebrain (Gibbs et al., 1997). Therefore, elevated *c-fos* mRNA in transgenic and DFP-treated mouse muscle could reflect regeneration processes. In brain, calcium-dependent elevations in *c-fos* mRNA were spatio-temporally correlated with elevated levels of AChE-R mRNA. This suggests that AChE-R represents a downstream, stress responsive element in the nervous system. The sequence homology (de la Escalera et al., 1990; Ichtchenko et al., 1995) and functional redundancy (Darboux et al., 1996; Grifman et al., 1998) between AChE and neuronal cell-cell interaction proteins with protruding intracellular domains such as neurotactin and neuroligin suggest a role for AChE in cell adhesion. In that case, stress responsive AChE-R could play a role in the neuronal remodeling that follows various stress insults. The core domain of AChE is likely to mediate the enzyme's non-catalytic functions, perhaps by regulating ligand-binding interactions between its homologous cell surface proteins and their natural binding partners (i.e. neurexins). Nevertheless, isoform-specific influences of AChE on cellular morphogenesis implies important, but yet undefined roles for the various alternative C-terminal peptides.

Cholinesterase inhibitors are routinely employed to treat various neurological disorders associated with cholinergic deficits. For example, the fluctuating muscle weakness suffered by individuals afflicted with myasthenia gravis is treated with chronic administration of neostigmine. Nevertheless, neostigmine has long been known to promote ultrastructural abnormalities of the post-synaptic NMJ membrane, terminal nerve branching, and myopathologies in normal rats (Engel et al., 1973; Hudson et al., 1978). For these reasons, it was suggested that anticholinesterase therapy may actually contribute to the progressive deterioration of muscle function in myasthenia gravis (Swash, 1975). Our current findings suggest that adverse responses to neostigmine might be mediated by feedback responses to AChE inhibition and consequent accumulation of AChE-R in muscle. Thus, our data point to feedback overexpression of AChE-R as a mechanism translating diverse physiological NMJ stresses into long-term neuromuscular pathologies. They therefore raise serious concern about excessive use of anticholinesterases for management of non-crisis medical situations. Perhaps it is not surprising, therefore, that muscle weakness is prominent among the complaints of Gulf War veterans having received 90 mg per day pyridostigmine as a prophylactic guard against anticipated exposure to chemical weapons (Haley et al., 1997). Thus, the indications that anticholinesterase drugs initiate potentially devastating feedback responses in mammalian muscle carries profound health implications for the relatively large group of individuals currently receiving, or targeted for, various anticholinesterase therapeutics. For example, the only drugs currently approved for Alzheimer's disease are potent AChE inhibitors. The efficient *in vivo* suppression of AChE overexpression achieved here with extremely low doses of antisense oligonucleotides to AChEmRNA suggests that antisense therapeutics may offer a viable alternative approach to conventional anticholinesterase therapy in the nervous system.

## Acetylcholinesterase monomer interactions with the anxiety-associated neuronal complexes of PKC $\beta$ II with RACK1

Physiological stress induces rapid, robust signaling processes in mammalian brain neurons. These suppress long term potentiation (LTP, Vereker *et al.*, 2000), augment long term depression (LTD, Xu *et al.*, 1997) and induce release of synaptic vesicles, potentiating neurotransmission (Stevens and Sullivan, 1998). At the longer term, stress-induced signaling attenuates the stress response, enabling the organism to be less excessively affected by a stressful event. This induces neuronal dendrite branching (Sousa *et al.*, 2000) and synapse re-organization (McEwen, 1999). However, the molecular pathway(s) leading from short - to long - term processes and which enable the adjustment to stressful stimuli, are not yet known.

Ample information suggests the involvement of specific protein kinases in at least some of these stress-induced processes. The enzymatic activity of certain subtypes of protein kinase C (PKC, Coussens *et al.*, 1986) was shown to be subject to changes (i.e. biochemical activation, membrane translocation) under physiological (Hu *et al.*, 1987; Wang and Feng, 1992), biochemical (Macek *et al.*, 1998) and cytoarchitectural (Tint *et al.*, 1992) responses at the cellular and organismal levels. A relevant mediator of the stress-related changes in PKC activities is likely to be largely absent from brain neurons under normal conditions, but should be induced rapidly and for long periods following stress insults. The putative mediator should further be intracellular in its location and capable of activating or translocating active PKC within neuronal perikarya. The “readthrough” acetylcholinesterase variant AChE-R is a promising candidate for this role (reviewed by Soreq and Seidman, 2001). Brain AChE-R is exceedingly rare in the adult, non-stressed brain. Various stress insults induce AChE-R overproduction through alternative splicing, creating a different C-terminal domain from that of synaptic AChE-S. AChE-R levels rise rapidly under acute psychological stress (Kaufer *et al.*, 1998) or chemical neurotoxication (Shapira *et al.*, 2000) and stay higher for over two weeks following head injury (Shohami *et al.*, 2000). Being a secretory protein AChE-R fulfills the extracellular function of reducing the stress-induced acetylcholine levels. In addition, however, it accumulates in neuronal cell bodies (Sternfeld *et al.*, 2000), where acetylcholine hydrolysis is unlikely. Transgenic mice overexpressing neuronal AChE-R, but not the normally abundant synaptic variant AChE-S, display reduced levels of stress-associated neuropathologies (Sternfeld *et al.*, 2000). This suggests for the AChE-R protein distinct stress-related function(s). Intriguingly, the unique C-terminal domain of AChE-R does not participate in acetylcholine hydrolysis for which the core domain, common to all of the AChE variants is sufficient (Duval *et al.*, 1992). Altogether, these findings made this C-terminal domain of AChE-R an attractive candidate for non-biased screening for potential protein partners that could be instrumental for stress-induced processes.

Of the many subtypes of PKC, PKC $\beta$ II appears more directly relevant than others to physiological stress responses. PKC $\beta$ II undergoes specific activation and membrane translocation under ischemia (Cardell and Wieloch, 1993). Its genomic disruption causes loss of learning faculties and induces deficits in both cued and conditional fear conditioning (Weeber *et al.*, 2000). Intracellularly stored PKC $\beta$ II molecules are translocated to those neuronal perikaryon sites where they function with the aid of RACK1, the intracellular receptor for activated protein kinase C (Ron *et al.*, 1999). RACK1 interacts with activated PKC $\beta$ II and facilitates its subcellular movement under exposure to phorbol ester, dopamine  $\beta_2$  agonists or ethanol (Ron *et al.*, 1999; Ron *et al.*, 2000). Some, although not all reports indicate RACK1 deficits in the brain of Alzheimer’s disease patients (Battaini *et al.*, 1999),

where phosphorylation impairments are a distinct feature of the disease phenotype (Buee *et al.*, 2000). However, RACK1, like PKC $\beta$ II, is ubiquitously present in numerous cell types, which makes it unlikely to be the primary inducer of PKC $\beta$ II-mediated stress related cascades. Using a yeast 2-hybrid screen, we discovered that the C-terminal domain of AChE-R forms tight, co-immunoprecipitable triple complexes with RACK1 and PKC $\beta$ II. Moreover, AChE-R interaction activates PKC $\beta$ II and facilitate its translocation into densely packed neuronal clusters that may be causally involved with the stress-protection capacity of overexpressed AChE-R.

### Materials and Methods

**Vectors employed.** A fragment of human AChE-R cDNA, nt 1796-1865 of hAChE, accession no. M55040, followed by nt 1-111 from the genomic hAChE I4-E5 domain (accession no. S71129, stop codon in position 86), was used as "bait" for the two-hybrid screen. Cloning into the *EcoRI/SmaI* sites of pGBK-T7 (Clontech, Palo Alto, CA), yielding the plasmid pGBK-ARP1. Cloning of the "bait" sequence into the *Bsp120I/XbaI* sites of pEGFP-C2 (Clontech) yielded the pGARP vector. The AChE-R expressing plasmid used for transfections has been described in detail (Seidman *et al.*, 1995).

**Two hybrid screening.** The "bait" *EcoRI/HpaI* fragment of AChE-R cDNA encodes the 51 amino acid long C-terminal fragment of AChE-R fused to the DNA-binding domain (BD) (amino acids 1-147) of the yeast GAL4 transcriptional activator. An amplified and CsCl gradient-purified human fetal brain cDNA library cloned into the AD vector (Chien *et al.*, 1991) encodes for a fusion protein with the yeast GAL4 activation domain AD, (amino acids 768-881). The AH109 yeast strain (Clontech) was sequentially transformed with the pGBK-ARP1 plasmid, and with 10-25  $\mu$ g of the library DNA, using the Yeastmaker transformation system (Clontech). A total number of 240,000 independent clones were screened.

**Recombinant RACK1 preparation.** A plasmid overexpressing MBP-RACK1 in *E. coli* pDEM31, a derivative of pMAL-c2 (New England Biolabs, Beverly, MA) (Rodriguez *et al.*, 1999), was a kind gift from Dr. Daria Mochly-Rosen, Stanford University. The pDEM31 vector expresses in *E. coli* recombinant RACK1 fused to the maltose binding protein, which was purified on an amylose affinity column (New England Biolabs). The 36 kDa RACK1 protein was released by proteolysis with factor Xa (New England Biolabs).

**Cell cultures and transfection experiments.** PC12 cells were transiently transfected with the plasmid encoding AChE-R, using Lipofectamine Plus (Life Technologies, Paisley, UK). Cells were lysed 24 h following transfection in lysis buffer (0.1 M phosphate buffer pH 7.4, 1% Triton X-100, and Complete mini protease inhibitor cocktail, Roche, Mannheim, Germany). Cell debris was removed by centrifugation at 12,000 x g for 10 min.

**Overlay assay.** Protein samples containing recombinant RACK1 were separated by SDS-PAGE. Following blotting, the nitrocellulose membrane was incubated in a blocking solution (3% non fat dried milk, 2% BSA, 0.2% Tween-20 in Tris buffered saline, TBS, 0.1 M Tris pH 7.4, 1.7 M NaCl) for 1 h. Overlay was in 6 ml of 1:20 diluted clear supernatant from homogenates of PC12 cells expressing either human AChE-R (Grifman *et al.*, 1998). The final protein concentration was 2mg/mL, in 50 mM Tris-HCl, pH 7.5, 0.2 M NaCl, 0.1% BSA, 0.1% polyethylene glycol (PEG), 12 mM  $\beta$ -mercaptoethanol and Complete mini-protease inhibitors cocktail (Roche), in a final concentration of 0.05% Triton X-100. Following incubation (1h, room temp.), unbound material was removed by 3 brief washes and

three 5 min washes in 0.05% Tween-20 in TBS. Following fixation with 4% paraformaldehyde (30 min, at 4°C), bound AChE was detected using goat polyclonal antibodies targeted to the N-terminal domain of hAChE (Cat. No. sc-6431, Santa Cruz Biotechnology, Santa Cruz, CA; dilution 1:500).

**Coimmunoprecipitation.** Clear supernatants of PC12 or COS cell homogenates (200 µL, 1.5 mg protein/mL) were prepared by manual homogenization, followed by 30 min centrifugation at 12,000 x g, 4 °C. Supernatants were diluted 5-fold with NET buffer (50 mM Tris-HCl, pH 7.4, 150 mM NaCl, 1 mM EDTA, 0.25% gelatin and Complete mini protease inhibitors cocktail, Roche), in a final concentration of 0.05% Triton X-100). Goat polyclonal antibodies (Santa Cruz) targeted to the N-terminal domain of hAChE (10 µL, 200 µg/mL) were added for overnight rotation at 4°C. 75 µL of Protein G MicroBeads (Miltenyi Biotec, Bergisch Galdbach, Germany) was added and incubation continued for another h. Mixtures were loaded on MACS magnetic separation columns (Miltenyi Biotec), washed 3 times with 200 µL of TBS buffer containing 0.05% Tween-20 and eluted with gel loading buffer. Elutes were separated by sodium dodecyl sulfate polyacrylamide gel electrophoresis (Bio-Rad, Hercules, CA), blotted and incubated with the noted detection antibodies. For immunoprecipitation, dissected mouse brain regions were homogenized in nine volumes of the lysis buffer. Homogenates were passed several times through a 21G needle. Insoluble debris was removed by a 30 min 12,000 x g centrifugation. Homogenates were kept frozen at -70°C until use.

**PKC activity** PKC activity was measured using a PKC assay kit (Upstate Biotechnology, Lake Placid, NY) according to the kit instructions. Radioactivity resulting from [ $\gamma$ <sup>32</sup>P]ATP phosphorylation of a specific substrate peptide (QKRPSQRSKYL), was evaluated by incubating PKC (Calbiochem, San Diego, CA) in 20 mM MOPS (pH 7.2), 25 mM  $\beta$ -glycerol phosphate, 1 mM sodium orthovanadate, 1mM DTT, 1mM CaCl<sub>2</sub>, 10 mM MgCl, 100 µM ATP/[ $\gamma$ <sup>32</sup>P]ATP in the presence or absence of 1 µg recombinant AChE-S (Sigma, Rehovot, Israel) and/or 1 µg RACK1. BSA was added to supplement the final protein concentration in all reactions to 0.1 mg/ml. Reactions were performed in the presence or absence of lipid activators (0.1 mg/ml phosphatidyl serine, 0.01 mg/ml diacylglycerol). Following a 10 min incubation at 30°C, reaction was started by substrate addition additional for 10 min incubation at 30°C. Aliquots of the reaction mixtures were then spotted on P81 phosphocellulose paper washed three times with 0.75% phosphoric acid and once with acetone, and counted by Cherenkov method in a scintillation counter (Beckman, Fullerton, CA). Background phosphorylation was determined in a reaction carried out without lipid activators in the presence of 10 mM EGTA, this value was subtracted from all data.

PKC activity in brain homogenates (100 µg total protein) of transgenic and control mice was measured as detailed above, with the addition of PKA/CaMK inhibitor cocktail supplied with the kit.

**Laboratory Animals and Stress Experiments.** Male 6-8 weeks old FVB/N mice were subjected to saline injection (0.2 ml, intraperitoneal) which induces mild psychological stress in this stress-sensitive strain. Stressed mice, control and AChE-R transgenic mice (Sternfeld *et al.*, 2000) were sacrificed 24 h post-injection. To prepare brain sections, four mice from each line were deeply anesthetized with Pental (pentobarbitone sodium 200mg/ml, CTS Chemical industries, Petah Tikva, Israel) at a dose of 100 mg/Kg and transcardially perfused with 4% (v/v) paraformaldehyde. Brains were post-fixed by immersion in 4% (v/v) paraformaldehyde (overnight, 2-8°C) and incubated in 12% (vol/vol) sucrose in 0.1M phosphate buffered saline (PBS). Coronal cryostat sections (30 µm) were floated in PBS and

kept at  $-20^{\circ}\text{C}$  in 40% (v/v) ethylene glycol and 1% polyvinylpyrrolidone in 0.1 M potassium acetate (pH 6.5) until staining.

**Antibodies and working dilutions.** Immunohistochemical analyses were essentially as previously described (Shoham and Ebstein, 1997; Sternfeld *et al.*, 2000), using rabbit anti-ARP (Sternfeld *et al.*, 2000) 1:100, rabbit anti PKC $\beta$ II (Cat. No. sc-210, Santa Cruz) 1:100, rabbit anti PKC $\beta$ II (Sigma-Israel) 1:250 and mouse anti RACK1 (Cat. No. R20620, Transduction Laboratories, San Diego, CA) 1:200. Immunoblot analyses were with rabbit anti-N-terminus AChE antibodies (Cat. No. N-19, Santa Cruz), 1:500; mouse monoclonal antibody against all isoforms of PKC of mouse, rat and human origin (Cat. No. sc-80, Santa Cruz), dilution 1:100, or mouse monoclonal antibody against RACK1 (R20620, Transduction Laboratories), dilution 1:2500.

Sections were incubated with the primary antibody and then with biotin-conjugated donkey anti-rabbit antibody (Cat No. AP132B, Chemicon, Temecula, CA; 1 h, room temp., overnight at  $2-8^{\circ}\text{C}$ ) and extravidin-peroxidase (Sigma). RACK1 staining was further preceded by trypsin type II treatment (Sigma), 1  $\mu\text{g}/\text{ml}$  with  $\text{CaCl}_2$  0.001% for 2 min, at room temp., which required the addition of 0.001% soybean trypsin inhibitor (Sigma) during staining. Detection was with horseradish peroxidase-conjugated goat anti-mouse antibody (1:100 dilution, Sigma). Pre-incubation of anti-RACK1 with 10  $\mu\text{M}$  RACK1 for 1 h at room temp totally eliminated staining with anti-RACK1, demonstrating specificity. For all antibodies, staining was intensified with 0.075% diaminobenzidine and 0.05% nickel ammonium sulfate.

**Fluorescence double labeling.** RACK1 and ARP: Primary staining solutions contained 0.001% trypsin inhibitor (Sigma type IIS), 0.3% Triton X100, 0.05% Tween 20, 2% normal goat serum, 2% normal donkey serum, rabbit anti-ARP1 (1:100) and mouse anti-RACK1 (1:100). The secondary antibody solution contained 0.3% Triton X100, 0.05% Tween 20, 2% normal goat serum, 2% normal donkey serum, donkey-anti-rabbit conjugated to fluorescein (Chemicon, AP182F) diluted 1:100 and goat-anti-mouse conjugated with tetra-methyl-rhodamine (Sigma, T7782) diluted 1:800. Sections were mounted on SuperFrost slides (Menzel Glaser, Freiburg, Germany), air-dried, covered in Immumount (Shandon, Pittsburgh, PA) and covered for microscopy.

PKC $\beta$ II and ARP1: The primary staining solution contained 0.3% Triton X100, 0.05% Tween 20, 2% normal goat serum, 2% normal donkey serum, rabbit anti-ARP (1:100) and mouse-anti-PKC $\beta$ II (Sigma, P8083), diluted 1:500. Secondary antibody solutions and preparation for microscopy were as specified above for ARP and RACK1.

**Confocal microscopy.** Slices were scanned using a Bio-Rad MRC-1024 scanhead (Hemel Hempstead Herts.,UK) coupled to an inverted Zeiss Axiovert 135M microscope with a 40X oil immersion objective (N.A. 1.3). Excitation wavelength was 488nm (using 10% of a 100mW laser power). Fluorescence emission was measured using a 580df32 bandpass interference filter ( $580\text{ nm} \pm 16\text{ nm}$ ) for detecting tetra-methyl-rhodamine and a 525/40 filter for detecting fluorescein. The confocal iris was set to 3mm. Conditions of scanning took into consideration the overlap of fluorescein fluorescence into the rhodamine filter (as were determined by control experiments). Images were then further processed using Image pro Plus 4.01 program (version 4.0, Media Cybernetics, Silver Spring, MD).

## Results

**Two-hybrid screening for protein partners of AChE-R.** The AChE-R Readthrough peptide 1 (ARP1), composed of the C-terminal 51-amino acids of AChE-R served as “bait” for the Gal4 two-hybrid system. AChE-R is intensively expressed in the embryonic brain (Soreq and Seidman, 2001). Therefore, we screened a two-hybrid cDNA library from human fetal brain for ARP1 interacting proteins.

Fig. 1 presents the origin of AChE-R, its accumulation in neurons and the ARP1 sequence and its position in the AChE protein.

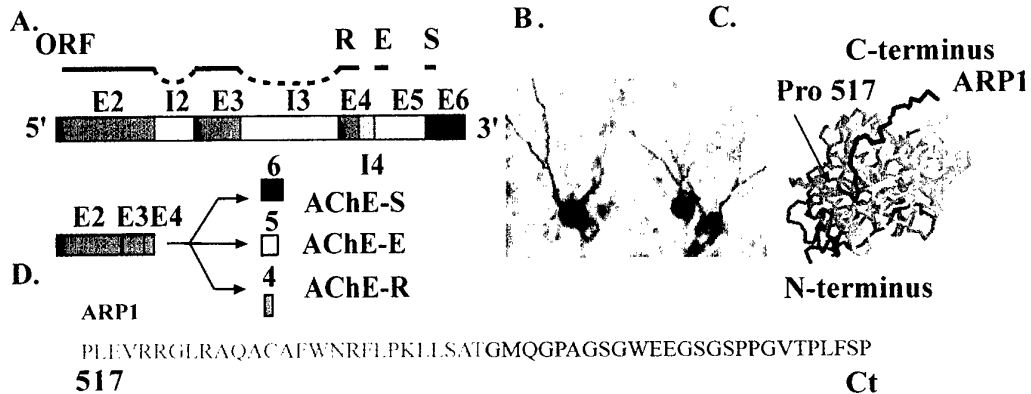


**Fig. 1: The ARP1 C-terminal domain of AChE**

(A) Alternative splicing products of the single ACHE gene. Shown is a schematic diagram of the human ACHE gene (E= exon, I= intron, ORF= open reading frame) with its three C-terminal alternative splicing products: AChE-S (S, for synaptic), AChE-E (E, for erythrocytic), and “readthrough” AChE-R. (B) immunohistochemistry of CA1 hippocampal neurons from AChE-R transgenics stained toward AChE-R. Note the intensified intra-neuron staining. (C) 3-D structure of mouse AChE (<http://www.rcsb.org/pdb/index.html>, accession no. 1C2B). Residues 1-517 are required for acetylcholine hydrolysis, whereas the C-terminal 51 residues (ARP1) are not. The structure of the distal 26 residues is not known. (D) The ARP1 domain. Shown is the ARP1 sequence. The black part is unique to the AChE-R isoform.

Several clones identified in this screen carried heterogeneous fragments of RACK1 cDNA (Fig. 2A and sequence data not shown).  $\beta$ -galactosidase ( $\beta$ -gal) activity staining, revealed for the isolated ARP1/RACK1 expressing yeast cells up to 80% of the enzyme activity induced by p53 - T-antigen interaction, which displays a dissociation constant of  $2 \times 10^8 \text{ M}^{-1}$  (Kuhn *et al.*, 1999). Lamin C interactions were negative, making false positive interaction unlikely. All of the  $\beta$ -gal inducing RACK1 clones included large parts of the WD domains 5 and 6 (out of 7 domains in the RACK1 protein), suggesting that the N-terminal region of the RACK1 protein is ineffective in ARP1- RACK1 interactions (Fig. 2A,B). RACK1 clones which included WD domain 5,6 and 7 appeared less effective in inducing  $\beta$ -gal activity than clones with domain 5,6 alone (Fig. 2A), in contrast to  $\beta$ -integrin interaction which requires domains 5-7 (Liliental and Chang, 1998). This attributed ARP1 binding capacity to a 71 residues long region from WD domain 5 and 6.

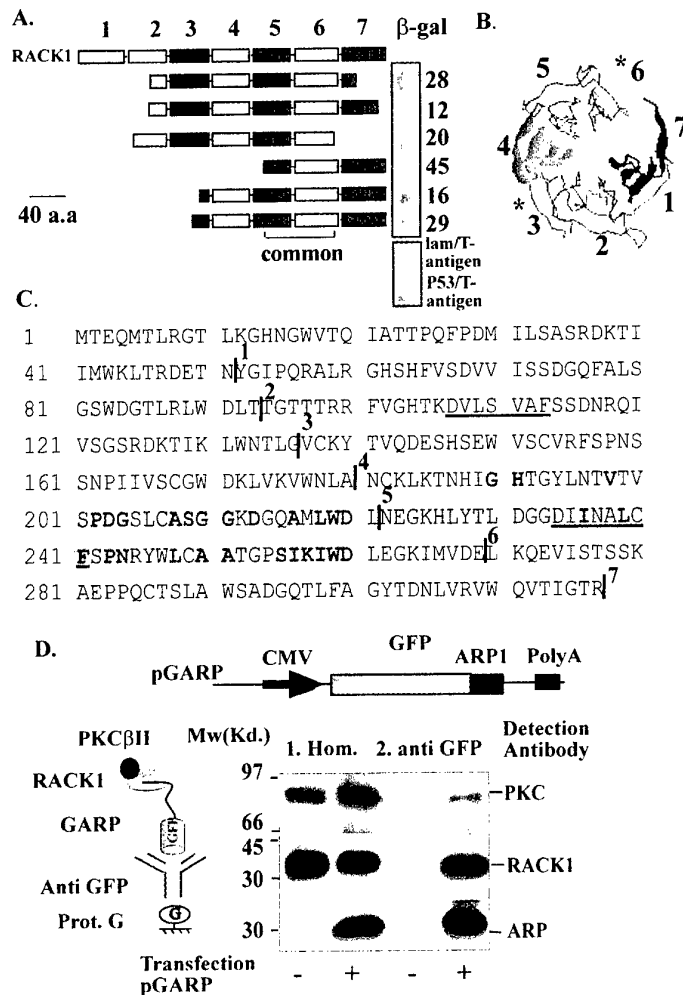


**Fig. 2: Two-hybrid positive RACK1 clones**

**A. Schematic alignment of RACK1 clones with its consensus WD domains.** Shown are scaled drawings of the 7 WD domains (boxes numbered above) in RACK1 (top) and the six RACK1 clones of human fetal brain origin, which showed ARP1 interaction in the two-hybrid system. The intensity of ARP1-RACK1 interactions as tested for representative colonies expressing the different clones is shown by staining for (blue spots) and densitometric quantification of  $\beta$ -gal activity (columns). p53 - T-antigen interaction in yeast (bottom spot) served as a positive control, lamin C-T antigen (above) was used as a negative control. The regions in WD domains 5 and 6, that were common to all clones are underlined. **B. RACK1 amino acid sequence.** Shown is the amino acid sequence of human RACK1. Shaded in yellow (for WD domain 5) and gray (for WD

domain 6) are the common domains, with residues which fit the WD consensus marked in red (Smith *et al.*, 1999). Repeat boundaries (1-7) are numbered, and the PKC $\beta$ II binding peptides underlined (red). **C. Schematic structure of the G protein  $\beta$  subunit** (<http://pdb.ccdc.cam.ac.uk/pdb/>, accession no. 1gp2). Highlighted in color are the concentric antiparallel 4 strands which constitute the blade composition of WD proteins. The WD domains are numbered. Starred are the RACK1 regions necessary for binding PKC $\beta$ II. **D. ARP1 promotes AChE-R/RACK1/PKC $\beta$ II triple complex formation in transfected COS cells.** Top scheme shows the CMV-based vector encoding pGARP, a GFP fusion protein with ARP1. Side drawing presents the experimental concept. 1. Homogenates: Shown are immunolabeled RACK1 and PKC $\beta$ II (but not ARP1) in non-transfected COS cell homogenates (-). When GARP transfected (+), COS cells are also positive for anti-ARP antibodies. 2. Anti-GFP: Immunoprecipitation with anti-GFP antibodies precipitates and PKC $\beta$ II, ARP and RACK1 in transfected but not in non-transfected COS cells.

RACK1 is identical to the propeller part of G protein  $\beta$ . polypeptide 2 like 1 (Genbank accession no. mAAH00214) and homologous to other G proteins. These include the G protein  $\beta$ 2 subunit, a prototypic member of the WD domain family (Smith *et al.*, 1999) (RACK1 sequence Blast identity 26%, similarity 44%; accession no. AAH04186), suggesting that RACK1 shares its structure. All of the WD domain proteins form wheel-like propeller

structures, composed of uniconcentric blades including  $\alpha$ -helix strands and  $\beta$ -pleated sheets (Smith *et al.*, 1999). Interestingly, the RACK1 domain which conferred binding to ARP1 in the two-hybrid system covered large parts of blades 5 and 6, with 27 out of the 71 amino acid residues in this region compatible with the accepted WD consensus (Fig. 2B). The ARP1 interacting region further included the domain 6 peptide reported as one of the binding sites of PKC $\beta$ II to RACK1 (Rodriguez *et al.*, 1999) (Fig. 2B). Another PKC $\beta$ II binding site, on blade No. 3, emerged as not associated with ARP1 interaction. Fig. 2 presents the G-protein structural organization with the presumed PKC $\beta$ II binding sites of RACK1 labeled on the corresponding blades.

**The AChE synaptic variant C-terminus also binds RACK1.** A peptide containing 67 amino acids, 40 of them unique to the synaptic variant of AChE served as another bait for screening of the same human fetal brain library using the same two-hybrid system. Out of 250,000 clones screened only one interacted with RACK1. This clone did not interact with lamin C and was stained blue by  $\beta$ -gal both serving as controls to eliminate false positives. Since AChE-R is the variant which is the variable involved in stress responses we continued our research checking mainly this isoform and its interactions with RACK1. Although the binding of AChE to RACK1 is probably in an area common to the C-terminus of the synaptic and readthrough variants.

**ARP1 promotes triple complex formation with RACK1 and PKC $\beta$ II.** To test whether ARP1, further promotes triple complex formation with PKC $\beta$ II and RACK1 in mammalian cells, we used pGARP. This vector encodes a fusion protein of green fluorescent protein (GFP) with ARP1 under the CMV promoter (Fig. 2D). When transfected into COS cells, which do not express AChE, anti-ARP antibodies immunodetected GARP expression in cell homogenates. Anti-GFP antibodies were ineffective in non-transfected cells but immunoprecipitated GARP, RACK1 and PKC $\beta$ II from homogenates of GARP – transfected COS cells (Fig. 2D).

**Overlay demonstration of RACK1 binding to hAChE-R.** To test for RACK1 interaction with the full AChE-R protein, we combined an *in vitro* overlay assay with protein blot analysis. A fusion between maltose-binding protein (MBP) and RACK1, expressed in *E. coli*, was purified by affinity chromatography to maltose. RACK1 was released from the fusion protein by site-specific factor Xa protease, separated by PAGE and transferred onto a nitrocellulose membrane (Fig 3A). Anti-RACK1 antibodies labeled the fusion protein, proteolytically-released RACK1 and fragments thereof, but not MBP (Fig 3B). Parallel membranes were overlaid with a homogenate obtained from rat pheochromocytoma PC12 cells transfected with a plasmid encoding AChE-R (Seidman *et al.*, 1995). Antibodies to the N-terminus of human AChE detected in the overlaid membrane specific binding of AChE to the intact RACK1 protein but not to its degradation products or to MBP (Fig. 3C). Non-overlaid membrane remained unlabeled when incubated with these antibodies, demonstrating AChE-R dependence (Fig. 3D).

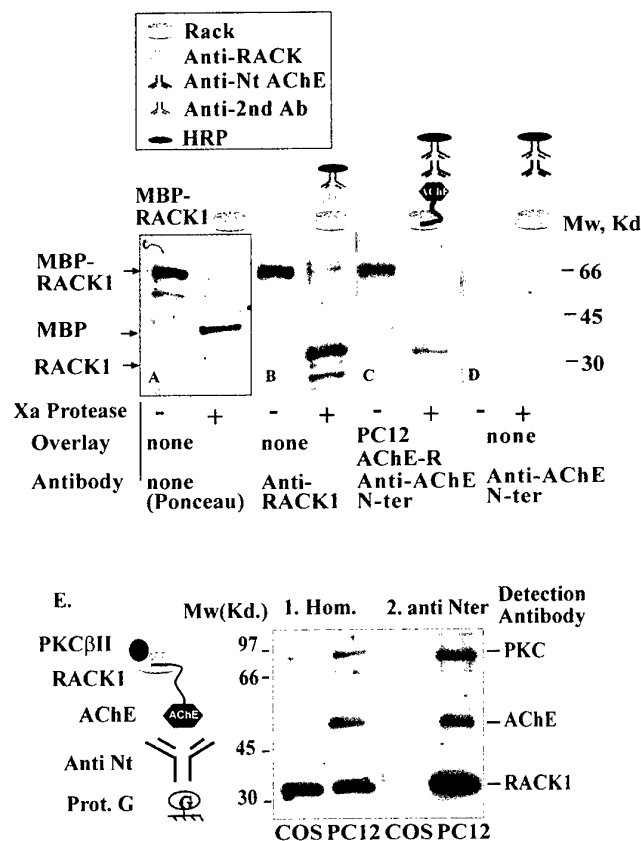


**Fig. 3: From overlay AChE-R/RACK1 interactions to immunoprecipitated AChE-R/RACK1/ PKCβII complexes**

A-D: Shown are membrane protein blots subjected to various labeling experiments. (A) Ponceau S staining of purified RACK1 fused to bacterial maltose binding protein (MBP-RACK1,-) or the 36 kDa RACK1 protein released by factor Xa proteolysis (+). Maltose binding protein (MBP) served as an internal control. (B) Horseradish peroxidase (HRP) immunolabeled RACK1 and its MBP complex and degradation products. Anti-RACK1 labeling either in fusion with MBP or alone, but not with MBP itself, demonstrated binding specificity. (C) RACK1-AChE-R complexes labeled by overlay with a PC12 cell homogenate overproducing recombinant AChE-R, followed by development with antibody to AChE N-terminus. (D) AChE N-terminus antibody

showed no signal in membranes that were not overlaid previously with AChE-R overproducing cell homogenate (negative control). (E) RACK1 and PKCβII co-immunoprecipitate with anti-AChE antibodies. Drawing shows the experimental concept. 1. Homogenates (Hom): Shown are immunodetected PKCβII and RACK1 in homogenates of COS cells, which do not express AChE, and PKCβII, RACK1 and AChE in PC12 cell homogenates. 2. Anti-AChE N ter: Dissolved immunoprecipitation complexes created with antibodies to the N-terminus of AChE display no signals in COS cells, but are positive for all 3 partner proteins in PC12 cells, demonstrating AChE requirement for the creation of these complexes.

**AChE-R promotes in native PC12 cells triple complexes with RACK1 and PKCβII.** Both COS and PC12 cells express RACK1 and PKCβII in their native state, whereas only PC12 express AChE-R, as observed in immunoblots of the soluble fraction of cell homogenates (Fig. 3E1). Antibodies targeted to the N-terminal domain of AChE co-immunoprecipitated both PKCβII and RACK1 in PC12 but not COS cells, supporting the notion of tight linkage for AChE-R/RACK1/ PKCβII in these PC12 cell complexes (Fig. 3E2).

**Stress induces neuronal co-accumulation of immunoreactive AChE-R and RACK1.** The *in vivo* relevance of AChE-R/RACK1 interactions, was explored in normal and post-stress mouse brain. Immunoreactive RACK1 was observed in the cytoplasm and closely proximal processes of pyramidal neurons, in layers 3 and 5 of the frontal and parietal cortex, in both superficial and deep layers of the piriform cortex, and in regions CA1-3 of the hippocampus. A subset of these neurons also over-expresses AChE-R under acute psychological stress (Fig. 4 and data not shown). Stress-induced increase of RACK1 was seen in parietal cortex layer 5

(compare Fig 4, 3 to 5 and 7 to 9). Unlike RACK1, AChE-R antibodies also stained cells with glial morphology. Also, in some regions, such as hippocampal CA1, RACK1 staining formed an almost continuous pattern, whereas AChE-R was localized to a subset of the pyramidal neurons. For both AChE-R and RACK1, uneven perikarial accumulation and increased neurite labeling were observed under stress (Fig. 4).

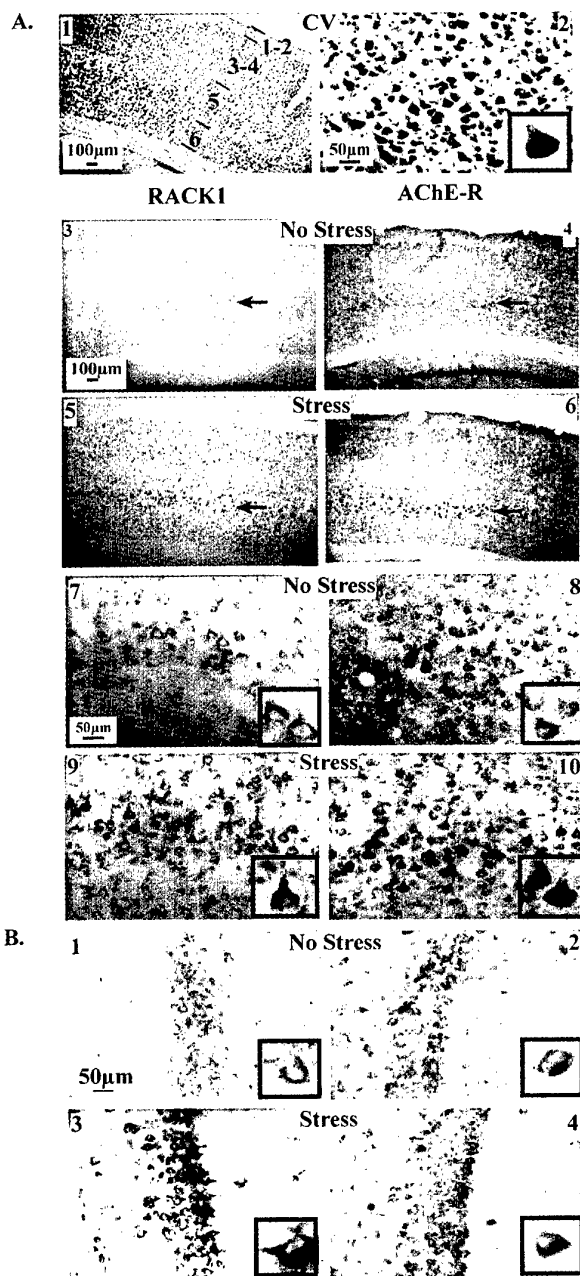


**Fig. 4. RACK1 and AChE-R co-expression in parietal cortex and CA1 neurons under stress**

Shown are parietal cortex sections stained with cresyl violet (1,2, top) or with anti-RACK1 (left) or anti-AChE-R antibodies (right)(3-10). Note uneven labeling patterns of both proteins in the cytoplasm and proximal processes of individual pyramidal neurons in the parietal cortex and hippocampus CA1 (insets). Note RACK1 and AChE-R expression increases in layers 5 (arrows) of the parietal cortex under stress.

**Transgenic AChE-R overexpression elevates brain RACK1 levels and intensifies the formation of neuronal PKC $\beta$ II clusters.** To test if AChE-R overproduction modulates the levels, properties and/or neuronal localization of its RACK1 and PKC $\beta$ II partner proteins, we tested hippocampal homogenates from AChE-R overexpressing transgenics (Sternfeld *et al.*, 2000). These displayed significant increases over control FVB/N levels of neuronal AChE-R

and RACK1, as well as a faster migrating PKC $\beta$ II band that was only faintly detected in a control hippocampus (Fig. 5A).

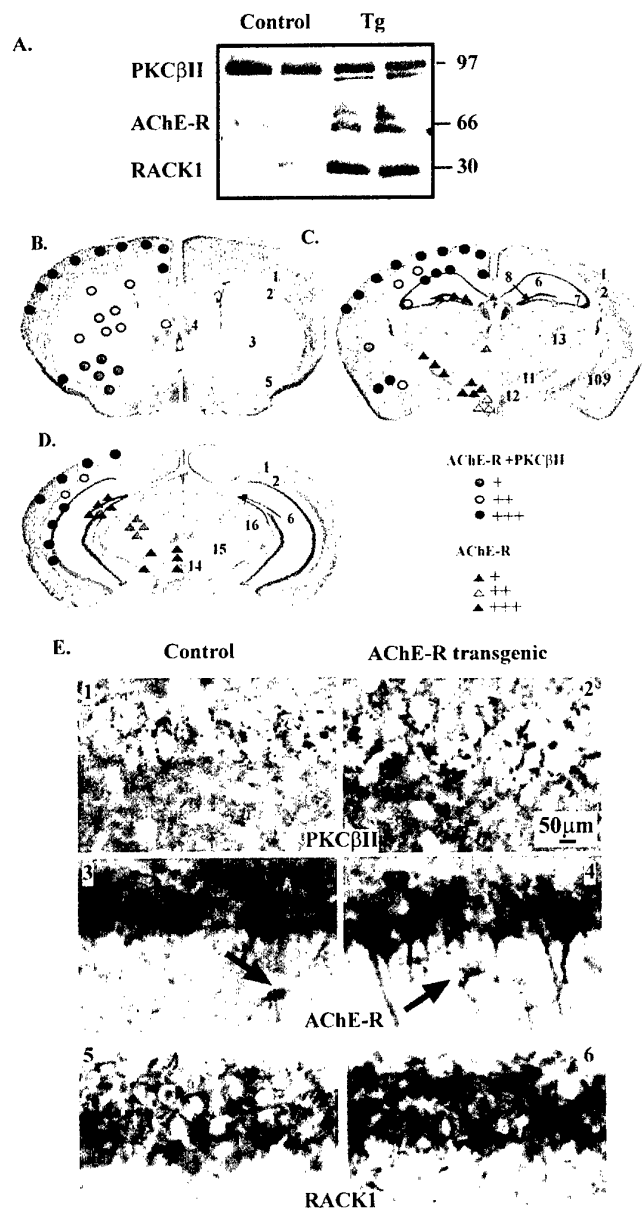


**Fig. 5. Transgenic AChE-R overexpression intensifies neuronal RACK1 and PKC $\beta$ II labeling in hippocampal CA1 neurons.**

**A. Immunoblot analysis.** Shown are immunoblot signals for PKC $\beta$ II, AChE-R and RACK1 following gel electrophoresis of clear hippocampal homogenates from 2 FVB/N controls and 2 sex and age-matched AChE-R transgenic mice (Tg). Note the intensified staining in transgenics and the fast migrating additional PKC $\beta$ II band, which could not be detected in controls. Representative results from 5 reproducible experiments. **B-D. Partial overlaps in neuronal AChE-R accumulation and PKC $\beta$ II distributions.** Shown are selected brain sections (posterior to Bregma 0.0-0.2 mm, 1.5-1.7 mm and 2.9-3.1mm respectively) and the corresponding subregions where AChE-R accumulation (triangles) or PKC $\beta$ II co-labeling in AChE-R accumulating neurons (circles) were detected. Staining intensity was low (green,+), medium (yellow,++) or high (red,+++). The corresponding subregions are numbered as follows: 1, Cortex upper layers; 2, Cortex lower layers; 3, striatum; 4, lateral septum; 5, piriform cortex; 6,

hippocampus CA1; 7, hippocampus CA3; 8, hippocampus dentate gyrus; 9, basolateral amygdala; 10, central amygdala; 11, lateral hypothalamus; 12, ventromedial hypothalamus; 13, ventral lateral thalamus; 14, Edinger-Westphal nucleus; 15, Red nucleus; 16, Pre-tectal area. **E. Hippocampal immunohistochemistry.** Shown are parallel CA1 regions from representative control and AChE-R transgenics stained with antibodies toward PKC $\beta$ II, AChE-R or RACK1. Note the intensified non-homogeneous staining of hippocampal neurons in the brain of transgenics for both AChE-R and RACK1, the relatively high background staining of PKC $\beta$ II and the microglia (arrows) positive for AChE-R.

Of the three target proteins, RACK1 and AChE-R appeared more widely distributed and could be detected in numerous brain regions (Fig. 5B and data not shown). In the brain of

AChE-R transgenics AChE-R overexpression was particularly conspicuous in neuron groups expressing punctiform PKC $\beta$ II staining (Fig. 5B-D). PKC $\beta$ II labeling, in contrast, appeared higher than control levels in only part of the AChE-R overexpressing subregions. Finally, RACK1 staining was intensified in the AChE-R expressing hippocampal CA1 and dentate gyrus neurons, and less prominently also in the parietal cortex. This suggested facilitation by AChE-R/RACK1/PKC $\beta$ II interactions of the intracellular retention of the secretory AChE-R protein.

**Diverse subcellular distributions of PKC $\beta$ II.** In control mice, PKC $\beta$ II antibodies displayed diffuse staining (Weeber *et al.*, 2000) in sub-regions of layers 5,6 in the cortex, in the stratum oriens and stratum radiatum layers of the hippocampus CA1 field, in the striatum matrix, and in the substantia nigra pars reticulata. Axonal bundles including the nigro-striatal tract were also labeled (data not shown). Another, novel staining pattern consisted of dense PKC $\beta$ II clusters in neuronal perikaria and in the axonal stems. This punctiform pattern appeared in upper layers of the parietal, temporal and piriform cortex, dorsal striatum, basolateral amygdala, hippocampal CA1 and lateral septum. In general, cells in AChE-R transgenic mice that displayed prominent AChE-R labeling were positive for RACK1 and presented PKC $\beta$ II punctiform staining (Fig. 5,B-E). AChE-R labeling in cells which in control mice included AChE-R and RACK1 but PKC $\beta$ II punctation did not intensify in AChE-R transgenics. These include neurons in the globus pallidus, substantia nigra, superior culliculus, medial septum and diagonal band (Fig. 5B-E and data not shown). Yet other neurons were AChE-R-filled in control and yet more so in AChE-R transgenics but had no PKC $\beta$ II punctiform staining. These resided in the lateral and ventro-medial hypothalamus, central nucleus of the amygdala, the hippocampal dentate gyrus, ventro-lateral thalamus, and Edinger-Westphal nucleus (Fig. 5C, D). As Weeber *et al* (2000) did not mention the punctated staining pattern in C57B6J mice, we re-tested that strain. In our hands, a weaker but discernible punctiform signal was also observed in C57B6J mice in the same cell populations as in the stress-prone FVB/N strain, our controls (data not shown).

**Inter-related AChE-R/RACK1/PKC $\beta$ II distributions.** In AChE-R transgenics, anti-PKC $\beta$ II antibodies detected basically similar diffuse and axonal staining patterns to those observed in the parental FVB/N strain. However, the punctated pattern was altered. Intensified, denser clusters of PKC $\beta$ II were located on the perikaryal circumference of a larger fraction of hippocampal CA1 neurons (Fig. 5E2). Transgenic mice overexpressing the major synaptic isoform of AChE (Beerli *et al.*, 1995) did not show such changes in PKC $\beta$ II, suggesting that this *in vivo* effect depended on chronic AChE-R excess and/or that it was prevented by AChE-S excess (data not shown). AChE-R labeling in the transgenic brain was prominent in the cell bodies and proximal processes of many, but not all CA1 hippocampal neurons, suggesting that a specific subset of these neurons was especially amenable for such accumulation (Fig. 5E3,4). Sparse cells with morphology reminiscent of microglia were also positive for AChE-R staining, both in controls and transgenics (Fig. 5E5, 6). Intensified labeling of perikaria and closely proximal neurites of CA1 pyramidal neurons was also observed by staining with RACK1 antibodies (Fig. 5E3, 4).

**Overlapping subcellular distributions of AChE-R, RACK1 and PKC $\beta$ II.** Confocal micrographs of upper layer neurons from the parieto-temporal cortex were double labeled with antibodies toward AChE-R and RACK1 or PKC $\beta$ II. Compound field projections displayed distinct yet overlapping distributions for the three partner proteins within neuronal perikarya. As expected, AChE-R labeling was conspicuously more intense in AChE-R transgenics than in FVB/N controls (compare Fig. 6B1 to 4 and C7 to 10). This

overexpression and the associated overlapping increases in the two partner proteins were reflected in different colors (Fig. 6B and C).

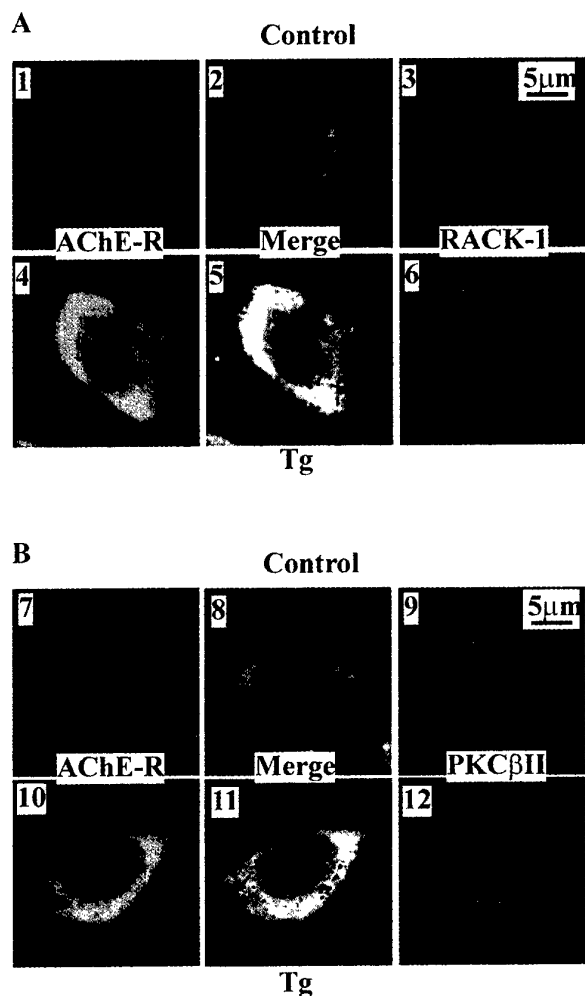


**Fig. 6. Double-labeling highlights the AChE-R modulation of AChE-R/RACK1/ PKCβII complexes.**

Shown are merged confocal micrographs from individual upper layer parietal cortex neurons of FVB/N and AChE-R overexpressing transgenic mice, co-immunolabeled with AChE-R/RACK1 (A) or AChE-R/PKCβII (B). Staining was with antibodies to AChE-R (green) and RACK1 or PKCβII (red); merged micrographs show yellow signals for overlap staining, with orange regions reflecting high partner levels. Note the uneven, distinct distributions of the analyzed antigens in cortical neurons, with AChE-R labeling demonstrating perikaryal circumference distribution, RACK1 more mobilized toward the perikaryal circumference identified in top sections (No. B5) and PKCβII highlighted in dense clusters co-localized with both RACK1 and AChE-R (No. C11).

Proteins destined to be secreted are initially concentrated near the nucleus, where their processing takes place, whereas proteins that are associated with the perikaryal cytoskeleton, plasma membrane and/or proximal process structures are distributed more peripherally. In cortical neurons from control mice, both AChE-R and RACK1 immunostaining formed peri-nuclear accumulations (compare Fig. 6, B1 to 3). In contrast, RACK1 concentrations in AChE-R transgenics were especially high around the perikaryal circumference (compare Fig. 6, B5 to B2), suggesting subcellular translocation under AChE-R excess. PKCβII clusters, too, were removed from the peri-nuclear domain in the control mice (Fig. 6, C8) to uneven distribution in larger cellular spaces in transgenics (Fig. 6, C11). In control mice, PKCβII patterns differed from both those of AChE-R and RACK1 in that they demonstrated both diffuse staining and punctated clusters of protein complexes, compatible with the parallel light microscopy patterns. Constitutive AChE-R overexpression further enlarged the perikaryal space occupied by AChE-R, RACK1 and PKCβII and apparently increased the intracellular density of their complexes.

## Discussion

Using the non-biased yeast 2-hybrid screening approach, we found two potential links explaining the function of intraneuronal AChE-R. Tight, co-immunoprecipitable and naturally co-localized complexes of AChE-R appeared to connect the C-terminal domain ARP1 with PKC $\beta$ II and its intracellular shuttling protein RACK1 and activate PKC. Intensified labeling and neuronal mobilization of both RACK1 and PKC $\beta$ II was observed in the stress-protected transgenic mice constitutively overexpressing AChE-R. Transgenic AChE-R overexpression translocated RACK1 to the perikaryal circumference and intensified PKC $\beta$ II clustering in pyramidal neurons, and activated PKC suggesting functional relevance for AChE-R overexpression in the stress-suppressing cascades of neuronal signal transduction.

**Structural Considerations.** The variety of RACK1 clones that were identified and their capacity to induce intense  $\beta$ -gal staining in the yeast cell context strengthen the notion that AChE-R/RACK1 interactions are both common and tight in the embryonic brain from which the screened library originated. The cell biology tests point at neuronal accumulation and/or subcellular mobilization as the outcome of these interactions under *in vivo* stress or transgenic overexpression. That the RACK1 region which was found to be essential for AChE-R interaction consists of two antiparallel four strand "blades" which together cover ca. 30% of the of the RACK1 perimeter. The large number of conserved WD domain residues in this part of RACK1 may highlight the requirement for correct blade folding as essential for ARP1 interactions. The AChE-R-induced changes in the intensity of RACK1/PKC $\beta$ II interactions, which are implicated from our study, may also be physiologically relevant.

**The RACK1 scaffold protein performs multiple shuttling functions.** WD proteins can simultaneously bind different partners to various regions in their multi-blade rings (Smith *et al.*, 1999), which provides flexibility and combinatorial diversity. Thus, RACK1 is a scaffold for cell-cell interaction proteins such as  $\beta$ -integrin (Liliental and Chang, 1998), members of signaling cascades like cAMP phosphodiesterase (Yarwood *et al.*, 1999), C2-containing proteins such as phospholipase C- $\gamma$ 1 (Disatnik *et al.*, 1994), src kinase (Chang *et al.*, 1998) and PH domain-containing proteins such as the  $\beta$ -adrenergic receptor (Rodriguez *et al.*, 1999). Interaction between RACK1 and AChE-R would likely compete with other associations, changing the subcellular balance between these variable complexes. Alternatively, or in addition, AChE-R/RACK1 interactions may promote the formation of additional triple complexes with other proteins. Diverse links between AChE and other signaling molecules may, in turn, explain its capacity to exert various non-catalytic intracellular functions, a possibility which awaits further investigation.

**PKC activation.** Several RACK1 reports have addressed the effect of PKC-RACK interactions on PKC activity. Addition of RACK1 to PKC in the presence of PKC activators did not significantly change PKC activity (Chang *et al.*, 1998), yet PKC activators induced RACK1 interaction with PKC, *Src* (Chang *et al.*, 2001) and integrin  $\beta$ 1 (Liliental and Chang, 1998), presumably by inducing a conformational change in RACK1 which exposes it to the binding of other proteins. PKC activation is also known to induce the MAPK pathway associated with stress responses (Gil *et al.*, 2000; Kaneki *et al.*, 1999). Our current findings demonstrate elevated PKC activity under increased RACK and AChE concentrations *in vitro*, in the absence of PKC activators, and in brain homogenates of AChE-R transgenics. The order of the events inducing the conformational change and the relevance to the MAPK pathway will have to be further investigated.

**AChE-R as a multidomain responder to diverse external stimuli.** In addition to its primary function of acetylcholine hydrolysis, AChE was shown to initiate adhesive cell-cell interactions through its core domain and promote mammalian neurite extension in a manner similar to that of its non-enzyme membrane protein homolog neuroligin (reviewed by Soreq and Seidman, 2001). Nevertheless, the neurotogenic activities of distinct AChE variants appeared to depend on their unique C-termini, which to date were not found to share sequence homologies with other proteins. In hematopoietic cells, the 26 C-terminal residues of the stress-induced AChE-R protein exert proliferative and growth factor activities (Grisaru *et al.*, 2001); however, it is not yet known whether these activities depend on extra- or intracellular interactions. Also, neither the molecular mechanism(s) nor the nervous system relevance of such activities were yet explored. Our current findings reveal that at least part of the C-terminus specific non-catalytic effects of AChE-R, are intracellular and PKC $\beta$ II-mediated.

**AChE-R interaction with PKC $\beta$ II is indirect, mediated by the PKC $\beta$ II shuttling protein RACK1;** this offers several functional advantages. Thus, PKC $\beta$ II and RACK1 are readily available in neurons, albeit in inactive and possibly, non-associated or, loosely attached compositions. We now find that stress responses and the subsequent accumulation of AChE-R (Kaufer *et al.*, 1998) facilitate the formation of triple, tightly bound AChE-R/RACK1/PKC $\beta$ II complexes. These are mobilized from their resting state intracellular location, translocating RACK1 to the perikaryal circumference and PKC $\beta$ II into densely packed clusters. Modified properties and location of PKC $\beta$ II in stress-responding neurons may possibly change the stress-induced kinase activation, phosphodiesterase mobilization, or other processes.

**Punctiform PKC $\beta$ II labeling joins AChE-R and RACK1 in neural circuits suppressing stress responses.** The presence of PKC $\beta$ II in the deep cortical layers and in the stratum oriens and stratum radiatum of CA1 in hippocampus, may reflect signal transmission across synapses between axons coming from outside the region. Staining in axon bundles such as the nigro-striatal tract may indicate that PKC $\beta$ II is distributed along the entire axon of some neurons. Finally, the currently observed perikaryal punctiform pattern, is compatible both with RACK1 interactions and with different functions, as considered below.

Transgenic AChE-R -filled neurons with both punctiform PKC $\beta$ II and RACK1 labeling are mostly relevant to stress-response inhibitory pathways (Herman and Cullinan, 1997). These were located in cortical upper layers, the hippocampal CA1 region, the lateral septum and the basolateral amygdala. PKC $\beta$ II punctiform patterns also appeared in a subset of basolateral amygdala neurons, which are generally considered excitatory to psychological stress. However, the existence in this region of stress-inhibitory neurons, has been discussed with regards to the regulation of fearful behavior (Davis *et al.*, 1994). These neurons presumably suppress other basolateral amygdala neurons that are stress-excitatory, consistent with the limited stress-related neuropathology hallmarks in the brain of AChE-R transgenic mice (Sternfeld *et al.*, 2000). The neuronal location of AChE-R/RACK1/PKC $\beta$ II complexes further suggests relevance to the PKC-activated down regulation of transient K<sup>+</sup> channels in dendrites of hippocampal CA1 pyramidal neurons (Hoffman and Johnston, 1998). Such downregulation may contribute to the reduced stress overload of AChE-R overexpressing mice.

**PKC $\beta$ II association with stress responses.** In general, PKC is mainly referred to as a morphologically active kinase. However, PKC $\beta$ II has been shown to be associated with oxidative (Paola *et al.*, 2000) and ischemic stresses (Cardell and Wieloch, 1993) and essential

for fear conditioning (Weeber *et al.*, 2000). Intriguingly, genomic disruption of the glucocorticoid receptor, which upregulates AChE-R production (Grisaru *et al.*, 2001) abolished anxiety responses (Tronche *et al.*, 1999). Our current findings therefore propose a chain of events that may assist in overcoming traumatic stress responses. This cascade initiates with glucocorticoid hormone release, proceeds with transcriptional activation and alternative splicing to elevate AChE-R levels and results in RACK1 and PKC $\beta$ II mobilization. AChE-R thus emerges as a modulator and PKC $\beta$ II – an initiator of long-term morphological responses to stress. Relevant processes include the reported PKC-induced inhibition of presynaptic metabotropic glutamate receptors (Macek *et al.*, 1998), coupling to the cAMP response element binding protein in CA1 neurons (Roberson *et al.*, 1999) and the PKC-regulated release of vesicle pools (Stevens and Sullivan, 1998). The increase in neuronal PKC $\beta$ II in AChE-R transgenic mice further proposes that when such changes become permanent they can confer stress protection, whereas the PKC $\beta$ II disruption study indicates that chronic impairments in this cascade may be detrimental. Nevertheless, excessive AChE-R production may also be detrimental, at least for recovery from closed head injury (Shohami *et al.*, 2000).

Based on the above arguments, AChE-R and/or PKC $\beta$ II levels should be tested in patients with post-traumatic stress disorder (McEwen, 1999), post-stroke phenomena and inherited susceptibility to processes in which PKC $\beta$ II plays a major role, e.g. panic attacks (Gorman *et al.*, 2000), where fear conditioning is intimately involved. Likewise, the dissociation between RACK1 and PKC $\beta$ II under ethanol exposure (Ron *et al.*, 2000) may be relevant to the stress-suppressing effect of alcohol. In addition, this study calls for testing PKC $\beta$ II levels and subcellular localization in patients hypersensitive to anticholinesterases (e.g. Alzheimer's disease drugs) which also induce AChE-R overproduction (Kaufer *et al.*, 1998; Shapira *et al.*, 2000).

**Downstream mechanistic considerations.** Triple AChE-R/RACK1/PKC $\beta$ II complexes are likely involved with the neuronal redistribution of PKC $\beta$ II in brain development (Gallicano *et al.*, 1997), aging (Battaini *et al.*, 1999) and neurodegeneration (McNamara *et al.*, 1999), all of which involve considerable modulations in AChE-R levels. AChE-R is further expressed in other RACK1/PKC $\beta$ II producing tissues, including epithelial, muscle, hematopoietic, and germ cells (Soreq and Seidman, 2001) where its capacity to induce PKC $\beta$ II - mediated changes should be examined.

**Combinatorial aspects of stress-induced proteins.** The signaling cascades involving AChE-R/RACK1/PKC $\beta$ II complexes may well be just one thread in a complex network of many pathways attenuating stress responses. Transgenic overexpression of AChE-R could, *a priori*, be expected to be seen in all cells; however, in practice transgenic AChE-R accumulation is limited to certain specific neurons. This may reflect different transcription factor combinations in specific neuronal subsets. Additionally, or alternatively AChE-R-filled neurons in transgenic mice, may belong to specific neural circuitries in which part of the intracellular signal transduction requires PKC $\beta$ II participation. That AChE-R -filled neurons also appeared in cell populations devoid of PKC $\beta$ II punctiform staining, suggests that AChE-R is involved, in addition, in physiological mechanisms other than those that engage PKC $\beta$ II. Finally, those neurons in transgenic mice which are not AChE-R -enriched may likewise be part of physiological mechanisms which do not engage PKC $\beta$ II activities.

It is noteworthy that each of the components in the triple AChE-R/RACK1/PKC $\beta$ II complexes represents one out of several options. Thus, other PKC isoforms most likely interact with different shuttling proteins, with distinct and different effects on the complex physiological phenomena that follow traumatic experiences. Likewise, RACK1 operates as a shuttling vector to many other proteins, and at least part of these interactions (e.g. phosphodiesterase) are likely to compete with the currently described one and ameliorate its consequences. Finally, the AChE-R protein is one out of three diverse AChE isoforms, each with its own C-terminal peptide and possibly different interactions. Further screening efforts should shed more light on the potential partners of other AChE variants, as well as on AChE-R interacting proteins in other tissues and developmental phases.

## Conditionally transgenic mice—Preliminary findings (task 7)

### A. Inducible antisense and ribozyme suppression of acetylcholinesterase gene expression in transfected cells

The function of acetylcholinesterase (AChE) in terminating cholinergic neurotransmission is well recognized. However, this enzyme has gained new importance since it has been found to be involved in other processes, such as cell motility, division, development, growth, and stress responses. These attribute to the AChE protein non-catalytic morphogenic activities that may be deleterious to the nervous system and peripheral organs and suggest that interference with its accumulation may be therapeutically beneficial. Moreover, modulation of the cellular level of this protein would be instrumental for elucidating the mechanisms of its complex function. In particular, the role of AChE in late-onset neurodegeneration of cholinergic neurons is of utmost importance. To establish conditional down-regulation of the *ACHE* gene, we use tetracycline controlled expression of antisense/ribozyme constructs targeted to the domain on AChE mRNA that we have found to be especially vulnerable to ribozyme degradation (Birikh et al., 1997; Grifman et al., 1998). Ribozyme and antisense expressing constructs were first demonstrated to suppress human AChE in vitro and in CHO tet-off cells as well as to prevent the accumulation of endogenous rat AChE in PC12 tet-on cells treated with nerve growth factor.

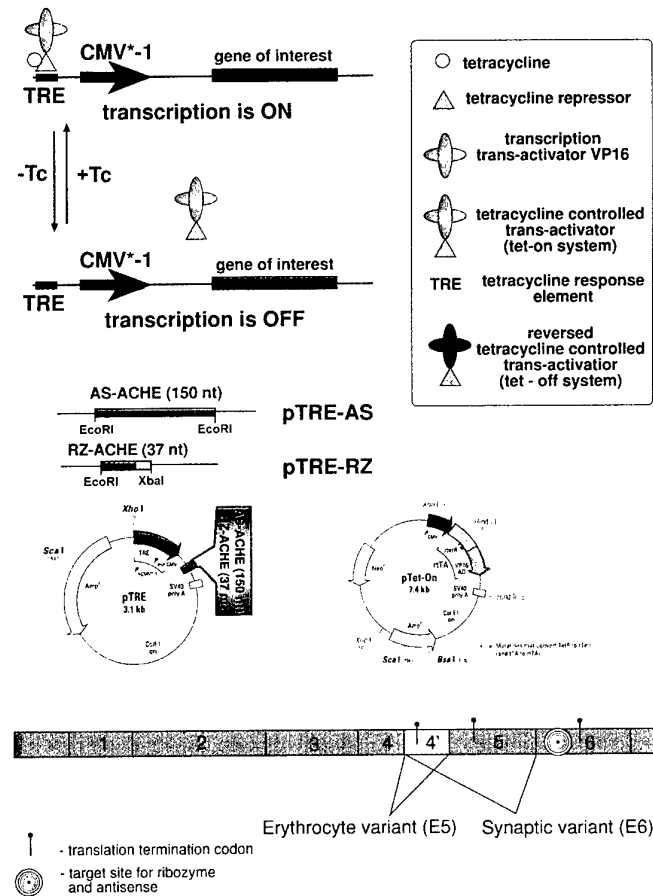


**Fig. 1. The experimental concept.**

We are developing an inducible gene expression protocol for controlled delivery of antisense RNA targeted against AChE mRNA in cells and tissues. The strategy takes advantage of the tetracycline (tet) resistance operon of *E. coli*. In its earliest form, the tet repressor (rT) was placed under control of a constitutive basal promoter to generate the tet-controlled transactivator protein (rTA; Furth et al., 1994). When co-transfected with a plasmid containing the ribozyme (RZ) coding sequence under control of the tet operator and a CMV promoter element (PhCMV\*-1), constitutive expression of the gene is subject to repression by exogenous tetracycline in a dose-dependent manner. A notable improvement of this "tet-off" strategy includes the "reverse" rTA (rrTA), the activation of which depends upon the presence of tetracycline ("tet-on"), not its absence. To construct the relevant vectors, we introduced into

commercial pTRE plasmids (Clontech) the AS-ACHE and RZ-ACHE sequences.



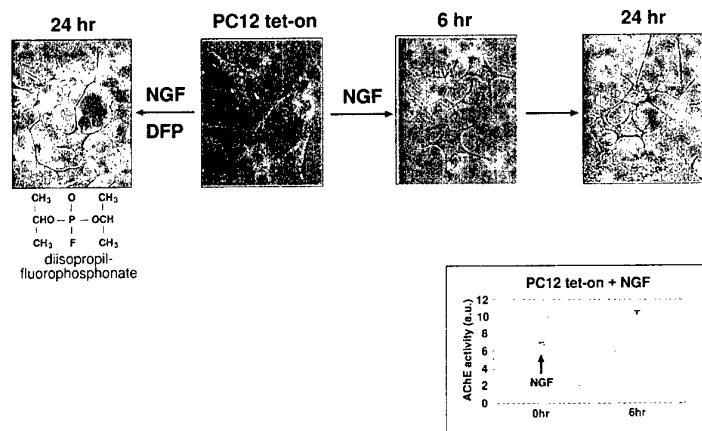


**Fig. 4.** PC12, the rat neuroendocrine pheochromocytoma cell line, was chosen in our study as an experimental model for antisense/ribozyme inhibition of AChE. When subjected to Nerve growth factor (NGF) treatment, these cells switch to differentiation towards a cholinergic phenotype with increased AChE activity and neurite like processes. AChE

was implicated as a potential mediator of these cytoarchitectural changes, as stable suppression of its production prevented the NGF effect (Grifman et al., 1998). Conditional depletion of AChE synthesis should allow more specific investigation of the phase where its function contributes toward cell differentiation processes. NGF induced differentiation of PC12 tet-on cells (CLONTECH) is associated with an increase of AChE levels. Moreover, the NGF-induced extension of neurites from PC12 tet-on cells is not prevented by DFP inhibition of AChE's catalytic activity. This leaves the non-catalytic role(s) of AChE as potentially involved with PC12 neuritogenesis. To ensure that these cells provide an appropriate system for addressing this question, we ascertained that alterations in AChE expression pattern during this process are not affected by doxycycline alone.

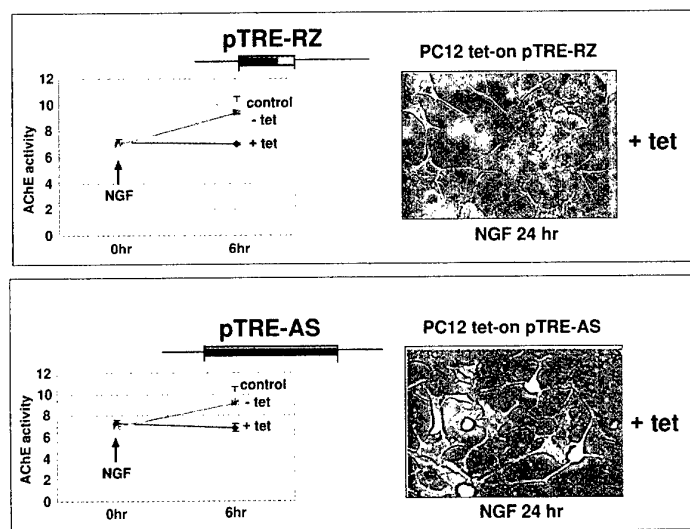


**Fig. 5. Both AS and ribozyme prevent elevation of AChE levels.**

PC12 tet-on cells were transiently transfected with ribozyme or antisense expressing plasmids (pTRE-ribozyme or pTRE-AS, respectively). After 24 hr, doxycycline (tetracycline analog) was added into half of the samples to initiate transcription of the ribozyme or AS. Cells were incubated for another 24 hr to allow accumulation of the ribozyme or AS transcripts. Then AChE expression was stimulated

by NGF. AChE activity was measured at the time of NGF addition (0 hr) and after 6 hr. PC12 tet-on cells transfected with pTRE plasmid served as a control.

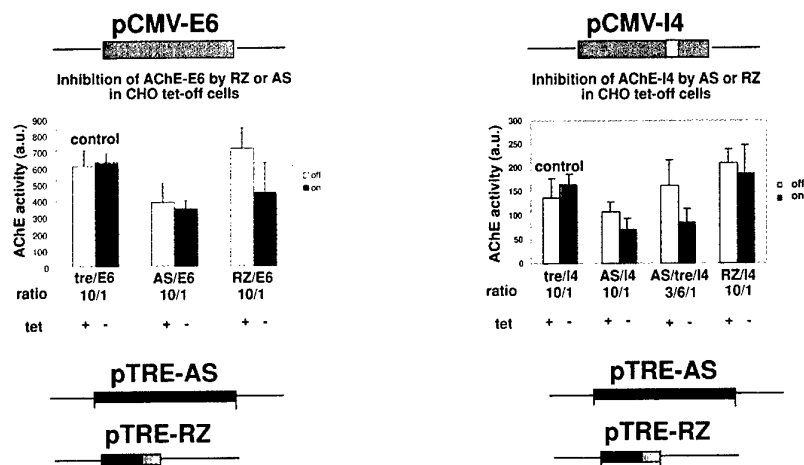


**Fig. 6. AS and ribozyme action in transfected cells.**

CHO tet-off cells (CLONTECH) were transiently co-transfected with pTRE-RZ/AS or pTRE as a control plasmid and with a plasmid encoding for one of the human AChE isoforms behind the CMV promoter (pCMV-AChE-E6/I4).

Immediately after transfection, doxycycline was added to half of the samples to induce AS/ribozyme synthesis. AChE activity was measured after 48 h. Note, that (1) in the "off" mode (white bars) AS shows reduction of AChE activity as compare to the control, probably due to leakiness of the system under transient transfection conditions. The leakiness can be compromised by lowering the ratio between the AS plasmid and the CMV-AChE (3/1 instead of 10/1 for the CMV-I4 plasmid); (2) in the "on" mode (pink bars) both ribozyme and AS reduce accumulation of the recombinant human AChE-E6 by about 50% of the control; antisense reduces AChE-I4 as well to the same extent. The remaining AChE activity may be partially attributed to synthesis of the enzyme before AS/ribozyme concentration in the cell becomes sufficient for suppression. This implicates that both ribozyme and AS are capable of cleavage of human AChE mRNA, but antisense provides a stronger suppression.

### Conclusions

- Antisense and ribozyme constructs were developed which are capable of suppressing rat and human AChE mRNA in cultured cells in a doxycycline-dependent manner.
- Prevention of AChE elevation under NGF treatment as well as inhibition of AChE catalytic activity by DFP does not prevent the initial phase of neurite outgrowth in PC12 cells.
- Development stably transgenic mouse pedigrees should provide long term inhibition of AChE and be instrumental in elucidation of its functions.

### B. Establishment of AS- and ribozyme-transgenic mouse pedigrees

Transgenic mouse pedigrees were created with the tet/AS and tet/ribozyme sequences. In the first pedigree created, the tet/ribozyme transgene was not expressed in the tissues of carrier mice at detectable levels (using RT-PCR tests). Another tet/ribozyme pedigree is currently being raised. In contrast, a mouse pedigree carrying the tet/AS transgenes yielded detectable mRNA transcripts in some, but not all of the tested tissues. An additional line, with the AS but not the tet sequence (-/AS), served as control.

Under treatment with doxycycline (2 mg/ml drinking water for 7 consecutive days prior to testing), tet/AS but not -/AS mice should overproduce the antisense sequence, which would prevent AChE-R accumulation under stressful insults. Under no antibiotic treatment, however, the tet/AS transgene should not be expressed. Therefore, the predicted response of these conditionally transgenic mice under no antibiotic treatment should be essentially that of controls. However, previous reports note that the tetracycline control tends to be "leaky" in transgenic mice, a possibility of which we were aware and for which we tested.

We have used bacterial lipopolysaccharide injection (*E. coli* LPS, 50 µg/Kg) as stressor and tested catalytic AChE activity and electrophoretic migration as reporter properties. 6 hrs post-injection, mice were sacrificed and tissues prepared for analysis.

LPS is an endotoxin, derived from the outer cell wall of Gram-negative bacteria, that binds to the cell surface molecule CD14 (Ulevitch & Tobias, 1994). This interaction induces, through the Jak/stat pathway, transcriptional over-production of 2'-5'-oligoadenylate synthetase (Hartmann et al., 1998; Zhou et al., 1993). Other inducers of 2'-5'-oligoadenylate synthetase are single and double stranded RNA aptamers. The resultant reactions products, 2'-5'-linked oligoadenylates of up to 30 monomers, act as allosteric activators of latent endoribonuclease, RNaseL, which degrades single-stranded viral or cellular RNA (Zhou et al., 1997) and induces a pro-apoptotic state (Ghosh et al., 2001).

Because of the stress response that is induced by LPS, one would expect AChE-R accumulation under exposure. However, mRNAs with low stability, such as AChE-R mRNA, are likely to be particularly sensitive to RNaseL and therefore to be quickly degraded, even under LPS induction. Indeed, we found AChE-R mRNA to be especially sensitive to antisense-catalyzed destruction (Grisaru et al., 2001; Galyam et al., 2001), a sensitivity which can, at least in part, be explained by the capacity of double-stranded antisense-mRNA hybrids to induce 2'-5' oligoadenylate synthetase and RNaseL. Exposure of tet/AS mice to LPS can assist in differentiating these two pathways, as the difference between control and tet/AS mice in AChE-R mRNA levels following LPS exposure should reflect the net contribution of the antisense transcripts to the destruction of the LPS-induced AChE-R mRNA.

Preliminary tests of these new mouse lines yielded the following outcomes:

mouse no.	genotype	doxy-cycline	LPS	AChE activity (units/mg protein)				
				plasma	hippo-campus	cortex	intestine	muscle
257	xx,-/AS	+	+	0.133	0.42	0.65	61.	77.
187	xx,-/AS	+	+	0.094	0.40	0.86	71.	124.
263	xx,-/AS	+	+	0.120	0.51	0.87	66.	
251	xx,-/AS	+	+	0.078	0.28	0.93	75.	66.
262	xx,tet/AS	-	+			0.45		63.
252	xx,tet/AS	-	+			0.50		70.
242	xx,tet/AS	+	+	0.091	0.36	0.41	43.	118.
248	xx,tet/AS	+	+			0.75		101.
129	xy,tet/AS	+	+	0.066	0.34	0.56	50.	184.
137	xy,tet/AS	+	-	0.101	0.49	0.61	50.	86.

These studies are obviously preliminary, yet they help us plan future experiments. There is as yet no control group (-/-), and the sizes of each group are as yet too small to perform a meaningful statistical analysis.

To the extent that any conclusion, however tentative, may be drawn, it seems that catalytic activities tended to be lower in both male and female tet/AS mice than their -/AS controls, whether or not LPS exposure occurred. This, perhaps, indicates continuous "leakage" of the tet transgene, conferring consistent AS expression and therefore lower AChE activities. This possibility is currently being tested.

Further tests and optimization of the experimental conditions are in progress.

## Autism, stress and chromosome 7 genes (task 8)

Autism, a disorder that affects 4 out of 10,000 individuals in the general population, is classified as a pervasive developmental disorder. It becomes apparent by the third year of life and its characteristic impairments persist into adulthood. Whereas the inheritance of this disorder does not follow a simple Mendelian pattern, there is compelling evidence for strong genetic basis. This fact places autism in the category of complex genetic traits and predicts difficulties in any attempt to unravel the various genes that contribute to the disorder, genes that may even have different contributions in different populations. Recently, the rising interest in autism has spawned quite a few multinational efforts aimed at identification of these genes. The projects, taking advantage of experimental approaches especially designed for the study of complex genetic traits, succeeded in identifying several candidate loci. However, none of these loci was identified with certainty. Among this group of candidate loci, several appear to be more prominent than the rest. The long arm of chromosome 7 (7q) is one of those.

The main characteristics of autism are social and communicative impairments, as well as repetitive and stereotyped behaviors and interests. However, there are also reports of stress response-like behavior in autistic children. Such reports strongly suggest that autism is associated with inherited impairments in stress responses. However, this association has yet to be confirmed. An interesting link that relates impairments in stress responses to autism is found in the chromosome 7 gene *ACHE*, which encodes the enzyme acetylcholinesterase (AChE). The expression of this gene is robustly and persistently up-regulated under stress and was recently found to be affected by a novel mutation in the gene's extended promoter.

This chapter will describe the recent advances in the identification of genes or gene loci that contribute to the autistic phenotype, concentrating on what appears to be one of the best candidate loci, 7q. It will further describe the reports that suggest an association between autism and impairments in stress responses and will elaborate on putative molecular mechanism(s) that underlie stress responses in conjunction with autism. Finally, to follow the suggested link that connects autism with stress, through the candidate locus 7q, we present in this chapter the results of a survey, which determined the frequency of the *ACHE* up-stream mutation in affected and non-affected American families. These results show an extremely low incidence of this mutation, failing to confirm its association with autism in American families. Nonetheless, the results do not rule out a role for this polymorphism in the etiology of autism in the Israeli population where the mutation is present a higher frequency.

### Autism as a complex trait, candidate loci and genes

Multigenic diseases differ from monogenic ones in that their occurrence cannot be linked to one specific gene, but is, rather, affected by changes in several genes. They include some of modern medicine's chief concerns, such as risk of cardiac failure, diabetes mellitus and a plethora of neurologic disorders. Among these, autism is an intriguing disorder both from the aspect of its behavioral symptoms, the scope of which is difficult to define, and due to its complex etiology. The frequency of autism is 4 in 10,000 for the classically defined syndrome (with males affected 4 times more frequently than females (Smalley, Asarnow, & Spence, 1988)). Inclusion of the

related Pervasive Development Disorders, Not Otherwise Specified (PDD-NOS) and Asperger syndrome increases this incidence to 16 in 10,000 (Rodier, 2000).

It was previously believed that drugs such as the teratogens thalidomide and valproic acid may be risk factors for autism (Rodier, Ingram, Tisdale, Nelson, & Romano, 1996). Although a certain contribution of such environmental factors may exist, it is now known that the main factors for the disorder are genetic (Folstein & Rutter, 1977). The strongest evidence for the contribution of inherited factors to autism comes from studies on twins (Bailey et al., 1995; Folstein & Rutter, 1977; Steffenburg et al., 1989; Wahlstrom, Steffenburg, Hellgren, & Gillberg, 1989). These studies showed a much higher concordance rate (the chance that a child will be diagnosed as autistic when his twin has already been confirmed as autistic) in monozygotic (MZ, identical) twin pairs compared to dizygotic pairs (DZ). The concordance rates found in the largest of these studies (Bailey et al., 1995) were 60% in MZ pairs compared to 0% in DZ pairs. This enabled calculation of the heritability of autism, which was found to be greater than 90%. Moreover, in many of the twin pairs showing a discordance, the non-autistic co-twins presented language impairments in childhood and social deficits that persisted into adulthood (Le Couteur et al., 1996). This supports the understanding of autism as a multigenic and multifactorial disease with a large array of partially-overlapping symptoms representing disorders with similar physiological bases. Such similar disorders are sometimes pooled into a related diagnostic group of PDD-NOS. That the concordance rate in MZ twin pairs does not reach the 100% expected for a pure genetic disorder implies that autism, as many other multifactorial diseases, is also affected by environmental factors that are associated with life history. Individual responses to life history, however, are also affected by the genetic make-up of the individual. The assumption is that individuals with genetic susceptibility to adverse responses to certain life events (e.g. a traumatic experience) are more likely to develop autism than others who are similarly exposed, yet do not have the inherited susceptibility. One of the twin studies (Steffenburg et al., 1989) reported that in most of the twin pairs discordant for autism, the autistic twin had more perinatal stress. This possible link of autism with stress will be further discussed below.

With the genetic basis of autism well established, the next and more challenging goal is to identify the genes linked to it. So far, no clear-cut linkage has been found between any particular gene or genetic locus and autism. This may be attributed to misdiagnosis of individuals, but probably also stems from the genetic heterogeneity of autism, with affecting genes varying in their contribution within different populations. It is believed that more than 14 loci may be associated with autism (Risch et al., 1999). Table 1 presents a summary of the current candidate loci and genes, most of which were determined in recent genome-wide screens. Whereas the majority of these chromosomes are implicated in autism based on a single identification, a few loci came up more than once and are therefore considered more seriously as containing genes that contribute significantly to the etiology of autism. Among these, the most prominent locus is 7q, with most of the markers pointing to the q32-q35 region but with some cytogenetical evidence suggesting q21-q22 as well (Ashley-Koch et al., 1999). Another locus that appears to be a serious candidate for harboring relevant genes based on cytological studies, is 15q11-q13 (for example, see Cook et al., 1997). However, this locus is not favored by results of the genetic screens. The reason for

this may be the sampling of individuals for the genetic screens, which excludes those carrying chromosomal abnormalities.

**Table 1. Candidate genes and genetic loci associated with autism<sup>a</sup>**

<sup>b</sup> chromosomal locus	<sup>c</sup> candidate genes	reference
1p(13)		Risch et al., 1999
2q(24-31)		IMGSAC, 1998; Philippe et al., 1999
4q(34-35)		Philippe et al., 1999
5p		Philippe et al., 1999
6q (16)	MACS, GRIK6, GPR6	Philippe et al., 1999
7q(31-35, 21-22 <sup>d</sup> )	GPR37, <sup>d</sup> SPCH1, PTPRZ1, EPHB6, ACHRM1, PTN, NEDD2/ICH1/CASP2, GRM8,	IMGSAC, 1998; Barrett et al., 1999; Philippe et al., 1999; Risch et al., 1999
10q(26)		(Philippe et al., 1999)
13q(21-32)		(Risch et al., 1999)
15q11-q13	GABRB3, UBE3A	Cook et al., 1998); (Martin et al., 2000) but see Barrett et al., 1999; Risch et al., 1999
16p(12-13)		IMGSAC, 1998; Philippe et al., 1999
17q11.1-q12	HTT, NF1	Cook et al., 1997; Mbarek et al., 1999
17p	HOX1A <sup>e</sup>	Risch et al., 1999
18q(22)		Philippe et al., 1999
19p(13)		IMGSAC, 1998; Philippe et al., 1999
Xp(21-22)		Philippe et al., 1999

<sup>a</sup>Compiled mostly from 4 full-genome screens performed in the past 2 years (IMGSAC, 1998; Barrett et al., 1999; Philippe et al., 1999; Risch et al., 1999).

<sup>b</sup>Whenever available, the exact location of the linked region is designated. When no exact location has been suggested the position of the markers used for the genetic screening was added (in brackets).

<sup>c</sup>Whenever proposed in the cited papers.

<sup>d</sup>See Ashley-Koch et al. (1999).

<sup>e</sup>See Rodier (2000).

Before further focusing on chromosome 7, a few of the candidate genes believed to contribute to the etiology of autism are worth mentioning. Most of the proposed candidate genes are believed to be causally involved in autism based on their known contribution to neuronal activity or development, combined with linkage analysis of their chromosomal locations. In certain cases, such as with the serotonin transporter, the gene was proposed as a candidate based on a phenotypic abnormality, the high serotonin levels shown by autistic individuals (Cook et al., 1997), a suggestion that was re-enforced by genetic association studies (Klauck, Poustka, Benner, Lesch, & Poustka, 1997). Similarly, the neurofibromatosis type 1 gene (NF1; Mbarek et al., 1999) was found to be over-expressed in autistic patients. NF1 is known to regulate the activity of Ras proteins, of which one shows an association with autism (Comings, Wu, Chiu, Muhleman, & Sverd, 1996). A different case involved the  $\gamma$ -aminobutyric

acid receptor  $\beta 3$ -subunit gene (GABRB3; Cook et al., 1998). This receptor is activated by GABA, the principal inhibitory neurotransmitter in the brain. Its importance in control of brain excitability, as well as its developmentally regulated expression, indicated possible involvement in the autistic phenotype.

So far, however, genetic screens have failed to unequivocally verify the association of these genes. In most cases, new allelic markers were identified in the gene regions, but not in the same position as the preliminarily associated markers (Martin et al., 2000; Risch et al., 1999). The next 2 sections will point up the stress-related symptoms of autism that have been somewhat neglected in recent years, and which may suggest new candidate genes based on their involvement in such symptoms.

### Is autism associated with inherited impairments in stress responses?

Once a genetic basis of autism was established, environmental factors, which had previously been the focus of attention, were pushed aside. However, we now believe that there is reason to consider an interaction of genetic and environmental factors. The correlation of autism with inherited susceptibility to extreme stress responses has been discussed extensively, so far without resolution. Several observations suggest such correlation. First, autistic patients show an exaggerated response to external stimuli that are not stressful in healthy individuals (Bergman & Escalona, 1949; Hutt, Hutt, Lee, & Ounsted, 1964), perhaps suggesting inherited differences in their levels of perceived stress; second, such an exaggerated response to such stimuli may indicate an inherited tendency to impaired control over stress responses (Hutt, Hutt, Lee, & Ounsted, 1965); and third, the long-lasting nature of their repetitive behavior phenotype hints at inherited difficulties in termination of stress responses. Similarly, the impairments in socio-emotional reciprocity that are characteristic of autism (Wing & Gould, 1979), the communication impairments and anxiety (Muris, Steerneman, Merckelbach, Holdrinet, & Meesters, 1998), the susceptibility to epileptic seizures (Giovanardi Rossi, Posar, & Parmeggiani, 2000) and the restricted repertoire of activities and interests (Wing & Gould, 1979) may all be associated with inherited defects in the intricate processes that control human responses to stress. In addition, autism is associated with a mild, but reproducible and apparently specific elevation in the stress-related hormones  $\beta$ -endorphin and ACTH (Tordjman et al., 1997) (Fig. 1). All this calls for investigating those nervous system pathways and the corresponding genes that contribute to stress responses. One such pathway involves cholinergic neurotransmission.

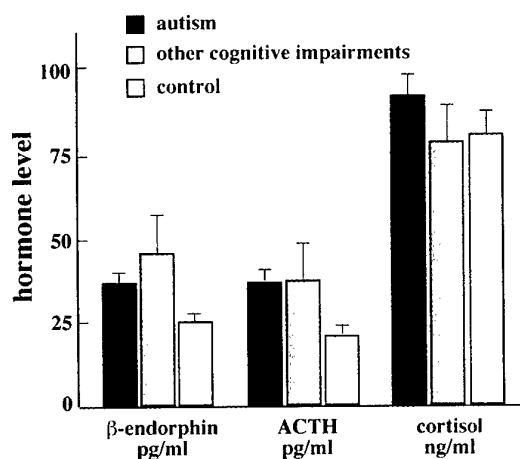


**Fig. 1. Plasma stress hormones in autism.** Shown in columns are results taken from Tordjman et al. (1997) of data from autistic patients (n=46-48), patients with mental retardation or other cognitive impairments (n=15-16) and normal subjects (n=23-26). Statistics was performed on log-transformed data, as described in the reference.

Neurons that communicate by the neurotransmitter acetylcholine (ACh) are tightly involved in mammalian stress responses. Hyperexcitation of cholinergic neurotransmission has been reported under stress (Kaufer & Soreq, 1999); persistent changes were observed in the expression patterns of the key genes that encode the ACh-synthesizing enzyme choline acetyl transferase, the packaging protein vesicular ACh transporter and the ACh-hydrolyzing enzyme AChE (Kaufer, Friedman, Seidman, & Soreq, 1998), all of which lead to a decrease in cholinergic hyperexcitation and to re-establishment of normal neurotransmission. These stress-induced changes take place primarily in the hippocampus, which has been reported to develop abnormally in autistic individuals (Piven, 1997). The change in AChE expression, its increase under stress conditions, is mimicked in AChE-over-producing transgenic mice. These mice display progressive stress-related pathologies, including high density of curled neuronal processes in the somatosensory cortex, accumulation of clustered heat shock protein 70-immunopositive neuronal fragments in the hippocampus, and a high incidence of reactive astrocytes (Sternfeld et al., 2000). They also present progressive impairments in learning, memory and social behavior (Beeri et al., 1995; Beeri et al., 1997; Cohen, O. et al, personal communication), and appear extremely sensitive to head injury (Shohami et al., 2000) and AChE inhibitors (Shapira et al., 2000b). Moreover, stress was shown to increase the blood-brain barrier permeability (Friedman et al., 1996), thereby allowing potentially harmful xenobiotics to enter the brain. A subset of such xenobiotics, the AChE inhibitors, are commonly used in agriculture and in the household as insecticides. Upon entering the brain, AChE inhibitors may cause the above-mentioned persistent increase in AChE expression; and excess of this protein may lead to neuropathological changes and to impairment of cognitive and social skills such as those observed in the transgenic mice. Altogether, these data suggest that individuals with an inherited susceptibility to adverse stress responses, itself probably a complex trait, will present exaggerated AChE expression. Similarly, individuals with an inherited abnormal AChE expression may develop a susceptibility to adverse stress responses. The autism-associated symptoms which, appear to indicate increased stress responses, may point to the *ACHE* gene and its transcriptional control as promising ground in which to explore for correlations with the autistic phenotype.

Consider (a) that in everyone, there is a toll in brain neuropathologies to be paid for the daily load of stress, and in experimental animals the appearance of these pathologies seems to exacerbated under AChE over-expression (Sternfeld et al., 2000); (b) this toll may be magnified in individuals with an inherited predisposition to exaggerated responses to stress and to anti-AChE agents, as in some cases hypersensitivity to anti-AChEs was discovered to be associated with a genomic variation that induces constitutive over-expression of AChE (Shapira et al., 2000b); and (c) an additional factor may be a previous exposure to AChE inhibitors, which under stress can cross the blood-brain barrier (Friedman et al., 1996) and induce progressive damage to glia and neurons. Each of these effects, and especially the sum of them, may facilitate the developmental impairments characteristic of autism.

#### **Chromosome 7 and autism**

The long arm of chromosome 7 was marked as a locus of genes which contribute to autism in all of the full genome screens performed so far (IMGSAC, 1998; Barrett et

al., 1999; Philippe et al., 1999; Risch et al., 1999) and in a few more restricted screens, e.g. by Ashley-Koch et al. (1999). While the linked loci extend from bands q32 to q35, several genes located outside of this region may be equally important. This assumption is based on identified mapping inaccuracies and ambiguities (Hauser, Boehnke, Guo, & Risch, 1996), on the assumption that certain genetic aberrations may involve not only the genetically-linked region but also neighboring genes and on potentially relevant functions of the respective gene products, which make them appropriate candidates for association with different aspects of the autistic phenotype. One such candidate gene, *SPCHI*, which fulfills all 3 criteria, was proposed recently. Mapped to 7q31, *SPCHI* is associated with a severe speech and language disorder (Fisher, Vargha-Khadem, Watkins, Monaco, & Pembrey, 1998) and thus may be responsible for the language difficulties observed in autistic children. A family with three affected children, two with autism and one with a language disorder, was recently investigated (Ashley-Koch et al., 1999). Affected members of this family were found to carry an inversion that spans bands 7q21 to 7q34. Further screening of additional families for markers located in the inversion region pointed to part of this inversion region being associated with 25-40% of autism cases (Ashley-Koch et al., 1999). However, with the set of chromosome 7 markers included in that screen, the *SPCHI* gene itself was not linked to this syndrome.

We have recently examined the possible involvement of aberrant regulation of another chromosome 7 gene, *ACHE*, located close to *SPCHI*, in the susceptibility to development of the autistic phenotype. Mapped to 7q22, *ACHE* encodes the enzyme AChE which is responsible for hydrolyzing the neurotransmitter ACh and thus for terminating neurotransmission across cholinergic synapses (Massoulie et al., 1998). In addition, *ACHE* is involved in plasticity responses in many more tissues through non-catalytic activities (reviewed in Grisaru, Sternfeld, Eldor, Glick, & Soreq, 1999). Yet more importantly, over-production of AChE was reported under acute psychological stress (Kaufer et al., 1998). The proximity of the *ACHE* gene to the autism related 7q32-35 region, its inclusion in the inversion region found in the autism family (reported in Ashley-Koch et al., 1999) and its association with stress responses all make it a plausible candidate. In addition, *ACHE* is expressed in early stages of brain development, long before the formation of functioning synapses (Layer, 1995), which implies that its aberrant regulation can contribute to the developmental defects that are associated with autism. In addition, it should be noted that stress-induced over-expression of 7q22 genes is not limited to *ACHE*; at least one additional gene, *ARS* which is associated with arsenite resistance, and possibly others at this locus, also appear to be over-expressed (Shapira, Grant, Korner, & Soreq, 2000a).

Although total blockade of ACh hydrolysis is incompatible with life, polymorphisms that modulate the transcriptional control of AChE may cause a milder effect, which is manifested as an inherited susceptibility to changes in cholinergic neurotransmission. Following a search for such polymorphisms (Shapira et al., 2000b), we have recently identified a 4-base pair deletion that disrupts one of two binding sites for the transcription factor HNF3B (Kaestner, Hiemisch, Luckow, & Schutz, 1994; Qian, Samadani, Porcella, & Costa, 1995). This deletion is located in a distal enhancer domain, 17 Kb up-stream from the transcription start site of *ACHE*, a region dense with binding motifs for other factors, including glucocorticoid hormones (Shapira et al., 2000b) (Fig. 2). This *ACHE* promoter deletion induces constitutive AChE over-

production, which in turn causes an impaired capacity for up-regulating AChE production under chemical stress insults and results in hypersensitivity to such insults. Because of the molecular mechanisms common to chemical and psychological stress responses, i.e. elevated expression of stress-associated transcription factors such as AP1 or HNF3, of AChE (Kaufer & Soreq, 1999) and of heat shock proteins (Sternfeld et al., 2000), we suspect that carriers of this promoter polymorphism are also hypersensitive to psychological stressors. An extension of this concept implies that autism and susceptibility to stressors share common molecular abnormalities. It may also be that a primary stress event would induce an acquired susceptibility to exaggerated responses to subsequent stress. Under a certain genetic make-up, the risk of developing the full autistic phenotype may also increase. To examine one of the molecular markers associated with such susceptibility, we determined the incidence of the transcriptionally activating deletion in the *ACHE* promoter in US families with autistic children as compared with screened healthy individuals from Israel and the USA.

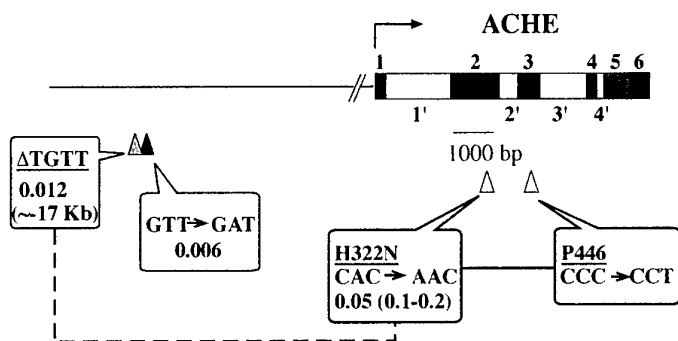


**Fig. 2. *ACHE* polymorphisms** Shown is a drawn-to-scale scheme of the *ACHE* locus with all known polymorphisms depicted. Exons are depicted as numbered filled boxes, introns as numbered open boxes and

mutations as wedges. A solid line connecting mutations indicates complete linkage between the variants. A broken line represents strong incomplete linkage. Mutation frequencies are taken from Ehrlich et al. (1994) for the coding region mutations (open wedges).

In the examined Israeli population, the tested deletion displayed an allele frequency of 0.012 and was strongly linked to the catalytically neutral H322N point mutation in the AChE coding sequence. The H322N mutation, responsible for the rare Yt<sup>b</sup> blood group, is considerably more frequent in Middle Eastern populations (Ehrlich et al., 1994), than in the USA (Giles, Metaxas-Buhler, Romanski, & Metaxas, 1967). Therefore, we predicted that the *ACHE* promoter polymorphism would occur less frequently in the US population, regardless of the autistic status. This was, indeed, found to be the case, with 8 heterozygous carriers out of 333 screened Israelis (2.4% incidence) but only 5 carriers in 816 US individuals (0.6%) (Table 2). The low incidence of this polymorphism further complicated the data analysis, as it was found in 3 out of 616 normal US individuals (0.5%) as compared with 2 out of 190 affected ones (1.0%). We conclude that if indeed this specific polymorphism is involved with in the susceptibility to extreme responses in the US survey of autistic patients, its effect is minimal.

**Table 2. Screening autism families for  $\Delta 4$  *ACHE* promoter polymorphism**

US autism families		US individuals carriers			Israeli individuals carriers		total individuals carriers	
singleton <sup>a</sup>	103	normal	616	3 <sup>c</sup>	333	8	949	11
multiplex <sup>b</sup>	82	affected	190	2 <sup>d</sup>	-		190	2
unconfirmed multiplex	18	unclear status	18	-	-		18	-
total	203		816	5	333	8	949	13

<sup>a</sup>Nuclear families with an affected child.

<sup>b</sup>Families with at least two affecteds, usually sibs.

<sup>c</sup>Of two families, one female, one male and his grandson.

<sup>d</sup>Two affected males.

### Prospects

The current status of this study leaves us with more questions than answers. Because of the rarity of the analyzed promoter polymorphism, we cannot confirm that it is associated with the autistic phenotype in the studied families. The conflicting evidence regarding candidate genes suggests that its genomic basis may differ **from** one population to another. This is highlighted by the different allelic frequency of the *ACHE* promoter polymorphism in the US and Israeli populations that were screened. In addition, the wealth of transcription factor binding motifs in the extended *ACHE* promoter suggests multiple contributions toward its control, both under normal and stress conditions. Therefore, the over-all post-transcriptional pattern of *ACHE* gene expression may be more relevant to autism than sequence polymorphisms in particular elements of its promoter.

We do believe, however, that it is worthwhile paying attention to environmental factors, such as stress, that, given a certain genetic make-up, may affect the development of autism. More than identifying affecting environmental factors per se, this approach may offer hints of additional genetic factors, that indirectly contribute to the etiology of autism by processing environmental influences.

### Key research accomplishments

- Neuronal overexpression of "readthrough" acetylcholinesterase is associated with antisense-suppressible behavioral impairments
- Developmental reduction in AChE gene expression is associated with acquired learning behavior in honey bees
- Synaptogenesis and myopathy under AChE over-expression
- Modified testicular expression of stress-associated "readthrough" acetylcholinesterase predicts male infertility
- Development of AChE variant-specific antibodies for the demonstration of differential expression of variants in hematopoietic cells
- Complex host cell responses to antisense suppression of *ACHE* gene expression
- Relief of neuromuscular weakness in experimental autoimmune myasthenia gravis by antisense oligonucleotides
- Search for the connections among autism, stress and chromosome 7 genes
- The C-terminal sequence of AChE-R interacts with RACK1, a PKC intracellular receptor and a WD-type protein
- A system for inducible antisense suppression of *ACHE* gene expression has been constructed

## Reportable outcomes

The following new articles have appeared or will shortly appear in peer-reviewed journals:

- Galyam, N., Grisar, D., Grifman, M., Melamed-Book, N., Eckstein, F., Seidman, S., Eldor, A., and Soreq, H. (2001). Complex host cell responses to antisense suppression of ACHE gene expression. *Antisense Nucl Acid Drug Dev* 11, 51-57.
- Lev-Lehman, E., Evron, T., Broide, E. S., Meshorer, E., Ariel, I., Seidman, S., and Soreq, H. (2000). Synaptogenesis and myopathy under acetylcholinesterase overexpression. *J. Mol. Neurosci.* 14, 93-105.
- Mor I., Grisar, D., Titelbaum, L. , Evron, T., Richler, C., Wahrman, J. , Sternfeld, M., Yogev, L., Meiri, N., Shlomo Seidman, S. and Hermona Soreq, H. (2001). Modified testicular expression of stress-associated "readthrough" acetylcholinesterase predicts male infertility. *FASEB J.* 15, 2039-2041.
- Shapira, M., Thompson, C.K., Soreq, H. and Robinson, G.E. (2001) Changes in neuronal acetylcholinesterase gene expression and division of labor in honey bee colonies. *J. Mol. Neurosci.* 17 (in press).
- Soreq, H., and Seidman, S. (2001). Acetylcholinesterase - new roles for an old actor. *Nature Rev. Neurosci.* 2, 294-302.

The following review articles have appeared:

- Soreq, H. and Seidman, S. (2000) Anti-sense approach to anticholinesterase therapeutics. *Isr. Med. Assn. J.* 2 Suppl. 81-85.
- Shapira, M., Glick, D., Gilbert, J.P., and Soreq, H. (2000). Autism, stress and chromosome 7 genes. In : *The Research Basis of Autism Intervention.* . E. Schloper, L. Marcus, C. Shulman and N. Yirmiya, eds. (New York: Kluwer Academic/Plenum Publishers), pp. 103-113.
- Soreq, H., and Glick, D. (2000). Novel roles for cholinesterases in stress and inhibitor responses. In: *Cholinesterases and Cholinesterase Inhibitors: Basic, Preclinical and Clinical Aspects*, E. Giacobini, ed. (London: Martin Dunitz), pp. 47-61.
- Soreq, H., Kaufer, D., Friedman, A. and Glick, D. (2000) Blood-Brain Barrier modulations and low-level exposure to Xenobiotics. In: *Chemical Warfare Agents: Low Level Toxicity*, S. M. Somani and J. A. Romano, eds. (Boca Raton: CRC Press), pp. 121-144.

## Degrees granted

Michael Shapira received his PhD from Hebrew University for "Neurogenetics approach to the transcriptional control of acetylcholinesterase production".

## Employment opportunities resulting from work on this grant

Christina Erb, a former post-doctoral fellow is now employed by Bayer AG, Pharma Research CNS at Wuppertal, Germany.

Michael Shapira, a former student, received a Dean's Fellowship for post-doctoral studies at Stanford University.

#### Awards

An honorary professorship was conferred upon Prof. Soreq by Maimonides University School of Medicine, Buenos Aires, May 2001

Inbal Mor, a doctoral candidate, was awarded the Hebrew University of Jerusalem Pollack Prize for excellence in research and studies.

Cesar Flores-Flores, was awarded an extension of his Long-Term FEBS Fellowship for post-graduate studies at the Hebrew University

#### Funding applied for based on work supported by this grant

“Human acetylcholinesterase isoforms from transgenic plants: a robust system for the production and delivery of effective countermeasures against non-conventional warfare agents”, award 030 7461 from Defense Advanced Research Projects Agency of the US Department of Defense (with Tsafir Mor and Charles Arntzen, Arizona State University)

“Functional genomics of neurogenic variability: cholinesterase and glycine receptor polymorphisms”, awarded by German-Israeli Foundation (with Cord-Michael Becker, Erlangen University)

#### Collaborations initiated

Prof. Charles Arntzen, Arizona State University, Tempe

Prof. Cord-Michael Becker, Erlangen University, Nuremberg, Germany

#### Training of personnel

A neurologist from Soroka Hospital (Beersheva), Tatiana Vander, MD, has been receiving training at Hebrew University to enable the Beersheva group, under Dr. Friedman, perform AChE enzyme and protein concentration assays and determine genomic polymorphisms. The standardization of these assays, and improved shared protocols for extraction of DNA from blood samples, will facilitate the collection of information on human subjects when the conditionally approved HSRRB certification process for these studies is completed.

## Conclusions

In focusing this year's work on the potentially distinct functions of the different AChE variants, we have found the neuronal overexpression of the stress-induced AChE-R variant to be associated with behavioral impairments in mice. Another animal model, the honey bee, showed consistent improvement of behavioral functions during their normal developmental reduction of *ache* gene expression and also under mild rivastigmine exposure. In the neuromuscular system, we observed AChE-R overexpression under mouse exposure to DFP and in an experimental autoimmune myasthenia gravis model in rats. This overexpression was associated with impaired muscle structure and myopathy (in mice) and with electromyographic deterioration (in rats). Both effects were preventable by systemic administration of antisense oligonucleotides, which also transiently improved the behavioral abnormalities associated with AChE-R overproduction.

Modulated AChE-R production was also noted in differentiating hematopoietic and sperm cells; in AChE-R transgenic mice, this induced male infertility, and unusual AChE-R distribution was also observed in human sperm samples from the male partners of some couples with unexplained infertility. Finally, at least part of these intriguing AChE-R properties could be traced to a cascade response leading to modulated activities of PCK $\beta$ II, a protein kinase variant known to control anxiety responses.

## References

- Adey, N.B., Kay, B.K. (1997) Isolation of peptides from phage-displayed random peptide libraries that interact with the talin-binding domain of vinculin. *Biochem J* 324, 523-528.
- Agrawal, S., Kandimalla, E.R. (2000). Antisense therapeutics: is it as simple as complementary base recognition? *Mol Med Today* 6, 72-81.
- Alvarez, A., Alarcon, R., Opazo, C., Campos, E.O., Munoz, F.J., Calderon, F.H., Dajas, F., Gentry, M.K., Doctor, B.P., De Mello, F.G., Inestrosa, N.C. (1998) Stable complexes involving acetylcholinesterase and amyloid- $\beta$  peptide change the biochemical properties of the enzyme and increase the neurotoxicity of Alzheimer's fibrils. *J Neurosci* 18, 3213-3223.
- Andres, C., Beeri, R., Friedman, A., Lev-Lehman, E., Henis, S., Timberg, R., Shani, M., Soreq, H. (1997). Acetylcholinesterase-transgenic mice display embryonic modulations in spinal cord choline acetyltransferase and neurexin 1 $\beta$  gene expression followed by late-onset neuromotor deterioration. *Proc Natl Acad Sci USA* 94, 8173-8178.
- Andres, C., Seidman, S., Beeri, R., Timberg, R., Soreq, H. (1998) Transgenic acetylcholinesterase induces enlargement of murine neuromuscular junctions but leaves spinal cord synapses intact. *Neurochem Int*, 32, 449-456.
- Anglister, L., Stiles, J.R., Salpeter, M.M. (1994). Acetylcholinesterase density and turnover number at frog neuromuscular junctions, with modeling of their role in synaptic function. *Neuron* 12, 783-794.
- Ashley-Koch, A., Wolpert, C.M., Menold, M.M., Zaeem, L., Basu, S., Donnelly, S.L., Ravan, S. A., Powell, C.M., Qumsiyeh, M.B., Aylsworth, A.S., Vance, J.M., Gilbert, J.R., Wright, H.H., Abramson, R.K., DeLong, G.R., Cuccaro, M.L., Pericak-Vance, M.A. (1999). Genetic studies of autistic disorder and chromosome 7. *Genomics* 61, 227-236.
- Atherton, E., Sheppard, R.C. (1989) Solid phase peptide synthesis: a practical approach. IRL Press, Oxford.
- Bailey, A., Le Couteur, A., Gottesman, I., Bolton, P., Simonoff, E., Yuzda, E., Rutter, M. (1995). Autism as a strongly genetic disorder: evidence from a British twin study. *Psychol Med* 25, 63-77.
- Barrett, S., Beck, J.C., Bernier, R., Bisson, E., Braun, T. A., Casavant, T.L., Childress, D., Folstein, S.E., Garcia, M., Gardiner, M.B., Gilman, S., Haines, J.L., Hopkins, K., Landa, R., Meyer, N.H., Mullane, J.A., Nishimura, D.Y., Palmer, P., Piven, J., Purdy, J., Santangelo, S. L., Searby, C., Sheffield, V., Singleton, J., Slager, S., et al. (1999). An autosomal genomic screen for autism. Collaborative linkage study of autism. *Am J Med Genet* 88, 609-615.
- Battaini, F., Pascale, A., Lucchi, L., Pasinetti, G.M., Govoni, S. (1999) Protein kinase C anchoring deficit in postmortem brains of Alzheimer's disease patients. *Exp Neurol* 159, 559-564.
- Beeri, R., Andres, C., Lev-Lehman, E., Timberg, R., Huberman, T., Shani, M., Soreq, H. (1995). Transgenic expression of human acetylcholinesterase induces progressive cognitive deterioration in mice. *Curr Biol* 5, 1063-1071.
- Beeri, R., Le Novere, N., Mervis, R., Huberman, T., Grauer, E., Changeux, J.P., Soreq, H. (1997). Enhanced hemicholinium binding and attenuated dendrite branching in cognitively impaired acetylcholinesterase-transgenic mice. *J Neurochem* 69, 2441-2451.
- Beltinger, C., Saragovi, H.U., Smith, R. M., Lesauteur, L., Shah, N., Dedionisio, L., Christensen, L., Raible, A., Jarett, L., Gweirtz, A.M. (1995). Binding, uptake, and intracellular trafficking of phosphorothioate-modified oligodeoxynucleotides. *J Clin Invest* 95, 1814-1823.

- Belzunces, L.P., Toutant, J.P., Bounias, M. (1988). Acetylcholinesterase from *Apis mellifera* head. Evidence for amphiphilic and hydrophilic forms characterized by Triton X-114 phase separation. *Biochem J* 255, 463-470.
- Ben Aziz Aloya, R., Seidman, S., Timberg, R., Sternfeld, M., Zakut, H., Soreq, H. (1993). Expression of a human acetylcholinesterase promoter-reporter construct in developing neuromuscular junctions of *Xenopus* embryos. *Proc Natl Acad Sci USA*, 90, 2471-2475.
- Bergman, P., Escalona, S. (1949). Unusual sensitivities in very young children. *Psychoanal Study Child* 34, 333-352.
- Bigbee, J.W., Sharma, K.V., Chan, E.L., Bogler, O. (2000) Evidence for the direct role of acetylcholinesterase in neurite outgrowth in primary dorsal root ganglion neurons. *Brain Res* 861, 354-362.
- Birikh, K., Berlin, Y.A., Soreq, H., Eckstein, F. (1997). Probing accessible sites for ribozymes on human acetylcholinesterase RNA. *RNA* 3, 429-437.
- Bluthe, R. M., Schoenen, J., Dantzer, R. (1990). Androgen-dependent vasopressinergic neurons are involved in social recognition in rats. *Brain Res* 519, 150-157.
- Boneva, N., Brenner, T., Argov, Z. (2000). Gabapentin may be hazardous in myasthenia gravis. *Muscle Nerve* 23, 1204-1208.
- Boschetti, N., Brodbeck, U., Jensen, S.P., Koch, C., Norgaard-Pedersen, B. (1996) Monoclonal antibodies against a C-terminal peptide of human brain acetylcholinesterase distinguish between erythrocyte and brain acetylcholinesterases. *Clin Chem* 42, 19-23.
- Buee, L., Bussiere, T., Buee-Scherrer, V., Delacourte, A., Hof, P.R. (2000) Tau protein isoforms, phosphorylation and role in neurodegenerative disorders. *Brain Res Brain Res Rev*, 33, 95-130.
- Cano Lozano, V., Gauthier, M. (1998). Effects of the muscarinic antagonists atropine and pirenzepine on olfactory conditioning in the honeybee. *Pharmacol Biochem Behav* 59, 903-7.
- Cardell, M., Wieloch, T. (1993) Time course of the translocation and inhibition of protein kinase C during complete cerebral ischemia in the rat. *J Neurochem* 61, 1308-1314.
- Carlson, N.R. (1994). *Physiology of Behavior*, 5th Edition (Needham Heights, MA: Allyn and Bacon).
- Chan, R.Y., Adatia, F.A., Krupa, A.M., Jasmin, B.J. (1998). Increased expression of acetylcholinesterase T and R transcripts during hematopoietic differentiation is accompanied by parallel elevations in the levels of their respective molecular forms. *J Biol Chem* 273, 9727-9733.
- Chang, B.Y., Conroy, K.B., Machleder, E.M., Cartwright, C.A. (1998) RACK1, a receptor for activated C kinase and a homolog of the beta subunit of G proteins, inhibits activity of src tyrosine kinases and growth of NIH 3T3 cells. *Mol Cell Biol* 18, 3245-3266.
- Changeux, J.P., Galzi, J.L., Devillers-Thiery, A., Bertrand, D. (1992). The functional architecture of the acetylcholine nicotinic receptor explored by affinity labelling and site-directed mutagenesis. *Q Rev Biophys* 25, 395-432.
- Chien, C.T., Bartel, P.L., Sternglanz, R., Fields, S. (1991) The two-hybrid system: a method to identify and clone genes for proteins that interact with a protein of interest. *Proc Natl Acad Sci USA* 88, 9578-9582.
- Chollat-Namy, A., Delamanche, I.S., Bouchaud, C. (1993) Variation in the expression of c-fos after intoxication by soman. Comparative study using in situ hybridization and immunohistochemistry. *Brain Res* 603, 32-37.

- Chothia, C., Lesk, A.M. (1987) Canonical structures for the hypervariable regions of immunoglobulins. *J Mol Biol* 196, 901-917.
- Clarke, R.N., Klock, S.C., Geoghegan, A., Travassos, D.E. (1999). Relationship between psychological stress and semen quality among in- vitro fertilization patients. *Hum Reprod* 14, 753-758.
- Cohan, S.L., Pohlmann, J.L., Mikszewski, J., O'Doherty, D.S. (1976). The pharmacokinetics of pyridostigmine. *Neurology* 26, 536-539.
- Comings, D.E., Wu, S., Chiu, C., Muhleman, D., Sverd, J. (1996). Studies of the c-Harvey-Ras gene in psychiatric disorders. *Psychiatry Res* 63, 25-32.
- Cook, E.H., Jr., Courchesne, R.Y., Cox, N. J., Lord, C., Gonen, D., Guter, S.J., Lincoln, A., Nix, K., Haas, R., Leventhal, B.L., Courchesne, E. (1998). Linkage-disequilibrium mapping of autistic disorder, with 15q11-13 markers. *Am J Hum Genet* 62, 1077-1083.
- Cook, E.H., Jr., Lindgren, V., Leventhal, B.L., Courchesne, R., Lincoln, A., Shulman, C., Lord, C., Courchesne, E. (1997). Autism or atypical autism in maternally but not paternally derived proximal 15q duplication. *Am J Hum Genet* 60, 928-934.
- Coussens, L., Parker, P.J., Rhee, L., Yang-Feng, T.L., Chen, E., Waterfield, M.D., Francke, U., Ullrich, A. (1986) Multiple, distinct forms of bovine and human protein kinase C suggest diversity in cellular signaling pathways. *Science* 233, 859-866.
- Coyle, J.T., Price, D.L., DeLong, M.R. (1983) Alzheimer's disease: a disorder of cortical cholinergic innervation. *Science* 219, 1184-1190.
- Crooke, S.T. (2000). Progress in antisense technology: the end of the beginning. *Methods Enzymol* 313, 3-45.
- Cummings, J.L., Back, C. (1998). The cholinergic hypothesis of neuropsychiatric symptoms in Alzheimer's disease. *Am J Geriatr Psychiatry* 6, S64-78.
- Darboux, I., Barthalay, Y., Piovant, M., Hipeau Jacquotte, R. (1996) The structure-function relationships in *Drosophila* neurotactin show that cholinesterasic domains may have adhesive properties. *EMBO J* 15, 4835-4843.
- Davis, M., Rainnie, D., Cassell, M. (1994) Neurotransmission in the rat amygdala related to fear and anxiety. *Trends Neurosci* 17, 208-214.
- de Belle, J.S., Heisenberg, M. (1994). Associative odor learning in *Drosophila* abolished by chemical ablation of mushroom bodies. *Science* 263, 692-695.
- de Kruif, J., Boel, E., Logtenberg, T. (1995) Selection and application of human single chain Fv antibody fragments from a semi-synthetic phage antibody display library with designed CDR3 regions. *J Mol Biol* 248, 97-105.
- de la Escalera, S., Bockamp, E.O., Moya, F., Piovant, M., Jimenez, F. (1990) Characterization and gene cloning of neurotactin, a *Drosophila* transmembrane protein related to cholinesterases. *EMBO J* 9, 3593-3601.
- de Quervain, D.J., Roozendaal, B., McGaugh, J.L. (1998). Stress and glucocorticoids impair retrieval of long-term spatial memory. *Nature* 394, 787-790.
- Diamond, D.M., Fleshner, M., Ingersoll, N., Rose, G.M. (1996). Psychological stress impairs spatial working memory: relevance to electrophysiological studies of hippocampal function. *Behav Neurosci* 110, 661-672.
- Disatnik, M.H., Hernandez-Sotomayor, S.M., Jones, G., Carpenter, G., Mochly-Rosen, D. (1994) Phospholipase C-gamma 1 binding to intracellular receptors for activated protein kinase C. *Proc Natl Acad Sci USA* 91, 559-563.

- Donger, C., Krejci, E., Serradell, A. P., Eymard, B., Bon, S., Nicole, S., Chateau, D., Gary, F., Fardeau, M., Massoulie, J., Guicheney, P. (1998). Mutation in the human acetylcholinesterase-associated collagen gene, COLQ, is responsible for congenital myasthenic syndrome with end-plate acetylcholinesterase deficiency (Type Ic). *Am J Hum Genet* 63, 967-975.
- Drachman, D.B. (1994). Myasthenia gravis. *N Engl J Med* 330, 1797-1810.
- Duval, N., Massoulie, J., Bon, S. (1992) H and T subunits of acetylcholinesterase from Torpedo, expressed in COS cells, generate all types of globular forms. *J Cell Biol* 118, 641-653.
- Dwivedi, C., Long, N.J. (1989). Effect of cholinergic agents on human spermatozoa motility. *Biochem Med Metab Biol* 42, 66-70.
- Egbunike, G.N. (1980). Changes in acetylcholinesterase activity of mammalian spermatozoa during maturation. *Int J Androl* 3, 459-468.
- Ehrlich, G., Patinkin, D., Ginzberg, D., Zakut, H., Eckstein, F., Soreq, H. (1994). Use of partially phosphorothioated "antisense" oligodeoxynucleotides for sequence-dependent modulation of hematopoiesis in culture. *Antisense Res Dev* 4, 173-183.
- Engel, A.G., Lambert, E.H., Santa, T. (1973) Study of long-term anticholinesterase therapy. Effects on neuromuscular transmission and on motor end-plate fine structure. *Neurology* 23, 1273-1281.
- Engelhardt, J.I., Siklos, L., Appel, S.H. (1997) Immunization of guinea pigs with human choline acetyltransferase induces selective lower motoneuron destruction. *J Neuroimmunol* 78, 57-68.
- Erb, C., Troost, J., Kopf, S., Schmitt, U., Loffelholz, K., Soreq, H., Klein, J. (2001). Compensatory mechanisms enhance hippocampal acetylcholine release in transgenic mice expressing human acetylcholinesterase. *J Neurochem* 77, 638-646.
- Evoli, A., Batocchi, A.P., Tonali, P. (1996) A practical guide to the recognition and management of myasthenia gravis. *Drugs* 52, 662-670.
- Farris, S.M., Robinson, G.E., Davis, R.L., Fahrbach, S.E. (1999). Larval and pupal development of the mushroom bodies in the honey bee, *Apis mellifera*. *J Comp Neurol* 414, 97-113.
- Fibiger, H.C., Damsma, G., Day, J.C. (1991). Behavioral pharmacology and biochemistry of central cholinergic neurotransmission. *Adv Exp Med Biol* 295, 399-414.
- Fisher, S.E., Vargha-Khadem, F., Watkins, K.E., Monaco, A.P., Pembrey, M.E. (1998). Localisation of a gene implicated in a severe speech and language disorder. *Nat Genet* 18, 168-170.
- Flores-Flores, C., Nissim, A., Shochat, S., Soreq, H. (in press). Phage display selection and characterization of myc-tagged humanized monoclonal antibodies to synaptic acetylcholinesterase. *J. Neural Transm Supp.*
- Folstein, S., Rutter, M. (1977). Infantile autism: a genetic study of 21 twin pairs. *J Child Psychol Psychiatry* 18, 297-321.
- Fresquet, N., Fournier, D., Gauthier, M. (1998). A new attempt to assess the effect of learning processes on the cholinergic system: studies on fruitflies and honeybees. *Comp Biochem Physiol B Biochem Mol Biol* 119, 349-353.
- Friedman, A., Kaufer, D., Shemer, J., Hendler, I., Soreq, H., Tur-Kaspa, I. (1996) Pyridostigmine brain penetration under stress enhances neuronal excitability and induces early immediate transcriptional response. *Nat Med* 2, 1382-1385.
- Furth, P.A., St Onge, L., Boger, H., Gruss, P., Gossen, M., Kistner, A., Bujard, H., Hennighausen, L. (1994). Temporal control of gene expression in transgenic mice by a tetracycline-responsive promoter. *Proc Natl Acad Sci USA* 91, 9302-9306.

- Futerman AH, Low MG, Michaelson DM, Silman I (1985) Solubilization of membrane-bound acetylcholinesterase by a phosphatidylinositol-specific phospholipase C. *J Neurochem* 45: 1487-1494.
- Galiotta, L.J., Rasola, A., Rugolo, M., Zottini, M., Mastrocola, T., Gruenert, D.C., Romeo, G. (1992). Extracellular 2-chloroadenosine and ATP stimulate volume-sensitive Cl<sup>-</sup> current and calcium mobilization in human tracheal 9HTEo- cells. *FEBS Lett* 304, 61-65.
- Gallicano, G.I., Yousef, M.C., Capco, D.G. (1997) PKC- $\alpha$  a pivotal regulator of early development. *Bioassays* 19, 29-36.
- Galyam, N., Grisaru, D., Grifman, M., Melamed-Book, N., Eckstein, F., Seidman, S., Eldor, A., Soreq, H. (2001). Complex host cell responses to antisense suppression of ACHE gene expression. *Antisense Nucl Acid Drug Dev* 11, 51-57.
- Garner, D.L., Thomas, C.A. (1999). Organelle-specific probe JC-1 identifies membrane potential differences in the mitochondrial function of bovine sperm. *Mol Reprod Dev* 53, 222-229.
- Gauthier, M., Belzunces, L. P., Zaoujal, A., Colin, M. E., Richad, D. (1992). Modulatory effect of learning and memory on honey bee brain acetylcholinesterase activity. *Comp. Biochem. Physiol.* 103C, 91-95.
- Gauthier, M., Cano-Lozano, V., Zaoujal, A., Richard, D. (1994). Effects of intracranial injections of scopolamine on olfactory conditioning retrieval in the honeybee. *Behav Brain Res* 63, 145-149.
- Gerace, L. (1995). Nuclear export signals and the fast track to the cytoplasm. *Cell* 82, 341-344.
- Gheusi, G., Bluthe, R. M., Goodall, G., Dantzer, R. (1994). Ethological study of the effects of tetrahydroaminoacridine (THA) on social recognition in rats. *Psychopharmacology (Berl)* 114, 644-650.
- Ghosh, A., Sarkar, S.N., Rowe, T.M., Sen, G.C. (2001). A specific isozyme of 2'-5' oligoadenylate synthetase is a dual function proapoptotic protein of the Bcl-2 family. *J Biol Chem* 276, 25447-25455.
- Giacobini, E. (2000). Present and future of Alzheimer therapy. *J Neural Transm Suppl* 59, 231-242.
- Gibbs, R.B., Martynowski, C. (1997). Nerve growth factor induces Fos-like immunoreactivity within identified cholinergic neurons in the adult rat basal forebrain. *Brain Res* 753, 141-151.
- Giblin, P.T., Poland, M.L., Moghissi, K.S., Ager, J.W., Olson, J.M. (1988). Effects of stress and characteristic adaptability on semen quality in healthy men. *Fertil Steril* 49, 127-132.
- Gil, C., Chaib-Oukadour, I., Pelliccioni, P., Aguilera, J. (2000) Activation of signal transduction pathways involving trkA, PLC $\gamma$ -1, PKC isoforms and ERK-1/2 by tetanus toxin. *FEBS Lett*, 481, 177-182.
- Giles, C.M., Metaxas-Buhler, M., Romanski, Y., Metaxas, M.N. (1967). Studies on the Yt blood group system. *Vox Sang* 13, 171-180.
- Giovanardi Rossi, P., Posar, A., Parmeggiani, A. (2000). Epilepsy in adolescents and young adults with autistic disorder. *Brain Dev.* 22, 102-106.
- Gnagey, A.L., Forte, M., Rosenberry, T.L. (1987). Isolation and characterization of acetylcholinesterase from *Drosophila*. *J Biol Chem* 262, 13290-13298.
- Gorlich, D. (1998). Transport into and out of the cell nucleus. *Embo J* 17, 2721-7.
- Gorman, J.M., Kent, J.M., Sullivan, G.M., Coplan, J.D. (2000) Neuroanatomical hypothesis of panic disorder, revised. *Am J Psychiatry* 157, 493-505.

- Griffiths AD, Malmqvist M, Marks JD, Bye JM, Embleton MJ, McCafferty J, Baier M, Holliger KP, Gorick BD, Hughes-Jones NC, Hoogenboom HR, Winter G (1993) Human anti-self antibodies with high specificity from phage display libraries. *EMBO J* 12: 725-734.
- Grifman, M., Galyam, N., Seidman, S., Soreq, H. (1998) Functional redundancy of acetylcholinesterase and neuroligin in mammalian neuritogenesis. *Proc Natl Acad Sci USA* 95, 13935-13940.
- Grifman, M., Soreq, H. (1997). Differentiation intensifies the susceptibility of pheochromocytoma cells to antisense oligodeoxynucleotide-dependent suppression of acetylcholinesterase activity. *Antisense Nucleic Acid Drug Dev* 7, 351-359.
- Grisaru, D., Deutch, V., Shapira, M., Galyam, N., Lessing, B., Eldor, A., Soreq, H. (2001). ARP, a peptide derived from the stress-associated acetylcholinesterase variant, has hematopoietic growth promoting activities. *Mol Med* 7, 93-105.
- Grisaru, D., Lev-Lehman, E., Shapira, M., Chaikin, E., Lessing, J. B., Eldor, A., Eckstein, F., Soreq, H. (1999). Human osteogenesis involves differentiation-dependent increases in the morphogenetically active 3' alternative splicing variant of acetylcholinesterase. *Mol Cell Biol* 19, 788-795.
- Grisaru, D., Sternfeld, M., Eldor, A., Glick, D., Soreq, H. (1999). Structural roles of acetylcholinesterase variants in biology and pathology. *Eur J Biochem* 264, 672-686.
- Habib, K.E., Weld, K.P., Rice, K.C., Pushkas, J., Champoux, M., Listwak, S., Webster, E.L., Atkinson, A.J., Schulkin, J., Contoreggi, C., Chrousos, G.P., McCann, S.M., Suomi, S.J., Higley, J.D., Gold, P.W. (2000). Oral administration of a corticotropin-releasing hormone receptor antagonist significantly attenuates behavioral, neuroendocrine, and autonomic responses to stress in primates. *Proc Natl Acad Sci USA* 97, 6079-6084.
- Haley, R.W., Kurt, T.L., Hom, J. (1997) Is there a Gulf War Syndrome? Searching for syndromes by factor analysis of symptoms. *JAMA* 277, 215-222.
- Hammer, M., Menzel, R. (1995). Learning and memory in the honeybee. *J Neurosci* 15, 1617-1630.
- Harrinson JL, Williams SC, Winter G, Nissim A (1996) Screening of phage antibody libraries. *Methods Enzymol* 267: 83-109.
- Hartmann, R., Norby, P.L., Martensen, P.M., Jorgensen, P., James, M.C., Jacobsen, C., Moestrup, S.K., Clemens, M.J., Justesen, J. (1998). Activation of 2'-5' oligoadenylate synthetase by single-stranded and double-stranded RNA aptamers. *J. Biol Chem* 273, 3236-3246.
- Hauser, E.R., Boehnke, M., Guo, S. W., Risch, N. (1996). Affected-sib-pair interval mapping and exclusion for complex genetic traits: sampling considerations. *Genet Epidemiol.* 13, 117-137.
- He, F., Xu, H., Qin, F., Xu, L., Huang, J., He, X. (1998). Intermediate myasthenia syndrome following acute organophosphates poisoning--an analysis of 21 cases. *Hum Exp Toxicol* 17, 40-45.
- Henderikx P, Kandilogiannaki M, Petrarca C, von Mensdorff-Pouilly S, Hilgers JHM, Krambovitis E, Arends J, Hoogenboom HR (1998) Human single-chain Fv antibodies to MUC1 core peptide selected from phage display libraries recognize unique epitopes and predominantly bind adenocarcinoma. *Cancer Res* 58: 4324-4332.
- Herman, J.P., Cullinan, W.E. (1997) Neurocircuitry of stress: central control of the hypothalamo-pituitary- adrenocortical axis. *Trends Neurosci*, 20, 78-84.
- Herman, J.P., Cullinan, W.E. (1997) Neurocircuitry of stress: central control of the hypothalamo-pituitary- adrenocortical axis. *Trends Neurosci* 20, 78-84.

- Hillegaart, V., Ahlenius, S. (1994). Time course for synchronization of spontaneous locomotor activity in the rat following reversal of the daylight (12:12 h) cycle. *Physiol Behav* 55, 73-5.
- Hoffman, D.A., Johnston, D. (1998) Downregulation of transient K<sup>+</sup> channels in dendrites of hippocampal CA1 pyramidal neurons by activation of PKA and PKC. *J Neurosci* 18, 3521-3528.
- Hoogenboom HR, Lutgerink JT, Pelsers MM, Rousch MJ, Coote J, van Neer N, De Bruine A, Van Nieuwenhoven FA, Glatz JF, Arends JW (1999) Selection-dominant and nonaccessible epitopes on cell-surface receptors revealed by cell-panning with a large phage antibody library. *Eur J Biochem* 260: 774-784.
- Hu, G.Y., Hvalby, O., Walaas, S.I., Albert, K.A., Skjeflo, P., Andersen, P., Greengard, P. (1987) Protein kinase C injection into hippocampal pyramidal cells elicits features of long term potentiation. *Nature* 328, 426-429.
- Huang, D., Shi, F. D., Giscombe, R., Zhou, Y., Ljunggren, H. G., Lefvert, A. K. (2001). Disruption of the IL-1beta gene diminishes acetylcholine receptor- induced immune responses in a murine model of myasthenia gravis. *Eur J Immunol* 31, 225-232.
- Hudson, C.S., Rash, J.E., Tiedt, T.N., Albuquerque, E.X. (1978) Neostigmine-induced alterations at the mammalian neuromuscular junction. II. Ultrastructure. *J Pharmacol Exp Ther* 205, 340-356.
- Hutt, C., Hutt, S.J., Lee, D., Ounsted, C. (1964). Arousal and childhood autism. *Nature* 204, 908.
- Hutt, C., Hutt, S.J., Lee, D., Ounsted, C. (1965). A behavioural and electroencephalographic study of autistic children. *J Psychiatry Res* 3, 181-197.
- Ichtchenko, K., Hata, Y., Nguyen, T., Ullrich, B., Missler, M., Moomaw, C., Sudhof, T.C. (1995). Neuroligin 1: a splice site-specific ligand for beta-neurexins. *Cell* 81, 435-443.
- Im, S.H., Barchan, D., Fuchs, S., Souroujon, M.C. (1999). Suppression of ongoing experimental myasthenia by oral treatment with an acetylcholine receptor recombinant fragment. *J Clin Invest* 104, 1723-1730.
- IMGSAC, International Molecular Genetic Study of Autism Consortium (1998). A full genome screen for autism with evidence for linkage to a region on chromosome 7q. *Hum Mol Genet* 7, 571-578
- Ito, K., Suzuki, K., Estes, P., Ramaswami, M., Yamamoto, D., Strausfeld, N. J. (1998). The organization of extrinsic neurons and their implications in the functional roles of the mushroom bodies in *Drosophila melanogaster* Meigen. *Learn Mem* 5, 52-77.
- Jasmin, B.J., Lee, R.K., Rotundo, R.L. (1993) Compartmentalization of acetylcholinesterase mRNA and enzyme at the vertebrate neuromuscular junction. *Neuron* 11, 467-477.
- Jolly, C., Morimoto, R.I. (1999). Stress and the cell nucleus: dynamics of gene expression and structural reorganization. *Gene Expr* 7, 261-270.
- Kaestner, K. H., Hiemisch, H., Luckow, B., Schutz, G. (1994). The HNF-3 gene family of transcription factors in mice: gene structure, cDNA sequence, and mRNA distribution. *Genomics*, 20, 377-385.
- Kaneki, M., Kharbanda, S., Pandey, P., Yoshida, K., Takekawa, M., Liou, J., Stone, R., Kufe, D. (1999) Functional role for protein kinase Cbeta as a regulator of stress-activated protein kinase activation and monocytic differentiation of myeloid leukemia cells. *Molecular and Cellular Biology*, 19, 461-470.
- Kaneto, H. (1997). Learning/memory processes under stress conditions. *Behav Brain Res* 83, 71-74.

- Karpel, R., Ben Aziz-Aloya, R., Sternfeld, M., Ehrlich, G., Ginzberg, D., Tarroni, P., Clementi, F., Zakut, H., Soreq, H. (1994) Expression of three alternative acetylcholinesterase messenger RNAs in human tumor cell lines of different tissue origins. *Exp Cell Res* 210: 268-277.
- Kaufer, D., Friedman, A., Seidman, S., Soreq, H. (1998) Acute stress facilitates long-lasting changes in cholinergic gene expression. *Nature* 393, 373-377.
- Kaufer, D., Friedman, A., Soreq, H. (1999) The vicious circle of stress and anticholinesterase responses. *Neuroscientist* 5, 173-183.
- Kaufer, D., Soreq, H. (1999). Tracking cholinergic pathways from psychological and chemical stressors to variable neurodeterioration paradigms. *Curr Opin Neurol* 12, 739-743.
- Kawabuchi, M., Osame, M., Watanabe, S., Igata, A., Kanaseki, T. (1976) Myopathic changes at the end-plate region induced by neostigmine methylsulfate. *Experientia* 32, 632-635.
- Klauck, S.M., Poustka, F., Benner, A., Lesch, K.P., Poustka, A. (1997). Serotonin transporter (5-HTT) gene variants associated with autism? *Hum Mol Genet* 6, 2233-2238.
- Knowles, M.R., Clarke, L.L., Boucher, R.C. (1991). Activation by extracellular nucleotides of chloride secretion in the airway epithelia of patients with cystic fibrosis. *N Engl J Med* 325, 533-538.
- Koenigsberger, C., Chiappa, S., Brimijoin, S. (1997) Neurite differentiation is modulated in neuroblastoma cells engineered for altered acetylcholinesterase expression. *J Neurochem* 69, 1389-1397.
- Kramer, T.H., Buckhout, R., Fox, P., Widman, E. et al. (1991). Effects of stress on recall. *Appl Cog Psychol* 5, 483-488.
- Kreissl, S., Bicker, G. (1989). Histochemistry of acetylcholinesterase and immunocytochemistry of an acetylcholine receptor-like antigen in the brain of the honeybee. *J Comp Neurol* 286, 71-84.
- Kristensen, P., Winter, G. (1998) Proteolytic selection for protein folding using filamentous bacteriophages. *Fold Des* 3: 321-328.
- Kronman, C., Chitlaru, T., Elhanany, E., Velan, B., Shafferman, A. (2000). Hierarchy of post-translational modifications involved in the circulatory longevity of glycoproteins. *J Biol Chem* 275, 29488-29502.
- Kucharski, R., Maleszka, R., Hayward, D.C., Ball, E.E. (1998). A royal jelly protein is expressed in a subset of Kenyon cells in the mushroom bodies of the honey bee brain. *Naturwissenschaften* 85, 343-346.
- Kuhn, C., Muller, F., Melle, C., Nasheuer, H.P., Janus, F., Deppert, W., Grosse, F. (1999) Surface plasmon resonance measurements reveal stable complex formation between p53 and DNA polymerase alpha. *Oncogene* 18, 769-774.
- Lapidot Lifson, Y., Patinkin, D., Prody, C. A., Ehrlich, G., Seidman, S., Ben Aziz, R., Benseler, F., Eckstein, F., Zakut, H., Soreq, H. (1992). Cloning and antisense oligodeoxynucleotide inhibition of a human homolog of cdc2 required in hematopoiesis. *Proc Natl Acad Sci U S A* 89, 579-583.
- Laping, N.J., Nichols, N.R., Day, J.R., Johnson, S.A., Finch, C.E. (1994). Transcriptional control of glial fibrillary acidic protein and glutamine synthetase in vivo shows opposite responses to corticosterone in the hippocampus. *Endocrinology* 135, 1928-1933.
- Laskowski, M.B., Olson, W.H., Dettbarn, W.D. (1975) Ultrastructural changes at the motor end-plant produced by an irreversible cholinesterase inhibitor. *Exp Neurol* 47, 290-306.
- Layer PG, Willbold E (1995) Novel functions of cholinesterases in development, physiology and disease. *Prog Histochem Cytochem* 29: 1-94.

- Layer, P.G. (1995). Nonclassical roles of cholinesterases in the embryonic brain and possible links to Alzheimer disease. *Alzheimer Dis Assoc Disord* 9, 29-36.
- Layer, P.G., Willbold, E. (1995) Novel functions of cholinesterases in development, physiology and disease. *Prog Histochem Cytochem* 29, 1-99.
- Le Couteur, A., Bailey, A., Goode, S., Pickles, A., Robertson, S., Gottesman, I., Rutter, M. (1996). A broader phenotype of autism: the clinical spectrum in twins. *J Child Psychol Psychiatry* 37, 785-801.
- Lee, S.W., Sullenger, B.A. (1997). Isolation of a nuclease-resistant decoy RNA that can protect human acetylcholine receptors from myasthenic antibodies. *Nat Biotechnol* 15, 41-5.
- Legay, C., Bon, S., Vernier, P., Coussen, F., Massoulie, J. (1993). Cloning and expression of a rat acetylcholinesterase subunit: generation of multiple molecular forms and complementarity with a Torpedo collagenic subunit. *J Neurochem* 60, 337-346.
- Leonhardt, H. (1993). Male genital organs. In: *Color Atlas and Textbook of Human Anatomy*, W. Kahle, H. Leonhardt and W. Platzer, eds. (New York: Thieme Flexibooks), pp. 274-289.
- Lev-Lehman, E., Deutsch, V., Eldor, A., Soreq, H. (1997). Immature human megakaryocytes produce nuclear-associated acetylcholinesterase. *Blood* 89, 3644-3653.
- Lev-Lehman, E., Evron, T., Broide, E. S., Meshorer, E., Ariel, I., Seidman, S., Soreq, H. (2000). Synaptogenesis and myopathy under acetylcholinesterase overexpression. *J. Mol. Neurosci.* 14, 93-105.
- Li, Y., Camp, S., Rachinsky, T.L., Getman, D., Taylor, P. (1991). Gene structure of mammalian acetylcholinesterase. Alternative exons dictate tissue-specific expression. *J Biol Chem* 266, 23083-23090.
- Liberzon, I., Lopez, J.F., Flagel, S. B., Vazquez, D. M., Young, E.A. (1999). Differential regulation of hippocampal glucocorticoid receptors mRNA and fast feedback: relevance to post-traumatic stress disorder. *J Neuroendocrinol* 11, 11-17.
- Light, D.B., Schwiebert, E.M., Fejes-Toth, G., Naray-Fejes-Toth, A., Karlson, K.H., McCann, F. V., Stanton, B.A. (1990). Chloride channels in the apical membrane of cortical collecting duct cells. *Am J Physiol* 258, F273-280.
- Liliental, J., Chang, D.D. (1998) Rack1, a receptor for activated protein kinase C, interacts with integrin beta subunit. *J Biol Chem* 273, 2379-2383.
- Lindstrom, J. (1998) Mutations causing muscle weakness. *Proc Natl Acad Sci USA* 95, 9070-9071.
- Livneh, A., Sarova, I., Michaeli, D., Pras, M., Wagner, K., Zakut, H., Soreq, H. (1988). Antibodies against acetylcholinesterase and low levels of cholinesterases in a patient with an atypical neuromuscular disorder. *Clin Immunol Immunopathol* 48, 119-131.
- Lofas S, Johnsson B (1990) A novel hydrogel matrix on gold surfaces in surface plasmon resonance sensors for fast and efficient covalent immobilization of ligands. *J Chem Soc Chem Commun* 21: 1526-1528.
- Loke, S.L., Stein, C.A., Zhang, X.H., Mori, K., Nakanishi, M., Subasinghe, C., Cohen, J.S., Neckers, L.M. (1989). Characterization of oligonucleotide transport into living cells. *Proc Natl Acad Sci USA* 86, 3474-3478.
- Luo, Z.D., Wang, Y., Werlen, G., Camp, S., Chien, K.R., Taylor, P. (1999). Calcineurin enhances acetylcholinesterase mRNA stability during C2-C12 muscle cell differentiation. *Mol Pharmacol* 56, 886-894.

- Ma, M., Benimetskaya, L., Lebedeva, I., Dignam, J., Takle, G., Stein, C.A. (2000). Intracellular mRNA cleavage induced through activation of RNase P by nuclease-resistant external guide sequences. *Nat Biotechnol* 18, 58-61.
- Macek, T.A., Schaffhauser, H., Conn, P.J. (1998) Protein kinase C and A3 adenosine receptor activation inhibit presynaptic metabotropic glutamate receptor (mGluR) function and uncouple mGluRs from GTP-binding proteins. *J Neurosci* 18, 6138-6146.
- Marks, J.D., Griffiths, A.D., Malmqvist, M., Clackson, T.P., Bye, J.M., Winter, G. (1992) By-passing immunization: building high affinity human antibodies by chain shuffling. *Biotechnology* 10: 779-783.
- Marks, J.D., Hoogenboom, H.R., Bonnert, T.P., McCafferty, J., Griffiths, A.D., Winter, G. (1991) By-passing immunization. Human antibodies from V-gene libraries displayed on phage. *J Mol Biol* 222: 581-597.
- Martin, E.R., Menold, M.M., Wolpert, C.M., Bass, M.P., Donnelly, S.L., Ravan, S.A., Zimmerman, A., Gilbert, J.R., Vance, J.M., Maddox, L.O., Wright, H.H., Abramson, R.K., DeLong, G.R., Cuccaro, M.L., Pericak-Vance, M.A. (2000). Analysis of linkage disequilibrium in gamma-aminobutyric acid receptor subunit genes in autistic disorder. *Am J Med Genet* 96, 43-48.
- Massoulie, J., Anselmet, A., Bon, S., Krejci, E., Legay, C., Morel, N., Simon, S. (1998). Acetylcholinesterase: C-terminal domains, molecular forms and functional localization. *J Physiol (Paris)* 92, 183-190.
- Massoulie, J., Pezzenti, L., Bon, S., Krejci, E., Vallette, F.M. (1993) Molecular and cellular biology of cholinesterases. *Prog Neurobiol* 41, 31-91.
- Matsuyama, S., Llopis, J., Deveraux, Q.L., Tsien, R.Y., Reed, J.C. (2000). Changes in intramitochondrial and cytosolic pH: early events that modulate caspase activation during apoptosis. *Nat Cell Biol* 2, 318-325.
- Mbarek, O., Marouillat, S., Martineau, J., Barthelemy, C., Muh, J. P., Andres, C. (1999). Association study of the NF1 gene and autistic disorder. *Am J Med Genet* 88, 729-732.
- McEwen, B.S. (1999) Stress and hippocampal plasticity. *Annu Rev Neurosci*, 22, 105-122.
- McEwen, B.S., Sapolsky, R.M. (1995). Stress and cognitive function. *Curr Opin Neurobiol* 5, 205-216.
- McNamara, R.K., Wees, E.A., Lenox, R.H. (1999) Differential subcellular redistribution of protein kinase C isozymes in the rat hippocampus induced by kainic acid. *J Neurochem* 72, 1735-1743.
- Melchior, F., Paschal, B., Evans, J., Gerace, L. (1993). Inhibition of nuclear protein import by nonhydrolyzable analogues of GTP and identification of the small GTPase Ran/TC4 as an essential transport factor. *J Cell Biol* 123, 1649-1659.
- Meller, V.H., Davis, R.L. (1996). Biochemistry of insect learning: lessons from bees and flies. *Insect Biochem Mol Biol* 26, 327-335.
- Mello, C., Nottebohm, F., Clayton, D. (1995). Repeated exposure to one song leads to a rapid and persistent decline in an immediate early gene's response to that song in zebra finch telencephalon. *J Neurosci* 15, 6919-6925.
- Menzel, R., Erber, J., Mashur, T. (1974). Learning and memory in the honey bee. In: *Experimental Analysis of Insect Behavior*, L. B. Browne, ed. (Berlin: Springer-Verlag), pp. 195-218.
- Mobbs, P.G. (1985). Brain structure. In: *Comprehensive Insect Physiology, Biochemistry and Pharmacology*, G. A. Kerkut and L. W. Gilbert, eds. (Oxford: Pergamon), pp. 299-370.

- Mor, I., Grisaru, D., Titelbaum, L., Evron, T., Richler, C., Wahrman, J., Sternfeld, M., Yogev, L., Meiri, N., Seidman, S., Soreq, H. (2001). Modified testicular expression of stress-associated "readthrough" acetylcholinesterase predicts male infertility. *FASEB J.* 15, 2039-2041
- Moran, D., Shapiro, Y., Meiri, U., Laor, A., Epstein, Y., Horowitz, M. (1996). Exercise in the heat: Individual impacts of heat acclimation and exercise training on cardiovascular performance. *J. Therm Biol.* 21, 171-181.
- Munro, S., Pelham, H.R. (1986) An Hsp70-like protein in the ER: identity with the 78 kd glucose-regulated protein and immunoglobulin heavy chain binding protein. *Cell* 46: 291-300.
- Murata, J., Matsukawa, K., Shimizu, J., Matsumoto, M., Wada, T., Ninomiya, I. (1999). Effects of mental stress on cardiac and motor rhythms. *J Auton Nerv Syst* 75, 32-37.
- Muris, P., Steerneman, P., Merckelbach, H., Holdrinet, I., Meesters, C. (1998). Comorbid anxiety symptoms in children with pervasive developmental disorders. *J Anxiety Disord* 12, 387-393.
- Negro-Vilar, A. (1993). Stress and other environmental factors affecting fertility in men and women: overview. *Environ Health Perspect* 101 Suppl 2, 59-64.
- Neri, D., Carnemolla, B., Nissim, A., Leprini, A., Querze, G., Balza, E., Pini, A., Tarli, L., Halin, C., Neri, P., Zardi, L., Winter, G. (1997) Targeting by affinity-matured recombinant antibody fragments of an angiogenesis associated fibronectin isoform. *Nat Biotechnol* 15: 1271-1275.
- Newcomb, R.D., East, P.D., Russell, R.J., Oakeshott, J.G. (1996). Isolation of alpha cluster esterase genes associated with organophosphate resistance in *Lucilia cuprina*. *Insect Mol Biol* 5, 211-216.
- Nissim, A., Hoogenboom, H. R., Tomlinson, I. M., Flynn, G., Midgley, C., Lane, D., Winter, G. (1994). Antibody fragments from a 'single pot' phage display library as immunochemical reagents. *EMBO J* 13, 692-698.
- Nordberg, A., Hellstrom-Lindahl, E., Almkvist, O., Meurling, L. (1999) Activity of acetylcholinesterase in CSF increases in Alzheimer's patients after treatment with tacrine. *Alzheimer's Reports* 2: 347-352.
- Oh, M.M., Power, J.M., Thompson, L.T., Moriearty, P.L., Disterhoft, J.F. (1999). Metrifonate increases neuronal excitability in CA1 pyramidal neurons from both young and aging rabbit hippocampus. *J Neurosci* 19, 1814-1823.
- Ohno, K., Engel, A.G., Brengman, J.M., Shen, X.M., Heidenreich, F., Vincent, A., Milone, M., Tan, E., Demirci, M., Walsh, P., Nakano, S., Akiguchi, I. (2000). The spectrum of mutations causing end-plate acetylcholinesterase deficiency. *Ann Neurol* 47, 162-170.
- Ostlie, N.S., Karachunski, P.I., Wang, W., Monfardini, C., Kronenberg, M., Conti-Fine, B.M. (2001). Transgenic expression of IL-10 in T cells facilitates development of experimental myasthenia gravis. *J Immunol* 166, 4853-4862.
- Palmero, S., Bardi, G., Coniglio, L., Falugi, C. (1999). Presence and localization of molecules related to the cholinergic system in developing rat testis. *Eur J Histochem* 43, 277-283.
- Paola, D., Domenicotti, C., Nitti, M., Vitali, A., Borghi, R., Cottalasso, D., Zaccheo, D., Odetti, P., Strocchi, P., Marinari, U.M., Tabaton, M., Pronzato, M.A. (2000) Oxidative stress induces increase in intracellular amyloid beta-protein production and selective activation of betaI and betaII PKCs in NT2 cells. *Biochem Biophys Res Commun* 268, 642-646.
- Penn, A.S., Rowland, L.P. (1995). Myasthenia Gravis. In: *Meritt's Textbook of Neurology*, 9th Ed., L.P. Rowland, ed. (Baltimore: Williams and Wilkins), pp. 754-761.
- Perio, A., Terranova, J.P., Worms, P., Bluthe, R. M., Dantzer, R., Biziere, K. (1989). Specific modulation of social memory in rats by cholinomimetic and nootropic drugs, by

- benzodiazepine inverse agonists, but not by psychostimulants. *Psychopharmacology* 97, 262-268.
- Persic, L., Horn, I.R., Rybak, S., Cattaneo, A., Hoogenboom, H.R., Bradbury, A. (1999) Single-chain variable fragments selected on the 57-76 p21Ras neutralising epitope from phage antibody libraries recognise the parental protein. *FEBS Lett* 443: 112-116.
- Philippe, A., Martinez, M., Guilloud-Bataille, M., Gillberg, C., Rastam, M., Sponheim, E., Coleman, M., Zappella, M., Aschauer, H., Van Maldergem, L., Penet, C., Feingold, J., Brice, A., Leboyer, M., van Maldergerme, L. (1999). Genome-wide scan for autism susceptibility genes. Paris Autism Research International Sibpair Study. *Hum Mol Genet* 8, 805-812.
- Pinkas-Kramarski, R., Stein, R., Lindenboim, L., Sokolovsky, M. (1992) Growth factor-like effects mediated by muscarinic receptors in PC12M1 cells. *J Neurochem* 59, 2158-2166.
- Piven, J. (1997). The biological basis of autism. *Curr Opin Neurobiol*, 7, 708-712.
- Prince, F.P. (1992). Ultrastructural evidence of indirect and direct autonomic innervation of human Leydig cells: comparison of neonatal, childhood and pubertal ages. *Cell Tissue Res* 269, 383-390.
- Qian, X., Samadani, U., Porcella, A., Costa, R.H. (1995). Decreased expression of hepatocyte nuclear factor 3 alpha during the acute-phase response influences transthyretin gene transcription. *Mol Cell Biol* 15, 1364-1376.
- Raju, R., Zhan, W.Z., Karachunski, P., Conti-Fine, B., Sieck, G.C., David, C. (1998). Polymorphism at the HLA-DQ locus determines susceptibility to experimental autoimmune myasthenia gravis. *J Immunol* 160, 4169-4174.
- Risch, N., Spiker, D., Lotspeich, L., Nouri, N., Hinds, D., Hallmayer, J., Kalaydjieva, L., McCague, P., Dimiceli, S., Pitts, T., Nguyen, L., Yang, J., Harper, C., Thorpe, D., Vermeer, S., Young, H., Hebert, J., Lin, A., Ferguson, J., Chiotti, C., Wiese-Slater, S., Rogers, T., Salmon, B., Nicholas, P., Myers, R. M. et al. (1999). A genomic screen of autism: evidence for a multilocus etiology. *Am J Hum Genet* 65, 493-507.
- Roberson, E.D., English, J.D., Adams, J.P., Selcher, J.C., Kondratick, C., Sweatt, J.D. (1999) The mitogen-activated protein kinase cascade couples PKA and PKC to cAMP response element binding protein phosphorylation in area CA1 of hippocampus. *J Neurosci* 19, 4337-4348.
- Robinson, G. (1999). Integrative animal behaviour and sociogenomics. *Trends Ecol. Evol.* 14, 202-205.
- Robinson, G.E., Heurse, L.M., LeConte, Y., Lenquette, F., Hollingworth, R.M. (1999) Neurochemicals improve bee nestmate recognition *Nature* 399, 534-535.
- Robinson, G.E., Page, R. (1989). Genetic determination of nectar foraging, pollen foraging, and nest-site scouting in honey bee colonies. *Behav. Ecol. Sociobiol.* 24, 317-323.
- Roden, L.D., Myzka, D. (1996) Global analysis of a macromolecular interaction measured on BIAcore. *Biochem Biophys Res Comm* 225: 1073-1077.
- Rodier, P.M. (2000). The early origins of autism. *Sci Am* 282, 56-63.
- Rodier, P.M., Ingram, J.L., Tisdale, B., Nelson, S., Romano, J. (1996). Embryological origin for autism: developmental anomalies of the cranial nerve motor nuclei. *J Comp Neurol* 370, 247-261.
- Rodriguez, M.M., Ron, D., Touhara, K., Chen, C.H., Mochly-Rosen, D. (1999) RACK1, a protein kinase C anchoring protein, coordinates the binding of activated protein kinase C and select pleckstrin homology domains in vitro. *Biochemistry* 38, 13787-13794.
- Ron, D., Jiang, Z., Yao, L., Vagts, A., Diamond, I., Gordon, A. (1999) Coordinated movement of RACK1 with activated betaIIPKC. *J Biol Chem* 274, 27039-27046.

- Ron, D., Vagts, A.J., Dohrman, D.P., Yaka, R., Jiang, Z., Yao, L., Crabbe, J., Grisel, J.E., Diamond, I. (2000) Uncoupling of betaIIIPKC from its targeting protein RACK1 in response to ethanol in cultured cells and mouse brain. *FASEB J* 14, 2303-2314.
- Rotundo, R.L. (1990). Nucleus-specific translation and assembly of acetylcholinesterase in multinucleated muscle cells. *J Cell Biol* 110, 715-719.
- Sanes, J.R., Lichtman, J.W. (1999) Development of the vertebrate neuromuscular junction. *Ann. Rev. Neurosci.* 22, 389-442.
- Sapolsky, R.M., Romero, L.M., Munck, A.U. (2000). How do glucocorticoids influence stress responses? Integrating permissive, suppressive, stimulatory, and preparative actions. *Endocr Rev* 21, 55-89.
- Sarkar, R., Mohanakumar, K.P., Chowdhury, M. (2000). Effects of an organophosphate pesticide, quinalphos, on the hypothalamo- pituitary-gonadal axis in adult male rats. *J Reprod Fertil* 118, 29-38.
- Schneider, L.S. (2001) Treatment of Alzheimer's disease with cholinesterase inhibitors. *Clin Geriatr Med* 17: 337-358.
- Schonbeck, S., Chrestel, S., Hohlfeld, R. (1990) Myasthenia gravis: prototype of the antireceptor autoimmune diseases. *Int Rev Neurobiol* 32, 175-200.
- Schwiebert, E.M., Karlson, K.H., Friedman, P.A., Dietl, P., Spielman, W.S., Stanton, B.A. (1992). Adenosine regulates a chloride channel via protein kinase C and a G protein in a rabbit cortical collecting duct cell line. *J Clin Invest* 89, 834-841.
- Seidman, S., Ben Aziz-Aloya, R., Timberg, R., Loewenstein, Y., Velan, B., Shafferman, A., Liao, J., Norgaard-Pedersen, B., Brodbeck, U., Soreq, H. (1994). Overexpressed monomeric human acetylcholinesterase induces subtle ultrastructural modifications in developing neuromuscular junctions of *Xenopus laevis* embryos. *J Neurochem* 62, 1670-1681.
- Seidman, S., Eckstein, F., Grifman, M., Soreq, H. (1999). Antisense technologies have a future fighting neurodegenerative diseases. *Antisense Nucleic Acid Drug Dev* 9, 333-340.
- Seidman, S., Sternfeld, M., Ben Aziz Aloya, R., Timberg, R., Kaufer Nachum, D., Soreq, H. (1995) Synaptic and epidermal accumulations of human acetylcholinesterase are encoded by alternative 3'-terminal exons. *Mol Cell Biol* 15, 2993-3002.
- Sekiguchi, R., Wolterink, G., and van Ree, J.M. (1991). Short duration of retroactive facilitation of social recognition in rats. *Physiol Behav* 50, 1253-1256.
- Shannon, H., Peters, S.C. (1990). A comparison of the effects of cholinergic and dopaminergic agents on scopolamine-induced hyperactivity in mice. *J Pharmacol Exp Ther* 255, 549-553.
- Shapira, M., Seidman, S., Sternfeld, M., Timberg, R., Kaufer, D., Patrick, J., Soreq, H. (1994). Transgenic engineering of neuromuscular junctions in *Xenopus laevis* embryos transiently overexpressing key cholinergic proteins. *Proc Natl Acad Sci U S A* 91, 9072-9076.
- Shapira, M., Grant, A., Korner, M., Soreq, H. (2000). Genomic and transcriptional characterization of the human ACHE locus: complex involvement with acquired and inherited diseases. *Isr Med Assoc J* 2, 470-473.
- Shapira, M., Tur-Kaspa, I., Bosgraaf, L., Livni, N., Grant, A.D., Grisar, D., Korner, M., Ebstein, R.P., Soreq, H. (2000). A transcription-activating polymorphism in the ACHE promoter associated with acute sensitivity to anti-acetylcholinesterases. *Hum Mol Genet* 9, 1273-1281.
- Shapira, J., Thompson, C.K., Soreq, H., Robinson, G.E. (2001). Changes in neuronal acetylcholinesterase gene expression and division of labor in honey bee colonies. *J. Mol. Neurosci.* 17,1-12.

- Sharma, K.V., Bigbee, J.W. (1998) Acetylcholinesterase antibody treatment results in neurite detachment and reduced outgrowth from cultured neurons: further evidence for a cell adhesive role for neuronal acetylcholinesterase. *J Neurosci Res* 53, 454-464.
- Shoham, S., Ebstein, R.P. (1997) The distribution of beta-amyloid precursor protein in rat cortex after systemic kainate-induced seizures. *Exp Neurol* 147, 361-376.
- Shohami, E., Kaufer, D., Chen, Y., Seidman, S., Cohen, O., Ginzberg, D., Melamed-Book, N., Yirmiya, R., Soreq, H. (2000). Antisense prevention of neuronal damages following head injury in mice. *J. Mol. Med.* 78, 228-236.
- Sirevaag, A.M., Black, J.E., Greenough, W.T. (1991). Astrocyte hypertrophy in the dentate gyrus of young male rats reflects variation of individual stress rather than group environmental complexity manipulations. *Exp Neurol* 111, 74-79.
- Sitaraman, S., Metzger, D.W., Belloto, R.J., Infante, A.J., Wall, K.A. (2000). Interleukin-12 enhances clinical experimental autoimmune myasthenia gravis in susceptible but not resistant mice. *J Neuroimmunol* 107, 73-82.
- Slotkin, T.A., McCook, E.C., Seidler, F.J. (1997) Cryptic brain cell injury caused by fetal nicotine exposure is associated with persistent elevations of c-fos protooncogene expression. *Brain Res* 750, 180-188.
- Smalley, S.L., Asarnow, R.F., Spence, M.A. (1988). Autism and genetics. A decade of research. *Arch Gen Psychiatry* 45, 953-961.
- Smith, T.F., Gaitatzes, C., Saxena, K., Neer, E.J. (1999) The WD repeat: a common architecture for diverse functions. *Trends Biochem Sci* 24, 181-185.
- Soreq, H., Glick, D. (2000). Novel roles for cholinesterases in stress and inhibitor responses. In: *Cholinesterases and Cholinesterase Inhibitors*, E. Giacobini, ed. (London: Martin Dunitz), pp. 47-61.
- Soreq, H., Seidman, S. (2001). Acetylcholinesterase--new roles for an old actor. *Nat Rev Neurosci* 2, 294-302.
- Sousa, N., Lukoyanov, N., Madeira, M., Almeida, O., Paula-Barbosa, M. (2000) Reorganization of the morphology of hippocampal neurites and synapses after stress-induced damage correlates with behavioral improvement. *Neuroscience* 97, 253-266.
- Steffenburg, S., Gillberg, C., Hellgren, L., Andersson, L., Gillberg, I. C., Jakobsson, G., Bohman, M. (1989). A twin study of autism in Denmark, Finland, Iceland, Norway and Sweden. *J Child Psychol Psychiatry* 30, 405-416.
- Sternfeld M, Ming G, Song H, Sela K, Timberg R, Poo M, Soreq H (1998) Acetylcholinesterase enhances neurite growth and synapse development through alternative contributions of its hydrolytic capacity, core protein, and variable C termini. *J Neurosci* 18: 1240-1249.
- Sternfeld, M., Patrick, J.D., Soreq, H. (1998) Position effect variegations and brain-specific silencing in transgenic mice overexpressing human acetylcholinesterase variants. *J Physiol (Paris)*, 92, 249-255.
- Sternfeld, M., Shoham, S., Klein, O., Flores-Flores, C., Evron, T., Idelson, G.H., Kitsberg, D., Patrick, J.W., Soreq, H. (2000). Excess "readthrough" acetylcholinesterase attenuates but the "synaptic" variant intensifies neurodeterioration correlates. *Proc. Natl. Acad. Sci. USA* 97, 8647-8652.
- Stevens, C.F., Sullivan, J.M. (1998) Regulation of the readily releasable vesicle pool by protein kinase C. *Neuron* 21, 885-893.
- Suer, C., Dolu, N., Ozesmi, C., Yilmaz, A., Sahin, O. (1998). Effect of reversed light-dark cycle on skin conductance in male rats. *Percept Mot Skills* 87, 1267-1274.

- Swash, M. (1975) Motor innervation of myasthenic muscles. *Lancet* 2, 663.
- Tainer, J.A., Getzoff, E.D., Alexander, H., Houghten, R.A., Olson, A.J., Lerner, R.A., Hendrickson, W.A. (1984) The reactivity of anti-peptide antibodies is a function of the atomic mobility of sites in a protein. *Nature* 312: 127-134.
- Taylor, P. (1996) Agents acting at the neuromuscular junction and autonomic ganglia. In: Hardman, J.G., Limbird, L.E., Molinoff, P.B., Ruddon, R.W. (eds.), *Goodman and Gilman's The Pharmacological Basis of Therapeutics*. McGraw-Hill, New York, pp. 177-197.
- Taylor, P., Radic, Z., Hosea, N. A., Camp, S., Marchot, P., Berman, H.A. (1995). Structural bases for the specificity of cholinesterase catalysis and inhibition. *Toxicol Lett* 82-83, 453-458.
- Thor, D.H., Holloway, W.R. (1982). Social memory of the male laboratory rat. *J Comp Psychol* 96, 1000-1006.
- Thornton, J.M., Edwards, M.S., Taylor, W.R., Barlow, D.J. (1986) Location of "continuous" antigenic determinants in the protruding regions of proteins. *EMBO J* 5: 409-413.
- Tielemans, E., van Kooij, R., te Velde, E.R., Burdorf, A., Heederik, D. (1999). Pesticide exposure and decreased fertilisation rates in vitro. *Lancet* 354, 484-485.
- Tint, I.S., Bonder, E.M., Feder, H.H., Reboulleau, C.P., Vasiliev, J.M., Gelfand, I.M. (1992) Reversible structural alterations of undifferentiated and differentiated human neuroblastoma cells induced by phorbol ester. *Proc Natl Acad Sci USA* 89, 8160-8164.
- Toma, D.P., Bloch, G., Moore, D., Robinson, G.E. (2000). Changes in period mRNA levels in the brain and division of labor in honey bee colonies. *Proc Natl Acad Sci U S A* 97, 6914-6919.
- Tomlinson IM, Walter G, Marks JD, Llewelyn MB, Winter G. (1992) The repertoire of human germline V<sub>H</sub> sequences reveals about fifty groups of V<sub>H</sub> segments with different hypervariable loops. *J Mol Biol* 227: 776-798.
- Tordjman, S., Anderson, G.M., McBride, P.A., Hertzog, M.E., Snow, M.E., Hall, L.M., Thompson, S.M., Ferrari, P., Cohen, D.J. (1997). Plasma beta-endorphin, adrenocorticotropin hormone, and cortisol in autism. *J Child Psychol Psychiatry* 38, 705-715.
- Tronche, F., Kellendonk, C., Kretz, O., Gass, P., Anlag, K., Orban, P., Bock, R., Klein, R., Schutz, G. (1999) Disruption of the glucocorticoid receptor gene in the nervous system results in reduced anxiety. *Nat Genet* 23, 99-103.
- Ulevitch, R.J., Tobias, P.S. (1994). Recognition of endotoxin by cells leading to transmembrane signaling. *Curr Opin Immunol* 6, 125-130.
- van der Heiden, M.G., Thompson, C.B. (1999). Bcl-2 proteins: regulators of apoptosis or of mitochondrial homeostasis? *Nat Cell Biol* 1, E209-E216.
- Vaughan, T.J., Williams, A.J., Pritchard, K., Osbourn, J.K., Pope, A.R., Earnshaw, J.C., McCafferty, J., Hodits, R.A., Wilton, J., Johnson, K.S. (1996) Human antibodies with sub-nanomolar affinities isolated from a large non-immunized phage display library. *Nat Biotechnol* 14: 309-314.
- Vereker, E., O'Donnell, E., Lynch, M.A. (2000) The inhibitory effect of interleukin-1beta on long-term potentiation is coupled with increased activity of stress-activated protein kinases. *J Neurosci* 20, 6811-6819.
- Vincent, A. (1999). Immunology of the neuromuscular junction and presynaptic nerve terminal. *Curr Opin Neurol* 12, 545-551.
- Wagener-Hulme, C., Kuehn, J. C., Schulz, D.J., Robinson, G.E. (1999). Biogenic amines and division of labor in honey bee colonies. *J Comp Physiol [A]* 184, 471-479.

- Wahlstrom, J., Steffenburg, S., Hellgren, L., Gillberg, C. (1989). Chromosome findings in twins with early-onset autistic disorder. *Am J Med Genet* 32, 19-21.
- Wang, J.H., Feng, D.P. (1992) Postsynaptic protein kinase C essential to induction and maintenance of long-term potentiation in the hippocampal CA1 region. *Proc Natl Acad Sci USA* 89, 2576-2580.
- Weeber, E.J., Atkins, C.M., Selcher, J.C., Varga, A.W., Mirnikjoo, B., Paylor, R., Leitges, M., Sweatt, J.D. (2000) A role for the beta isoform of protein kinase C in fear conditioning. *J Neurosci* 20, 5906-5914.
- Weiner, M. F., Vobach, S., Olsson, K., Svetlik, D., Risser, R.C. (1997). Cortisol secretion and Alzheimer's disease progression. *Biol Psychiatry* 42, 1030-1038.
- Wing, L., Gould, J. (1979). Severe impairments of social interaction and associated abnormalities in children: epidemiology and classification. *J Autism Dev Disord* 9, 11-29.
- Winslow, J.T., Camacho, F. (1995). Cholinergic modulation of a decrement in social investigation following repeated contacts between mice. *Psychopharmacology (Berl)* 121, 164-172.
- Winston M: *The Biology of the Honey Bee*. Cambridge, MA: Harvard University Press; 1987.
- Wirguin, I., Brenner, T., Sicsic, C., Argov, Z. (1994). Variable effect of calcium channel blockers on the decremental response in experimental autoimmune myasthenia gravis. *Muscle Nerve* 17, 523-527.
- Withers, G.S., Fahrbach, S.E., Robinson, G.E. (1993). Selective neuroanatomical plasticity and division of labour in the honeybee. *Nature* 364, 238-240.
- Wright, C.I., Geula, C., Mesulam, M.M. (1993) Neurological cholinesterases in the normal brain and in Alzheimer's disease: relationship to plaques, tangles, and patterns of selective vulnerability. *Ann Neurol* 34: 373-384.
- Wu, H., Lima, W.F., Crooke, S.T. (1999). Properties of cloned and expressed human RNase H1. *J Biol Chem* 274, 28270-28278.
- Xie, J., McCobb, D.P. (1998). Control of alternative splicing of potassium channels by stress hormones. *Science* 280, 443-446.
- Xu, B.Y., Huang, D., Pirskanen, R., Lefvert, A.K. (2000). beta2-adrenergic receptor gene polymorphisms in myasthenia gravis (MG). *Clin Exp Immunol* 119, 156-160.
- Xu, L., Anwyl, R., Rowan, M.J. (1997) Behavioural stress facilitates the induction of long-term depression in the hippocampus. *Nature*, 387, 497-500.
- Yarwood, S.J., Steele, M.R., Scotland, G., Houslay, M.D., Bolger, G.B. (1999) The RACK1 signaling scaffold protein selectively interacts with the cAMP-specific phosphodiesterase PDE4D5 isoform. *J Biol Chem* 274, 14909-14917.
- Yirmiya, R., Barak, O., Avitsur, R., Gallily, R., Weidenfeld, J. (1997). Intracerebral administration of *Mycoplasma fermentans* produces sickness behavior: role of prostaglandins. *Brain Res* 749, 71-81.
- Young, R.J., Laing, J.C. (1991). The binding characteristics of cholinergic sites in rabbit spermatozoa. *Mol Reprod Dev* 28, 55-61.
- Zhang, G.X., Xiao, B. G., Bai, X.F., van der Meide, P.H., Orn, A., Link, H. (1999). Mice with IFN-gamma receptor deficiency are less susceptible to experimental autoimmune myasthenia gravis. *J Immunol* 162, 3775-3781.
- Zhang, Q., Wang, X., Wolgemuth, D.J. (1999). Developmentally regulated expression of cyclin D3 and its potential in vivo interacting proteins during murine gametogenesis. *Endocrinology* 140, 2790-2800.

- Zhou, A., Hassel, B.A., Silverman, R.H. (1993). Expression cloning of 2-5A-dependent RNAase: a uniquely regulated mediator of interferon action. *Cell* 72, 753-765.
- Zhou, A., Paranjape, J., Brown, T.L., Nie, H., Naik, S., Dong, B., Chang, A., Trapp, B., Fairchild, R., Colmenares, C., Silverman, R.H. (1997). Interferon action and apoptosis are defective in mice devoid of 2',5'-oligoadenylate-dependent RNase L. *EMBO J* 16, 6355-6363.
- Ziegler, R., Engler, D.L., Davis, N.T. (1995). Biotin-containing proteins of the insect nervous system, a potential source of interference with immunocytochemical localization procedures. *Insect Biochem Mol Biol* 25, 569-574.



REPLY TO  
ATTENTION OF

DEPARTMENT OF THE ARMY  
OFFICE OF THE SURGEON GENERAL  
5109 LEESBURG PIKE  
FALLS CHURCH VA 22041-3258



JUL 20 2001

Office of Regulatory  
Compliance and Quality

SUBJECT: Protocol Entitled, "Acute and Long-Term Neurological Consequences of Anticholinesterase Exposure in Humans," Submitted by Hermona Soreq, Ph.D., The Alexander Silberman Institute of Life Sciences, Hebrew University of Jerusalem, Givat-Ram, Jerusalem, Israel, and Alon Friedman, M.D., Soroka University Medical Center, Beersheva, Israel, Proposal Log Number 98222016, Award Number DAMD17-99-1-9547, HSRRB Log Number A-9139

Hermona Soreq, Ph.D.  
The Alexander Silberman Institute of Life Sciences  
Hebrew University of Jerusalem  
Department of Biological Chemistry  
Jerusalem 91904  
Israel

Dear Doctor Soreq:

The subject protocol was reviewed at The Surgeon General's Human Subjects Research Review Board (HSRRB) meeting on July 11, 2001 for compliance with applicable human subjects protection regulations. It is requested that you make revisions in accordance with the enclosed recommendations. Final approval will be granted only if revisions are made to the protocol, the consent forms, the assent forms, the sample donation form, the data collection/recording form, and the advertisements/recruitment posters.

You are reminded not to initiate this study until you receive approval from the Contracting Officer and not to construe this correspondence as approval for any additional contract funding. Only the Contracting Officer can commit Federal government funds.

Submit your revisions as soon as possible by facsimile to (301) 619-7803 (Attention: Doctor Pranulis), by electronic mail to [maryann.pranulis@det.amedd.army.mil](mailto:maryann.pranulis@det.amedd.army.mil), or by mail to Commanding General, U.S. Army Medical Research and Materiel Command, ATTN: MCMR-RCQ-HR (Doctor Pranulis), 504 Scott Street, Fort Detrick, Maryland 21702-5012.

Please contact Doctor Pranulis at (301) 619-6237 for questions concerning this correspondence.

Sincerely,

*Julie K. Zadinsky*

Julie K. Zadinsky  
Colonel, Army Nurse Corps  
Acting Chair, Human Subjects  
Research Review Board

-2-

Enclosure

Copies Furnished:

U.S. Army Medical Research and Materiel Command, ATTN: MCMR-SGS (wo/enclosure)  
U.S. Army Medical Research and Materiel Command, ATTN: MCMR-PLC  
(Lieutenant Colonel Friedl) (w/enclosure)  
U.S. Army Medical Research Acquisition Activity, ATTN: MCMR-AAA-A (Ms. Labella)  
(w/enclosure)  
Zlotowski Center of Neuroscience, Soroka University Medical Center, ATTN: Doctor Friedman

**"Acute and Long-Term Neurological Consequences of Anticholinesterase Exposure in Humans," Submitted by Hermona Soreq, Ph.D., The Alexander Silberman Institute of Life Sciences, Hebrew University of Jerusalem, Givat-Ram, Jerusalem, Israel, and Alon Friedman, M.D., Soroka University Medical Center, Beersheva, Israel, Proposal Log Number 98222016, Award Number DAMD17-99-1-9547, HSRRB Log Number A-9139**

BOARD MEMBERS' RECOMMENDATIONS: Board members recommended approving this protocol with modifications. The Principal Investigator should address the following issues and submit a revised protocol and related documents to the Acting Chair, HSRRB.

a. Required documents and information.

- (1) Current CV for the neurologist who is joining the team of investigators.
- (2) Revised protocols for the prospective and retrospective studies that meet all of the human subjects protection regulations and adequately address the recommendations listed below.
- (3) Revised consent forms (prospective study and retrospective study), adult versions, that meets all of the human subjects protection regulations and adequately address the recommendations listed below.
- (4) Revised assent form, adolescent version, that meets all of the human subjects protection regulations and adequately addresses the recommendations listed below.
- (5) Revised assent form, child version, that meets all of the human subjects protection regulations and adequately addresses the recommendations listed below.
- (6) Revised sample donation form that meets all of the human subjects protection regulations and adequately addresses the recommendations listed below.
- (7) Documentation of ministry of health approval, English translation.
- (8) Completion of SPA application (biographical sketches for the members of the committee need to be submitted; all other documents are on file).
- (9) Documentation of Soroka University's IRB (Helsinki Committee) review and approval of the HSRRB-required revisions (pending approval of the HSRRB).

b. Revisions to be made to the prospective study protocol.

- (1) Include the neurologist as a member of the study team and provide a description of her role in the research role responsibilities.
- (2) Clarify who will be completing the detailed questionnaire pertaining to the patient's medical status on visits 3 thru 6 in the prospective protocol.
- (3) Clarify pregnancy as a criterion for exclusion only for the acute poisoning state. Provide adequate, empirically based justification for this exclusion.

incl

**“Acute and Long-Term Neurological Consequences of Anticholinesterase Exposure in Humans,” Submitted by Hermona Soreq, Ph.D., The Alexander Silberman Institute of Life Sciences, Hebrew University of Jerusalem, Givat-Ram, Jerusalem, Israel, and Alon Friedman, M.D., Soroka University Medical Center, Beersheva, Israel, Proposal Log Number 98222016, Award Number DAMD17-99-1-9547, HSRRB Log Number A-9139**

(4) Clarify in the recruitment/consent process that the adult patient will not be invited to participate in the study until she or he is clinically stable and capable of consenting for self.

(5) Clarify in the consent process that surrogate consent will not be sought for adult patients who are not able to consent for self.

(6) In the consent procedures describe how the illiterate patient will be informed about the study and how verbal consent will be obtained, verified, and documented.

(7) In the consent procedures describe how the patient's wishes will be respected in relation to whether or not she or he consents to future use of the specimens and the desire to be informed/consented in advance of use.

(8) In the assent procedures clarify which tests will be done for which age group.

(9) Clarify in the study procedures how the researchers will coordinate the study procedures with the patient's clinical testing to avoid subjecting the patient to unnecessary duplication of testing.

(10) In the study procedures correct the statements about the duration of the study. Indicate how long study enrollment will be open (when you will stop enrolling patients), how long the patient will participate in the study, and when the final data collection will be completed for the last patients that are enrolled in the study.

(11) In the study procedures indicate clearly what procedures will be done on the initial evaluation, what ones will be done weekly if the patient remains hospitalized, and what ones will be done just prior to hospital discharge.

(12) Clarify in the benefit section that the patient will be informed about the results of the study tests and that a written report will be provided to the patient's attending physician.

(13) Describe how the children will have the developmental testing, by whom, and under what conditions. If this will be done by referral to another service, provide documentation of the availability of the referral service. If the developmental testing is routinely done as a standard of care, then remove it from the list of research participation benefits.

(14) Clarify how the identifiers on the data will be addressed and how this will be coordinated with the DOD VRDB.

(15) Add the Serious Adverse Events Clause 1.02 [(AR 70-25, 2-5(C), 2-9(C)(4); OTSG 15-2, 4(e)(2)].

**"Acute and Long-Term Neurological Consequences of Anticholinesterase Exposure in Humans," Submitted by Hermona Soreq, Ph.D., The Alexander Silberman Institute of Life Sciences, Hebrew University of Jerusalem, Givat-Ram, Jerusalem, Israel, and Alon Friedman, M.D., Soroka University Medical Center, Beersheva, Israel, Proposal Log Number 98222016, Award Number DAMD17-99-1-9547, HSRRB Log Number A-9139**

c. Revisions to be made to the retrospective study protocol.

(1) Include the neurologist as a member of the study team and provide a description of her role in the research role responsibilities.

(2) Clarify who will be completing the detailed questionnaire pertaining to the patient's medical status on visit 1 in the retrospective protocol.

(3) Eliminate pregnancy as a criterion for exclusion.

(4) In the consent procedures describe how the illiterate patient will be informed about the study and how verbal consent will be obtained, verified, and documented.

(5) In the consent procedures describe how the patient's wishes will be respected in relation to whether or not she or he consents to future use of the specimens and the desire to be informed/consented in advance of use.

(6) In the assent procedures clarify which tests will be done for which age group.

(7) Clarify in the study procedures how the researchers will coordinate the study procedures with the patient's clinical testing to avoid subjecting the patient to unnecessary duplication of testing.

(8) Clarify in the benefit section that the patient will be informed about the results of the study tests and that a written report will be provided to the patient's attending physician.

(9) Describe how the children will have the developmental testing, by whom, and under what conditions. If this will be done by referral to another service, provide documentation of the availability of the referral service. If the developmental testing is routinely done as a standard of care, then remove it from the list of research participation benefits.

(10) Clarify how the identifiers on the data will be addressed and how this will be coordinated with the DOD VRDB.

(11) Add the Serious Adverse Events Clause 1.02 (AR 70-25, 2-5(C), 2-9(C)(4); OTSG 15-2, 4(e)(2).

d. Revisions to be made to the adult (or parent) version of the prospective study consent form.

(1) Eliminate pregnancy that occurs subsequent to enrollment in the study (the time of acute poisoning and hospitalization) as an exclusionary criterion.

**"Acute and Long-Term Neurological Consequences of Anticholinesterase Exposure in Humans," Submitted by Hermona Soreq, Ph.D., The Alexander Silberman Institute of Life Sciences, Hebrew University of Jerusalem, Givat-Ram, Jerusalem, Israel, and Alon Friedman, M.D., Soroka University Medical Center, Beersheva, Israel, Proposal Log Number 98222016, Award Number DAMD17-99-1-9547, HSRRB Log Number A-9139**

(2) Eliminate imaging as a benefit for children under 12: offer parents the option of having the MRI imaging done for children under 12.

(3) Eliminate BCT imaging as a benefit: this is a clinical not a research procedure.

(4) Clarify the genetic counseling and the language about the impact/usefulness of this information on their decisions about whether or not to have children.

(5) Include a description of the types of symptoms the patient might experience if she or he were sensitive to succinylcholine

(6) Include information about the institutional point of contact (e.g., Helsinki Committee) that the patient can contact for questions about his or her rights as a research subject, to report research-related injury, and request withdrawing from the study or to have their samples withdrawn from storage.

(7) Clarify which procedures will be done for children under 12 years of age.

(8) Add a statement that the investigator may terminate a subject's participation in the study and describe the possible reasons for this.

(9) Use the second person voice throughout the consent form.

e. Revisions to be made to the adult (or parent) version of the retrospective study consent

## The stress-induced “readthrough” acetylcholinesterase variant displays distinctive neurochemical properties

Asher Y. Salmon, Dalia Ginzberg, Meira Sternfeld, Inbal Mor, David Glick and Hermona Soreq  
Department of Biological Chemistry, Institute of Life Sciences, The Hebrew University of  
Jerusalem, Safra Campus, Jerusalem, Israel, 91904.

Address correspondence to: Hermona Soreq, Institute of Life Sciences, Hebrew University of  
Jerusalem, 91904 Israel; tel. 972-2-6585109; fax. 972-2-6520258; e-mail  
soreq@shum.huji.ac.il.

24 pages; 4 figures; 2 tables; 31 references, 250 abstract words; 46,827 characters

### Abbreviations:

*ACHE*, the acetylcholinesterase gene  
AChE, acetylcholinesterase  
AChE-C, core AChE, encoded by exons E2, E3 and E4  
AChE-E, erythrocytic AChE, encoded by E2, E3, E4 and E5  
AChE-R, “readthrough” AChE, encoded by E2, E3, E4 and I4  
AChE-S, synaptic AChE, encoded by E2, E3, E4 and E6  
ATCh, acetylthiocholine  
BuChE, butyrylcholinesterase  
ChE, cholinesterase  
CMV, cytomegalovirus  
DFP, diisopropylfluorophosphonate  
G1, globular monomer (of AChE)  
G2, globular dimer (of AChE)  
G4, globular tetramer (of AChE)  
iso-OMPA, tetraisopropylpyrophosphoramidate

There is strong evidence for an mRNA that encodes an acetylcholinesterase variant, AChE-R, which arises from readthrough of the pseudo-intron I4, but characterization of the protein has been hampered by its low level of expression. To address this issue, we have now expressed human AChE-R in the milk and muscle of transgenic mice. In electrophoresis it behaves as a 62 kDa protein, and sucrose gradient centrifugation shows that it is monomeric. An anti-human AChE-R that cross-reacts with mouse AChE-R has allowed the finding that under stress, endogenous mouse AChE-R constitutes a large fraction of the newly-expressed protein. The catalytic activity of transgenic human AChE-R was characterized by its susceptibility to inhibition by a number of organophosphate and carbamate inhibitors. While the actions of some anti-AChEs were the same on all AChE variants, others were not; rivastigmine, an anti-AChE used for the treatment of Alzheimer’s disease, inhibited AChE-R significantly more strongly than it did other variants. Because variants differ only in their C-terminal sequences, a new transgenic variant was created, one truncated at the point in the sequence where the identity of the natural variants ends. To clarify the role of the C-terminal sequences in the interaction with inhibitors, this core protein, AChE-C, was compared to the other variants. Its closer similarity to AChE-R than to AChE-S, suggests an involvement of the C-terminus in inhibitor interactions. We conclude that stress, through changes in alternative splicing, may modify the properties of brain AChE, as well as its sensitivity to some anti-AChE agents.

## Introduction

Alternative splicing of the nascent acetylcholinesterase (AChE) transcript gives rise to three 3 variant mRNAs (1-3). One encodes the synaptic form, AChE-S, another the erythrocytic form, AChE-E, and a third incorporates pseudo-intron I4 and forms the readthrough variant, AChE-R (4). AChE-S and AChE-E are well known and quite thoroughly studied, but the characterization of AChE-R lags behind, largely because it is normally present in very low amounts. In order to obtain sufficient quantities of this protein, we have tried the biopharming approach, and have begun by creating a line of transgenic mice that secrete the variant in their milk and muscle. Even so, the very limited quantities of the enzyme that are thus available allow only an initiation of its biochemical characterization.

AChE-R is of particular interest because its synthesis is up-regulated under stress, exposure to inhibitors of AChE and head injury (5-8). Unlike AChE-S and AChE-E, it is only monomeric and, thanks to its hydrophilic C-terminus, it is soluble. We have assumed that the increase in AChE-R offers short-term protection under stress and AChE inhibition (5). Its long-term protection from stress-induced neuropathology was subsequently demonstrated in transgenic mice (9). However, acute excess AChE-R overexpression was shown to be detrimental following head injury (6). We now report that AChE-R has its own distinctive inhibitor specificity profile. This demonstrates involvement of the C-terminus of AChE variants in ligand interactions.

## Methods

**Chemicals:** Human AChE-E, recombinant human AChE-S, tetraisopropylpyrophosphoramidate (iso-OMPA), acetylthiocholine (ATCh), pyridostigmine, tacrine (Cognex™, Parke Davis/Warner-Lambert), diisopropylfluorophosphonate (DFP), diethyl-*p*-nitrophenylphosphonate (paraoxon) and oxytocin were purchased from Sigma Chemical Co. (St. Louis, MO, USA). Rivastigmine (Exelon™, Novartis) was a gift of Dr. M. Weinstock (Jerusalem, Israel). Donepezil (Aricept™, Pfizer) was purchased commercially. Monoclonal mouse anti-human AChE antibodies were provided by Dr. Norgaard-Pedersen (Copenhagen, Denmark). Goat anti-rabbit and donkey anti-mouse, horseradish peroxidase-conjugated antibodies and ECL detection kit were purchased from Santa Cruz Biotechnology (Santa Cruz, CA, USA).

**Transgenic animals** included FVB/N mice carrying transgenic human (h) AChE-S cDNA under control of the proximal 600 bp of the human *ACHE* promoter (10), transgenics that strongly express hAChE-R under the cytomegalovirus (CMV) promoter (lines 45 and 70) (9) and an additional line of FVB/N transgenics expressing a truncated protein, hAChE-C, that retains only the core common to all variants, also under the CMV promoter (for a description of the hAChE-C transgene, see ref. 11). Confined swim stress, anti-AChE exposure and isolation of the brain of these animals were as described (5); homogenates prepared from these brains were kept at -70°C until use.

**Milk collection** was from nursing mice 7 days after parturition. Two hr following separation from their pups, the dams were injected with 0.3 I.U. oxytocin. Ten min later, the mammary glands were gently massaged and milk was collected in a capillary tube, diluted 1:4 with double distilled water, centrifuged to allow removal of lipid droplets and stored at -20°C.

**AChE-R antibodies:** Polyclonal rabbit antibodies against the C-terminal sequence of hAChE-R were prepared as described (9). Because of the extensive homology of the two enzymes, the antibody cross-reacted with the mouse enzyme.

**AChE activity and inhibitor assays:** AChE activity measurements and inhibition studies were performed in tissue homogenates or immunoadsorption-purified enzyme preparations, as described (11,12). For reversible inhibitors we used concentration ranges of 6 orders of magnitude and calculated  $K_i$  values by the method of Hobbiger and Peck (13), based on a  $K_m$  value of 0.14 mM ATCh for human AChE (9,14). For irreversible inhibitors, we used an antibody-coated microtiter plate assay as described (12). Protein concentrations were determined using the Bio-Rad DC Protein Assay kit (Bio-Rad Laboratories, Hercules, CA, USA). Enzyme rate data at low substrate concentration were used to determine an inhibitory efficiency for the irreversible inhibitors. The pseudo-first order inhibition rate constants at low concentration (i.e. low compared to the dissociation constant,  $K_i$ , of the reversible pre-reaction enzyme-inhibitor complex) are divided by the inhibitor concentration; this is the inhibitory efficiency,  $k_i/K_i$ , where  $k_i$  is the true first order rate constant for the conversion of the reversible enzyme-inhibitor complex to the irreversible complex. This is analogous to the treatment used to obtain the bimolecular rate constant for enzyme-substrate interaction, often called the catalytic efficiency,  $k_{cat}/K_m$ . In cases where the rate constants had been determined by other laboratories (14,15), the values we present are close, but identity cannot be expected because of the very different methods of their measurement.

**Polyacrylamide gel electrophoresis:** Denaturing polyacrylamide gel electrophoresis and blotting were performed as described (16) using the noted antibodies and histochemical staining procedure. **Immunoblot** analysis was as detailed (9). Immunodetection was with pooled goat anti-mouse and anti-human AChE antibodies, directed to an N-terminal sequence common to the different variants (N-19 and E-19; Santa Cruz Biotechnology) or to the C-terminal sequence unique to hAChE-R (see above).

**Sucrose gradient ultracentrifugation** was performed with 20-80  $\mu$ l samples containing a total AChE activity sufficient to achieve a  $\Delta A_{405}$  of approx. 2.4/min in the Ellman assay. This amount of activity enabled the analysis of the more dilute sedimentation fractions. Muscle extracts were loaded with high salt buffer and somatosensory cortex extracts, with low salt buffer. Samples were applied to 12 ml 5-20% linear sucrose density gradients. Ultracentrifugation was for 20 hr at 240,000  $\times g$  and 4°C in the presence of bovine catalase (Sigma) as a sedimentation marker (11.4 S). Fractions were collected in 96-well microtiter plates and assayed for AChE activity essentially as described above.

## Results

Several lines of transgenic mice were screened for the level of muscle AChE and for their secretion of the AChE variants in milk (Table 1). For AChE-R, the highest expressor, line 70, was chosen for subsequent studies.

**In vivo production of AChE-R in transgenic mice:** CMV-controlled expression in muscle of transgenic AChE-C and AChE-R mice was 46- and 350-fold higher, respectively, than in the muscle of non-transgenic control mice (Table 1). No increase in milk AChE activity was

observed in AChE-S transgenics, where the proximal human *ACHE* promoter limits expression to the nervous system (10). In contrast, milk enzyme activities were up to 14- and 230-fold higher than controls in AChE-C and AChE-R pedigrees, respectively (Table 1). In AChE-S transgenics, muscle AChE comprises both the host AChE-R and host and transgenic AChE-S (8). In AChE-R transgenics, either muscle or milk, in comparison, contained almost exclusively the transgenic enzyme (Fig. 1) and presented signal to noise ratios sufficiently high for testing inhibitor sensitivities of the AChE-R protein. Preincubation (10 min) of AChE-S or AChE-E with normal milk at the same dilution as that used in the assay of transgenic milk yielded the same activity and resulted in inhibition profiles indistinguishable from those of unmixed AChE preparations, as did preincubation with saline (data not shown), indicating that milk contains no AChE inhibitor. The enzyme activity in these tissues was stable with time and under freezing and thawing, which enabled accumulation of enzyme preparations for testing.

**AChE variants are subject to tissue-specific post-transcriptional modifications:** Non-denaturing gel electrophoresis followed by cytochemical staining for catalytic activity revealed a diffuse fast-migrating band for AChE-R in transgenic milk, which was absent in the milk of control mice (Fig. 1A). Muscle homogenates showed marked heterogeneity of staining, with 2 major diffuse bands, both different from the milk enzyme. This suggested tissue-specific post-transcriptional and/or post-translational modification. The transgene that expresses AChE-R also includes exon 5, which produces the C-terminal sequence characteristic of AChE-E (9). This raised the possibility that the slower migrating band in muscle homogenates represented AChE-E dimers produced by alternative splicing of the transgene. That purified AChE-E migrated yet more slowly, again indicated tissue specificity for the post-translational processing of AChE-S as compared with AChE-E, consistent with the variable AChE glycosylation reported by others (19). Recombinant AChE-S from HEK293 cells (20) migrated yet more slowly (not shown), as did mouse brain AChE, primarily composed of AChE-S; and plasma BuChE presented a relatively sharp band of the same mobility as AChE-E. A faint parallel band in the mouse milk probably represents the endogenous enzyme, as AChE is known to be secreted in milk (21).

**Transgenic milk and muscle AChE variants display distinct electrophoretic mobilities and multimeric structure:** When subjected to electrophoresis under denaturing conditions followed by reaction with an antibody directed to the common core of AChE variants, muscle homogenates from AChE-R transgenic mice revealed 2 bands, of 62 and 70 kD (Fig. 1B). The low level of endogenous AChE in control muscle escaped detection by this antibody. Two major proteins were labeled in mouse milk, probably because of their high concentration, yet a third 62 kD band, not detected by Ponceau staining, appeared only in the milk of AChE-R transgenics, suggesting that it is AChE-R. Finally, recombinant AChE-S yielded a single band of 70 kD. Also, a selective polyclonal rabbit antibody targeted to the AChE-R C-terminus detected a 66 kD protein present in the milk, and muscle of Tg mice as well as in extracts of AChE-R-producing COS cells. Cross-reactivity with host mAChE-R was observed in milk, but not muscle, and a short degradation product appeared in COS cells (Fig. 1B),

Sucrose gradient sedimentation profiles (Fig. 2) indicated that milk AChE-R and AChE-C are monomeric, with a relatively long shoulder in the AChE-R samples that could reflect significant interactions with additional, yet unknown macromolecules. Monomeric structure is consistent with AChE-R and AChE-C, each of which lacks the cysteine residue at its C-terminus, being

unable to form disulfide-bridged dimers. When subjected to immunoblot analysis, isolated fractions from the G1 peak were immunopositive for both a specific anti-AChE-R antibody, i.e. an antibody generated against the unique C-terminal sequence of AChE-R, and an anti-AChE-C antibody. In contrast, protein samples from the considerably smaller peak, including G2 material, reacted, albeit faintly, with only the anti-AChE-C antibody (Fig. 2, inset). This suggested that the dimeric enzyme did not include AChE-R; rather, this analysis indicated that the G2 dimers in the muscle of AChE-R transgenic mice most likely originated from AChE-E-containing transcripts in the muscle tissue.

**The inhibitor sensitivities of AChE-R are reflected in *ex vivo* tests:** The normally rare AChE-R isoform accumulates in the mammalian brain following exposure to anti-cholinesterases (anti-ChEs) (7,8) or stress (5). An increase in monomeric AChE may represent an accumulation of AChE-R in the stressed brain. This was tested by sucrose gradient centrifugation. Similar volumes of 1:10 (w/v) brain homogenates from AChE-R or AChE-S transgenics, untreated and stressed control mice revealed more intense immunolabeled bands with anti-AChE antibodies and higher hydrolytic activities in transgenics and stressed mice. In addition, different ratios were observed between monomers and tetramers in transgenic or stressed as compared to control mice (Fig. 3). The striking increase in the monomeric fraction following stress (with the G1:G4 ratio increasing from 0.14 to 1.05) indicated a massive accumulation of the AChE-R protein in stressed brain. In comparison, G1:G4 ratios in AChE-R and AChE-S transgenics were 0.65 and 0.12, respectively.

The AChE-R protein could constitute only part of the brain's acetylcholine-hydrolyzing activity, even in AChE-R transgenic mice and certainly in the post-stress brain of normal mice. However, when we tested two AChE inhibitors on brain extracts of AChE-R transgenic, stressed and control mice, we found significant differences in  $IC_{50}$  values. Sensitivity to rivastigmine in the brain of stressed or AChE-R transgenic mice was 2 times higher than in control mice, with  $IC_{50}$  values of 36 – 2, 39 – 11 and 78 – 8 nM, respectively. In contrast, sensitivities of all cortex preparations to donepezil were similar (Fig. 3C). We suspected that these differences were the result of the different proportions of AChE variants in the AChE-R transgenic and stressed normal vs. the unstressed control mouse brains. This hypothesis was further tested with a variety of AChE inhibitors using milk from AChE-R transgenic mice, the most enriched source of this variant.

**AChE-R displays inhibitor sensitivities distinct from other variants:** Inhibition studies of human AChE-R from transgenic mouse milk or muscle, where this enzyme constitutes the largest AChE fraction, revealed clearer differences between this variant and AChE-E or AChE-S purified from human red blood cells and transfected HEK 293 cells, respectively. Fig. 4 presents the inhibition curves for the different agents. These inhibition curves appeared similar for AChE-R from muscle and milk (data not shown), and Table 2 presents the inhibition constants for the variant enzymes with reversible and irreversible (including very slowly reversible) inhibitors. Note that activity in the presence of an irreversible inhibitor depends upon the time of incubation, whereas the kinetic constants are not so dependent. To minimize possible artifacts due to the use of different sources of the studied AChE isoforms, we enriched the tested enzyme by immunoabsorption to immobilized selective antibodies. Using this approach, we found AChE-S to be more sensitive to the peripheral site inhibitor propidium than AChE-E or AChE-R.

Conversely, AChE-R was more sensitive than AChE-S to rivastigmine and paraoxon. The greater sensitivity of AChE-R to rivastigmine is consistent with the observed selective affinity of rivastigmine for soluble brain AChE monomers (22), as AChE-R exists only as monomers. It is also consistent with the observed sensitivity of AChE monomers from rat hippocampus to this drug (23). Finally, both tacrine and donepezil inhibited the 3 natural AChE variants to the same extent (Table 2 and Fig. 4), corroborating the conclusions drawn from our brain enzyme analyses.

**Inhibition of AChE-R is affected by the presence of its unique C-terminal sequence:** We were interested in determining the role of the C-terminal sequence of AChE-R in the variant's inhibitor sensitivity. *A priori*, the observed inhibitor sensitivity of AChE-R could reflect (a) the sensitivity of the core AChE protein, with the C-terminal peptide of AChE-R contributing nothing to this sensitivity, and/or (b) the C-terminal peptides of each of the variants may characteristically affect inhibitor interactions. To resolve these possibilities we compared the inhibition constants of AChE-R and AChE-S with those of AChE-C for DFP, rivastigmine, paraoxon and pyridostigmine (Table 2). The characteristic C-termini of the natural AChE variants appeared in these analyses to affect the kinetics of their interactions with inhibitors. Furthermore, AChE-R was inhibited more efficiently than AChE-S by DFP and rivastigmine. In the case of rivastigmine, AChE-R was more sensitive than either AChE-S or AChE-C; in the case of paraoxon, AChE-R was again more sensitive than AChE-S, and was as sensitive as AChE-C. We conclude, therefore, that all of the 3 C-termini can affect the inhibition of the enzyme and that these effects may be either positive or negative. In contrast, substrate affinities were not dissimilar among the variants. All showed apparent  $K_m$  values close to 0.2 mM for ATCh; the  $K_i$  that characterizes substrate inhibition was also similar for the AChE-S, -R and -C variants, 2.7, 2.3 and 1.3 mM, respectively. Comparison of AChE-R and AChE-S with AChE-C indicates that the C-terminus must interact with or affect the architecture of the substrate-binding site, either by imposing a conformational change on the core of the protein, or through a direct effect of the C-terminal residues on the access of substrates or inhibitors to the active site.

## Discussion

Using three different lines of transgenic mice that overexpress the human splice variants of AChE, we found that the CMV promoter directs expression in muscle and milk and generates sufficient AChE-R or AChE-C for initiating their neurochemical characterization. Using muscle and milk of transgenic mice that over-produce the different human AChE variants, we observed significant differences in their electrophoretic mobilities, sensitivities to some inhibitors and in their degree of multimerization.

The gradient centrifugation studies show that AChE-R is only monomeric, confirming what was suspected on the basis of its lacking the cysteine residue by which AChE-S dimerizes, or the glycyl-glutamyl bond of the C-terminal sequence of AChE-E where a GPI moiety is inserted by transamidation. Being monomeric, the AChE-R variant is more able to diffuse to non-synaptic sites, where it may play an important physiological role. This is compatible with our previous electrophysiological analyses (5,24), which demonstrated suppression of the stress-induced neuronal hyperexcitation in conjunction with AChE-R overproduction. To that end, our sucrose gradient analyses extend previous qualitative reports that AChE-R activity increases under stress (5). Thus, a 30% increase in AChE activity in the brain of AChE-R transgenics leads to a G1:G4 ratio of 0.65, but 90 min post-stress, this ratio is even higher at 1.05. AChE-R may, therefore,

represent over a third of the brain enzyme in the post-stress state. Interestingly, it has been observed that the fraction of AChE monomers increases also in Alzheimer's disease (25), and following organophosphate exposure (26), both of which may be due to AChE-R overproduction.

During stress, there is a wave of acetylcholine secretion, and the physiological benefit of increased AChE at such times is apparent; the benefit of long-term up-regulation of AChE-R is less apparent, but may be related to the non-classical actions of the protein. On theoretical grounds, a soluble AChE can interfere with cell adhesion effected by AChE-like proteins (27) because AChE is homologous with the extracellular domains of a family of cell adhesion proteins that includes insect neurotactins (28) and mammalian neuroligins (29). By replacing its homolog in interaction with a binding partner on a neighboring cell, AChE-R would interrupt the attachment of two cells that depends, for instance, on a neurexin-neuroligin interaction. In fact, it has been shown *in vitro* that the core of AChE can replace neurotactin in a cell-adhesion model (30). This non-catalytic activity may restructure glutamatergic neurotransmission circuits, as neuroligin is apparently localized to excitatory, probably glutamatergic synapses (31), where the easily accessible AChE-R variant may affect its synaptic interactions. As the AChE-R concentration in the synapse increases in response to stress, it is, therefore, possible that the non-catalytic actions of AChE-R alter glutamatergic neurotransmission in the post-stress brain.

In conclusion, AChE-R has distinctive structural properties and inhibitor specificities that may be physiologically and clinically significant following anti-AChE exposure, under chronic anti-AChE treatment such as for Alzheimer's disease or myasthenia gravis, or under acute psychological stress.

#### Acknowledgements

This study was supported by the US-Israel Binational Science Foundation (1999/115), the US Army Medical Research and Development Command (DAMD17-99-1-9547), the Eric Roland Center for Neurodegenerative Diseases and Ester Neuroscience, Ltd. We thank Dr. B. Norgaard-Pedersen (Copenhagen) for the gift of anti-AChE antibodies and Dr. M. Weinstock (Jerusalem) for rivastigmine.

#### References

1. Chan, R. Y., Adataia, F. A., Krupa, A. M. & Jasmin, B. J. (1998) *J Biol Chem* **273**, 9727-9733.
2. Taylor, P., Luo, Z. D. & Camp, S. (2000) in *Cholinesterases and Cholinesterase Inhibitors*, ed. Giacobini, E. (Martin Dunitz, London), pp. 63-79.
3. Massoulie, J., Anselmet, A., Bon, S., Krejci, E., Legay, C., Morel, N. & Simon, S. (1998) *J Physiol Paris* **92**, 183-190.
4. Soreq, H. & Seidman, S. (2001) *Nature Reviews Neuroscience* **2**, 294-302.
5. Kaufer, D., Friedman, A., Seidman, S. & Soreq, H. (1998) *Nature* **393**, 373-377.
6. Shohami, E., Kaufer, D., Chen, Y., Seidman, S., Cohen, O., Ginzberg, D., Melamed-Book, N., Yirmiya, R. & Soreq, H. (2000) *J Mol Med* **78**, 228-236.
7. Shapira, M., Tur-Kaspa, I., Bosgraaf, L., Livni, N., Grant, A. D., Grisaru, D., Korner, M., Ebstein, R. P. & Soreq, H. (2000) *Hum Mol Genet* **9**, 1273-1281.
8. Lev-Lehman, E., Evron, T., Broide, E. S., Meshorer, E., Ariel, I., Seidman, S. & Soreq, H. (2000) *J. Mol. Neurosci.* **14**, 93-105.

9. Sternfeld, M., Shoham, S., Klein, O., Flores-Flores, C., Evron, T., Idelson, G. H., Kitsberg, D., Patrick, J. W. & Soreq, H. (2000) *Proc. Natl. Acad. Sci. USA* **97**, 8647-8652.
10. Beeri, R., Andres, C., Lev-Lehman, E., Timberg, R., Huberman, T., Shani, M. & Soreq, H. (1995) *Curr Biol* **5**, 1063-1071.
11. Sternfeld, M., Ming, G., Song, H., Sela, K., Timberg, R., Poo, M. & Soreq, H. (1998) *J Neurosci* **18**, 1240-1249.
12. Schwarz, M., Loewenstein Lichtenstein, Y., Glick, D., Liao, J., Norgaard Pedersen, B. & Soreq, H. (1995) *Brain Res Mol Brain Res* **31**, 101-110.
13. Hobbiger, F. & Peck, A. W. (1969) *Br J Pharmacol* **37**, 258-271.
14. Ordentlich, A., Barak, D., Kronman, C., Ariel, N., Segall, Y., Velan, B. & Shafferman, A. (1995) *J Biol Chem* **270**, 2082-2091.
15. Barak, D., Kronman, C., Ordentlich, A., Ariel, N., Bromberg, A., Marcus, D., Lazar, A., Velan, B. & Shafferman, A. (1994) *J Biol Chem* **269**, 6296-6305.
16. Seidman, S., Sternfeld, M., Ben Aziz Aloya, R., Timberg, R., Kaufer Nachum, D. & Soreq, H. (1995) *Mol Cell Biol* **15**, 2993-3002.
17. Andres, C., Beeri, R., Friedman, A., Lev-Lehman, E., Henis, S., Timberg, R., Shani, M. & Soreq, H. (1997) *Proc Natl Acad Sci U S A* **94**, 8173-8178.
18. Karnovsky, M. J. & Roots, L. (1964) *J. Histochem. Cytochem.* **12**, 219-221.
19. Meflah, K., Bernard, S. & Massoulie, J. (1984) *Biochimie* **66**, 59-69.
20. Kerem, A., Kronman, C., Bar Nun, S., Shafferman, A. & Velan, B. (1993) *J Biol Chem* **268**, 180-184.
21. Spitsyn, V. A. & Bychkovskaia, L. S. (1994) *Genetika* **30**, 172-175.
22. Weinstock, M., Razin, M., Chorev, M. & Enz, A. (1994) *J Neural Transm Suppl* **43**, 219-225.
23. Trabace, L., Cassano, T., Steardo, L., Pietra, C., Villetti, G., Kendrick, K. M. & Cuomo, V. (2000) *J. Pharmacol. Exp. Ther.* **294**, 187-194.
24. Friedman, A., Kaufer, D., Pavlovsky, L. & Soreq, H. (1998) *J Physiol Paris* **92**, 329-335.
25. Arendt, T., Bruckner, M. K., Lange, M. & Bigl, V. (1992) *Neurochem Int* **21**, 381-396.
26. Wilson, B. W. & Viola, G. A. (1972) *J Neurol Sci* **16**, 183-192.
27. Grifman, M., Galyam, N., Seidman, S. & Soreq, H. (1998) *Proc Natl Acad Sci USA* **95**, 13935-13940.
28. Auld, V. J., Fetter, R. D., Broadie, K. & Goodman, C. S. (1995) *Cell* **81**, 757-767.
29. Nguyen, T. & Sudhof, T. C. (1997) *J Biol Chem* **272** (41), 26032-26039.
30. Darboux, I., Barthalay, Y., Piovant, M. & Hipeau Jacquotte, R. (1996) *EMBO J* **15**, 4835-4843.
31. Song, J. Y., Ichtchenko, K., Sudhof, T. C. & Brose, N. (1999) *Proc Natl Acad Sci USA* **96**, 1100-1105.

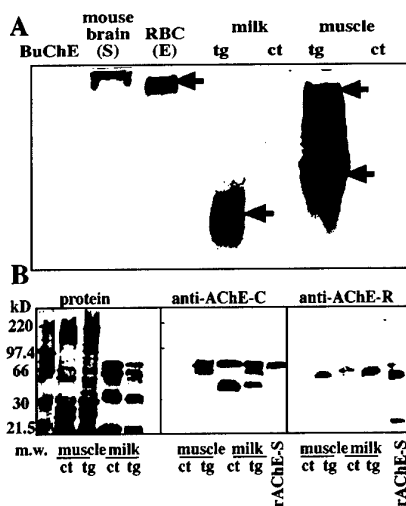


**Fig. 1. AChE-R transgenic mice produce characteristic AChE variants in muscle and milk.**

A. Activity gel. Samples of ChEs (activity of  $\Delta A_{405}$  of approx. 0.0004/min in the Ellman assay) were electrophoresed on non-denaturing polyacrylamide gels. ChE activity was detected using the Karnovsky method (18). Shown are (left to right): human serum BuChE; AChE-S from transgenic mouse brain; AChE-E from human erythrocytes; milk and gastrocnemius muscle extracts from AChE-R transgenic (tg) and control (ct) mice. Upper bands (upper arrows) are slowly migrating AChE-E. Lower bands (lower arrows) denote AChE-R. The different mobilities are probably due to different post-translational processing.

B. Immunodetection of recombinant human AChE in milk and muscle of transgenic mice. Right: Immunoblot; samples

of milk and muscle extracts (40  $\mu$ g protein) from AChE-R transgenic and control mice, and purified recombinant AChE-S (6 I.U.) were subjected to 8% denaturing gel electrophoresis and blotted onto nitrocellulose filters, then reacted with monoclonal antibodies raised against denatured AChE-C (core) and with horseradish peroxidase-conjugated goat anti-mouse IgG and subjected to chemiluminescent detection. Two bands (72 and 54 kD) appear both in transgenic and non-transgenic milk. The upper band, stained by the Ponceau reagent, co-migrates with mouse serum albumin, which is abundant in mouse milk. However, a 62 kD band, the size of the AChE-R protein, appears in the milk and muscle of AChE-R transgenic, but not control mice. In the transgenic muscle, an additional band of 70 kD was detected, but not in non-transgenic muscle. A single 62 kD protein was identified in both muscle and milk of hAChE-R Tg mice by a polyclonal anti-AChE-R antibody that also labeled a fainter co-migrating band in the milk of control mice and revealed the existence of a rapidly-migrating product in the extract of hAChE-R-expressing COS cells (right). Left: Ponceau staining of the proteins on the nitrocellulose filter.

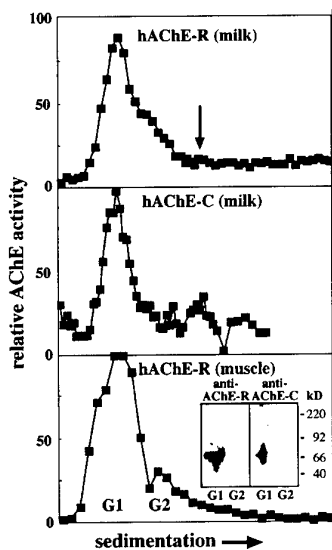


**Fig. 2. Sedimentation profiles of variant AChEs from milk and muscle of female transgenic mice**

Presented is 1 of 4 replicate sets of sedimentation profiles in 5-20% sucrose gradients of AChE activities from milk and whole gastrocnemius extract from mice expressing the AChE-R transgene and of milk from mice expressing AChE-C. All sedimentation profiles were aligned with bovine catalase as a marker (11.4 S), (arrow). Note the prominent peak of the monomer (G1), in milk of transgenics expressing either AChE-R or AChE-C. An additional shoulder of AChE-E dimers (G2) is detectable in muscle from AChE-R transgenics. Inset: immunoblot film, for G1 and G2 gradient peaks. The antibodies employed were targeted to AChE-R (9) (left) or AChE-C, the sequence common to all variants (right). Note that the G1 peak reacts with both antibodies, which identifies it as AChE-R, whereas the considerably smaller G2 peak is immunopositive only with the anti-core antibody, suggesting that it

represents AChE-E dimers.

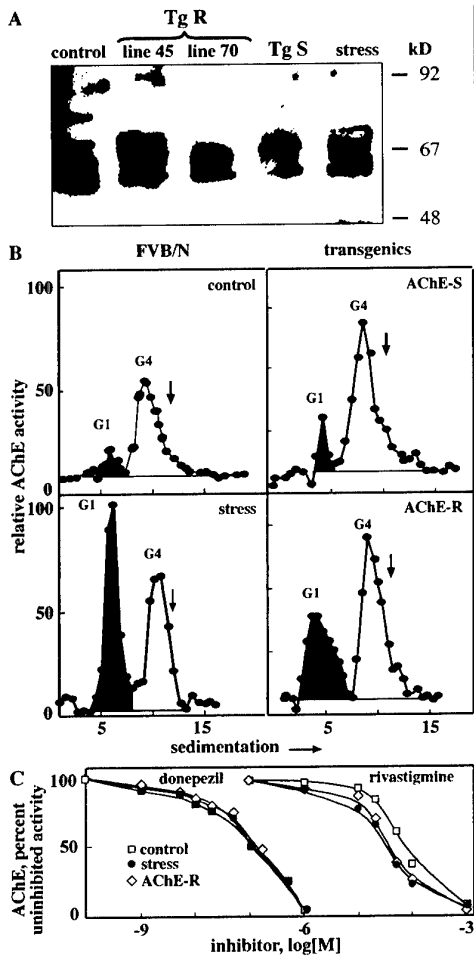
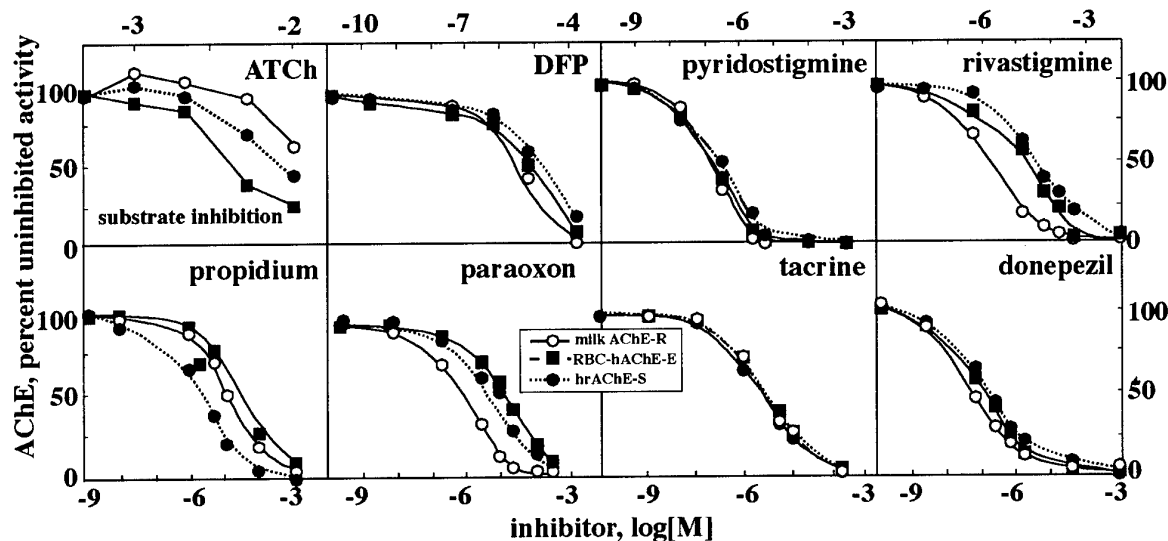


**Fig. 3. Transgenic- and stress-induced alterations in brain AChE sedimentation profiles and inhibitor sensitivities**

A. Immunoblot film, for cortical homogenates from transgenics and control and stressed control mouse brains. The antibody was targeted to the common core domain of human AChE; the multi-band signal obtained with this antibody in control mouse samples demonstrates massive cross reactivity with the mouse enzyme. Note the altered immune reactions with homogenates of the brains from transgenics expressing AChE-R (TgR) or AChE-S (TgS), as well as from the stressed brain.

B. Shown is 1 of 4 sets of sedimentation patterns of AChE activity from the somatosensory cortices of untreated and 90 min post-stress control mice and from untreated AChE-S and -R transgenic mice. The total AChE activity of the control preparation was 1.0 – 0.2; for the stressed group, 1.1 – 0.2; for the AChE-S transgenics, 1.5 – 0.3; and for the AChE-R transgenics, 1.4 – 0.2 nmol/min/mg wet tissue weight. The G1 activities were: control, 0.12; stress 0.56; AChE-S transgenic, 0.16 and AChE-R transgenic, 0.55 nmol/min/mg wet tissue weight..

C. Shown are inhibition curves of pooled somatosensory cortex homogenates ( $n = 4$  in each case), closely similar in dilution, of the above model systems (control and stressed control mice and AChE-R transgenics). Inhibition was with increasing doses of donepezil and rivastigmine. Note the increased sensitivity to the latter in experimental, as compared to control, samples.



g. 4. AChE from transgenic AChE-R mouse milk displays high sensitivity to inhibitors AChE from the milk of AChE-R transgenic mice, human red blood cells (RBC-hAChE-E) and human recombinant AChE-S (hrAChE-S) were pre-incubated for 10 min with the indicated concentrations of inhibitors in Ellman's reagent and AChE activity was measured. Data are presented for each AChE isoform as percent of uninhibited activity. Note that milk AChE-R, as expressed in AChE-R transgenic mice (open circles), is more sensitive to the organophosphate paraoxon and to the carbamate inhibitor rivastigmine than are the other AChE variants; AChE-R displays the same sensitivity as AChE-S and AChE-E to pyridostigmine and tacrine, and is less sensitive than AChE-E to propidium. Note also that the range of the abscissae for the upper 4 panels is shown above them, and for the lower 4, below them.

**Table 1. Production of human AChE variants in milk of transgenic mice<sup>a</sup>**

promoter	protein	milk total ChE activity	milk <sup>a</sup> AChE activity <sup>b</sup>	muscle AChE activity <sup>b</sup>
human	AChE-S	3.9 – 0.2	0.5 – 0.2	35.9 – 1.3 <sup>c</sup>
CMV	AChE-C	13 – 2	7.1 – 0.6	352 – 59 <sup>d</sup>
CMV	AChE-R (line 45)	11 – 1	7.4 – 0.3	190 – 23 <sup>e</sup>
CMV	AChE-R (line 70)	121 – 4	115 – 4.0	2700 – 250 <sup>e</sup>
	control	4.1 – 0.4	0.5 – 0.3	7.6 – 0.6 <sup>e</sup>

<sup>a</sup>Activity is expressed as nmol ATCh/min/l (milk) or /mg protein (muscle) – s.d.

<sup>b</sup>Activity determined in the presence of  $10^{-5}$  M iso-OMPA.

<sup>c</sup>Data taken from Andres et al. (17).

<sup>d</sup>Values from 2 male mice (personal communication from T. Evron, Jerusalem).

<sup>e</sup>Data taken from Sternfeld et al. (9).

**Table 2. Inhibitor affinities**

A.  $K_i$  values ( M) of human AChE variants for reversible inhibitors<sup>a</sup>

	donepezil	tacrine	propidium
AChE-R	0.098 – 0.011	0.034 – 0.002	1.3 – 0.2
AChE-S	0.18 – 0.02	0.040 – 0.003	0.32 – 0.04
AChE-E	0.19 – 0.001	0.046 – 0.007	2.9 – 0.6

B. Inhibitory efficiency ( $k_i/K_i$ ,  $\text{min}^{-1} \text{M}^{-1}$ ) of irreversible inhibitors<sup>b</sup>

	DFP	paraoxon	pyridostigmine	rivastigmin e
AChE-S	0.02	0.51	6.5	0.008
AChE-R	0.12	1.08	12.4	0.034
AChE-C	0.07	1.06	11.8	0.021

<sup>a</sup>The source of AChE-R was transgenic mouse milk and of AChE-S, commercial human recombinant and commercial human erythrocyte enzymes. The experiments were performed in triplicate; values are – s.d.

<sup>b</sup>For the determination of  $k_i/K_i$ , see Methods. The source of AChE-R and AChE-C was milk from the corresponding transgenic mice, and AChE-S was the commercial human recombinant enzyme. Note that assays were performed on immobilized immunoadsorbed enzyme preparations to minimize background artifacts.

## Antisense oligonucleotides relieve neuromuscular weakness in experimental autoimmune myasthenia gravis

Talma Brenner<sup>1</sup>, Yasmine Hamra<sup>1</sup>, Tama Evron<sup>2</sup>, Neli Boneva<sup>1</sup>, Shlomo Seidman<sup>2</sup> and Hermona Soreq<sup>2,3</sup>

<sup>1</sup>Department of Neurology, Hadassah University Hospital and Hebrew University Hadassah Medical School, Jerusalem, Israel 91120

<sup>2</sup>Department of Biological Chemistry, The Institute of Life Sciences and The Eric Roland Center for Neurodegenerative Diseases, The Hebrew University of Jerusalem, Israel 91904

<sup>3</sup>Corresponding author (tel: 972-2-658-5109; fax: 972-2-652-0258, e-mail: soreq@shum.huji.ac.il).

### Abstract

The neuromuscular weakness associated with myasthenia gravis (MG) can be transiently relieved by pharmacological inhibitors of acetylcholinesterase (AChE). Here, we expand the anticholinesterase repertoire to include partially 2'-oxymethyl-protected antisense oligonucleotides (AS-ONs) targeted to AChE mRNA. In rats with experimental autoimmune myasthenia gravis (EAMG), normal response to repetitive nerve stimulation was sequence and dose-dependently restored for up to several weeks following repeated oral administration of 1 to 20 nmol doses of AS-ON. This was accompanied by marked improvement in stamina and disease symptoms and the selective suppression of the alternatively spliced AChE-R mRNA variant and its protein product. In plasma from both EAMG rats and human MG patients, the elevated levels of AChE-R, attribute a previously unsuspected role to this splice variant in MG pathophysiology, suggesting its detection as a peripheral surrogate marker for MG monitoring and highlighting the potential advantages of AS-ON gene-targeted drug therapy for treating this chronic neuromuscular disorder.

### Key words

acetylcholinesterase  
electromyograph  
serologic tests  
stress

### Introduction

Myasthenia gravis (MG) is caused by a defect in neuromuscular transmission caused by autoantibodies that severely reduce the number of functional post-synaptic muscle nicotinic acetylcholine receptors (nAChR) (1, 2). MG is characterized by fluctuating muscle weakness that may be transiently improved by inhibitors of acetylcholinesterase (AChE) (3). The diagnostic electrophysiological abnormality is a progressive, rapid, decrement in the amplitude of compound muscle action potentials (CMAP) evoked by repetitive nerve stimulation at 3 or 5 Hz. To date, the standard treatment for MG includes immunosuppression combined with chronic administration of multiple daily doses of peripheral AChE inhibitors such as pyridostigmine (Mestinon<sup>TM</sup>) (3). While AChE inhibitors effectively restore muscle performance in MG patients, the effect is short-lived, calling for the development of more effective treatment.

Antisense technology offers an attractive, gene-based alternative to conventional anticholinesterase therapeutics. It exploits the rules of Watson-Crick base pairing to design

15-25 residue antisense oligonucleotides (AS-ONs), whose sequence is complementary to that of a target mRNA (4). Stretches of double-stranded oligonucleotide sequences resulting from hybridization of the AS-ON with its target are substrates for RNase H (5), which hydrolyzes the RNA of AS-ON-mRNA hybrids. As antisense therapeutics target RNA rather than proteins, they offer the potential to design highly specific drugs with effective concentrations in the nanomolar range (6). Both phosphorothioated and 3' terminally protected 2'-oxymethyl AS-ONs targeted to AChE mRNA were shown effective in blocking AChE expression *in vitro* in cultured human and rodent cells (6-8), and *in vivo* in brain (9).

Recently, we observed that treatment with the irreversible cholinesterase inhibitor diisopropylfluorophosphonate (DFP) induces overexpression of an otherwise rare, non-synaptic alternative splicing variant of AChE, AChE-R, in brain and intestine (10). Muscles from animals treated with DFP also overexpressed AChE-R, accompanied by exaggerated neurite branching, disorganized wasting fibers and proliferation of neuromuscular junctions (NMJs). Partially protected 2'-oxymethyl AS-ON targeted to AChE mRNA suppressed feedback upregulation of AChE and ameliorated DFP-induced NMJ proliferation (11). These observations demonstrated that stress induces overexpression of AChE-R in muscle and that antisense oligonucleotides can prevent the accumulation of such AChE-R excess. Therefore, we pursued overexpression of AChE-R in EAMG and MG and developed selective antisense suppression of AChE-R, which induced rapid and long-lasting improvement in muscle function of EAMG rats in a sequence and dose-dependent manner.

## Methods

**Human MG patients:** Serum samples from anonymous MG patients were used according to the guidelines of the Hebrew University's Bioethics Committee.

**Materials:** Unless otherwise specified, materials were purchased from Sigma Chemical Co. (St. Louis, MO).

**Animals:** EAMG was induced in female Lewis rats (120-150 g) purchased from the Jackson Laboratory (Bar Harbor, ME), and housed in the Animal Facility at the Hebrew University Faculty of Medicine, in accordance with NIH guidelines. Control FVB/N mice were bred from the FVB/N strain purchased from Harlan Biotech Israel (Rehovot, Israel). Transgenic FVB/N mice overexpressing AChE-R were as described (12).

**Oligonucleotides:** HPLC-purified, GLP grade oligodeoxynucleotides (purity >90% as verified by capillary electrophoresis) were purchased from Hybridon, Inc. (Worcester, MA). Lyophilized oligonucleotides were resuspended in sterile double distilled water (24 mg/ml), and stored at -20 °C. The three 3'-terminal residues in all of the employed AS-ON agents were substituted with methoxy groups at the 2' position. The primary sequences used in this study were:

rat EN101     5'-CTGCAATATTTTCTTGCA\*C\*C\*-3';  
rEN102       5'-GGGAGAGGAGGAGGAAGA\*G\*G\*- 3' ; and  
inv-rEN102   5'-GGAGAAGGAGGAGGAGAG\*G\*G\*-3'.  
(Asterisks denote 2'-oxymethyl protected residues.)

All of these AS-ONs are complementary or inverse to the coding sequence of the rat AChE mRNA sequence common to all variants (13).

**Antibodies:** Rabbit polyclonal Abs against the C-terminal sequence that is unique to AChE-R were prepared and purified as described (12). Goat polyclonal anti-nAChR (C-20, S.C.-1448) Abs were from Santa Cruz Biotechnology (Santa Cruz, CA). Biotinylated donkey anti-rabbit Ab (Chemicon International, Temecula, CA) and biotinylated donkey anti-goat Ab (Jackson ImmunoResearch Laboratories, West Grove, PA) were used as secondary antibodies.

**Induction of EAMG:** The *Torpedo* acetylcholine receptor (tAChR) was purified from *T. californica* electroplax by affinity chromatography on neurotoxin-Sepharose resin, as previously described (14). Rats were immunized with 40 µg of purified tAChR emulsified in CFA supplemented with 1 mg of *M. tuberculosis* H37Ra (Difco, Detroit MI). Subcutaneous injection in the hind footpads was followed by a booster injection of the same amount after 30 d. A third injection was administered to animals that did not develop EAMG after the second injection. Animals were weighed and inspected weekly during the first month, and daily after the booster immunization, for evaluation of muscle weakness. The muscle weakness status of the rats was graded according to: apparently healthy – Without definite weakness (treadmill running time, 23 ± 3 min), Mild – weight loss >10% during a week, accompanied by weak grip or audible complaint with fatigue (4-8 min run on the treadmill). Moderate – hunched posture at rest, head down and forelimb digit flexed, tremulous ambulation (1-3.5 min run on treadmill). Severe – general weakness, no audible complaint or grip (treadmill running time <1 min).

**Anti-AChR Ab determination:** Sera from EAMG animals and MG patients were assayed by direct radioimmunoassay, for <sup>125</sup>I-α-bungarotoxin (BgT) binding to tAChR or rat (r) AChR (14, 15). All the EAMG rats displayed high anti-tAChR and/or anti-rAChR titers, with serum mean ± SEM values of 82.1 ± 16.0 nM for anti-tAChR antibodies and 19.9 ± 1.8 nM for anti-rAChR.

**Quantification of nAChR:** AChR concentration in the gastrocnemius and tibialis muscles was determined using <sup>125</sup>I-α-BgT binding followed by precipitation in saturated ammonium sulfate as described previously (16).

**Electromyography:** Rats were anesthetized by *i.p.* injection of 2.5 mg/Kg pentobarbital, immobilized, and subjected to repetitive sciatic nerve stimulation, using a pair of concentric needle electrodes at 3 Hz. Baseline compound muscle action potential (CMAP) was recorded by a concentric needle electrode placed in the gastrocnemius muscle, following a train of repetitive nerve stimulations at supramaximal intensity. Decrease (percent) in the amplitude of the fifth vs. the first muscle action potential was determined in two sets of repetitive stimulations for each animal. A reduction of 7% or more was considered indicative of neuromuscular transmission dysfunction (15).

**Drug administrations:** Intravenous injections and blood sampling for anti-nAChR Ab determination, were via the right jugular vein under anesthesia. For oral administration, a special intubation feeding curved needle with a ball end (Stoelting, Wood Dale, IL) was used. Mestinon, administered in a dose of 1 mg/Kg per day, was purchased from Hoffmann La-Roche (Basel, Switzerland).

**Exercise training on treadmill:** To establish a physiological measure of neuromuscular performance in EAMG rats, animals were placed on an electrically powered treadmill (17) running at a rate of 25 m/min, a physical effort of moderate intensity, until visibly fatigued. The time the rats were able to run was recorded before and at the noted times after AS-ON or Mestinon treatment.

**In situ hybridization** was performed with fully 2'-oxymethylated AChE-R-or AChE-S-specific 50-mer cRNA probes complementary to pseudointron 4 or exon 6, respectively, in the *ACHE* gene (6). Detection was with alkaline phosphatase and Fast Red™ substrate (Molecular Probes, Eugene, OR). DAPI (Sigma) staining served to visualize nuclei.

**Immunohistochemistry:** Muscle sections (7 µm) were deparaffinized with xylene and were re-hydrated in graded ethanol solutions (100%, 90%, 70%) and PBS. Heat-induced antigen retrieval was performed by microwave treatment (850 W for rapid boil followed by 10 min at reduced intensity) in 0.01 M citrate buffer, pH 6.0. Slides were cooled to room temperature and rinsed in double distilled water. Non-specific binding was blocked by 4% naive donkey

serum in PBS with 0.3% Triton X-100 and 0.05% Tween 20 (1 h at room temperature). Primary Ab was diluted (1:100 and 1:30 for rabbit anti-AChE-R and goat anti-nAChR, respectively) in the same buffer and slides were incubated 1 h at room temperature following overnight incubation at 4 °C. Sections were rinsed and incubated with the appropriate biotinylated secondary Ab, diluted in the same blocking buffer 1 h at room temperature and then overnight at 4 °C. Detection was with streptavidin conjugated to alkaline phosphatase (Amersham Life Science, Arlington Heights, IL) and Fast Red substrate; slides were cover-slipped with Immunomount (Shandon Pittsburgh, PA).

**Patient serum analyses:** Blood samples were drawn from 19 MG patients who displayed Ab titers between 1 and 60 pmol/ml serum. Non-denaturing gel electrophoresis was as described (18), as were catalytic activity measurements of AChE in the serum of patients and experimental animals.

## Results

### Antisense oligonucleotides restore normal CMAP in myasthenic rats

To evaluate the severity of muscle pathology in tested animals, we performed electromyography recording from the gastrocnemius muscle. EAMG rats, but never control animals, displayed a characteristic decrement in CMAP in response to repeated stimulation at 3 and 5 Hz (Fig. 1A, inset and data not shown). The baseline decrement, calculated by measuring the decrease from the first to the fifth response, ranged from 7% to 36% (mean=13.0% ± 2.5%) as compared to a limited change of 4.0% ± 0.9% in control animals. To test the potential application of antisense technology in suppressing AChE activity in muscle, we treated EAMG rats with rEN101, a partially 2'-oxymethyl protected AS-ON targeted to a region of rAChE mRNA that is common to all 3 variants.

As expected, based on the vast clinical experience with cholinesterase inhibitors in the treatment of MG, *i.p.* administered neostigmine bromide (Prostigmine™, 1000 µg/Kg, which equals ca. 0.5 µmol/rat) rapidly and effectively reversed the myasthenic CMAP decrement in EAMG rats. The effects of cholinesterase blockade were evident starting 30 min after injection and up to 2-3 h post-injection, after which CMAP decrements reverted to baseline (Figure 1A). A control AS-ON with an inverse sequence to rAChE mRNA, invEN102, showed no effect at 50 µg/Kg, demonstrating that neither the injection itself nor the presence of an inert AS-ON would alter the CMAP ratio (Figure 1A). Following *i.v.* injection of EN101 at doses ranging from 50-500 µg/Kg, *i.e.* 2 to 20 nmol/rat, CMAP ratios changed to normal values within 1 h post-administration (Figure 1B). CMAP normalization was accompanied by visible improvement in motor activity associated with increased mobility, upright posture, stronger grip and reduced tremulous ambulation. A second, independent and similarly protected AS-ON, targeting a neighboring sequence in rAChE mRNA (EN102), produced similar rectification of decrements in CMAP in EAMG rats (Table 1), validating the specificity for the target protein. Nevertheless, antisense effects on neuromuscular activity were sequence-dependent, as comparable amounts of invEN102, the control oligonucleotide with inverse sequence, did not improve muscle function (Figure 1A and Table 1). The duration of CMAP restoration increased with the dose of EN101, from short-term improvement with 10 µg/Kg up to over 72 h with 500 µg/Kg. Fifty µg/Kg yielded 24 h improvement, and was therefore used for repetitive daily treatments (Figure 1B).

Since *i.v.* drug administration is of limited value in chronic treatment paradigms, and since oral administration of AS-ONs had been shown to be effective in some applications (4), we explored the activity of orally administered EN101. Fifty µg/Kg EN101 was administered via

an intubation feeding needle, to EAMG rats, and CMAP recordings were performed 1, 5, and 24 h later. The orally administered EN101 was as active as *i.v.* administered 25  $\mu\text{g}/\text{Kg}$  (Table 1 and Figure 2A). Orally administered Mestinon (pyridostigmine, 1000  $\mu\text{g}/\text{Kg}$ ) imparted predictable restoration of CMAP for up to several hours, and *inv*EN102 had no effect on CMAP. Under the oral administration route, EN102 appeared slower to affect CMAP than EN101, suggesting sequence-specific differences for this effect (Table 1). Individual variabilities in animal responses to the EN101 treatment may parallel the variable decrement observed in response to calcium channel blockers in EAMG (15). To compare repeated daily oral and *i.v.* administration routes, we treated EAMG rats with EN101 once a day for 5 days and performed CMAP recordings prior to each drug treatment. Neither oral nor *i.v.* repeated administration of EN101 appeared to produce resistance to the therapy, normal electrophysiological activities being recorded over the entire course of treatment (Figure 2B). Both the efficacy of EN101 treatment and its capacity to reduce the inter-animal variability were comparable to those of Mestinon, with the exceptions that Mestinon's effects were more rapid (data not shown), whereas EN101's effect was considerably longer-lasting. Also, the effect of daily single doses of Mestinon wore off within a day, causing drastic fluctuations in the treated animals' muscle strength (Table 1, Figure 2B and data not shown). Among the EAMG animals thus treated with single daily administration of Mestinon, 5 out of 6 died within these 5 days. In contrast, 6 out of 8 animals treated by single daily oral administration of EN101, which maintained consistently normal CMAP levels throughout the treatment period, survived the full 5 day period (Figure 2C). Although inconclusive, this experiment indicated EN101 as suitable for longer treatment evaluation.

#### **EN101 promotes muscle stamina in EAMG rats**

Placed on a treadmill at 25 m/min, control animals ran for  $23.0 \pm 3.0$  min after which time they displayed visible signs of fatigue. Myasthenic animals placed on the treadmill were able to run as short a time as only  $2.3 \pm 0.5$  min before signs of fatigue appeared, depending on the severity of symptoms. We then classified animals as mildly, moderately, or severely affected based on their stamina in the treadmill test and disease signs, and monitored their performance 24 h following administration of 250  $\mu\text{g}/\text{Kg}$  EN101 (Figure 3). All groups demonstrated improved stamina following injection. Thus, severely sick animals preformed, when treated, as well as untreated moderately sick ones, and treated moderately sick animals reached performance levels better than those of untreated mildly sick animals, amounting to 3-fold improved running times of  $6.5 \pm 1.5$ . EN101 had no significant effect on the running time of control rats (Figure 3).

In a yet longer-term treatment regimen, 7 out of 9 EAMG animals under daily EN101 administration presented improved treadmill performance 1 mo after initiation of treatment, 1 showed no improvement and 1 animal died. In contrast, of 5 similarly sick animals that received daily Mestinon treatment, 3 died, 2 performed worse, and none showed improved performance. Saline injection yielded similar results, 3 dead, 2 worse. Thus, daily EN101 administration appeared effective for long-term treatment, enabling EAMG animals with moderate to severe symptoms to thrive under conditions where untreated or Mestinon-treated animals did not survive.

#### **Stress-associated AChE-R accumulates in muscles of EAMG rats and is suppressed selectively by EN101**

Both the rare, unstable splicing variant known as readthrough AChE (18) and the corresponding AChE-R mRNA transcript (19) are intrinsically unstable. Therefore, EN101

mediates the preferential degradation of this transcript (8). AChE-R mRNA accumulates in muscle under chronic anticholinesterase exposure (11). The rapid and long-lasting effects of EN101 in restoring normal electrophysiological activity in muscles of EAMG rats, raised the possibility that AChE-R plays a previously unrecognized role in myasthenic muscle weakness.

To determine the involvement of AChE-R in the autoimmune-mediated myasthenic neuromuscular junction (NMJ), we performed *in situ* hybridization on sections of the triceps muscle from EAMG rats. Intensified expression of this splicing variant, evident as a punctated pattern of AChE-R mRNA labeling, was detected close to the sub-synaptic clusters of nuclei in muscles of EAMG as compared to control rats, which showed diffuse labeling (Figure 4A, top). In contrast, the primary "synaptic" AChE-S mRNA transcript maintained apparently similar sub-synaptic labeling patterns in both healthy and EAMG rats (Figure 4A, bottom). Following *i.v.* EN101 treatment, AChE-R mRNA labeling was drastically reduced, almost to the limit of detection, both in control and EAMG rats (Figure 4A, insets). AChE-S mRNA labeling was minimally affected, reconfirming the selectivity of the AS-ON effect (Figure 4B, insets).

Immunohistochemical staining with a polyclonal antiserum that selectively detects AChE-R (12), revealed positive signals in some, but not all muscle fibers of control rats. Pronounced cytoplasmic accumulation of AChE-R protein in muscle fibers from EAMG rats demonstrated an increase in this protein (Figure 4B, top). The dispersed cytoplasmic localization of immunodetected AChE-R in EAMG muscle was characteristic of this soluble AChE-R isoform as previously observed in transgenic models of AChE overexpression (20). No significant difference was observed in the expression of the AChE-S protein in EAMG compared to control rats, extending the *in situ* hybridization findings (data not shown). Twenty-four h following a single *i.v.* injection of 250 µg/Kg EN101, AChE-R protein levels were conspicuously suppressed in muscle from both control and EAMG rats (Figure 4B, top insets).

#### **AChE-R accumulation coincides with muscle nAChR reduction**

The association between muscle AChE-R accumulation and the EAMG disease state was confirmed by immunohistochemical staining for muscle nAChR protein. Sub-nuclear labeling of this receptor was observed in control triceps muscles. In EAMG muscle, marked reduction was observed, as expected in this disease, which is associated with nAChR loss (Figure 4B, bottom). EN101 treatment did not affect nAChR staining, supporting its specificity for preventing AChE-R production (Figure 4B, bottom insets). Muscle nAChR loss was confirmed by direct measurement of muscle AChR content, using labeled  $\alpha$ -bungarotoxin. The nAChR content in mild EAMG was reduced by 50% from the control and in severe EAMG it was reduced by 70-80% (average,  $n > 10$  in each group).

Because AChE-R is a secretory, soluble protein, we further searched for its levels in serum. Immunoblot analysis of non-denaturing gels loaded with serum samples from control rats demonstrated the presence of AChE-R in serum. EN101 treated control animals displayed conspicuously reduced AChE-R signals in the immunoblot analysis, whereas EAMG rats demonstrated massive accumulation of AChE-R in serum, as compared with healthy animals. AChE-R labeling was substantially decreased in myasthenic animals under EN101 treatment, reaching levels close to those observed in untreated control animals (Figure 4C).

### **AChE-R accumulates in plasma of human MG patients**

To explore the putative correlation between AChE-R overexpression and neuromuscular junction dysfunction in humans, and to examine the potential use of AChE-R as a surrogate marker of myasthenic muscle impairments, we searched for elevated levels of AChE-R in plasma collected from MG patients. In serum samples from several patients, we consistently observed the existence of rapidly migrating, catalytically active AChE isoform (Figure 5A). In contrast, serum samples from control, healthy individuals showed primarily a slowly migrating active enzyme, which could be effectively inhibited by  $5 \times 10^{-5}$  M of the AChE-specific inhibitor, BW284c51, but not by the butyrylcholinesterase-specific inhibitor iso-OMPA (Figure 5 and data not shown).

Serum samples from control mice subjected to confined swim stress (10), or transgenic mice overexpressing human AChE-R (12) displayed higher levels than non-stressed controls of a rapidly migrating AChE isoform. This activity, like the slowly migrating enzyme, was blocked by  $5 \times 10^{-5}$  M of the AChE specific inhibitor BW284c51, but not by  $5 \times 10^{-5}$  M iso-OMPA (Figure 5 and data not shown). This suggested that the rapidly migrating AChE is AChE-R. Thus, human MG patients, like stressed or AChE-R transgenic mice or EAMG rats, accumulate excess serum AChE-R. There was no apparent correlation between the intensity of AChE-R staining and the anti-AChR titers in the 12 analyzed patients (data not shown). Also, total AChE activity measurements in the serum of patients or of stressed and non-stressed mice showed no correlation with these AChE-R migration patterns, probably due to differences in released erythrocytic AChE due to hemolysis (Figure 5B). Thus, immunodetection or activity gel analyses appeared more informative than serum enzyme assay.

### **Discussion**

By targeting an orally delivered AS-ON drug to a long-known MG target, AChE, we achieved rapid, yet long-lasting physiological improvement, associated with reversal of the CMAP decremental response at 3 Hz nerve stimulation and increased muscle stamina in the treadmill test. The beneficial effect of AS-ON injection on the CMAP response began within 1 h post-treatment and lasted many more hours than the effect of the currently employed anticholinesterases, likely reflecting the mechanistic differences between these two groups of drugs.

Chemical anticholinesterases are stoichiometrically targeted at the large number of AChE molecules present in the NMJ -- density of 3000-5000 molecules/ $\mu\text{m}^2$  (21). In contrast, AChE mRNA chains exist in far lower quantities than their protein products, and are produced only by subsynaptic nuclei -- 1:200 of total muscle nuclei (22). Furthermore, AChE-R mRNA is normally the least abundant of the alternative splice variants of AChE mRNA. In addition, AS-ON agents that target the AChE-R mRNA transcripts can operate repeatedly, i.e. one AS-ON is responsible for hydrolysis of many mRNAs. This explains the over 100-fold difference in the molar dose of AS-ON as compared to Prostigmine or Mestinon that is effective in relieving EAMG weakness.

Because of the intrinsic instability of the AChE-R mRNA transcript (19), AS-ON agents targeted to the AChE mRNA sequence that is shared by all transcripts, will destroy primarily the longer, less G,C-rich AChE-R mRNA (8). This provides selectivity towards this normally rare transcript, while protecting most of the synaptic AChE-S variant from the antisense effect. Consequently, neuromuscular functioning is maintained while the disease-associated

damaging protein is efficiently removed. The 3' terminal 2'-oxymethyl protection of AS-ON chains increases the hybridization affinity while minimizing toxicity (6). This may further explain the beneficial effect of 2'-oxymethyl protected AS-ON agents following *i.v.* as well as oral administration. In comparison, conventional anticholinesterases would similarly inhibit the catalytic activity of the two variants, but would not remove the blocked enzyme from the system. This may be detrimental for three reasons: first, anticholinesterases induce a robust, multi-tissue feedback response of AChE-R overproduction; second, the overproduced protein apparently possesses additional, non-catalytic activities that are not necessarily blocked by anticholinesterases (reviewed in ref. (20)); third, prolonged exposure may cause tissue damage, as indeed is the case in DFP-exposed muscle. Together, these may explain the apparent absence under AS-ON treatment of adverse effects often associated with chronic anti-cholinesterase exposure. The long-term survival of animals receiving AS-ON by daily oral treatment, as compared with the poor survival of severely diseased animals under the physiologically fluctuating effects of a daily dose of Mestionon, may also reflect these differences.

Chemically protected RNA aptamers, capable of blocking the autoantibodies access to the nAChR, have been developed for the treatment of MG (23), however their reaction with the antibodies is stoichiometric, whereas the AS-ON reaction is catalytic, allowing a considerably lower dosage of the drug. In this context, two surprising properties of EN101 merit special discussion: the rapid onset and the long-lasting effect. The rapid onset of CMAP improvement that is offered by EN101 is most likely due to its easy accessibility to the highly metabolic muscle tissue combined with the instability of its target mRNA. The long-lasting functioning of this AS-ON agent probably reflects the fact that its neuromuscular effect may last after the AS-ON is totally degraded, to cease only when AChE-R accumulation passes a threshold beyond which this protein causes functional damage. This is compatible with the myasthenic symptoms reported in patients with acute anticholinesterase poisoning, which begin several hours after the acute phase (24). Pyridostigmine toxicity, reported in one myasthenic patient and in one healthy control (25), manifested weakness following drug administration, and displayed higher pyridostigmine blood levels than in myasthenic patients with satisfactory clinical response. This suggests individual differences in the clinical responsiveness to anticholinesterases that may depend on the individual rates of their metabolism.

A polymorphism at the HLA-DQ locus was reported to regulate the susceptibility to EAMG in mice (26), and polymorphisms in the  $\beta_2$  adrenergic receptor gene appear to have distinct distributions in human MG patients (27), indicating involvement of both immune modulators and general stress responses in the disease process and suggesting that overexpressed AChE-R may contribute to either or both of these levels of response. To this end, the beneficial effect of repeated AS-ON treatment likely reflects long-lasting changes in cytokine balances that contribute to the myasthenic syndrome. The complexity of relevant elements is evident from recently reported animal models that show, for example, that T cell overexpression of IL-10 facilitates EAMG development (28), whereas genomic disruption of the murine IL-1 $\beta$  gene diminishes the AChR-mediated immune response (29), and deficiency in IFN  $\gamma$  receptor limits both EAMG development and the negative feedback cascades that are induced by such development (30). Indeed, injected IL-12, a major inducer of IFN  $\gamma$  production, accelerates and enhances disease in AChR-immunized mice, but not in strain-matched mice with a disrupted IFN  $\gamma$  gene (31). The wide span of tissues involved, and the importance of altered cytokine relationships were reflected in the capacity of orally administered AChR fragments

to suppress on-going EAMG (32). Future studies should address the issue of whether AS-ON suppression of systemic AChE-R production affects myasthenic symptoms indirectly by eliminating the hematopoietically active AChE-R (8) and thus modulating cytokine production.

Apart from its obvious utility, this study, therefore, highlights the previously unperceived involvement of the AChE-R splice variant in MG etiology. Alternative splicing has recently emerged as a primary neuronal stress response, which affects different genes (33, 34). Our current findings suggest that synaptic muscle nuclei similarly respond to cholinergic stress by alternative splicing of their pre-mRNA products. MG patients are routinely treated by a combination of anticholinesterase, immune and glucocorticoid therapy. Both anticholinesterases and glucocorticoids would enhance AChE gene expression, further increasing the cumulative AChE-R load in treated MG patients. Due to the secretory nature of AChE-R, it also accumulates in the serum. Further studies will be required to test the applicability of AChE-R detection as a surrogate marker for MG; however, the accumulation of serum AChE-R in EAMG rats and human patients gives reason to believe that, unlike blood catalytic AChE activity, immunodetected serum AChE-R may reflect the severity of the disease state.

The pathogenesis of MG and EAMG is primarily related to the destructive effect of anti-AChR antibodies on the NMJ. In addition, neuromuscular weakness associated with cholinergic imbalance is known in patients with congenital myasthenic syndromes (34), where synaptic AChE is the only form missing, as well as following acute anticholinesterase poisoning, muscle dystrophy and in amyotrophic lateral sclerosis and post-traumatic stress disorder, among others. As AS-ONs targeted to AChE mRNA provide relief of cholinergic muscle malfunctioning, they should be useful for symptomatically treating these and many other diseases.

#### **Acknowledgements**

This research was supported by grants from the Association Française contre les Myopathies (to T.B) and from US Army Medical Research and Development Command (DAMD 17-99-1-9547, to H.S.) and Ester Neuroscience (to H.S. and T.B). We thank Drs. M. Horowitz, I. Wirguin and D. Glick (Jerusalem) for helpful discussions.

#### **References**

1. Drachman, D.B. 1994. Myasthenia gravis. *N Engl J Med.* 330:1797-1810.
2. Vincent, A. 1999. Immunology of the neuromuscular junction and presynaptic nerve terminal. *Curr Opin Neurol.* 12:545-551.
3. Penn, A.S., and Rowland, L.P. 1995. Myasthenia Gravis. In Meritt's Textbook of Neurology, 9th Ed. Williams and Wilkins, Baltimore. 754-761.
4. Agrawal, S., and Kandimalla, E.R. 2000. Antisense therapeutics: is it as simple as complementary base recognition? *Mol Med Today.* 6:72-81.
5. Crooke, S.T. 2000. Progress in antisense technology: the end of the beginning. *Methods Enzymol.* 313:3-45.
6. Galyam, N., Grisar, D., Grifman, M., Melamed-Book, N., Eckstein, F., Seidman, S., Eldor, A., and Soreq, H. 2001. Complex host cell responses to antisense suppression of *ACHE* gene expression. *Antisense Nucl Acid Drug Dev.* 11:51-57.

7. Koenigsberger, C., Chiappa, S., and Brimijoin, S. 1997. Neurite differentiation is modulated in neuroblastoma cells engineered for altered acetylcholinesterase expression. *J Neurochem.* 69 (4):1389-1397.
8. Grisaru, D., Deutch, V., Shapira, M., Galyam, N., Lessing, B., Eldor, A., and Soreq, H. 2001. ARP, a peptide derived from the stress-associated acetylcholinesterase variant, has hematopoietic growth promoting activities. *Mol Med.* 7:93-105.
9. Shohami, E., Kaufer, D., Chen, Y., Seidman, S., Cohen, O., Ginzberg, D., Melamed-Book, N., Yirmiya, R., and Soreq, H. 2000. Antisense prevention of neuronal damages following head injury in mice. *J Mol Med.* 78:228-236.
10. Shapira, M., Tur-Kaspa, I., Bosgraaf, L., Livni, N., Grant, A.D., Grisaru, D., Korner, M., Ebstein, R.P., and Soreq, H. 2000. A transcription-activating polymorphism in the ACHE promoter associated with acute sensitivity to anti-acetylcholinesterases. *Hum Mol Genet.* 9:1273-1281.
11. Lev-Lehman, E., Evron, T., Broide, E.S., Meshorer, E., Ariel, I., Seidman, S., and Soreq, H. 2000. Synaptogenesis and myopathy under acetylcholinesterase overexpression. *J. Mol. Neurosci.* 14:93-105.
12. Sternfeld, M., Shoham, S., Klein, O., Flores-Flores, C., Evron, T., Idelson, G.H., Kitsberg, D., Patrick, J.W., and Soreq, H. 2000. Excess "readthrough" acetylcholinesterase attenuates but the "synaptic" variant intensifies neurodeterioration correlates. *Proc. Natl. Acad. Sci. USA.* 97:8647-8652.
13. Legay, C., Bon, S., Vernier, P., Coussen, F., and Massoulie, J. 1993. Cloning and expression of a rat acetylcholinesterase subunit: generation of multiple molecular forms and complementarity with a Torpedo collagenic subunit. *J Neurochem.* 60:337-346.
14. Boneva, N., Brenner, T., and Argov, Z. 2000. Gabapentin may be hazardous in myasthenia gravis. *Muscle Nerve.* 23:1204-1208.
15. Wirguin, I., Brenner, T., Sicsic, C., and Argov, Z. 1994. Variable effect of calcium channel blockers on the decremental response in experimental autoimmune myasthenia gravis. *Muscle Nerve.* 17:523-527.
16. Changeux, J.P., Galzi, J.L., Devillers-Thierry, A., and Bertrand, D. 1992. The functional architecture of the acetylcholine nicotinic receptor explored by affinity labelling and site-directed mutagenesis. *Q Rev Biophys.* 25:395-432.
17. Moran, D., Shapiro, Y., Meiri, U., Laor, A., Epstein, Y., and Horowitz, M. 1996. Exercise in the heat: Individual impacts of heat acclimation and exercise training on cardiovascular performance. *J. Therm Biol.* 21:171-181.
18. Kaufer, D., Friedman, A., Seidman, S., and Soreq, H. 1998. Acute stress facilitates long-lasting changes in cholinergic gene expression. *Nature.* 393:373-377.
19. Chan, R.Y., Adatia, F.A., Krupa, A.M., and Jasmin, B.J. 1998. Increased expression of acetylcholinesterase T and R transcripts during hematopoietic differentiation is accompanied by parallel elevations in the levels of their respective molecular forms. *J Biol Chem.* 273:9727-9733.
20. Soreq, H., and Seidman, S. 2001. Acetylcholinesterase - new roles for an old actor. *Nature Reviews Neuroscience.* 2:294-302.
21. Anglister, L., Stiles, J.R., and Salpeter, M.M. 1994. Acetylcholinesterase density and turnover number at frog neuromuscular junctions, with modeling of their role in synaptic function. *Neuron.* 12:783-794.
22. Rotundo, R.L. 1990. Nucleus-specific translation and assembly of acetylcholinesterase in multinucleated muscle cells. *J Cell Biol.* 110:715-719.

23. Lee, S.W., and Sullenger, B.A. 1997. Isolation of a nuclease-resistant decoy RNA that can protect human acetylcholine receptors from myasthenic antibodies. *Nat Biotechnol.* 15:41-45.
24. He, F., Xu, H., Qin, F., Xu, L., Huang, J., and He, X. 1998. Intermediate myasthenia syndrome following acute organophosphates poisoning--an analysis of 21 cases. *Hum Exp Toxicol.* 17:40-45.
25. Cohan, S.L., Pohlmann, J.L., Mikszewski, J., and O'Doherty, D.S. 1976. The pharmacokinetics of pyridostigmine. *Neurology.* 26:536-539.
26. Raju, R., Zhan, W.Z., Karachunski, P., Conti-Fine, B., Sieck, G.C., and David, C. 1998. Polymorphism at the HLA-DQ locus determines susceptibility to experimental autoimmune myasthenia gravis. *J Immunol.* 160:4169-4174.
27. Xu, B.Y., Huang, D., Pirskanen, R., and Lefvert, A.K. 2000. beta2-adrenergic receptor gene polymorphisms in myasthenia gravis (MG). *Clin Exp Immunol.* 119:156-160.
28. Ostlie, N.S., Karachunski, P.I., Wang, W., Monfardini, C., Kronenberg, M., and Conti-Fine, B.M. 2001. Transgenic expression of IL-10 in T cells facilitates development of experimental myasthenia gravis. *J Immunol.* 166:4853-4862.
29. Huang, D., Shi, F.D., Giscoombe, R., Zhou, Y., Ljunggren, H.G., and Lefvert, A.K. 2001. Disruption of the IL-1beta gene diminishes acetylcholine receptor- induced immune responses in a murine model of myasthenia gravis. *Eur J Immunol.* 31:225-232.
30. Zhang, G.X., Xiao, B.G., Bai, X.F., van der Meide, P.H., Orn, A., and Link, H. 1999. Mice with IFN-gamma receptor deficiency are less susceptible to experimental autoimmune myasthenia gravis. *J Immunol.* 162:3775-3781
31. Sitaraman, S., Metzger, D.W., Belloto, R.J., Infante, A.J., and Wall, K.A. 2000. Interleukin-12 enhances clinical experimental autoimmune myasthenia gravis in susceptible but not resistant mice. *J Neuroimmunol.* 107:73-82
32. Im, S.H., Barchan, D., Fuchs, S., and Souroujon, M.C. 1999. Suppression of ongoing experimental myasthenia by oral treatment with an acetylcholine receptor recombinant fragment. *J Clin Invest.* 104:1723-1730
33. Xie, J., and McCobb, D.P. 1998. Control of alternative splicing of potassium channels by stress hormones. *Science.* 280:443-446.
34. Ohno, K., Engel, A.G., Brengman, J.M., Shen, X.M., Heidenreich, F., Vincent, A., Milone, M., Tan, E., Demirci, M., Walsh, P., Nakano, S., and Akiguchi, I. 2000. The spectrum of mutations causing end-plate acetylcholinesterase deficiency. *Ann Neurol.* 47:162-170.

### Figure Legends

#### Figure 1. EN101 elicits lasting improvement in muscle function of myasthenic rats.

Compound muscle action potentials (CMAP) were recorded from the gastrocnemius muscle of EAMG rats during repetitive stimulation at 3 Hz and the ratio between the 5<sup>th</sup> and 1<sup>st</sup> peaks determined (inset). Animals exhibiting a decrement, reflecting the fatigue characteristic of myasthenic muscles (CMAP ratio <90%), were treated with a single *i.v* injection (1000 µg/Kg) of the AChE inhibitor Prostigmine, increasing concentrations of EN101, or a control AS-ON with the 5'-3' nucleotide sequence of EN102 reversed (INV-EN102). Graphs display percent above baseline of average CMAP ratios (5<sup>th</sup> to 1<sup>st</sup>) measured at the specified times post-injection for at least 6 rats in each group. The average CMAP ratio of EAMG rats included in the study prior to treatment was 87 ± 2.5% of control animals. Inset: CMAP Ratio Improvement. Shown are the 1<sup>st</sup> and 5<sup>th</sup> depolarization peaks in EAMG muscle (top) and in EN101-treated EAMG muscle (bottom; 500 µg/Kg, 1 h post-treatment). Note the constant size of CMAP peaks under treatment (percent).

A. Prostigmine. Following administration of Prostigmine at a standard therapeutic dose of 1000 µg/Kg body weight, normal CMAP ratios ( $\geq 100\%$ ) were recorded within 30 min and for up to 2 h. The control AS-ON invEN102 had no effect on muscle responses to stimulation at 3 Hz from EAMG rats, demonstrating sequence-specificity for the AS-ON.

B. EN101. Shown are dose-dependently restored normal CMAPs from 1 h and up to 72 h under 10-500 µg/Kg EN101. Higher doses conferred longer-lasting relief.

**Figure 2. Effective oral administration of EN101.**

EAMG rats received EN101 (50 µg/Kg) or Mestion (1000 µg/Kg) once daily for up to 4 days via an intubation feeding needle. CMAP ratio was determined 1 and 5 h following the first drug administration and then every 24 h, prior to the administration of the subsequent dose.

A. Single dose. The graph depicts percent CMAP ratios above baseline measured at the noted time points following oral administration of EN101 ( $n=8$ ) or Mestion ( $n=4$ ). Orally administered Mestion and EN101 relieved decremental CMAP responses to repetitive stimulation within 1 h. Twenty-four h following administration of Mestion, CMAP ratios in muscles of treated rats returned to baseline. In contrast, no decrement was detected in rats treated with EN101.

B. Repeated daily doses. The graph depicts the equivalent improvement in muscle function elicited by oral ( $n=8$ ) as compared to *i.v.* ( $n=4$ ) administration of EN101. Note that repeated administration of EN101 conferred stable, long-term alleviation of CMAP decrements. Repeated daily administration of Mestion at 24 h intervals had no cumulative or long-term effect on CMAP ratios.

C. Survival. The graph depicts the percentage of EAMG rats still alive at specified days following initiation of treatment with repeated oral administrations of Mestion or EN101. Average CMAP values for each group at the starting day are noted. A greater fraction of animals treated with EN101 survived than those treated with Mestion at the given doses despite their poorer initial status, as indicated by initial CMAP ratios.

**Figure 3. EN101 improves stamina in myasthenic rats.**

EAMG rats with varying severity of symptoms (severe  $n=11$ , moderate  $n=4$ , mild  $n=5$ ) and control Lewis rats (none,  $n=7$ ) were prodded to run on an electrically powered treadmill (25 m/min, inset) until visibly fatigued. The time (in min  $\pm$  SEM) each rat was able to run was recorded before, and 24 h following, *i.v.* administration of 250 µg/Kg EN101. Note that EAMG rats run considerably less time than controls, and that running time is increased for each group by EN101.

**Figure 4. EN101 selectively suppresses elevated muscle AChE-R accumulation in EAMG rats.**

A. Muscle AChE mRNA variants. Shown are paraffin-embedded sections of triceps muscle from severely ill EAMG or control Lewis rats following *in situ* hybridization with 2'-O-methyl protected cRNA probes specific for AChE-S or -R mRNAs. The white size bar represents 50 µm. Fast Red (red) labeling reflects mRNA presence. DAPI (white) was used to visualize cell nuclei. Note the prominent sub-nuclear accumulation of AChE-R mRNA in preparations from EAMG, but not control animals. AChE-S mRNA displayed similar focal expression around subnuclear domains in control and EAMG rats. Twenty-four h following treatment with EN101 (250 µg/Kg), AChE-R mRNA was barely detectable in both control and EAMG rats, while AChE-S mRNA levels were not visibly affected (insets).

**B. Inverse intensities of AChE-R and AChR labeling in EAMG.** Shown is immunohistochemical staining observed using polyclonal rabbit antibodies to AChE-R (top) or to nAChR (bottom) and Fast Red. The white size bar represents 10  $\mu$ m. Immunostaining for AChE-R protein was prominently elevated in EAMG as compared to control rats, and suppressed by EN101 (insets). Consistent with their myasthenic pathology, staining of the nAChR is dramatically reduced in EAMG rats. nAChR was not affected by EN101.

**C. Serum AChE-R labeling.** Serum samples from EAMG and control rats were subjected to non-denaturing polyacrylamide gel electrophoresis and immunolabeling with anti-AChE-R antibodies. Note pronounced enhancement of a band representing AChE-R (arrow) in plasma of EAMG rats and its significant reduction in EN 101-treated control and EAMG animals.

**Figure 5. A rapidly migrating AChE variant accumulates in the serum of human MG patients.**

Shown is a non-denaturing polyacrylamide gel stained for catalytically active cholinesterases (left) and a bar graph representing the catalytic AChE activities in the serum of these patients and animals (right). Additional lanes depict the catalytically active isoforms in serum from confined-swim stressed mice (lane 1), control mice (lane 2) and AChE-R transgenic mice (lane 3), a healthy human volunteer (lane 4), a patient with an irrelevant metabolic disease (non-MG) (lane 5) and 4 MG patients (lanes 6-9). Note the presence of a rapidly migrating AChE isoform, parallel to AChE-R in its properties, in the serum of MG patients but not other individuals.

**Table 1. Summary of responses to treatments<sup>A</sup>**

	Oral <sup>B</sup>					Intravenous <sup>B</sup>			
	EN101 treated healthy	EN101-treated EAMG	EN102-treated EAMG	INV102-treated EAMG	Mestinon-treated EAMG	EN101 treated healthy	EN101-treated EAMG	EN102-treated EAMG	INV102-treated EAMG
0 h	101.5±0.9 (4)	83.6±3.0 (8)	82.3±2.0 (4)	78.4±5.5 (4)	89.5±1.0 (6)	100.5±0.4 (6)	86.7±1.2 (6)	84.7±5.6 (4)	88.8±2.4 (5)
1 h <sup>C</sup>	100.9±1.7 (4)	97.2±2.0 (8)	85.6±4.4 (3)	86.3±4.5 (4)	97.7±1.1 (6)	102.1±0.7 (7)	100.0±1.4 (4)	103.9±1.3 (4)	89.0±3.0 (5)
5 h	103.0±2.1 (4)	97.4±2.5 (7)	95.6±2.3 (4)	86.4±5.4 (4)	95.8±2.0 (6)	100.4±1.0 (6)	98.4±2.0 (4)	98.2±3.0 (4)	88.6±1.9 (5)
24 h	101.5± 0.7 (4)	101.0±1.3 (6)	94.8±2.8 (5)	81.2±7.5 (4)	87.2±2.4 (6)	102.0±0.9 (6)	100.0±0.0 (4)	100.3±1.1 (4)	89.7±1.7 (5)

<sup>A</sup>CMAP ratios were determined at the noted times following treatment and the averages  $\pm$  SEM are presented. Each treatment represents similarly, although not simultaneously treated rats, the numbers of which are shown in parentheses.

<sup>B</sup>Drug doses were 50  $\mu$ g/Kg for EN101, EN102 or INV102 and 1000  $\mu$ g/Kg for Mestinon, for both administration routes.

<sup>C</sup>Note the apparently delayed effect of orally administered EN102 as compared to EN101 or Mestinon.

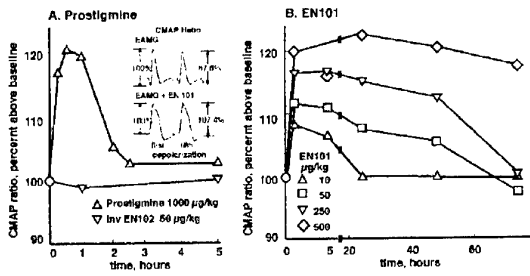


Fig. 1

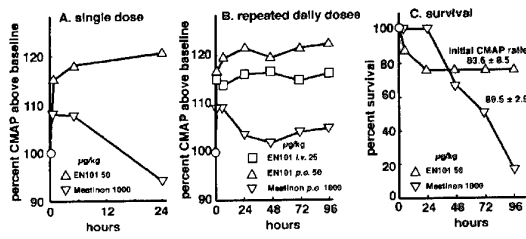


Fig. 2

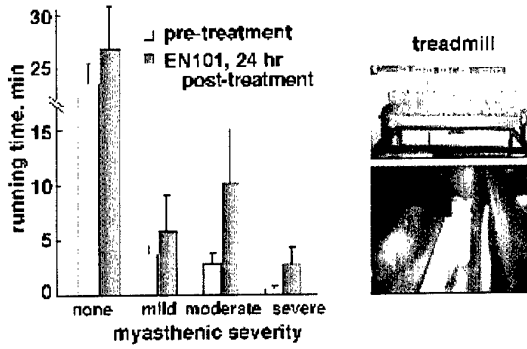


Fig. 3

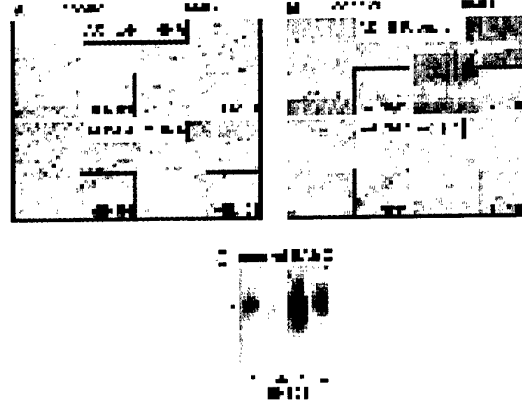


Fig. 4

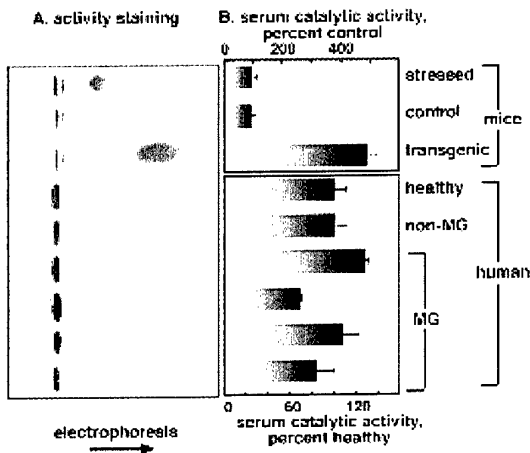


Fig. 5

**Neuronal overexpression of "readthrough" acetylcholinesterase is associated with antisense-suppressible behavioral impairments**

Cohen, O.\* , Erb, C.\* Ginzberg, D.\* Pollak, Y. , Seidman, S.\* ,  
Shoham, S. , Yirmiya, R. and Soreq, H.\*

\*Department of Biological Chemistry, The Hebrew University of Jerusalem, Jerusalem, 91904 Israel,  
Department of Psychology, The Hebrew University of Jerusalem, Jerusalem, 91905 Israel,  
Research Department, Herzog Hospital, Jerusalem, 91351 Israel

Running title: Cholinergic behavioral impairments

Key words: antisense circadian rhythm mouse psychological stress  
social recognition transgenic

Corresponding author: to R. Yirmiya, Department of Psychology, The Hebrew University of Jerusalem,  
Israel (fax: 972-2-588-2947, tel: 972-2-558-3695, e-mail: msrazy@mscc.huji.ac.il)

Abstract

Molecular origin(s) of the diverse behavioral responses to anticholinesterases were explored in behaviorally impaired transgenic (Tg) FVB/N mice expressing synaptic human acetylcholinesterase (hAChE-S). Untreated hAChE-S Tg, unlike naive FVB/N mice, presented variably intense neuronal overexpression of the alternatively spliced, stress-induced mouse "readthrough" mAChE-R mRNA. Both strains displayed similar diurnal patterns of locomotor activity that were impaired 3 days after a day-to-night switch. However, hAChE-S Tg, but not FVB/N mice responded to the circadian switch with irregular, diverse bursts of increased locomotor activity. In social recognition tests, controls displayed short-term recognition, reflected by decreased exploration of a familiar, compared to a novel juvenile conspecific as well as inverse correlation between social recognition and cortical and hippocampal AChE specific activities. In contrast, transgenics presented poor recognition, retrievable by tetrahydroaminoacridine (tacrine, 1.5 mg/Kg). Tacrine's effect was short-lived (<40 min), suggesting its effect was overcome by anticholinesterase-induced overproduction of mAChE-R. Consistent with this hypothesis, antisense oligonucleotides (2 daily intracerebroventricular injections of 25 ng) arrested mAChE-R synthesis, selectively reduced mAChE-R levels and afforded an extended (>24 hr) suppression of the abnormal social recognition pattern in transgenics. Efficacy of antisense treatment was directly correlated to AChE-R levels and the severity of the impaired phenotype, being most apparent in transgenics presenting highly abnormal pre-treatment behavior. These findings demonstrate that neuronal AChE-R overproduction is involved in various behavioral impairments and anticholinesterase responses, and point to the antisense strategy as a potential approach for re-establishing cholinergic balance.

Introduction

Social behavior is a complex phenotype, composed of the individual's general level of activity, cognitive perception and anticipation of the outcome of such behavior<sup>1</sup>. Working and storage memory and the ability to integrate information can also contribute towards social behavior, which is tightly linked to cholinergic neurotransmission. For example, the hypocholinergic features of Alzheimer's disease (AD)

patients include aggressive behavior and/or avoidance of novel social challenges<sup>2</sup>, as well as fears of social interactions alleviated by treatment with anticholinesterases<sup>3</sup>. Surprisingly, anticholinesterases, e.g. tacrine (tetrahydroaminoacridine, Cognex<sup>®</sup>, Parke-Davis), donepezil (Aricept<sup>®</sup>, Pfizer), rivastigmine (Exelon<sup>®</sup>, Novartis) and galantamine (Reminyl<sup>®</sup>, Janssen), were reported to cause more pronounced improvement in more severely affected patients. To explain the molecular basis of this phenomenon, re-evaluation is needed of the linkage between cholinergic neural pathways, social behavior and acetylcholinesterase (AChE).

Both anticholinesterase exposure and stressful insults, i.e. confined swim, induce in the mammalian brain a rapid *c-fos* elevation that mediates muscarinic responses and subsequent *ACHE* overexpression<sup>4</sup>. A stress-associated switch in alternative splicing<sup>5,6</sup> diverts AChE from the major, "synaptic" AChE-S to the normally rare "readthrough" AChE-R variant<sup>7</sup>. The distinctive non-catalytic activities of these AChE isoforms<sup>8</sup>, suggest links between AChE-R accumulation and behavioral anticholinesterase responses.

Transgenic (Tg) mice overexpressing human (h) AChE-S in brain neurons are amenable to pursuit of this linkage. These mice present , early-onset loss of learning and memory capacities<sup>9</sup>, progressive dendritic depletion<sup>10</sup>, stress-related neuropathology<sup>8</sup>, and modified anxiety responses<sup>11</sup>. However, their social behavior and psychological stress responses have not yet been addressed.

AChE-S Tg mice constitutively overexpress AChE-R mRNA in their intestinal epithelium. When exposed to an organophosphate anticholinesterase (DFP), they fail to increase further the already overproduced AChE-R, and present extreme DFP sensitivity. Humans with inherited AChE overexpression are likewise hypersensitive to the anticholinesterase pyridostigmine<sup>12</sup>. Our working hypothesis postulated that at appropriate levels, AChE-R accumulation in response to stress restores normal cholinergic activity and social behavior. However, under chronic stress, acute anti-AChE treatment or exposure, or in individuals with inherited AChE excess, AChE-R increases to a limit beyond which their cholinergic system cannot further respond and impaired social behavior is a result.

To test this hypothesis, we ascertained whether (a) AChE-S Tg mice display excessive response to a mildly stressful stimulus, a switch in the day/night cycle<sup>13</sup>, (b) examined AChE-R expression in their brain neurons; and (c) studied their social recognition behavior<sup>14</sup> before and after administration of tacrine or AS3, an antisense oligonucleotide (AS-ON) shown to selectively suppress AChE-R production<sup>15</sup>. Our findings demonstrate constitutive mAChE-R accumulation with inter-animal variability in brain neurons of hAChE-S Tg mice, associated with an exaggerated response to changes in circadian rhythm, and impaired social recognition, which are amenable to effective AS-ON suppression.

#### Materials and Methods

**Animals:** AChE-S Tg mice were obtained in a 100% FVB/N genotype from heterozygous breeding pairs (Beerl et al., 1995). Control, non-Tg FVB/N mice were obtained by littermate breeding. Adult, 8-20 wk old Tg and control male mice were housed 4-5/cage in a 12 hr dark/light cycle with free access to food and water. All experiments were conducted during the first half of the dark phase of a reversed 12 hr dark/light cycle, under dim illumination. Routine locomotor activity in the home cage was measured using a remote motility detector (MFU 2100, Rhema-Labortechnik, Hofheim, Germany) to quantify changes in the electromagnetic field.

**Telemetric measurements:** Battery operated biotelemetric transmitters (model VM-FH, Mini Mitter, Sun River, OR, USA) were implanted in the peritoneal cavity under ether anesthesia 12 days prior to the test. After implantation, mice were housed in separate cages with free access to food and water. Output was monitored by a receiver board (model RA-1010, Mini Mitter) placed under each animal's cage and fed into a peripheral processor (BCM 100) connected to a desktop computer. Locomotor activity after the dark/light shift was measured by detecting changes in signal strength as animals moved about in their cages, so that the number of pulses that were generated by the transmitter was proportional to the distance the animal moved. The cumulative number of pulses generated over the noted periods was recorded<sup>16</sup>. Recording lasted 24 consecutive hrs, starting at 9:30 am, with the light phase of a 12:12 hr dark / light cycle beginning at 7:00 a.m. To initiate a day/night switch, the dark/light periods were reversed and recording started 72 hr after the switch and lasted 24 hr. Following intraperitoneal injection of AS-ONs (see below), recording proceeded for an additional 3 hr.

**Social exploration tests:** Each mouse was placed in a semicircular, transparent observation box and allowed 15 min for habituation, following which a juvenile male mouse (23-29 days old) was introduced. The time spent by the experimental mouse in social exploration consisted mainly of body and anogenital sniffing, chasing, attacking and crawling over the juvenile. Measurements covered a 4-min period, using a computerized event recorder. Each mouse underwent 2 successive social exploration sessions at the noted inter-session intervals. The first session was considered as baseline. In the second session (test), either the same or a different juvenile was introduced. Social recognition was calculated as percentage of tested out of baseline exploration time recorded for each mouse.

**In situ hybridization and AChE activity measurements:** Animals were sacrificed by cervical dislocation, and brains were removed and dissected or fixed for *in situ* hybridization. AChE activity was measured in hippocampus, cortex and cerebellum extracts as described<sup>17</sup>. Protein determination was performed using a detergent-compatible kit (DC, Bio-Rad, München, Germany). Immunoblot detection of specific AChE isoforms was as reported<sup>15</sup>.

For *in situ* hybridization, 5 µm paraffin sections of brain tissue were prepared after fixation by transcardial perfusion of anaesthetized mice with 4% paraformaldehyde in PBS (pH 7.4). A 50-mer fully 2'-O-methylated 5'-biotinylated AChE-R cRNA probe was applied as described<sup>4</sup>. Following probe detection with a streptavidin-alkaline phosphatase conjugate (Amersham Pharmacia Biotech Ltd., Little Chalfont, UK) and Fast Red as the reaction substrate (Roche Diagnostics, Mannheim, Germany), micrographs of hippocampal and cortical neurons were subjected to semi-quantitative evaluation of Fast Red staining. Mean signal intensities of light micrographs (taken with a Real-14 color digital camera, CRI, Boston, MA, USA) were analyzed using Image Pro Plus (Media Cybernetics, Silver Spring, MD, USA) image analysis software. The mean intensity of Fast Red labeling was measured in CA3 hippocampal and cortical neurons and corrected for background staining in each picture.

**Cytochemistry** of glial fibrillary acidic protein (GFAP) was performed as described<sup>8</sup>. Briefly, floating, formalin-fixed, 30 µm, coronal cryostat-sections were pretreated with trypsin (type II, Sigma Chemical Co., St. Louis, MO, USA) 0.001% for 1 min. Sections were incubated overnight at 4°C with a mouse anti-glial fibrillary acidic protein (GFAP) antibody (clone GA-5, Sigma-Isreal, Rehovot, Israel), diluted 1:500. Then sections were incubated overnight at 4°C with horseradish peroxidase-labeled goat-anti-mouse antibody (Sigma-Isreal), diluted 1:100. Color was developed by reaction with diaminobenzidine 0.0125%, nickel

ammonium sulfate 0.05% and hydrogen peroxide (0.00125%). Sections were counterstained with cresyl violet.

Quantitative analysis of the hippocampal stratum lacunosum moleculare (SLM) was performed at the level of posterior 2.5 mm from bregma. Using a 40x objective, consecutive fields of the SLM were visualized with a Nikon microscope and processed using an AnalySIS image analysis system. A total of 35 astrocytes were sampled from each group (control vs. Tg). The variables that were compared were intensity of staining of the soma (arbitrary units from a range of 256 shades of gray), soma size ( $\mu\text{m}^2$ ), and thickness of the largest process (dendrite) of each astrocyte at the process stem ( $\mu\text{m}$ ). Statistical comparisons were made using Student's t-test, with 68 degrees of freedom.

**Considerations for designing antisense tests:** *In vivo* antisense suppression of *de novo* AChE-R synthesis was employed throughout the current study to provide a proof of concept (i.e. demonstrate the causal involvement of the secretory, soluble mAChE-R variant in the excessive locomotor activity and the impaired social recognition of Tg mice). Two types of experiments were performed: (1) intracerebroventricular (*i.c.v.*) AS3 injection of animals subjected to longitudinal social exploration tests (up to one week post-treatment) and (2) *i.c.v.* injection followed by 1-day social exploration test, immunochemical detection and measurement of catalytic activity of brain AChE. Both of these were associated with certain inherent limitations, as is detailed below, yet each test provided evidence to support part of the explored concept.

Intracranial AS-ON injection is inherently more powerful when centrally controlled behavioral parameters are sought; limitations in this case involve the duration of tests (as the animals are all at a post-surgery state) and the requirement to control for the outcome of this surgical procedure in addition to the behavioral test itself. To avoid excessive complications, we refrained from employing double operations (and, therefore, could not use telemetric measurements, which require transmitter implantation, on *i.c.v.*-injected animals).

The experimental controls, as well, were chosen after careful consideration. Each test should involve both Tg and control animals, as well as sham treatment (injection of either saline or an irrelevant oligonucleotide) and comparison between pre- and post-treatment phenotypes. Whenever possible, animals were self-compared, requiring careful time-of-day comparisons; in other cases, groups of animals with similar pre-treatment behavior patterns were compared to each other with regard to the efficacy of the antisense treatment. Neither of these tests is conclusive by itself, however, their cumulative outcome substantially supported the possibility of employing antisense knockdown in careful behavioral tests.

**Cannula implantation:** Mice under sodium pentobarbital anesthesia (50 mg/Kg, *i.p.*) were placed in a stereotaxic apparatus. Skulls were exposed and a burr hole was drilled. Implantation was with a 26-gauge stainless steel guide cannula (Plastics-One Inc., Roanoke, VA, USA). The tip of the guide cannula was positioned 1 mm above the left lateral ventricle according to the following coordinates: A: -0.4 -0.66\* (bl-3.8), (bl = bregma-lambda); L: 1.5; D: -2.2. The guide cannula was secured to the skull with 3 stainless-steel screws and dental cement, and was closed by a dummy cannula. Mice were housed in individual cages and allowed postoperative recovery of 10-14 days before experiments.

**Preparation of AS-ON:** For *i.c.v.* injection, 2'-O-methyl protected (three-3 nucleotides) oligonucleotides (5 M) targeted against murine AChE (AS3) or BuChE (ASB) mRNA<sup>15</sup> were combined with 13 M of the

lipophilic transfection reagent DOTAP (Roche Diagnostics) in PBS and incubated for 15 min at 37°C prior to injection. One  $\mu$ l (25 ng) of this oligonucleotide solution was injected in each treatment.

***I.c.v.* administration of AS-ON:** For intracranial microinjections, solutions were administered through a 33-gauge stainless steel internal cannula (Plastic One Inc.), which was 1 mm longer than the guide cannula. A PE20 tube connected the internal cannula to a microsyringe pump (KD Scientific Instruments, Boulder, CO, USA). Solutions were administered at a constant rate during 1 min, followed by 1 min during which the internal cannula was left within the guide cannula, to avoid spillage from the guide cannula. Correct positioning of the cannula was verified following each experiment by injection of trypan blue through the cannula and testing dye distribution after removal of the brains.

**Statistical analysis:** The results of the *in situ* hybridization experiment were analyzed by a t-test. The results of the circadian shift (Fig. 3C) were analyzed by a three-way, repeated measures ANOVA (genotype x day (routine/reversed) x circadian phase (dark/light)). The results of the social recognition test (Fig. 4) were analyzed by a three-way, repeated measures ANOVA (genotype x stimulus animal (same or different juvenile) x intersession interval). The results of the experiment on tacrine's effect on social recognition (Fig. 5) were analyzed by a three-way ANOVA (genotype x stimulus animal (same or different juvenile) x drug (tacrine/saline)). The results of the effect of AS3 on social recognition (Fig. 6A) were analyzed by a two-way, repeated measures ANOVA (pretreatment (short/long explorers) x time (days after injection)). The results of the specificity of AS3 effect (Fig. 7) were analyzed by a three-way ANOVA (genotype x drug (AS3/ASB) x time (before/after the treatment)). All ANOVAs were followed by post-hoc tests with the Fisher PLSD procedure.

### Results

**Transgenic mice overexpress host AChE-R:** To explore the specific contribution of variant AChE mRNA transcripts towards neuronal *ACHE* gene expression, Tg mice overexpressing hAChE-S in the nervous system were tested by high resolution *in situ* hybridization using cRNA probes selective for each of the two major AChE variants. Excessive labeling was observed in hAChE-S Tg mice as compared with controls in which hybridization was performed with the AChE-S selective probe. This was consistent with the expected cumulative contribution of the overexpressed human transgene and the host mouse (m)AChE-S mRNA transcript<sup>9,10</sup>. However, hAChE-S Tg mice also displayed variably excessive labeling with the AChE-R cRNA probe, decorating mouse (m)AChE-R mRNA. Fig. 1 presents a representative micrograph of mAChE-R mRNA overexpression in the cortex and hippocampus of a Tg as compared to a control mouse. Neuronal mAChE-R mRNA overproduction in these Tg mice was heterogeneous in its extent, yet significantly higher than that in control mice. Analysis of Fast Red staining showed an increase from an average of 20  $\pm$  3 arbitrary intensity units ( $\pm$  standard error of the mean, S.E.M.) in 5 control animals to 41  $\pm$  5.5 in 6 transgenics ( $t(9) = 10.27$ ,  $p < 0.05$ ). This suggested an inherited predisposition to constitutive AChE-R overproduction in Tg mice. Because AChE-R overproduction is associated with psychological stress, this further called for evaluating its neuroanatomical and behavioral manifestations.

**Hypertrophy in hippocampal astrocytes reflects elevated stress in hAChE-S Tg mice:** Immunocytochemical labeling of glial fibrillary acidic protein (GFAP) was used in search of an independent parameter for evaluating the stress-prone state of hAChE-S Tg mice. Hippocampal astrocytes are known from previous studies to be sensitive to various forms of stress<sup>18,19</sup>. This property is manifest in morphological changes, increased size of cell soma and of astrocytic processes (dendrites) collectively called hypertrophy and which is accompanied by increased expression of GFAP. The hippocampal SLM

is particularly enriched in astrocytes, which appeared to be hypertrophic in hAChE-S Tg mice (Fig. 2, B,D) as compared to age-matched controls (Fig. 2, A,C). Astrocytes in other regions, such as cortex appeared unchanged (Fig. 2, E,F). Fig. 2 presents this selective hippocampal change, which is generally considered to reflect the cumulative load of stressful insults in the mammalian brain and is frequently associated with impaired cognitive and behavioral properties<sup>20</sup>.

Intensity of staining of GFAP-like immunoreactivity in the astrocytic soma was significantly higher in Tg mice ( $176.3 \pm 4.0$ , arbitrary units) compared to control mice ( $147.8 \pm 3.5$ ,  $t = 5.3$ ,  $p < 0.0001$ ). Cross-sectional area of the astrocytic soma was significantly increased in Tg ( $45.9 \pm 1.4 \text{ m}^2$ ) compared to control mice ( $35.4 \pm 1.5$ ,  $t = 5.16$ ,  $p < 0.0001$ ). The stem thickness of the large astrocytic process (dendrite) was greater in Tg mice ( $1.75 \pm 0.05 \text{ m}$ ) compared to control mice ( $1.32 \pm 0.05$ ,  $t = 6.21$ ,  $p < 0.0001$ ). Taken together, these data form a picture of 20-30% hypertrophy in hippocampal astrocytes of hAChE-S Tg mice, consistent with the earlier reports of stress-associated and pathology-associated astrocytic hypertrophy<sup>18,19</sup>.

**AChE overexpression predisposes to hypersensitivity to changed circadian cycle:** Behavioral differences between Tg and control mice were first sought by recording locomotion patterns. Under routine conditions, both genotypes displayed similar home cage activity (Fig. 3A). Their circadian rhythms included, as expected, significantly more frequent and pronounced locomotor activity during the dark phase of the circadian cycle ( $F(1,24) = 18.16$ ,  $p < 0.001$ ) (summarized in Fig. 3C). Seventy-two hr following reversal of the light/dark phases both genotypes lost most of the circadian rhythm in their locomotor activity, as reported by others<sup>21</sup>, but presented distinctive behavioral patterns (Fig. 3B and 3C). After the shift, hAChE-S Tg mice showed a general increase in activity, which was reflected in a significant genotype by day (routine vs. reversed) interaction ( $F(1,24) = 4.68$ ,  $p < 0.05$ ). Post-hoc tests demonstrated in Tg mice significantly increased activity in the reversed cycle (compared with activity in the routine cycle), both during the dark and the light phases ( $p < 0.05$ ). In addition, activity in the dark phase of the reversed cycle, was significantly greater in Tg compared with control mice. These findings indicate that adjustment to the circadian insult was markedly impaired in Tg mice, suggesting that these mice display a genetic predisposition to abnormal responses to changes in the circadian rhythm. The transgenics intensified activity was found to be suppressed for a short time ( $< 3 \text{ hr}$ ) by intravenous administration of AS-ONS targeted to AChE mRNA (preliminary data, data not shown).

**Impaired social recognition due to AChE excess:** In the social recognition paradigm, control mice could recognize a previously encountered ( same ) juvenile. This is manifest as a reduction in exploration time in the second exposure of the mice to the same, but not to a different juvenile, provided that the time interval from the end of the first encounter with that juvenile to the beginning of the memory test did not exceed 15 min. As expected, this memory decayed with increased intersession interval. In contrast, Tg mice tended to explore the previously introduced juvenile longer than control mice and did not display social recognition even after a short interval of 5 min (Fig. 4). These findings were reflected by a significant statistical interaction between the genotype (control vs. Tg) and the stimulus juvenile (same/different) ( $F(1,76) = 9.93$ ,  $p < 0.01$ ). In Tg mice, post-hoc analysis revealed significant reduction in exploration time only when Tg mice were tested immediately after the baseline (0 interval) with the same juvenile. These results are consistent with the cholinergic modulation of social recognition behavior<sup>22</sup>.

The reversible AChE inhibitor, tacrine, has been clinically used for blocking acetylcholine hydrolysis and extending the impaired memory of Alzheimer s disease patients<sup>3</sup>. Therefore, we tested the capacity of

tacrine (1.5 mg/Kg), injected immediately following a baseline encounter with a juvenile mouse, to improve the social recognition of Tg mice. Injected mice were tested with either the same or a different juvenile following a 10-min interval. As expected from previous reports on the beneficial effects of tacrine on social recognition in rats<sup>23</sup>, injection of Tg mice with tacrine induced a significant improvement in recognition memory, with post-treatment performance similar to that displayed by untreated control mice. In contrast, Tg mice displayed no recognition of the same juvenile when injected with saline, and non-Tg control mice maintained unchanged recognition performance when injected with either tacrine or saline (Fig. 5). These findings were reflected by a significant 3-way interaction between the genotype, (control/Tg), the stimulus juvenile (same/different) and the drug (tacrine/saline) ( $F(1,52) = 4.18, p < 0.05$ ). In a similar experiment, in which the injections preceded the social recognition test by 40, rather than 10 min, tacrine had no effect in either Tg or control mice (data not shown). Therefore, tacrine facilitated memory consolidation when administered during the consolidation process, but did not affect acquisition of memory when given in advance.

**Explorative behavior is inversely correlated with brain AChE activity:** Apart from its improvement of memory, tacrine suppressed the exploration behavior toward a different juvenile in control ( $p < 0.05$ ) but not in Tg mice. Decreased locomotor activity under tacrine treatment was suggested to reflect cholinergic mediation of social exploration behavior<sup>24</sup>. To further investigate this concept, control mice were divided into 3 equal groups ( $n = 10$ ), presenting short, intermediate or long exploration time of same juveniles. AChE activity was determined in the cortex and hippocampus of each subgroup, 24 hr following social recognition tests of the "same" juvenile (presented 10 min following first exposure). Mice with lower levels of cortical and hippocampal AChE activity spent more interaction time with the same juvenile than mice with high AChE activity levels (Table 1), so that their explorative behavior was inversely correlated with cortical and hippocampal AChE activity levels (correlation magnitude,  $r = -0.49$  and  $0.41$ , respectively). Compared to shorter explorers, longer explorer mice exhibited a 29% reduction in cortical AChE activity, corresponding to a >80% increase in social exploration time. The significance of the difference between the shorter and longer explorers was verified by ANOVA ( $F(2,27) = 4.89, p < 0.05$ ) and post-hoc tests.

The lack of tacrine effect on the social recognition performance in control mice, and its improvement effect on the social recognition in transgenics, with approximately 50% excess AChE<sup>8</sup>, presented an apparent contradiction to the inverse correlation between AChE catalytic activity and social exploration. One potential explanation to this complex situation was that the inverse correlation in control mice reflected primarily the levels of the synaptic enzyme AChE-S; in contrast, the massive mAChE-R excess in the Tg brain could cause their impaired social recognition behavior. According to this working hypothesis, selective suppression of AChE-R should improve the social recognition performance. To test this hypothesis, we adopted *i.c.v.* injection of AS3 to prevent *de-novo* mAChE-R production<sup>15</sup>. Mice were tested in the social exploration paradigm once before (baseline) and then 1, 3 and 6 days after 2 daily injections of AS3. Fig. 6A presents the experimental design of these tests.

**AS3 improvement of social exploration increases in efficacy and duration in animals with severe pre-treatment impairments:** Post-treatment follow-up of social exploration was performed 1, 3 and 6 days following AS3 treatment in animals with short, medium and long pre-treatment social exploration behavior ( $n = 5-6$ /group). As expected, there was a significant overall difference between the short and the long groups in exploration time ( $F(1,24) = 10.81, p < 0.05$ ). However, post-hoc tests revealed that these groups differed significantly only during the pre-treatment day ( $p < 0.05$ ), and not after the AS3 treatment (Fig. 6B). Furthermore, within the long, but not the short explorers group, social exploration of the same

juvenile was significantly reduced ( $p < 0.05$ ) one day after the AS3 injection (attesting to the efficacy of this treatment), with progressive increases in social exploration time during the 5 subsequent days. Because of the pre-treatment differences, the severely impaired animals sustained a certain level of improvement even at the sixth post-treatment day (Fig. 6B) (i.e., even on this day there was no resumption of the pre-treatment difference between the short and long explorers). This experiment thus demonstrated reversibility of the antisense treatment, however with exceedingly long duration, especially in animals with severe pre-treatment impairments and in comparison to the short-term efficacy of tacrine.

**Antisense AChE-R mRNA suppression selectively reduces brain AChE-R protein:** Tg mice with long pre-treatment explorative behavior displayed a significant improvement in social exploration of the same juvenile 24 hr following the second treatment with AS3, but not with the irrelevant AS-ON ASB (Fig. 8A) ( $F(1,10) = 33.95$ ,  $p < 0.001$ ). ASB, targeted to the related enzyme, butyrylcholinesterase, served as a sequence specificity control. Control mice with either long or short pre-treatment social exploration showed no response to either AS3 or ASB (Fig. 7A and data not shown), attesting to the selectivity of this treatment for treating AChE-R overexpressing animals and its sequence-specificity in reversing the AChE-R induced impairment of behavior.

Catalytic activity measurements performed 24 hr after the last AS-ON injection failed to show differences, perhaps due to the limited number of animals and the variable enzyme levels. However, immunodetected AChE-R protein levels were significantly lower in AS3 treated mice as compared with ASB treated mice, regardless of their genotype or pre-treatment behavior pattern (Fig 7B and data not shown,  $F(1,22) = 19.63$ ,  $p < 0.001$ ). In contrast, densitometric analysis of immunodetected total AChE protein (detected by an antibody targeted to the N-terminus, common to both isoforms) revealed essentially unchanged signals (data not shown). In further tests for potential association, post-treatment AChE-R levels were plotted as a function of the social exploration values. Data points clustered separately before the AS-ON treatment (Fig. 8A), with both AChE-R levels and exploration times of controls clearly different from transgenics. After treatment, long explorer transgenics shifted to short exploration values (Fig. 8B). Intriguingly, the explorative behavior of long explorer controls was not affected by the treatment, indicating that the reduction in mAChE-R following AS3 treatment affected only animals that were behaviorally impaired before the treatment.

#### Discussion

Combination of behavioral, molecular and biochemical analyses revealed multileveled contributions of cholinergic neurotransmission and *ACHE* gene expression, towards the general activity and social behavior of adult Tg mice over-expressing neuronal AChE. In addition to inherited excess of hAChE-S, these Tg mice display conspicuous yet heterogeneous overexpression of the stress-associated "readthrough" mAChE-R in their cortical and hippocampal neurons. Nevertheless, they present close to normal activity patterns under normal maintenance conditions with minimal external challenges. In contrast, their capacity to adjust to behavioral changes in response to external signals appears to be compromised, suggesting that they suffer genetic predisposition for adverse responses to stressful stimuli<sup>20</sup>.

**Behavioral and learning impairments of cholinergic origin:** When subjected to a day/night switch, hAChE-S Tg mice respond with excessive bursts of locomotor activity, particularly during the dark phase, but also during the light phase of the post-shift diurnal cycle. In preliminary experiments, this excessive activity could be transiently suppressed by antisense oligonucleotides, which was especially encouraging in view of the progressively impaired neuromotor functioning in these mice<sup>25</sup>. Matched controls, unlike

transgenics, display, as expected, relatively suppressed locomotor activity during the post-shift dark phase<sup>26</sup>. When confronted twice with a conspecific young mouse, hAChE-S Tg mice spend significantly longer periods than controls in the social interactions characterizing such confrontations. Similarly, in a new environment, hAChE-S Tg mice displayed increased locomotor activity as compared with controls<sup>11</sup>. In the social recognition paradigm, they failed to remember a conspecific juvenile, even following a delay interval of only 5 min. This extends previous reports on their spatial learning and memory impairments<sup>9,10</sup> and agrees with previous reports<sup>22,27</sup> on the social behavior changes associated with cholinergic impairments.

Several other neurotransmission systems, e.g. vasopressin<sup>28</sup>, are most likely related, as well, with impaired social interactions. In hAChE-S Tg mice, however, this phenotype may be attributed to hypo-cholinergic functioning due to AChE excess, as is evident from the capacity of the AChE inhibitor tacrine to retrieve their social recognition. Nevertheless, tacrine's effects appeared surprisingly short-lived, consistent with findings of others<sup>29</sup>. In contrast, exceedingly low doses of oligonucleotides suppressing AChE-R synthesis exerted considerably longer-term improvement of the social recognition skills of Tg mice. This suggested non-catalytic activities as an alternative explanation(s) for the behavioral and cognitive impairments caused by AChE-R excess<sup>30</sup>.

**Circadian switch as a behavioral stressor:** Cholinergic neurotransmission circuits are known to be subject to circadian changes<sup>1</sup> and control the sensorimotor cortical regions regulating such activity<sup>31</sup>. Therefore, the intensified response of hAChE-S Tg mice to the circadian switch suggested that their hypo-cholinergic state is the cause. The variable nature of the excessive locomotor activity in the Tg mice indicates an acquired basis for its extent and duration. A potential origin of such heterogeneity could be the variable extent of neuronal mAChE-R mRNA in the sensorimotor cortex and hippocampal neurons. Both psychological<sup>4</sup> and physical stressors<sup>15</sup> induce neuronal AChE-R overproduction. Exaggerated stress responses, such as the intense locomotor response to the mild stress of a circadian switch, can hence be expected to exacerbate the hypo-cholinergic state of these already compromised animals,

In social behavior tests, hAChE-S Tg mice display impaired recall processes causing poor recognition when confronted with a conspecific young mouse. Therefore AChE-R overexpression, which is also induced under stress<sup>4</sup>, may be causally involved with the reported suppression of recall processes under stress<sup>32</sup> as well as with the apparent correlation between stress and hippocampal dysfunction<sup>33</sup>. This suggests that excess AChE-R can simultaneously impair recall processes and induce excessive locomotion. Stress-induced effects on learning and memory processes have been reported by others<sup>34</sup>, but were not correlated with AChE levels. Our current findings of improvement in transgenics' exploration behavior following tacrine injection, which would be expected to augment cholinergic neurotransmission, strongly indicate that their hypo-cholinergic state was the cause.

**Advantages and limitations of anticholinesterases:** In control mice, with low AChE-R levels, tacrine did not affect the normal social recognition capacity. This suggests that suppression of AChE activity may have distinct effects under normal and stress-induced conditions. Tg mice with higher AChE levels have accommodated themselves to this state, and it may be this accommodation that renders them incapable of facing a challenge by an anti-ChE. One option is that of a threshold AChE-R activity that would be compatible both with satisfactory memory and normal locomotion. This balance is impaired in the Tg mice and may also be disrupted under inducers of long-term AChE-R overproduction, e.g. stress or exposure to anticholinesterases<sup>6</sup>. This, in turn, implies that the effect of anticholinesterases would depend on the initial

levels of specific AChE variants in the treated mammal. Above the behaviorally-compatible threshold of AChE-R, anticholinesterases would exert behavioral improvement, whereas below it, their effects would be limited, which can explain their differential efficacy in patients with different severity of symptoms.

**Glucocorticoid regulation of cholinergic behavioral patterns:** The separation between general behavior patterns and learning paradigms as those relate to cholinergic transmission may explain why AChE transgenics, so dramatically impaired in their learning capacities, display such subtle deficiencies in their daily behavior. According to this concept, a constitutive hypocholinergic condition would be evident as a failure to learn and remember, however, its behavioral effect will be far less pronounced, unless challenged. This predisposition to drastic responses to external insults is indeed reminiscent of the reported behavior of demented patients. It had been initially attributed to their elevated cortisol levels<sup>35</sup>, which matches recent findings in primates<sup>36</sup>. Indeed, cortisol upregulates *ACHE* gene expression and elevates AChE-R levels<sup>37</sup>, possibly above the required threshold. In addition, both psychological stress and glucocorticoid hormones were reported to impair spatial working memory<sup>38,39</sup>, consistent with such impairments in the hAChE-S Tg mice. The intensive overexpression of mAChE-R in these mice mimics a situation in which the individual capacity for AChE-R overproduction would be tightly correlated both with the severity of the behavioral impairments induced under cholinergic hypofunction and with the capacity of anticholinesterases to affect learning and behavior properties.

**Low dose and long duration of efficacy for antisense agents:** The short duration of the behavioral and memory improvements afforded by administration of tacrine parallels the time scale reported for the induction by such inhibitors of a transcriptional activation<sup>4</sup>. Together with a shift in alternative splicing this feedback response causes secondary AChE-R accumulation facilitating the hypocholinergic condition<sup>40</sup>. Recent reports demonstrate AChE accumulation in the cerebrospinal fluid of anticholinesterases-treated Alzheimer's disease patients<sup>41</sup>, suggesting that such feedback response occurs also in humans with cholinergic deficiencies<sup>42</sup> and perhaps explaining the gradual increase in anticholinesterase dosage that is necessary to maintain their palliative value in patients.

Unlike tacrine, the temporary antisense suppression of AChE synthesis improves social recognition in Tg mice for up to 6 days. This requires exceedingly low doses (25 ng per daily treatment) of the antisense agent, about  $10^4$ -fold lower in molar terms than tacrine concentrations. Active site enzyme inhibitors should be administered in stoichiometric ratios with the large numbers of their protein target molecules. Moreover, the action of such inhibitors terminates when they reach their target. In contrast, a single chemically protected antisense molecule can cause the destruction of numerous mRNA transcripts, each capable of producing dozens of protein molecules. Assuming translation rates of approximately half-hour per chain and an average half-life of several hours for each transcript, destruction of each mRNA chain would prevent the production of many protein molecules. Therefore, the cumulative efficacy of antisense agents can exceed that of protein blockers by several orders of magnitude<sup>43,44</sup>. Moreover, the palliative effects of AS-ON destroying AChE-R mRNA should extend long after the AS-ON is destroyed, because AChE-R-induced adverse consequences would occur only above a certain threshold which takes time to accumulate. Therefore, the dose dependent nature of the adverse consequences of AChE-R excess makes it particularly attractive as a target for antisense therapeutics.

We have recently found that AChE-R mRNA, having a long 3' untranslated domain, is significantly more sensitive to antisense destruction than the synaptic transcript<sup>15,37</sup>. AChE-R mRNA transcripts would hence be preferentially destroyed, so that the excess of AChE-R, but not much of the synaptic enzyme,

would decrease. This effect may explain the extended duration and increased efficacy of the antisense treatment in modifying behavior and learning exclusively in those mice with disturbed social recognition.

In conclusion, our study provides a tentative explanation for the behavioral impairments under imbalanced cholinergic neurotransmission, attributes much of these impairments to the stress-related effects of the AChE-R variant and suggests the development of antisense approach to selectively ameliorate these effects.

#### Acknowledgements

The authors are grateful to Prof. Konrad L ffelholz and Drs. Franz-Josef van der Staay (Germany), Menno Pieter Gerkema (The Netherlands) and David Glick (Israel) for discussions and help with experiments. This study was supported by the US-Israel Binational Science Foundation (1999/115), the US Army Medical Research and Development Command (DAMD 17-99-1-9547) and Ester Neuroscience, Ltd. (to H.S.). R.Y. and H.S. are members of the Eric Roland Center for Neurodegenerative Diseases of The Hebrew University of Jerusalem. C.E. was the incumbent of a post-doctoral fellowship from the Minerva Foundation.

#### References

1. Carlson, N.R. *Physiology of Behavior*, (Allyn and Bacon, Needham Heights, MA, 1994).
2. Cummings, J.L. & Back, C. The cholinergic hypothesis of neuropsychiatric symptoms in Alzheimer's disease. *Am J Geriatr Psychiatry* 1998; **6**: S64-78.
3. Giacobini, E. Present and future of Alzheimer therapy. *J Neural Transm Suppl* 2000; **59**: 231-242.
4. Kaufer, D., Friedman, A., Seidman, S. & Soreq, H. Acute stress facilitates long-lasting changes in cholinergic gene expression. *Nature* 1998; **393**: 373-377.
5. Xie, J. & McCobb, D.P. Control of alternative splicing of potassium channels by stress hormones. *Science* 1998; **280**: 443-446.
6. Kaufer, D. & Soreq, H. Tracking cholinergic pathways from psychological and chemical stressors to variable neurodeterioration paradigms. *Curr Opin Neurol* 1999; **12**: 739-743.
7. Grisaru, D., Sternfeld, M., Eldor, A., Glick, D. & Soreq, H. Structural roles of acetylcholinesterase variants in biology and pathology. *Eur J Biochem* 1999; **264**: 672-686.
8. Sternfeld, M. *et al.* Excess "readthrough" acetylcholinesterase attenuates but the "synaptic" variant intensifies neurodeterioration correlates. *Proc. Natl. Acad. Sci. USA* 2000; **97**: 8647-8652.
9. Beeri, R. *et al.* Transgenic expression of human acetylcholinesterase induces progressive cognitive deterioration in mice. *Curr Biol* 1995; **5**: 1063-1071.
10. Beeri, R. *et al.* Enhanced hemicholinium binding and attenuated dendrite branching in cognitively impaired acetylcholinesterase-transgenic mice. *J Neurochem* 1997; **69**: 2441-2451.
11. Erb, C. *et al.* Compensatory mechanisms enhance hippocampal acetylcholine release in transgenic mice expressing human acetylcholinesterase. *J Neurochem* 2001; **77**: 638-646.
12. Shapira, M. *et al.* A transcription-activating polymorphism in the ACHE promoter associated with acute sensitivity to anti-acetylcholinesterases. *Hum Mol Genet* 2000; **9**: 1273-1281.
13. Suer, C., Dolu, N., Ozesmi, C., Yilmaz, A. & Sahin, O. Effect of reversed light-dark cycle on skin conductance in male rats. *Percept Mot Skills* 1998; **87**: 1267-1274.
14. Thor, D.H. & Holloway, W.R. Social memory of the male laboratory rat. *J Comp Psychol* 1982; **96**: 1000-1006.
15. Shohami, E. *et al.* Antisense prevention of neuronal damages following head injury in mice. *J Mol Med* 2000; **78**: 228-236.

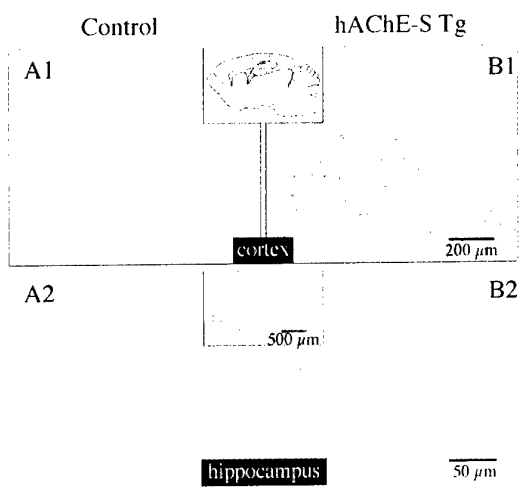
16. Yirmiya, R., Barak, O., Avitsur, R., Gallily, R. & Weidenfeld, J. Intracerebral administration of *Mycoplasma fermentans* produces sickness behavior: role of prostaglandins. *Brain Res* 1997: **749**: 71-81.
17. Sternfeld, M. *et al.* Acetylcholinesterase enhances neurite growth and synapse development through alternative contributions of its hydrolytic capacity, core protein, and variable C termini. *J Neurosci* 1998: **18**: 1240-1249.
18. Laping, N.J., Nichols, N.R., Day, J.R., Johnson, S.A. & Finch, C.E. Transcriptional control of glial fibrillary acidic protein and glutamine synthetase in vivo shows opposite responses to corticosterone in the hippocampus. *Endocrinology* 1994: **135**: 1928-1933.
19. Sirevaag, A.M., Black, J.E. & Greenough, W.T. Astrocyte hypertrophy in the dentate gyrus of young male rats reflects variation of individual stress rather than group environmental complexity manipulations. *Exp Neurol* 1991: **111**: 74-79.
20. McEwen, B.S. & Sapolsky, R.M. Stress and cognitive function. *Curr Opin Neurobiol* 1995: **5**: 205-216.
21. Hillegaart, V. & Ahlenius, S. Time course for synchronization of spontaneous locomotor activity in the rat following reversal of the daylight (12:12 h) cycle. *Physiol Behav* 1994: **55**: 73-75.
22. Winslow, J.T. & Camacho, F. Cholinergic modulation of a decrement in social investigation following repeated contacts between mice. *Psychopharmacology (Berl)* 1995: **121**: 164-172.
23. Gheusi, G., Bluthe, R.M., Goodall, G. & Dantzer, R. Ethological study of the effects of tetrahydroaminoacridine (THA) on social recognition in rats. *Psychopharmacology (Berl)* 1994: **114**: 644-650.
24. Shannon, H.E. & Peters, S.C. A comparison of the effects of cholinergic and dopaminergic agents on scopolamine-induced hyperactivity in mice. *J Pharmacol Exp Ther* 1990: **255**: 549-553.
25. Andres, C. *et al.* Acetylcholinesterase-transgenic mice display embryonic modulations in spinal cord choline acetyltransferase and neurexin I $\beta$  gene expression followed by late-onset neuromotor deterioration. *Proc Natl Acad Sci U S A* 1997: **94**: 8173-8178.
26. Murata, J. *et al.* Effects of mental stress on cardiac and motor rhythms. *J Auton Nerv Syst* 1999: **75**: 32-37.
27. Perio, A. *et al.* Specific modulation of social memory in rats by cholinomimetic and nootropic drugs, by benzodiazepine inverse agonists, but not by psychostimulants. *Psychopharmacology* 1989: **97**: 262-268.
28. Bluthe, R.M., Schoenen, J. & Dantzer, R. Androgen-dependent vasopressinergic neurons are involved in social recognition in rats. *Brain Res* 1990: **519**: 150-157.
29. Sekiguchi, R., Wolterink, G. & van Ree, J.M. Short duration of retroactive facilitation of social recognition in rats. *Physiol Behav* 1991: **50**: 1253-1256.
30. Soreq, H. & Seidman, S. Acetylcholinesterase--new roles for an old actor. *Nat Rev Neurosci* 2001: **2**: 294-302.
31. Fibiger, H.C., Damsma, G. & Day, J.C. Behavioral pharmacology and biochemistry of central cholinergic neurotransmission. *Adv Exp Med Biol* 1991: **295**: 399-414.
32. Kramer, T.H., Buckhout, R., Fox, P., Widman, E. & *et-al.* Effects of stress on recall. *Appl Cog Psychol* 1991: **5**: 483-488.
33. Liberzon, I., Lopez, J.F., Flagel, S.B., Vazquez, D.M. & Young, E.A. Differential regulation of hippocampal glucocorticoid receptors mRNA and fast feedback: relevance to post-traumatic stress disorder. *J Neuroendocrinol* 1999: **11**: 11-17.
34. Kaneto, H. Learning/memory processes under stress conditions. *Behav Brain Res* 1997: **83**: 71-74.

35. Weiner, M.F., Vobach, S., Olsson, K., Svetlik, D. & Risser, R.C. Cortisol secretion and Alzheimer's disease progression. *Biol Psychiatry* 1997: **42**: 1030-1038.
36. Habib, K.E. *et al.* Oral administration of a corticotropin-releasing hormone receptor antagonist significantly attenuates behavioral, neuroendocrine, and autonomic responses to stress in primates. *Proc Natl Acad Sci U S A* 2000: **97**: 6079-6084.
37. Grisaru, D. *et al.* ARP, a peptide derived from the stress-associated acetylcholinesterase variant, has hematopoietic growth promoting activities. *Mol Med* 2001: **7**: 93-105.
38. Diamond, D.M., Fleshner, M., Ingersoll, N. & Rose, G.M. Psychological stress impairs spatial working memory: relevance to electrophysiological studies of hippocampal function. *Behav Neurosci* 1996: **110**: 661-672.
39. de Quervain, D.J., Roozendaal, B. & McGaugh, J.L. Stress and glucocorticoids impair retrieval of long-term spatial memory. *Nature* 1998: **394**: 787-790.
40. Kaufer, D., Friedman, A., Seidman, S. & Soreq, H. Anticholinesterases induce multigenic transcriptional feedback response suppressing cholinergic neurotransmission. *Chem Biol Interact* 1999: **119-120**: 349-360.
41. Nordberg, A., Hellstrom-Lindahl, E., Almkvist, O. & Meurling, L. Activity of acetylcholinesterase in CSF increases in Alzheimer's patients after treatment with tacrine. *Alzheimer's Reports* 1999: **2**: 347-352.
42. Coyle, J.T., Price, D.L. & DeLong, M.R. Alzheimer's disease: a disorder of cortical cholinergic innervation. *Science* 1983: **219**: 1184-1190.
43. Seidman, S., Eckstein, F., Grifman, M. & Soreq, H. Antisense technologies have a future fighting neurodegenerative diseases. *Antisense Nucleic Acid Drug Dev* 1999: **9**: 333-340.
44. Galyam, N. *et al.* Complex host cell responses to antisense suppression of AChE gene expression. *Antisense Nucleic Acid Drug Dev* 2001: **11**: 51-57.

**Table 1: Social exploration behavior and brain AChE activities.**

	exploration time percent of baseline	specific AChE activity nmol ATCh hydrolyzed/min/mg protein	
		hippocampus	cortex
<b>total population</b>	80 – 4	87 – 4	90 – 5
<b>shorter exploration time</b>	57 – 3	96 – 6	104 – 10
<b>intermediate exploration time</b>	78 – 2	95 – 6	92 – 10
<b>longer exploration time</b>	104 – 3	71 – 7**	74 – 8*

Control FVB/N male mouse population (n = 30) (3-5 months) was divided into three equal groups (n = 10) with short, intermediate and long exploration time of the same juvenile (shown as average – S.E.M. percent of baseline). Intersession interval was 10 min for all groups. Mice were sacrificed 24 hr after the behavior test and AChE specific activities were measured in hippocampus and cortex extracts. Asterisks mark significantly lower AChE specific activity in control long explorers as compared with short explorers (p <0.01 for hippocampus and p <0.05 for cortex; ANOVA followed by post-hoc tests with the Fisher PLSD procedure).



**Figures**  
**Fig 1: Intensive neuronal AChE-R mRNA expression in Tg mice**  
 Shown are representative micrographs of *in situ* hybridization in parietal cortex (A<sub>1</sub>, B<sub>1</sub>) and hippocampus (A<sub>2</sub>, B<sub>2</sub>) using an AChE-R cRNA probe and Fast Red detection. Insets: schematic drawing (top) or low-magnification micrograph presenting the location of higher magnification micrographs in the cortex and hippocampal CA3 region. Note the intense AChE-R expression in cortical and hippocampal neurons of Tg mice.

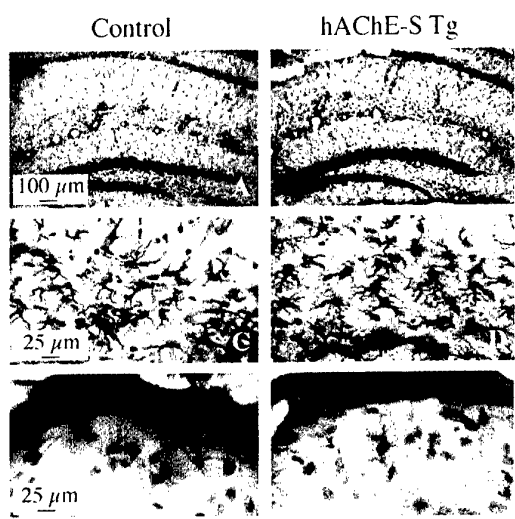


**Fig. 2: Intensified GFAP staining in hypertrophic hippocampal astrocytes of hAChE-S Tg mice .**  
 Shown are light microscopy micrographs of GFAP immunocytochemical staining in the brain of control (A,C,E) and Tg (B, D, F) mice. Note the intensified cell body staining in hippocampal (A-D) but not in cortical astrocytes (E,F) and the thickened process extensions in the transgenics' astrocytes.

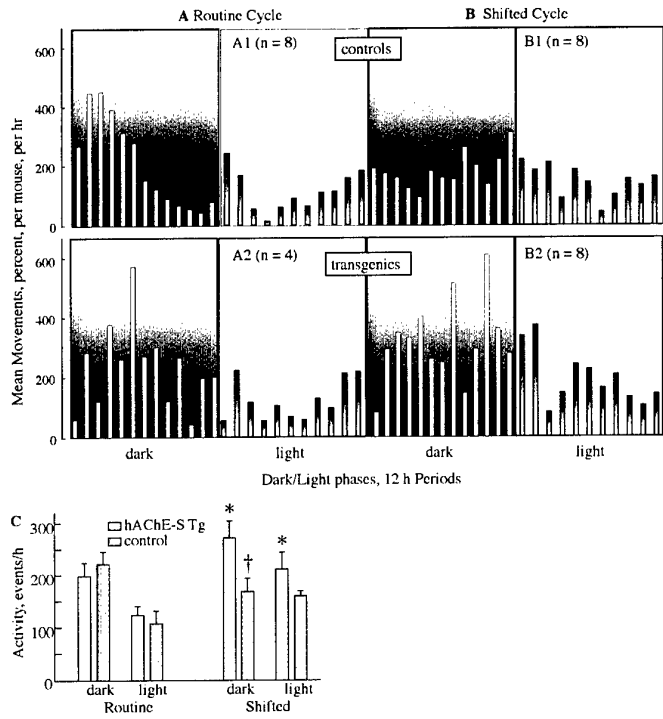


**Fig 3: Spontaneous locomotor activity of control and Tg mice under routine dark/light cycle and following cycle reversal.**

Locomotor activity was detected by biotelemetric-recorded movements for 24 hr and is displayed as percent of the mean movements per mouse per hr. Shaded areas in the figure indicate the dark phases of the light/dark cycle. A, routine cycle; B, shifted cycle.; C. summated activity intensification. Shown are values of locomotor activity during the dark and light phases in the daily cycle for Tg and age-matched control mice under routine and reversed cycles. \*Significantly different from the corresponding group in the routine condition ( $p < 0.05$ ). †Significantly different from Tg mice in the dark phase of the reversed condition.

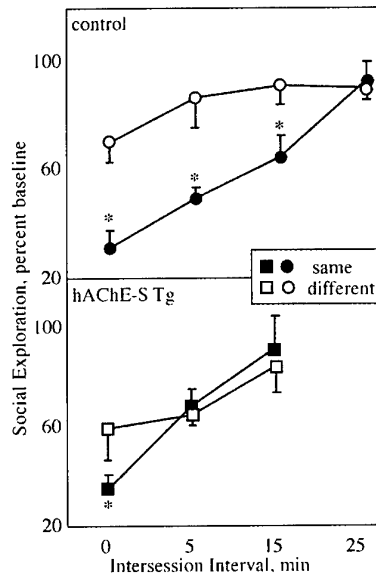


**Fig. 4: Working memory deficiency in Tg mice**

Shown is percent of baseline social exploration time for 8-11 wk old Tg and control male mice as a function of the intersession interval. Average baseline exploration time was 143 – 5 and 153 – 5 (sec – S.E.M.) for transgenics ( $n = 42$ ) and control mice ( $n = 48$ ), respectively. Asterisks mark significant reductions of exploration time toward the same juvenile ( $p < 0.05$ ), as compared to a different juvenile, i.e. short-term working memory. Increased exploration time of the same juvenile with increasing intersession intervals reflects time-dependent decay in the working memory of control mice. After a 5 min interval, Tg mice displayed no reduction in exploration time toward the same juvenile, indicating that they did not remember the same mouse for even 5 min.

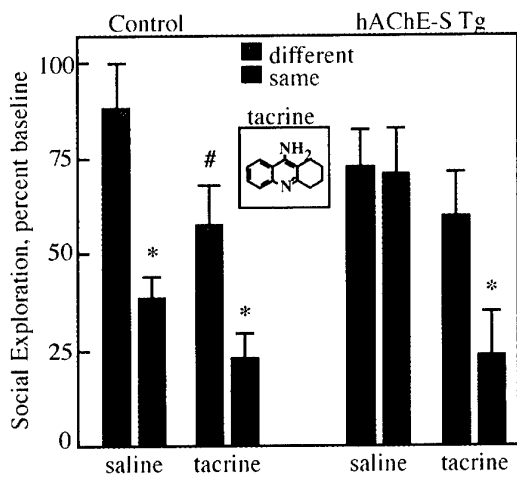


**Fig 5: Tacrine improves working memory of Tg mice**

Presented is the mean social exploration time – S.E.M. as percentage of baseline time for 29 control and 32 Tg mice (12-15 wk. old, 7-8 mice/group) where either tacrine (1.5 mg/Kg) or saline (10 ml/Kg body weight) was administered intraperitoneally immediately following the baseline exploration period. The intersession interval was 10 min for all groups. Note the post-treatment shortening of explorative time of Tg mice, reflecting improved working memory. Asterisks mark significant reduction of exploration time toward the same juvenile ( $p < 0.05$ ) as compared to a different juvenile. # marks a significant tacrine-induced reduction of exploration time toward the different juvenile ( $p < 0.05$ ).

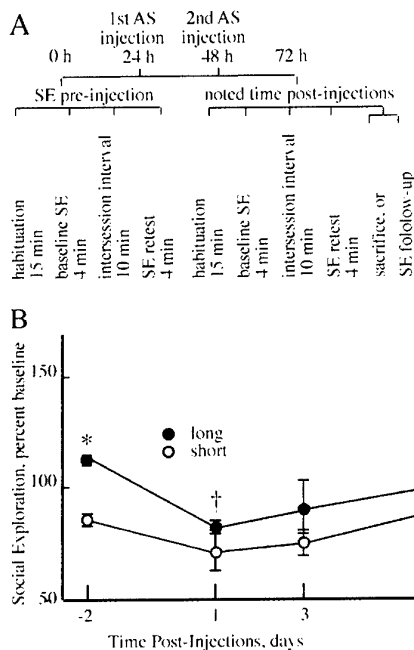


**Fig. 6: *I.c.v.* antisense effect on the excessive social exploration behavior of Tg mice. A. The experimental paradigm.**

Shown is the order of procedures and tests of the social exploration capacity in cannula-implanted mice following antisense treatment. See Materials and Methods for details. B. Long-term reversibility and correlation of treatment efficacy with the severity of pre-treatment symptoms. Shown are social exploration values, in percent of baseline performance, for cannulated hAChE-S Tg mice with short and long pre-treatment exploration of the same juvenile, following *i.c.v.* AS3 treatment ( $n = 5$  mice per group). Note that both the efficacy and the duration of the suppression effect are directly correlated to the severity of pre-treatment symptoms. \*Significantly different from mice with short exploration time, at day -2 ( $p < 0.05$ ). †Significantly different from mice with long exploration time, at day -2 ( $p < 0.05$ ).

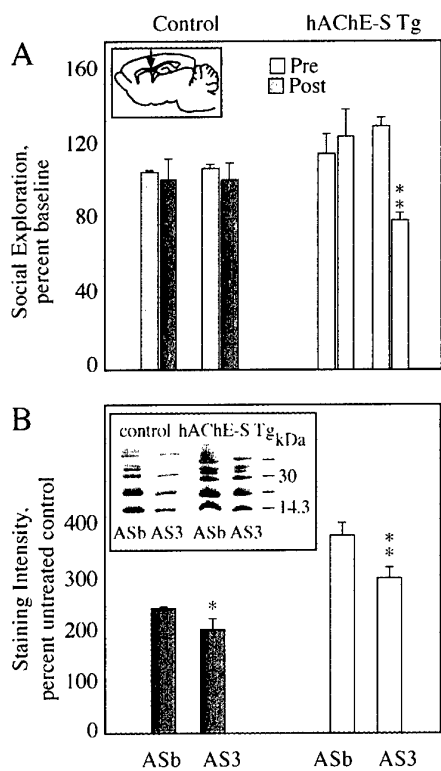


**Fig 7: AS3 decreases brain AChE-R levels and ameliorates social recognition deficits in Tg-mice**

Tg (n = 36) and control (n = 22) cannula-implanted mice, 10-20 wk old, were injected *i.c.v.* with AS-ONs targeted against AChE (AS3) or butyrylcholinesterase (ASB) on 2 consecutive days. Social exploration of the "same" juvenile was tested 24 hr before (pre) and 24 hr after (post) injections. Mice were sacrificed immediately after the last social recognition test and brain homogenates subjected to immunodetection of AChE-R. A. Social exploration behavior. Shown are mean social exploration of the same juvenile (percent of baseline – S.E.M.) before (pre) and 24 hr after (post) AS-ON treatment for long explorer mice (see Table 1). Asterisk marks significant reduction of social exploration time after AS3 treatment (p <0.05). Inset: Location of icv cannula in the brain (arrow). B. Immunodetected AChE-R. Mean – S.E.M. densitometry values for immunodetected AChE-R in cortex extracts of the noted groups post-treatment. AChE-R levels in uncannulated control mice were considered 100%. Asterisks mark significant reduction of AChE-R levels in AS3 as compared to ASB treated mice (\*\*: p <0.05, \*: p <0.1). Note the significant reduction of immunodetected AChE-R and fragments thereof in cortices from both groups treated with AS3 as compared with those

treated with the control reagent, ASB.

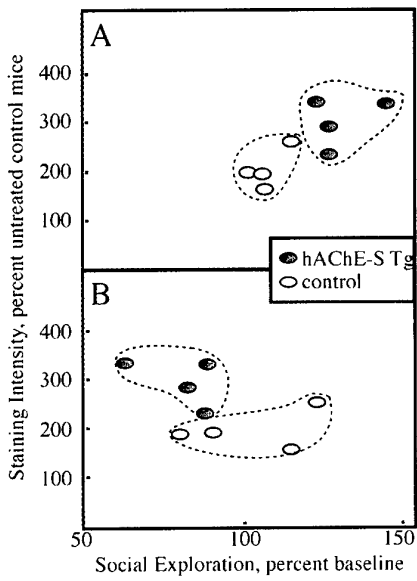


**Fig. 8: Decreased AChE-R levels correlate with reduced social exploration time in Tg mice.**

Presented are cortical AChE-R levels (immunodetected protein, percent of levels in uncannulated controls) as a function of social exploration for each mouse before (A) and after (B) AS3 treatment. Long-explorer mice, each represented by a dot, were sorted by their genetic backgrounds (control and Tg). Note the exclusive post-treatment shift in the clustered distribution of the Tg long explorers, with excessive mAChE-R levels, as compared with the non-shifted cluster of long-explorer controls.

## Brief Communication

# Complex Host Cell Responses to Antisense Suppression of *ACHE* Gene Expression

N. GALYAM,<sup>1</sup> D. GRISARU,<sup>1,2,3</sup> M. GRIFMAN,<sup>1</sup> N. MELAMED-BOOK,<sup>1</sup> F. ECKSTEIN,<sup>4</sup>  
S. SEIDMAN,<sup>1</sup> A. ELDOR,<sup>3</sup> and H. SOREQ<sup>1</sup>

### ABSTRACT

3'-End-capped, 20-mer antisense oligodeoxynucleotides (AS-ODN) protected with 2'-O-methyl (Me) or phosphorothioate (PS) substitutions were targeted to acetylcholinesterase (AChE) mRNA and studied in PC12 cells. Me-modified AS-ODN suppressed AChE activity up to 50% at concentrations of 0.02–100 nM. PS-ODN was effective at 1–100 nM. Both AS-ODN displayed progressively decreased efficacy above 10 nM. *In situ* hybridization and confocal microscopy demonstrated dose-dependent decreases, then increases, in AChE mRNA. Moreover, labeling at nuclear foci suggested facilitated transcription or stabilization of AChE mRNA or both under AS-ODN. Intracellular concentrations of biotinylated oligonucleotide equaled those of target mRNA at extracellular concentrations of 0.02 nM yet increased only 6-fold at 1  $\mu$ M ODN. Above 50 nM, sequence-independent swelling of cellular, but not nuclear, volume was observed. Our findings demonstrate suppressed AChE expression using extremely low concentrations of AS-ODN and attribute reduced efficacy at higher concentrations to complex host cell feedback responses.

### INTRODUCTION

ANTISENSE OLIGODEOXYNUCLEOTIDES (AS-ODN) are powerful tools for sequence-dependent suppression of target genes (Agrawal and Kandimalla, 2000; Crooke, 2000). AS-ODN are presumed to act by facilitating the action of ribonuclease on mRNA-ODN hybrids (Ma et al., 2000; Wu et al., 1999). To exert their effects, AS-ODN must enter the cell, interact with their target mRNA long enough for the nuclease to act, and then attach to another mRNA. Much effort has been devoted to understanding the cellular uptake and mechanism of action of AS-ODN (Beltinger et al., 1995). In contrast, less is known about host cell responses to this process. For example, it is not known whether AS-ODN-treated cells compensate for lost mRNA. This issue is important, as feedback upregulation of a targeted gene may mask antisense effects and encourage the use of excessively high concentrations of ODN.

Another important issue to address relates to the effects of

foreign DNA and AS-ODN degradation products, such as free nucleotides, on cellular physiology. Nucleotides and their analogs modulate cell volume through several independent mechanisms (Galiotta et al., 1992). Under physiologic steady-state conditions, cell volume is held constant by a pump-leak mechanism. The osmotic pressure arising from impermeable cytoplasmic solutes is balanced by the Na<sup>+</sup>/K<sup>+</sup> pump, accompanied by the constant expenditure of metabolic energy (Hoffmann, 1992). Micromolar or lower adenosine concentrations, such as those expected to accumulate by degradation of ODN, were shown to activate the A1 adenosine receptor and a Cl<sup>-</sup> channel in the apical membrane of RCCT-28A endothelial cells (Light et al., 1990; Schwiebert et al., 1992). Extracellular ATP, UTP, and related compounds similarly stimulate Cl<sup>-</sup> secretion and affect cell volume in the nasal epithelium of both normal and cystic fibrosis patients (Knowles et al., 1991). Once they enter the cell, nucleotides affect the nucleocytoplasmic shuttle of proteins and RNA (Gerace, 1995), whereas nonhydrolyzable

<sup>1</sup>Department of Biological Chemistry, The Institute of Life Sciences, The Hebrew University of Jerusalem, Israel 91904.

<sup>2</sup>Department of Obstetrics and Gynecology, and <sup>3</sup>Institute of Hematology, Tel-Aviv Sourasky Medical Center, The Sackler School of Medicine, Tel Aviv University, Israel.

<sup>4</sup>Max Planck Institute for Experimental Medicine, D-37075 Gottingen, Germany.

GTP analogs inhibit this shuttle (Melchior et al., 1993). Changes in nuclear protein import may affect several levels of cellular metabolism (Gorlich, 1998) but have not yet been examined under AS-ODN treatment. These observations predict sequence-nonspecific cellular responses to AS-ODN treatments. Therefore, both the balance of ion homeostasis and nuclear-cytoplasmic interactions must be considered in AS-ODN studies.

Acetylcholinesterase (AChE) is an appropriate model to investigate host cell responses to AS-ODN. The single *ACHE* gene produces three 3'-alternatively spliced mRNA transcripts, AChE-S, AChE-E, and AChE-R (Grisaru et al., 1999b). AChE is ubiquitously expressed at variable levels in diverse tissues and cell types and undergoes transcript-specific, differentiation-dependent stabilization (Chan et al., 1998). We previously demonstrated that AChE mRNA and protein are overexpressed in rodent brain and muscle following acute pharmacologic blockade of catalytic activity (Friedman et al., 1996; Kaufer et al., 1998; Lev-Lehman et al., 2000). However, it was not known whether antisense blockade of AChE synthesis would elicit similar feedback responses. In addition, it was shown that plasmid-encoded AS-cRNA suppressing *ACHE* gene expression alters the growth properties of mouse neuroblastoma cells (Koenigsberger et al., 1997) and rat neuroendocrine PC12 cells (Grifman et al., 1998). These studies suggested complex cellular responses to antisense-mediated AChE deficiencies. Two AS-ODN targeted to AChE mRNA, AS1 and AS3, suppressed AChE expression in PC12 cells (Grifman and Soreq, 1997), human osteosarcoma Saos-2 cells (Grisaru et al., 1999a), and hematopoietic CD34<sup>+</sup> cells from umbilical cord blood (Grisaru et al., 2001), with corresponding physiologic effects. Here, we studied cellular responses of PC12 cells to AChE AS-ODN-mediated suppression of AChE activity.

## MATERIALS AND METHODS

### *PC12 rat pheochromocytoma cells*

PC12 cells were grown in a fully humidified atmosphere at 37°C and 5% CO<sub>2</sub> in Dulbecco modified Eagle medium (DMEM) containing 8% each fetal bovine serum (FBS) and horse serum (HS) (tissue culture reagents from Biological Industries, Beth Haemek, Israel). To induce differentiation, 50 ng/ml nerve growth factor (NGF) (Alomone, Jerusalem, Israel) was added to the medium with 1% FBS and 1% HS. Tissue culture plates or coverslips were coated with 10 µg/ml collagen (type IV) (Sigma, St. Louis, MO).

### *AS-ODN*

AS-ODN targeted to exon 2 of mouse AChE mRNA (AS1, AS3) have been described previously (Grifman and Soreq, 1997). Oligonucleotides targeted to butyrylcholinesterase (BChE) mRNA (ASB) served as control (Ehrlich et al., 1994): AS1, 5-GGGAGAGGAGGAGGAAGAGG-3; AS3, 5-CTGCAATAT-TTCTTGACC-3; ASB, 5-GACTTTGCTATGCAT-3.

All ODN were end-capped with either 2'-O-methyl RNA substitutions (Me) or phosphorothioate (PS) modification at their three 3'-terminal positions. As lipofectamine was previously shown to be cytotoxic in differentiating PC12 cells (Grif-

man and Soreq, 1997), AS-ODN was added directly to the culture medium without carrier.

*In situ* hybridization was performed with a fully 2'-O-methylated 50-mer AChE cRNA probe complementary to alternative exon E6 in the *ACHE* gene (Kaufer et al., 1998). As PC12 cells contain endogenous biotin, 5'-digoxigenin (5'-DIG)-labeled probes were employed. Detection was with alkaline phosphatase and Fast Red<sup>®</sup> substrate (Molecular Probes, Eugene, OR). Hybridization was as detailed elsewhere (Grisaru et al., 1999a). RT-PCR was performed essentially as described (Grifman and Soreq, 1997).

Confocal microscopy was carried out using a Bio-Rad MRC-1024 confocal scanhead (Hemel Hempstead, Hertfordshire, U.K.) coupled to an inverted Zeiss Axiovert 135 microscope (Oberkochen, Germany) equipped with a plan apochromat 63X/1.4 oil immersion objective. Fast Red was excited at 488 nm, and emission was measured through a 580df32 bandpass interference filter (580 nm ± 16 nm). The confocal iris was set to 3 mm. Sections were scanned every 0.44 µm, corrected for immersion oil/mounting medium index of refraction mismatch. The sections were processed in the following way. First, a maximum value projection was created from a set of sections. Intensity-based thresholding was used to both isolate the cell from the background and identify Fast Red precipitates. The threshold was at first selected manually and, later, using the automatic object identification capability of Image Pro Plus (version 4.0) (Media Cybernetics, Silver Spring, MD). Fast Red precipitates were considered to be those objects that contained five or more pixels and exceeded the selected intensity threshold. This threshold was selected so that control cells always showed identical levels of labeling in order to correct for the variables in preparation (e.g., alkaline phosphatase reaction time, probe efficiency). The total area covered by the Fast Red precipitates was then measured. The data were not normalized to cell volume because the spread in cell volumes was very small.

Nuclear and cytoplasmic volume calculations were based on average values of nuclear and cell diameter as measured in the imaged sections. The measured cells and their nuclei were assumed to be spherical, and cytoplasmic volume was taken as the cell minus nuclear volume.

## RESULTS

### *Peak inhibition of AChE activity at very low concentrations of AS-ODN*

We previously studied AS-ODN targeted to various regions of AChE mRNA using end-capped 20-mer oligonucleotides in which PS-modified bases were incorporated into the three 3'-terminal positions (Grifman and Soreq, 1997). Two AS-ODN, AS1 and AS3, targeted to the common exon 2 shared by all AChE mRNA splice variants reduced AChE activity in differentiating PC12 cells by up to 30%. To improve uptake and stability while reducing toxicity, we prepared 3'-end-capped, Me-modified versions of AS1 and AS3 and compared their potency to their PS-modified counterparts. Both PS-capped and Me-capped AS1 suppressed AChE catalytic activity in NGF-stimulated PC12 cells to about 50% of controls in a dose-dependent

and sequence-dependent manner within 48 hours. AS1-Me displayed significant effects at an extracellular concentration of 0.05 nM, and maximum suppression of AChE activity was observed at 2 nM AS-ODN (Fig. 1A). In contrast, 2 nM AS1-PS was required to exert prominent suppression of AChE activity in PC12 cells. Sequence specificity was shown by the insignificant effects exerted by either PS-protected or Me-protected AS-ODN targeting BChE (Fig. 1, inset). Curiously, increasing the concentrations of AS1 above 2 nM reduced AS-ODN efficacy to the extent that PC12 cells exposed to 1  $\mu$ M AS1, AS1-PS, or AS1-Me displayed only minor loss of AChE activity.

To confirm the observation that increasing concentrations of oligonucleotide neutralize the potency of AS-ODN targeted to AChE mRNA, we used *in situ* hybridization (ISH) to label AChE-S mRNA in cells treated with AS3-Me for 48 hours. Generally, AChE-S mRNA appeared concentrated in one or two cytoplasmic areas close to the nuclear margin, possibly in the Golgi apparatus where AChE would be translated, folded, and rendered catalytically active. To quantify ISH signals detecting cytoplasmic AChE mRNA, we applied confocal microscopy and computerized image analysis. This analysis revealed a U-shaped dose-response curve for AS3 that closely paralleled the curve obtained with AS1 using AChE catalytic activity as the measure of antisense potency (compare Fig. 1B to 1A). Dose-dependent increases and decreases in AChE-R

mRNA levels were matched by corresponding changes in cell-associated AChE activity as determined by cytohistochemical staining (Fig. 1B, inset). Nevertheless, AChE mRNA appeared more sensitive than AChE protein to the higher AS-ODN concentration. We observed similar dose-dependent effects on RNA and protein in human Saos-2 cells with AS1 (Grisaru et al., 1999a; data not shown). In contrast, ASB-Me did not elicit significant changes in ISH signals. These findings demonstrated effective suppression of AChE expression by two independent AS-ODN targeted to AChE mRNA, demonstrated the enhanced potency and wide effective window conferred by Me modification of AChE AS-ODN, and raised the question of why increasing concentrations of AS-ODN fail to elicit reliable suppression of AChE activity in these cells.

#### AS-ODN treatment stimulates nuclear accumulation of AChE mRNA

Control PC12 cells never displayed intranuclear staining following ISH. However, at low concentrations of AS3-Me (0.2–2 nM), cells often displayed one or two small intranuclear foci of ISH signal (Fig. 2). At higher concentrations of 100–1000 nM AS3-Me, intense nuclear staining of AChE-S mRNA was commonly observed in up to two highly defined focal points. Similar nuclear labeling was also noted in AS-ODN-treated, multi-

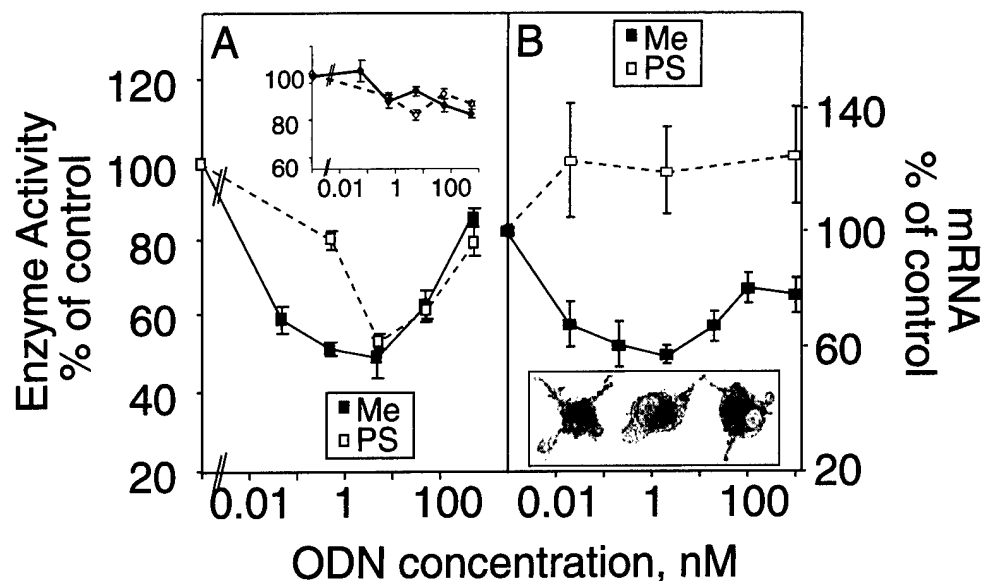


**FIG. 1.** 2'-O-Methyl (Me) AS-AChE displays a wide effective window at extremely low concentrations. Varying concentrations of phosphorothioate (PS) and Me AS1 or ASB were added to PC12 cells once daily for 2 days following 24-hour exposure to NGF, and cells were analyzed for AChE catalytic activity or mRNA encoding AChE-S. (A) AChE catalytic activity was measured using a colorimetric assay and acetylthiocholine as substrate. Results are expressed as percent of activity in control cells  $\pm$  standard error of the mean (SEM) for five to nine triplicate measurements for each point. Note that Me-modified AS1 elicited significant suppression of AChE at the extremely low concentration of 0.02 nM, whereas PS modification of the same three bases yielded an AS-ODN that exhibited effective suppression of AChE activity only at concentrations above 2 nM. Both oligonucleotides displayed decreasing efficacy at ODN concentrations above 2 nM. The nonrelevant control AS-ODN ASB had minimal effects on AChE activity at concentrations up to 100 nM in both the Me-modified and PS-modified forms (inset). (B) *In situ* hybridization with an exon 6-specific AChE cRNA probe was employed to detect AChE-S mRNA in AS3-treated cells. Quantification of AChE-S mRNA levels was by confocal microscopy and computer-assisted image analysis. Shown are average  $\pm$  SEM of AChE-S mRNA levels as a percentage of that observed in untreated cells. Note that AS3 induced a dose-dependent decrease in AChE-S mRNA levels that was reversed at about 2 nM AS-ODN. ASB had no detectable effect on AChE-S mRNA levels in these cells. (inset) Cells from the same experiment following cytohistochemical staining for catalytically active AChE. From left to right are representative cells from cultures treated with 0.2, 2, and 1000  $\mu$ M AS3, respectively.

nucleated Saos-2 cells, where multiple nuclear sites of labeling were observed (Grisaru et al., 1999a; data not shown). These observations suggested a direct association between focal nuclear staining and the number of transcription sites and hinted at *de novo* accumulation of heteronuclear (hn)-AChE mRNA in AS-ODN-treated cells. To further examine AChE mRNA levels in antisense-treated PC12 cells, we performed RT-PCR on RNA extracted from cultures treated with AS3 for 48 hours following NGF-stimulated differentiation. RT-PCR revealed both a short mRNA representing mature 3'-spliced AChE-S mRNA and a longer, unspliced transcript presumably representing hn-AChE in differentiating PC12 cells (Fig. 2B, inset). Both the long and the short transcript were noted to be about 2-fold higher in cells treated with 100 nM as compared with 10 nM AS3. The nuclear accumulation of AChE mRNA under AS-ODN treatment suggests that the reduced potency of >2 nM AChE AS-ODN in PC12 cells reflects feedback upregulation of the AChE gene in response to highly effective primary antisense effects or to the presence of excess AS-ODN or their degradation products. Moreover, it advances the notion that antisense, like pharmacologic, inhibition of AChE below a certain threshold initiates feedback upregulation of AChE expression in multiple cell types. Together, these data point to the need to strike a balance in antisense studies between antisense effects and dose-dependent compensatory host cell responses.

#### *Cellular uptake of AS-ODN*

The role of AS-ODN uptake in host cell feedback responses was evaluated using 5'-DIG-tagged AS3-Me and the image analysis strategy of ISH. To estimate the sensitivity of the confocal approach, we mixed a 1-nM solution of DIG-tagged AS-ODN into a PC12 cell extract, dried a 50- $\mu$ l drop on a microscope slide, and performed image analysis (Galyam, 1999; data not shown). In AS-ODN-treated PC12 cells, this quantification procedure revealed concentration-dependent increases in intracellular oligonucleotide (Fig. 3A), although increasing extracellular concentrations between 20 pM and 1  $\mu$ M AS3-Me resulted in exceedingly limited increases in intracellular ODN (approximately 6-fold for the 5000-fold increased external concentration) for both AS1-Me and AS3-Me (Fig. 3A). We calculated 10–100 AS-ODN molecules per 10 pl cell volume under 0.02 nM treatment conditions, close to the external concentrations of oligonucleotide. Therefore, 20 pM external concentration of AS3 sufficed to introduce AS3 into PC12 cells at a concentration similar to that of its complementary AChE mRNA (see Discussion). From 0.02 nM, 10-fold increases in external ODN concentration resulted in nonproportional increases in intracellular concentration. Nevertheless, these data indicate that low external concentrations of AS-ODN elicited dose-dependent antisense effects in PC12 cells that are approximately proportional to internal AS-ODN concentrations (compare with Fig. 1). At higher concentrations, however, nonspecific cellular effects may result from extracellular effects of oligonucleotides, their degradation products, or both.

#### *Excess AS-ODN mediates sequence-independent increases in cytoplasmic volume*

In search of mechanism(s) controlling the increased AChE gene activity observed at AS-ODN concentrations >2 nM, we

used the confocal microscope to measure cell volume. This analysis revealed >25% increases in cytoplasmic, but not nuclear, volume of PC12 cells exposed to AS-ODN over a range of 10–500 nM (Fig. 3B). The changes in cytoplasmic volume were sequence independent, as they were common to cells treated with either antisense or inverse AChE AS-ODN. Sustained nuclear volume under these conditions attested to the fact that no apoptotic changes took place. Therefore, increased cytoplasmic volume in this effective range of ODN concentrations may include a host cell response to the extracellular or intracellular presence of >2 nM ODN or their degradation products or both.

## DISCUSSION

Several key responses of PC12 cells to the extracellular presence of oligonucleotides were noted when using a wide range of AS-ODN concentrations. (1) Above 50 pM and up to 20 nM AS-ODN, AChE activity was suppressed by up to 50%, with Me-capped ODN displaying improved activity compared with PS-modified oligos. (2) Above 50 nM AS-ODN, AChE activity was refractory to AS-ODN treatment and sequence-dependent increases in nuclear labeling suggestive of transcriptional activation of the target gene. (3) Above 10 nM AS-ODN, cytoplasmic volume increased by >25%, reflecting a sequence-independent host cell response.

#### *Nanomolar doses of Me AS-ODN suffice to destroy their target mRNA*

AChE mRNA concentrations in differentiating PC12 cells were estimated to be 1–10 molecules/pl, or 1–10 pM, assuming approximately  $1 \times 10^8$  cells/ml and 10–100 molecules of a nonabundant target mRNA per cell. Assuming that each AS-ODN chain can inactivate many target molecules, the concentrations of AS1 and AS3 that were used in the present study should be sufficient to destroy all the AChE mRNA molecules in treated cells, even in neurons, where AChE levels are highest (see Lev-Lehman et al., 2000; Li et al., 1991, for quantitative estimates of AChE mRNA amounts in various cell types). Reversal of the dose-response curve at 50% inhibition, therefore, suggests that this represents the limit of blockade beyond which the AChE feedback loop is activated. Me-end-capped AS-ODN suppressed AChE activity in PC12 cells at 100-fold lower concentrations than the corresponding PS-ODN. Thus, Me protection reduced the quantity of ODN needed to suppress AChE expression, in addition to preventing the cytotoxicity associated with PS protection (Ehrlich et al., 1994).

#### *Micromolar AS-ODN induces AChE mRNA accumulation*

In the micromolar range, sequence-dependent refractoriness to AS-ODN was observed. AS-ODN concentration-dependent decreases and increases in AChE mRNA and enzyme activity suggest that the inefficacy of high levels of oligonucleotide represents a cellular response triggered by changes in cellular AChE concentrations. Changes in AChE gene expression under antisense inhibition may be expected to include enhanced transcription, changes in specific splicing patterns, selective

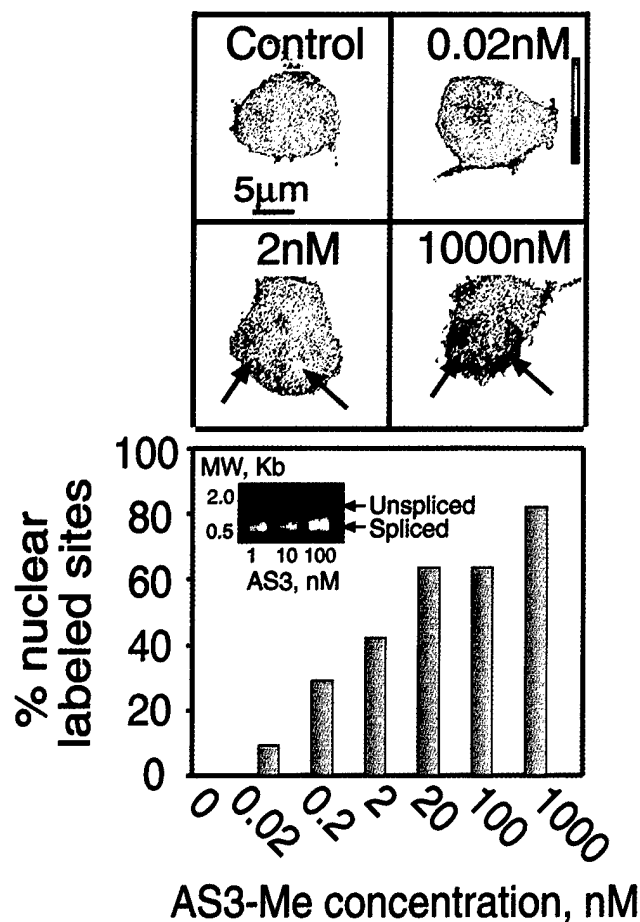


**FIG. 2.** Focal nuclear accumulation of AChE mRNA in AS-ODN-treated PC12 cells. (A) Pseudocolored compound confocal images of representative PC12 cells following incubation with Me RNA-protected AS3 and *in situ* hybridization with a probe detecting AChE-S mRNA and *in situ* hybridization with a probe detecting AChE-S mRNA. Color coding (upper right) correlates with intensity of Fast Red staining and, therefore, AChE-S mRNA levels. Note that increasing concentrations of AS3 were associated with the appearance of punctate nuclear staining for AChE-S mRNA (red arrows) and reduced antisense efficacy as presented in Figure 1. (B) Graph depicts the percentage of total potential nuclear sites (assuming two per cell) labelled by *in situ* hybridization at the noted concentrations of AS3. Note the prominent concentration-dependent increase in the fraction of nuclei labeled for AChE mRNA and the almost universal labeling of nuclei at 1 μM AS-ODN. These data indicate feedback transcription or stabilization or both of nascent hn-AChE mRNA under treatment with AS3. (Inset) Ethidium bromide-stained products of RT-PCR performed on RNA extracted from PC12 cells treated with the noted concentrations of AS3. Note that in addition to product representing mature, spliced AChE-S mRNA, a band of high molecular weight product presumed to represent unspliced hn-AChE mRNA is present. Both bands are intensified above 10 nM AS3, corresponding to the appearance of focal nuclear staining observed by *in situ* hybridization.

stabilization of certain mRNA transcripts, or all of these combined. The intense nuclear labeling of AChE mRNA suggests enhanced transcription or nuclear stabilization (or both) of nascent transcripts under AS-ODN concentrations > 2 nM. The cytoplasmic accumulation of AChE mRNA could reflect selective stabilization, similar to that observed in differentiating nerve and muscle (Luo et al., 1999) and hematopoietic cells

(Chan et al., 1998). Diversion of default 3'-alternative splicing patterns may also be involved, similar to the selective increases in unspliced AChE-R mRNA observed under stress or exposure to AChE inhibitors (Kaufer et al., 1998). Disproportionate increases in AChE-R would account for the apparent discrepancy between full recovery of AChE activity above 100 nM AS-ODN and the only partial recovery of AChE-S mRNA (Fig. 1).

#### ODN may regulate cellular volume

In the picomolar-nanomolar range, AS-ODN induced the destruction of its target AChE mRNA. In the presence of increas-

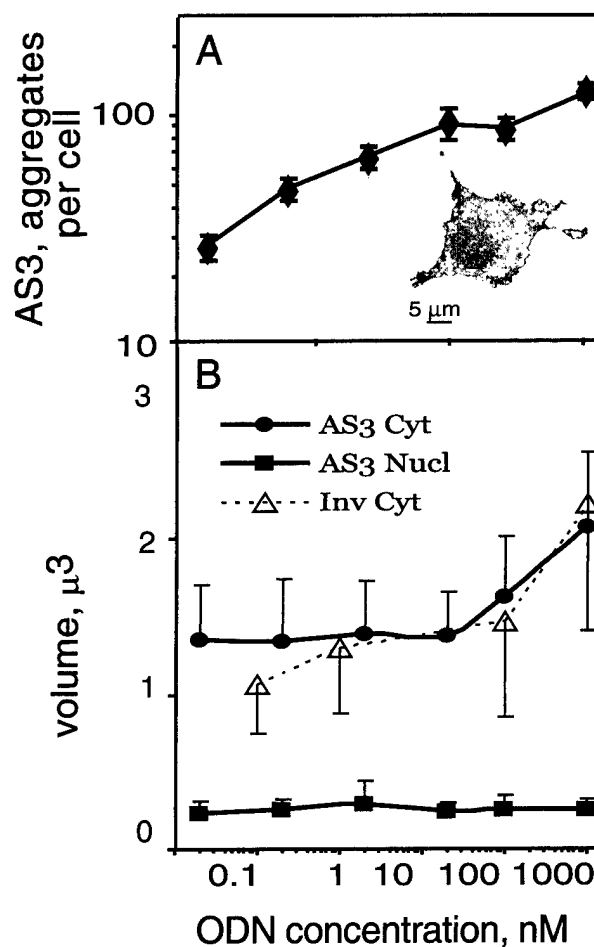


**FIG. 3.** AS3 uptake and its effect on cell volume. (A) Limited AS3 penetrance under increasing concentrations. Differentiated PC12 cells were incubated for 24 hours with biotinylated AS3, treated with alkaline phosphatase-conjugated streptavidin, and subjected to Fast Red detection. Fast Red signals from 20 cells were quantified as in Figure 1. Note that large changes in extracellular ODN concentrations result in relatively small changes in intracellular ODN concentration. (Inset) A representative projection of a single PC12 cell incubated with 1 μM ODN. (B) Cytoplasmic but not nuclear volume changes under increasing concentrations of AS3. Total cellular and nuclear volumes of AS-ODN-treated PC12 cells were determined using confocal microscopy as described in Materials and Methods. Note that cytoplasmic volume increased in a dose-dependent but sequence-independent manner above 10 nM extracellular ODN, whereas nuclear volume remained constant over the entire tested range of ODN concentrations.

ing extracellular concentrations ( $>10$  nM) of AS-ODN, confocal microscopy revealed sequence-independent changes in cytoplasmic volume. Reports on the cellular effects of low nucleotide concentrations point to the extracellular increase in nucleotide breakdown products of AS-ODN, in particular increases in adenosine, as a likely cause for these changes (see Galiotta et al., 1992, for example). Another important consideration refers to the extent of change in cytoplasmic volume. Because the cytoplasm is crowded with cytoskeletal elements, ribosomes, and endoplasmic reticulum, a change of 25%–50% may imply a considerably larger change in the volume of the liquid microenvironment where biochemical reactions regulating cellular physiology take place. This would be expected to impose metabolic disequilibrium and could initiate cellular stress responses. As AChE is proving to be a ubiquitous stress response element, this could contribute to the feedback response initiated by reduced intracellular AChE levels. These data, therefore, caution against the use of unnecessarily high concentrations of AS-ODN and suggest reevaluation of our concepts of the oligonucleotide concentrations previously believed to be physiologically relevant. This conclusion is particularly relevant in light of reported saturation of ODN uptake at concentrations as low as 160 nM (Nakai et al., 1996).

In summary, our findings indicate that Me-protected AChE AS-ODN effectively suppress AChE activity in cell types of different origins in the picomolar-nanomolar range. These concentrations are much lower than those reported previously for AChE-targeted AS-ODN and considerably lower than commonly used concentrations (50 nM–1  $\mu$ M) for AS-ODN targeted to various other mRNAs. Notably, increasing the extracellular AS-ODN above these levels neither elevated their intracellular concentrations proportionally nor increased their ultimate effectiveness. In the yet higher micromolar range, the antisense strategy was relatively ineffective, apparently because of feedback activation of AChE gene activity. These findings may explain inconsistencies reported with numerous AS-ODN. Furthermore, they call for *in vivo* experiments using similarly reduced concentrations of AS-ODN. Recently, we successfully used low doses of AS3 to suppress overexpressed AChE-R mRNA in brain of head-injured mice (Shohami et al., 2000) and in muscles of anticholinesterase-treated mice (Lev-Lehman et al., 2000) and rats with experimental myasthenia gravis (T. Brenner and H. Soreq, unpublished observations). The advantages of greatly reduced AS-ODN concentrations are many, including reduced side effects and increased cost effectiveness.

#### ACKNOWLEDGMENTS

We are grateful to Dr. A. Cohen, Boston, for advice and assistance and to Dr. Aryeh Weiss, Jerusalem, for critical review of this manuscript. This work was supported by grants from the Medical Research and Materiel Command of the US Army (DAMD 17-99-1-9547), the German-Israeli Fund (I 512 206 / 96), and Ester Neuroscience, Ltd. (to H.S.).

#### REFERENCES

- AGRAWAL, S., and KANDIMALLA, E.R. (2000). Antisense therapeutics: Is it as simple as complementary base recognition? *Mol. Med. Today* **6**, 72–81.
- BELTINGER, C., SARAGOVI, H.U., SMITH, R.M., LESAUTEUR, L., SHAH, N., DEDIONISIO, L., CHRISTENSEN, L., RAIBLE, A., JARETT, L., and GEWIRTZ, A.M. (1995). Binding, uptake, and intracellular trafficking of phosphorothioate-modified oligodeoxynucleotides. *J. Clin. Invest.* **95**, 1814–1823.
- CHAN, R.Y., ADATIA, F.A., KRUPA, A.M., and JASMIN, B.J. (1998). Increased expression of acetylcholinesterase T and R transcripts during hematopoietic differentiation is accompanied by parallel elevations in the levels of their respective molecular forms. *J. Biol. Chem.* **273**, 9727–9733.
- CROOKE, S.T. (2000). Progress in antisense technology: The end of the beginning. *Methods Enzymol.* **313**, 3–45.
- EHRlich, G., PATINKIN, D., GINZBERG, D., ZAKUT, H., ECKSTEIN, F., and SOREQ, H. (1994). Use of partially phosphorothioated "antisense" oligodeoxynucleotides for sequence-dependent modulation of hematopoiesis in culture. *Antisense Res. Dev.* **4**, 173–183.
- FRIEDMAN, A., KAUFER, D., SHEMER, J., HENDLER, I., SOREQ, H., and TUR-KASPA, I. (1996). Pyridostigmine brain penetration under stress enhances neuronal excitability and induces early immediate transcriptional response. *Nat. Med.* **2**, 1382–1385.
- GALIOTTA, L.J., RASOLA, A., RUGOLO, M., ZOTTINI, M., MASTROCOLA, T., GRUENERT, D.C., and ROMEO, G. (1992). Extracellular 2-chloroadenosine and ATP stimulate volume-sensitive  $Cl^-$  current and calcium mobilization in human tracheal 9HTeO-cells. *FEBS Lett* **304**, 61–65.
- GALYAM, N. (1999). Neuronal and hematopoietic consequences of antisense acetylcholinesterase suppression. M.Sc. thesis, The Hebrew University of Jerusalem.
- GERACE, L. (1995). Nuclear export signals and the fast track to the cytoplasm. *Cell* **82**, 341–344.
- GORLICH, D. (1998). Transport into and out of the cell nucleus. *EMBO J.* **17**, 2721–2727.
- GRIFMAN, M., GALYAM, N., SEIDMAN, S., and SOREQ, H. (1998). Functional redundancy of acetylcholinesterase and neuroigin in mammalian neuritogenesis. *Proc. Natl. Acad. Sci. USA* **95**, 13935–13940.
- GRIFMAN, M., and SOREQ, H. (1997). Differentiation intensifies the susceptibility of pheochromocytoma cells to antisense oligodeoxynucleotide-dependent suppression of acetylcholinesterase activity. *Antisense Nucleic Acid Drug Dev.* **7**, 351–359.
- GRISARU, D., DEUTCH, V., SHAPIRA, M., PICK, M., STERNFELD, M., MELAMED-BOOK, N., KAUFER, D., GALYAM, N., GAIT, M., OWEN, D., LESSING, J., ELDOR, A., and SOREQ, H. (2001). ARP, a peptide derived from the stress-associated acetylcholinesterase variant, has hematopoietic growth-promoting activities. *Mol. Med. In press.*
- GRISARU, D., LEV-LEHMAN, E., SHAPIRA, M., CHAIKIN, E., LESSING, J.B., ELDOR, A., ECKSTEIN, F., and SOREQ, H. (1999a). Human osteogenesis involves differentiation-dependent increases in the morphogenically active 3' alternative splicing variant of acetylcholinesterase. *Mol. Cell. Biol.* **19**, 788–795.
- GRISARU, D., STERNFELD, M., ELDOR, A., GLICK, D., and SOREQ, H. (1999b). Structural roles of acetylcholinesterase variants in biology and pathology. *Eur. J. Biochem.* **264**, 672–686.
- HOFFMAN, E.K. (1992). Cell swelling and volume regulation. *Can. J. Physiol. Pharmacol.* **70**, 310–313.
- KAUFER, D., FRIEDMAN, A., SEIDMAN, S., and SOREQ, H. (1998). Acute stress facilitates long-lasting changes in cholinergic gene expression. *Nature* **393**, 373–377.

- KNOWLES, M.R., CLARKE, L.L., and BOUCHER, R.C. (1991). Activation by extracellular nucleotides of chloride secretion in the airway epithelial of patients with cystic fibrosis [see Comments]. *N. Engl. J. Med.* **325**, 533–538.
- KOENIGSBERGER, C., CHIAPPA, S., and BRIMIJOIN, S. (1997). Neurite differentiation is modulated in neuroblastoma cells engineered for altered acetylcholinesterase expression. *J. Neurochem.* **69**, 1389–1397.
- LEV-LEHMAN, E., EVRON, T., BROIDE, R.S., MESHORER, E., ARIEL, I., SEIDMAN, S., and SOREQ, H. (2000). Synaptogenesis and myopathy under acetylcholinesterase overexpression. *J. Mol. Neurosci.* **14**, 93–105.
- LI, Y., CAMP, S., RACHINSKY, T.L., GETMAN, D., and TAYLOR, P. (1991). Gene structure of mammalian acetylcholinesterase. Alternative exons dictate tissue-specific expression. *J. Biol. Chem.* **266**, 23083–23090.
- LIGHT, D.B., SCHWIEBERT, E.M., FEJES-TOTH, G., NARAY-FEJES-TOTH, A., KARLSON, K.H., McCANN, F.V., and STANTON, B.A. (1990). Chloride channels in the apical membrane of cortical collecting duct cells. *Am. J. Physiol.* **258**, F273–F280.
- LOKE, S.L., STEIN, C.A., ZHANG, X.H., MORI, K., NAKANISHI, M., SUBASINGHE, C., COHEN, J.S., and NECKERS, L.M. (1989). Characterization of oligonucleotide transport into living cells. *Proc. Natl. Acad. Sci. USA* **86**, 3474–3478.
- LUO, Z.D., WANG, Y., WERLEN, G., CAMP, S., CHIEN, K.R., and TAYLOR, P. (1999). Calcineurin enhances acetylcholinesterase mRNA stability during C2-C12 muscle cell differentiation. *Mol. Pharmacol.* **56**, 886–894.
- MA, M., BENIMETSKAYA, L., LEBEDEVA, I., DIGNAM, J., TAKLE, G., and STEIN, C.A. (2000). Intracellular mRNA cleavage induced through activation of RNase P by nuclease-resistant external guide sequences. *Nat. Biotechnol.* **18**, 58–61.
- MELCHIOR, F., PASCHAL, B., EVANS, J., and GERACE, L. (1993). Inhibition of nuclear protein import by nonhydrolyzable analogues of GTP and identification of the small GTPase Ran/TC4 as an essential transport factor [published erratum appears in *J. Cell. Biol.* 1994 **124**, 217]. *J. Cell. Biol.* **123**, 1649–1659.
- NAKAI, D., SEITA, T., TERASAKI, T., IWASA, S., SHOJI, Y., MIZUSHIMA, Y., and SUGIYAMA, Y. (1996). Cellular uptake mechanism for oligonucleotides: involvement of endocytosis in the uptake of phosphodiester oligonucleotides by a human colorectal adenocarcinoma cell line, HCT-15. *J. Pharmacol. Exp. Ther.* **278**, 1362–1372.
- SCHWIEBERT, E.M., KARLSON, K.H., FRIEDMAN, P.A., DIETL, P., SPIELMAN, W.S., and STANTON, B.A. (1992). Adenosine regulates a chloride channel via protein kinase C and a G protein in a rabbit cortical collecting duct cell line. *J. Clin. Invest.* **89**, 834–841.
- SHOHAMI, E., KAUFER, D., CHEN, Y., SEIDMAN, S., COHEN, O., GINZBERG, D., MELAMED-BOOK, N., YIRMIYA, R., and SOREQ, H. (2000). Antisense prevention of neuronal damages following head injury in mice. *J. Mol. Med.* **78**, 228–236.
- WU, H., LIMA, W.F., and CROOKE, S.T. (1999). Properties of cloned and expressed human RNase H1. *J. Biol. Chem.* **274**, 28270–28278.

Address reprint requests to:

*Dr. H. Soreq  
Department of Biological Chemistry  
The Institute of Life Sciences  
The Hebrew University of Jerusalem  
Jerusalem  
Israel 91904*

Received August 11, 2000; accepted in revised form October 17, 2000.

## Synaptogenesis and Myopathy Under Acetylcholinesterase Overexpression

**Efrat Lev-Lehman,<sup>1,\*\*</sup> Tamah Evron,<sup>1</sup> Ron Shruga Broide,<sup>1,\*\*</sup>  
Eran Meshorer,<sup>1</sup> Ilana Ariel,<sup>1,2</sup> Shlomo Seidman,<sup>1</sup> and Hermona Soreq<sup>\*,1</sup>**

<sup>1</sup>Department of Biological Chemistry, The Life Sciences Institute, The Hebrew University of Jerusalem, Jerusalem, Israel 91904; <sup>2</sup>Department of Pathology, Hadassah University Hospital, Mount Scopus, Jerusalem, Israel

### Abstract

Environmental, congenital, and acquired immunological insults perturbing neuromuscular junction (NMJ) activity may induce a variety of debilitating neuromuscular pathologies. However, the molecular elements linking NMJ dysfunction to long-term myopathies are unknown. Here, we report dramatically elevated levels of mRNA encoding *c-Fos* and the "readthrough" (R) variant of acetylcholinesterase (AChE) in muscles of transgenic mice overexpressing synaptic (S) AChE in motoneurons and in control mice treated with the irreversible cholinesterase inhibitor diisopropylfluorophosphonate (DFP). Tongue muscles from DFP-treated and AChE-S transgenic mice displayed exaggerated neurite branching and disorganized, wasting fibers. Moreover, diaphragm muscles from both transgenic and DFP-treated mice exhibited NMJ proliferation. 2'-O-methyl-protected antisense oligonucleotides targeted to AChE mRNA suppressed feedback upregulation of AChE and ameliorated DFP-induced NMJ proliferation. Our findings demonstrate common transcriptional responses to cholinergic NMJ stress of diverse origin, and implicate deregulated AChE expression in excessive neurite outgrowth, uncontrolled synaptogenesis, and myopathology.

**Index Entries:** Acetylcholinesterase/antisense; cholinesterase inhibitors; physiological stress; muscle pathology; neuromuscular junction.

\*Author to whom all correspondence and reprint requests should be addressed.

\*\*Current address: Departments of Human and Molecular Genetics (E.L.L.) and Neuroscience (R.S.B), Baylor College of Medicine, Houston, TX

## Introduction

Neuromuscular junctions (NMJ) are highly specialized, morphologically distinct, and well-characterized cholinergic synapses (Sanes and Lichtman, 1999). Chronic impairments in NMJ activity induce neuromuscular disorders characterized by deterioration of muscle structure and function. Thus, etiologically diverse insults interfering with acetylcholine-mediated neurotransmission cause a variety of "myasthenic" syndromes presenting muscle weakness and fatigue (Livneh et al., 1988; Schonbeck et al., 1990; Engelhart et al., 1997; Donger et al., 1998; Lindstrom, 1998). The molecular and cellular mechanisms leading from compromised NMJ activity to muscle wasting have not been elucidated. However, it is likely that physiological stress imposed on the nerve and/or muscle under conditions of NMJ dysfunction initiate changes in gene expression. Inhibitors of the acetylcholine-hydrolyzing enzyme, AChE, induce neuromuscular pathologies sharing features with the myasthenic syndromes. Among the delayed effects of anticholinesterase intoxication are degeneration of synaptic folds, terminal nerve branching, enlargement of motor endplates, and disorganization of muscle fibers (Laskowski et al., 1975; Kawabuchi et al., 1976). Cholinesterase inhibitors promoting myopathy include organophosphate poisons such as DFP and paraoxon (the toxic metabolite of the agricultural insecticide parathion), and carbamate drugs like pyridostigmine and neostigmine, used to treat myasthenia gravis (Evoli et al., 1996). The similarities between the neuromuscular impairments resulting from anticholinesterase exposure and that of pathophysiological NMJ dysfunction suggest overlapping and/or convergent pathways involving AChE.

RNA transcribed from the mammalian *ACHE* gene is subject to 3' alternative splicing yielding mRNAs encoding a "synaptic" (S) isoform, a "erythropoietic" (E) isoform, and the stress-related "readthrough" AChE-R derived from the 3'-unspliced transcript (Ben Aziz-Aloya et al., 1993; Massoulie et al., 1993). In addition to their hydrolytic activities, the various AChEs exert sequence-specific morphogenic effects on neurite outgrowth (Layer et al., 1995; Koenigsberger et al., 1997; Grifman et al., 1998; Sharma et al., 1998; Stern-

feld et al., 1998) and NMJ structure (Shapira et al., 1994; Seidman et al., 1995). Transgenic mice overexpressing human AChE-S in spinal cord motoneurons displayed progressive neuromotor impairments that were associated with changes in NMJ ultrastructure (Andres et al., 1997, 1998). However, the molecular mechanisms mediating neuromuscular deterioration in these mice were unclear. Elevated intracellular calcium was previously implicated in anticholinesterase-mediated myopathologies (Laskowski et al., 1975). Electromyography (EMG) data revealed exaggerated post-synaptic responses in muscles of transgenic mice that indicated similarly enhanced calcium influx. In rodent brain, we found that both stress and cholinesterase inhibitors induce dramatic calcium-dependent overexpression of AChE-R (Kaufer et al., 1998). We therefore predicted that feedback overexpression of AChE-R would also occur in muscles of both anticholinesterase-treated control and NMJ-stressed AChE transgenic mice. Moreover, we expected that overexpressed AChE would have morphogenic implications for the nerves and/or muscles. To test these hypotheses, we examined AChE expression, motor endplate organization, neurite outgrowth, and muscle integrity in AChE-S transgenic mice and in normal mice treated with DFP with or without coadministration of antisense oligonucleotides to AChE mRNA. Our findings identify the AChE feedback loop as a molecular response common to both physiological NMJ stress and anticholinesterase exposure in muscle. Furthermore, they suggest that induced overexpression of AChE-R contributes to neuromuscular deterioration under diverse conditions leading to disease and demonstrate *in vivo* antisense blockade of the AChE feedback response to NMJ stress.

## Materials and Methods

### *Animals and Tissue Preparations*

FVB/N mice, aged postnatal day (P) 0, 15, 30 and 4 mo (M) were sacrificed and their tongues removed into liquid nitrogen for polymerase chain reaction (PCR) and biochemical analyses. For *in situ* hybridization and silver staining, 2-mm<sup>3</sup> cubes of tongue tissue were incubated in 3.7% formaldehyde overnight at room temperature and then

paraffin embedded. Sections were cut (5  $\mu$ m) and placed on 3-aminopropyltriethoxysilane-treated slides, dried at 37°C overnight, and kept at 4°C until use. For cytochemistry, whole diaphragms were fixed for 1 h in 4% paraformaldehyde at 22°C, rinsed twice in phosphate-buffered saline (PBS), and stained for catalytically active AChE activity as previously described (Andres et al., 1997).

### Chronic DFP Treatment

Mouse pups were housed with the dam in a light- and temperature-controlled room. Animals were injected subcutaneously (s.c.) once daily with either 1.0 mg/kg DFP (Aldrich Chemical Co., Milwaukee, WI) dissolved in corn oil or with corn oil alone during the first 2 postnatal weeks. To minimize central nervous system (CNS) toxicity, pups were pretreated with 10 mg/kg (ip) atropine sulfate (Sigma Chemical Co., St. Louis, MO) in saline 15 min before injection. At P15, about 4 h after the last injection, pups were sacrificed and their tongues removed.

### DFP/Antisense Experiments

Adult FVB/N mice were coinjected intraperitoneally (ip) once daily for 4 consecutive days with DFP alone or together with 5  $\mu$ g/kg of an antisense oligonucleotide (AS3; 3'CCA GCT TCT TTT ATA ACG TCs) targeted to exon E2 in the mouse acetylcholinesterase gene. AS3 included 2'-O-methyl ribonucleotide substitutions at the three 3'-terminal positions to stabilize it against nucleolytic degradation.

### RT-PCR Analysis

RNA from tongue samples was extracted by RNA Clean (PeqLab, Heidelberg, Germany) according to manufacturer's instructions. Reverse transcription (RT)-PCR reactions were performed as previously described using a common upstream (+) primer and downstream (-) primers selective for each of the alternative AChE mRNA exons (Fig. 1A):

- E3: 1361(+) {5'-CCGGGTCTATGCCTACAT-CTTGAA-3'}  
 E6: 1844(-){5'CACAGGTCTGAGCAGCGCTCC-TGCTTG-CTA-3'}  
 E5: 240(-) {5'-AAGGAAGAAGAGGAGGGA-CAGGGCTAAG-3'}  
 I4: 74(-) {5'-TTGCCGCCTTGTGCATTCCCT-3'}

To detect *c-Fos* mRNA, we used the primer pair 1604(+)/2306(-) (Kaufer et al., 1998). PCR products sampled every third cycle from cycles 24–36 for the AChE and *c-Fos* mRNAs, and from cycles 18–24 for  $\beta$ -actin mRNA were electrophoresed on 1.5% agarose gels and stained with ethidium bromide.

### In Situ Hybridization

2'-O-methylated, 5'-biotinylated cRNA probes were used to decorate selectively alternative mouse (m) AChE mRNAs. Detection was with alkaline phosphatase-conjugated streptavidin and ELF™ detection kit (Molecular Probes).

- mI4: (-79) 5'-AACCCUUGCCGCCUUGUG-CAUCCUGCUCUCCCCACUCCAUGCGC-CUA-C-3'(-29);  
 mE6: (209) 5'-CCCCUAGUGGGAGGAAGUCG-GGGAGGAGUGGACAGGGCCUGGGGGCU-CGG-3'(258);  
 mE5: (-249) 5'-GAGGAGGAAAAGGAAGAA-GAGGAGGGACAGGGCUAAGUCCGGCCC-GGGC-3'(-200);

Paraffin-embedded tongue sections were deparaffinized and dehydrated in a methanol/PBT (PBS, 0.1% Tween-20) series. Hybridization included preclearing in H<sub>2</sub>O<sub>2</sub> (6% in PBT, 30 min), proteinase treatment, glycine wash, and refixation (4% paraformaldehyde, 20 min), all essentially as described elsewhere (Kaufer et al., 1998; Grisaru et al., 1999) except that 1% sodium dodecyl sulfate (SDS) was added to the hybridization buffer and to solution 1 and 0.1% Tween-20 was added to solution 2.

### Neurites Silver Stain

Paraffin-embedded tongue muscle sections were stained for neuronal fibers using silver nitrate (20%, 60 min at 37°C), distilled water washes and incubation in ammonium hydroxide-silver nitrate solution (60 min). Color was developed for 24–36 h. For fixation, slides were dipped in sodium thiosulfate (2 s), washed in water, and dehydrated.

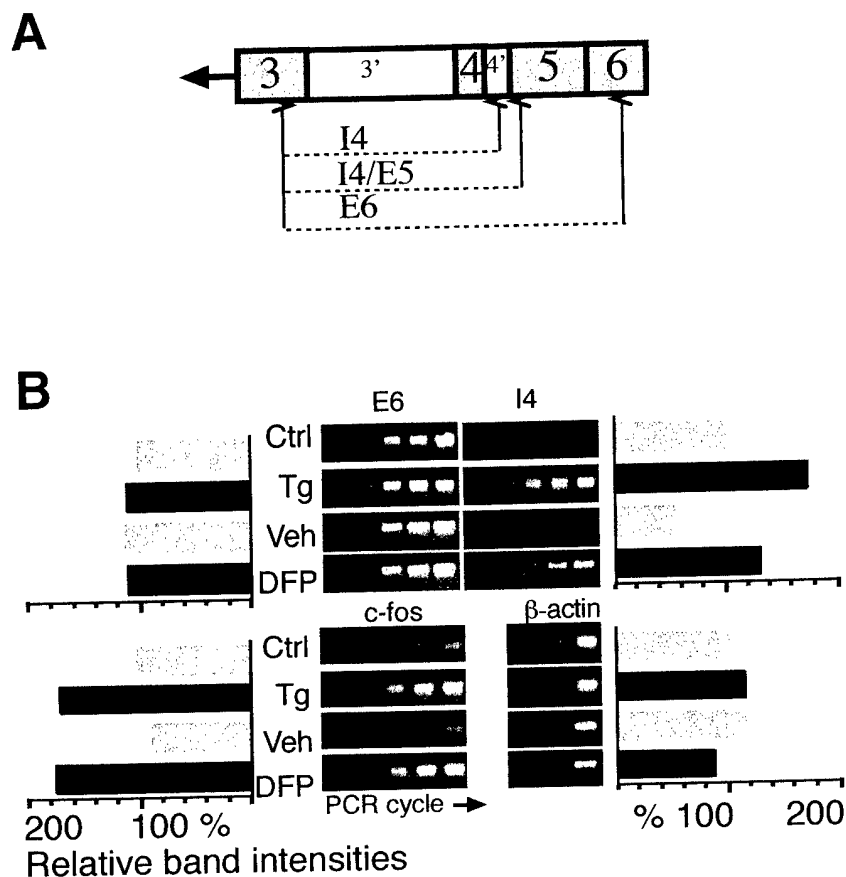


Fig. 1. Transgenic AChE-S and DFP similarly induce enhanced *c-fos* and AChE-R mRNA production in muscle. (A) The mouse ACHE gene and alternative splicing products. Presented is a schematic illustration of coding exons 3, 4, 5, and 6 (shaded boxes) and introns 3 to 4 (white boxes) in the mouse ACHE gene. The "synaptic" AChE-S mRNA transcript (E6) results from splicing of exons 4 to 6; the "erythropoietic" AChE-H mRNA transcript (E5) from splicing of exons 4 to 5; *readthrough* AChE-R mRNA retains intron I4 in a mature unspliced transcript. Arrowheads indicate PCR primer pairs detecting the individual mRNA transcripts. (B) RT-PCR analyses. RT-PCR was performed using primers specific for the various alternative AChE mRNAs (See Materials and Methods section). Presented are PCR products of AChE mRNA derived from tongue muscle of control (Ctrl) or AChE transgenic (Tg) newborn mice or from control mice treated for 2 wk with either DFP or vehicle (Veh). Note the increased levels of both endogenous mouse AChE-R and *c-fos* mRNAs in transgenic vs control mice and in control mice injected with DFP. Neither endogenous AChE-S or the unrelated  $\beta$ -actin mRNAs responded to either transgenic AChE overexpression or AChE inhibition. Displayed are PCR reactions sampled every third cycle from cycle 24 for AChE and *c-fos*, and from cycle 18 for  $\beta$ -actin. One of four experiments for each mRNA in the presented PCR images as determined by densitometric analysis. Quantification was performed at cycle 33 for AChE and *c-fos* mRNAs and at cycle 24 for  $\beta$ -actin mRNA, within the exponential phase of product accumulation.

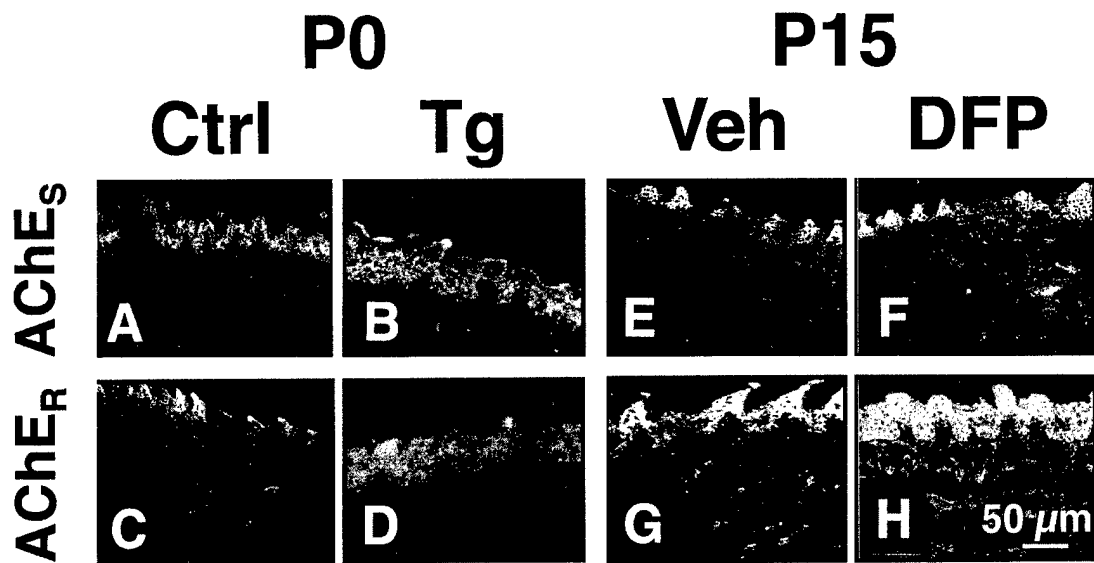


Fig. 2. Overexpressed transgenic AChE-S and DFP induce accumulation of endogenous AChE-R mRNA in both epithelium and muscle. *In situ* hybridization was performed on 7- $\mu$ m sections of tongue from newborn (P0) control (A,C) and AChE transgenic (B,D) mice, or 15-d-old (P15) control mice injected with either vehicle (E,G) or the AChE inhibitor DFP (F,H). Note enhanced and delocalized fluorescent labeling of AChE-R but not AChE-S mRNA in epithelial cells and muscle fibers from both transgenic and DFP-treated mice as compared to controls.

## Results

### **Chronic Cholinesterase Blockade and Transgenic Overexpression of Synaptic Neuronal AChE Promote Elevated *c-Fos* and readthrough AChE mRNAs in Muscle**

Both acute stress and cholinesterase inhibitors were shown to trigger overexpression of AChE-R in rodent brain via a *c-fos*-mediated pathway (Kaufer et al., 1998). To investigate whether the AChE feedback loop is active in muscle, we performed RT-PCR on mRNA extracted from tongue of 2-wk-old (P15) mice injected daily, from birth, with 1 mg/kg DFP. This dose of DFP blocked approx 80% of muscle AChE activity, but did not elicit overt symptoms of cholinergic poisoning. In parallel, RT-PCR was performed on tongue RNA from transgenic mice overexpressing AChE-S in spinal cord motoneurons. Semi-quantitative analyses performed with primers detecting mouse mRNAs encoding either *c-fos* or AChE-R revealed over twofold elevated levels of both transcripts following either chronic inhibition or congenital overex-

pression of AChE (Fig. 1). In contrast, neither endogenous AChE-S- nor AChE-E-mRNA levels were detectably affected by either DFP or transgenic AChE (Fig. 1 and data not shown).  $\beta$ -actin mRNA displayed similar levels among all groups, indicating equal starting amounts of RNA in all reactions (Fig. 1). These data demonstrated that both chronic overproduction and acute blockade of AChE catalytic activity stimulate selective *de novo* synthesis of AChE-R in muscle.

### **Readthrough AChE mRNA Accumulates in Both Muscle and Epithelium Under Cholinesterase Blockade and Transgenic AChE Overexpression**

To determine the localization of induced AChE-R mRNA in tongue, we employed high resolution, fluorescent *in situ* hybridization. Fluorescent hybridization signals obtained using an AChE-S mRNA-specific probe exhibited similar moderate intensities and bandwidth in epithelium of newborn transgenic and control mice (Fig. 2A,B). AChE-E mRNA was also detected at low levels in the epithelium of both control and transgenic mice

(not shown). AChE-R mRNA was barely detectable in sections from control mice, consistent with the PCR data. In contrast, pronounced expression of AChE-R mRNA was observed in tongue epithelium of newborn transgenic mice (figure 2C,D). With DFP, no significant differences were observed in the expression of AChE-S mRNA in treated- vs vehicle-injected mice (Fig. 2E,F). However, 15-d-old DFP-treated, but not their littermate controls, exhibited high levels of AChE-R mRNA across the entire width of the tongue epithelium, extending into the muscle (Fig. 2G,H). In general, hybridization with the AChE-S mRNA probe gave moderate and somewhat punctuated staining, consistent with the localization of this message around junctional nuclei (Jasmin et al., 1993). In contrast, staining with the AChE-R mRNA-specific probe yielded a more diffuse staining pattern, especially following DFP treatment, suggesting extrajunctional synthesis. These data demonstrated that both transgenic overexpression and inhibitor-mediated blockade of AChE promote a specific induction of AChE-R mRNA that takes place in both muscle and epithelium.

### **Transgenic Mice Display Delocalized Overexpression of Catalytically Active AChE in Muscle**

High-salt/detergent extracts of tongue revealed a developmental increase in AChE enzyme activity in control mice ( $12 \pm 2$  nmol substrate hydrolyzed/min/mg protein at P7 versus  $24 \pm 4$  at P15;  $n = 8$ ). Two-fold increased levels of catalytically active AChE were observed in tongue homogenates from transgenic over control mice at P7, but only 25% at P15. These findings suggested that adjustments in the feedback response take place over time and/or during development. To localize overexpressed AChE in the tongue, we performed cytohistochemical staining for AChE on sections from 1-mo-old control and transgenic mice. In control mice, activity staining was pale except for intense, highly localized staining observed at motor endplates (Fig. 3A,B). In contrast, transgenic mice displayed overall darker staining of the muscle layers, particularly near the submucosal epithelium (Fig. 3C). In transgenic mice, intense staining was observed along muscle fibers, not restricted to endplate regions (Fig. 3D). This staining pattern

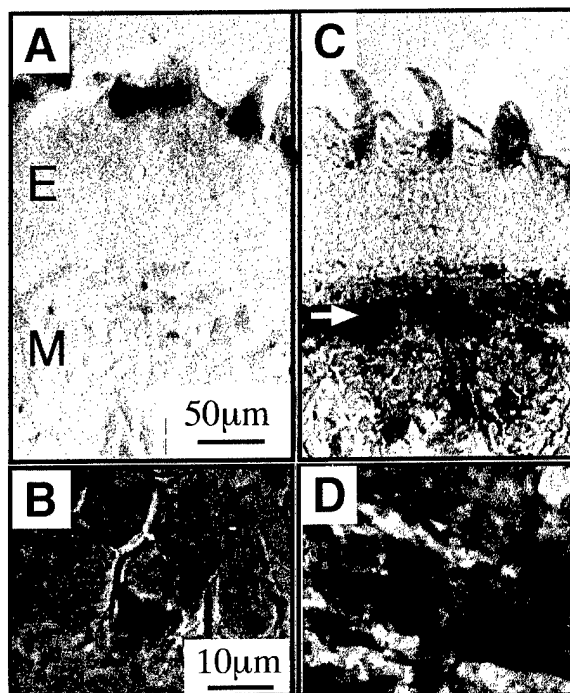


Fig. 3. AChE-Transgenic mice display pronounced nonjunctional enzyme activity in muscle. Tongue sections from 1-mo-old control and transgenic mice were stained for catalytically active AChE. (A) At low magnification, diffuse, light staining of both epithelium (E) and muscle (M) layers was observed in sections from control mice (B). Higher magnification revealed strong AChE activity localized to motor endplates (C). In sections from transgenic mice, minimal levels of AChE are visible in the epithelium, (C, arrow; D) whereas intense staining is evident in the muscle layer, widely distributed along muscle fibers.

was reminiscent of AChE-S overexpressed in myotomes of microinjected *Xenopus* embryos (Seidman et al., 1995). The relative contributions of endogenous AChE-R and transgenic AChE-S isoforms to this overexpression pattern were not discernable in this experiment. Nevertheless, AChE-R mRNA displayed pronounced overexpression in epithelium of transgenic mice that contrasted with the accumulation of catalytically active protein that was primarily limited to muscle.

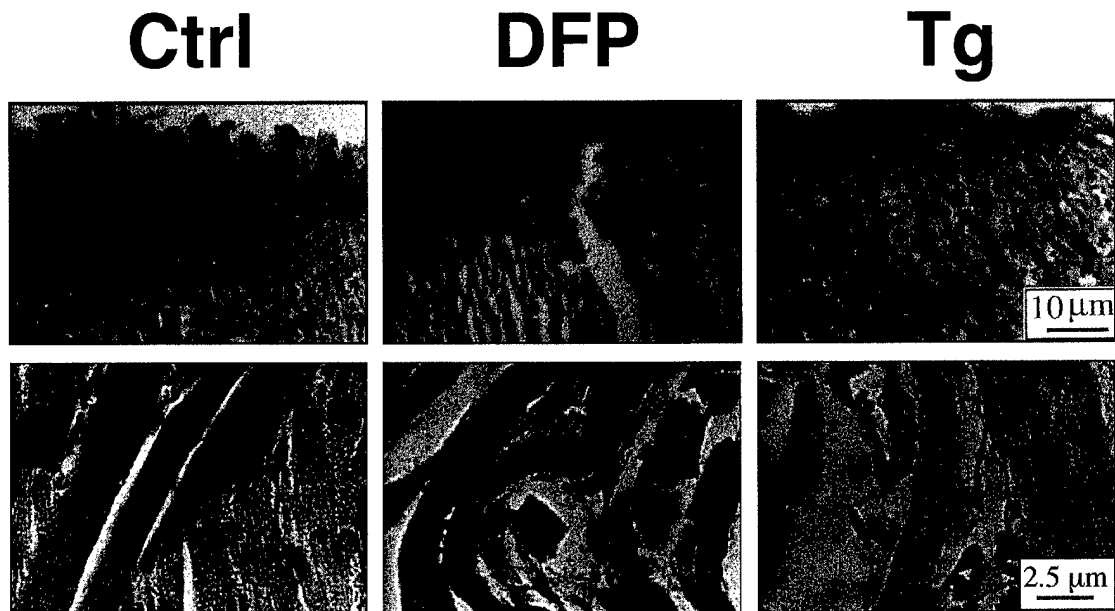


Fig. 4. Transgenic and DFP-induced AChE excesses associated with muscle pathologies. Tongue muscle from P15 untreated control (Ctrl), chronic-DFP-treated control (DFP), or untreated AChE transgenic (Tg) mice was stained with hematoxylin-eosin and evaluated for gross morphological features. Muscle tissue of control mice displayed a high degree of organization, with fibers closely aligned in regular parallel arrays. In control mice injected daily with DFP, and in untreated transgenic mice, the corresponding tissues appeared distorted, with apparently atrophic, disorganized muscle fibers. Upper panels present low magnification photomicrographs that include epithelial and muscle layers. Lower panels display high magnification of the muscle layer alone.

### ***Cholinesterase Inhibition and Overexpressed AChE Cause Similar Muscle Pathologies***

We previously reported aberrant NMJ ultrastructure and progressive neuromotor dysfunction among adult AChE transgenic mice. We hypothesized that induced AChE-R contributes to this neuromuscular deterioration. In that case, DFP, as an instigator of the AChE feedback loop, would be expected to elicit parallel myopathologies. To determine if the ability of cholinesterase inhibition to promote deterioration of muscle is correlated with overexpressed AChE-R, we studied the gross morphological features of tongue muscle. Muscle fibers from 15-d-old untreated control mice were organized in a linear fashion within parallel bundles. In contrast, muscle fibers from both DFP-treated of the FVB/N strain mice and AChE-transgenic mice displayed chaotic disorder (Fig. 4). At higher magnification, severely atrophic, vacuolated muscles

could be observed in both experimental systems. Despite these muscle malformations, transgenic pups suckled normally and displayed normal growth in their first weeks, suggesting a fairly large safety margin for nonstrenuous muscle activity.

### ***Both Transgenic and Anti-AChE Insults Cause Excessive Muscle Reinnervation***

Neurite-growth promoting activities have been demonstrated for AChE *in vitro*. We therefore hypothesized that overexpressed AChE may exert morphogenic activities on motoneurons. To test this hypothesis, we used silver staining to characterize the distribution of motor axons in tongue muscle from DFP-treated FVB/N and untreated AChE transgenic mice as compared to untreated control mice. Large bundles of neurites (Fig. 5A) were observed in muscles of all three groups in similar numbers, suggesting similar primary nerve input to the tongue in all mice. However, both DFP-

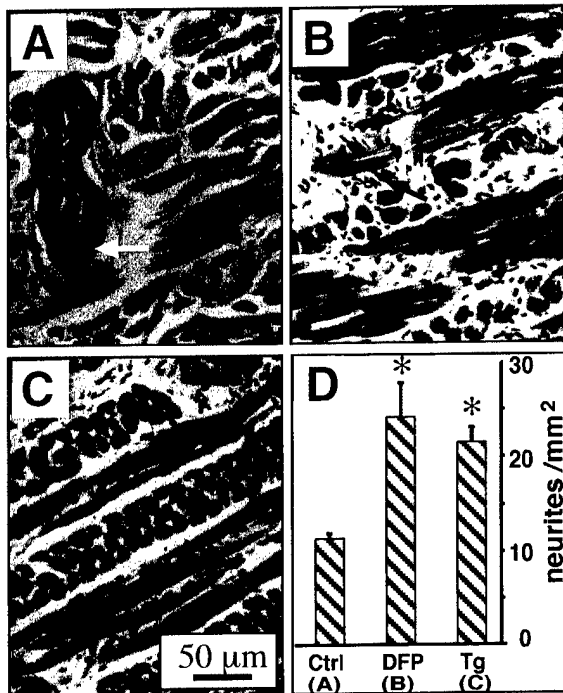


Fig. 5. Both transgenic AChE and DFP induce neurite sprouting. Silver-stained tongue-muscle neurites are shown in parallel sections from (A) 15-d-old control, (B) DFP-injected control, and (C) AChE transgenic mice. Both DFP-treated and transgenic mice displayed numerous small ( $<200\ \mu\text{m}^2$ ) bundles of neurites as compared with untreated controls (black arrows). Shown are representative photomicrographs in an equivalent location beneath the tongue epithelium. White arrow indicates a representative large ( $>1000\ \mu\text{m}^2$ ) neurite bundle observed in all groups in similar numbers. Sections from vehicle-injected animals were indistinguishable from untreated controls (not shown). Bar graph represents number of small neurites per  $\text{mm}^2$  (average  $\pm$  SEM) for at least three animals from each group. Asterisk indicates statistically significant difference compared to control ( $p < 0.05$ , ANOVA)

injected and AChE transgenic mice displayed two-fold increases in the number of small ( $<200\ \mu\text{m}^2$ ), apparently unbundled neurites as compared to both untreated and vehicle-injected controls (Fig. 5B,C). These results indicated axon branching in AChE-R overexpressing muscles, and hinted at a process of denervation-reinnervation in muscles of both DFP-treated and AChE transgenic mice.

### Elevated AChE Induces Antisense-Blocked Expansion of Motor Endplate Fields

The observed increase in small, silver-stained neurites in transgenic and DFP-treated mice suggested that cholinergic insults may be associated with reinnervation processes and the formation of new endplates. To examine this possibility, we counted motor endplates in intact diaphragms from adult control and transgenic mice, and from control mice 1 mo following a course of four daily ip injections of DFP (1 mg/kg). In diaphragms from DFP-treated mice, we observed a twofold increase over controls in the average number of endplates per  $\text{mm}^2$  as measured along the length of the innervating nerve ( $16.14 \pm 2.44$  vs  $8.52 \pm 2.42$  [ $\pm$ SEM]) (Fig. 6A,B). In diaphragms from transgenic mice, we observed a 50% increase in the density of motor endplates compared to controls ( $12.61 \pm 0.49$  NMJs/ $\text{mm}^2$ ) (Fig. 6C). Overall, these endplates appeared smaller than endplates from control mice. However, in addition to the many small endplates, we often observed abnormal, elongated endplates in muscles from both DFP-treated and transgenic mice. Two weeks after treatment with DFP, muscles from FVB/N mice displayed AChE activity that was elevated approximately twofold above controls ( $10.2 \pm 2.3$  vs  $6.1 \pm 2.1$  nanomoles substrate hydrolyzed/min/mg tissue;  $n \geq 6$ ). However, coadministration of as little as 80  $\mu\text{g}/\text{kg}$  of a 3'-end-capped, 2'-O-methyl antisense oligonucleotide against AChE (Grisaru et al., 1999) prevented accumulation of catalytically active enzyme by 60% and largely suppressed DFP-induced increases in the number of diaphragm motor endplates; Fig. 6D). AS3 alone reduced NMJ densities to values well below those measured in control muscles without dramatically altering AChE activity. Together with data indicating a relative sensitivity of AChE-R mRNA over AChE-S mRNA to AS3-mediated destruction (Grisaru et al., 1999; Golyam et al., manuscript in preparation), these observations suggest that AChE-R represents a minor but physiologically significant component of total muscle AChE in control untreated animals.

### Discussion

We observed common molecular and cellular responses in mouse muscle to transgenic overex-

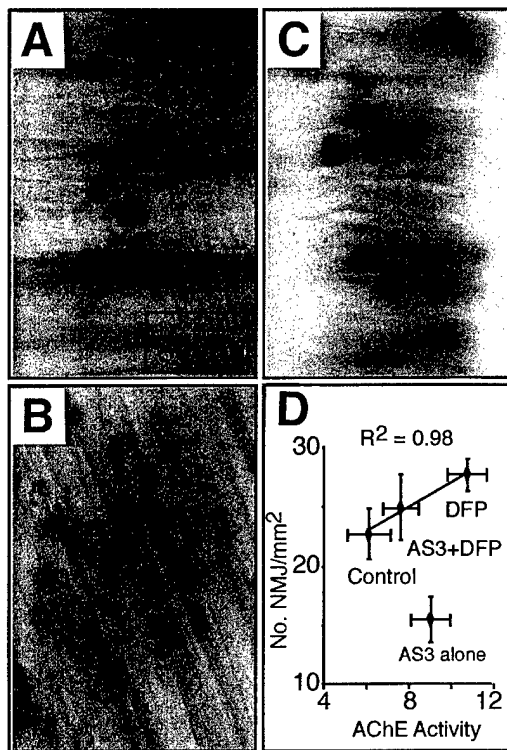


Fig. 6. Transgenic AChE and DFP promote proliferation of motor endplates. Diaphragm motor endplates from (A) 4 mo-old control mice, (B) control mice 1 mo following repeated treatment with DFP, and (C) AChE-transgenic mice visualized by staining for catalytically active AChE. Both DFP-treated control mice and AChE-transgenic mice displayed an increased number of small synapses as compared to controls. (D) Graph represents the number of synapses (average  $\pm$  SEM;  $n \geq 3$ ) per  $\text{mm}^2$  tissue as a function of AChE catalytic activity (average  $\pm$  SEM;  $n \geq 6$ ) as determined in high salt/detergent extracts by the acetylthiocholine colorimetric assay (Seidman et al., 1995). AChE activity is expressed as nanomoles acetylthiocholine hydrolyzed/min/mg tissue. Note that the NMJ/activity ratio in diaphragms from AS3-treated control mice deviates significantly from that expected given the correlation established in the DFP + AS3 paradigm.

pression of neuronal AChE and to chronic administration of the potent AChE inhibitor DFP. On the surface, the convergent outcome of these two experimental manipulations appears paradoxical. DFP imposes a rapid, irreversible blockade of the acetylcholine-hydrolyzing activity of AChE, leading to

acetylcholine excess and cholinergic excitation (Taylor, 1995; Friedman et al., 1996). In contrast, transgenic overexpression of AChE in motoneurons is predicted to elevate locally acetylcholine-hydrolyzing activity at the NMJ, presumably resulting in an acetylcholine deficit and cholinergic hypoactivity. Yet, in both cases, we observed elevated levels of *c-fos* and AChE-R mRNAs associated with changes in the number and structure of motor endplates, branching of motor axons, and severe myopathologies. These findings suggest that both gain and loss of synaptic activity impose a physiological stress on the muscle that is translated into changes in gene expression having long-term implications for neuromuscular function. In transgenic mice, abnormally intense electrophysiological activity suggested that long-term adaptation to overexpressed synaptic AChE promotes enhanced cholinergic activity at some sites (Andres et al., 1997; Farchi et al., unpublished data). In that case, even normal neuromotor activity would elicit cholinergic hyperexcitation and induce expression of AChE-R in muscles of transgenic mice. Nevertheless, AChE overexpression following either stress or anticholinesterase intoxication carries dire implications for neuromuscular structure and function in vivo. These findings in muscle parallel the overexpression of AChE-R observed in rodent brain under stress and anticholinesterase exposure. The profound impact of AChE-R overexpression on the structure and organization of NMJs, advances the notion that overexpressed AChE-R in the CNS plays a role in the delayed psychopathologies associated with trauma or anticholinesterase intoxication (reviewed by Kaufer et al., 1999). It is noteworthy that transgenic mice overexpressing very high levels of AChE-R (Sternfeld et al., 1998) display dramatic fourfold elevated NMJ densities (T. Evron and M. Soreq, unpublished observation).

Until recently, the low-level basal expression of AChE-R precluded characterization of this protein from natural sources. Nonetheless, heterologous expression studies demonstrated AChE-R to be a soluble, secreted, nonsynaptic, catalytically active form of the enzyme (Seidman et al., 1995). In microinjected *Xenopus* embryos, expression of AChE-R was restricted to secretory epidermal cells. This is consistent with our observations of induced AChE-R mRNA in tongue epithelium. However, the absence of significant AChE activity in the

tongue epithelium suggests that excess AChE-R is excreted from, rather than retained within, this tissue as well. Normally, the accumulation of AChE in mature NMJs is accomplished by focal transcription at subjunctional nuclei combined with restrictions on diffusion of AChE mRNA or protein to nonjunctional sites (Jasmin et al., 1993). The diffuse localization of overexpressed AChE-R mRNA and of AChE enzyme in transgenic and DFP-treated muscle is consistent with a nonjunctional disposition for this enzyme. Moreover, it suggests that transcription of AChE mRNA is activated following DFP in otherwise "quiescent" nonjunctional nuclei. Nevertheless, the extent of overexpressed AChE in transgenic mice displayed a downward trend during postnatal development. Our current findings indicate adjustments of the AChE feedback loop and would explain our previous detection of only slightly elevated AChE activity in muscles of adult transgenic mice (Andres et al., 1997).

Increased numbers of small neurites were associated with increased numbers of small, immature endplates in diaphragms of DFP and transgenic mice. This suggests that NMJ stress stimulates compensatory mechanisms designed to increase the number of functional synapses. I.p. injections of antisense oligonucleotides to AChE mRNA ameliorated both induced AChE overexpression and motor endplate expansion. Because oligonucleotides are not known to cross the blood-brain barrier unassisted (Seidman et al., 1999), the observation that systemic administration of AS3 effectively blocked DFP-promoted synaptogenesis indicates a prominent role for muscle-derived AChE-R in this phenomenon. Neurite-growth-promoting functions attributed to the synaptic AChE-S variant were shown to be independent of catalytic activity (Sternfeld et al., 1998). In the current study, repeated DFP treatments were associated with elevated levels of AChE-R mRNA and enhanced neurite branching even though *de novo* synthesized enzyme would be rapidly inactivated by residual inhibitor. This is compatible with the idea that catalytically inactive AChE-R exerts morphogenetic activities on mammalian motoneurons. Moreover, recent studies in our laboratory demonstrate long-term (at least 1 mo) overproduction of AChE-R in brain following exposure to DFP (Friedman et al., manuscript in preparation). This could

help explain the devastating myopathic effects of even a single exposure to this agent (Taylor, 1996). As DFP promotes overexpression of AChE in central neurons, the signal driving changes in neurite structure could originate from either the muscle or the motoneurons themselves. Similarly, the effects of DFP on muscle may reflect its status as a target tissue of neurons overexpressing AChE-R. This latter possibility suggests further studies into the potential effects of overexpressed neuronal AChE on other target tissues such as adrenal gland and intestine.

A massive and transitory increase in *c-fos* mRNA and Fos protein was reported to occur in rats intoxicated by a single dose of Soman, a highly toxic irreversible inhibitor of cholinesterase (Chollat et al., 1993). In our study, both DFP and transgenic AChE promoted elevated levels of *c-fos* mRNA in muscle. Upregulation of this nuclear transcription factor could be owing to muscle necrosis and cell death because chronic elevation of Fos usually accompanies cell injury or apoptosis (Slotkin et al., 1997). However, induction of *c-Fos* was also reported to follow nerve growth factor administration in cholinergic neurons of the adult rat basal forebrain (Gibbs et al., 1997). Therefore, elevated *c-fos* mRNA in transgenic and DFP-treated mouse muscle could reflect regeneration processes. In brain, calcium-dependent elevations in *c-fos* mRNA were spatiotemporally correlated with elevated levels of AChE-R mRNA. This suggests that AChE-R represents a downstream, stress-responsive element in the nervous system. The sequence homology (de la Escalera et al., 1990; Ichtchenko et al., 1995) and functional redundancy (Darboux et al., 1996; Grifman et al., 1998) between AChE and neuronal cell-cell interaction proteins with protruding intracellular domains such as neurotactin and neuroligin suggest a role for AChE in cell adhesion. In that case, stress-responsive AChE-R could play a role in the neuronal remodeling that follows various stress insults. The core domain of AChE is likely to mediate the enzyme's noncatalytic functions, perhaps by regulating ligand-binding interactions between its homologous cell surface proteins and their natural binding partners (i.e., neurexins). Nevertheless, isoform-specific influences of AChE on cellular morphogenesis implies important, but yet undefined roles for the various alternative C-terminal peptides.

Cholinesterase inhibitors are routinely employed to treat various neurological disorders associated with cholinergic deficits. For example, the fluctuating muscle weakness suffered by individuals afflicted with myasthenia gravis is treated with chronic administration of neostigmine. Nevertheless, neostigmine has long been known to promote ultrastructural abnormalities of the postsynaptic NMJ membrane, terminal nerve branching, and myopathologies in normal rats (Engel et al., 1973; Hudson et al., 1978). For these reasons, it was suggested that anticholinesterase therapy may actually contribute to the progressive deterioration of muscle function in myasthenia gravis (Swash, 1975). Our current findings suggest that adverse responses to neostigmine might be mediated by feedback responses to AChE inhibition and consequent accumulation of AChE-R in muscle. Thus, our data point to feedback overexpression of AChE-R as a mechanism translating diverse physiological NMJ stresses into long-term neuromuscular pathologies. They therefore raise serious concern about excessive use of anticholinesterases for management of noncrisis medical situations. Perhaps it is not surprising, therefore, that muscle weakness is prominent among the complaints of Gulf War veterans having received 90 mg/d pyridostigmine as a prophylactic guard against anticipated exposure to chemical weapons (Haley et al., 1997). Thus, the indications that anticholinesterase drugs initiate potentially devastating feedback responses in mammalian muscle carries profound health implications for the relatively large group of individuals currently receiving, or targeted for, various anticholinesterase therapeutics. For example, the only drugs currently approved for Alzheimer's disease are potent AChE inhibitors. The efficient *in vivo* suppression of AChE overexpression achieved here with extremely low doses of antisense oligonucleotides to AChE mRNA suggests that antisense therapeutics may offer a viable alternative approach to conventional anticholinesterase therapy in the nervous system.

## Acknowledgments

The authors would like to thank Drs. Asher Meshorer and Naomi Melamed-Book for helpful discussions and Ms. M. Maman-Sapir and Ms. D. Nathan, for excellent technical assistance.

This research has been supported by the US Army Medical Research and Development Command (DAMD 17-99-1-9547), The Israel Science Foundation (590/97), and the US-Israel Binational Science Foundation (96-001100) (to H.S.).

## References

- Andres C., Beeri R., Friedman A., Lev-Lehman E., Henis S., Timberg R., et al. (1997). Acetylcholinesterase-transgenic mice display embryonic modulations in spinal cord choline acetyltransferase and neurexin Ibeta gene expression followed by late-onset neuromotor deterioration. *Proc. Natl. Acad. Sci. USA* **94**, 8173-8178.
- Andres C., Seidman S., Beeri R., Timberg R., and Soreq H. (1998) Transgenic acetylcholinesterase induces enlargement of murine neuromuscular junctions but leaves spinal cord synapses intact. *Neurochem Int.* **32**, 449-456.
- Ben Aziz Aloya R., Seidman S., Timberg R., Sternfeld M., Zakut H., and Soreq H. (1993). Expression of a human acetylcholinesterase promoter-reporter construct in developing neuromuscular junctions of *Xenopus* embryos. *Proc. Natl. Acad. Sci. USA* **90**, 2471-2475.
- Chollat Namy A., Delamanche I. S., and Bouchaud C. (1993) Variation in the expression of *c-fos* after intoxication by soman. Comparative study using *in situ* hybridization and immunohistochemistry. *Brain Res.* **603**, 32-37.
- Darbox I., Barthalay Y., Piovant M., and Hipeau Jacquotte R. (1996) The structure-function relationships in *Drosophila* neurotactin show that cholinesterasic domains may have adhesive properties. *EMBO J.* **15**, 4835-4843.
- de la Escalera S., Bockamp E. O., Moya F., Piovant M., and Jimenez F. (1990) Characterization and gene cloning of neurotactin, a *Drosophila* transmembrane protein related to cholinesterases. *EMBO J.* **9**, 3593-3601.
- Donger C., Krejci E., Serradell A. P., Eymard B., Bon S., Nicole S., et al. (1998). Mutation in the human acetylcholinesterase-associated collagen gene, COLQ, is responsible for congenital myasthenic syndrome with end-plate acetylcholinesterase deficiency (Type Ic). *Am. J. Hum. Genet.* **63**, 967-975.
- Engel A. G., Lambert E. H., and Santa T. (1973) Study of long-term anticholinesterase therapy. Effects on neuromuscular transmission and on motor end-plate fine structure. *Neurology* **23**, 1273-1281.

- Engelhardt J. I., Siklos L., and Appel S. H. (1997) Immunization of guinea pigs with human choline acetyltransferase induces selective lower motoneuron destruction. *J. Neuroimmunol.* **78**, 57–68.
- Evoli A., Batocchi A. P., and Tonali P. (1996) A practical guide to the recognition and management of myasthenia gravis. *Drugs* **52**, 662–670.
- Friedman A., Kaufer D., Shemer J., Hendler I., Soreq H., and Tur Kaspas I. (1996). Pyridostigmine brain penetration under stress enhances neuronal excitability and induces early immediate transcriptional response. *Nat. Med.* **2**, 1382–1385.
- Gibbs R. B. and Martynowski C. (1997). Nerve growth factor induces Fos-like immunoreactivity within identified cholinergic neurons in the adult rat basal forebrain. *Brain Res.* **753**, 141–151.
- Grifman M., Galyam N., Seidman S., and Soreq H. (1998) Functional redundancy of acetylcholinesterase and neurexins in mammalian neurite outgrowth. *Proc. Natl. Acad. Sci. USA* **95**, 13,935–13,940.
- Grisaru D., Lev-Lehman E., Shapira M., Chaikin E., Lessing J. B., Eldor A., et al. (1999) Human osteogenesis involves differentiation-dependent increases in the morphogenetically active 3' alternative splicing variant of acetylcholinesterase. *Mol. Cell Biol.* **19**, 788–795.
- Haley R. W., Kurt T. L., and Hom J. (1997) Is there a Gulf War Syndrome? Searching for syndromes by factor analysis of symptoms. *JAMA* **277**, 215–222.
- Hudson C. S., Rash J. E., Tiedt T. N., and Albuquerque E. X. (1978) Neostigmine-induced alterations at the mammalian neuromuscular junction. II. Ultrastructure. *J. Pharmacol. Exp. Ther.* **205**, 340–356.
- Ichtchenko K., Hata Y., Nguyen T., Ullrich B., Missler M., Moomaw C., and Sudhof T. C. (1995). Neurexins: a splice site-specific ligand for beta-neurexins. *Cell* **81**, 435–443.
- Jasmin B. J., Lee R. K., and Rotundo R. L. (1993) Compartmentalization of acetylcholinesterase mRNA and enzyme at the vertebrate neuromuscular junction. *Neuron* **11**, 467–477.
- Kaufer D., Friedman A., and Soreq H. (1999) The vicious circle of stress and anticholinesterase responses. *Neuroscientist* **5**, 173–183.
- Kaufer D., Friedman A., Seidman S., and Soreq H. (1998) Acute stress facilitates long-lasting changes in cholinergic gene expression. *Nature* **393**, 373–377.
- Kawabuchi M., Osame M., Watanabe S., Igata A., and Kanaseki T. (1976) Myopathic changes at the endplate region induced by neostigmine methylsulfate. *Experientia* **32**, 632–635.
- Koenigsberger C., Chiappa S., and Brimijoin S. (1997) Neurite differentiation is modulated in neuroblastoma cells engineered for altered acetylcholinesterase expression. *J. Neurochem.* **69**, 1389–1397.
- Laskowski M. B., Olson W. H., and Dettbarn W. D. (1975) Ultrastructural changes at the motor endplate produced by an irreversible cholinesterase inhibitor. *Exp. Neurol.* **47**, 290–306.
- Layer P. G. and Willbold E. (1995) Novel functions of cholinesterases in development, physiology and disease. *Prog. Histochem. Cytochem.* **29**, 1–99.
- Lindstrom J. (1998) Mutations causing muscle weakness. *Proc. Natl. Acad. Sci. USA* **95**, 9070,9071.
- Livneh A., Sarova I., Michaeli D., Pras M., Wagner K., Zakut H., and Soreq H. (1988). Antibodies against acetylcholinesterase and low levels of cholinesterases in a patient with an atypical neuromuscular disorder. *Clin. Immunol. Immunopathol.* **48**, 119–131.
- Massoulié J., Pezzementi L., Bon S., Krejci E., and Vallette F. M. (1993) Molecular and cellular biology of cholinesterases. *Prog. Neurobiol.* **41**, 31–91.
- Sanes J. R. and Lichtman J. W. (1999) Development of the vertebrate neuromuscular junction. *Ann. Rev. Neurosci.* **22**, 389–442.
- Schonbeck S., Chrestel S., and Hohlfeld R. (1990) Myasthenia gravis: prototype of the antireceptor autoimmune diseases. *Int. Rev. Neurobiol.* **32**, 175–200.
- Seidman S., Sternfeld M., Ben Aziz Aloya R., Timberg R., Kaufer Nachum D., and Soreq H. (1995). Synaptic and epidermal accumulations of human acetylcholinesterase are encoded by alternative 3'-terminal exons. *Mol. Cell Biol.* **15**, 2993–3002.
- Seidman S., Eckstein F., Grifman M., and Soreq H. Antisense technologies have a future combating neurodegenerative disease. *Antisense Res. Drug Dev.* **9**, 333–340.
- Shapira M., Seidman S., Sternfeld M., Timberg R., Kaufer D., Patrick J., and Soreq H. (1994). Transgenic engineering of neuromuscular junctions in *Xenopus laevis* embryos transiently overexpressing key cholinergic proteins. *Proc. Natl. Acad. Sci. USA* **91**, 9072–9076.
- Sharma K. V. and Bigbee J. W. (1998) Acetylcholinesterase antibody treatment results in neurite detachment and reduced outgrowth from cultured neurons: further evidence for a cell adhesive role for neuronal acetylcholinesterase. *J. Neurosci. Res.* **53**, 454–464.

- Slotkin T. A., McCook E. C., and Seidler F. J. (1997) Cryptic brain cell injury caused by fetal nicotine exposure is associated with persistent elevations of c-fos protooncogene expression. *Brain Res.* **750**, 180–188.
- Sternfeld M., Ming G., Song H., Sela K., Timberg R., Poo M., and Soreq H. (1998). Acetylcholinesterase enhances neurite growth and synapse development through alternative contributions of its hydrolytic capacity, core protein, and variable C termini. *J. Neurosci.* **18**, 1240–1249.
- Sternfeld M., Patrick J. D., and Soreq H. (1998) Position effect variegations and brain-specific silencing in transgenic mice overexpressing human acetylcholinesterase variants. *J. Physiol. (Paris)* **92**, 249–255.
- Swash M. (1975) Motor innervation of myasthenic muscles (Letter). *Lancet* **2**, 663.
- Taylor P. (1996) Agents acting at the neuromuscular junction and autonomic ganglia, in *Goodman and Gilman's The Pharmacological Basis of Therapeutics* (Hardman J. G., Limbird L. E., Molinoff P. B., and Ruddon R. W., eds.), McGraw-Hill, New York, pp. 177–197.
- Taylor P., Radic Z., Hosea N. A., Camp S., Marchot P., and Berman H. A. (1995). Structural bases for the specificity of cholinesterase catalysis and inhibition. *Toxicol. Lett.* **82–83**, 453–458.

## Modified testicular expression of stress-associated “readthrough” acetylcholinesterase predicts male infertility

Inbal Mor\*, Dan Grisaru\*<sup>‡</sup>, Lior Titelbaum\*, Tamah Evron\*, Carmelit Richler<sup>†</sup>, Jacob Wahrman<sup>†</sup>, Meira Sternfeld\*, Leah Yogev<sup>§</sup>, Noam Meiri<sup>#</sup>, Shlomo Seidman\*, and Hermona Soreq\*

\*Department of Biological Chemistry and <sup>†</sup>Department of Genetics, The Life Sciences Institute, The Hebrew University of Jerusalem, Jerusalem, Israel; <sup>‡</sup>Dept. of Gynecology and <sup>§</sup>Institute for the Study of Fertility, Surasky Medical Center and Sackler School of Medicine, Tel Aviv, Israel; <sup>#</sup>Institute of Animal Science, ARO, Volcani Center, Bet Dagan, Israel

Corresponding author: Hermona Soreq, Department of Biological Chemistry, The Life Sciences Institute, The Hebrew University of Jerusalem, Jerusalem, Israel; E-mail: soreq@cc.huji.ac.il

### ABSTRACT

Male infertility is often attributed to stress. However, the protein or proteins that mediate stress-related infertility are not yet known. Overexpression of the “readthrough” variant of acetylcholinesterase (AChE-R) is involved in the cellular stress response in a variety of mammalian tissues. Here, we report testicular overexpression of AChE-R in heads, but not tails, of postmeiotic spermatozoa from mice subjected to a transient psychological stress compared with age-matched control mice. Transgenic mice overexpressing AChE-R displayed reduced sperm counts, decreased seminal gland weight, and impaired sperm motility compared with age-matched nontransgenic controls. AChE-R was prominent in meiotic phase spermatocytes and in tails, but not heads, of testicular spermatozoa from AChE-R transgenic mice. Head-localized AChE-R was characteristic of human sperm from fertile donors. In contrast, sperm head AChE-R staining was conspicuously reduced in samples from human couples for whom the cause of infertility could not be determined, similar to the pattern found in transgenic mice. These findings indicate AChE-R involvement in impaired sperm quality, which suggests that it is a molecular marker for stress-related infertility.

Key words: psychological stress • sperm motility • spermatogenesis

**M**ale gamete production, spermatogenesis, takes place in the seminiferous tubules of the testes. Progression through this process is accompanied by migration of cells from the tubule periphery towards the central cavity. At the periphery of the tubules are diploid stem cells, spermatogonia, which pass through proliferative mitotic divisions to generate spermatocytes. Spermatocytes give rise to round haploid spermatids through meiosis. Spermatids elongate and differentiate to form spermatozoa that are released to the genital duct system. In the epididymis, spermatozoa acquire motility and fertilization ability (1).

Reduced male fertility is one of the known consequences of psychological stress (2–4). The molecular pathways translating stress into depressed male reproductive potency are not yet known but likely involve stress-hormone-induced alterations in gene expression (5).

Glucocorticoid hormones released by the adrenal gland in response to stress (6) are known to exert long-lasting effects on gene expression. We reported previously activation of the gene encoding the acetylcholine hydrolyzing enzyme acetylcholinesterase (AChE; EC 3.1.1.7) by forced swim stress and pharmacological inhibitors of AChE in brain (7), muscle (8), hematopoietic cells (9), and intestinal epithelium (10). In all these cases, overexpressed AChE appeared as an otherwise rare splicing variant known as "readthrough" AChE, or AChE-R. Stress-induced overexpression of AChE-R likely involves both glucocorticoid-sensitive (9) and glucocorticoid-insensitive (7) components.

The classical function of AChE, acetylcholine hydrolysis (11), plays a crucial role in cholinergic neurotransmission. AChE was also observed in spermatozoa (12, 13), where its presence was attributed to cholinergic mechanism(s) involved in sperm motility (14, 15). Nevertheless, it has been shown recently that AChE exerts morphogenic and/or developmental activities unrelated to acetylcholine hydrolysis (16). Furthermore, AChE inhibitors in use as agricultural insecticides were associated with yet unexplained impairments in spermatogenesis and sperm properties (17, 18). For these reasons, we explored the influence of AChE-R on spermatogenesis and sperm properties.

## MATERIALS AND METHODS

### **Animals and tissue collection**

Male FVB/N mice (2–6 months old) were killed 24 h after four successive daily forced swim sessions as detailed (7). Control mice, and mice that have a transgene encoding human AChE-R inserted into their genome, were killed with no previous treatment. We prepared serum from blood samples allowed to clot 1 h at room temperature and overnight at 4°C, followed by centrifugation and supernatant collection. Testes and seminal vesicles were excised and weighed. One testis from each animal was fixed in 4% paraformaldehyde or Bouin's fixative, the other was kept at -70°C for protein extraction.

### **Serum hormone levels**

Serum corticosterone concentrations were determined by radioimmunoassay (ICN Pharmaceuticals, Inc., Costa Mesa, CA).

### **Sperm evaluation**

Live, motile sperm were counted manually in isolates prepared from a single cauda epididymis shredded in 1 ml saline. Sperm concentration was measured by using the Improved Neubauer chamber (Heinz Herenz, Hamburg, Germany). For staining with the fluorogenic dye JC-1, epididymal sperm cells were incubated 20 min at room temperature in the presence of 3 µM JC-1 and 12 µM Propidium Iodide (Molecular Probes, Inc., Eugene, OR), essentially as detailed (19). Samples were centrifuged at 500 g for 7 min to remove excess dye. A drop of the suspended cells was placed on a coverslip and covered by a second coverslip. Viable motile cells that reached the drop's periphery were subjected to fluorescence microscopy and quantitative

evaluation of JC-1 emission at 525 nm (green) and 585 nm (red). The ratio between red and green fluorescence was considered to reflect mitochondrial membrane potential.

### **AChE analysis**

AChE activity assay, 5%–20% sucrose gradient and immunoblot analysis were performed essentially as described (20) on testes tissue homogenized in 1 M NaCl, 0.01 M EGTA, 0.01 M Tris HCl pH 7.4, 1% TritonX100. AChE-R was detected with a polyclonal antibody targeted at the C-terminal peptide of AChE-R (20). Band intensities of two lanes loaded with protein from individual mice of each group were quantified by using Adobe Photoshop 5.0 software.

### ***In situ* hybridization**

*In situ* hybridization was performed as detailed elsewhere (7) on 7- $\mu$ m-thick paraformaldehyde-fixed paraffin-embedded sections using 50-mer, biotinylated, 2'-O-methyl cRNA probes targeted to either pseudointron I4 or exon E6 in AChEmRNA transcripts. ELF<sup>TM</sup> (Molecular Probes, Inc., Eugene, OR) was used as a fluorogenic alkaline phosphatase substrate.

### **Immunohistochemistry**

Detection of the AChE isoforms was performed on 7- $\mu$ m-thick paraffin-embedded sections with polyclonal antibodies targeted at the C-terminal peptide of synaptic AChE-S (C-16; Santa Cruz Biotechnology, Santa Cruz, CA) or of AChE-R(20). Biotinylated secondary antibodies were detected with streptavidin-alkaline phosphatase conjugate (Amersham Pharmacia Biotech, Piscataway, NJ). Fast Red (Roche Molecular Biochemicals, Mannheim, Germany) was used as a chromogenic substrate. PCNA was detected by using a dedicated staining kit (Zymed Laboratories, San Francisco, CA); nuclear counterstaining was with hematoxylin (Sigma, St. Louis, MO). All immunodetections were performed after heat-induced antigen retrieval.

### **Confocal analysis**

An MRC-1024 BioRad (Hemel Hempstead, Hertfordshire, U.K.) confocal microscope equipped with an inverted microscope was used to scan the Fast Red precipitate used for immunodetection. Fluorescence was excited at 488 nm, and emission was measured with a 580df32 filter. To examine mouse testicular spermia in tissue sections, we scanned a confocal plane every 0.35 $\mu$ m using a 63X/1.4 oil immersion objective and a three-dimensional projection created from all sections. To examine human sperm smears, a confocal plane was scanned every 0.30  $\mu$ m by using a 40X/1.3 oil immersion objective; three-dimensional projections of the signal were overlaid on a phase contrast image of the cells.

## **RESULTS**

### **AChE-R is overexpressed in testes from mice exposed to forced swimming**

To examine the effects of acute stress on AChE expression in the male gonads, we subjected adult male FVB/N mice to four successive daily sessions of confined swim (7). Stressed mice displayed fivefold elevated serum corticosterone levels ( $171.0 \pm 62.4$  ng/ml serum (Avg.  $\pm$  SE);  $n=4$ ) compared with naïve mice ( $31.6 \pm 7.5$ ;  $n=3$ ;  $P \leq 0.04$ , Mann-Whitney). Elevated glucocorticoid levels were accompanied by mildly increased AChE activities in testicular extracts ( $0.3 \pm 0.03$  nmoles substrate/min/mg protein after stress vs.  $0.1 \pm 0.01$  nmoles/min/mg protein in controls). To identify the cell population(s) that respond to stress by increasing *ACHE* gene activity, we used *in situ* hybridization (7). A selective 2'-O-methyl biotinylated cRNA probe revealed a circumferential distribution of AChE-R mRNA in testicular tubules from naïve mice (Fig. 1A). In stressed mice 24 h after the last swim session, AChE-R mRNA signals were notably intensified and extended into all cell layers (Fig. 1B). Immunodetection with an antibody selective for AChE-R (20) produced no detectable staining in testes from control mice (Fig. 1C). In contrast, anti-AChE-R antibodies intensively labeled internal cell layers in tubules of stressed mice (Fig. 1D), particularly the innermost stratum containing maturing spermatozoa. Stress therefore induced AChE-R mRNA overproduction in cells undergoing early spermatogenesis and caused accumulation of AChE-R protein at later stages of sperm formation.

#### **Transgenic mice as a model for chronic testicular overexpression of AChE-R**

To establish a model for chronic gonadal overexpression of AChE-R, we exploited mice that were transgenic for human AChE-R (20). Transgenic mice displayed 700-fold excess testicular AChE activity (Fig. 2A). Elevated levels of a 66 KDa immunoreactive band comigrating with recombinant AChE-R protein was accompanied by unchanged labeling of a slightly faster migrating band (Fig. 2B), potentially reflecting another AChE variant (21), different glycosylation patterns (22) or proteolytic cleavage of the AChE protein, which was previously observed in the serum of stressed mice (9). Sucrose gradient centrifugation (5%–20%) demonstrated the excess AChE to migrate as a single peak of globular monomeric enzyme, as expected from AChE-R (Fig. 2C). Using *in situ* hybridization, we detected high levels of AChE-R mRNA in the peripheral layers of testicular tubules from transgenic compared with control FVB/N mice (Fig. 3A, B). Elevation of AChE-R mRNA levels in the circumference of tubules was similar to that observed in nontransgenic mice following stress (compare with Fig. 1B). The peripheral layers are the cell layers harboring both mitotic spermatogonia and postmitotic spermatocytes. Using anti-AChE-R antibodies, we could not detect the AChE-R protein in sections from control nonstressed mice (Fig. 3C). In contrast, 65% of stained tubules from transgenic mice displayed pronounced deposition of AChE-R in a single peripheral cell layer (Fig. 3D). The remaining 35% were divided evenly between tubules with AChE-R deposits in the inner cell layers harboring spermatozoa heads (similar to the stress pattern) and tubules with labeling within the tubular cavity into which the spermatozoa tails project (data not shown). Some tubules stained in the periphery were also stained in the inner layer (12% of stained tubules) or the cavity (26%). Thus, AChE-R expression in testes of transgenic mice resembled that of mice subjected to repeated acute stress at the level of the mRNA but exhibited a more complex pattern of cellular distribution at the level of the protein. In contrast, the expression of the "synaptic" AChE-S splicing variant appeared largely unaffected by either stress or transgenic overexpression of AChE-R (data not shown).

### **Accumulated AChE-R in postmitotic sperm progenitors imposes a partial block to postmeiotic differentiation**

We observed recently that AChE-R promotes expansion of hematopoietic progenitor cells (9) and terminal differentiation of osteoblasts (23). We therefore considered the possibility that overproduction of AChE-R may affect the proliferation of male germ cell progenitors. To quantify replicating cells, we stained for proliferating cell nuclear antigen (PCNA). In both naïve FVB/N and AChE-R transgenic mice, PCNA staining was confined to the most peripheral cell layer consisting exclusively of spermatogonia, the proliferative spermatogenic progenitors (Fig. 3E and data not shown). AChE-R was undetectable in this cell layer (Fig. 3F), being concentrated in the next inner layer of postmitotic spermatocytes of transgenic mice. In spermatocytes, AChE-R displayed a subcellular disposition that included diffuse cytoplasmic distribution in addition to focal perinuclear sites of accumulation (Fig. 3F, inset). The average number of PCNA labeled cells was identical in transgenic and control mice ( $67.5 \pm 2.8$  vs.  $67.2 \pm 2.0$  cells/normalized tubule perimeter, respectively). In addition, we did not observe any changes in the organization of spermatogonia in testes from transgenic mice (data not shown). In contrast, the number of postmeiotic, differentiating spermatozoa surrounding the tubular cavity was reduced significantly in transgenic mice compared with control mice ( $82 \pm 12$  vs.  $97 \pm 15$  cells/normalized tubule perimeter, respectively;  $n=3$ , 8–10 tubules per mouse,  $P < 0.0005$ , Student's *t*-test).

### **Transgenic testicular overproduction of AChE-R is associated with impaired sperm properties**

As predicted by the reduced number of spermatozoa in testicular tubules, epididymal sperm counts were also significantly lower in transgenic compared with control mice (Fig. 4). However, the 45% reduction in epididymal sperm cells exceeded the cell loss observed in tubules by 30%, indicating that additional cell loss takes place following the release of spermatozoa from the seminiferous tubules. In addition, motility of surviving sperm appeared compromised in transgenic mice compared with controls (Fig. 4). Although suggestive of functional impairments, the sperm motility data were not statistically significant. Using JC-1 (19) to assess mitochondrial activity of motile transgenic epididymal sperm, we observed hyperpolarization rather than hypopolarization of mitochondrial membranes (data not shown). This observation excluded reduced cellular respiration as a cause for reduced sperm motility but raised the possibility that mitochondrial hyperpolarization foreshadows apoptotic events that contribute to reduced sperm counts (24, 25). In addition to sperm properties, seminal gland weight of transgenic mice was also reduced compared with controls (Fig. 4).

### **AChE-R may serve as a marker of stress-related male infertility**

Testicular tubules from stressed mice and a large portion (~60%) of those from transgenic mice displayed accumulation of AChE-R in differentiated spermatozoa residing at the inner cell layer surrounding the cavity. To characterize the expression of AChE-R in mouse spermatozoa, and to explore the relevance of the mouse models to human fertility, we performed confocal microscopy. Anti-AChE-R antibodies failed to label testicular spermatozoa from control mice (Fig. 5A). In contrast, repeated acute stress facilitated strong, punctate, intracellular labeling that

was limited to spermatozoa heads (Fig. 5B), with few cells also stained at the neck. Spermatozoa from AChE-R transgenics were either unlabeled (40%), or stained at the neck (35%) or head (25%) (Fig. 5C). We then examined human sperm in air-dried smears of ejaculates from apparently fertile donors or from the male partner of couples with unexplained infertility. Men from infertile couples were healthy, did not suffer from hypogonadism, and displayed sperm concentration within the same range as fertile subjects ( $44\text{--}241$  and  $60\text{--}137 \times 10^6$  sperm cells/ml, respectively). These men were selected because they did not display any abnormal sperm parameter to which the couple infertility could be attributed. Sperm in samples from fertile donors were stained in both the head and neck regions. In contrast, samples from infertility patients presented large fractions of sperm with intense labeling in the neck region but no detectable head-associated AChE-R (Fig. 5D). Cumulative analysis by a blind observer of approximately 40 sperm cells from each of 3 individuals in each group demonstrated a significantly decreased proportion ( $P < 0.05$ , Mann Whitney) of head-stained sperm from male partners of infertile couples as compared to sperm-bank donors.

## DISCUSSION

### **Testicular AChE is subject to stress-induced changes in alternative splicing**

Our current findings associate stress with testicular overproduction of AChE-R and suggest that stress insults of varying duration or severity may initiate graded increases in AChE-R in spermatogenic cells (Fig. 6). The increase in AChE expression following stress is consistent with the presence of a recently discovered consensus sequence for a putative glucocorticoid response element in the upstream promoter region of the human *ACHE* gene locus (10). AChE overexpression following stress was highly selective as it was observed only for the AChE-R isoform. This finding suggests active diversion of 3' alternative splicing of AChE mRNA. This pattern of stress-mediated *ACHE* gene expression parallels that observed in other tissues and strengthens the concept of shifted alternative splicing and the resultant AChE-R protein as universal stress response elements in multiple mammalian organs, including the gonads. It would be interesting to test if the effect of stress on testis is reversible and, if so, how long it takes to reverse.

### **Massive AChE-R elevation could impair spermatogenesis and sperm function in a noncatalytic manner**

Compared with psychologically-stressed FVB/N mice, transgenic mice exhibiting massive AChE-R overproduction displayed heterogeneity in the cellular and subcellular localization of AChE-R. It is yet unclear whether this difference between stressed and transgenic mice reflects the high levels of overexpression achieved in the transgenic model, or a property resulting from chronic congenital overexpression of the transgenic protein. The greatly elevated expression of AChE-R in transgenic mice was accompanied by decreased sperm counts, sperm motility, and seminal gland weight. The decline in postmitotic spermatozoa numbers in AChE-R transgenics suggests that AChE-R excess may impose yet undefined restrictions on spermatogenesis following mitotic cell division. Although the reduction in seminal gland weight potentially reflects systemic effects of chronic AChE-R overexpression and its impact on autonomous

cholinergic innervation(26), not all the effects should necessarily be attributed to increased cholinesterase activity. The high accumulation of AChE-R in sperm cell progenitors suggests that the primary impact of its transgenic overexpression on spermatogenesis and/or sperm properties results from direct effects of the protein on cellular processes. In this light, noncatalytic cell signaling capacities now well established for nervous system AChE (27-29) may be relevant. Our findings therefore emphasize the need to identify the yet unknown protein partner(s) of AChE-R and its putative signal transduction pathways. The perinuclear localization of AChE-R in spermatocytes resembled the nuclear association of megakaryocytic AChE (30). In hematopoietic progenitors, AChE regulation is tightly associated with that of CHED, a CDC-related protein kinase (31), which suggests potential involvement in cell cycle processes and calling for a search for potential correlation between cyclin regulation during mammalian gametogenesis (32) and AChE-R.

#### **AChE-R is potentially involved in the detrimental effects of psychological stress on male fertility**

The transgenic mouse model demonstrates the potentially detrimental effects of high levels of dispersed testicular AChE-R on mammalian sperm maturation and/or properties. Absence of AChE-R from heads of testicular spermatozoa, as was observed primarily in AChE-R transgenic mice, also appeared to be characteristic of sperm from the male partners of human couples with unexplained infertility, but not of sperm from fertile controls. These results support the notion of a role for stress-related changes in AChE expression in impaired sperm quality in humans as well. The differential AChE-R staining patterns observed in the two human groups suggest AChE-R labeling as a possible useful marker for stress-related male infertility, and strengthen the notion that stress-associated overexpression of AChE-R may be a risk factor in fertility disturbances. Scientists are examining whether the observed changes affect male reproduction and fertility.

#### **AChE-R as a molecular target for understanding and resolving various aspects of male infertility**

As anticholinesterases were shown to induce overproduction of AChE-R (see introductory paragraph), our findings may also explain the impaired sperm properties and male infertility associated with exposure to agricultural insecticides or other anticholinesterase agents (17, 18). If so, these findings further imply potential modes of intervention, including blockade of AChE feedback overexpression, prevention of the shift in alternative splicing from AChE-S to AChE-R, and selective antisense suppression of AChE-R (33). In the brain, AChE feedback overexpression was shown to be independent of the hypothalamus-pituitary axis (7). Nevertheless, the recent demonstration of a functional glucocorticoid response element in the extended AChE promoter (9) suggests a glucocorticoid-mediated component to stress-related AChE overexpression. This finding could be examined in glucocorticoid-receptor knockout mice (5, 34). AChE-R thus presents a previously unrecognized target for studying, analyzing, and treating stress-induced human male infertility.

#### **ACKNOWLEDGMENTS**

The authors are grateful to G. Paz and H. Yavetz, Tel Aviv, for fruitful discussions and N. Melamed-Book for assistance with the confocal microscopy. This study was supported by grants to H. S. from the German-Israeli Foundation (no. I-512-206.01/96), the U.S.-Israel Binational Science Foundation (no. 1999-115), and the U.S. Army Medical Research and Materiel Command (DAMD 17-99-1-9547).

1. Leonhardt, H. (1993) Male genital organs. In *Color Atlas and Textbook of Human Anatomy* (Kahle, W., Leonhardt, H., and Platzer, W., eds.) Vol. 2, Internal Organs pp. 274–289, Thieme Flexibooks: New York
2. Giblin, P. T., Poland, M. L., Moghissi, K. S., Ager, J. W., and Olson, J. M. (1988) Effects of stress and characteristic adaptability on semen quality in healthy men. *Fertil. Steril.* **49**, 127–132
3. Clarke, R. N., Klock, S. C., Geoghegan, A., and Travassos, D. E. (1999) Relationship between psychological stress and semen quality among *in vitro* fertilization patients. *Hum. Reprod.* **14**, 753–758
4. Negro-Vilar, A. (1993) Stress and other environmental factors affecting fertility in men and women: overview. *Environ. Health Perspect.* **101 Suppl 2**, 59–64
5. Jolly, C., and Morimoto, R. I. (1999) Stress and the cell nucleus: dynamics of gene expression and structural reorganization. *Gene Expr.* **7**, 261–270
6. Sapolsky, R. M., Romero, L. M., and Munck, A. U. (2000) How do glucocorticoids influence stress responses? Integrating permissive, suppressive, stimulatory, and preparative actions. *Endocr. Rev.* **21**, 55–89
7. Kaufe, D., Friedman, A., Seidman, S., and Soreq, H. (1998) Acute stress facilitates long-lasting changes in cholinergic gene expression. *Nature (London)* **393**, 373–377
8. Lev-Lehman, E., Evron, T., Broide, R. S., Meshorer, E., Ariel, I., Seidman, S., and Soreq, H. (2000) Synaptogenesis and myopathy under acetylcholinesterase overexpression. *J. Mol. Neurosci.* **14**, 93–105
9. Grisaru, D., Deutch, V., Shapira, M., Pick, M., Sternfeld, M., Melamed-Book, N., Kaufe, D., Galyam, N., Gait, M., Owen, D., Lessing, J., Eldor, A., and Soreq, H. (2001) ARP, a peptide derived from the stress-associated acetylcholinesterase variant has hematopoietic growth promoting activities. *Mol. Med.* **7**, 93–105
10. Shapira, M., Tur-Kaspa, I., Bosgraaf, L., Livni, N., Grant, A. D., Grisaru, D., Korner, M., Ebstein, R. P., and Soreq, H. (2000) A transcription-activating polymorphism in the AChE promoter associated with acute sensitivity to anti-acetylcholinesterases. *Hum. Mol. Genet.* **9**, 1273–1281

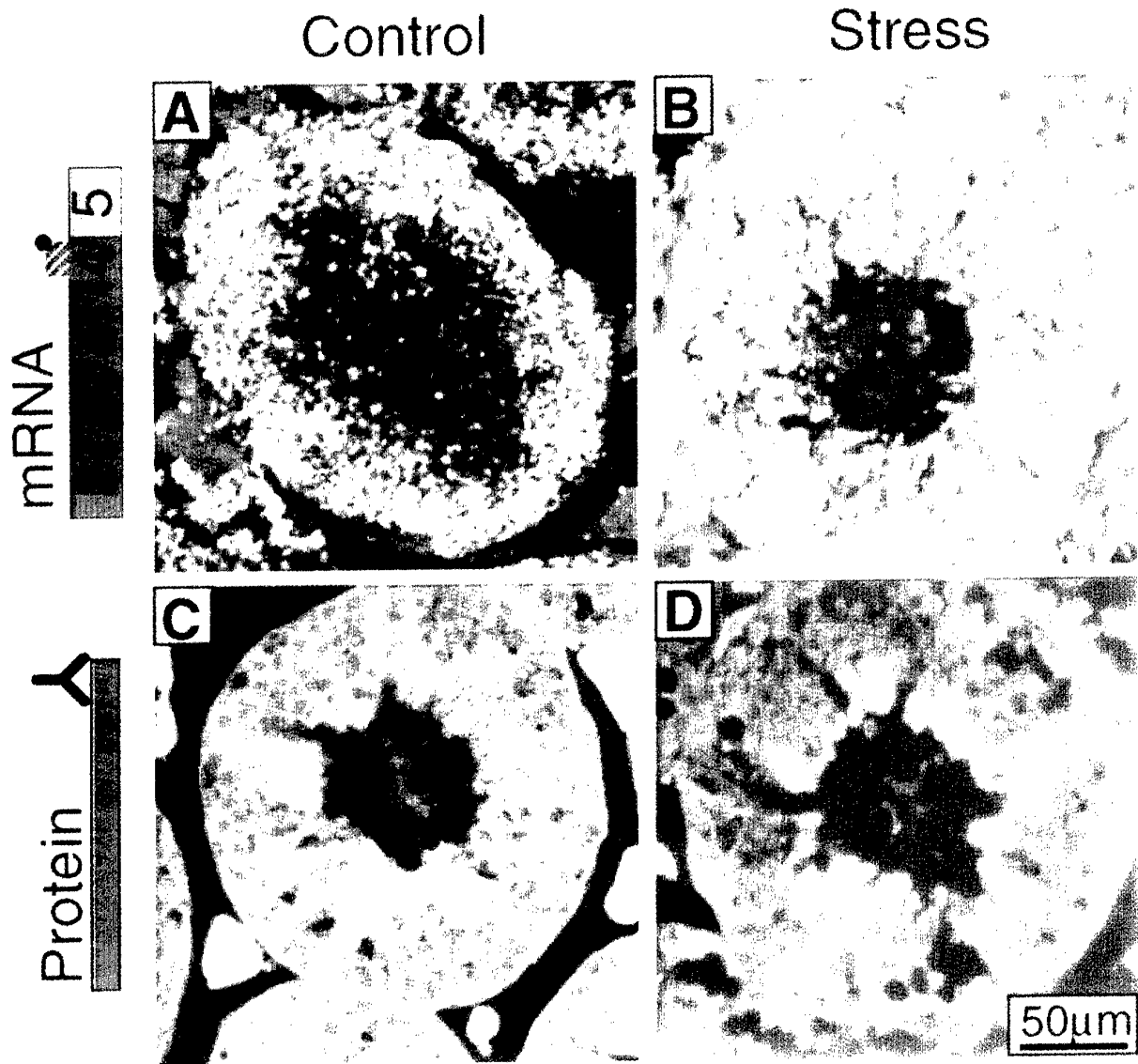
11. Taylor, P. (1996) Agents acting at the neuromuscular junction and autonomic ganglia. In *Goodman and Gilman's The Pharmacological Basis of Therapeutics* (Hardman, J. G., Limbird, L. E., Molinoff, P. B., and Ruddon, R. W., eds) pp. 177–197, McGraw-Hill: New York
12. Egbunike, G. N. (1980) Changes in acetylcholinesterase activity of mammalian spermatozoa during maturation. *Int. J. Androl.* **3**, 459–468
13. Palmero, S., Bardi, G., Coniglio, L., and Falugi, C. (1999) Presence and localization of molecules related to the cholinergic system in developing rat testis. *Eur. J. Histochem.* **43**, 277–283
14. Young, R. J., and Laing, J. C. (1991) The binding characteristics of cholinergic sites in rabbit spermatozoa. *Mol. Reprod. Dev.* **28**, 55–61
15. Dwivedi, C., and Long, N. J. (1989) Effect of cholinergic agents on human spermatozoa motility. *Biochem. Med. Metab. Biol.* **42**, 66–70
16. Grisaru, D., Sternfeld, M., Eldor, A., Glick, D., and Soreq, H. (1999) Structural roles of acetylcholinesterase variants in biology and pathology. *Eur. J. Biochem.* **264**, 672–686
17. Tielemans, E., van Kooij, R., te Velde, E. R., Burdorf, A., and Heederik, D. (1999) Pesticide exposure and decreased fertilisation rates *in vitro*. *Lancet* **354**, 484–485
18. Sarkar, R., Mohanakumar, K. P., and Chowdhury, M. (2000) Effects of an organophosphate pesticide, quinalphos, on the hypothalamo-pituitary-gonadal axis in adult male rats. *J. Reprod. Fertil.* **118**, 29–38
19. Garner, D. L., and Thomas, C. A. (1999) Organelle-specific probe JC-1 identifies membrane potential differences in the mitochondrial function of bovine sperm. *Mol. Reprod. Dev.* **53**, 222–229
20. Sternfeld, M., Shoham, S., Klein, O., Flores-Flores, C., Evron, T., Idelson, G. H., Kitsberg, D., Patrick, J. W., and Soreq, H. (2000) Excess "readthrough" acetylcholinesterase attenuates but the "synaptic" variant intensifies neurodeterioration correlates. *Proc. Natl. Acad. Sci. USA* **97**, 8647–8652
21. Soreq, H., and Glick, D. (2000) Novel roles for cholinesterases in stress and inhibitor responses. In *Cholinesterases and Cholinesterase Inhibitors* (Giacobini, E., ed.) pp. 47–61, Martin Dunitz: London
22. Kronman, C., Chitlaru, T., Elhanany, E., Velan, B., and Shafferman, A. (2000) Hierarchy of post-translational modifications involved in the circulatory longevity of glycoproteins. Demonstration of concerted contributions of glycan sialylation and subunit assembly to the pharmacokinetic behavior of bovine acetylcholinesterase. *J. Biol. Chem.* **275**, 29488–29502

23. Grisaru, D., Lev-Lehman, E., Shapira, M., Chaikin, E., Lessing, J. B., Eldor, A., Eckstein, F., and Soreq, H. (1999) Human osteogenesis involves differentiation-dependent increases in the morphogenically active 3' alternative splicing variant of acetylcholinesterase. *Mol. Cell Biol.* **19**, 788–795
24. Matsuyama, S., Llopis, J., Deveraux, Q. L., Tsien, R. Y., and Reed, J. C. (2000) Changes in intramitochondrial and cytosolic pH: early events that modulate caspase activation during apoptosis. *Nat. Cell Biol.* **2**, 318–325
25. Vander Heiden, M. G., and Thompson, C. B. (1999) Bcl-2 proteins: regulators of apoptosis or of mitochondrial homeostasis? *Nat. Cell Biol.* **1**, E209–E216
26. Prince, F. P. (1992) Ultrastructural evidence of indirect and direct autonomic innervation of human Leydig cells: comparison of neonatal, childhood and pubertal ages. *Cell Tissue Res.* **269**, 383–390
27. Koenigsberger, C., Chiappa, S., and Brimijoin, S. (1997) Neurite differentiation is modulated in neuroblastoma cells engineered for altered acetylcholinesterase expression. *J. Neurochem.* **69** (4), 1389–1397
28. Sternfeld, M., Ming, G., Song, H., Sela, K., Timberg, R., Poo, M., and Soreq, H. (1998) Acetylcholinesterase enhances neurite growth and synapse development through alternative contributions of its hydrolytic capacity, core protein, and variable C termini. *J. Neurosci.* **18**, 1240–1249
29. Bigbee, J. W., Sharma, K. V., Chan, E. L., and Bogler, O. (2000) Evidence for the direct role of acetylcholinesterase in neurite outgrowth in primary dorsal root ganglion neurons. *Brain Res.* **861**, 354–362
30. Lev-Lehman, E., Deutsch, V., Eldor, A., and Soreq, H. (1997) Immature human megakaryocytes produce nuclear-associated acetylcholinesterase. *Blood* **89**, 3644–3653
31. Lapidot Lifson, Y., Patinkin, D., Prody, C. A., Ehrlich, G., Seidman, S., Ben Aziz, R., Benseler, F., Eckstein, F., Zakut, H., and Soreq, H. (1992) Cloning and antisense oligodeoxynucleotide inhibition of a human homolog of cdc2 required in hematopoiesis. *Proc. Natl. Acad. Sci. USA* **89**, 579–583
32. Zhang, Q., Wang, X., and Wolgemuth, D. J. (1999) Developmentally regulated expression of cyclin D3 and its potential in vivo interacting proteins during murine gametogenesis. *Endocrinology* **140**, 2790–2800
33. Shohami, E., Kaufer, D., Chen, Y., Seidman, S., Cohen, O., Ginzberg, D., Melamed-Book, N., Yirmiya, R., and Soreq, H. (2000) Antisense prevention of neuronal damages following head injury in mice. *J. Mol. Med.* **78**, 228–236

34. Tronche, F., Kellendonk, C., Kretz, O., Gass, P., Anlag, K., Orban, P. C., Bock, R., Klein, R., and Schutz, G. (1999) Disruption of the glucocorticoid receptor gene in the nervous system results in reduced anxiety. *Nat. Genet.* **23**, 99–103

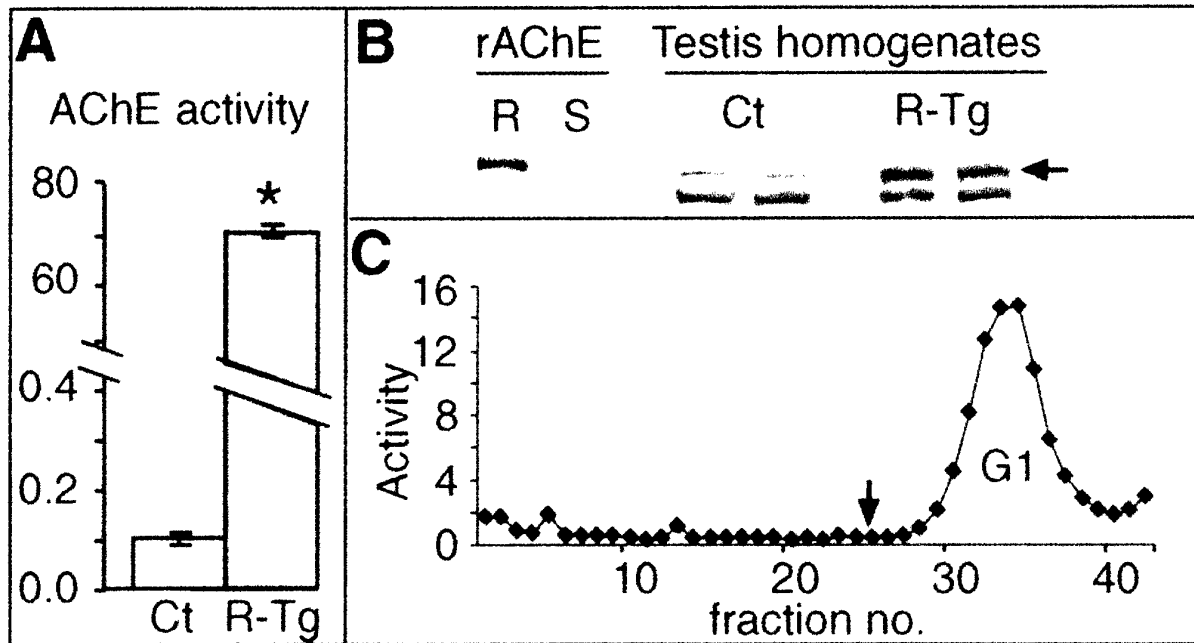
*Received December 20, 2000; revised April 3, 2001.*

Fig. 1



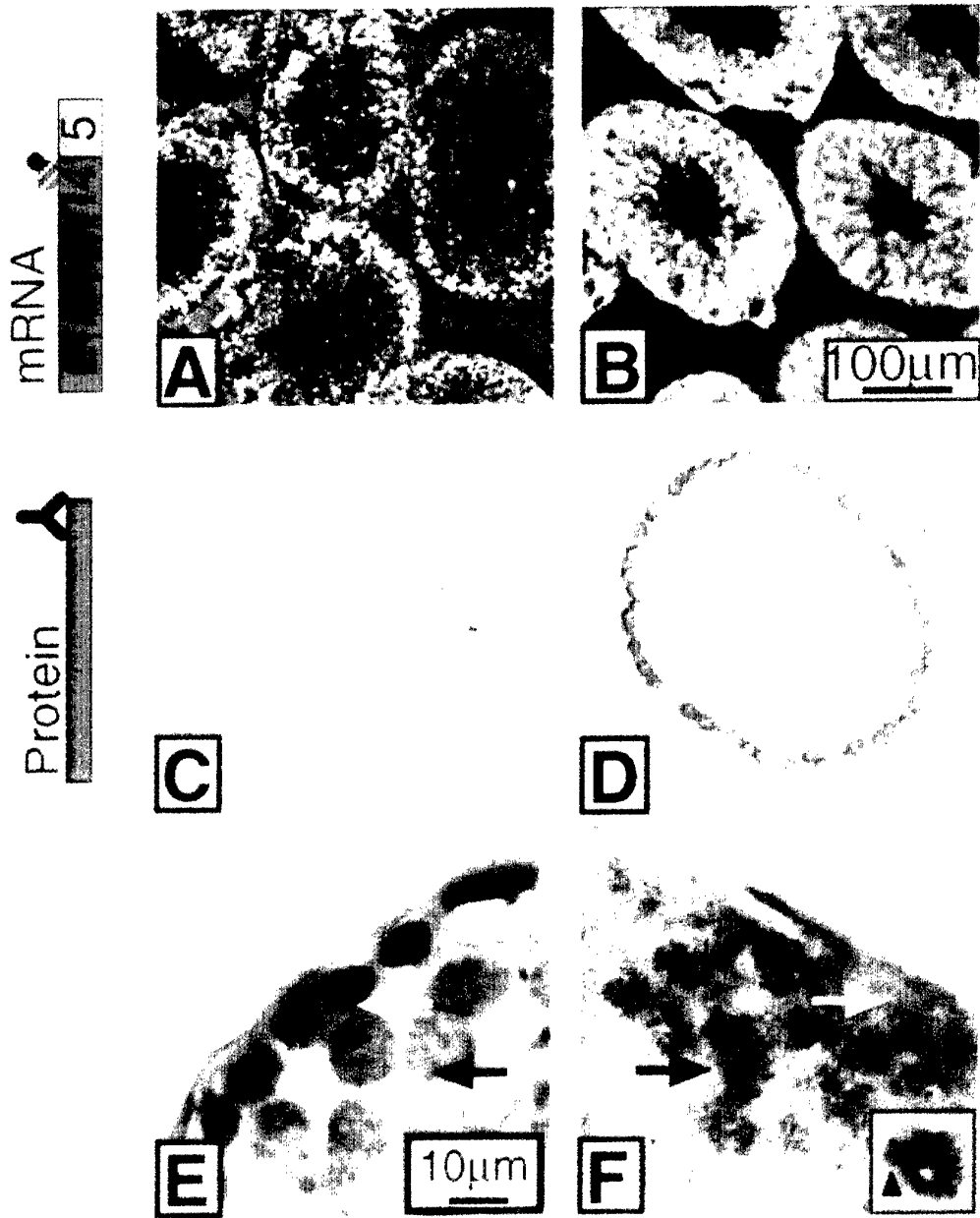
**Figure 1. Repeated forced swim stress induces testicular AChE-R overexpression.** **A, B)** In situ hybridization was performed on sections of seminiferous testicular tubules from naïve and stressed FVB/N mice. Yellow fluorescence is the product of alkaline phosphatase-mediated hydrolysis of ELF<sup>TM</sup> (Molecular Probes, Inc.) and indicates sites of AChE-R mRNA accumulation. Note the intense, dispersed signal in tubules from stressed mice. **C, D)** Immunohistochemistry with antibodies selective for AChE-R. Signal is orange. Note that in stressed mice, AChE-R protein product is localized primarily, but not exclusively, to the inner cell layer harboring maturing testicular spermatozoa. Schemes present probe location for the hybridization experiment (A, B) and the antibody-targeted domain for the immunostaining (C, D).

Fig. 2



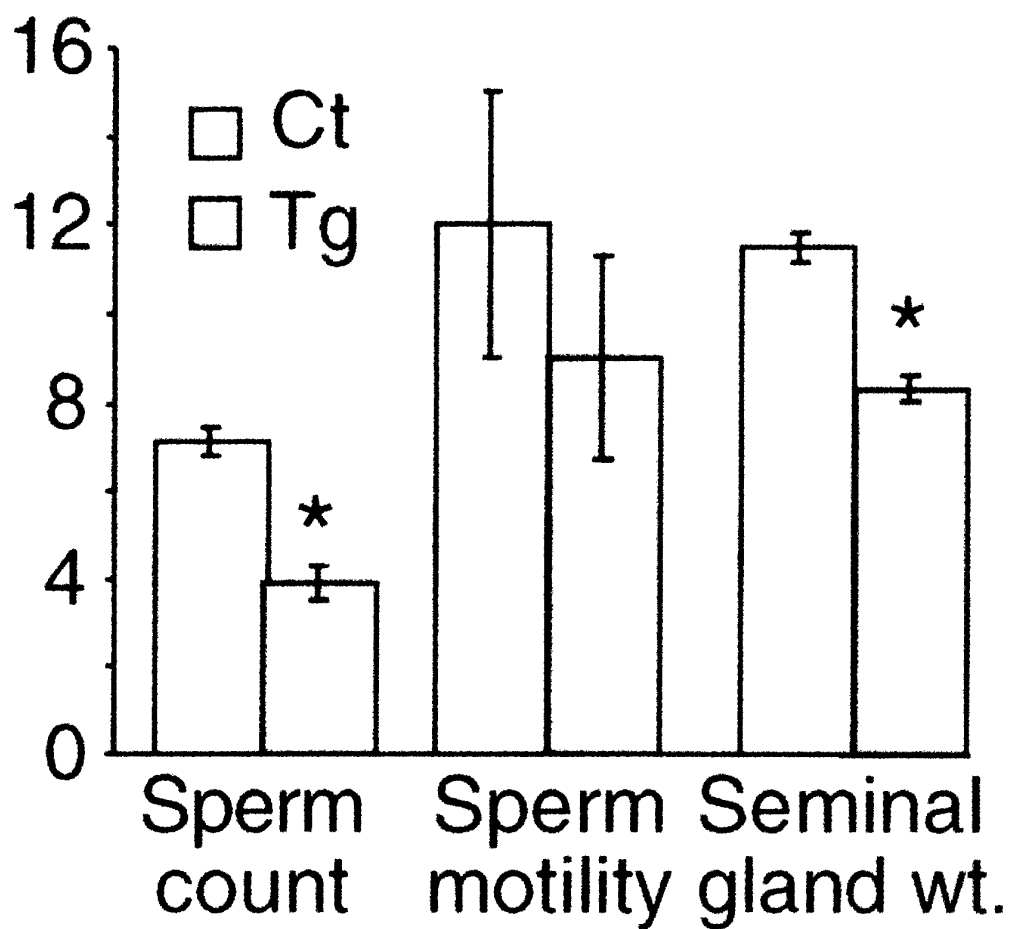
**Figure 2. Testicular AChE-R overproduction in transgenic mice.** **A)** Presented are average  $\pm$  SE specific AChE activity (nmol acetylthiocholine hydrolyzed/min/mg protein) from duplicate measurements performed in testicular homogenates from three adult male FVB/N (Ct) or AChE-R-overexpressing transgenic (R-Tg) mice (20). Stars note statistical significance ( $P < 0.05$ , Mann-Whitney). **B)** Testicular homogenates were subjected to SDS-polyacrylamide gel electrophoresis and the resultant blots incubated with antibodies directed at the C-terminal peptide unique to AChE-R (20) (R). Shown is an immunoblot with each two lanes loaded with homogenates from individual mice of the noted pedigree. Of the two bands observed, the top one (~66 Kd, arrow) co-migrated with recombinant AChE-R produced in transfected phaeochromocytoma PC12 cells (left lane). Recombinant AChE-S (S, second lane from left, Sigma) remained unlabeled, demonstrating selectivity of the antibody. **C)** Presented are AChE activities (nmol acetylthiocholine hydrolyzed/min/mg protein) in fractions collected following sucrose gradient centrifugation of a testicular homogenate from an AChE-R transgenic mouse. The observed sedimentation coefficient of 4.50–5.0S reflects globular monomers (G1), consistent with the AChE-R isoform. Arrow notes the localization of alkaline phosphatase (6.1S), which served as a sedimentation marker. One of two analyses.

Fig. 3



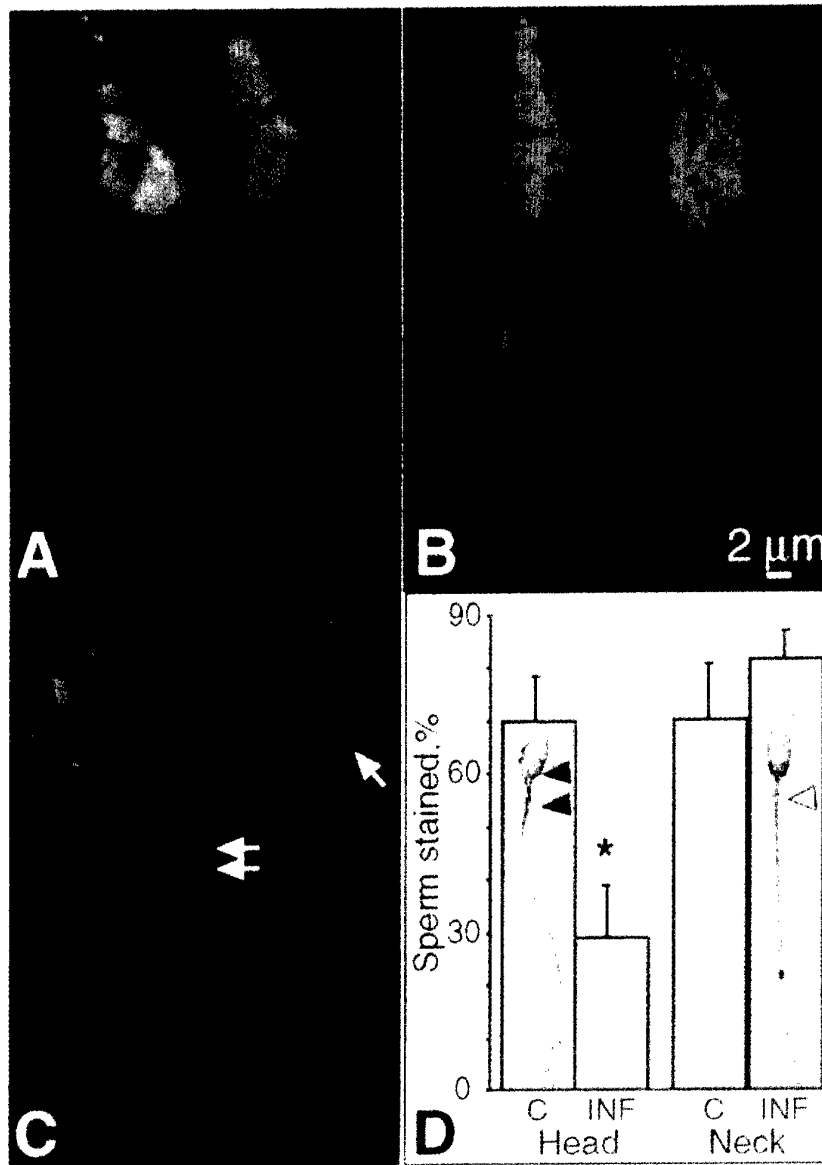
**Figure 3. AChE-R accumulates in spermatocytes of transgenic mice.** In situ hybridization (A–B, yellow) and immunohistochemistry (C–D, red) of representative tubules from naïve adult FVB/N or AChE-R transgenic mice. Tubules of transgenic mice (B) display high levels of dispersed AChE-R mRNA compared with controls (A). Restricted localization of AChE-R protein to a single peripheral cell layer was observed in transgenics (D) but not in controls (C). Antibodies toward proliferating cell nuclear antigen (PCNA) detected mitotic cells undergoing DNA replication in the outermost cell layer containing spermatogonia in all mice (E). In contrast, AChE-R immunoreactivity appeared in the next inner layer harboring meiotic spermatocytes only in transgenic mice (F). White arrows indicate spermatogonia; black arrows, spermatocytes. Nuclei were counterstained with hematoxylin. F) Inset: high-magnification image demonstrates focal perinuclear accumulation of AChE-R in spermatocytes.

Fig. 4



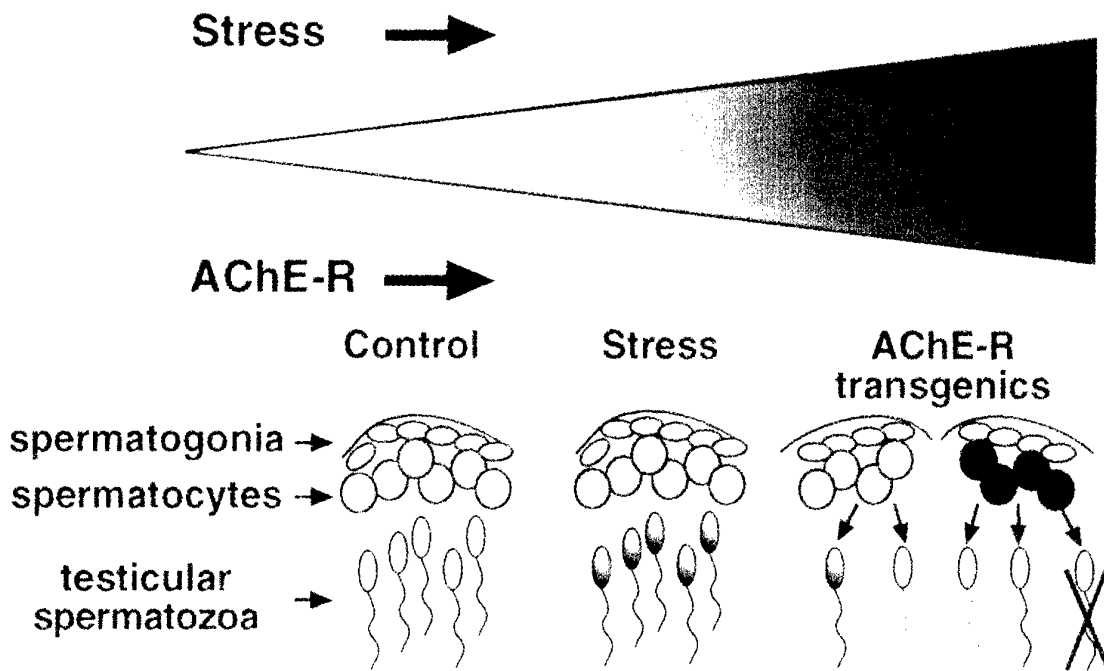
**Figure 4. Testicular AChE-R overproduction is associated with impaired sperm properties.** Bar graph represents data from 3–5 adult male FVB/N (Ct) or AChE-R-overexpressing transgenic (Tg) mice. Average  $\pm$  SE values are shown for sperm counts (cells/epidymis  $\times 10^{-6}$ ), sperm motility (percent motile of total sperm cells), and seminal gland weight (mg/gr body weight). Stars note statistical significance ( $P < 0.05$ , Mann-Whitney).

Fig. 5



**Figure 5. AChE-R sperm-head staining intensifies in stressed mice and decreases in transgenic mice and in subjects with unexplained infertility.** A-C) Shown are representative compound confocal images of testicular spermatozoa reaching the central space within testicular tubules following immunohistochemical staining with anti-AChE-R antibodies and Fast Red. Note the pronounced labeling in heads of spermatozoa from mice subjected to forced swim stress compared with those from both naïve FVB/N and transgenic mice. Spermatozoa from transgenic mice were divided among those unstained and those stained primarily in the tail region or in the head (white arrows; see text for details). D) Bar graph shows percentage of sperm labeled by anti-AChE-R antibodies (average  $\pm$  SE) in the head or neck regions for approximately 40 cells from each of three healthy human donors (C) and three male partners from infertile couples (INF). Star notes a statistically significant difference between controls and patients ( $P < 0.05$ , Mann Whitney). Shown in the outside columns are representative compound confocal images of a sperm from a donor (right) or infertility patient (left). Note labeling of the postacrosomal region of sperm heads and neck in control cells (black arrowheads) compared with limited sperm head labeling in the patient (white arrowhead).

Fig. 6



**Figure 6. Graded increases in AChE-R associated with its altered spermatogenic localization.** Shown is a schematic representation of seminiferous tubules. Following stress, AChE-R levels increase in spermatocytes and all other spermatogenic cells with the most marked elevation in the head of testicular spermatozoa. A greater or more persistent increase in AChE-R expression, represented by the transgenic model, might be found under intense or prolonged stress. Under such conditions, spermatocytes are stained while AChE-R is either excluded from testicular spermatozoa altogether or is localized to the tail, with only a smaller fraction of the spermatids displaying head staining. AChE-R overexpression in spermatocytes could impede spermatogenesis, which could thereby explain reduced sperm counts in transgenic mice.

## Autism, Stress and Chromosome 7 Genes

Michael Shapira<sup>1</sup>, David Glick<sup>1</sup>, John R. Gilbert<sup>2</sup> and Hermona Soreq<sup>1,3</sup>

<sup>1</sup>Department of Biological Chemistry, Institute of Life Sciences, The Hebrew University of Jerusalem, Jerusalem 91904, Israel

<sup>2</sup>Department of Medicine and Center for Human Genetics, Duke University, Durham, North Carolina 27710, USA.

<sup>3</sup>To whom correspondence should be addressed

### Introduction

Autism, a disorder affecting 4 out of 10,000 individuals in the general population, is classified as a pervasive developmental disorder. It becomes apparent by the third year of life and its characteristic impairments persist into adulthood. Whereas the inheritance of this disorder does not follow a simple Mendelian pattern, there is compelling evidence for strong genetic basis. This fact places autism in the category of complex genetic traits and predicts difficulties in any attempt to unravel the various genes that contribute to the disorder, genes that may even have different contributions in different populations. Recently, the rising interest in autism has spawned quite a few multinational efforts aimed at identification of these genes. The projects, taking advantage of experimental approaches designed for the study of complex genetic traits, succeeded in identifying several candidate loci. However, none of these loci was identified with certainty. Among this group of candidate loci, several appear to be more prominent than the rest. The long arm of chromosome 7 (7q) is one of those.

The main characteristics of autism are social and communicative impairments, as well as repetitive and stereotyped behaviors and interests. However, there are also reports of stress response-like behavior in autistic children. Such reports strongly suggest that autism is associated with inherited impairments in stress responses. However, this association has yet to be confirmed. An interesting link that relates impairments in stress responses to autism is found in the chromosome 7 gene *ACHE*, which encodes the enzyme acetylcholinesterase (AChE). The expression of this gene is robustly and persistently up-regulated under stress and was recently found to be affected by a novel mutation in the gene's extended promoter.

This chapter will describe the recent advances in the identification of genes or gene loci that contribute to the autistic phenotype, concentrating on what appears to be one of the best candidate loci, 7q. It will further describe the reports that suggest an association between autism and impairments in stress responses and will elaborate on putative molecular mechanism(s) that underlie stress responses in conjunction with autism. Finally, to follow the suggested link that connects autism with stress, through the candidate locus 7q, we present in this chapter the results of a survey, which determined the frequency of the *ACHE* up-stream mutation in affected and non-affected American families. These results show an extremely low incidence of this mutation, failing to confirm its association with autism in American families. Nonetheless, the results do not rule out a role for this polymorphism in the etiology of autism in the Israeli population where the mutation is present in a higher frequency.

### **Autism as a complex trait, candidate loci and genes**

Multigenic diseases differ from monogenic ones in that their occurrence cannot be linked to one specific gene, but is, rather, affected by changes in several genes. They include some of modern medicine's chief concerns, such as risk of cardiac failure, diabetes mellitus and a plethora of neurologic disorders. Among these, autism is an intriguing disorder both from the aspect of its behavioral symptoms, the scope of which is difficult to define, and due to its complex etiology. The frequency of autism is 4 in 10,000 for the classically defined syndrome (with males affected 4 times more frequently than females (Smalley, Asarnow, & Spence, 1988)). Inclusion of the related Pervasive Development Disorders, Not Otherwise Specified (PDD-NOS) and Asperger syndrome increases this incidence to 16 in 10,000 (Rodier, 2000).

It was previously believed that drugs such as the teratogens thalidomide and valproic acid may be risk factors for autism (Rodier, Ingram, Tisdale, Nelson, & Romano, 1996). Although a certain contribution of such environmental factors may exist, it is now known that the main factors for the disorder are genetic (Folstein & Rutter, 1977). The strongest evidence for the contribution of inherited factors to autism comes from studies on twins (Bailey et al., 1995; Folstein & Rutter, 1977; Steffenburg et al., 1989; Wahlstrom, Steffenburg, Hellgren, & Gillberg, 1989). These studies showed a much higher concordance rate (the chance that a child will be diagnosed as autistic when his twin has already been confirmed as autistic) in monozygotic (MZ, identical) twin pairs compared to dizygotic pairs (DZ). The concordance rates found in the largest of these studies (Bailey et al., 1995) were 60% in MZ pairs compared to 0% in DZ pairs. This enabled calculation of the heritability of autism, which was found to be greater than 90%. Moreover, in many of the twin pairs showing a discordance, the non-autistic co-twins presented language impairments in childhood and social deficits that persisted into adulthood (Le Couteur et al., 1996). This supports the understanding of autism as a multigenic and multifactorial disease with a large array of partially-overlapping symptoms representing disorders with similar physiological bases. Such similar disorders can be pooled into a related diagnostic group of PDD-NOS. That the concordance rate in MZ twin pairs does not reach the 100% expected for a pure genetic disorder implies that autism, as many other multifactorial diseases, is also affected by environmental factors that are associated with life history. Individual responses to life history, however, are also affected by the genetic make-up of the individual. The assumption is that individuals with genetic susceptibility to adverse responses to certain life events (e.g. a traumatic experience) are more likely to develop autism than others who are similarly exposed, yet do not have the inherited susceptibility. One of the twin studies (Steffenburg et al., 1989) reported that in most of the twin pairs discordant for autism, the autistic twin had more perinatal stress. This possible link of autism with stress will be further discussed below.

With the genetic basis of autism well established, the next and more challenging goal is to identify the genes linked to it. So far, no clear-cut linkage has been found between any particular gene or genetic locus and autism. This may be attributed to misdiagnosis of individuals, but probably also stems from the genetic heterogeneity of autism, with affecting genes varying in their contribution within different populations. It is believed that more than 14 loci may be associated with autism (Risch et al.,

1999). Table 1 presents a summary of the current candidate loci and genes, most of which were determined in recent genome-wide screens. Whereas the majority of these chromosomes are implicated in autism based on a single identification, a few loci came up more than once and are therefore considered more seriously as containing genes that contribute significantly to the etiology of autism. Among these, the most prominent locus is 7q, with most of the markers pointing to the q32-q35 region but with some cytogenetical evidence suggesting q21-q22 as well (Ashley-Koch et al., 1999). Another locus that appears to be a serious candidate for harboring relevant genes based on cytological studies, is 15q11-q13 (for example, see Cook et al., 1997). However, this locus is not favored by results of the genetic screens. The reason for this may be the sampling of individuals for the genetic screens, which excludes those carrying chromosomal abnormalities.

[Table 1 about here]

Before further focusing on chromosome 7, a few of the candidate genes believed to contribute to the etiology of autism are worth mentioning. Most of the proposed candidate genes are believed to be causally involved in autism based on their known contribution to neuronal activity or development, combined with linkage analysis of their chromosomal locations. In certain cases, such as with the serotonin transporter (HTT), the gene was proposed as a candidate based on a phenotypic abnormality, the high serotonin levels shown by autistic individuals (Cook et al., 1997), a suggestion that was re-enforced by genetic association studies (Klauck, Poustka, Benner, Lesch, & Poustka, 1997). Similarly, the neurofibromatosis type 1 gene (NF1; Mbarek et al., 1999) was found to be over-expressed in autistic patients. NF1 is known to regulate the activity of Ras proteins, of which one shows an association with autism (Comings, Wu, Chiu, Muhleman, & Sverd, 1996). A different case involved the  $\gamma$ -aminobutyric acid receptor  $\beta$ 3-subunit gene (GABRB3; Cook et al., 1998). This receptor is activated by GABA, the principal inhibitory neurotransmitter in the brain. Its importance in control of brain excitability, as well as its developmentally regulated expression, indicated possible involvement in the autistic phenotype.

So far, however, genetic screens have failed to unequivocally verify the association of these genes. In most cases, new allelic markers were identified in the gene regions, but not in the same position as the preliminarily associated markers (Martin et al., 2000; Risch et al., 1999). The next 2 sections will point up the stress-related symptoms of autism that have been somewhat neglected in recent years, and which may suggest new candidate genes based on their involvement in such symptoms.

### **Is autism associated with inherited impairments in stress responses?**

Once a genetic basis of autism was established, environmental factors, which had previously been the focus of attention, were pushed aside. However, we now believe that there is reason to consider an interaction of genetic and environmental factors. The correlation of autism with inherited susceptibility to extreme stress responses has been discussed extensively, so far without resolution. Several observations suggest such correlation. First, autistic patients show an exaggerated response to external stimuli that are not stressful in healthy individuals (Bergman & Escalona, 1949; Hutt, Hutt, Lee, & Ounsted, 1964), perhaps suggesting inherited differences in their levels of perceived stress; second, such an exaggerated response to external stimuli may indicate an inherited tendency to impaired control over stress responses (Hutt, Hutt, Lee, & Ounsted, 1965); and third, the long-lasting nature of their repetitive behavior

phenotype hints at inherited difficulties in termination of stress responses. Similarly, the impairments in socio-emotional reciprocity that are characteristic of autism (Wing & Gould, 1979), the communication impairments and anxiety (Muris, Steerneman, Merckelbach, Holdrinet, & Meesters, 1998), the susceptibility to epileptic seizures (Giovanardi Rossi, Posar, & Parmeggiani, 2000) and the restricted repertoire of activities and interests (Wing & Gould, 1979) may all be associated with inherited defects in the intricate processes that control human responses to stress. In addition, autism is associated with a mild, but reproducible and apparently specific elevation in the stress-related hormones  $\beta$ -endorphin and ACTH (Tordjman et al., 1997) (Fig. 1). All this calls for investigating those nervous system pathways and the corresponding genes that contribute to stress responses. One such pathway involves cholinergic neurotransmission.

[Figure 1 about here]

Neurons communicating by the neurotransmitter acetylcholine (ACh) are tightly involved in mammalian stress responses. Hyperexcitation of cholinergic neurotransmission has been reported under stress (Kaufer & Soreq, 1999); persistent changes were observed in the expression patterns of the key genes that encode the ACh-synthesizing enzyme choline acetyl transferase, the packaging protein vesicular ACh transporter and the ACh-hydrolyzing enzyme AChE (Kaufer, Friedman, Seidman, & Soreq, 1998), all of which lead to a decrease in cholinergic hyperexcitation and to re-establishment of normal neurotransmission. These stress-induced changes take place primarily in the hippocampus, which has been reported to develop abnormally in autistic individuals (Piven, 1997). The change in AChE expression, its increase under stress conditions, is mimicked in AChE-over-producing transgenic mice. These mice display progressive stress-related pathologies, including high density of curled neuronal processes in the somatosensory cortex, accumulation of clustered heat shock protein 70-immunopositive neuronal fragments in the hippocampus, and a high incidence of reactive astrocytes (Sternfeld et al., 2000). They also present progressive impairments in learning, memory and social behavior (Beeri et al., 1995; Beeri et al., 1997; Cohen, O. et al, personal communication), and appear extremely sensitive to head injury (Shohami et al., 2000) and AChE inhibitors (Shapira et al., 2000b). Moreover, stress was shown to increase the blood-brain barrier permeability (Friedman et al., 1996), thereby allowing potentially harmful xenobiotics to enter the brain. A subset of such xenobiotics, the AChE inhibitors, are commonly used in agriculture and in the household as insecticides. Upon entering the brain, AChE inhibitors may cause the above-mentioned long-lasting increase in AChE expression; and persistent excess of this protein may lead to neuropathological changes and to impairment of cognitive and social skills such as those observed in the transgenic mice. Altogether, these data suggest that individuals with an inherited susceptibility to adverse stress responses, itself probably a complex trait, will present exaggerated AChE expression. Similarly, individuals with an inherited abnormal AChE expression may develop a susceptibility to adverse stress responses. The autism-associated symptoms, which appear to indicate increased stress responses, may point to the *ACHE* gene and its transcriptional control as promising ground in which to explore for correlations with the autistic phenotype.

Consider (a) that in everyone, there is a toll in brain neuropathologies to be paid for the daily load of stress, and in experimental animals the appearance of these pathologies seems to exacerbated under AChE over-expression (Sternfeld et al.,

2000); (b) this toll may be magnified in individuals with an inherited predisposition to exaggerated responses to stress and to anti-AChE agents, as in some cases hypersensitivity to anti-AChEs was discovered to be associated with a genomic variation that induces constitutive over-expression of AChE (Shapira et al., 2000b); and (c) an additional factor may be a previous exposure to AChE inhibitors, which under stress can cross the blood-brain barrier (Friedman et al., 1996) and induce progressive damage to glia and neurons. Each of these effects, and especially the sum of them, may facilitate the developmental impairments characteristic of autism.

### **Chromosome 7 and autism**

The long arm of chromosome 7 was marked as a locus of genes which contribute to autism in all of the full genome screens performed so far (IMGSAC, 1998; Barrett et al., 1999; Philippe et al., 1999; Risch et al., 1999) and in a few more restricted screens, e.g. by Ashley-Koch et al. (1999). While the linked loci extend from bands q32 to q35, several genes located outside of this region may be equally important. This assumption is based on identified mapping inaccuracies and ambiguities (Hauser, Boehnke, Guo, & Risch, 1996), on the assumption that certain genetic aberrations may involve not only the genetically-linked region but also neighboring genes and on potentially relevant functions of the respective gene products, which make them appropriate candidates for association with different aspects of the autistic phenotype. One such candidate gene, SPCH1, which fulfills all 3 criteria, was proposed recently. Mapped to 7q31, SPCH1 is associated with a severe speech and language disorder (Fisher, Vargha-Khadem, Watkins, Monaco, & Pembrey, 1998) and thus may be responsible for the language difficulties observed in autistic children. A family with three affected children, two with autism and one with a language disorder, was recently investigated (Ashley-Koch et al., 1999). Affected members of this family were found to carry an inversion spanning bands 7q21 to 7q34. Further screening of additional families for markers located in the inversion region pointed to part of this inversion region being associated with 25-40% of autism cases (Ashley-Koch et al., 1999). However, with the set of chromosome 7 markers included in that screen, the SPCH1 gene itself was not linked to this syndrome.

We have recently examined the possible involvement of aberrant regulation of another chromosome 7 gene, *ACHE*, located close to SPCH1, in the susceptibility to development of the autistic phenotype. Mapped to 7q22, *ACHE* encodes the enzyme AChE which is responsible for hydrolyzing the neurotransmitter ACh and thus for terminating neurotransmission across cholinergic synapses (Massoulie et al., 1998). In addition, *ACHE* is involved in plasticity responses in many more tissues through non-catalytic activities (reviewed in Grisaru, Sternfeld, Eldor, Glick, & Soreq, 1999). Yet more importantly, over-production of AChE was reported under acute psychological stress (Kaufer et al., 1998). The proximity of the *ACHE* gene to the autism related 7q32-35 region, its inclusion in the inversion region found in the autism family (reported in Ashley-Koch et al., 1999) and its association with stress responses all make it a plausible candidate. In addition, *ACHE* is expressed in early stages of brain development, long before the formation of functioning synapses (Layer, 1995), which implies that its aberrant regulation can contribute to the developmental defects that are associated with autism. In addition, it should be noted that stress-induced over-expression of 7q22 genes is not limited to *ACHE*; at least one additional gene, *ARS*

which is associated with arsenite resistance, and possibly others at this locus, also appear to be over-expressed (Shapira, Grant, Korner, & Soreq, 2000a).

Although total blockade of ACh hydrolysis is incompatible with life, polymorphisms that modulate the transcriptional control of AChE may cause a milder effect, which is manifested as an inherited susceptibility to changes in cholinergic neurotransmission. Following a search for such polymorphisms (Shapira et al., 2000b), we have recently identified a 4-base pair deletion that disrupts one of two binding sites for the transcription factor HNF3 $\beta$  (Kaestner, Hiemisch, Luckow, & Schutz, 1994; Qian, Samadani, Porcella, & Costa, 1995). This deletion is located in a distal enhancer domain, 17 Kb up-stream from the transcription start site of *ACHE*, a region dense with binding motifs for other factors, including glucocorticoid hormones (Shapira et al., 2000b) (Fig. 2). This *ACHE* promoter deletion induces constitutive AChE over-production, which in turn causes an impaired capacity for up-regulating AChE production under chemical stress insults and results in hypersensitivity to such insults. Because of the molecular mechanisms common to chemical and psychological stress responses, i.e. elevated expression of stress-associated transcription factors such as AP1 or HNF3, of AChE (Kaufer & Soreq, 1999) and of heat shock proteins (Sternfeld et al., 2000), we suspect that carriers of this promoter polymorphism are also hypersensitive to psychological stressors. An extension of this concept implies that autism and susceptibility to stressors share common molecular abnormalities. It may also be that a primary stress event would induce an acquired susceptibility to exaggerated responses to subsequent stress. Under a certain genetic make-up, the risk of developing the full autistic phenotype may also increase. To examine one of the molecular markers associated with such susceptibility, we determined the incidence of the transcriptionally activating deletion in the *ACHE* promoter in US families with affected children as compared with screened healthy individuals from Israel and the USA.

[Figure 2 about here]

In the examined Israeli population, the tested deletion displayed an allele frequency of 0.012 and was strongly linked to the biochemically neutral H322N point mutation in the AChE coding sequence. The H322N mutation, responsible for the rare Yt<sup>b</sup> blood group, is considerably more frequent in Middle Eastern populations (Ehrlich et al., 1994), much more than in the USA (Giles, Metaxas-Buhler, Romanski, & Metaxas, 1967). Therefore, we predicted that the *ACHE* promoter polymorphism would occur less frequently in the US population, regardless of the autistic status. This was, indeed, found to be the case, with 8 heterozygous carriers out of 333 screened Israelis (2.4% incidence) but only 5 carriers in 816 US individuals (0.6%) (Table 2). The low incidence of this polymorphism further complicated the data analysis, as it was found in 3 out of 616 normal US individuals (0.5%) as compared with 2 out of 190 affected ones (1.0%). We conclude that if indeed this specific polymorphism is involved in the susceptibility to extreme stress responses in the US survey of autistic patients, its effect is minimal.

[Table 2 about here]

### Prospects

The current status of this study leaves us with more questions than answers. Because of the rarity of the analyzed promoter polymorphism, we cannot confirm that it is associated with the autistic phenotype in the studied families. The conflicting evidence regarding candidate genes suggests that the genomic basis of autism may

differ from one population to another. This is highlighted by the different allelic frequency of the *ACHE* promoter polymorphism in the US and Israeli populations that were screened. In addition, the wealth of transcription factor binding motifs in the extended *ACHE* promoter suggests multiple contributions toward its control, both under normal and stress conditions. Therefore, the over-all post-transcriptional pattern of *ACHE* gene expression may be more relevant to autism than sequence polymorphisms in particular elements of its promoter.

We do believe, however, that it is worthwhile paying attention to environmental factors, such as stress, that, given a certain genetic make-up, may affect the development of autism. More than identifying affecting environmental factors *per se*, this approach may offer hints of additional genetic factors, that indirectly contribute to the etiology of autism by processing environmental influences.

### References

- Ashley-Koch, A., Wolpert, C. M., Menold, M. M., Zaeem, L., Basu, S., Donnelly, S. L., Ravan, S. A., Powell, C. M., Qumsiyeh, M. B., Aylsworth, A. S., Vance, J. M., Gilbert, J. R., Wright, H. H., Abramson, R. K., DeLong, G. R., Cuccaro, M. L., & Pericak-Vance, M. A. (1999). Genetic studies of autistic disorder and chromosome 7. *Genomics*, 61(3), 227-236.
- Bailey, A., Le Couteur, A., Gottesman, I., Bolton, P., Simonoff, E., Yuzda, E., & Rutter, M. (1995). Autism as a strongly genetic disorder: evidence from a British twin study. *Psychol Med*, 25(1), 63-77.
- Barrett, S., Beck, J. C., Bernier, R., Bisson, E., Braun, T. A., Casavant, T. L., Childress, D., Folstein, S. E., Garcia, M., Gardiner, M. B., Gilman, S., Haines, J. L., Hopkins, K., Landa, R., Meyer, N. H., Mullane, J. A., Nishimura, D. Y., Palmer, P., Piven, J., Purdy, J., Santangelo, S. L., Searby, C., Sheffield, V., Singleton, J., Slager, S., & et al. (1999). An autosomal genomic screen for autism. Collaborative linkage study of autism. *Am J Med Genet*, 88(6), 609-615.
- Beeri, R., Andres, C., Lev Lehman, E., Timberg, R., Huberman, T., Shani, M., & Soreq, H. (1995). Transgenic expression of human acetylcholinesterase induces progressive cognitive deterioration in mice. *Curr Biol*, 5(9), 1063-1071.
- Beeri, R., Le Novere, N., Mervis, R., Huberman, T., Grauer, E., Changeux, J. P., & Soreq, H. (1997). Enhanced hemicholinium binding and attenuated dendrite branching in cognitively impaired acetylcholinesterase-transgenic mice. *J Neurochem*, 69(6), 2441-2451.
- Bergman, P., & Escalona, S. (1949). Unusual sensitivities in very young children. *Psychoanal Study Child*, 34, 333-352.
- Comings, D. E., Wu, S., Chiu, C., Muhleman, D., & Sverd, J. (1996). Studies of the c-Harvey-Ras gene in psychiatric disorders. *Psychiatry Res*, 63(1), 25-32.
- Cook, E. H., Jr., Courchesne, R. Y., Cox, N. J., Lord, C., Gonen, D., Guter, S. J., Lincoln, A., Nix, K., Haas, R., Leventhal, B. L., & Courchesne, E. (1998). Linkage-disequilibrium mapping of autistic disorder, with 15q11-13 markers. *Am J Hum Genet*, 62(5), 1077-1083.
- Cook, E. H., Jr., Lindgren, V., Leventhal, B. L., Courchesne, R., Lincoln, A., Shulman, C., Lord, C., & Courchesne, E. (1997). Autism or atypical autism in maternally but not paternally derived proximal 15q duplication. *Am J Hum Genet*, 60(4), 928-934.
- Ehrlich, G., Patinkin, D., Ginzberg, D., Zakut, H., Eckstein, F., & Soreq, H. (1994). Use of partially phosphorothioated "antisense" oligodeoxynucleotides for

- sequence-dependent modulation of hematopoiesis in culture. *Antisense Res Dev*, 4(3), 173-183.
- Fisher, S. E., Vargha-Khadem, F., Watkins, K. E., Monaco, A. P., & Pembrey, M. E. (1998). Localisation of a gene implicated in a severe speech and language disorder. *Nat Genet*, 18(2), 168-170.
- Folstein, S., & Rutter, M. (1977). Infantile autism: a genetic study of 21 twin pairs. *J Child Psychol Psychiatry*, 18(4), 297-321.
- Friedman, A., Kaufer, D., Shemer, J., Hendler, I., Soreq, H., & Tur-Kaspa, I. (1996). Pyridostigmine brain penetration under stress enhances neuronal excitability and induces early immediate transcriptional response. *Nat Med*, 2, 1382-1385.
- Giles, C. M., Metaxas-Buhler, M., Romanski, Y., & Metaxas, M. N. (1967). Studies on the Yt blood group system. *Vox Sang*, 13(2), 171-180.
- Giovanardi Rossi, P., Posar, A., & Parmeggiani, A. (2000). Epilepsy in adolescents and young adults with autistic disorder. *Brain Dev*, 22(2), 102-106.
- Grisaru, D., Sternfeld, M., Eldor, A., Glick, D., & Soreq, H. (1999). Structural roles of acetylcholinesterase variants in biology and pathology. *Eur J Biochem*, 264, 672-686.
- Hauser, E. R., Boehnke, M., Guo, S. W., & Risch, N. (1996). Affected-sib-pair interval mapping and exclusion for complex genetic traits: sampling considerations. *Genet Epidemiol*, 13(2), 117-137.
- Hutt, C., Hutt, S. J., Lee, D., & Ounsted, C. (1964). Arousal and childhood autism. *Nature*, 204, 908.
- Hutt, C., Hutt, S. J., Lee, D., & Ounsted, C. (1965). A behavioural and electroencephalographic study of autistic children. *J Psychiatry Res*, 3, 181-197.
- IMGSAC, International Molecular Genetic Study of Autism Consortium (1998). A full genome screen for autism with evidence for linkage to a region on chromosome 7q. *Hum Mol Genet*, 7(3), 571-578
- Kaestner, K. H., Hiemisch, H., Luckow, B., & Schutz, G. (1994). The HNF-3 gene family of transcription factors in mice: gene structure, cDNA sequence, and mRNA distribution. *Genomics*, 20(3), 377-385.
- Kaufer, D., Friedman, A., Seidman, S., & Soreq, H. (1998). Acute stress facilitates long-lasting changes in cholinergic gene expression. *Nature*, 393(6683), 373-377.
- Kaufer, D., & Soreq, H. (1999). Tracking cholinergic pathways from psychological and chemical stressors to variable neurodeterioration paradigms. *Curr Opin Neurol*, 12(6), 739-743.
- Klauck, S. M., Poustka, F., Benner, A., Lesch, K. P., & Poustka, A. (1997). Serotonin transporter (5-HTT) gene variants associated with autism? *Hum Mol Genet*, 6(13), 2233-2238.
- Layer, P. G. (1995). Nonclassical roles of cholinesterases in the embryonic brain and possible links to Alzheimer disease. *Alzheimer Dis Assoc Disord*, 9(Suppl 2), 29-36.
- Le Couteur, A., Bailey, A., Goode, S., Pickles, A., Robertson, S., Gottesman, I., & Rutter, M. (1996). A broader phenotype of autism: the clinical spectrum in twins. *J Child Psychol Psychiatry*, 37(7), 785-801.
- Martin, E. R., Menold, M. M., Wolpert, C. M., Bass, M. P., Donnelly, S. L., Ravan, S. A., Zimmerman, A., Gilbert, J. R., Vance, J. M., Maddox, L. O., Wright, H. H., Abramson, R. K., DeLong, G. R., Cuccaro, M. L., & Pericak-Vance, M. A. (2000). Analysis of linkage disequilibrium in gamma-aminobutyric acid receptor subunit genes in autistic disorder. *Am J Med Genet*, 96(1), 43-48.

- Massoulie, J., Anselmet, A., Bon, S., Krejci, E., Legay, C., Morel, N., & Simon, S. (1998). Acetylcholinesterase: C-terminal domains, molecular forms and functional localization. *J Physiol Paris*, 92(3-4), 183-190.
- Mbarek, O., Marouillat, S., Martineau, J., Barthelemy, C., Muh, J. P., & Andres, C. (1999). Association study of the NF1 gene and autistic disorder. *Am J Med Genet*, 88(6), 729-732.
- Muris, P., Steerneman, P., Merckelbach, H., Holdrinet, I., & Meesters, C. (1998). Comorbid anxiety symptoms in children with pervasive developmental disorders. *J Anxiety Disord*, 12(4), 387-393.
- Philippe, A., Martinez, M., Guilloud-Bataille, M., Gillberg, C., Rastam, M., Sponheim, E., Coleman, M., Zappella, M., Aschauer, H., Van Maldergem, L., Penet, C., Feingold, J., Brice, A., Leboyer, M., & van Malldergerme, L. (1999). Genome-wide scan for autism susceptibility genes. Paris Autism Research International Sibpair Study. *Hum Mol Genet*, 8(5), 805-812.
- Piven, J. (1997). The biological basis of autism. *Curr Opin Neurobiol*, 7(5), 708-712.
- Qian, X., Samadani, U., Porcella, A., & Costa, R. H. (1995). Decreased expression of hepatocyte nuclear factor 3 alpha during the acute-phase response influences transthyretin gene transcription. *Mol Cell Biol*, 15(3), 1364-1376.
- Risch, N., Spiker, D., Lotspeich, L., Nouri, N., Hinds, D., Hallmayer, J., Kalaydjieva, L., McCague, P., Dimiceli, S., Pitts, T., Nguyen, L., Yang, J., Harper, C., Thorpe, D., Vermeer, S., Young, H., Hebert, J., Lin, A., Ferguson, J., Chiotti, C., Wiese-Slater, S., Rogers, T., Salmon, B., Nicholas, P., Myers, R. M., & et al. (1999). A genomic screen of autism: evidence for a multilocus etiology. *Am J Hum Genet*, 65(2), 493-507.
- Rodier, P. M. (2000). The early origins of autism. *Sci Am*, 282(2), 56-63.
- Rodier, P. M., Ingram, J. L., Tisdale, B., Nelson, S., & Romano, J. (1996). Embryological origin for autism: developmental anomalies of the cranial nerve motor nuclei. *J Comp Neurol*, 370(2), 247-261.
- Shapira, M., Grant, A., Korner, M., & Soreq, H. (2000a). Genomic and transcriptional characterization of the human ACHE locus: complex involvement with acquired and inherited diseases. *Isr Med Assoc J*, 2(6), 470-473.
- Shapira, M., Tur-Kaspa, I., Bosgraaf, L., Livni, N., Grant, A. D., Grisaru, D., Korner, M., Ebstein, R. P., & Soreq, H. (2000b). A transcription-activating polymorphism in the ACHE promoter associated with acute sensitivity to anti-acetylcholinesterases. *Hum Mol Genet*, 9(9), 1273-1281.
- Shohami, E., Kaufer, D., Chen, Y., Cohen, O., Ginzberg, D., Melamed-Book, N., Seidman, S., Yirmiya, R., & Soreq, H. (2000). Antisense prevention of neuronal damages following head injury in mice. *J Mol Med*, 78, 228-236.
- Smalley, S. L., Asarnow, R. F., & Spence, M. A. (1988). Autism and genetics. A decade of research. *Arch Gen Psychiatry*, 45(10), 953-961.
- Steffenburg, S., Gillberg, C., Hellgren, L., Andersson, L., Gillberg, I. C., Jakobsson, G., & Bohman, M. (1989). A twin study of autism in Denmark, Finland, Iceland, Norway and Sweden. *J Child Psychol Psychiatry*, 30(3), 405-416.
- Sternfeld, M., Shoham, S., Klein, O., Flores-Flores, C., Evron, T., Idelson, G. H., Kitsberg, D., Patrick, J. W., & Soreq, H. (2000). Excess "read-through" acetylcholinesterase attenuates but the "synaptic" variant intensifies neurodeterioration correlates. *Proc Natl Acad Sci USA*, 97(15), 8647-8652.
- Tordjman, S., Anderson, G. M., McBride, P. A., Hertzog, M. E., Snow, M. E., Hall, L. M., Thompson, S. M., Ferrari, P., & Cohen, D. J. (1997). Plasma beta-endorphin,

adrenocorticotropin hormone, and cortisol in autism. *J Child Psychol Psychiatry*, 38(6), 705-715.

Wahlstrom, J., Steffenburg, S., Hellgren, L., & Gillberg, C. (1989). Chromosome findings in twins with early-onset autistic disorder. *Am J Med Genet*, 32(1), 19-21.

Wing, L., & Gould, J. (1979). Severe impairments of social interaction and associated abnormalities in children: epidemiology and classification. *J Autism Dev Disord*, 9(1), 11-29.

**Table 1. Candidate genes and genetic loci associated with autism<sup>a</sup>**

chromosomal locus <sup>b</sup>	candidate genes <sup>c</sup>	reference
1p(13)		Risch et al., 1999
2q(24-31)		IMGSAC, 1998; Philippe et al., 1999
4q(34-35)		Philippe et al., 1999
5p		Philippe et al., 1999
6q (16)	MACS, GRIK6, GPR6	Philippe et al., 1999
7q(31-35, 21-22) <sup>d</sup>	GPR37, <sup>d</sup> SPCH1, PTPRZ1, EPHB6, ACHRM1, PTN, NEDD2/ICH1/CASP2, GRM8	IMGSAC, 1998; Barrett et al., 1999; Philippe et al., 1999; Risch et al., 1999
10q(26)		Philippe et al., 1999
13q(21-32)		Risch et al., 1999
15q11-q13	GABRB3, UBE3A	Cook et al., 1998); Martin et al., 2000 but see Barrett et al., 1999; Risch et al., 1999
16p(12-13)		IMGSAC, 1998; Philippe et al., 1999
17q11.1-q12	HTT, NF1	Cook et al., 1997; Mbarek et al., 1999
17p	HOX1A <sup>e</sup>	Risch et al., 1999
18q(22)		Philippe et al., 1999
19p(13)		IMGSAC, 1998; Philippe et al., 1999
Xp(21-22)		Philippe et al., 1999

<sup>a</sup>Compiled mostly from 4 full-genome screens performed in the past 2 years (IMGSAC, 1998; Barrett et al., 1999; Philippe et al., 1999; Risch et al., 1999).

<sup>b</sup>Whenever available, the exact location of the linked region is designated. When no exact location has been suggested the position of the markers used for the genetic screening was added (in brackets).

<sup>c</sup>Whenever proposed in the cited papers.

<sup>d</sup>See Ashley-Koch et al. (1999).

<sup>e</sup>See Rodier (2000).

**Table 2. Screening autism families for  $\Delta 4$  *ACHE* promoter polymorphism**

US autism families		US			Israeli		total	
		Individuals	carriers		Individuals	carriers	Individuals	carriers
singleton <sup>a</sup>	103	normal	616	3 <sup>c</sup>	333	8	949	11
multiplex <sup>b</sup>	82	affected	190	2 <sup>d</sup>	-		190	2
unconfirmed multiplex	18	unclear status	18	-	-		18	-
total	203		816	5	333	8	949	13

<sup>a</sup>Nuclear families with an affected child.

<sup>b</sup>Families with at least two affecteds, usually sibs.

<sup>c</sup>Of two families, one female, one male and his grandson.

<sup>d</sup>Two affected males.

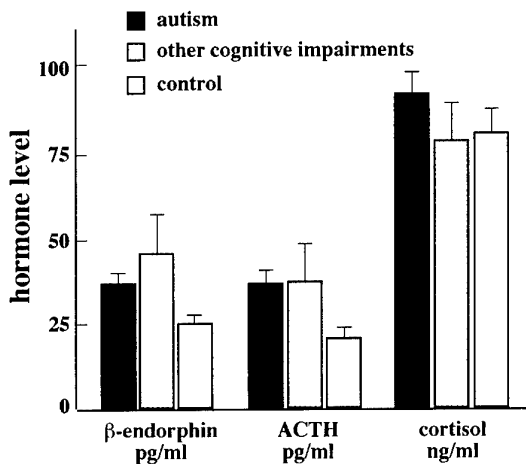


**Figure legends**

**Figure 1. Plasma stress hormones in autism.** Shown in columns are results taken from Tordjman et al. (1997) of data from autistic patients (n=46-48), patients with mental retardation or other cognitive impairments (n=15-16) and normal subjects (n=23-26). Statistics was performed on log-transformed data, as described in the reference.

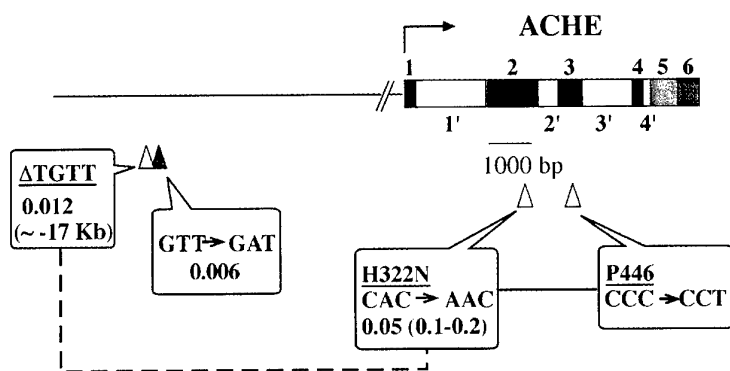


**Figure 2. *ACHE* polymorphisms**

Shown is a drawn-to-scale scheme of the *ACHE* locus with all known polymorphisms depicted. Exons are depicted as numbered filled boxes, introns as numbered open boxes and mutations as wedges. A solid line

connecting mutations indicates complete linkage between the variants. A broken line represents strong incomplete linkage. Mutation frequencies are taken from Ehrlich et al. (1994) for the coding region mutations (open wedges).

## Changes in neuronal acetylcholinesterase gene expression and division of labor in honey bee colonies

Shapira, M.<sup>1</sup>, Thompson, C.K.<sup>2</sup> Soreq, H.<sup>1,3</sup> and Robinson, G.E.<sup>4</sup>

<sup>1</sup> Department of Biological Chemistry, the Life Sciences Institute, the Hebrew University of Jerusalem, Givat Ram, 91904.

<sup>2</sup> Howard Hughes Research Fellow, Department of Entomology, University of Illinois, 505 S. Goodwin Ave. Urbana, IL 61801.

<sup>3</sup> To whom correspondence should be addressed (Tel. 972-2-6585109, Fax 972-2-6520258, email: soreq@shum.huji.ac.il).

<sup>4</sup> Department of Entomology and Neuroscience Program, University of Illinois, 505 S. Goodwin Ave. Urbana, IL 61801 USA

Running title: *Ache* expression and bee division of labor

### Abstract

Division of labor in honey bee colonies is highlighted by adult bees making a transition at 2-3 weeks of age from working in the hive to foraging for nectar and pollen outside. This behavioral development involves acquisition of new tasks that may require advanced learning capabilities. Because acetylcholinesterase (AChE) hydrolyzes acetylcholine, a major neurotransmitter associated with learning in the insect brain, we searched for changes in AChE expression in the brain during bee behavioral development. Biochemical aspects of the AChE protein were similar in foragers and "nurse" bees that work in the hive tending brood. However, catalytic AChE activity was significantly lower in foragers. Cloning of bee AChE cDNA enabled mRNA analysis, which demonstrated that the forager-related decrease in AChE activity was associated with decreased AChE mRNA levels. This was particularly apparent in the mushroom bodies, a brain region known to be involved with olfactory and visual learning and memory. In addition, treatment with the AChE-inhibitor metrifonate improved performance in an olfactory learning assay. These findings demonstrate long-term, naturally occurring developmental down-regulation of *AChE* gene expression in the bee brain, and suggest that this genomic plasticity can contribute to facilitated learning capabilities in forager bees.

Index entries: Honey bee, acetylcholinesterase, expression, behavioral development

### Introduction

The European honey bee, *Apis mellifera*, is one of the best-studied social insects. Its relatively rich but stereotyped behavioral repertoire can be studied and manipulated under natural conditions (e.g. Schulz and Robinson, 1999; Wagener-Hulme et al., 1999), thus making it a useful and convenient model for studying neurochemical aspects of behavioral development. Because some processes underlying behavioral development, such as motor control, sensory input processing, and learning appear to share common molecular components across insects and vertebrates (Acampora et al., 1998; Hammer and Menzel, 1995), the bee may also be a good model for studying molecular underpinnings of behavioral development.

One particularly interesting aspect of bee behavioral development is age polyethism, age-related changes in the performance of different tasks associated with colony growth and development

(reviewed in (Winston, 1987)). This behavioral development gives rise to an age-related division of labor among adult worker honey bees: Young “nurse” bees primarily feed and care for larvae and the queen, middle-age bees maintain the hive and store food, and the oldest bees forage for nectar and pollen and defend the hive. A bee usually begins to forage at about 21 days of age but this can be delayed or accelerated by a variety of environmental and intrinsic factors (reviewed in Robinson, 1992), including colony age demography (Huang and Robinson, 1992), pheromones (Pankiw et al., 1998), endocrine signaling (reviewed in Fahrbach and Robinson, 1996), or neuromodulators such as octopamine (Schulz and Robinson, 1999; Wagener-Hulme et al., 1999). Variation in the rate of behavioral development also is due to genetic variation, which may be related to some of the factors listed above (Giray et al., 2000; Giray and Robinson, 1994).

The tasks performed by forager bees are very different from those performed by hive bees such as nurses. Foragers tasks involve flying and navigating along relatively great distances and memorizing the location of food sources. These tasks may require better modules for sensory input processing, as well as enhanced learning and memory capabilities (reviewed in Fahrbach and Robinson, 1995). There is only limited evidence for differences in the learning performance of nurse bees and foragers (Ben-Shahar et al., 2000; Ray and Ferneyhough, 1999). However, several studies have shown that there are substantial structural differences in their brains. Volumetric differences have been found in the antennal lobes (Sigg et al., 1997; Withers et al., 1993) and the mushroom bodies (Withers et al., 1993); both structures are implicated in sensory input processing and learning. The mushroom bodies, in particular, are known to be a convergence site for olfactory and visual information (Mobbs, 1982) and are essential for olfactory learning (de Belle and Heisenberg, 1994; Hammer and Menzel, 1995; Meller and Davis, 1996). Foragers have a larger volume of the neuropil of the mushroom bodies relative to younger bees (Durst et al., 1994; Withers et al., 1993). This volume increase is associated with increased dendritic arborization of the intrinsic cells of the mushroom bodies, the Kenyon cells (Farris S.M et al., 1999. *Soc Neurosci abstr*) rather than with proliferation (Fahrbach et al., 1995).

Kenyon cells are responsive to cholinergic signaling (Kreissl and Bicker, 1989). Inhibition of either muscarinic (Cano Lozano and Gauthier, 1998; Gauthier et al., 1994) or nicotinic (Lozano et al., 1996) cholinergic receptors has been shown to impair olfactory conditioning, thus implicating cholinergic neurotransmission in learning-related phenomena in the mushroom bodies. A key cholinergic protein is acetylcholinesterase (AChE; EC 3.1.1.7; Massoulie et al., 1998), the enzyme responsible for hydrolyzing the neurotransmitter acetylcholine (ACh) and thus terminating the signal at cholinergic synapses. Experimentally decreased levels of AChE lead to increased cholinergic neurotransmission in vertebrates, which is the basis for drugs used to treat the symptoms of Alzheimer’s disease (Winkler et al., 1998). However, little is known about whether long-term changes in AChE activity occur naturally during behavioral maturation (Mesulam and Geula, 1991). Given that the life of the forager bee is more cognitively challenging than the life of a hive bee, and given that cholinergic neurotransmission may play a role in honey bee learning, we hypothesized that foragers have lower AChE brain activity than do nurse bees. We tested this hypothesis by comparing the expression of AChE both at the protein and the mRNA levels. We also began to explore whether manipulation of AChE levels in the bee brain can influence performance in a laboratory learning assay.

## Materials and methods

**Materials.** All chemicals were purchased from Sigma, St. Louis, MI. We used acetylthiocholine (ATCh), butyrylthiocholine (BTCh), 1,5-bis(4-allyldimethylammoniumphenyl)pentan-3-one dibromide (BW284C51), tetraisopropyl pyrophosphoramidate

(iso-OMPA) and (2,2,2-trichloro-1-hydroxy-ethyl)phosphonic acid dimethyl ester (Metrifonate).

**Bee colonies.** Bee colonies were maintained in the field according to standard commercial techniques either at the Tsrifin Bee Station in Israel or the University of Illinois Bee Research Facility, Urbana, IL. Bees in both locations are a mixture of European races of *Apis mellifera*. For AChE activity analyses, we used both typical colonies (each with a population of ~40000 workers and a naturally mated queen) and single-cohort colonies. A single-cohort colony is made by placing a queen, ~2000 one-day-old (0-24-hrs old) bees into a small hive box with one empty frame and a second frame containing a small amount of pollen and nectar. One-day-old bees were obtained by transferring honeycombs with pupae from a source colony to a 33°C incubator. In the absence of older bees, 5-10% of the individuals in a single-cohort colony will accelerate their behavioral development and become precocious foragers by 7-10 days of age (Robinson and Page, 1989). All bees in each single-cohort colony were marked with a spot of paint on the thorax; this was done to prevent sampling of bees that may have strayed from another hive. Bees from other (unrelated) typical colonies were used for the other experiments.

**Behavioral identification.** We collected nurse bees and foragers of unknown age from typical colonies (it can be assumed that nurses were about 1-2 weeks old and foragers were about 3 weeks old), and age-matched nurse bees and precocious foragers from single-cohort colonies. Nurse bees and foragers were identified according to standard criteria (Wagener-Hulme et al., 1999); nurses were individuals with their heads in cells containing larvae and foragers were bees returning to their hive with pollen loads (the brightly colored pollen loads are very easy to see). To facilitate collection of foragers, we temporarily obstructed the hive entrance with a piece of 8-mesh hardware cloth. Bees for analysis were collected with a vacuum device directly into liquid nitrogen (Wagener-Hulme et al., 1999) so that measurements of AChE mRNA and protein would reflect as much as possible the levels that existed naturally during the performance of the behavior.

**Brain dissection.** Dissections were performed on a dish cooled by dry ice, keeping the brains frozen throughout the procedure. Hypopharyngeal glands and the suboesophageal ganglion were removed and discarded.

**Brain homogenates.** Dissected brains were homogenized either separately or in groups of 4-5 in 1 % Triton X-100 and 10 mM Tris-HCl pH 7.4 (Solution A, 50 µl/brain) or in Solution A containing 1 M NaCl and 2 mM EDTA.

**Cholinesterase assays.** We measured activity levels of both AChE and the closely related enzyme butyrylcholinesterase (BuChE) with a colorimetric assay that measures rates of ATCh or BTCh hydrolysis (Loewenstein Lichtenstein et al., 1995). The AChE inhibitor, BW284C51, or the BuChE inhibitor, iso-OMPA, were both added at a concentration of 10 µM, 30 min prior to substrate addition. Quantification was performed on a  $V_{max}$  kinetic microplate reader (Molecular Devices Corp. Manlo Park CA) equipped with the Softmax program. AChE activity was quantified in brains of nurses and foragers from 5 typical colonies (N = 1-15 samples/colony, 1-10 bees/sample) and in brains of nurses and precocious foragers from 4 single-cohort colonies (N = 5-15 samples/colony, 1-4 bees/sample).

**Nondenaturing gel electrophoresis.** Electrophoresis was performed in 7% polyacrylamide gels and was followed by AChE activity staining (Seidman et al., 1995).

**Sucrose gradient centrifugation.** AChE multimeric assembly was examined by sedimentation in 5-20 % sucrose gradients, followed by catalytic AChE activity measurements (Seidman et al., 1994).

**RT-PCR with partially degenerate primers.** Since very limited codon usage information is available for the honey bee, we used data from the *Drosophila melanogaster* codon frequency table (as found in the University of Wisconsin GCG software package) to design partially

degenerate, 21- or 24-mer primers, for 2 highly conserved regions of AChE, SEDCLYLN/D and RVGT/AFGF. RT-PCR was performed as described (Grisaru et al., 1999a) with PCR annealing temperature of 48°C. PCR products separated on agarose gels were extracted using the Boehringer Mannheim (Germany) gel extraction kit. Subcloning was done with the TA cloning kit (Invitrogen, Carlsbad, CA) and sequences determined for several clones using vector-derived primers and an ABI377 automated sequencer.

**Rapid Amplification of cDNA Edges (RACE).** Primers designed according to a PCR-amplified fragment with high sequence similarity to other AChEs were used together with the 5'/3' RACE kit (Boehringer Mannheim), to amplify the 5'-terminus of the AmAChE mRNA. This was achieved using the 21-mer 791(-) specific primer (numbered as in the AmAChE cDNA sequence, Genebank accession number AF213012) for reverse transcription and a nested 20-mer reverse primer, 768(-), for PCR amplification using the Expand High Fidelity PCR system (Boehringer Mannheim). For the 3'-terminus, a bee cDNA library (Uni-ZAP™ XR library; Stratagene, La Jolla, CA) served as a template for PCR amplification with a specific 24-mer forward primer, 646(+), and the T7 primer (using the Expand High Fidelity PCR system). Both 5'- and 3'-termini were subcloned as described above.

**In situ hybridization (ISH).** High resolution non-radioactive ISH was performed as previously described (Grifman et al., 1998). Since insect brains contain high levels of endogenous biotin (Ziegler et al., 1995), sections were pre-treated for 1 h at room temperature with 10 µg/ml streptavidin (Amersham Life Sciences Products, Little Chalfont, Buckinghamshire, England) prior to pre-hybridization. Briefly, 7-µm thick paraffin-embedded brain sections were hybridized with the 680(-) 50-mer, 5'-biotinylated, 2'-o-methylated cRNA probe specific for AmAChE mRNA. Following incubation with a streptavidin-alkaline phosphatase (AP) conjugate (Amersham Life Sciences Products, Piscataway, NJ), transcripts were detected using either the ELF fluorogenic AP substrate (Molecular Probes Inc., Eugene, OR) and a fluorescent Zeiss Axioplan microscope or the Fast Red AP substrate (Boehringer-Mannheim) and an inverted Olympus microscope equipped with an MRC-1024 Bio-Rad confocal attachment (Hemel Hempstead Herts., UK). Fast Red precipitate was excited at 488 nm and emission was measured with a 580df32 filter. Sections were scanned every 0.54 µm and 3D projections were created from all scans, both for Fast Red and for autofluorescent signals. Signal density, representing AChE mRNA levels, was measured in regions of the mushroom bodies containing Kenyon cell bodies using the Image-Pro 3.0 software (Media Cybernetics, Silver Spring, MD). Final signal values were obtained by subtracting autofluorescent signal from Fast Red signal values. ISH was performed on brains from nurses and foragers taken from a typical colony unrelated to those used above.

**In vivo AChE inhibition and olfactory conditioning test.** Forager bees were injected in the abdomen with 1 µl, 2 mg/ml of the organophosphate AChE inhibitor metrifonate (Oh et al., 1999; Scali et al., 1997) in bee saline (Huang et al., 1991), or with saline alone. We used a well-established associative learning paradigm (Menzel et al., 1974; Fig.4, Top) to evaluate the effect of AChE inhibition on such abilities. Learning trials began 45 min after each bee was injected, an interval which eliminates obvious injection effects (Robinson et al., 1999). Each bee was exposed to the odor (geraniol) 4 times with an inter-exposure interval of 20 min. Odor exposure was coupled with a reward of 0.5 M sucrose which is the unconditioned stimulus that elicits the unconditioned response, the proboscis extension reflex (PER). A positive response was a complete extension of the proboscis that was observed during odor presentation but before reward presentation. Four trials of this experiment were performed (37-94 bees/group/trial; 216 metrifonate-injected and 233 saline-injected bees total). We used bees from two different, unrelated, colonies (two colonies were each used in two trials). ANOVA

(SAS) revealed no significant differences between trials, so data were pooled for the analysis presented below.

## Results

**Acetylcholinesterase from the brains of nurses and foragers is biochemically similar.** Acetylthiocholine (ATCh) hydrolysis, reflecting AChE activity, was found to be 20-fold higher in brain homogenates than butyrylthiocholine (BTCh) hydrolysis, reflecting activity of the closely related enzyme butyrylcholinesterase (BuChE). ATCh hydrolysis was almost completely abolished by the AChE-specific inhibitor BW248C51, whereas BTCh hydrolysis was only slightly inhibited by the classical BuChE inhibitor iso-OMPA (Fig. 1A). This demonstrates that AChE accounts for about 95% of the total cholinesterase activity in the bee brain and suggests that it is responsible for both ATCh and BTCh hydrolysis. These characteristics were identical for nurse and forager bees.

There also were no differences between nurses and foragers in electrophoretic migration and oligomeric assembly for catalytically active brain AChE. Bee AChE migrated as a single band and showed similar electrophoretic mobility to that of recombinant human AChE (Sigma; Fig. 1B and data not shown). It also displayed a single peak in sucrose gradient analysis, with a ca. 6S sedimentation coefficient (as was previously described (Belzunces et al., 1988)), which most likely corresponds to AChE dimers (Fig. 1B).

**Brain AChE catalytic activity decreases during behavioral development.** In contrast to its unchanged biochemical characteristics, the catalytic activity of AChE in brain extracts was 20-65% lower in foragers compared to nurses (Fig. 1C, left). Differences between foragers and nurses were significant and robust; these results were obtained over two different years, from five unrelated typical colonies (and therefore with different genetic contents) maintained under field conditions.

According to the basic structure of division of labor in bee colonies, hive work always precedes foraging; foragers are therefore both older and more behaviorally advanced than nurses. This means that the detected changes in AChE catalytic activity may: 1) anticipate or coincide with the transition to foraging; 2) relate to the acquisition of new tasks once foraging has already begun; and/or 3) relate to chronological aging that is independent of behavioral status. We used "precocious foragers" to determine whether hypothesis 1 is a more likely explanation than hypotheses 2 and 3. Precocious foragers are bees from experimental single-cohort colonies that are induced to start foraging as early as 7 days of age due to the absence of older individuals (Robinson and Page, 1989). There was no significant difference in brain AChE catalytic activity in 7-10-day-old nurses and precocious foragers collected from 4 single-cohort colonies (Fig. 1C, right).

**Bee AChE cloned.** To test whether the changes in AChE activity between nurse bee and foragers described above are caused by transcriptional regulation, we cloned the cDNA sequence encoding the *Apis mellifera* (Am)AChE in order to measure brain mRNA levels. RT-PCR, with partially-degenerate primers, yielded two main products, 187 and 245 bp long. The predicted protein encoded by the shorter product (accession no. AF213011) displayed 40% and 35% identity to alpha-esterases of the blowfly, *Lucilia cuprina*, and the fruitfly *D. melanogaster*, respectively (accession no. aaa91812 and aaB01149), enzymes which are important for organophosphate resistance (Newcomb et al., 1996). The protein sequence encoded by the longer product showed high sequence identity with AChEs from various organisms. We obtained a 1715 bp cDNA sequence using the sequence of the longer product by rapid amplification of cDNA and PCR amplification from a bee brain cDNA library as template. The 492 AA translation-product showed 67.1%, 61% and 39.9% identity to AChE from the beetle *Leptinotarsa decemlineata*, *D. melanogaster* and *H. sapiens*, respectively (Fig. 2). This comparison confirmed the identity of this cDNA as part of the *Ache* gene of the honey

bee, *Apis mellifera* (*AmAChE*). Interestingly, the *AmAChE* coding sequence was not less conserved than the predicted amino acid sequence (64%, 64% and 50%, respectively).

Most of the key amino acid residues important for AChE activity were found to be conserved in *AmAChE* compared to other insects. These include two residues of the catalytic triad (the third is yet undetermined due to the truncation of our sequence), the residues comprising the peripheral anionic site (Y104, M170, Q335 and W336; Fig. 2, numbering according to the *AmAChE* sequence), the choline binding residue M115 and the acetyl binding one, F345.

**AChE brain mRNA levels decrease during behavioral development, especially in the mushroom bodies.** High-resolution fluorescent *in situ* hybridization (FISH) showed AChE mRNA localization in several brain regions known to be involved with processing of olfactory and visual information, such as the mushroom bodies, the medulla and lamina of the optic lobes, and the area surrounding the antennal lobes (Fig 3A). These results agree with histochemical and immunocytochemical analyses of other components of the cholinergic system (Kreissl and Bicker, 1989). FISH revealed particularly strong AChE expression in the somata of the Kenyon cells (Fig 3A). Quantitative analysis of confocal microscopy images revealed a significantly lower density of mRNA labeling in the Kenyon cells of foragers relative to nurses (Fig. 3B left). Differences were especially striking in the centrally located cells (Fig. 3A, insets). Support for this observation comes from an analysis of the distribution of signal densities for all calyces analyzed (Fig. 3B right). Though the distributions for nurses and foragers overlap broadly, they do differ significantly ( $P < 0.001$ , G-test), with an apparent second peak in the low values of signal density for calyces from foragers. Given that sections ( $N = 21$  per behavioral group) were taken randomly with respect to position in the calyx, these results suggest that spatial patterns of AChE expression within the calyces of the mushroom bodies differ between nurses and foragers.

**Treatment with an AChE inhibitor causes improved performance on a learning assay.** Metrifonate-treated bees exhibited a significantly higher number of correct responses than did saline-treated bees in the olfactory conditioning test (Fig. 4, Bottom;  $2.48 \pm 0.26$  SE vs.  $1.93 \pm 0.24$ ,  $P < 0.03$ , ANOVA). This apparently was not a consequence of a difference in arousal; there were no significant differences in the percentages of metrifonate-treated and saline-treated bees that showed a positive response to the first odor exposure ( $P = 0.07$ ,  $DF = 3$ , Breslow-Day Multi-Way Test for Homogeneity, SAS). Significant differences between metrifonate-treated and saline-treated bees were also detected for analyses conducted on the data for Exposures 2-4 only.

## Discussion

We have used the process of honey bee behavioral development to look for long-term, naturally occurring changes in AChE regulation during adulthood. Our results indicate that such changes do occur, the first such report for this important enzyme. We did not extensively examine the functional consequences of such a change, but it is possible that forager bees have increased cholinergic neurotransmission efficacy relative to younger bees working in the hive. Similarly, increased dendritic arborization of the Kenyon cells of the mushroom bodies (Farris S.M *et al.*, 1999. *Soc Neurosci abstr*) also may increase neurotransmission efficacy. It is not known whether AChE regulation and the dendritic arborization are causally related, but we have found that overexpressed AChE reduces dendritic arborization in the brain of transgenic mice (Beeri *et al.*, 1997). Thus, although it is not clear whether foragers have higher cognitive capacities relative to younger hive bees, our current findings provide plausible explanations for such differences, if they occur.

Biochemical analyses of bee brain AChE revealed similarities between the enzyme in bees and *Drosophila*. As in flies, AChE appears to be the only cholinesterase in the bee brain,

responsible for both ATCh and BTCh hydrolysis, and exists mainly as a dimer (Gnagey et al., 1987). In contrast, in vertebrate central nervous system neurons, both AChE and BuChE are expressed, the main enzyme form being membrane-associated tetramers (Massoulié et al., 1998; Sternfeld et al., 2000). Whereas the bee and fly enzymes appear to share many characteristics, the bee system offers advantages for behaviorally-related analyses of AChE. Such analyses in flies are quite rare (e.g. Incardona and Rosenberry, 1996) and are much more difficult to interpret, because unlike honey bees, flies do not exhibit a well developed pattern of adult behavioral development.

While there are no differences between nurse and forager honey bees in the properties of AChE studied here, our developmental analyses revealed strong differences in measurements of catalytic activity. The decrease in brain AChE catalytic activity in foragers compared to nurses apparently does not occur prior to, or even immediately following the transition to foraging, as precocious foragers did not show it consistently. This leaves both chronological aging and experience-dependent changes as possible causal factors. We speculate that AChE activity in the bee brain is influenced, at least in part, by foraging experience. Foragers from typical colonies presumably had as much as one or two weeks of foraging experience before they were collected and showed a robust decrease in AChE activity. In contrast, precocious foragers had only one or two days of foraging experience before collection; perhaps this is not enough to consistently influence AChE. This speculation agrees with the observation that results for precocious foragers from two colonies did show decreases comparable to those seen in foragers from typical colonies. Further studies are necessary to determine whether the decrease in brain AChE activity in foragers is due to aging or experience.

That at least a part of the decrease observed in forager AmAChE activity levels is caused by reduced AChE gene expression is suggested by lower AmAChE mRNA levels measured in the mushroom bodies. Low levels of expression in these regions may reflect the fact that the forager calyx has a lower cell density than that of nurse bees (Ito et al., 1998). However, our comparative analysis of mRNA signal density in the Kenyon cells of foragers relative to nurses cannot be confounded by the cell density issue. The biggest decrease in forager AChE gene expression was found to occur in the centrally located cells of the mushroom bodies. These cells are the youngest of the Kenyon cell population, where the earliest born cells are pushed outward (Farris et al., 1999). This observation supports the notion that the decrease in AChE expression is not a degenerative process related to the age of cells, but rather a regulated process that may be inversely correlated with differentiation of Kenyon cells. An involvement of AChE in the differentiation of nerve cells was previously suggested for *Xenopus* motoneurons (Sternfeld et al., 1998) and for murine pheochromocytoma cells (Grifman et al., 1998). In both cases, the non-catalytic activities of AChE (Grisaru et al., 1999b) are believed to take part. Our results also provide additional support for the emerging recognition that the mushroom bodies of the insect brain are composed of heterogeneous populations of cells (e.g., (Farris et al., 1999)).

Inhibition of brain AChE activity by metrifonate was found to improve the performance of forager bees in an olfactory conditioning test. These results are consistent with most of the previous studies (Cano Lozano and Gauthier, 1998; Gauthier et al., 1994) that correlated enhanced cholinergic neurotransmission with improved performance (c.f. Fresquet et al., 1998). Studies involving nurse bees, a broader array of cholinergic pharmacological agents, and perhaps additional types of behavioral assays are required before the significance of the observed downregulation with respect to learning can be fully determined.

Another possibility is that AChE downregulation makes forager bees less sensitive than nurses to natural and synthetic xenobiotic agents such as organophosphate pesticides. This suggestion is based on the finding (Shapira et al., 2000) that a relatively small increase in AChE

constitutive expression (ca. 1.5 fold) in transgenic mice can impair the transcriptional response of the *ACHE* gene to various AChE inhibitors and therefore heighten sensitivity to such agents.

Changes in neural function that underlie long-term changes in memory are caused in part by transcription-dependent mechanisms (Kaufer et al., 1998). Our results indicate that similar mechanisms may be involved in the long-term changes in neural function that are associated with behavioral development in honey bees. There is only limited evidence for changes in gene expression in the brain that are associated with changes in behavior of animals in their natural environment (Mello et al., 1995; Robinson, 1999). However, this is probably due to the little attention this topic has received. In honey bees, there are only two other known cases of developmental regulation of brain gene expression. There are age-related increases in royal jelly protein-3 mRNA in the brain, the function of which is still unknown (Kucharski et al., 1998). There also are similar increases in brain mRNA levels of *period*, a gene well known for its role in circadian rhythms (Toma et al., 2000). These results, coupled with our findings, suggest that transcription-dependent mechanisms may play diverse roles in naturally occurring behavioral plasticity.

### Acknowledgements

We thank the staff at Tsrifin Bee Station for access to bees in Israel; A.J. Ross for assistance with bee colonies in Illinois; S.M. Farris, J. Mehren, S. O'Brien, and A.J. Ross for brain dissections; S. Aref for statistical analyses; and D. Glick and members of the Robinson lab for comments that improved the manuscript. Thanks to the University of Illinois Center for Advanced Study, the Fulbright Foundation and the Charles E. Smith Laboratory of Psychobiology for enabling G.E.R. to spend a sabbatical in the laboratory of H.S., during which this study was initiated. Other funding for this study came from the U.S. Army Medical Research and Development Command (DAMD17-99-1-9547; HS), the Israeli Ministry of Science (9433-1-97; HS), and the US National Institute of Health (DC3008; GER).

### References

- Acampora, D., Avantaggiato, V., Tuorto, F., Barone, P., Reichert, H., Finkelstein, R., and Simeone, A. (1998). Murine *Otx1* and *Drosophila otd* genes share conserved genetic functions required in invertebrate and vertebrate brain development. *Development* **125**, 1691-1702.
- Beeri, R., Le Novere, N., Mervis, R., Huberman, T., Grauer, E., Changeux, J. P., and Soreq, H. (1997). Enhanced hemicholinium binding and attenuated dendrite branching in cognitively impaired acetylcholinesterase-transgenic mice. *J. Neurochem.* **69**, 2441-2451.
- Belzunces, L. P., Toutant, J. P., and Bounias, M. (1988). Acetylcholinesterase from *Apis mellifera* head. Evidence for amphiphilic and hydrophilic forms characterized by Triton X-114 phase separation. *Biochem. J.* **255**, 463-470.
- Ben-Shahar, Y., Thompson, C. K., Smith, B. H., and Robinson, G. E. (2000). Reversal learning and division of labor in honey bees. *Animal Cognition* *In press*.
- Cano Lozano, V., and Gauthier, M. (1998). Effects of the muscarinic antagonists atropine and pirenzepine on olfactory conditioning in the honeybee. *Pharmacol. Biochem. Behav.* **59**, 903-907.
- de Belle, J. S., and Heisenberg, M. (1994). Associative odor learning in *Drosophila* abolished by chemical ablation of mushroom bodies. *Science* **263**, 692-695.
- Durst, C., Eichmuller, S., and Menzel, R. (1994). Development and experience lead to increased volume of subcompartments of the honeybee mushroom body. *Behav. Neural Biol.* **62**, 259-263.
- Fahrbach, S. E., and Robinson, G. E. (1995). Behavioral development in the honey bee: toward the study of learning under natural conditions. *Learn. Mem.* **2**, 199-224.

- Fahrbach, S. E., and Robinson, G. E. (1996). Juvenile hormone, behavioral maturation, and brain structure in the honey bee. *Dev. Neurosci.* **18**, 102-114.
- Fahrbach, S. E., Strande, J. L., and Robinson, G. E. (1995). Neurogenesis is absent in the brains of adult honey bees and does not explain behavioral neuroplasticity. *Neurosci. Lett.* **197**, 145-148.
- Farris, S. M., Robinson, G. E., Davis, R. L., and Fahrbach, S. E. (1999). Larval and pupal development of the mushroom bodies in the honey bee, *Apis mellifera*. *J. Comp. Neurol.* **414**, 97-113.
- Fresquet, N., Fournier, D., and Gauthier, M. (1998). A new attempt to assess the effect of learning processes on the cholinergic system: studies on fruitflies and honeybees. *Comp. Biochem. Physiol. B Biochem. Mol. Biol.* **119**, 349-353.
- Gauthier, M., Cano-Lozano, V., Zaoujal, A., and Richard, D. (1994). Effects of intracranial injections of scopolamine on olfactory conditioning retrieval in the honeybee. *Behav. Brain Res.* **63**, 145-149.
- Giray, T., Guzman-Novoa, E., Huang, Z.-Y., and Robinson, G. E. (2000). Physiological correlates of genotypic variation in rate of honey bee behavioral development. *Behav. Ecol. Sociobiol.* **47**, 17-28.
- Giray, T., and Robinson, G. (1994). Effects of intracolony variability in behavioral development on plasticity of division of labor in honey bee colonies. *Behav. Ecol. Sociobiol.* **35**, 13-20.
- Gnagey, A. L., Forte, M., and Rosenberry, T. L. (1987). Isolation and characterization of acetylcholinesterase from *Drosophila*. *J. Biol. Chem.* **262**, 13290-13298.
- Grifman, M., Galyam, N., Seidman, S., and Soreq, H. (1998). Functional redundancy of acetylcholinesterase and neuroigin in mammalian neuritogenesis. *Proc. Natl. Acad. Sci. U S A* **95**, 13935-13940.
- Grisaru, D., Lev-Lehman, E., Shapira, M., Chaikin, E., Lessing, J. B., Eldor, A., Eckstein, F., and Soreq, H. (1999a). Human osteogenesis involves differentiation-dependent increases in the morphogenetically active 3' alternative splicing variant of acetylcholinesterase. *Mol. Cell. Biol.* **19**, 788-795.
- Grisaru, D., Sternfeld, M., Eldor, A., Glick, D., and Soreq, H. (1999b). Structural roles of acetylcholinesterase variants in biology and pathology. *Eur. J. Biochem.* **264**, 672-686.
- Hammer, M., and Menzel, R. (1995). Learning and memory in the honeybee. *J. Neurosci.* **15**, 1617-1630.
- Huang, Z.-H., Robinson, G. E., Tobe, S. S., Yagi, K. J., Strambi, C., Strambi, A., and Stay, B. (1991). Hormonal regulation of behavioural development in the honey bee is based on changes in the rate of juvenile hormone biosynthesis. *J. Insect Physiol.* **37**, 733-741.
- Huang, Z. Y., and Robinson, G. E. (1992). Honeybee colony integration: worker-worker interactions mediate hormonally regulated plasticity in division of labor. *Proc. Natl. Acad. Sci. U S A* **89**, 11726-11729.
- Incardona, J. P., and Rosenberry, T. L. (1996). Replacement of the glycoinositol phospholipid anchor of *Drosophila* acetylcholinesterase with a transmembrane domain does not alter sorting in neurons and epithelia but results in behavioral defects. *Mol. Biol. Cell* **7**, 613-630.
- Ito, K., Suzuki, K., Estes, P., Ramaswami, M., Yamamoto, D., and Strausfeld, N. J. (1998). The organization of extrinsic neurons and their implications in the functional roles of the mushroom bodies in *Drosophila melanogaster* Meigen. *Learn. Mem.* **5**, 52-77.
- Kaufer, D., Friedman, A., Seidman, S., and Soreq, H. (1998). Acute stress facilitates long-lasting changes in cholinergic gene expression. *Nature* **393**, 373-377.

- Kreissl, S., and Bicker, G. (1989). Histochemistry of acetylcholinesterase and immunocytochemistry of an acetylcholine receptor-like antigen in the brain of the honeybee. *J. Comp. Neurol.* **286**, 71-84.
- Kucharski, R., Maleszka, R., Hayward, D. C., and Ball, E. E. (1998). A royal jelly protein is expressed in a subset of Kenyon cells in the mushroom bodies of the honey bee brain. *Naturwissenschaften* **85**, 343-346.
- Loewenstein Lichtenstein, Y., Schwarz, M., Glick, D., Norgaard Pedersen, B., Zakut, H., and Soreq, H. (1995). Genetic predisposition to adverse consequences of anti-cholinesterases in 'atypical' BCHE carriers. *Nat. Med.* **1**, 1082-1085.
- Lozano, V. C., Bonnard, E., Gauthier, M., and Richard, D. (1996). Mecamylamine-induced impairment of acquisition and retrieval of olfactory conditioning in the honeybee. *Behav. Brain Res.* **81**, 215-222.
- Massoulie, J., Anselmet, A., Bon, S., Krejci, E., Legay, C., Morel, N., and Simon, S. (1998). Acetylcholinesterase: C-terminal domains, molecular forms and functional localization. *J. Physiol. Paris* **92**, 183-190.
- Meller, V. H., and Davis, R. L. (1996). Biochemistry of insect learning: lessons from bees and flies. *Insect Biochem. Mol. Biol.* **26**, 327-335.
- Mello, C., Nottebohm, F., and Clayton, D. (1995). Repeated exposure to one song leads to a rapid and persistent decline in an immediate early gene's response to that song in zebra finch telencephalon. *J. Neurosci.* **15**, 6919-6925.
- Menzel, R., Erber, J., and Masuhr, T. (1974). Learning and memory in the honey bee, in *Experimental analysis of insect behavior*, (L. B. Browne, ed.e), pp. 195-218. Springer-Verlag, Berlin.
- Mesulam, M. M., and Geula, C. (1991). Acetylcholinesterase-rich neurons of the human cerebral cortex: cytoarchitectonic and ontogenetic patterns of distribution. *J. Comp. Neurol.* **306**, 193-220.
- Mobbs, P. (1982). The brain of the honey bee *Apis mellifera*. The connections and spatial organization of the mushroom bodies. *Trans. R. Soc. Lond. B Biol. Sci.* **298**, 309-354.
- Newcomb, R. D., East, P. D., Russell, R. J., and Oakeshott, J. G. (1996). Isolation of alpha cluster esterase genes associated with organophosphate resistance in *Lucilia cuprina*. *Insect Mol. Biol.* **5**, 211-216.
- Oh, M. M., Power, J. M., Thompson, L. T., Moriearty, P. L., and Disterhoft, J. F. (1999). Metrifonate increases neuronal excitability in CA1 pyramidal neurons from both young and aging rabbit hippocampus. *J. Neurosci.* **19**, 1814-1823.
- Pankiw, T., Huang, Z., Winston, M., and Robinson, G. (1998). Queen mandibular gland pheromone influences worker honey bee (*Apis mellifera* L.) foraging ontogeny and juvenile hormone titers. *J. Insect Physiol.* **44**, 685-692.
- Ray, S., and Ferneyhough, B. (1999). Behavioral development and olfactory learning in the honeybee (*Apis mellifera*). *Dev. Psychobiol.* **34**, 21-27.
- Robinson, G., and Page, R. (1989). Genetic determination of nectar foraging, pollen foraging, and nest-site scouting in honey bee colonies. *Behav. Ecol. Sociobiol.* **24**, 317-323.
- Robinson, G. E. (1992). Regulation of division of labor in insect societies. *Annu. Rev. Entomol.* **37**, 637-665.
- Robinson, G. E. (1999). Integrative animal behaviour and sociogenomics. *Trends in ecology and evolution* **14**, 202-205.
- Robinson, G. E., Heuser, L. M., LeConte, Y., Lenquette, F., and Hollingworth, R. M. (1999). Neurochemicals improve bee nestmate recognition. *Nature* **399**, 534-535.
- Scali, C., Giovannini, M. G., Bartolini, L., Prosperi, C., Hinz, V., Schmidt, B., and Pepeu, G. (1997). Effect of metrifonate on extracellular brain acetylcholine and object recognition in aged rats. *Eur. J. Pharmacol.* **325**, 173-180.

- Schulz, D. J., and Robinson, G. E. (1999). Biogenic amines and division of labor in honey bee colonies: behaviorally related changes in the antennal lobes and age-related changes in the mushroom bodies. *J. Comp. Physiol. [A]* **184**, 481-488.
- Seidman, S., Aziz Aloya, R. B., Timberg, R., Loewenstein, Y., Velan, B., Shafferman, A., Liao, J., Norgaard Pedersen, B., Brodbeck, U., and Soreq, H. (1994). Overexpressed monomeric human acetylcholinesterase induces subtle ultrastructural modifications in developing neuromuscular junctions of *Xenopus laevis* embryos. *J. Neurochem.* **62**, 1670-1681.
- Seidman, S., Sternfeld, M., Ben Aziz Aloya, R., Timberg, R., Kaufer Nachum, D., and Soreq, H. (1995). Synaptic and epidermal accumulations of human acetylcholinesterase are encoded by alternative 3'-terminal exons. *Mol. Cell. Biol.* **15**, 2993-3002.
- Shapira, M., Tur-Kaspa, I., Bosgraaf, L., Livni, N., Grant, A. D., Grisaru, D., Korner, M., Ebstein, R. P., and Soreq, H. (2000). A transcription-activating polymorphism in the ACHE promoter associated with acute sensitivity to anti-acetylcholinesterases. *Hum. Mol. Genet.* **9**, 1273-1281.
- Sigg, D., Thompson, C. M., and Mercer, A. R. (1997). Activity-dependent changes to the brain and behavior of the honey bee, *Apis mellifera* (L.). *J. Neurosci.* **17**, 7148-7156.
- Sternfeld, M., Ming, G., Song, H., Sela, K., Timberg, R., Poo, M., and Soreq, H. (1998). Acetylcholinesterase enhances neurite growth and synapse development through alternative contributions of its hydrolytic capacity, core protein, and variable C termini. *J. Neurosci.* **18**, 1240-1249.
- Sternfeld, M., Shoham, S., Klein, O., Flores-Flores, C., Evron, T., Idelson, G. H., Kitsberg, D., Patrick, J. W., and Soreq, H. (2000). Excess "read-through" acetylcholinesterase attenuates but the "synaptic" variant intensifies neurodeterioration correlates. *Proc. Natl. Acad. Sci. U S A* **97**, 8647-8652.
- Toma, D. P., Moore, D., Bloch, G., and Robinson, G. E. (2000). Changes in *period* expression in the brain and division of labor in honey bee colonies. *Proc. Natl. Acad. Sci. USA*, (in press).
- Wagener-Hulme, C., Kuehn, J. C., Schulz, D. J., and Robinson, G. E. (1999). Biogenic amines and division of labor in honey bee colonies. *J. Comp. Physiol. [A]* **184**, 471-479.
- Winkler, J., Thal, L. J., Gage, F. H., and Fisher, L. J. (1998). Cholinergic strategies for Alzheimer's disease. *J. Mol. Med.* **76**, 555-567.
- Winston, M. (1987). *The biology of the honey bee* (Cambridge, MA: Harvard University Press).
- Withers, G. S., Fahrbach, S. E., and Robinson, G. E. (1993). Selective neuroanatomical plasticity and division of labour in the honeybee. *Nature* **364**, 238-240.
- Ziegler, R., Engler, D. L., and Davis, N. T. (1995). Biotin-containing proteins of the insect nervous system, a potential source of interference with immunocytochemical localization procedures. *Insect Biochem. Mol. Biol.* **25**, 569-574.

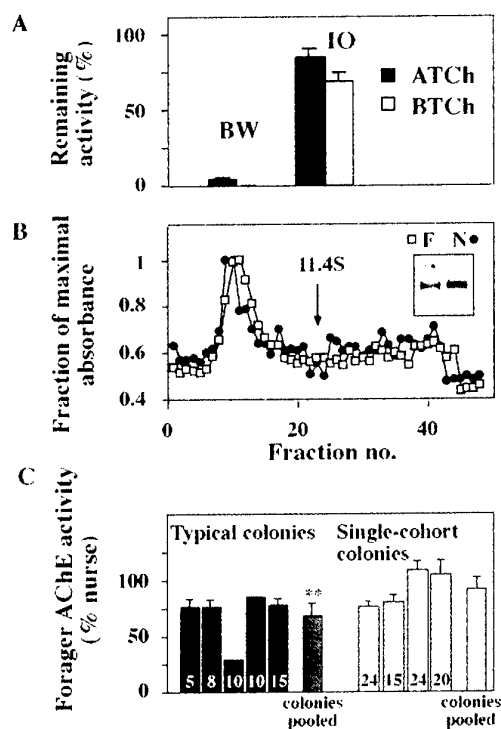


**Figure 1. Biochemical analyses of AChE from the brains of nurse and forager honey bees.** **A. Substrate and inhibitor specificities.** Mean ( $\pm$ SE) specific cholinesterase activity in brain homogenates from nurse bees, normalized to activity without inhibitors (2-3 measurements of one sample, 5 brains/sample). BTCh hydrolyzing activity was ca. 5% of ATCh hydrolyzing activity. BW: BW 248C51; IO: iso-OMPA. **B. Similar sedimentation and electromobility profiles for nurse and forager AChE.** Extracts representing 10 brains each were subjected to sucrose density centrifugation followed by an ATCh hydrolysis assay (Seidman et al., 1994). Arrow marks the position of bovine liver catalase. **Inset. AChE from nurses and foragers migrates similarly in activity gels.** AChE activity staining following gel electrophoresis. Note the single band with similar electromobility in brain homogenates prepared from foragers or

nurses (each sample is a 5- $\mu$ l aliquot of brain homogenate). **C. Differences in brain AChE catalytic activity in foragers and nurses.** **Left.** Mean ( $\pm$  SE) AChE brain activity levels (nmol ATCh hydrolyzed/min/mg total protein) in forager bees from typical colonies (N = 5), normalized to the mean level for nurse bees from the same colony (Sample sizes for brains in bars). Columns without SEs represent colonies where all brains were pooled into one homogenate; dotted bar represents the grand mean across all 5 colonies. 2-way ANOVA (randomized complete block on log-transformed data; SAS, Cary, NC) revealed significant variation between colonies ( $P < 0.05$ ) and between nurses and foragers ( $P < 0.01$ ). Similar results were obtained when excluding the one colony with the lowest forager catalytic activity. Absolute rates of ATCh hydrolysis varied greatly from colony to colony (the median was ca. 100 nmol ATCh hydrolyzed/min/mg total protein). **Right.** Similar results for bees from single-cohort colonies (N=4). 2-way ANOVA revealed significant variation between colonies ( $P < 0.05$ ) but no significant differences between nurses and precocious foragers ( $P > 0.7$ ).



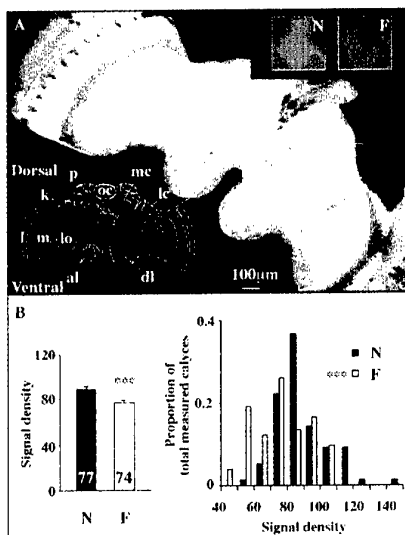


**Figure 3 AChE brain mRNA levels are lower in foragers than nurses, especially in the mushroom bodies.** A. AChE mRNA labeling in the bee brain.

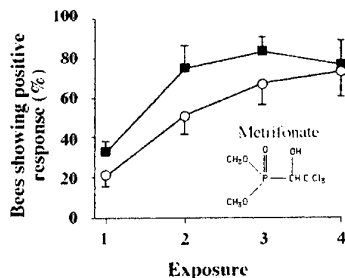
A representative coronal section through the brain of a worker honey bee labeled for AmAChE mRNA. Detection of transcripts was achieved using the ELF AP substrate (main image). White rectangle delineates the position of a calyx region of a mushroom body shown, magnified, in the top right images. **Top right.** Representative confocal microscope images (N = nurse, F = forager) of calyces from similar brain sections labeled for AmAChE mRNA using the Fast Red AP substrate. **Bottom left.** Schematic depiction of the bee brain (after Kreissl and Bicker, 1989). mc and lc, medial and lateral calyces of the mushroom bodies; k, Kenyon cell bodies region; p, pons; oc, one of three ocelli; l, m and lo, lamella, medula and lobula of the optical lobe; al, antennal lobe; dl, dorsal lobe.

**B. AChE mRNA levels are lower in Kenyon cells of foragers than nurses.** **Left.** Mean  $\pm$  SE signal densities (arbitrary units) of AmAChE mRNA from calyces (enclosing a population of Kenyon cell bodies) of nurses (N) and foragers (F) brains. The analysis was based on 2-4 calyces/section, 3 sections/brain, 7 brains/behavioral group, for a total of 77 calyx sections for nurses and 74 for foragers. ( $P < 0.00005$ , t-test). No significant differences in signal densities between medial and lateral calyces were detected (results not shown). **Right.** Frequency distribution of signal densities for all analyzed calyces. Since the sampling of sections through the calyces was random, with respect to position in the calyx, we can infer from this distribution conclusions regarding changes in mRNA density in different areas of the calyx. Asterisks denote a statistically significant difference in the distribution of signal density values.



**Figure 4. Metrifonate improves bee performance on olfactory learning test.** **Top.** A scheme of the learning assay (picture taken by Brian Smith, Ohio State University).

Odor exposure (a puff of geraniol-saturated air) was coupled with a reward of sucrose solution (droplet), which elicits the unconditioned response, the proboscis (arrow) extension reflex. See **Materials and methods** for a detailed explanation. **Bottom.** Mean ( $\pm$  SE) number of bees showing positive responses at each odor exposure. Grand means are based on data from four trials, with bees from 2 different, unrelated, colonies, 37-94 bees/group/trial; 216 metrifonate-injected (filled squares) and 233 saline-injected (open circles) bees total. Statistical analyses (see text) were conducted on the total number of correct responses/bee. Inset shows the chemical structure of trichloro-metrifonate.



**READTHROUGH ACETYLCHOLINESTERASE (ACHE-R)  
IS AN ANTISENSE-SUPPRESSIBLE STRESS-RESPONSE ELEMENT**

**Hermona Soreq and David Glick**

Department of Biological Chemistry, The Institute of Life Sciences,  
The Hebrew University of Jerusalem, Israel 91904  
tel: 972-2-6585109; fax: 972-2-652 0258; e-mail: soreq@shum.huji.ac.il

**Summary**

Acetylcholinesterase (AChE) signals important physiological messages. Best appreciated of its roles is in the termination of neurotransmission. More recently its role in morphogenesis and cell adhesion has been recognized. Alternative splicing of the single human *ACHE* gene transcript gives rise to three AChE variants, which immediately raises the question of whether each of the variants participates equally in all the identified functions, or whether there is a division of labor among the variants. Some of the morphogenic effects of nervous system AChE, we find, are AChE variant-specific. AChE is known to interact with several other proteins that putatively function in morphogenesis and cell adhesion, particularly in the nervous system. Therefore, we propose that the variants signal their unique cell adhesion and morphogenic instructions via variant-specific interactions with intrinsic and trans-membrane protein ligands. These morphogenic properties may be inseparable from the integrity of the entire variant protein, the small variant-specific domains imposing on the entire protein a conformation that allows these newer properties. A similar, but pathological, case seems to be the role of AChE in Alzheimer's disease: catalytically active enzyme is found in the fibrils and plaques that characterize the disease, and it accelerates formation of the structures and contributes to their neurotoxicity. Conventional AChE-inhibitor drugs, used in Alzheimer's disease therapy and myasthenia gravis, are either non-selective or insufficiently selective among the AChE variants. Moreover, inhibiting the hydrolytic activity of AChE would not necessarily prevent its morphogenic activities. Therefore, an attractive alternative to conventional chemical inhibitors is the selective suppression of the production of single variants by antisense oligodeoxynucleotides. Recent *in vivo* studies demonstrate such selectivity for antisense agents targeted at the *ACHE* gene.

**Introduction**

AChE is a signalling molecule in several senses. It has a well-established role in terminating cholinergic activity by hydrolysis of the neurotransmitter, acetylcholine to acetate and choline (Hoffman et al., 1996). More recently, non-classical activities, morphogenesis and cell adhesion properties, have been recognized. Evidence for these newer activities came first from the finding of the protein in unexpected places (Appleyard, 1992; Greenfield, 1984; Grisaru et al., 1999b), such as decidedly non-cholinergic cells and tissues: blood cells, notably erythrocytes and megakaryocytes (Lapidot Lifson et al., 1992; Lev-Lehman et al., 1997; Patinkin et al., 1994; Paulus et al., 1981; Soreq et al., 1994), developing avian cartilage (Layer, 1990) and mammalian bone (Grisaru et al., 1999a), and developing oocytes and sperm (Malingier et al., 1989; Sastry et al., 1981; Soreq et al., 1990). Even in the nervous system there is no simple relation of location to cholinergic function (Broide et al., 1999; Greenfield, 1991). Cell proliferation and/or invasive migration capacities were attributed to AChE in several tumor types (Drews, 1975; Noda et al., 1998; Zakut et al., 1990). During development of the nervous system, AChE contributes to the sprouting of neurites, which are process extensions from the cell body on which the synapses develop (Layer, 1991; Weikert et al., 1990). Coinciding with neuron proliferation and axon outgrowth, AChE is transiently expressed in the developing brain (Karpel et al., 1994; Karpel et al., 1996; Lapidot Lifson et al., 1992; Layer, 1991; Layer, 1990; Layer et al., 1987). The discovery of non-catalytic AChE-like proteins with documented roles in cell adhesion and axon guidance (Hortsch et al., 1990) further strengthened the conviction that there are

additional biological roles of AChE; cell culture experiments then provided an explanation in molecular terms of these new roles (Grifman et al., 1998; Koenigsberger et al., 1997; Sternfeld et al., 1998a)

#### **Alternative splicing of the common pre-mRNA creates three C-terminal variants**

The pre-mRNA transcript of the single human ACHE gene undergoes alternative splicing to yield several variant proteins. In addition to the well known "synaptic" (S) and "erythrocytic" (E) isoforms of AChE, molecular cloning has revealed the existence of a third, "readthrough" (R) isoform (Ben Aziz-Aloya et al., 1993; Li et al., 1991). These three isoforms share a core of 543 amino acid residues which is catalytically competent, but they differ in their C-terminal sequences. AChE-S terminates with the sequence DTLDEAERQWKAEFHRWSSYVMVHWKNQFDHYSKQDRCSDL; AChE-E with ASEAPSTCPGFTHG; and AChE-R with GMQGPAGSGWEEGSGSPPGVTPPLFSP. AChE-R is a soluble hydrophilic protein, unlike the better known AChE-S variant, which exists as dimers connected by disulfide bridges between the cysteine residues near their C-termini. These may be bundled to a collagen-like tail or a brain-specific structural subunit, whereas dimers of the AChE-E variant are bound to a glycosphosphatidoinositide moiety that is embedded in the erythrocyte membrane (Haas et al., 1996; Massoulié et al., 1998). AChE-R, being soluble, is readily accessible for interaction with immobile extracellular elements of its milieu.

#### **AChE has a potential for interaction with a variety of proteins**

AChE is now recognized as a member of a family of proteins that includes *Drosophila* neurotactin (Darboux et al., 1996; Hortsch et al., 1990) and gliotactin (Auld et al., 1995), known for their roles in maintenance of cellular adhesion, especially (for gliotactin) in the hemolymph-neuron barrier, which is the *Drosophila* analogue of the blood-brain barrier. They are intrinsic membrane proteins; their AChE-homologous domain is extracellular, and their intracellular domain interacts with proteins such as coracle (Baumgartner et al., 1996), a band 4.1 homologue, which is a mediator of signals to the cytoskeleton or discs lost (Dlt), a multi-PDZ element which serves as an anchor for cytoskeletal proteins (Bhat et al., 1999). This series of interactions, therefore, traces a sequence that potentially transduces signals from the cell membrane to the cytoskeleton via AChE-like proteins. That this may, indeed, be the case is attested by the findings that AChE can replace neurotactin in cell adhesion models (Darboux et al., 1996), and its effects on morphogenesis are duplicated by another AChE homologue, neuroligin, in phaeochromocytoma PC12 cells (Grifman et al., 1998).

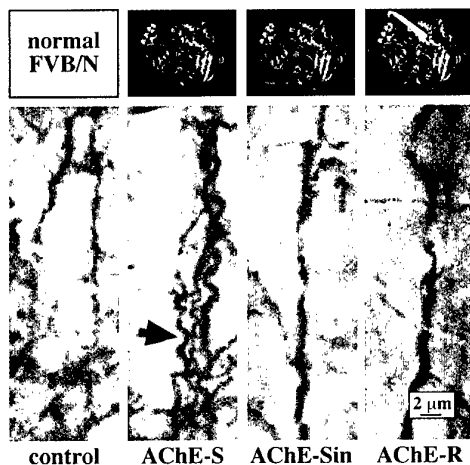
#### **The non-classical functions of AChE are variant-specific**

Studies of the morphogenic roles of AChE have been facilitated by the construction of transgenic mouse lines that over-express a specific AChE variant, AChE-S (Beeri et al., 1995) or AChE-R (Sternfeld et al., 1998b), by the use of stably transfected cell lines (Bigbee et al., 1999; Grifman et al., 1998; Koenigsberger et al., 1997), or primary neurons over-expressing AChE variants (Sternfeld et al., 1998a) and by producing small quantities of the recombinant variants. In several of these model systems, human AChE-R emerged as having capacities distinct from those of AChE-S. In cultured glioblastoma cells, over-expressed AChE-R confers a phenotype of small, round, rapidly dividing cells as opposed to the AChE-S phenotype of process growth (Karpel et al., 1994). Antisense suppression of AChE-R mRNA in PC12 cells was associated with complete loss of neuritogenesis, which was retrieved by re-transfection with AChE-S (Koenigsberger et al., 1997) as well as AChE-R or their non-catalytic homolog, neuroligin (Grifman et al., 1998). In DFP-exposed mice, over-expressed AChE-R increases the density of diaphragm neuromuscular junctions by around 5-fold in an antisense-preventable manner (Lev-Lehman et al., 2000). However, neuronal AChE-S over-production does not increase synaptogenesis (Andres et al., 1997), perhaps due to a synaptogenic function of AChE-R that is distinct from that of AChE-S.

### AChE-R is over-produced under the influence of several stressors

Acute psychological and physical stress (the forced-swim paradigm) (Kaufer et al., 1998), exposure to anti-cholinesterases (Kaufer et al., 1999) or trauma (closed head injury) (Shohami et al., 2000) rapidly induce robust and persistent over-production of AChE-R in mammalian brain and muscle. The resultant facilitation of the capacity for acetylcholine hydrolysis provides useful short-term suppression of the cholinergic hyperexcitation that is associated with stress responses. This can prevent epileptic seizures or muscle spasms, respectively. However, in the long run, these forms of stress or trauma — acute psychological stress, exposure to anti-cholinesterases, head injury — all can lead to delayed neurodeterioration. Further studies will be required to determine whether the association of AChE-R with these physiological conditions reflects a causal relationship to neurodeterioration, or whether the expression of AChE-R is a protective mechanism that is not always sufficient to prevent the deterioration.

There is the tantalizing possibility that synthetic peptides with sequences of the unique C-terminal domains which define the the variants will share with them their characteristic morphogenic properties. On the other hand, the C-terminal domains may impose these new biological properties on the entire protein, an effect best understood as forcing on the core protein a conformational change that adapts it to its new role. The figure below shows the effect of several AChE variants on the formation of pathological corkscrew neurite structures. The representations of the core AChE molecule and the C-terminal sequences show them essentially apart from the globular domain, or closely interacting with it. Future studies will be required to choose between these two possibilities.



### Neuropathologies induced by transgenic AChE-S

Above are representations of the core AChE molecule with C-terminal sequences arbitrarily represented as conformationally independent of the globular domain (AChE-S) or closely interacting with it (AChE-R). Below are sections of cortex taken from normal, transgenic human AChE-S, transgenic human AChE-Sin (an inactive engineered variant of AChE-S in which a 7-residue sequence interrupts the active site), and AChE-R. The pathological corkscrew structures (red arrow) appear in the brains of the AChE-S transgenics, but not in the brains of control, AChE-Sin or AChE-R transgenics.

*On the basis of these variant-specific non-classical properties of AChE, we propose that the three variants signal their unique cell adhesion and morphogenic instructions via their interactions with intrinsic and trans-membrane protein ligands.*

### **A pathological case of AChE in AD fibrils and plaques**

We presume that the interactions of AChE with other cell elements is a normal physiological function, but this line of reasoning may be extended to include the association of AChE with pathological structures, namely the interaction of AChE with the fibrils and plaques that characterize Alzheimer's disease (AD) (Arendt et al., 1992; Mesulam et al., 1992; Sberna et al., 1997) and to which are attributed the neurotoxicity that causes the characteristic AD deterioration. AChE has been located in these defining variant-specific morphogenic effects.

### **Conventional AChE inhibitors are either non-selective or insufficiently selective among the AChE variants**

AChE inhibitors have been designed with one end in mind, the abolition of catalytic activity. The variation of their effectiveness against the various molecular forms of AChE (Ogane et al., 1992), therefore seems only fortuitous. It is unsurprising, therefore, that these have no consistent effect on the newly-recognized properties of AChE, which are unrelated to catalysis. In the case of AChE in AD fibrils and plaques, the interaction is known to be at a peripheral site, so conventional AChE inhibitors would not be expected to interrupt the interaction. Cumulative experience with the already-approved anti-AChE drugs for AD demonstrates a divergence of their efficacy as AChE inhibitors from their behavioral and cognitive effects (Giacobini, 1998; Thal et al., 1996). The basis of this seeming paradox may lie in the variant-specific morphogenic effects.

*A non-conventional approach to suppression of AChE, therefore is required, especially one that would offer specificity to the several AChE variants. Such an approach is the suppression of AChE by antisense oligodeoxynucleotides (AS-ODNs).*

### **Selective suppression of a single variant may be achieved with an AS-ODN**

When the three 3'-terminal phosphodiester bonds are protected by 2'-O-methyl substitution, nanomolar doses of a 20-mer AS-ODN targeted to AChE mRNA effectively suppress AChE-R levels in cultured human Saos2 osteosarcoma cells (Grisaru et al., 1999a) and in the mouse brain *in vivo* (Shohami et al., 2000). The shorter AChE-S mRNA transcript is more resistant to such destruction, which makes the AS-ODN effect relatively selective for AChE-R even when targeted toward regions shared by the two transcripts (Seidman et al., 1999). The physiological effectiveness of AS-ACHE ODNs was demonstrated in several *in vivo* model systems. A single *i.c.v.* AS-ODN injection (2.5 mg/Kg) shortly after head injury prevents AChE-R over-production, improves survival by 2.5-fold for AChE-S transgenic animals, improves recovery to the rate observed for control mice and protects hippocampal neurons from post-injury death (Shohami et al., 2000). Moreover, similar AS-ODN treatment improved the post-injury recovery of control FVB/N mice, as measured by their performance in the beam walk test. When it is injected *i.p.* into DFP-treated mice, the AS-ACHE ODN prevents AChE-R over-production and the associated increase in the density of diaphragm neuromuscular junctions (Lev-Lehman et al., 2000).

### **Prospects**

The multiple physiological roles of AChE and their division among the three AChE variants requires further refinement of the therapeutic strategies aimed at prevention of the adverse consequences of AChE excess, especially for the management of AD. The expression of a characteristic form of AChE (Navaratnam et al., 1991; Saez-Valero et al., 1997; Saez-Valero et al., 1999), and modified ratios among AChE forms in favor of soluble monomers, is known in AD and following exposure to anti-AChE agents (Grisaru et al., 1999b). Such monomers may include AChE-R and/or unassembled AChE-S protomers. Whether either type of such monomers contribute toward neurodegeneration, and therefore should be a target of pharmacological intervention, or whether they are part of a physiological protective mechanism and should be maintained at a certain level will be the focus of future studies. In either case, the available armamentarium of anti-AChE

drugs should be supplemented with agents that are variant-specific. The AS-ODN strategy is an attractive such approach for both basic research and therapeutic programs.

#### Acknowledgements

For support of the work reported here, we thank the U.S. Army Medical Research and Materiel Command (DAMD17-99-1-9483), The U.S.-Israel Binational Science Foundation (96/00110), The German-Israeli Foundation (I-512-206.01/96), the Israel Science Foundation (590/97), and Ester Neuroscience, Ltd.

#### References

- Andres, C., Beeri, R., Friedman, A., Lev-Lehman, E., Henis, S., Timberg, R., Shani, M., and Soreq, H. (1997). Acetylcholinesterase-transgenic mice display embryonic modulations in spinal cord choline acetyltransferase and neurexin Ibeta gene expression followed by late-onset neuromotor deterioration. *Proc Natl Acad Sci U S A* 94, 8173-8178.
- Appleyard, M. E. (1992). Secreted acetylcholinesterase: non-classical aspects of a classical enzyme. *Trends Neurosci* 15, 485-490.
- Arendt, T., Bruckner, M. K., Lange, M., and Bigl, V. (1992). Changes in acetylcholinesterase and butyrylcholinesterase in Alzheimer's disease resemble embryonic development--a study of molecular forms. *Neurochem Int* 21, 381-396.
- Auld, V. J., Fetter, R. D., Broadie, K., and Goodman, C. S. (1995). Gliotactin, a novel transmembrane protein on peripheral glia, is required to form the blood-nerve barrier in *Drosophila*. *Cell* 81, 757-767.
- Baumgartner, S., Littleton, J. T., Broadie, K., Bhat, M. A., Harbecke, R., Lengyel, J. A., Chiquet Ehrismann, R., Prokop, A., and Bellen, H. J. (1996). A *Drosophila* neurexin is required for septate junction and blood-nerve barrier formation and function. *Cell* 87, 1059-1068.
- Beeri, R., Andres, C., Lev-Lehman, E., Timberg, R., Huberman, T., Shani, M., and Soreq, H. (1995). Transgenic expression of human acetylcholinesterase induces progressive cognitive deterioration in mice. *Curr Biol* 5, 1063-1071.
- Ben Aziz-Aloya, R., Sternfeld, M., and Soreq, H. (1993). Promoter elements and alternative splicing in the human ACHE gene. *Prog Brain Res* 98, 147-153.
- Bhat, M. A., Izaddoost, S., Lu, Y., Cho, K. O., Choi, K. W., and Bellen, H. J. (1999). Discs Lost, a novel multi-PDZ domain protein, establishes and maintains epithelial polarity. *Cell* 96, 833-845.
- Bigbee, J. W., Sharma, K. V., Gupta, J. J., and Dupree, J. L. (1999). Morphogenic Role for Acetylcholinesterase in Axonal Outgrowth during Neural Development. *Environ Health Perspect* 107 Suppl 1, 81-87.
- Broide, R. S., Grifman, M., Loewenstein, A., Grisaru, D., Timberg, R., Stone, J., Shani, M., Patrick, J. W., and Soreq, H. (1999). Manipulations of ACHE gene expression suggest non-catalytic involvement of acetylcholinesterase in the functioning of mammalian photoreceptors but not in retinal degeneration. *Brain Res Mol Brain Res* 71, 137-148.
- Darboux, I., Barthalay, Y., Piovant, M., and Hipeau Jacquotte, R. (1996). The structure-function relationships in *Drosophila* neurotactin show that cholinesterasic domains may have adhesive properties. *EMBO J* 15, 4835-4843.
- Drews, U. (1975). Cholinesterase in embryonic development. *Prog Histochem Cytochem* 7, 1-52.
- Giacobini, E. (1998). Invited review: Cholinesterase inhibitors for Alzheimer's disease therapy: from tacrine to future applications. *Neurochem Int* 32, 413-419.
- Greenfield, S. A. (1984). Acetylcholinesterase may have novel functions in the brain. *Trends Neurosci* 7, 364-368.
- Greenfield, S. A. (1991). A noncholinergic action of acetylcholinesterase (AChE) in the brain: from neuronal secretion to the generation of movement. *Cell Mol Neurobiol* 11, 55-77.

- Grifman, M., Galyam, N., Seidman, S., and Soreq, H. (1998). Functional redundancy of acetylcholinesterase and neurologin in mammalian neuritogenesis. *Proc Natl Acad Sci U S A* *95*, 13935-13940.
- Grisaru, D., Lev-Lehman, E., Shapira, M., Chaikin, E., Lessing, J. B., Eldor, A., Eckstein, F., and Soreq, H. (1999a). Human osteogenesis involves differentiation-dependent increases in the morphogenetically active 3 alternative splicing variant of acetylcholinesterase. *Mol Cell Biol* *19*, 788-795.
- Grisaru, D., Sternfeld, M., Eldor, A., Glick, D., and Soreq, H. (1999b). Structural roles of acetylcholinesterase variants in biology and pathology. *Eur J Biochem* *264*, 672-686.
- Haas, R., Jackson, B. C., Reinhold, B., Foster, J. D., and Rosenberry, T. L. (1996). Glycoinositol phospholipid anchor and protein C-terminus of bovine erythrocyte acetylcholinesterase: analysis by mass spectrometry and by protein and DNA sequencing. *Biochem J* *314*, 817-825.
- Hoffman, B. B., Lefkowitz, R. J., and Taylor, P. (1996). Neurotransmission: the autonomic and somatic motor nervous systems. In Goodman & Gilman's *The Pharmacological Basis of Therapeutics*, J. G. Hardman and L. E. Limbird, eds. (New York: McGraw-Hill), pp. 105-139.
- Hortsch, M., Patel, N. H., Bieber, A. J., Traquina, Z. R., and Goodman, C. S. (1990). Drosophila neurotactin, a surface glycoprotein with homology to serine esterases, is dynamically expressed during embryogenesis. *Development* *110*, 1327-1340.
- Inestrosa, N. C., and Alarcon, R. (1998). Molecular interactions of acetylcholinesterase with senile plaques. *J Physiol Paris* *92*, 341-344.
- Inestrosa, N. C., Alvarez, A., Perez, C. A., Moreno, R. D., Vicente, M., Linker, C., Casanueva, O. I., Soto, C., and Garrido, J. (1996). Acetylcholinesterase accelerates assembly of amyloid-beta-peptides into Alzheimer's fibrils: possible role of the peripheral site of the enzyme. *Neuron* *16*, 881-891.
- Karpel, R., Ben Aziz Aloya, R., Sternfeld, M., Ehrlich, G., Ginzberg, D., Tarroni, P., Clementi, F., Zakut, H., and Soreq, H. (1994). Expression of three alternative acetylcholinesterase messenger RNAs in human tumor cell lines of different tissue origins. *Exp Cell Res* *210*, 268-277.
- Karpel, R., Sternfeld, M., Ginzberg, D., Guhl, E., Graessmann, A., and Soreq, H. (1996). Overexpression of alternative human acetylcholinesterase forms modulates process extensions in cultured glioma cells. *J Neurochem* *66*, 114-123.
- Kaufer, D., Friedman, A., Seidman, S., and Soreq, H. (1998). Acute stress facilitates long-lasting changes in cholinergic gene expression. *Nature* *393*, 373-377.
- Kaufer, D., Friedman, A., Seidman, S., and Soreq, H. (1999). Anticholinesterases induce multigenic transcriptional feedback response suppressing cholinergic neurotransmission. *Chem Biol Interact* *119-120*, 349-360.
- Koenigsberger, C., Chiappa, S., and Brimijoin, S. (1997). Neurite differentiation is modulated in neuroblastoma cells engineered for altered acetylcholinesterase expression. *J Neurochem.* *69*, 1389-1397.
- Lapidot Lifson, Y., Patinkin, D., Prody, C. A., Ehrlich, G., Seidman, S., Ben Aziz, R., Benseler, F., Eckstein, F., Zakut, H., and Soreq, H. (1992). Cloning and antisense oligodeoxynucleotide inhibition of a human homolog of *cdc2* required in hematopoiesis. *Proc Natl Acad Sci U S A* *89*, 579-583.
- Layer, P. G. (1991). Cholinesterases during development of the avian nervous system. *Cell Mol Neurobiol* *11*, 7-33.
- Layer, P. G. (1990). Cholinesterases preceding major tracts in vertebrate neurogenesis. *Bioessays* *12*, 415-420.
- Layer, P. G., Alber, R., and Sporns, O. (1987). Quantitative development and molecular forms of acetyl- and butyrylcholinesterase during morphogenesis and synaptogenesis of chick brain and retina. *J Neurochem* *49*, 175-182.
- Lev-Lehman, E., Broide, E. S., Evron, T., Meshorer, E., Ariel, E., and Soreq, H. (2000). Synaptogenesis and myopathy under acetylcholinesterase overexpression. *J. Mol. Neurosci.*, (in press).

- Lev-Lehman, E., Deutsch, V., Eldor, A., and Soreq, H. (1997). Immature human megakaryocytes produce nuclear-associated acetylcholinesterase. *Blood* 89, 3644-3653.
- Li, Y., Camp, S., Rachinsky, T. L., Getman, D., and Taylor, P. (1991). Gene structure of mammalian acetylcholinesterase. Alternative exons dictate tissue-specific expression. *J Biol Chem* 266, 23083-23090.
- Malinger, G., Zakut, H., and Soreq, H. (1989). Cholinceptive properties of human primordial, pre-antral and antral oocytes: In situ hybridization and biochemical evidence for expression of cholinesterase genes. *J Molec Neuroscience* 1, 77-84.
- Massoulie, J., Anselmet, A., Bon, S., Krejci, E., Legay, C., Morel, N., and Simon, S. (1998). Acetylcholinesterase: C-terminal domains, molecular forms and functional localization. *J Physiol Paris* 92, 183-190.
- Mesulam, M., Carson, K., Price, B., and Geula, C. (1992). Cholinesterases in the amyloid angiopathy of Alzheimer's disease. *Ann Neurol* 31, 565-569.
- Munoz, F. J., and Inestrosa, N. C. (1999). Neurotoxicity of acetylcholinesterase amyloid beta-peptide aggregates is dependent on the type of Aβ peptide and the AChE concentration present in the complexes. *FEBS Lett* 450, 205-209.
- Navaratnam, D. S., Priddle, J. D., McDonald, B., Esiri, M. M., Robinson, J. R., and Smith, A. D. (1991). Anomalous molecular form of acetylcholinesterase in cerebrospinal fluid in histologically diagnosed Alzheimer's disease. *Lancet* 337, 447-50.
- Noda, S., Lammerding-Koppel, M., Oetting, G., and Drews, U. (1998). Characterization of muscarinic receptors in the human melanoma cell line SK-Mel-28 via calcium mobilization. *Cancer Lett* 133, 107-114.
- Ogane, N., Giacobini, E., and Messamore, E. (1992). Preferential inhibition of acetylcholinesterase molecular forms in rat brain. *Neurochem Res* 17, 489-495.
- Patinkin, D., Lev-Lehman, E., Zakut, H., Eckstein, F., and Soreq, H. (1994). Antisense inhibition of butyrylcholinesterase gene expression predicts adverse hematopoietic consequences to cholinesterase inhibitors. *Cell Mol Neurobiol* 14, 459-73.
- Paulus, J. M., Maigne, J., and Keyhani, E. (1981). Mouse megakaryocytes secrete acetylcholinesterase. *Blood* 58, 1100-1106.
- Saez-Valero, J., Sberna, G., McLean, C. A., Masters, C. L., and Small, D. H. (1997). Glycosylation of acetylcholinesterase as diagnostic marker for Alzheimer's disease. *Lancet* 350, 929.
- Saez-Valero, J., Sberna, G., McLean, C. A., and Small, D. H. (1999). Molecular isoform distribution and glycosylation of acetylcholinesterase are altered in brain and cerebrospinal fluid of patients with Alzheimer's disease. *J Neurochem* 72, 1600-1608.
- Sastry, B. V., Janson, V. E., and Chaturvedi, A. K. (1981). Inhibition of human sperm motility by inhibitors of choline acetyltransferase. *J Pharmacol Exp Ther* 216, 378-384.
- Sberna, G., Saez Valero, J., Beyreuther, K., Masters, C. L., and Small, D. H. (1997). The amyloid beta-protein of Alzheimer's disease increases acetylcholinesterase expression by increasing intracellular calcium in embryonal carcinoma P19 cells. *J Neurochem* 69, 1177-1184.
- Seidman, S., Eckstein, F., Grifman, M., and Soreq, H. (1999). Antisense technologies have a future fighting neurodegenerative diseases. *Antisense Nucleic Acid Drug Dev* 9, 333-340.
- Shohami, E., Kaufer, D., Chen, Y., Cohen, O., Ginzberg, D., Melamed-Book, N., Seidman, S., Yirmiya, R., and Soreq, H. (2000). Antisense prevention of neuronal damages following head injury in mice. *J. Mol. Med.* (in press).
- Soreq, H., Katz, A., Richler, C., Malinger, G., and Zakut, H. (1990). Expression of cholinesterase genes in human germline cells: implications on reproduction. *Is J Obst Gynecol* 1, 111-113.
- Soreq, H., Patinkin, D., Lev-Lehman, E., Grifman, M., Ginzberg, D., Eckstein, F., and Zakut, H. (1994). Antisense oligonucleotide inhibition of acetylcholinesterase gene expression induces progenitor cell expansion and suppresses hematopoietic apoptosis ex vivo. *Proc Natl Acad Sci U S A* 91, 7907-7911.

- Sternfeld, M., Ming, G., Song, H., Sela, K., Timberg, R., Poo, M., and Soreq, H. (1998a). Acetylcholinesterase enhances neurite growth and synapse development through alternative contributions of its hydrolytic capacity, core protein, and variable C termini. *J Neurosci* 18, 1240-1249.
- Sternfeld, M., Patrick, J. D., and Soreq, H. (1998b). Position effect variegations and brain-specific silencing in transgenic mice overexpressing human acetylcholinesterase variants. *J Physiol Paris* 92, 249-255.
- Thal, L. J., Schwartz, G., Sano, M., Weiner, M., Knopman, D., Harrell, L., Bodenheimer, S., Rossor, M., Philpot, M., Schor, J., and Goldberg, A. (1996). A multicenter double-blind study of controlled-release physostigmine for the treatment of symptoms secondary to Alzheimer's disease. Physostigmine Study Group. *Neurology* 47, 1389-1395.
- Weikert, T., Rathjen, F. G., and Layer, P. G. (1990). Developmental maps of acetylcholinesterase and G4-antigen of the early chicken brain: long-distance tracts originate from AChE-producing cell bodies. *J Neurobiol* 21, 482-498.
- Wright, C. I., Guela, C., and Mesulam, M. M. (1993). Protease inhibitors and indoleamines selectively inhibit cholinesterases in the histopathologic structures of Alzheimer disease. *Proc Natl Acad Sci U S A* 90, 683-686.
- Zakut, H., Ehrlich, G., Ayalon, A., Prody, C. A., Malinger, G., Seidman, S., Ginzberg, D., Kehlenbach, R., and Soreq, H. (1990). Acetylcholinesterase and butyrylcholinesterase genes coamplify in primary ovarian carcinomas. *J Clin Invest* 86, 900-908.

# 4

## Novel roles for cholinesterases in stress and inhibitor responses

*Hermona Soreq, David Glick*

The first and best known function of acetylcholinesterase (AChE), termination of cholinergic neurotransmission by hydrolysis of acetylcholine (ACh), stimulated the development of organophosphate compounds that were potent cholinesterase (ChE) inhibitors and which found uses as insecticides and chemical warfare agents. More recently, several therapeutic uses have been established for some of these and carbamate anti-ChEs.<sup>1</sup> With the growing recognition of new roles for AChE and butyrylcholinesterase (BuChE), it is appropriate to re-explore the effects of ChE inhibitors and the first steps toward novel approaches to the therapeutic suppression of excess ChE activities.

### *BuChE operates as a scavenger of anti-ChEs*

As a catalyst, BuChE is very similar to AChE. It is less specific for the acetate ester of choline, and it is inhibited by a wider spectrum of compounds, but as a catalyst, it is almost as efficient as AChE.<sup>2</sup> The two human proteins are also similar in sequence and tertiary structure. Their separate identities were established by cloning the two respective genes,<sup>3,4</sup> and locating them on separate chromosomes: *BCHE* to 3q26-*ter*<sup>5,6</sup> and *ACHE* to 7q22<sup>7,8</sup> (Fig. 4.1). Although AChE is the primary ChE of the nervous system and BuChE is present largely in the serum, BuChE was long

thought to be a 'back-up' to AChE.

Inconsistent with a role as a terminator of neurotransmission is the highly polymorphic nature of the *BCHE* gene. Over 40 natural mutations have been identified which result in distinct gene products (Fig. 4.2). These mutations generate a range of proteins, including some which are functionally indistinguishable from the typical BuChE, as well as others having no hydrolytic activity whatsoever.<sup>10</sup> That such mutations persist in the population without obvious detriment, even to homozygous carriers, is a good indication that whatever function BuChE performs it is non-essential. However, some BuChE mutations confer a genetic predisposition to adverse responses to AChE inhibitors.<sup>11</sup>

Because of the broad specificity of BuChE, every anti-AChE is also an anti-BuChE. An anti-AChE entering the body will react with BuChE before ever coming into contact with AChE at neuromuscular junctions or brain synapses. The individual is thus protected by the ability of BuChE to absorb AChE inhibitors. Consistent with being a molecular decoy for AChE are also the prominence of BuChE in the serum, its capacity to react quickly with a wide spectrum of compounds, and even the polymorphism of its gene. The polymorphism of *BCHE* has been surveyed extensively, originally by studying the variant characteristic susceptibility to inhibitors of the serum activity<sup>11</sup> and more recently by molecu-

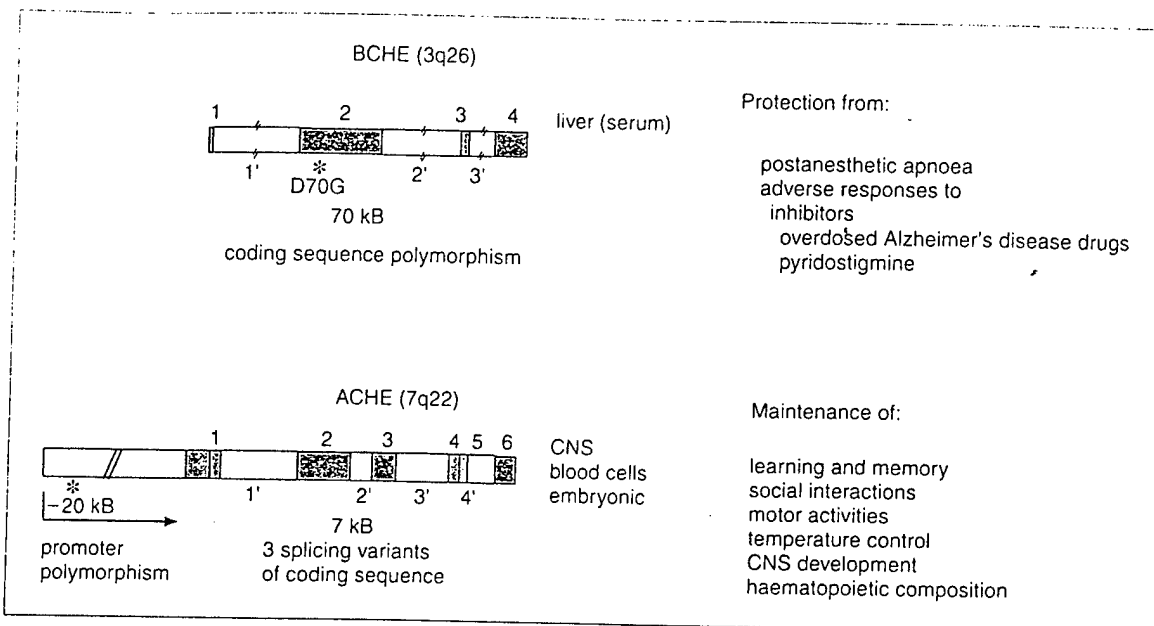


**Figure 4.1**

*The human cholinesterase genes. The BCHE gene, located on chromosome 3q26, is expressed in the liver and its BuChE protein secreted into the serum. (It also is expressed in the nervous system and, transiently, in many embryonic tissues.<sup>9</sup>) Of the known natural mutations, the most prominent is the D70G ('atypical') substitution (green asterisk). The biological role of BuChE appears to be as a decoy to protect AChE from inhibition. The AChE gene, AChE, located on chromosome 7q22, is expressed in the nervous system and in developing tissues. Polymorphisms 17 kb upstream from the coding sequence affect expression. Besides its classical role in neurotransmission, it appears to be involved in the plasticity of cholinergic and non-cholinergic neuronal tissues and in developing tissues, such as bone marrow.*

lar genotyping.<sup>13</sup> A common variant is 'atypical' BuChE, the product of a single base substitution which replaces aspartate with glycine at the secondary substrate/inhibitor binding site<sup>14-16</sup> (see Fig. 4.2). As a consequence, 'atypical' BuChE has a lower affinity for many inhibitors and unnatural substrates. Under normal conditions, this has no adverse consequences. However, anesthesiologists use the anti-AChE succinylcholine as a muscle relaxant, and for recovery depend upon its slow hydrolysis by BuChE. Homozygous carriers of

'atypical' BCHE show a much delayed return to spontaneous breathing following the use of succinylcholine. Less drastic effects, such as slower than normal recovery of spontaneous breathing, may be the consequence of dietary intake of natural anti-AChEs.<sup>19</sup> The very uneven geographical distribution of 'atypical' BCHE, with high or low frequencies notable among historically isolated groups, may reflect an evolutionary adaptation to local environment factors. One hypothesis concerns the interplay of the presence of mildly inhibitory

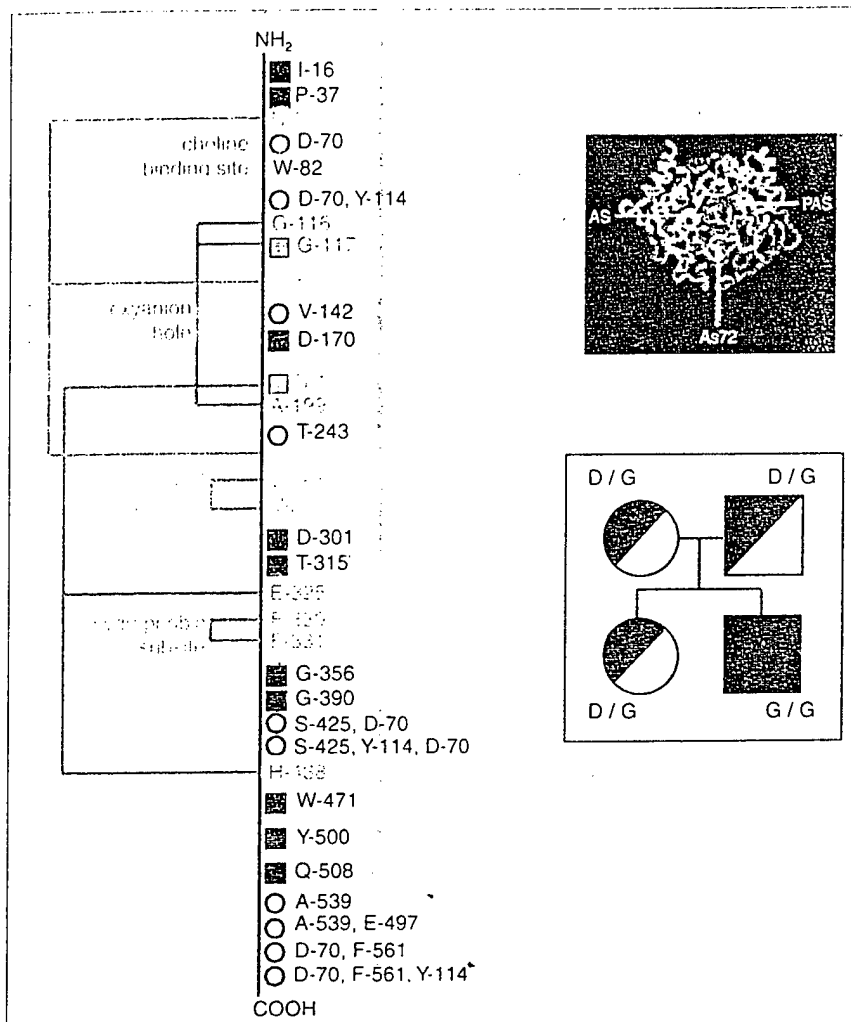


**Figure 4.2**  
 Natural mutations of BCHE. Among the sites in BuChE at which mutations have been localized<sup>10,12,17</sup> are the catalytic triad (green-blue), the acyl binding site (green), the choline binding site (magenta), the oxyanion hole (blue) and the peripheral anionic site (red-orange). The squares indicate mutations that abolish catalytic activity; the circles indicate mutations that result in moderate changes in activity. (a) A ribbon diagram of Torpedo AChE, showing the catalytic triad active site (AS), peripheral anionic site (PAS) and the aspartate residue, which is the cognate of D70 of human BuChE. The end of the helix in the upper left is the site of attachment of the carboxy-terminal residue, which is indistinct in the X-ray crystallography model.<sup>18</sup> (b) The pedigree of a soldier who carries two copies of the D70G 'atypical' BCHE mutation (filled square), and who displayed post-anaesthesia apnoea under succinylcholine administration, as well as deep depression, insomnia and massive weight loss following pyridostigmine treatment during the Gulf War.<sup>11</sup> In the failure of the 'atypical' enzyme to protect AChE from this anti-AChE, this case history strikingly illustrates the role of the typical BuChE as an anti-AChE scavenger.

alkaloids in *Solanaceae* food plants (potatoes, tomatoes, aubergines and peppers) and the appearance of BuChE in the placenta, to explain the co-occurrence of a high frequency of the 'atypical' allele and the traditional consumption of these foods; because 'atypical' BuChE has a low affinity for these alkaloids, it survives to play other protective roles during pregnancy.<sup>20,21</sup>

### *Multi-organ indications of non-catalytic roles*

The occurrence of AChE on the surface of erythrocytes is a paradox of long standing: there, it has no known cholinergic role. Early hints at non-classical roles for AChE and BuChE came from their presence in non-neuronal tissues such as the blood cells,<sup>22,23</sup> developing avian cartilage<sup>24</sup> and developing oocytes and sperm,<sup>25,26</sup> where no catalytic role for AChE is likely. Also, within the nervous system there is not always a correlation between the occurrence of AChE and other cholinergic proteins.<sup>27-29</sup> Furthermore, non-neuronal brain cells, the meninges,<sup>30</sup> blood vessel endothelium<sup>31</sup> and glia<sup>32</sup> also express AChE. Genomic studies have placed AChE in other unexpected contexts. The human *ACHE* gene undergoes massive amplification under diverse conditions: leukaemias,<sup>33</sup> ovarian carcinomas,<sup>34</sup> thrombocytopenia<sup>35</sup> and exposure to organophosphate ChE inhibitors.<sup>36</sup> These first indications of unexpected long-term danger in exposure to ChE inhibitors initiated a systematic search for cells and tissues in which *CHE* genes are expressed. As expected, expression of *ACHE*, i.e. the presence of the corresponding mRNA, was prominent in mammalian brain, but surprisingly AChE and BuChE mRNA were observed also in developing human oocytes,<sup>26</sup> which correlates with the report of an inherited amplification of the *BCHE* gene following

exposure to insecticides. Human *CHE* expression was also observed in primary carcinomas,<sup>37</sup> placental chorionic villi,<sup>38</sup> developing blood cells<sup>39</sup> and embryonic bone.<sup>40</sup> The ubiquitous expression of human *CHEs* in developing tissues reinforced the hypothesis that these proteins are involved in function(s), beyond ACh hydrolysis. Also, cytological and functional studies of neurons indicated a correlation of AChE with the morphology of neurites, which was not easily explained solely by the cholinergic function of these structures.<sup>41-43</sup>

### *Alternative splicing leads to AChE variants with distinct structural functions*

The single *ACHE* gene may give rise to different protein products by alternative splicing in the coding region of the original transcript. Production of carboxy-terminal (C-terminal) variant protein isoforms was observed in embryonic tissues<sup>44</sup> and in tumour cell lines.<sup>32</sup> Among the consequences of this alternative splicing are synaptic or epidermal accumulation of C-terminal distinct AChE isoforms in *Xenopus* tadpoles,<sup>45</sup> modulation of process extension in rat glioma cells<sup>46</sup> and induction of neurite growth in cultured *Xenopus* motor neurons.<sup>47</sup> Most of these functions of AChE are independent of its catalytic ability, as they survive insertion of a seven-residue polypeptide sequence into the active site.

A schematic diagram of alternative splicing in the coding region of human AChE mRNA is shown in Fig. 4.3. In all three *ACHE* mRNAs the common core, exons 2, 3 and 4, is sufficient for catalytic activity of the protein. Alternate splicing gives rise to AChE isoforms with different C-termini; these confer characteristic hydrodynamic properties, capacities for multimerization and/or attachment to



### Readthrough AChE accumulates following stress

In vivo and in cultured hippocampal brain slices, long-lasting accumulation of readthrough AChE is induced in response to acute stress and to anti-ChE exposure<sup>39</sup>

(Fig. 4.4). In the short term, excess of AChE-R would be advantageous, as it can suppress the initial excitation state by enhancing ACh hydrolysis. However in the long term, this accumulation may be harmful. Many of the delayed consequences of inhibitor exposure, notably cognitive impairments and neuro-

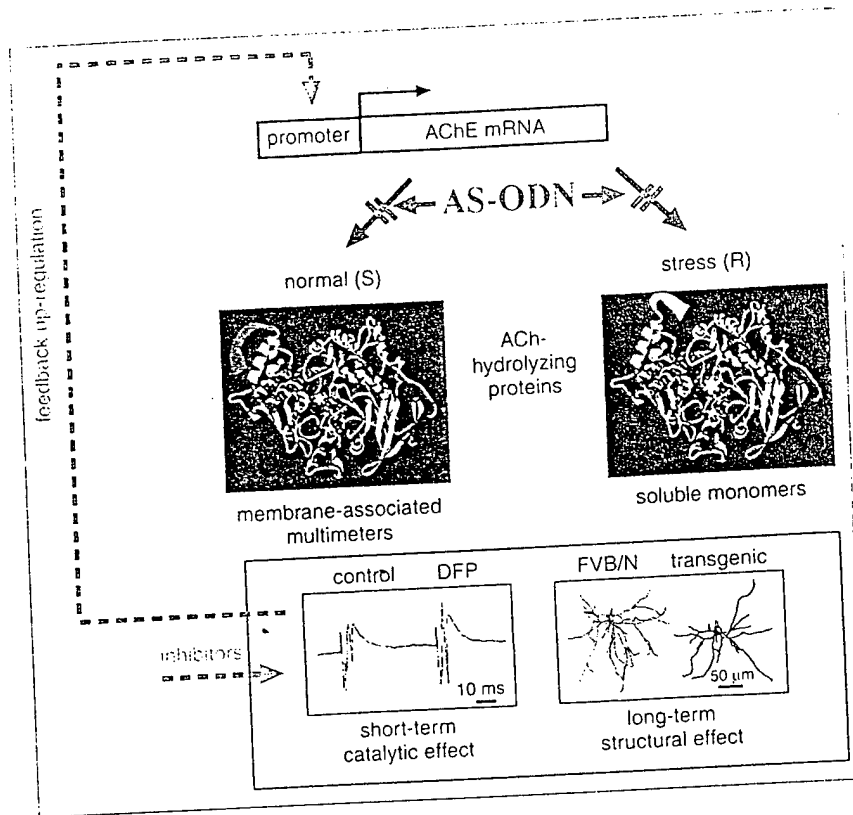


**Figure 4.4** Feedback regulation of AChE expression. Inhibition of synaptic AChE-S, for instance by an organophosphate, causes changes in neurotransmission, evident as increases in the electrophysiological excitation due to inhibition of membrane-associated AChE-S multimers (short-term) (lower left inset). At the transcriptional control level, such excitation leads to c-fos and/or egr-mediated increase in AChE gene expression (arrow pointing right) and causes accumulation of extrasynaptic AChE-R soluble monomers. AChE accumulation is associated with long-term structural effects on neuron morphology and plasticity. This is evident, among other pathologies, as thinning of the dendritic trees of pyramidal neurons in the somatosensory cortex of AChE transgenic mice (lower right inset). This feedback, and the expression of all variants (see Fig. 4.6), as such agents prevent oligodeoxynucleotides (AS-ODNs) targeted to the AChE gene, may be blocked by antisense AChE accumulation, reducing the catalytic and structural effects associated with AChE overproduction.

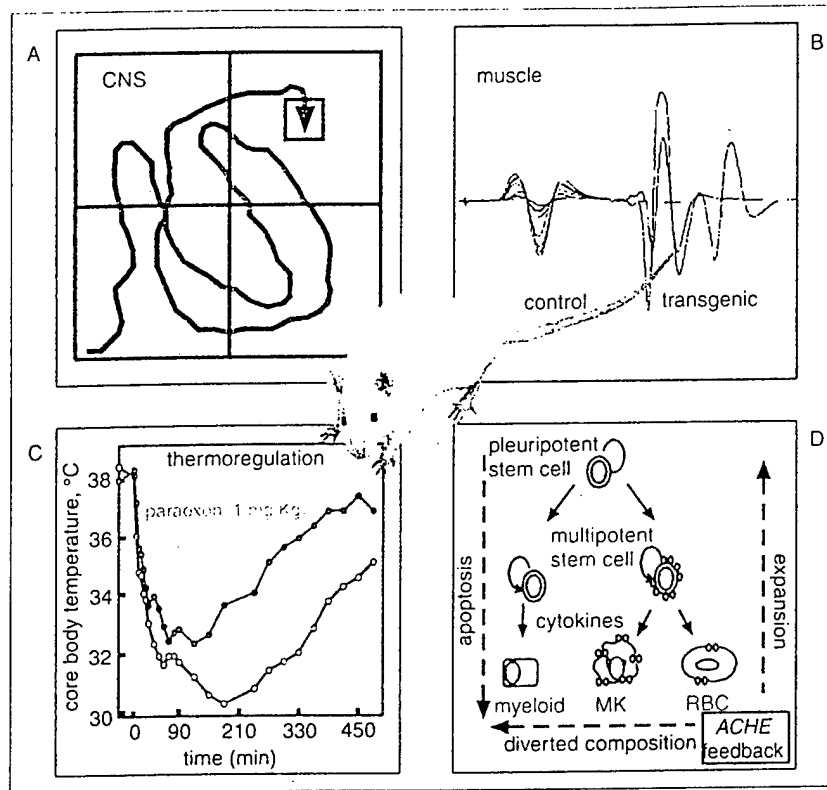


**Figure 4.5**

*Multi-organ consequences of AChE overproduction. AChE-transgenic mice, which overexpress AChEs in their brain neurons, have been characterized as suffering cognitive impairments, evident as failure to perform the Morris water maze tasks (CNS: a).<sup>56</sup> They also display progressive neuromotor deterioration, evident as rapid fatigue in their electromyographic response (muscle; b).<sup>51</sup> At the level of drug responses, these mice fail to adjust their body temperature under paraoxon exposure (thermoregulation: c).<sup>50</sup> In cultured primary haematopoietic cells, AChE overproduction is associated with enhanced expansion of multipotent stem cells and diversion of their differentiation toward myeloid lineages<sup>57</sup> (D Grisaru, unpublished observations).*

tor deficits, are strikingly similar to effects noted in transgenic mice that express human AChE (hAChE) in their CNS<sup>50,51</sup> (Fig. 4.5 (a,b)). What these experimental models have in common is elevated levels of AChE-R, due, in the case of exposure to anti-ChEs, to long-term up-regulation of AChE expression, and in the case of AChE-transgenic animals, to

increased gene dose. Under normal conditions, the blood-brain barrier is practically impermeable to many AChE inhibitors, especially those that are not lipophilic.<sup>52</sup> However, under acute psychological stress, there is an efficient penetration by inhibitors and other large compounds of the blood-brain barrier.<sup>53</sup> This would lead to AChE-R accumulation through

the above-described feedback response. However, our transgenic animal studies suggested that elevated levels of AChE are harmful, and indeed, this is supported by findings in a study of closed-head-injury animals (E. Shohami, unpublished observations). The extent of neuronal survival and recovery (evaluated from a panel of physical performance tasks to which injured animals were subjected) were both decreased in AChE-S-transgenic mice as compared to controls. Stress-induced accumulation of AChE-R was also observed in blood. To investigate this issue, the haematopoietic response to stress was mimicked *in vitro* by submitting human umbilical stem cells to hydrocortisone levels which are characteristic of stress and noting the accumulation of both AChE-R and its C-terminal peptide. Surprisingly, a synthetic peptide representing the 26 C-terminal residues of AChE-R improved the survival of cultured human stem cells, potentiated their AChE-R mRNA levels and enhanced their *ex vivo* expansion by early acting cytokines (D. Grisaru, unpublished observations). These findings identify the C-terminal peptide of AChE-R as an autoregulatory stress-responsive haematopoietic element promoting the myeloid and megakaryocytic expansion characteristic of acute and chronic stress responses.

### *Novel transgenic animal models reveal cortical neuropathologies*

Besides the extensively studied hAChE-S-transgenic mouse, additional transgenic strains have been created:<sup>54</sup> two transgenics for human AChE-R, and another which expresses a control variant of AChE-S that is catalytically inactive because of a seven-residue peptide inserted near the active site (IN-AChE-S).

Immunohistochemical detection of neurofilaments revealed in the brains of these mice pathological 'corkscrew' patterns of curled axons with sinusoidal regularity at the somatosensory cortex. Cumulative length measurements of these processes demonstrated a significantly more severe pathology in brains of AChE-S and IN-AChE-S transgenics than in AChE-R transgenics or non-transgenic controls. Corkscrew pathology is known to occur in degenerating cortical pyramidal neurons following exposure to phencyclidine (PCP), which blocks NMDA receptors of cortical  $\gamma$ -aminobutyric acid releasing (GABAergic) interneurons.<sup>55</sup> However, GABAergic cell counts and morphological properties of transgenic somatosensory cortices were indistinguishable from controls, suggesting that the corkscrew phenotype reflects acutely imbalanced cholinergic inputs to pyramidal neurons due to AChE-S overproduction. The neuropathologies of IN-AChE-S mice indicate that deleterious consequences of AChE increases, induced by AChE inhibitors, are primarily due to the structural properties of AChE and may therefore occur also in the presence of the inhibitor-blocked enzyme. At the same time, the limited pathology in AChE-R transgenics indicates that this soluble, extrasynaptic protein is designed to cause minimal damage under conditions of its stress-induced overproduction.

Very possibly AChE mediates other stress-related responses that are currently being investigated. Closed-head injury increases the risk of late-onset neuropathologies in humans.<sup>58</sup> It also promotes cholinergic hyperexcitation and facilitates initiation of the feedback loop of AChE overproduction (E. Shohami, unpublished observations). This denotes a convergent outcome of acute psychological stress, chemical inhibition and traumatic injury. Together with the demonstration that a long-term excess of AChE promotes

neurodeterioration, this suggests that elevated expression of *ACHE* due to various initial causes, may mediate delayed neurodegenerative deterioration. This further implies that genetic variabilities which affect the activity of the *CHE* genes or their protein products represent important risk factors that can determine susceptibility to neurodeterioration.

### *Implications for anti-AChE therapies*

AChE inhibitors are increasingly used in therapy. They had long been used to treat glaucoma (the organophosphate, tetraiso-propylpyrophosphoramidate) and some symptoms of myasthenia gravis (the carbamate, physostigmine).<sup>1</sup> More recently, and much more extensively, they have been used to protect soldiers from the anticipated use of chemical warfare agents (pyridostigmine) and as Alzheimer disease (AD) drugs (tacrine, donepezil, rivastigmine, etc.). If our findings in experimental animals are applicable to humans, and we fear they are, the short-term benefits of AChE inhibitor therapies will have to be weighed against the long-term dangers of neuromuscular and cognitive deterioration.<sup>59</sup> In fact, the danger is posed not only by the use of AChE inhibitors, but also by any condition that results in long-term up-regulation of AChE, such as seen in the closed-head injury and stressed animals.

The use of AChE inhibitors for treatment of neurodegenerative diseases is a rational approach to cholinergic imbalances.<sup>60,61</sup> Deficient cholinergic neurotransmission, it was reasoned, can be enhanced by partially blocking the hydrolysis of the neurotransmitter through the inhibition of AChE. (However, the presence of AChE in the pathological AD plaques<sup>62</sup> and its potential function in their formation,<sup>63</sup> complicate this neat picture.)

Until very recently, the only established function of AChE was termination of cholinergic neurotransmission. Therefore, all of the consequences of its inhibition might be evaluated by the efficiency of inhibition of AChE enzymatic activity and observation of cholinergic processes, such as cognition in AD patients. Now that additional functions of AChE are established, the effects of AChE inhibitors must be more broadly considered. This is especially so as one of these newly recognized effects is the up-regulation of *ACHE* expression and the other concerns changes in neurite growth. We see abnormal responses to anti-AChE as well as detrimental effects of AChE overproduction in experimental animals,<sup>54,56</sup> and suspect that they will be recognized in humans, as well. In line with this is the finding that in anti-AChE treatment of AD patients, the amelioration of cognitive decline is both limited and temporary.

### *Toward genome-based antisense therapy*

That the morphological effects of AChE are unrelated to the catalytic capacity of AChE warns us that the detrimental consequences of elevated AChE will not necessarily be alleviated by AChE inhibitors. Moreover, the feedback response to such inhibition increases the amount of the AChE protein in the brain of treated patients (A Nordberg, personal communication). Therefore, we have investigated the effects of blocking ChE production by specifically interfering with *ACHE* expression. Antisense oligodeoxynucleotides (AS-ODNs) targeted to AChE mRNA suppressed the development of cultured platelet-forming megakaryocytes.<sup>17</sup> Conversely, the subsequent increases in AChE-R were associated with induced progenitor cell expansion and suppressed haematopoietic apoptosis<sup>64</sup> (see Fig. 4.5(d)). An antisense cRNA, capable of

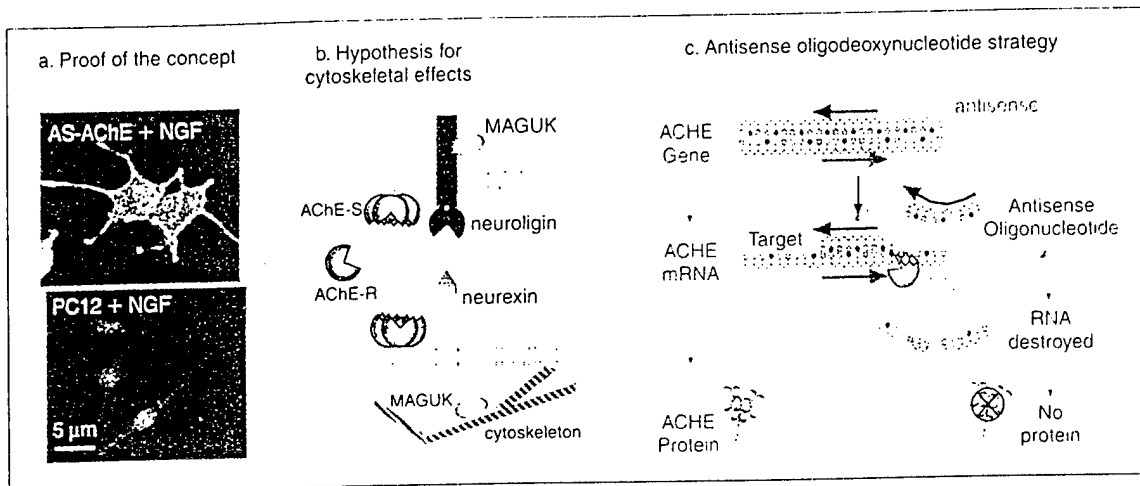


**Figure 4.6**

The antisense approach to suppression of AChE production. (a) Proof of the concept. When treated with nerve growth factor (NGF), PC12 cells extend neurites and express the AChE protein, detected on the cell surface with an antibody directed against the core AChE protein and visualized with a fluorescein-labelled secondary antibody (top). Transfection with a DNA plasmid encoding antisense AS-AChE cRNA to exon 6 yielded a stable phenotype with 80% lowered AChE levels and failure to extend neurites under NGF (bottom). Retransfection of the AS-AChE cells with vectors encoding catalytically active or inactive AChE or the AChE-homologous protein, neuroigin, rescued the neurite extension capacity of AS-AChE cells.<sup>65</sup> This proves that antisense suppression can deplete neurons of their AChE protein, that such depletion reversibly impairs neurite growth and that in affecting this growth process, AChE competes with neuroigin. (b) Hypothesis for cytoskeletal effects. AChE-S multimers, but not AChE-R monomers, associate with the plasma membrane through their amphipathic C-terminal tail and/or structural subunits (e.g. ColQ tails<sup>67</sup>). Proteins with single transmembrane domains and with AChE-like extracellular domains, such as neuroigin, can transduce signals into the cell which expresses them through interactions of their cytoplasmic carboxy-terminal domains with membrane-associated guanylate kinase (MAGUK) proteins. Extracellular interaction of neuroigin with neurexin<sup>68</sup> would further transduce signals, through yet other MAGUK proteins, into the other cell. MAGUK proteins are known to modulate the properties of cytoskeletal elements, thus potentially affecting neurite growth.<sup>69,70</sup> Therefore, competition between AChE-S and/or AChE-R and neuroigin (or, possibly, other AChE-like proteins), can explain the involvement of AChE with neuritogenesis, synapse plasticity under drug exposure and stress and perhaps the disruption of blood-brain barrier under stress. (c) Antisense oligodeoxynucleotide strategy. The 'sense' strand (rightward arrow) of the AChE gene is transcribed to yield the AChE mRNA product. Chemically protected 'antisense' oligonucleotides are directed inversely and form DNA-mRNA hybrids with their target AChE mRNA.<sup>66</sup> These hybrids are destroyed by induced RNase activities, preventing production of the AChE protein and reducing both its catalytic and its non-catalytic activities.<sup>71</sup>

suppressing AChE activity, suppressed neurite growth in mammalian neuroendocrine PC12 cells cultured with nerve growth factor.<sup>65</sup> Neurite growth was rescued by retransfecting

these cells (Fig. 4.6(a)) with the AChE-homologous protein, neuroigin, which was the basis for our theory of the redundant function of these two proteins (Fig. 4.6(b)).

Following characterization and optimization of AS-ODNs in cultured cells,<sup>66</sup> AS-AChEs are being used *in vivo* for improving recovery from injury and for enhancing short-term memory in the cognitively impaired transgenic mice with excess human AChE-S in their neurons.

Intracerebroventricular injection of 1 µg/kg doses of AS-AChE ODNs (Fig. 4.6(c)) reduces AChE-R levels and improves short-term memory for at least 24 h at similar efficiency with the AD drug tacrine, which is used in 1000-fold higher doses and at closely spaced intervals.<sup>72</sup> In developing the next generation of antisense agents, we have synthesized selective ribozymes for catalytic destruction of AChE mRNA transcripts.<sup>73</sup> If successful, such agents may lead to a novel approach for therapeutic suppression of AChE levels in those diseases where conventional inhibitors are now being used.

## Discussion

Accumulated findings implicate genetic polymorphism and recently described regulatory processes that control expression of the *CHE* genes in unexpected responses to ChE inhibitors. In particular, induction of a prolonged and exaggerated *ACHE* expression, associated with both immediate and long-term changes in ACh metabolism following acute psychological stress, closed-head injury (itself, a known AD risk factor) and exposure to ChE inhibitors. All of these insults elicit rapid, transient excitation of cholinergic neurons in the CNS. Such excitation activates a feedback response that dramatically up-regulates AChE production, mediated by early immediate transcription factors such as *c-fos* and *egr*<sup>74</sup> and dependent on increases in free intracellular calcium. Together with parallel down-regulation of the genes encoding the ACh-synthesiz-

ing and ACh-packaging proteins choline acetyltransferase and vesicular ACh transporter, this leads to delayed yet persistent suppression of electrophysiological activity in the hippocampus.<sup>75</sup> This response causes, within 1 h and for at least several days, a beneficial calming of brain hyperactivity by suppression of the increased ACh levels. However, studies with AChE-transgenic mice suggest that excesses of the AChE protein in neurons can also cause late-onset limitation of dendrite branching and depletion of dendritic spines (i.e. impaired networks) in cortical pyramidal neurons. This leads to progressively impaired performance in tests of memory and muscle strength. These findings suggest that at least some of the delayed phenomena induced by AChE excess are caused by the AChE protein *per se*, independently of its hydrolytic activity.

The biomedical and environmental implications of hAChE research indicate that genomic polymorphisms in the coding sequence and/or promoters of the *ACHE* and *BCHE* genes (and possible additional loci) may modulate individual responses to ChE inhibitors in a complex and yet not fully predictable manner, affecting both the nervous and the haematopoietic systems. Recent cosmid sequencing and genotyping efforts have revealed novel polymorphisms in the *ACHE* upstream promoter sequence.<sup>76</sup> Such polymorphisms can alter *ACHE* expression and/or properties, affecting both short- and long-term manifestations of cholinergic functions in a manner that may increase the risk for neurodegenerative disease due to physical, chemical or psychological insults.

## Acknowledgements

This research has been supported by grants from the US Army Medical Research and Development Command (DAMD 17-97-1-

7007), the Israel Science Foundation (590/97), the US-Israel Binational Science Foundation (96-00110) and Ester Neuroscience, Ltd.

## References

1. Taylor P. Agents acting at the neuromuscular junction and autonomic ganglia. In: Hardman JG, Limbird LE, Molinoff PB, Ruddon RW, eds. *Goodman and Gilman's The Pharmacological Basis of Therapeutics*. New York: McGraw-Hill, 1996: 177-197.
2. Chatonnet A, Lockridge O. Comparison of butyrylcholinesterase and acetylcholinesterase. *Biochem J* 1989; 260: 625-634.
3. Prody CA, Zevin-Sonkin D, Gnatt A, Goldberg O, Soreq H. Isolation and characterization of full-length cDNA clones coding for cholinesterase from fetal human tissues. *Proc Natl Acad Sci USA* 1987; 84: 3555-3559.
4. Soreq H, Ben-Aziz R, Prody CA *et al*. Molecular cloning and construction of the coding region for human acetylcholinesterase reveals a G + C-rich attenuating structure. *Proc Natl Acad Sci USA* 1990; 87: 9688-9692.
5. Gnatt A, Prody CA, Zamir R, Lieman-Hurwitz J, Zakut H, Soreq H. Expression of alternatively terminated unusual human butyrylcholinesterase messenger RNA transcripts, mapping to chromosome 3q26-ter, in nervous system tumors. *Cancer Res* 1990; 50: 1983-1987.
6. Allderdice PW, Gardner HA, Galutira D, Lockridge O, LaDu BN, McAlpine PJ. The cloned butyrylcholinesterase (BChE) gene maps to a single chromosome site, 3q26. *Genomics* 1991; 11: 452-454.
7. Ehrlich G, Viegas Pequignot E, Ginzberg D, Sindel L, Soreq H, Zakut H. Mapping the human acetylcholinesterase gene to chromosome 7q22 by fluorescent in situ hybridization coupled with selective PCR amplification from a somatic hybrid cell panel and chromosome-sorted DNA libraries. *Genomics* 1992; 13: 1192-1197.
8. Getman DK, Eubanks JH, Camp S, Evans GA, Taylor P. The human gene encoding acetylcholinesterase is located on the long arm of chromosome 7. *Am J Hum Genet* 1992; 51: 170-177.
9. Soreq H, Zakut H. *Human Cholinesterases and Anticholinesterases*. San Diego: Academic Press, 1993.
10. Primo-Parmo SL, Bartels CF, Wiersema B, van der Spek AF, Innis JW, La Du BN. Characterization of 12 silent alleles of the human butyrylcholinesterase (BCHE) gene. *Am J Hum Genet* 1996; 58: 52-64.
11. Loewenstein Lichenstein Y, Schwarz M, Glick D, Norgaard Pedersen B, Zakut H, Soreq H. Genetic predisposition to adverse consequences of anti-cholinesterases in 'atypical' BCHE carriers. *Nat Med* 1995; 1: 1082-1085.
12. Whittaker M. *Cholinesterase*. Basel: Karger, 1986.
13. La Du BN. Identification of human serum cholinesterase variants using the polymerase chain reaction amplification technique. *Trends Pharmacol Sci* 1989; 10: 309-313.
14. McGuire MC, Nogueira CP, Bartels CF *et al*. Identification of the structural mutation responsible for the dibucaine-resistant (atypical) variant form of human serum cholinesterase. *Proc Natl Acad Sci USA* 1989; 86: 953-957.
15. Neville LF, Gnatt A, Loewenstein Y, Soreq H. Aspartate-70 to glycine substitution confers resistance to naturally occurring and synthetic anionic-site ligands on in-ovo produced human butyrylcholinesterase. *J Neurosci Res* 1990; 27: 452-460.
16. Neville LF, Gnatt A, Loewenstein Y, Seidman S, Ehrlich G, Soreq H. Intramolecular relationships in cholinesterases revealed by oocyte expression of site-directed and natural variants of human BCHE. *EMBO J* 1992; 11: 1641-1649.
17. Schwarz M, Glick D, Loewenstein Y, Soreq H. Engineering of human cholinesterases explains and predicts diverse consequences of administration of various drugs and poisons. *Pharmacol Ther* 1995; 67: 283-322.
18. Sussman JL, Harel M, Frolow F *et al*. Atomic structure of acetylcholinesterase from *Torpedo californica*: a prototypic acetylcholine-binding protein. *Science* 1991; 253: 872-879.
19. Krasowski MD, McGehee DS, Moss J. Natural inhibitors of cholinesterases: implications for adverse drug reactions. *Can J Anaesth* 1997; 44: 525-534.

20. Ehrlich G, Ginzberg D, Loewenstein Y *et al.* Population diversity and distinct haplotype frequencies associated with *ACHE* and *BCHE* genes of Israeli Jews from trans-Caucasian Georgia and from Europe. *Genomics* 1994; 22: 288-295.
21. Sternfeld M, Rachmilewitz J, Loewenstein-Lichtenstein Y *et al.* Normal and atypical butyrylcholinesterases in placental development, function, and malfunction. *Cell Mol Neurobiol* 1997; 17: 315-332.
22. Paoletti F, Mocali A, Vannucchi AM. Acetylcholinesterase in murine erythroleukemia (Friend) cells: evidence for megakaryocyte-like expression and potential growth-regulatory role of enzyme activity. *Blood* 1992; 79: 2873-2879.
23. Patinkin D, Lev Lehman E, Zakut H, Eckstein F, Soreq H. Antisense inhibition of butyrylcholinesterase gene expression predicts adverse hematopoietic consequences to cholinesterase inhibitors. *Cell Mol Neurobiol* 1994; 14: 459-473.
24. Alber R, Sporns O, Weikert T, Willbold E, Layer PG. Cholinesterases and peanut agglutinin binding related to cell proliferation and axonal growth in embryonic chick limbs. *Anat Embryol Berlin* 1994; 190: 429-438.
25. Beeri R, Gnatt A, Lapidot Lifson Y *et al.* Testicular amplification and impaired transmission of human butyrylcholinesterase cDNA in transgenic mice. *Hum Reprod* 1994; 9: 284-292.
26. Soreq H, Malinger G, Zakut H. Expression of cholinesterase genes in human oocytes revealed by in-situ hybridization. *Hum Reprod* 1987; 2: 689-693.
27. Levey AI, Wainer BH, Rye DB, Mufson EJ, Mesulam MM. Choline acetyltransferase-immunoreactive neurons intrinsic to rodent cortex and distinction from acetylcholinesterase-positive neurons. *Neuroscience* 1984; 13: 341-353.
28. Mesulam MM, Geula C. Acetylcholinesterase-rich neurons of the human cerebral cortex: cytoarchitectonic and ontogenetic patterns of distribution. *J Comp Neurol* 1991; 306: 193-220.
29. Appleyard ME. Secreted acetylcholinesterase: non-classical aspects of a classical enzyme. *Trends Neurosci* 1992; 15: 485-490.
30. Razon N, Soreq H, Roth E, Bartal A, Silman I. Characterization of activities and forms of cholinesterases in human primary brain tumors. *Exp Neurol* 1984; 84: 681-695.
31. Pakaski M, Kasa P. Glial cells in coculture can increase the acetylcholinesterase activity in human brain endothelial cells. *Neurochem Int* 1992; 21: 129-133.
32. Karpel R, Ben Aziz Aloya R, Sternfeld M *et al.* Expression of three alternative acetylcholinesterase messenger RNAs in human tumor cell lines of different tissue origins. *Exp Cell Res* 1994; 210: 268-277.
33. Lapidot-Lifson Y, Prody CA, Ginzberg D, Meytes D, Zakut H, Soreq H. Coamplification of human acetylcholinesterase and butyrylcholinesterase genes in blood cells: correlation with various leukemias and abnormal megakaryocytopoiesis. *Proc Natl Acad Sci USA* 1989; 86: 4715-4719.
34. Zakut H, Ehrlich G, Ayalon A *et al.* Acetylcholinesterase and butyrylcholinesterase genes coamplify in primary ovarian carcinomas. *J Clin Invest* 1990; 86: 900-908.
35. Zakut H, Lapidot-Lifson Y, Beeri R, Ballin A, Soreq H. In vivo gene amplification in non-cancerous cells: cholinesterase genes and oncogenes amplify in thrombocytopenia associated with lupus erythematosus. *Mutat Res* 1992; 276: 275-284.
36. Prody CA, Dreyfus P, Zamir R, Zakut H, Soreq H. De novo amplification within a 'silent' human cholinesterase gene in a family subjected to prolonged exposure to organophosphorous insecticides. *Proc Natl Acad Sci USA* 1989; 86: 690-694.
37. Zakut H, Even L, Birkenfeld S, Malinger G, Zisling R, Soreq H. Modified properties of serum cholinesterases in primary carcinomas. *Cancer* 1988; 61: 727-737.
38. Zakut H, Lieman Hurwitz J, Zamir R, Sindell L, Ginzberg D, Soreq H. Chorionic villus cDNA library displays expression of butyrylcholinesterase: putative genetic disposition for ecological danger. *Prenat Diagn* 1991; 11: 597-607.
39. Lev-Lehman E, Deutsch V, Eldor A, Soreq H. Immature human megakaryocytes produce nuclear-associated acetylcholinesterase. *Blood* 1997; 89: 3644-3653.

40. Grisaru D, Lev-Lehman E, Shapira M *et al*. Human osteogenesis involves differentiation-dependent increases in the morphogenetically active 3' alternative splicing variant of acetylcholinesterase. *Mol Cell Biol* 1999; 19: 788-795.
41. Llinas RR, Greenfield SA. On-line visualization of dendritic release of acetylcholinesterase from mammalian substantia nigra neurons. *Proc Natl Acad Sci USA* 1987; 84: 3047-3050.
42. Dupree JL, Maynor EN, Bigbee JW. Inverse correlation of acetylcholinesterase (AChE) activity with the presence of neurofilament inclusions in dorsal root ganglion neurons cultured in the presence of a reversible inhibitor of AChE. *Neurosci Lett* 1995; 197: 37-40.
43. Koenigsberger C, Chiappa S, Brimijoin S. Neurite differentiation is modulated in neuroblastoma cells engineered for altered acetylcholinesterase expression. *J Neurochem* 1997; 69: 1389-1397.
44. Massoulie J, Pezzementi L, Bon S, Krejci E, Vallette FM. Molecular and cellular biology of cholinesterases. *Prog Neurobiol* 1993; 41: 31-91.
45. Seidman S, Sternfeld M, Ben Aziz Aloya R, Timberg R, Kaufer Nachum D, Soreq H. Synaptic and epidermal accumulations of human acetylcholinesterase are encoded by alternative 3'-terminal exons. *Mol Cell Biol* 1995; 15: 2993-3002.
46. Karpel R, Sternfeld M, Ginzberg D, Guhl E, Graessmann A, Soreq H. Overexpression of alternative human acetylcholinesterase forms modulates process extensions in cultured glioma cells. *J Neurochem* 1996; 66: 114-123.
47. Sternfeld M, Ming G, Song H *et al*. Acetylcholinesterase enhances neurite growth and synapse development through alternative contributions of its hydrolytic capacity, core protein, and variable C termini. *J Neurosci* 1998; 18: 1240-1249.
48. Futerman AH, Low MG, Ackermann KE, Sherman WR, Silman I. Identification of covalently bound inositol in the hydrophobic membrane-anchoring domain of Torpedo acetylcholinesterase. *Biochem Biophys Res Commun* 1985; 129: 312-317.
49. Kaufer D, Friedman A, Seidman S, Soreq H. Acute stress facilitates long-lasting changes in cholinergic gene expression. *Nature* 1998; 393: 373-377.
50. Beeri R, Andres C, Lev Lehman E *et al*. Transgenic expression of human acetylcholinesterase induces progressive cognitive deterioration in mice. *Curr Biol* 1995; 5: 1063-1071.
51. Andres C, Beeri R, Friedman A *et al*. Acetylcholinesterase-transgenic mice display embryonic modulations in spinal cord choline acetyltransferase and neurexin IB gene expression followed by late-onset neuromotor deterioration. *Proc Natl Acad Sci USA* 1997; 94: 8173-8178.
52. Mollgard K, Dziegielewska KM, Saunders NR, Zakur H, Soreq H. Synthesis and localization of plasma proteins in the developing human brain. Integrity of the fetal blood-brain barrier to endogenous proteins of hepatic origin. *Dev Biol* 1988; 128: 207-221.
53. Friedman A, Kaufer D, Shemer J, Hendler I, Soreq H, Tur Kaspas I. Pyridostigmine brain penetration under stress enhances neuronal excitability and induces early immediate transcriptional response. *Nat Med* 1996; 2: 1383-1385.
54. Sternfeld M, Patric, JD, Soreq H. Position effect variegations and brain-specific silencing in transgenic mice overexpressing human acetylcholinesterase variants. *J Physiol (Paris)* 1998; 92: 249-255.
55. Shoham S, Sternfeld M, Milay T, Patrick JW, Soreq H. Transgenic human AChE variants display different capacities of inducing 'corkscrew-like' neuronal processes in mouse somatosensory cortex. *Neurosci Lett* 1998; 51(Suppl): S38.
56. Beeri R, Le Novere N, Mervis R *et al*. Enhanced hemicholinium binding and attenuated dendrite branching in cognitively impaired acetylcholinesterase-transgenic mice. *J Neurochem* 1997; 69: 2441-2451.
57. Soreq H, Patinkin D, Lev-Lehman E *et al*. Antisense oligonucleotide inhibition of acetylcholinesterase gene expression induces progenitor cell expansion and suppresses hematopoietic apoptosis *ex vivo*. *Proc Natl Acad Sci USA* 1994; 91: 7907-7911.
58. Gennarelli TA, Graham DI. Neuropathology of the head injuries. *Semin Clin Neuropsychiatry* 1998; 3: 160-175.

59. Grisaru D, Sternfeld M, Eldor A, Glick D, Soreq H. Structural roles of acetylcholinesterase variants in biology and pathology. *Eur J Biochem* 1999; 264: 672-686.
60. Coyle JT, Price DL, DeLong MR. Alzheimer's disease: a disorder of cortical cholinergic innervation. *Science* 1983; 219: 1184-1190.
61. Giacobini E. Cholinergic foundations of Alzheimer's disease therapy. *J Physiol Paris* 1998; 92: 283-287.
62. Wright CI, Guela C, Mesulam MM. Protease inhibitors and indoleamines selectively inhibit cholinesterases in the histopathologic structures of Alzheimer disease. *Proc Natl Acad Sci USA* 1993; 90: 683-686.
63. Inestrosa NC, Alvarez A, Perez CA *et al.* Acetylcholinesterase accelerates assembly of amyloid- $\beta$ -peptides into Alzheimer's fibrils: possible role of the peripheral site of the enzyme. *Neuron* 1996; 16: 881-891.
64. Ehrlich G, Patinkin D, Ginzberg D, Zakut H, Eckstein F, Soreq H. Use of partially phosphorothioated 'antisense' oligodeoxynucleotides for sequence-dependent modulation of hematopoiesis in culture. *Antisense Res Dev* 1994; 4: 173-183.
65. Grifman M, Galyam N, Seidman S, Soreq H. Functional redundancy of acetylcholinesterase and neuroligin in mammalian neuritogenesis. *Proc Natl Acad Sci USA* 1998; 95: 13 935-13 940.
66. Grifman M, Soreq H. Differentiation intensifies the susceptibility of pheochromocytoma cells to antisense oligodeoxynucleotide-dependent suppression of acetylcholinesterase activity. *Antisense Nucleic Acid Drug Dev* 1997; 7: 351-359.
67. Donger C, Krejci E, Serradell AP *et al.* Mutation in the human acetylcholinesterase-associated collagen gene, COLQ, is responsible for congenital myasthenic syndrome with endplate acetylcholinesterase deficiency (Type Ic). *Am J Hum Genet* 1998; 63: 967-975.
68. Ichtchenko K, Nguyen T, Sudhof TC. Structures, alternative splicing, and neurexin binding of multiple neuroligins. *J Biol Chem* 1996; 271: 2676-2682.
69. Hata Y, Butz S, Sudhof TC. CASK: a novel dlg/PSD95 homolog with an N-terminal calmodulin-dependent protein kinase domain identified by interaction with neurexins. *J Neurosci* 1996; 16: 2488-2494.
70. Irie M, Hata Y, Takeuchi M *et al.* Binding of neuroligins to PSD-95. *Science* 1997; 277: 1511-1515.
71. Seidman S, Eckstein F, Grifman M, Soreq H. Antisense technologies have a future fighting neurodegenerative diseases. *Antisense Nucleic Acid Drug Dev* 1999; 9: 333-340.
72. Seidman S, Cohen O, Ginsberg D *et al.* Multi-level approaches to AChE-induced impairments in learning and memory. In: Doctor BP, Taylor P, Quinn DM, Rotundo RL, Gentry MK, eds. *Structure and Function of Cholinesterases and Related Proteins*. New York: Plenum Press, 1998: 183-184.
73. Birikh KR, Berlin YA, Soreq H, Eckstein F. Probing accessible sites for ribozymes on human acetylcholinesterase RNA. *RNA* 1997; 3: 429-437.
74. von der Kammer H, Mayhaus M, Albrecht C, Enderich J, Wegner M, Nitsch RM. Muscarinic acetylcholine receptors activate expression of the EGR gene family of transcription factors. *J Biol Chem* 1998; 273: 14 538-14 544.
75. Kaufer D, Friedman A, Soreq H. The vicious circle: long-lasting transcriptional modulation of cholinergic neurotransmission following stress and anticholinesterase exposure. *Neuroscientist* 1999; 5: 173-183.
76. Shapira M, Korner M, Bosgraaf L, Tur-Kaspa I, Soreq H. The human AChE locus includes a polymorphic enhancer domain 17 kb upstream from the transcription start site. In: Doctor BP, Taylor P, Quinn DM, Rotundo RL, Gentry MK, eds. *Structure and Function of Cholinesterases and Related Proteins*. New York: Plenum Press, 1998: 111.

## Acetylcholinesterase — new roles for an old actor

Hermona Soreq and Shlomo Seidman

The discovery of the first neurotransmitter — acetylcholine — was soon followed by the discovery of its hydrolysing enzyme, acetylcholinesterase. The role of acetylcholinesterase in terminating acetylcholine-mediated neurotransmission made it the focus of intense research for much of the past century. But the complexity of acetylcholinesterase gene regulation and recent evidence for some of the long-suspected 'non-classical' actions of this enzyme have more recently driven a profound revolution in acetylcholinesterase research. Although our understanding of the additional roles of acetylcholinesterase is incomplete, the time is ripe to summarize the evidence on a remarkable diversity of acetylcholinesterase functions.

Acetylcholine-mediated neurotransmission<sup>1,2</sup> is fundamental for nervous system function. Its abrupt blockade is lethal and its gradual loss, as in Alzheimer's disease<sup>3</sup>, multiple system atrophy<sup>4</sup> and other conditions<sup>5</sup>, is associated with progressive deterioration of cognitive, autonomic and neuromuscular functions. Acetylcholinesterase (AChE) hydrolyses (FIG. 1) and inactivates acetylcholine, thereby regulating the concentration of the transmitter at the synapse (BOX 1). Termination of activation is normally dependent on dissociation of acetylcholine from the receptor and its subsequent diffusion and hydrolysis, except in diseases where acetylcholine levels are limiting or under AChE inhibition, conditions that increase the duration of receptor activation<sup>6</sup>.

Acetylcholine hydrolysis can also be catalysed by a related, less-specific enzyme — butyrylcholinesterase (BuChE, also known as serum cholinesterase or pseudo-cholinesterase)<sup>7</sup>. BuChE can replace AChE by hydrolysing acetylcholine and it can also act as a molecular decoy for natural anti-AChEs by reacting with these toxins before they reach AChE<sup>8</sup>. However, AChE seems to have many more functions than BuChE as, for example, changes in levels and properties of AChE are associated with responses to numerous external stimuli. Here, we discuss our current

understanding of AChE functions beyond the classical view and suggest the molecular basis for its functional heterogeneity.

### From early to recent discoveries

The unique biochemical properties and physiological significance of AChE make it an interesting target for detailed structure-function analysis. AChE-coding sequences have been cloned so far from a range of evolutionarily diverse vertebrate and invertebrate species that include insects, nematodes, fish, reptiles, birds and several mammals, among them man. Sequence data were shortly followed by the first crystal model for AChE from *Torpedo californica*<sup>9</sup>, which historically had been one of the main sources of AChE for research. Later on, crystal structures from mouse<sup>10</sup>, *Drosophila*<sup>11</sup> and man<sup>12</sup> were obtained and found to be fundamentally similar. Surprisingly for an enzyme with an extraordinarily rapid catalytic reaction, the acetylcholine site was found to reside at the bottom of a deep, narrow gorge (FIG. 1a). Site-directed mutagenesis studies<sup>13</sup> have also delineated many of the ligand-binding features of this enzyme, particularly a peripheral binding site that had been identified in kinetic studies and that seems to be fundamental for some of the 'non-classical' functions of AChE.

AChE can be classified in several ways. Mechanistically, it is a serine hydrolase. Its catalytic site contains a catalytic triad — serine, histidine and an acidic residue (TABLE 1) — as do the catalytic sites of the serine proteases such as trypsin, several blood clotting factors, and others. However, the acidic group in AChE is a glutamate, whereas in most other cases it is an aspartate residue. The nucleophilic nature of the carboxylate is transferred through the imidazole ring of histidine to the hydroxyl group of serine, allowing it to displace the choline moiety from the substrate, forming an acetyl-enzyme intermediate (FIG. 1b). A subsequent hydrolysis step frees the acetate group. Understanding of the catalytic properties of the protein has assisted in our understanding of its inhibition by organophosphate and carbamate inhibitors (BOX 2). However, several questions remain to

be answered regarding AChE catalysis; for example, the mechanism behind the extremely fast turnover rate of the enzyme. Despite the fact that the substrate has to navigate a relatively long distance to reach the active site, AChE is one of the fastest enzymes<sup>14</sup>. One theory to explain this phenomenon has to do with the unusually strong electric field of AChE. It has been argued that this field assists catalysis by attracting the cationic substrate and expelling the anionic acetate product<sup>15</sup>. Site-directed mutagenesis, however, has indicated that reducing the electric field has no effect on catalysis<sup>16</sup>. However, the same approach has indicated an effect on the rate of association of fasciculins, a peptide that can inhibit AChE<sup>17</sup>.

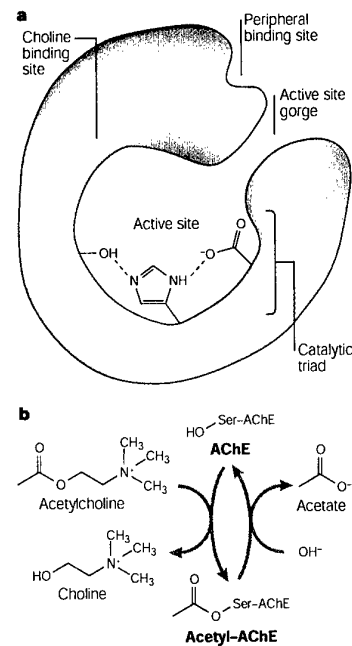


**Figure 1 | Acetylcholinesterase.** **a** | Structural features of the enzyme. X-ray crystallography has identified an active site at the bottom of a narrow gorge, lined with hydrophobic amino-acid side chains. At the time, the catalytic triad was unique among serine hydrolases in having a glutamate side chain in lieu of the familiar aspartate side chain. A choline-binding site featured hydrophobic tryptophan residues instead of the expected anionic groups; a peripheral binding site has also been identified by site-directed mutagenesis. **b** | The acetylcholinesterase (AChE) reaction. AChE promotes acetylcholine hydrolysis by forming an acetyl-AChE intermediate with the release of choline, and the subsequent hydrolysis of the intermediate to release acetate.

Crystallography and sequence analysis have identified a group of related enzymes and non-catalytic proteins. Some of these are transmembrane proteins with cytoplasmic domains and extracellular AChE-homologous domains that share the unique topography of AChE and its strong electric field (TABLE 1)<sup>18</sup>. On the basis of their structures, all of these are classified as  $\alpha/\beta$ -fold proteins; on the basis of their electric fields, they are classified as electroactins<sup>19</sup>.

AChE genes from different species are organized and sequentially spliced in a manner associated with distinct domains in their protein products. They include sites for alternative splicing of the pre-mRNA both at the 5' (REFS 20,21) and 3' ends<sup>22</sup>. Alternative splicing allows the production of three distinct AChE variants, each with a different carboxy-terminal sequence — the 'synaptic' (S), 'erythrocytic' (E) and 'readthrough' (R) AChE isoforms. The carboxy-terminal sequences determine their homologous assembly into AChE oligomers and their heterologous association with non-catalytic subunits that direct the subcellular localization of the protein. In AChE-S, a cysteine located three residues from the carboxyl terminus of the human protein allows dimerization by disulphide bridging. Two additional monomers can become associated by hydrophobic interactions<sup>23</sup>. These tetramers can attach covalently to a hydrophobic P subunit or to a collagen-like protein known as the T subunit<sup>24</sup>. The collagen-like subunit has a polyproline sequence that can form a triple-helical structure that bundles together 4, 8 or 12 AChE-S subunits<sup>23</sup>. In AChE-E, a glycol bond near the carboxyl terminus undergoes transamidation to attach a glycosylphosphatidylinositol group to the protein, which anchors the mature AChE-E to the outer surface of erythrocytes<sup>25</sup>. AChE-R does not seem to have any feature that allows for its attachment to other molecules and it remains monomeric and soluble. Last, it must be pointed out that another nomenclature labels the synaptic and erythropoietic variants according to properties of the proteins<sup>26</sup> — they are termed T (tailed), and H (hydrophobic), respectively. The many guises in which AChE-T occurs are also known as G for globular and A for asymmetric.

#### Multiple activities of AChE

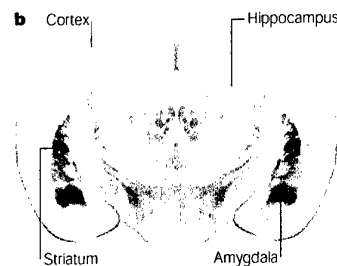
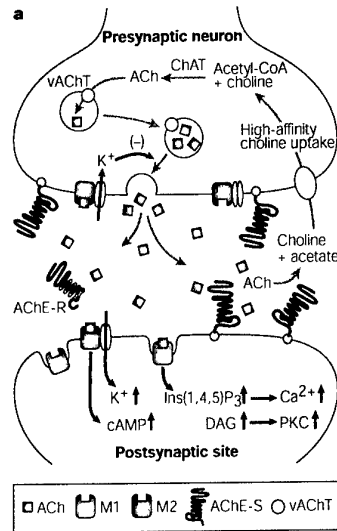
The idea that AChE has multiple, unrelated biological functions is not obvious and, indeed, was not readily accepted. Cytochemical data, however, attested to spatiotemporally regulated expression of AChE during very early embryogenesis<sup>27</sup>, during

#### Box 1 | The cholinergic synapse

In the presynaptic neuron, choline-acetyltransferase (ChAT) catalyses the synthesis of acetylcholine (ACh) from choline and acetyl-coenzyme A (panel a). ACh is packaged in synaptic vesicles via a vesicular ACh transporter (vAChT). Action potentials trigger the release of ACh into the synaptic cleft, where ACh can bind to muscarinic receptors located on the pre- and postsynaptic membrane. Muscarinic M2 receptors on the presynaptic membrane regulate ACh release via a negative feedback response. At the postsynaptic site, M1 receptors transduce signals through a pathway involving diacylglycerol (DAG), inositol-1,4,5-trisphosphate (Ins(1,4,5)P<sub>3</sub>) and a Ca<sup>2+</sup>-dependent protein kinase (PKC). In the hippocampus, most of the postsynaptic receptors are of the M1 subtype; in the cortex M2 receptors might also be located on the postsynaptic membrane. Genomic disruption of the M1 receptor impairs the activation of several signal-transduction pathways and explains why muscarinic excitation is the primary cause of seizures<sup>106</sup>. ACh is hydrolysed in the synaptic cleft by AChE tetramers, which are indirectly attached to the neuromuscular junction by a collagen-like tail<sup>5</sup>, or by another structural subunit to brain synapses<sup>107</sup>. AChE-R monomers would remain soluble within the synaptic cleft. A high-affinity choline-uptake mechanism returns choline to the presynaptic neuron.

Brain distribution of AChE includes both acetylcholine-releasing and cholinergic neurons. Panel b shows a cranial section of a brain stained for AChE activity (reproduced with permission from REF 108 © (1997) Harcourt). Note pronounced activity in the amygdala and caudate-putamen (striatum), and clearly detectable activity in the cortex and hippocampus.

embryonic neurite extension and muscle development and before synaptogenesis<sup>28,29</sup>. In addition, the enzyme was also found in adult non-cholinergic neurons, and in haematopoietic, osteogenic and various neoplastic cells. Early reports of a soluble, secreted, monomeric form of AChE<sup>30</sup> prompted the idea that this enzyme could have non-enzymatic functions. Gradually, this encouraged a small but persistent group of investigators to argue for the existence of 'non-classical' activities for AChE<sup>31</sup>. Some of the currently proposed functions are based merely on correlations and circumstantial evidence, and might yet be disproved. For example, the suggestion that AChE has intrinsic proteolytic activity was argued for several years (for example, REF. 32), but eventually was proved wrong by careful separation of the two activities<sup>33</sup>. Other activities,



however, have been confirmed and several research groups have established their molecular foundations.

**Neuritogenesis.** The first non-classical activity of AChE that was clearly distinguished from its hydrolytic capacity was its role in neuritogenesis. Exogenous purified AChE promoted neurite growth from chick nerve cells in culture and, whereas several active-site inhibitors failed to attenuate this effect<sup>34</sup>, an inhibitor of the peripheral site did block neuritogenesis<sup>35</sup>. Transfection with AChE or with antisense AChE cRNA-encoding vectors subsequently showed neuritogenic activity of the enzyme in neuroblastoma cells<sup>36</sup>, in pheochromocytoma (PC12) cells<sup>37</sup> and in primary dorsal root ganglion neurons<sup>38</sup>. Similarly, *Xenopus* motor neurons that expressed human AChE-S showed enhanced neurite growth rates (FIG. 2).

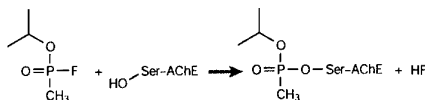
## PERSPECTIVES

### Box 2 | Natural and man-made anti-cholinesterases

Owing to its critical role in acetylcholine-mediated neurotransmission, AChE is a sensitive target for both natural and synthetic cholinergic toxins. Among the natural anti-AChEs are plant-derived carbamates and glycoalkaloid inhibitors<sup>109</sup>. A natural inhibitor of AChE was also found in a mollusc<sup>110</sup>. Blue-green algae are equipped with anatoxins<sup>111</sup>, highly effective toxins that block the active site. Green mamba venom includes the neurotoxic peptide fasciculin, which blocks entrance to the active and the peripheral sites of AChE<sup>10</sup>. Use of anti-AChEs as defence and attack weapons in nature, therefore, preceded their use by humans.

Synthetic anti-AChEs were first studied and manufactured as highly poisonous organophosphate and carbamate nerve gases and insecticides. In the clinic, controlled use of AChE inhibitors has proved valuable for the treatment of diseases that involve compromised acetylcholine-mediated neurotransmission (BOX 4).

The phosphate or carboxylate group of the active-site inhibitor acts like the carboxyl-ester group of a substrate to produce a stable phosphate or carboxylate ester, analogous to the acetyl-enzyme intermediate of catalysis. In this form, the enzyme is unavailable for its physiological function. The figure shows the reaction of AChE with the organophosphate, sarin, a chemical warfare agent.



After inhibition of AChE by organophosphates and carbamates, a slow spontaneous hydrolysis of the blocked enzyme regenerates an active enzyme. However, with organophosphate poisons, some of the acidic hydroxyl groups on the phosphate are esterified; slow spontaneous hydrolysis of these ester groups renders the phosphoryl-AChE permanently inactive. Antidotes for such poisoning have been developed to accelerate enzyme regeneration<sup>112</sup>. The slow reactivation of AChE was the basis of the use of pyridostigmine during the Gulf War as a prophylactic in anticipation of the use of organophosphate poisons (see BOX 3). It was argued that the prior blocking of AChE with pyridostigmine (a physostigmine derivative) prevents reaction with an organophosphate, and the slow reactivation regenerates AChE activity after the threat of poisoning has passed. The feedback response to anti-AChEs, including pyridostigmine<sup>64</sup>, indicates that AChE over-production might function as an additional protective mechanism against organophosphate poisoning.

**Cell adhesion.** The adhesive properties of the AChE core domain with the variant-specific carboxyl termini removed were studied in culture experiments using *Drosophila* cells. Chimeras were constructed in which the AChE-homologous domain of the cell-adhesion protein neurotactin<sup>39</sup> was replaced with the homologous *Drosophila* or *Torpedo* AChE core. These chimeras retained the adhesive properties in a homotypic cell-aggregation assay<sup>40</sup>, whereas AChE alone showed no such cell-adhesion property. However, AChE, unlike neurotactin, lacks a transmembrane domain. It was therefore argued that soluble AChE (that is, AChE-R) might compete with its structural homologues for their binding partners, and thus convey or interrupt morphogenic signals into neurons<sup>37</sup> (FIG. 3). However, the participation of AChE in interactions of this type remains to be directly shown.

**Synaptogenesis.** A synaptogenic function of AChE that depended on its catalytic properties<sup>41</sup> has been observed in microinjected *Xenopus* tadpoles. However, synaptogenic activity has been also shown for neurotactin,

another non-catalytic transmembrane protein that has an AChE-homologous extracellular domain and a carboxy-terminal cytoplasmic tail. When expressed in non-neuronal cells, neurotactin induced synaptic vesicle clustering and presynaptic differentiation in adjacent axons. This phenomenon was prevented by the addition of the extracellular domain of  $\beta$ -neurexin, a binding partner of neurotactin<sup>42</sup>, which can presumably also bind AChE. Combined with the immunohistochemical proof of the presence of neurotactin in adult excitatory brain synapses<sup>43</sup>, these findings indicate a probable involvement of neurotactin in synapse development and remodelling. Again, the actual role of AChE in this phenomenon, if any, remains to be tested in a more direct manner.

**Activation of dopamine neurons.** Real-time chemiluminescence has been used to visualize AChE release from dendrites of dopamine neurons in mammalian substantia nigra<sup>44</sup>. Purified recombinant AChE was later shown by the same group to enhance dopamine release from midbrain dopamine neurons<sup>45</sup>.

This non-classical autocrine phenomenon remains to be independently confirmed by the use of other approaches, but it might prove to be of physiological relevance.

**Amyloid fibre assembly.** AChE has been reported to promote amyloid fibre assembly<sup>46</sup>. The same group found that this activity was blocked by the peripheral-site inhibitor propidium, but not by the active-site AChE inhibitor edrophonium, clearly identifying this assembly-promoting activity as a non-classical AChE function. AChE-amyloid- $\beta$  complexes showed AChE activity that was resistant to low pH, lacked the substrate inhibition that is characteristic of the enzyme and had reduced sensitivity to anti-AChEs, properties that had previously been shown histochemically for AChE activity associated with Alzheimer's disease plaques<sup>3</sup>. The limitations of this study, however, include the high concentration of AChE that was needed to bind and promote amyloid fibre formation. In addition, only AChE binds amyloid fibrils *in vitro*, but both AChE and BuChE bind it *in vivo*.

**Haematopoiesis and thrombopoiesis.** Haematopoietic and thrombopoietic activities were first proposed for AChE on the basis of its presence in blood-cell progenitors<sup>47,48</sup>. Recent analyses have shown transcriptional activation of *ACHE* during haemagglutinin-induced lymphocyte activation. Inhibitor tests have suggested a mixed involvement of both catalytic and non-classical properties in this process<sup>49</sup>. Transient suppression and subsequent overproduction of AChE after treatment with antisense oligodeoxynucleotides induced myeloid proliferation in mouse

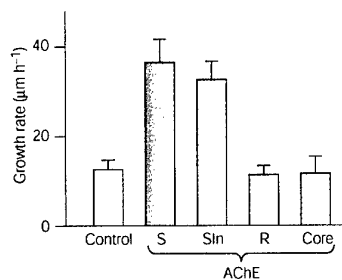


Figure 2 | **Neuritogenesis.** The growth of neurites in cultured motor neurons from *Xenopus* tadpoles was studied by time-lapse photography<sup>41</sup>. Rates of growth were observed in normal tadpoles and transgenics bearing coding sequences for human AChE-S (S), AChE-R (R), an enzyme with no variant-specific carboxyl terminus (core), or an enzymatically inactive AChE-S into which a seven-amino-acid stretch was inserted near the active site (Sln). Comparison with control values is shown.

Table 1 | The  $\alpha/\beta$ -fold superfamily\*

Protein	Origin	Triad residues	Intra-molecular disulphides	Splicing variants	Trans-membrane domain	Glyco-phospholipid linkage	Assembly potential
<b>Cholinesterases</b>							
Acetylcholinesterase	Mammalian	S E H	1 2 3	+	-	+	+
Acetylcholinesterase	<i>Torpedo</i>	S E H	1 2 3	+	-	+	+
Butyrylcholinesterase	Mammalian	S E H	1 2 3	-	-	-	+
Cholinesterase	Insect	S E H	1 2 3	-	-	+	+
<b>Other esterases</b>							
Carboxylesterases	Mammalian	S E H	1 2 -	-	-	-	-
Cholesterol esterase	Mammalian	S D H	1 2 -	-	-	-	-
Esterases 6 and P	Insect	S D H	1 2 -	-	-	-	-
Esterase B1	<i>Culex</i>	S E H	1 - -	-	-	-	-
Juvenile hormone esterase	<i>Heliothis</i>	S E H	1 - -	-	-	-	-
D2 esterase	<i>Dictostelium</i>	S E H	1 2 3	-	-	-	-
Crystal protein	<i>Dictostelium</i>	S E H	1 2 3	-	-	-	-
Lipases	<i>Geothricum, Candida</i>	S E H	1 2 -	-	-	-	-
<b>Non-enzyme proteins</b>							
Thyroglobulin	Mammalian	- - H	1 2 3	-	-	-	-
Neuroigin	Mammalian	- E H	1 2 -	+	+	-	-
Neurotactin	<i>Drosophila</i>	- E H	1 2 3	-	+	-	-
Glutactin	<i>Drosophila</i>	- - -	1 2 -	-	-	-	-
Gliotactin	<i>Drosophila</i>	- - -	1 2 -	-	+	-	-

\*Three related subfamilies belong to the  $\alpha/\beta$ -fold superfamily on the basis of their protein-folding patterns: cholinesterases, other esterases and non-enzyme proteins. Sequence alignments show two prototypic 'signatures' in all of these, one near the serine at the enzyme active site (prosite accession no. PS00122) and the other close to the amino terminus, with a conserved cysteine involved in disulphide bridging (prosite accession no. PS00941). The non-enzyme proteins include a growing number with AChE-homologous extracellular domains and, in some cases, a single transmembrane region with a protruding cytoplasmic domain that can interact with intracellular signalling proteins. Note that the possibilities of glyco-phospholipid linkage and multisubunit assembly are unique to the cholinesterases, whereas the conserved positions of the three (presumed) intramolecular disulphide bonds have been evolutionarily conserved in many of the members of this superfamily. The triad is complete only in those members of the superfamily that are enzymes. These findings are summarized from REF. 18.

bone-marrow-cell cultures<sup>50</sup>. This finding might explain the increased risk of leukaemia among users of anti-AChE pesticides<sup>51</sup>, as anti-AChEs induce AChE overproduction<sup>52</sup>. A related issue is whether AChE can itself be tumorigenic. The *ACHE* gene is frequently amplified, mutated or deleted in DNA from leukaemic patients<sup>53,54</sup>, supporting the idea that it is involved in myeloid proliferation. However, no mechanism has yet been proposed to explain this effect, and it is not known whether the mechanism is directly related to enzyme activity.

The heterogeneity of non-classical functions of AChE is further complicated by the difficulty of distinguishing these functions from its classical regulatory role in terminating acetylcholine-mediated neurotransmission. For example, it is likely that AChE would have both types of activity at acetylcholine neurons. However, inhibitor blockade of its hydrolytic activity does not necessarily block its non-classical functions. To understand the relationship between the forms and functions of AChE, a deeper insight is needed into the molecular origins of the functional heterogeneity of AChE.

#### Regulation of *ACHE* expression

Functional heterogeneity in AChE activity is regulated at the transcriptional, post-transcriptional and post-translational levels, leading to complex expression patterns that reflect tissue and cell-type specificity, differentiation state, physiological condition and response to external stimuli. The concentration of AChE in a tissue, the distribution of its alternative isoforms, its mode of oligomeric assembly, and its subcellular disposition, glycosylation<sup>55</sup> and proteolytic processing, are all subject to modulation through mechanisms that are not fully understood. Changes in most of these steps have indeed been shown to regulate the functional heterogeneity of AChE variants (for example, REFS 56-58).

**Transcription-regulated heterogeneity.** Transcriptional control of AChE production depends on a principal and an alternative proximal promoter<sup>21,59</sup>, on a distal enhancer domain<sup>60</sup>, and on an internal enhancer positioned within the first intron<sup>61</sup>. Sequential splicing of AChE pre-mRNA and regulation at the 5' and 3' ends yields tissue-, cell-type- and developmental-state-specific regulation

that provides rapid responses to physiological stimuli (FIG. 4).

Physiological cues that induce *ACHE* transcription include cell differentiation<sup>62</sup>, reduced AChE levels<sup>63</sup> and acetylcholine-mediated excitation elicited by exposure to anti-AChE agents and various traumatic insults<sup>64,65</sup>. AChE production increases during nervous system development in avian<sup>28</sup> and mammalian systems (for example, REF. 66), and is subject to regulation by the nerve growth factor receptor TrkA<sup>67</sup>. *In situ* hybridization and cytochemical studies have shown transient AChE activation in thalamic neurons during mammalian development<sup>68</sup>, and muscle differentiation is associated with transcriptional activation of the *ACHE* gene in subsynaptic nuclei<sup>62</sup>.

The *ACHE* gene retains a certain level of plasticity in the adult. In neocortical and hippocampal neurons, various external stimuli induce rapid, long-lasting activation of *ACHE* expression. In fact, psychological stress<sup>64</sup>, environmental stimuli (anti-AChE intoxication)<sup>60</sup> and head injury<sup>69</sup> increase *ACHE* transcription (FIG. 4). It is presumed that the initial stimulus induces excitation through acetylcholine

## PERSPECTIVES

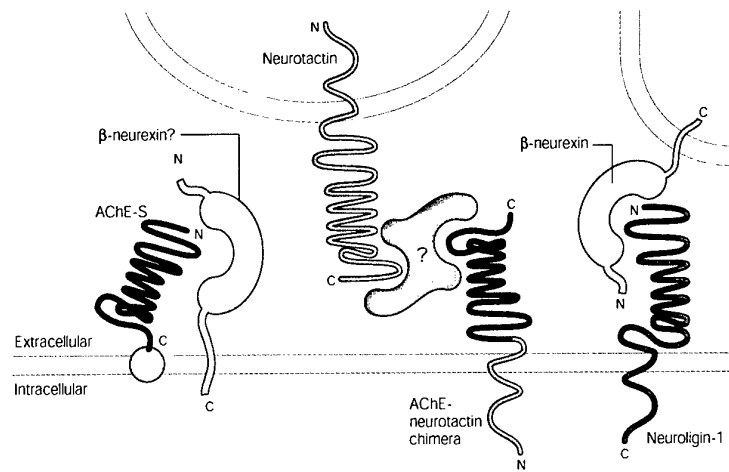


**Figure 3 | Proposed mechanism of some non-classical AChE functions.** AChE-S (blue) is shown by a folded line, as are the homologous regions of neurotactin (magenta) and neuroigin-1 (green). AChE-S linked to the membrane through a structural subunit (orange) might be associated with  $\beta$ -neurexin (yellow) in a neighbouring molecule or one embedded in the same membrane (left). Alternatively, if they are embedded in pre- and postsynaptic sites, neuroigin and  $\beta$ -neurexin might mediate cell-cell adhesion (right). Neurotactin might adhere to another neurotactin molecule (not shown), or be linked to AChE through a yet-to-be identified bridging protein (? , purple). Core AChE, or similar proteins cannot form any of these interactions by themselves. However, when the homologous region of AChE replaced a region of neurotactin, the chimeric protein retained the cell-cell adhesion capacity of the original neurotactin<sup>60</sup>. It has therefore been proposed<sup>37</sup> that AChE-R, which lacks the anchor to the membrane, might compete with neurotactin, neuroigin-1 or AChE-S and modify cell-cell interactions and intracellular signalling.

release and feedback overexpression of AChE acts to dampen excessive neurotransmission back towards normal levels<sup>64</sup>. This is important both for acetylcholine-mediated neurotransmission and for other brain circuits modulated by acetylcholine, for example, glutamate-mediated transmission in the hippocampus<sup>70</sup>. Excess AChE can also protect the organism from anti-AChEs toxicity, which has been shown in injection experiments<sup>71</sup>.

Transcriptional activation is common to many genetically determined responses to drugs and has been observed, for example, for cytochrome P450 proteins<sup>72</sup>. However, in addition to transcriptional activation, AChE mRNA transcripts in neuron, muscle and blood cells are subject to calcineurin-controlled, differentiation-induced stabilization<sup>56,73</sup>. Both these processes can increase the amount of AChE when and where it is needed, with AChE-R mRNA being significantly less stable than AChE-S mRNA<sup>56</sup>. This fact should be of specific interest, as anti-AChEs are routinely used in the treatment of patients with Alzheimer's disease<sup>74</sup>.

Chronically overproduced AChE can be expected to change acetylcholine balance, inducing activity-dependent, secondary feedback responses in the nervous system. In

AChE-overproducing transgenic mice, acetylcholine levels are reduced but acetylcholine-mediated neurotransmission is compensated by increases in high-affinity choline transport and acetylcholine synthesis<sup>75</sup>.

Last, transcriptional activation would also impinge on the non-classical actions of AChE. The consequences associated with this effect are still unknown but they might be relevant to ongoing discussions on Gulf War syndrome<sup>76</sup> (BOX 3) and the danger of terrorist attacks with nerve gas<sup>77</sup>.

**Mutation-related phenotypes.** Congenital myasthenia has been traced to a mutation not in *ACHE* itself but in the *COLQ* gene, which encodes the collagen-like structural subunit of neuromuscular AChE-S<sup>24,78</sup>. Natural amplification or mutation of the *Drosophila ache* gene results in insecticide resistance<sup>79</sup>, which is an inherited response to environmental exposure. Amplification of the human *BChE* gene, which encodes BuChE, has also been shown in the case of one family of farmers exposed to similar insecticides<sup>80</sup>. Nucleotide polymorphisms in the human *ACHE* gene are rare, and have a mild or no effect on the protein properties. Histidine substitution for asparagine at posi-

tion 322 creates the  $Y_{10}$  blood group, indicating that this residue might be part of an exposed epitope in AChE-E. Its frequency is higher in the Middle East as compared with European populations<sup>81,82</sup>. Nevertheless, the H322N mutation has no effect on the catalytic properties of the enzyme. The negligible polymorphism in the *ACHE* gene, in comparison with the abundant mutations in the homologous *BChE* gene<sup>83</sup>, has been interpreted as a reflection of the absolute necessity of a functional AChE. Chemical hypersensitivity to anti-AChEs was found in human carriers of an autosomal-dominant transcription-activating deletion in a distal *ACHE* enhancer domain<sup>60</sup>. Parallel hypersensitivity associated with progressive learning, memory and neuromuscular impairments was found in mice with a moderate overproduction of transgenic human AChE-S<sup>84</sup>, indicating that the level of this protein must be kept within a narrow window. It was therefore surprising that genomic disruption of the mouse *ACHE* gene yielded unhealthy, yet viable homozygotes<sup>85</sup>. However, whereas AChE can be temporarily replaced by BuChE, its absence becomes lethal within three weeks<sup>8</sup>. One possibility to explain this finding is that AChE, unlike BuChE, has three alternative variants, with potentially distinct functions. It is therefore important to discuss the functional significance of alternative splicing of the *ACHE* gene.

### Specific functions for splice variants?

Transcriptional activation of *ACHE* is often associated with a shift in its splicing pattern, leading to accumulation of the rare AChE-R variant. For example, AChE-R mRNA levels increased considerably within 30 minutes of confined swim stress, or after exposure to anti-AChEs or acetylcholine analogues. Similar effects have been observed in mammalian brain neurons *in vivo* after stress, in cortical and hippocampal neurons in brain slices and in cultured HEK293 cells. This shift depends on neuronal activity, muscarinic signalling and intracellular  $Ca^{2+}$  levels. In fact, AChE-R accumulation can be inhibited in brain slices by tetrodotoxin or by the  $Ca^{2+}$  chelator BAPTA-AM<sup>64</sup>, and it is facilitated by transfection with the M1 muscarinic receptor in HEK293 cells<sup>86</sup>. After head injury, neuronal AChE-R accumulation persists for over two weeks<sup>69</sup>.

Stress-induced alternative splicing also modifies  $K^+$  channels<sup>87</sup> and is regulated by neuronal activity-dependent transcriptional changes in several splicing regulatory proteins<sup>88</sup> (FIG. 4). In *ACHE* gene expression, alternative splicing changes the ratio of the

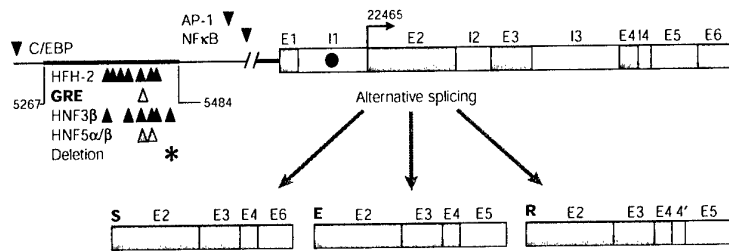


**Figure 4 | The human *AChE* gene and its alternative messenger RNAs.** The core of human *AChE* is encoded by three exons and parts of additional regions encode the variant-specific carboxy-terminal sequences. Transcription begins at E1, and E2 encodes a leader sequence that does not appear in any mature protein. In addition to a proximal promoter (red line adjacent to E1), a distal enhancer region (more distal red line) is rich in potential regulatory sequences, some of which are shown as wedges. The transcriptional activation of *AChE* by cortisol<sup>56</sup> is probably due to the distal glucocorticoid response element (GRE). A deletion mutation in this region disrupts one of two HNF3 (hepatocyte nuclear factor 3) binding sites, a factor that also activates transcription<sup>60</sup>. Intron 1 (I1) contains an enhancer sequence<sup>56,57</sup> indicated by a red dot. Nucleotide numbers are those of GeneBank cosmid AF002993. Normally, much more *AChE-S* than *AChE-R* mRNA is produced, but under stress or inhibition of *AChE*, alternative splicing produces much more of the *AChE-R* mRNA.

▶ Animated online

multimeric *AChE-S* to the monomeric *AChE-R* variant. These variants share a similar hydrolytic activity, but differ in their cellular and subcellular distribution and might have distinct non-classical functions. In nematodes, for example, four different genes encode distinct *AChE* variants. They resemble the mammalian variants in their carboxyl termini<sup>69</sup>, further emphasizing the likelihood of isoform-specific functions. Unequivocal evidence for variant-specific differences in the non-classical functions of *AChE* is still sparse. Nevertheless, some information attesting to such functions now exists.

**Variant-specific protein transport.** The location of *AChE-S* in the neuromuscular junction (NMJ) has been studied in great detail<sup>90</sup>. Enzyme clustering was found to be mediated by the heparan sulphate proteoglycan perlecan and to involve complex formation with dystroglycan<sup>91</sup>. In microinjected *Xenopus* tadpoles, transgenic *AChE-S* accumulated in the NMJ, whereas *AChE-R* was found in epidermal cells<sup>92</sup>. *AChE-S*, but not *AChE-R*, would adhere to the active zone at the NMJ (see REF. 93 for a tomographic microscopic analysis of these junctions). Transgenic mice with a disrupted *ColQ* collagen-like *AChE-S* subunit have congenital myasthenia<sup>94</sup>, demonstrating that *AChE-S* is an essential component of the NMJ. However, the secretory, soluble *AChE-R* might also change acetylcholine balance in the synaptic cleft<sup>92</sup> and/or compete with *AChE*-homologous proteins (for example, neuroligin) for interaction with their binding partners (BOX 1).

**Induction of process extension.** When expressed in developing *Xenopus* motor neurons, human *AChE-S* but not *AChE-R* or a carboxy-terminal truncated *AChE*, promoted neurite extension. This neurotogenic function was independent of the catalytic capacity, as a catalytically inactive *AChE-S* variant retained this function<sup>41</sup>. This finding argues for a neurotogenic activity of the carboxy-terminal sequence that is unique to *AChE-S*. A limitation of this study, however, is that it tested a

biological function of the human protein in the evolutionarily remote *Xenopus* system. However, differences between *AChE-S* and *AChE-R* were also observed in mammalian glia. In rat C6 glioma, transfected *AChE-S* induced process extension but *AChE-R* facilitated the formation of small, round cells<sup>95</sup>. No molecular mechanism has yet been proposed for this function.

**Regulation of stress-induced disorders.** Transgenic mice expressing human *AChE-R* show lower levels of stress-associated hallmarks of pathology (accumulation of heat-shock proteins, presence of reactive glia and curled neurites), whereas transgenic animals with human *AChE-S* show accelerated stress-related pathology<sup>96</sup>. *AChE-S* transgenic animals, which fail to respond to external stimuli by *AChE-R* overproduction, are exceptionally sensitive to closed-head injury<sup>99</sup> and to exposure to *AChE* inhibitors<sup>60</sup>. This indicates a probable physiological relevance for the alternative splicing of *AChE* in response to stressors, although it is not yet clear whether the stress-induced changes in *AChE* expression are a cause or an effect. In addition, the stress-induced *AChE-R* protein seems to be cleaved to yield its unique carboxy-terminal peptide (which by itself has haematopoietic growth-factor-like action), increasing DNA replication and survival of CD34<sup>+</sup> progenitors in human blood cell cultures and in mice subjected to confined swim stress<sup>98</sup>.

### Box 3 | Gulf War syndrome

The heterogeneous cognitive and physiological impairments reported by veterans of the 1991 Persian Gulf War are informally referred to as the Gulf War syndrome (GWS). During the war, soldiers were exposed to harsh weather conditions, high levels of anti-*AChE* insecticides and numerous vaccinations. In addition, the peripherally acting carbamate anti-*AChE*, pyridostigmine bromide, was administered as a prophylactic in anticipation of chemical warfare. In short-term peacetime tests, pyridostigmine caused no incapacitation and elicited minimal central nervous system effects<sup>113</sup>. However, factor analysis indicated delayed, but significant, impairment of cognition, ataxia and arthro-myoneuropathy in some veterans. These symptoms were interpreted to reflect exposure to centrally acting anti-*AChEs*<sup>114</sup>. The idea that GWS is related, at least in part, to the use of anti-*AChEs* in the war suggested a role for polymorphism in the *AChE*, *BChE* and paraoxonase genes (for example, REF. 60), or battlefield stress<sup>115</sup> as factors promoting neurological symptoms and muscle weakness. It was argued that the psychological stress associated with war conditions impaired the integrity of the blood-brain barrier (BBB), allowing penetration of the otherwise peripheral-acting inhibitor pyridostigmine into the brain<sup>116</sup>, where it activated *AChE* transcription<sup>64</sup>. Although stress-induced BBB leakage was difficult to reproduce by some<sup>117,118</sup> (perhaps because perfusion removed the over-produced secretory, soluble *AChE-R*), more recent studies confirmed the stress-promoted BBB disruption and attributed at least part of it to brain mast-cell activation<sup>119</sup>. Moreover, anti-*AChEs* were reported to facilitate viral invasion of the nervous system<sup>120</sup>, and stress was found to increase lethality of low levels of an anti-*AChE* pesticide<sup>121</sup>, further strengthening the links between stress, *AChE* and BBB integrity. So, the possibility that exposure to anti-*AChEs* together with acute stress and a compromised immune system might have contributed to the cholinergic consequences of GWS cannot be ruled out, a conclusion also of the Rand Corp report on the pyridostigmine and GWS literature.

## Box 4 | Reassessing the role of AChE in neurological disease

Pharmacological inhibitors of AChE are important in controlling diseases that involve impaired acetylcholine-mediated neurotransmission. For example, Alzheimer's disease involves selective loss of cholinergic neurons in the brain<sup>122</sup>. In myasthenia gravis, auto-antibodies reduce the number of nicotinic acetylcholine receptors at the neuromuscular junction<sup>123</sup>. AChE inhibition increases the synaptic concentration of acetylcholine and allows a higher occupancy rate and longer duration at its receptor<sup>124</sup>. Nevertheless, anti-AChE therapeutics do not address the aetiology of the diseases for which they are used.

**Neurodegeneration**

Neuritic plaques from Alzheimer's patients include catalytically active AChE<sup>3</sup>. Transgenic mice overexpressing AChE show progressive cognitive deficits and neuropathological markers (for example, cortical dendrite and spine loss) reminiscent of Alzheimer's disease<sup>125</sup>. Also, AChE-amyloid- $\beta$  complexes were more neurotoxic than amyloid- $\beta$  peptides alone<sup>126</sup>, suggesting that AChE imbalances might be involved in neurodeterioration. Last, increased AChE levels were reported in the brains of transgenic mice that express the carboxy-terminal fragment of the amyloid- $\beta$  protein<sup>127</sup>. Reconsideration of the rationale and expectations of conventional anti-AChE therapeutics is therefore required, as anti-AChEs induce AChE accumulation in cerebrospinal fluid<sup>65</sup>.

**Neuromotor dysfunction**

In chickens, muscle dystrophy is associated with changes in AChE properties<sup>128,129</sup>. In humans, congenital myasthenia might be caused by ColQ mutations<sup>5,24</sup>, and standard treatment of myasthenia gravis includes life-long administration of AChE inhibitors. However, AChE inhibitors promote overexpression of AChE-R in muscle, and exert dire effects on muscle integrity and neuromuscular junction structure in healthy mice<sup>52</sup>. This suggests that AChE-R might participate in the aetiology of myopathic syndromes and questions the potential long-term effects of anti-AChE drugs on disease progression. The unexplained muscle weakness reported by some of the Gulf War veterans who were exposed to various anti-AChEs might also be relevant here (see BOX 3).

**Antisense suppression makes sense**

*In vivo* antisense suppression of AChE mRNA using chemically protected oligonucleotides directed against AChE messenger RNA prevents AChE overproduction induced by organophosphate AChE inhibitors in muscle<sup>52</sup>, arrests the haematopoietic process elicited by this overproduction under acute psychological stress<sup>58</sup> and improves survival and recovery from closed-head injury<sup>69</sup>. Antisense agents, therefore, emerge as a promising alternative to anti-AChE therapeutics, especially as this is the only approach that promises a degree of selectivity among the several variants of AChE<sup>58</sup>.

**Prospects**

There are many challenges left regarding the non-classical functions of AChE. First, it is necessary to substantiate the nature of the protein regions and the amino-acid residues that mediate non-classical activities. Second, additional AChE binding partners that transfer morphogenic signals into the cell must be identified. Third, the intracellular signalling cascades that translate AChE-mediated events into altered cellular properties should be delineated and the physiological significance of such cascades should be tested. To this end, two-hybrid<sup>97</sup> and/or phage-display<sup>98</sup> screens can guide us to new protein partners. Mutagenesis and co-crystallization of these protein pairs can reveal the nature of their interactions. Conditional genetic disruption of AChE variants and their protein partners<sup>99</sup> combined with DNA-microarray analyses<sup>100</sup> can reveal the biological pathway(s) in which these interactions are involved.

At the level of the whole organism, the various animal models with up- or down-reg-

ulated *AChE* gene expression permit behavioural, electrophysiological and developmental studies. Mating AChE-overexpressing mice with transgenic animals that overexpress the human amyloid- $\beta$  might probe the involvement of AChE in the aetiology of Alzheimer's disease (BOX 4). Moreover, the morphogenic capacities that are peculiar to AChE indicate that it might modify the differentiation of embryonic stem cells<sup>101</sup>. Finally, positron emission tomography of AChE activity might be developed to the level of real-time imaging of this enzyme in the human brain. Tracers that are hydrolysed by AChE already permit measurement and imaging of AChE activity in humans and have shown a reduction of cerebral AChE activity in Alzheimer's<sup>102</sup> and Parkinson's diseases<sup>103</sup>. Further development of this approach can make AChE a sensitive, reliable biosensor of changes in acetylcholine-mediated neurotransmission, perhaps even under stressful conditions.

One of the key challenges in this field is to search for the physiological functions of the

different splice variants. Whereas pharmacological theories on the involvement of AChE in neurophysiology were largely limited to acetylcholine-mediated neurotransmission, acetylcholine is known to modulate additional circuits, for example, glutamate-mediated hippocampal activity<sup>70</sup>. It would be very interesting to know, for example, if the soluble AChE-R monomers secreted under stress transmission or affect the stress-induced changes in long-term potentiation<sup>104</sup> or long-term depression<sup>105</sup>.

Together, data obtained by geneticists, neurobiologists and biochemists during the past few years forcefully argue that the AChE story continues. Once again, the infinite complexity of nature is shining through, demanding a new look at an old friend.

Hermona Soreq and Shlomo Seidman are at the Department of Biological Chemistry, Institute of Life Sciences, The Hebrew University of Jerusalem, Israel 91904. Correspondence to H.S. e-mail: soreq@cc.huji.ac.il

**Links**

**DATABASE LINKS** AChE | BuChE | COLQ  
**FURTHER INFORMATION** The ESTHER database | GWS literature  
**ENCYCLOPEDIA OF LIFE SCIENCES**  
Acetylcholine

- Dale, H. The action of certain esters and ethers of choline, and their relation to muscarine. *J. Pharmacol. Exp. Therap.* **6**, 147-190 (1914).
- Loewi, O. & Navratil, E. Über humorale Übertragbarkeit der Herznervenwirkung. X Mitteilung. *Pflüger's Arch.* **214**, 678-688 (1926).
- Wright, C. I., Geula, C. & Mesulam, M. M. Neurological cholinesterases in the normal brain and in Alzheimer's disease: relationship to plaques, tangles, and patterns of selective vulnerability. *Ann. Neurol.* **34**, 373-384 (1993).
- Palinsky, R. J., Holmes, K. V., Brown, R. T. & Weise, V. CSF acetylcholinesterase levels are reduced in multiple system atrophy with autonomic failure. *Neurology* **39**, 40-44 (1989).
- Ohno, K. et al. The spectrum of mutations causing end-plate acetylcholinesterase deficiency. *Ann. Neurol.* **47**, 162-170 (2000).
- Silver, A. A histochemical investigation of cholinesterases at neuromuscular junctions in mammalian and avian muscle. *J. Physiol. (Lond.)* **169**, 386-393 (1963).
- Augustinsson, K. B. & Nachmansohn, D. Distinction between acetylcholinesterase and other choline ester-splitting enzymes. *Science* **110**, 98-99 (1949).
- Li, B. et al. Abundant tissue butyrylcholinesterase and its possible function in the acetylcholinesterase knockout mouse. *J. Neurochem.* **75**, 1320-1331 (2000).
- Sussman, J. L. et al. Atomic structure of acetylcholinesterase from *Torpedo californica*: a prototypic acetylcholine-binding protein. *Science* **253**, 872-879 (1991).
- Bourne, Y., Taylor, P. & Marchot, P. Acetylcholinesterase inhibition by fasciculin: crystal structure of the complex. *Cel* **83**, 503-512 (1995).
- Harel, M. et al. Three-dimensional structures of *Drosophila melanogaster* acetylcholinesterase and of its complexes with two potent inhibitors. *Protein Sci.* **9**, 1063-1072 (2000).
- Kryger, G. et al. Structures of recombinant native and E202Q mutant human acetylcholinesterase complexed with the snake-venom toxin fasciculin-II. *Acta Crystallogr. D Biol. Crystallogr.* **56**, 1385-1394 (2000).
- Shafferman, A. et al. Mutagenesis of human acetylcholinesterase. Identification of residues involved in

- catalytic activity and in polypeptide folding. *J. Biol. Chem.* **267**, 17640–17648 (1992).
14. Nair, H. K., Seravali, J., Arbuckle, T. & Quinn, D. M. Molecular recognition in acetylcholinesterase catalysis: free-energy correlations for substrate turnover and inhibition by trifluoro ketone transition-state analogs. *Biochemistry* **33**, 8566–8576 (1994).
  15. Ripoll, D. R., Faerman, C. H., Axelsen, P. H., Silman, I. & Sussman, J. L. An electrostatic mechanism for substrate guidance down the aromatic gorge of acetylcholinesterase. *Proc. Natl Acad. Sci. USA* **90**, 5128–5132 (1993).
  16. Shaffer, A. et al. Electrostatic attraction by surface charge does not contribute to the catalytic efficiency of acetylcholinesterase. *EMBO J.* **13**, 3448–3455 (1994).
  17. Radic, Z., Kirchhoff, P. D., Quinn, D. M., McCammon, J. A. & Taylor, P. Electrostatic influence on the kinetics of ligand binding to acetylcholinesterase. Distinctions between active center ligands and fasciculins. *J. Biol. Chem.* **272**, 23265–23277 (1997).
  18. Taylor, P., Luo, Z. D. & Camp, S. in *Cholinesterases and Cholinesterase Inhibitors* (ed. Giacobini, E.) 63–79 (Martin Dunitz, London, 2000).
  19. Botti, S. A., Felder, C. E., Sussman, J. L. & Silman, I. Electrostatics: a class of adhesion proteins with conserved electrostatic and structural motifs. *Protein Eng.* **11**, 415–420 (1998).
  20. Luo, Z. D., Camp, S., Muter, A. & Taylor, P. Splicing of 5' Introns dictates alternative splice selection of acetylcholinesterase pre-mRNA and specific expression during myogenesis. *J. Biol. Chem.* **273**, 28486–28495 (1998).
  21. Atanasova, E., Chiappa, S., Wieben, E. & Brimijoin, S. Novel messenger RNA and alternative promoter for murine acetylcholinesterase. *J. Biol. Chem.* **274**, 21078–21084 (1999).
  22. Li, Y., Camp, S., Rachinsky, T. L., Getman, D. & Taylor, P. Gene structure of mammalian acetylcholinesterase. Alternative exons dictate tissue-specific expression. *J. Biol. Chem.* **266**, 23083–23090 (1991).
  23. Bon, S., Coussens, F. & Massoulié, J. Quaternary association of acetylcholinesterase. II. The polyproline attachment domain of the collagen tail. *J. Biol. Chem.* **272**, 3016–3021 (1997).
  24. Donger, C. et al. Mutation in the human acetylcholinesterase-associated collagen gene, COLQ, is responsible for congenital myasthenic syndrome with end-plate acetylcholinesterase deficiency (Type Ic). *Am. J. Hum. Genet.* **63**, 967–975 (1998).
  25. Futeran, A. H., Low, M. G., Ackermann, K. E., Sherman, W. R. & Silman, I. Identification of covalently bound inositol in the hydrophobic membrane-anchoring domain of Torpedo acetylcholinesterase. *Biochem. Biophys. Res. Commun.* **129**, 312–317 (1985).
  26. Massoulié, J. et al. The polymorphism of acetylcholinesterase: post-translational processing, quaternary associations and localization. *Chem. Biol. Interact.* **119–120**, 29–42 (1999).
  27. Fitzpatrick-McElligott, S. & Stent, G. S. Appearance and localization of acetylcholinesterase in embryos of the leech *Helobdella triseriata*. *J. Neurosci.* **1**, 901–907 (1981).
  28. Betz, H., Bourgeois, J. P. & Changeux, J. P. Evolution of cholinergic proteins in developing slow and fast skeletal muscles in chick embryo. *J. Physiol.* **302**, 197–218 (1980).
  29. Layer, P. G. Cholinesterases preceding major tracts in vertebrate neurogenesis. *Bioessays* **12**, 415–420 (1990).
  30. Kreutzberg, G. W. Neuronal dynamics and axonal flow. IV. Blockage of intra-axonal enzyme transport by colchicine. *Proc. Natl Acad. Sci. USA* **62**, 722–728 (1969).
  31. Appleyard, M. E. Secreted acetylcholinesterase: non-classical aspects of a classical enzyme. *Trends Neurosci.* **15**, 485–490 (1992).
  32. Small, D. H. Non-cholinergic actions of acetylcholinesterases: proteases regulating cell growth and development? *Trends Biochem. Sci.* **15**, 213–216 (1990).
  33. Checler, F., Grassi, J. & Vincent, J. P. Cholinesterases display genuine arylacylamidase activity but are totally devoid of intrinsic peptidase activities. *J. Neurochem.* **62**, 756–763 (1994).
  34. Layer, P. G., Weikert, T. & Alber, R. Cholinesterases regulate neurite growth of chick nerve cells *in vitro* by means of a non-enzymatic mechanism. *Cell Tissue Res.* **273**, 219–226 (1993).
  35. Small, D. H., Reed, G., Whitefield, B. & Nurcombe, V. Cholinergic regulation of neurite outgrowth from isolated chick sympathetic neurons in culture. *J. Neurosci.* **15**, 144–151 (1995).
  36. Koenigsberger, C., Chiappa, S. & Brimijoin, S. Neurite differentiation is modulated in neuroblastoma cells engineered for altered acetylcholinesterase expression. *J. Neurochem.* **69**, 1389–1397 (1997).
  37. Grifman, M., Galyam, N., Seidman, S. & Soreq, H. Functional redundancy of acetylcholinesterase and neuroigin in mammalian neurogenesis. *Proc. Natl Acad. Sci. USA* **95**, 13935–13940 (1998).
  38. Bigbee, J. W., Sharma, K. V., Chan, E. L. & Bogler, O. Evidence for the direct role of acetylcholinesterase in neurite outgrowth in primary dorsal root ganglion neurons. *Brain Res.* **861**, 354–362 (2000).
  39. de la Escalera, S., Bockamp, E. O., Moya, F., Piovant, M. & Jimenez, F. Characterization and gene cloning of neurotactin, a *Drosophila* transmembrane protein related to cholinesterases. *EMBO J.* **9**, 3593–3601 (1990).
  40. Darboux, I., Barthaly, Y., Piovant, M. & Hipeau Jacquotte, R. The structure-function relationships in *Drosophila* neurotactin show that cholinesterase domains may have adhesive properties. *EMBO J.* **15**, 4835–4843 (1996).
  41. Sternfeld, M. et al. Acetylcholinesterase enhances neurite growth and synapse development through alternative contributions of its hydrolytic capacity, core protein, and variable C termini. *J. Neurosci.* **18**, 1240–1249 (1998).
  42. Scheiffele, P., Fan, J., Choih, J., Fetter, R. & Serafini, T. Neuroigin expressed in nonneuronal cells triggers presynaptic development in contacting axons. *Cell* **101**, 657–669 (2000).
  43. Song, J. Y., Ichtchenko, K., Sudhof, T. C. & Brose, N. Neuroigin 1 is a postsynaptic cell-adhesion molecule of excitatory synapses. *Proc. Natl Acad. Sci. USA* **96**, 1100–1105 (1999).
  44. Linas, R. R. & Greenfield, S. A. On-line visualization of dendritic release of acetylcholinesterase from mammalian substantia nigra neurons. *Proc. Natl Acad. Sci. USA* **84**, 3047–3050 (1987).
  45. Holmes, C., Jones, S. A., Budd, T. C. & Greenfield, S. A. Non-cholinergic, trophic action of recombinant acetylcholinesterase on mid-brain dopaminergic neurons. *J. Neurosci.* **9**, 207–218 (1989).
  46. Inestrosa, N. C. et al. Acetylcholinesterase accelerates assembly of amyloid- $\beta$  peptides into Alzheimer's fibrils: possible role of the peripheral site of the enzyme. *Neuron* **16**, 881–891 (1996).
  47. Paoletti, F., Mocali, A. & Vannucchi, A. M. Acetylcholinesterase in murine erythroleukemia (Friend) cells: evidence for megakaryocyte-like expression and potential growth-regulatory role of enzyme activity. *Blood* **79**, 2873–2879 (1992).
  48. Lev-Lehman, E., Deutsch, V., Eldor, A. & Soreq, H. Immature human megakaryocytes produce nuclear-associated acetylcholinesterase. *Blood* **89**, 3644–3653 (1997).
  49. Kawashima, K. & Fujii, T. Extraneuronal cholinergic system in lymphocytes. *Pharmacol. Ther.* **86**, 29–48 (2000).
  50. Soreq, H. et al. Antisense oligonucleotide inhibition of acetylcholinesterase gene expression induces progenitor cell expansion and suppresses hematopoietic apoptosis *ex vivo*. *Proc. Natl Acad. Sci. USA* **91**, 7907–7911 (1994).
  51. Brown, L. M. et al. Pesticide exposure and other agricultural risk factors for leukemia among men in Iowa and Minnesota. *Cancer Res.* **50**, 6585–6591 (1990).
  52. Lev-Lehman, E. et al. Synaptogenesis and myopathy under acetylcholinesterase overexpression. *J. Mol. Neurosci.* **14**, 93–105 (2000).
  53. Lapidot-Lifson, Y. et al. Coamplification of human acetylcholinesterase and butyrylcholinesterase genes in blood cells: correlation with various leukemias and abnormal megakaryocytopoiesis. *Proc. Natl Acad. Sci. USA* **86**, 4715–4719 (1989).
  54. Stephenson, J., Czepulkowski, B., Hirst, W. & Muftic, G. Deletion of the acetylcholinesterase locus at 7q22 associated with myelodysplastic syndromes (MDS) and acute myeloid leukaemia (AML). *Leuk. Res.* **20**, 235–241 (1996).
  55. Velan, B. et al. N-glycosylation of human acetylcholinesterase: effects on activity, stability and biosynthesis. *Biochem. J.* **296**, 649–656 (1993).
  56. Chan, R. Y., Adatia, F. A., Krupa, A. M. & Jasmin, B. J. Increased expression of acetylcholinesterase T and R transcripts during hematopoietic differentiation is accompanied by parallel elevations in the levels of their respective molecular forms. *J. Biol. Chem.* **273**, 9727–9733 (1998).
  57. Camp, S. & Taylor, P. in *Structure and Function of Cholinesterases and Related Proteins* (eds Doctor, B. P., Taylor, P., Quinn, D. M., Rotundo, R. L. & Gentry, M. K.) 51–55 (Plenum, New York, 1998).
  58. Grisaru, D. et al. ARP, a peptide derived from the stress-associated acetylcholinesterase variant has hematopoietic growth promoting activities. *Mol. Med.* (in press).
  59. Li, Y., Camp, S., Rachinsky, T. L., Bongiorno, C. & Taylor, P. Promoter elements and transcriptional control of the mouse acetylcholinesterase gene. *J. Biol. Chem.* **268**, 3563–3572 (1993).
  60. Shapira, M. et al. A transcription-activating polymorphism in the AChE promoter associated with acute sensitivity to anti-acetylcholinesterases. *Hum. Mol. Genet.* **9**, 1273–1281 (2000).
  61. Chan, R. Y., Boudreau-Lariviere, C., Angus, L. M., Mankal, F. A. & Jasmin, B. J. An intronic enhancer containing an N-box motif is required for synapse- and tissue-specific expression of the acetylcholinesterase gene in skeletal muscle fibers. *Proc. Natl Acad. Sci. USA* **96**, 4627–4632 (1999).
  62. Rotundo, R. L. Nucleus-specific translation and assembly of acetylcholinesterase in multinucleated muscle cells. *J. Cell Biol.* **110**, 715–719 (1990).
  63. Galyam, N. et al. Complex host cell responses to antisense suppression of AChE gene expression. *Antisense Nucl. Acid Drug Dev.* **11**, 51–57 (2001).
  64. Kaufer, D., Friedman, A., Seidman, S. & Soreq, H. Acute stress facilitates long-lasting changes in cholinergic gene expression. *Nature* **393**, 373–377 (1998).
  65. Nordberg, A., Hellstrom-Lindahl, E., Almkvist, O. & Meurling, L. Activity of acetylcholinesterase in CSF increases in Alzheimer's patients after treatment with tacrine. *Alzheimer's Reports* **2**, 347–352 (1999).
  66. Grisaru, D. et al. Human osteogenesis involves differentiation-dependent increases in the morphogenetically active 3' alternative splicing variant of acetylcholinesterase. *Mol. Cell Biol.* **19**, 788–795 (1999).
  67. Schober, A. et al. Reduced acetylcholinesterase (AChE) activity in adrenal medulla and loss of sympathetic preganglionic neurons in TrkA-deficient, but not TrkB-deficient, mice. *J. Neurosci.* **17**, 891–903 (1997).
  68. Robertson, R. T. et al. Do subplate neurons comprise a transient population of cells in developing neocortex of rats? *J. Comp. Neurol.* **426**, 632–650 (2000).
  69. Shohami, E. et al. Antisense prevention of neuronal damages following head injury in mice. *J. Mol. Med.* **78**, 228–236 (2000).
  70. Gray, R., Rajan, A. S., Radcliffe, K. A., Yakehiro, M. & Dani, J. A. Hippocampal synaptic transmission enhanced by low concentrations of nicotine. *Nature* **393**, 713–716 (1996).
  71. Ashani, Y. et al. Butyrylcholinesterase and acetylcholinesterase prophylaxis against organophosphorus poisoning in mice. *Biochem. Pharmacol.* **41**, 37–41 (1991).
  72. Evans, W. E. & Relling, M. V. Pharmacogenomics: translating functional genomics into rational therapeutics. *Science* **286**, 487–491 (1999).
  73. Luo, Z. D. et al. Calcineurin enhances acetylcholinesterase mRNA stability during C2-C12 muscle cell differentiation. *Mol. Pharmacol.* **56**, 896–894 (1999).
  74. Giacobini, E. in *Cholinesterases and Cholinesterase Inhibitors* (ed. Giacobini, E.) 181–226 (Martin Dunitz, London, 2000).
  75. Erb, C. et al. Compensatory mechanisms facilitate hippocampal acetylcholine release in transgenic mice expressing human acetylcholinesterase. *J. Neurochem.* (in press).
  76. Pollet, C. et al. Medical evaluation of Persian Gulf veterans with fatigue and/or chemical sensitivity. *J. Med.* **29**, 101–113 (1998).
  77. Okumura, T. et al. Report on 640 victims of the Tokyo subway sarin attack. *Ann. Emerg. Med.* **28**, 129–135 (1996).
  78. Ohno, K., Brengman, J., Tsubino, A. & Engel, A. G. Human endplate acetylcholinesterase deficiency caused by mutations in the collagen-like tail subunit (ColQ) of the asymmetric enzyme. *Proc. Natl Acad. Sci. USA* **95**, 9654–9659 (1998).
  79. Fournier, D. et al. *Drosophila melanogaster* acetylcholinesterase gene: Structure, evolution and mutations. *J. Mol. Biol.* **210**, 15–22 (1989).
  80. Prody, C. A., Dreyfus, P., Zamir, R., Zuker, H. & Soreq, H. *De novo* amplification within a "silent" human cholinesterase gene in a family subjected to prolonged exposure to organophosphorus insecticides. *Proc. Natl Acad. Sci. USA* **86**, 690–694 (1989).
  81. Bartels, C. F., Zelinski, T. & Lockridge, O. Mutation at codon 322 in the human acetylcholinesterase (AChE)

## PERSPECTIVES

- gene accounts for YT blood group polymorphism. *Am. J. Hum. Genet.* **52**, 928–936 (1993).
82. Ehrlich, G. *et al.* Population diversity and distinct haplotype frequencies associated with AChE and BCHE genes of Israeli Jews from trans-Caucasian Georgia and from Europe. *Genomics* **22**, 288–295 (1994).
  83. La Du, B. N. *et al.* Phenotypic and molecular biological analysis of human butyrylcholinesterase variants. *Clin. Biochem.* **23**, 423–431 (1990).
  84. Beeri, R. *et al.* Transgenic expression of human acetylcholinesterase induces progressive cognitive deterioration in mice. *Curr. Biol.* **5**, 1063–1071 (1995).
  85. Xie, W. *et al.* Postnatal developmental delay and supersensitivity to organophosphate in gene-targeted mice lacking acetylcholinesterase. *J. Pharmacol. Exp. Ther.* **293**, 895–902 (2000).
  86. von der Kammer, H. *et al.* Muscarinic acetylcholine receptors activate expression of the EGR gene family of transcription factors. *J. Biol. Chem.* **273**, 14538–14544 (1998).
  87. Xie, J. & McCobb, D. P. Control of alternative splicing of potassium channels by stress hormones. *Science* **280**, 443–446 (1998).
  88. Daoud, R., Da Penha Berzaghi, M., Siedler, F., Hubener, M. & Stamm, S. Activity-dependent regulation of alternative splicing patterns in the rat brain. *Eur. J. Neurosci.* **11**, 788–802 (1999).
  89. Combes, D., Fedon, Y., Grauso, M., Toutant, J. P. & Arpagaus, M. Four genes encode acetylcholinesterases in the nematodes *Caenorhabditis elegans* and *Caenorhabditis briggsae*. cDNA sequences, genomic structures, mutations and *in vivo* expression. *J. Mol. Biol.* **300**, 727–742 (2000).
  90. Anglister, L., Siles, J. R. & Salpeter, M. M. Acetylcholinesterase density and turnover number at frog neuromuscular junctions: with modeling of their role in synaptic function. *Neuron* **12**, 783–794 (1994).
  91. Peng, H. B., Xie, H., Rossi, S. G. & Rotundo, R. L. Acetylcholinesterase clustering at the neuromuscular junction involves perlecan and dystroglycan. *J. Cell Biol.* **145**, 911–921 (1999).
  92. Seidman, S. *et al.* Synaptic and epidermal accumulations of human acetylcholinesterase are encoded by alternative 3'-terminal exons. *Mol. Cell Biol.* **15**, 2993–3002 (1995).
  93. Harlow, M. L., Ress, D., Stoschek, A., Marshall, R. M. & McMahan, U. J. The architecture of active zone material at the frog's neuromuscular junction. *Nature* **409**, 479–484 (2001).
  94. Feng, G. *et al.* Genetic analysis of collagen Q: roles in acetylcholinesterase and butyrylcholinesterase assembly and in synaptic structure and function. *J. Cell Biol.* **144**, 1349–1360 (1999).
  95. Karpel, R. *et al.* Overexpression of alternative human acetylcholinesterase forms modulates process extensions in cultured glioma cells. *J. Neurochem.* **66**, 114–123 (1996).
  96. Sternfeld, M. *et al.* Excess 'readthrough' acetylcholinesterase attenuates but the 'synaptic' variant intensifies neurodegeneration correlates. *Proc. Natl Acad. Sci. USA* **97**, 8647–8652 (2000).
  97. Chien, C. T., Bartel, P. L., Sternglanz, R. & Fields, S. The two-hybrid system: a method to identify and clone genes for proteins that interact with a protein of interest. *Proc. Natl Acad. Sci. USA* **88**, 9578–9582 (1991).
  98. Nissim, A. *et al.* Antibody fragments from a 'single pot' phage display library as immunochemical reagents. *EMBO J.* **13**, 692–698 (1994).
  99. Mayford, M., Abel, T. & Kandel, E. R. Transgenic approaches to cognition. *Curr. Opin. Neurobiol.* **5**, 141–148 (1995).
  100. Young, R. A. Biomedical discovery with DNA arrays. *Cell* **102**, 9–15 (2000).
  101. Mezey, E., Chandross, K. J., Harta, G., Maki, R. A. & McKercher, S. R. Turning blood into brain: cells bearing neuronal antigens generated *in vivo* from bone marrow. *Science* **290**, 1779–1782 (2000).
  102. Kuhl, D. E. *et al.* *In vivo* mapping of cerebral acetylcholinesterase activity in aging and Alzheimer's disease. *Neurology* **52**, 691–699 (1999).
  103. Shinotoh, H. *et al.* Positron emission tomographic measurement of acetylcholinesterase activity reveals differential loss of ascending cholinergic systems in Parkinson's disease and progressive supranuclear palsy. *Ann. Neurol.* **46**, 62–69 (1999).
  104. Vereker, E., O'Donnell, E. & Lynch, M. A. The inhibitory effect of interleukin-1 $\beta$  on long-term potentiation is coupled with increased activity of stress-activated protein kinases. *J. Neurosci.* **20**, 6811–6819 (2000).
  105. Xu, L., Anwyl, R. & Rowan, M. J. Behavioural stress facilitates the induction of long-term depression in the hippocampus. *Nature* **387**, 497–500 (1997).
  106. Hamilton, S. E. *et al.* Disruption of the m1 receptor gene ablates muscarinic receptor-dependent M current regulation and seizure activity in mice. *Proc. Natl Acad. Sci. USA* **94**, 13311–13316 (1997).
  107. Gennari, K., Brunner, J. & Brodbeck, U. Tetrameric detergent-soluble acetylcholinesterase from human caudate nucleus: subunit composition and number of active sites. *J. Neurochem.* **49**, 12–18 (1987).
  108. Franklin, R. B. J. & Paxinos, G. *The Mouse Brain in Stereotaxic Coordinates* (Academic, San Diego, 1997).
  109. Holmstedt, B. *in Cholinesterases and Cholinesterase Inhibitors: Basic, Preclinical and Clinical Aspects* (ed. Giacobini, E.) 1–8 (Martin Dunitz, London, 2000).
  110. Abramson, S. N., Radic, Z., Manker, D., Faulkner, D. J. & Taylor, P. Onchidal: a naturally occurring irreversible inhibitor of acetylcholinesterase with a novel mechanism of action. *Mol. Pharmacol.* **36**, 349–354 (1989).
  111. Carmichael, W. The toxins of cyanobacteria. *Sci. Am.* **270**, 78–86 (1994).
  112. Wilson, I. B. Molecular complementarity and antidotes for alkylphosphate poisoning. *Fed. Proc.* **18**, 752–758 (1959).
  113. Keeler, J. R., Hurst, C. G. & Dunn, M. A. Pyridostigmine used as a nerve agent pretreatment under wartime conditions. *J. Am. Med. Assoc.* **266**, 693–695 (1991).
  114. Haley, R. W., Kurt, T. L. & Hom, J. Is there a Gulf War Syndrome? Searching for syndromes by factor analysis of symptoms. *J. Am. Med. Assoc.* **277**, 215–222 (1997).
  115. Sapolsky, R. M. The stress of Gulf War syndrome. *Nature Med.* **3**, 308–309 (1998).
  116. Friedman, A. *et al.* Pyridostigmine brain penetration under stress enhances neuronal excitability and induces early immediate transcriptional response. *Nature Med.* **2**, 1382–1385 (1996).
  117. Grauer, E., Alkalai, D., Kapon, J., Cohen, G. & Raveh, L. Stress does not enable pyridostigmine to inhibit brain cholinesterase after parenteral administration. *Toxicol. Appl. Pharmacol.* **164**, 301–304 (2000).
  118. Lallemand, G. *et al.* Heat stress, even extreme, does not induce penetration of pyridostigmine into the brain of guinea pigs. *Neurotoxicology* **19**, 759–766 (1998).
  119. Esposito, P. *et al.* Acute stress increases permeability of the blood-brain-barrier through activation of brain mast cells. *Brain Res.* **888**, 117–127 (2001).
  120. Grauer, E. *et al.* Viral neuroinvasion as a marker for BBB integrity following exposure to cholinesterase inhibitors. *Life Sci.* **68**, 985–990 (2001).
  121. Relyea, R. A. & Mills, N. Predator-induced stress makes the pesticide carbaryl more deadly to gray treefrog tadpoles (*Hyla versicolor*). *Proc. Natl Acad. Sci. USA* **98**, 2491–2496 (2001).
  122. Coyle, J. T., Price, D. L. & DeLong, M. R. Alzheimer's disease: a disorder of cortical cholinergic innervation. *Science* **219**, 1184–1190 (1983).
  123. Patrick, J. & Lindstrom, J. Autoimmune response to acetylcholine receptor. *Science* **180**, 871–872 (1973).
  124. Keesey, J. C. Contemporary opinions about Mary Walker: a shy pioneer of therapeutic neurology. *Neurology* **51**, 1433–1439 (1998).
  125. Beeri, R. *et al.* Enhanced hemicholinium binding and attenuated dendrite branching in cognitively impaired acetylcholinesterase-transgenic mice. *J. Neurochem.* **69**, 2441–2451 (1997).
  126. Alvarez, A. *et al.* Stable complexes involving acetylcholinesterase and amyloid- $\beta$  peptide change the biochemical properties of the enzyme and increase the neurotoxicity of Alzheimer's fibrils. *J. Neurosci.* **18**, 3213–3223 (1998).
  127. Sberna, G. *et al.* Acetylcholinesterase is increased in the brains of transgenic mice expressing the C-terminal fragment (CT100) of the  $\beta$ -amyloid protein precursor of Alzheimer's disease. *J. Neurochem.* **71**, 723–731 (1998).
  128. Wilson, B. W. & Viola, G. A. Multiple forms of acetylcholinesterase in nutritional and inherited muscular dystrophy of the chicken. *J. Neurol. Sci.* **16**, 183–192 (1972).
  129. Silman, I., di Giambardino, L., Lyles, L., Couraud, J. Y. & Barnard, E. A. Parallel regulation of acetylcholinesterase and pseudocholinesterase in normal, denervated and dystrophic chicken skeletal muscle. *Nature* **280**, 160–162 (1979).

### We welcome correspondence

Has something in the journal caught your attention?

If so, please write to us about it by sending an email to: [naturereviews@nature.com](mailto:naturereviews@nature.com) and flag it for the attention of the *Nature Reviews Neuroscience* editors.

Correspondence to the journal will be selected by the editors for publication on the *Nature Reviews Neuroscience* Website at <http://www.nature.com/reviews/neuroscience/> where it will be linked to the relevant article.

# Anti-Sense Approach to Anticholinesterase Therapeutics

Hermona Soreq PhD and Shlomo Seidman PhD

Department of Biological Chemistry, Life Sciences Institute, The Hebrew University, Jerusalem, Israel

Key words: anti-sense, acetylcholinesterase, myasthenia gravis, stress, head injury, Alzheimer's disease, cholinesterase inhibitors

## Abstract

The acetylcholine-hydrolyzing enzyme, acetylcholinesterase, is the molecular target of approved drugs for Alzheimer's disease and myasthenia gravis. However, recent data implicate AChE splicing variants in the etiology of complex diseases such as AD and MG. Despite the large arsenal of anti-AChE drugs, therapeutic inhibitors are primarily targeted towards an active site shared by all variants. In contrast, anti-sense oligonucleotides attack unique mRNA sequences rather than tertiary protein structures. AS-ODNs thus offer a means to target gene expression in a highly discriminative manner using very low concentrations of drug. In light of the likely role(s) of specific AChE variants in various diseases affecting cholinergic neurotransmission, the potential contribution that anti-sense technology can make towards improved approaches to anti-AChE therapeutics deserves serious attention.

*IMAJ 2000;2(Suppl):81-85*

## The high specificity of anti-sense oligonucleotides

Anti-sense oligonucleotides are short synthetic DNA chains, usually 15–25 nucleotides long, that have been designed to hybridize with a target messenger RNA according to the rules of Watson-Crick base-pairing [1,2]. The cellular uptake of oligonucleotides is not well understood. However, once inside the cell, the AS-ODN finds its complementary mRNA and forms an RNA-ODN duplex. The action of RNaseH upon the nascent hybrid results in AS-ODN-mediated destruction of the target RNA. To protect AS-ODNs from nucleolytic degradation, chemically modified analogs have been developed that display both prolonged and enhanced anti-sense effects. Common modifications include substitution of a non-bridging oxygen in the phosphodiester backbone with sulfur (phosphorothioate modification), and replacement of the 5' and/or 3' terminal bases of the ODN with 2'-O-methyl ribonucleotides. Since each of these modifications

AChE = acetylcholinesterase  
AD = Alzheimer's disease  
MG = myasthenia gravis  
AS-ODNs = anti-sense oligonucleotides

has its own unique advantages and disadvantages, it is becoming accepted to combine variably modified nucleotides into what are known as mixed-base oligonucleotides. AS-ODNs have been used to study a variety of medically relevant nervous system proteins, including ion channels, neurotransmitter receptors, neuropeptides and enzymes [Table 1]. Indeed, remarkable success has been reported using anti-sense technology to dissect the roles of closely related and pharmacologically indistinguishable proteins in the central nervous system [3].

## Current anticholinesterase pharmacology

Acetylcholinesterase is responsible for the control of neurotransmission at cholinergic synapses and neuromuscular junctions by hydrolyzing acetylcholine. Rapid hydrolysis of ACh removes excess neurotransmitter from the synapse, preventing overstimulation and tetanic excitation of the postsynaptic cell. For this reason, AChE is the target protein of pesticides and chemical warfare

Table 1. Examples of nervous system proteins studied using anti-sense oligonucleotides

Potassium channels	N. Meiri, et al., <i>Proc Natl Acad Sci USA</i> 1997;94:4430–4 N. Meiri, et al., <i>Proc Natl Acad Sci USA</i> 1998;95:15037–42
Dopamine receptors	J.M. Tepper, et al., <i>J Neurosci</i> 1997;17:2519–30.
cAMP response element-binding protein (CREB)	S.B. Lane Ladd, et al., <i>J Neurosci</i> 1997;17:7890–901 R. Lamprecht, et al., <i>J Neurosci</i> 1997;17:8443–50.
Neuropeptide Y; galanin	P.S. Kalra, et al., <i>Methods Enzymol</i> 2000;314:184–200
Opioid receptors	G.W. Pasternak, Y X. Pan, <i>Methods Enzymol</i> 2000;2314:51–60 P. Sanchez-Blazquez, et al., <i>Antisense Nucleic Acid Drug Dev</i> 1999;9:253–60
Neuronal nitrous oxide synthetase (nNOS)	Y.A. Kolesnikov, et al., <i>Proc Natl Acad Sci USA</i> 1997;94:8220–5
Cyclic nucleotide phosphodiesterases (PDE)	P.M. Epstein, <i>Methods</i> 1998;14:21–33

ACh = acetylcholine

agents [4,5]. At the same time, controlled use of AChE inhibitors plays a leading role in therapeutic strategies designed to enhance the cholinergic system. The rationale behind the clinical use of anticholinesterases is that AChE blockade extends the half-life of released ACh, thereby enhancing postsynaptic signals in patients with compromised cholinergic function. Indeed, the extensive use of anticholinesterase therapies highlights their clinical value. Nevertheless, accumulated experience attests to the limited extent and duration of clinical effects achieved with pharmacological AChE inhibitors. Recent advances in molecular and cellular biology suggest several explanations to account for limitations of classic anticholinesterase therapeutics and suggest a novel genome-based approach.

### Specificity in anticholinesterase pharmaceuticals

A primary challenge confronting anticholinesterase pharmacology is to overcome the structural and functional homology between AChE and butyrylcholinesterase, also known as "serum cholinesterase" [6,7]. AChE and BChE are carboxylesterase type B serine hydrolases with 52% identity [8]. Both enzymes degrade acetylcholine. However, AChE is very specific in its substrate recognition, while BChE recognizes a broad range of substrates. For this reason, it has been suggested that circulating plasma BChE serves a scavenging function, protecting AChE from naturally occurring inhibitors. At the same time, however, BChE will also scavenge anticholinesterase drugs, elevating the dose necessary to achieve inhibition at the target organ. To complicate the issue, the large number of polymorphic BChE variants with differing affinities for inhibitors was predicted to confer inheritable variations in the sensitivity of individuals to anti-AChE drugs and poisons [9]. The AChE/BChE specificity problem has been partially overcome with the development of AChE inhibitors, demonstrating up to 1,000-fold preference for AChE [10]. Nevertheless, the minimal homology displayed by AChE and BChE at the level of the gene makes these sequences completely non-overlapping targets for an anti-sense-based drug.

### AChE variants

A new dimension to the question of specificity with regard to AChE inhibitors emerged as molecular cloning revealed that alternative splicing gives rise to three distinct AChE isoforms [11,12]. The presumed target of all anticholinesterase therapeutics is the "synaptic" AChE-S isoform with its unique 40 amino acid, amphiphilic, C-terminal peptide. A second, erythrocyte-bound form, AChE-E, is presumed to participate with BChE in scavenging blood-borne inhibitors, including drugs of abuse [13]. Until recently, AChE-S and AChE-E were considered the primary factors in the development of anticholinesterase

drugs. Recently, the rare "readthrough" AChE-R isoform was discovered to undergo dramatic upregulation under some conditions, including acute psychological stress, closed head injury, and exposure to AChE inhibitors [14,15]. This finding suggested that AChE-R plays a role in the body's response to stress [16,17]. In addition, it raised the possibility that the balance between AChE-R and AChE-S carries important implications for health and disease. These studies therefore challenge us to develop inhibitors that selectively target specific AChE variants. However, the differences in the affinities of inhibitors for AChE-S and AChE-R are small (Salmon et al., submitted), suggesting an anti-sense approach to the problem of isoform-specific inhibition of AChE.

### Transgenic models of AChE over-expression

The discovery that traumatic insults and AChE inhibitors elicit feedback over-expression of AChE-R highlights the complexity of anticholinesterase therapeutics on the one hand, and the need to understand the physiological role of AChE-R on the other. To examine these issues, we produced transgenic mice over-expressing various AChE isoforms. Mice over-expressing AChE-S in CNS neurons displayed an age-dependent tendency for increased AChE-R that was associated with neuromotor and cognitive impairments that presented features of human neurological diseases [18-20]. In contrast, transgenic mice over-expressing AChE-R from birth were relatively free of age-dependent markers of neuronal stress [21]. These studies indicate that the long-term balance between AChE-S and AChE-R may be a critical element mediating outcomes of AChE responses.

### Avoiding feedback

Electrophysiological recordings in hippocampal brain slices indicated that overproduction of AChE-R is initiated by the acute cholinergic stimulation resulting from abrupt pharmacological blockade of AChE [14]. Moreover, novel polymorphisms in the upstream promoter region of the human ACHE gene locus encoding AChE have been associated with acute hypersensitivity to anticholinesterase drugs [22]. Anti-sense technology offers two solutions to this problem. First, the relative instability of AChE-R vs. AChE-S mRNA [23] suggests that AS-ODNs could be aimed primarily at AChE-R, leaving AChE-S and cholinergic neurotransmission intact. Moreover, by blocking production of new AChE rather than neutralizing existing AChE, anti-sense suppression of enzyme activity occurs more slowly than that of conventional drugs. Gradual inhibition allows the target tissue to adapt to graded increases in ACh concentrations. Finally, thanks to the anti-mRNA nature of anti-sense blockade, oligonucleotide doses can be tailored to suppress *de novo* expression of the ACHE gene (N. Galyam and H. Soreq, unpublished data).

## Non-catalytic activities of AChE

In addition to its long-recognized role in hydrolyzing acetylcholine, AChE exerts profound effects on neurite outgrowth and cell adhesion [7,24]. These activities were proven to be independent of ACh hydrolysis [25] and were tentatively attributed to homologies between AChE and cholinesterase-like cell adhesion molecules like *Drosophila* neurotactin and mammalian neuroligins [26–28]. Non-catalytic activities of AChE have been tentatively mapped to the peripheral anionic site, but were not yet shown to be affected by conventional anticholinesterase drugs. Moreover, since damaging effects of over-expressed AChE-R may be related to non-catalytic activities, cholinesterase inhibitors may actually aggravate certain conditions by elevating the levels of catalytically inactivated AChE via the feedback loop. Since anti-sense technology targets production of the protein, rather than the activity of existing enzyme, AS-ODNs offer a potential solution to this problem as well.

## Anti-AChE anti-sense oligonucleotides – where do we stand?

AS-ODNs to AChE have been demonstrated effective *in vitro* and *in vivo*, especially in the hematopoietic system [29–31]. First-generation anti-AChE AS-ODNs were prepared in unmodified or fully phosphorothioated forms [32] and then in partially phosphorothioated form. Reducing the phosphorothioate content minimized cytotoxicity without compromising activity [33]. Two AChE AS-ODNs, AS1 and AS3 [23], demonstrated potent inhibition of AChE in rat pheochromocytoma PC12 cells (up to 50%) at extremely low nanomolar concentrations. Substitution of 2'-O-methyl-modified ribonucleotides at the three terminal 3' positions conferred a wide effective window (0.02–200 nM; N. Galyam and H. Soreq, manuscript in preparation) and became the routine configuration for AS-ODN synthesis in our laboratory. In osteosarcoma Saos-2 cells, 2 nM AS-ODN blocked AChE and modified proliferation, reinforcing evidence that AChE plays a role in mammalian osteogenesis [34]. The pronounced effects elicited by such low concentrations of AS-ODN predict reduced costs and minimal non-specific side effects of future anti-sense therapies.

## Potential applications

### Anticholinesterase exposures

The association between AChE inhibitors, AChE feedback, and neuromuscular impairments [7,35] suggests AChE AS-ODNs for treating anticholinesterase intoxication. During the Persian Gulf War, several hundred thousand soldiers received the carbamate AChE inhibitor pyridostigmine to protect them against threatened chemical warfare. A recent Rand Corporation report (Document no. MR-1018/2-OSD) prompted the U.S. Defense Department to acknowledge that pyridostigmine cannot be ruled out as a possible contributor to various

unexplained symptoms experienced by Gulf War veterans, including muscle weakness [36]. In light of our knowledge about the AChE feedback loop, the detrimental effects of over-expressed AChE on muscle [37], and the fact that no clinical protocol has been implemented to treat muscle weakness among Gulf War veterans, we suggest that this may represent an appropriate arena in which to test the utility of anti-sense therapy for neuromuscular impairments. The regrettably high incidence of agricultural anticholinesterase poisoning incidents in Israel alone (about 500 per year) suggests another potential application for anti-AChE ODN drugs.

### Neuromuscular disease

Myasthenia gravis is a debilitating neuromuscular disease characterized by muscle weakness and deterioration of neuromotor function [38]. MG results from autoimmune antibody-mediated depletion of acetylcholine receptors from neuromuscular junctions. AChE inhibitors such as Mestinon – a commercial formulation of pyridostigmine – treat the symptoms of MG but do not slow its progression [39]. Moreover, the pharmacological effects of anticholinesterase drugs are short-lasting, and relatively high doses of these medications must be taken up to six times per day for many years. It has even been suggested that pyridostigmine may contribute to progressive deterioration in muscle function [40]. In this light, it is not surprising that a promising AChE inhibitor for Alzheimer's disease was withdrawn from clinical trials after some patients reported muscle weakness (SCRIP World Pharmaceutical News, 1998, No. 2374, P. 19). We demonstrated that the AChE feedback loop is active in muscle, and that AS3 suppresses inhibitor-induced over-expression of AChE in mice [37]. In that study, 80 µg/kg AS3 blocked anticholinesterase-induced accumulation of catalytically active AChE in muscle by 60%, and suppressed the accompanying increase in motor endplates. These experiments proved that AS-ODNs can suppress both catalytic and morphogenic activities of muscle AChE *in vivo*. Tests in rats with experimental autoimmune myasthenia are in progress (in collaboration with T. Brenner).

### Head trauma

Closed head injury is a major cause of death among young adults [41,42] and a risk factor in non-familial Alzheimer's disease [43]. Effective treatment should therefore consider survival, recovery, and prevention of delayed neurological disorders. We observed elevated AChE-R mRNA in brains of mice subjected to CHI [14]. A single intracerebroventricular administration of 0.5 µg AS3 within one hour of injury blocked the accumulation of AChE-R mRNA and the excessive dendritic growth accompanying it. In AChE transgenic mice, anti-sense treatment reduced mortality, facilitated recovery and protected CA3 hippocampal neurons. These findings demonstrated the potential of anti-sense therapeutics in emergency medicine and

suggest the application of AChE AS-ODN to protect against the long-term consequences of traumatic insults to the nervous system.

### Neurodegenerative disease

Alzheimer's disease is a debilitating neurodegenerative disease characterized by progressive deterioration of cognitive faculties including learning, memory, problem solving and abstract thinking. The cholinergic theory of AD suggests that loss of cholinergic neurons leaves a relative deficit of acetylcholine in the brain regions that mediate learning and memory [44]. The only approved drugs for AD are potent AChE inhibitors [45]. Nevertheless, the cognitive improvement afforded by conventional anticholinesterase therapy is limited. Moreover, recent studies suggest that AChE plays a role in AD that goes beyond the cholinergic theory [46,47]. Indeed, the putative role of AChE as an active component in the progress of AD may explain the disappointing performance of AChE inhibitors in providing effective long-term improvement. Using surgically implanted cannulae to deliver nanomolar quantities of AS3 to the cerebrospinal fluid of cognitively impaired transgenic mice, we are testing the effects of anti-sense therapy on performance in behavior models such as social exploration and spatial navigation (O. Cohen et al., Abstract to the Israel Society of Neuroscience, Eilat, 1999). Nevertheless, the challenge of bringing AS-ODN technology to CNS therapeutics faces yet unresolved technical limitations. Among the most difficult issues to resolve is the poor transport of oligonucleotides across the blood-brain-barrier [2]

### Conclusions

Advances in our understanding of the molecular and cellular mechanisms of action of AChE allow us to postulate mechanisms explaining the limitations of conventional anticholinesterase pharmacology. These limitations are likely based on non-catalytic activities of AChE isoforms and a feedback loop leading to over-expression of AChE following acute blockade of enzymatic activity. At the same time, cloning of the human ACHE gene opened the door to novel strategies to suppress AChE biosynthesis using anti-sense technology. These advances in basic research allow us to think ahead to the application of AS-ODN-based drugs to future anticholinesterase therapeutics.

**Acknowledgements:** The work presented here was supported by Israel Ministry of Health, the U.S. Army Medical Research and Development Command, the Israel Science Foundation, the U.S.-Israel Binational Science Foundation, the Eric Roland Center for Neurodegenerative Diseases, and Ester Neurosciences, Ltd., Tel Aviv.

### References

- Agrawal S, Kandimalla ER. Antisense therapeutics: is it as simple as complementary base recognition? *Mol Med Today* 2000;6:72-81.
- Seidman S, Eckstein F, Grifman M, Soreq H. Antisense technologies have a future fighting neurodegenerative diseases. *Antisense Nucleic Acid Drug Dev* 1999;9:333-40.
- McCarthy MM. Use of antisense oligonucleotides in the central nervous system: why such success? In: Stein CA, Krieg AM, eds. *Allied Antisense Oligonucleotide Technology*. New York: Wiley-Liss, Inc., 1998:283-96.
- Soreq H, Zakut H, eds. In: *Human Cholinesterases and Anticholinesterases*. San Diego: Academic Press, 1993.
- Taylor P. Agents acting at the neuromuscular junction and autonomic ganglia. In: Hardman JG, Limbird LE, Molinoff PB, Ruddon RW, eds. *Goodman and Gilman's The Pharmacological Basis of Therapeutics*. Ninth edition. New York: McGraw-Hill, 1996:177-177.
- Schwarz M, Glick D, Loewenstein Y, Soreq H. Engineering of human cholinesterases explains and predicts diverse consequences of administration of various drugs and poisons. *Pharmacol Ther* 1995;67:283-322.
- Soreq H, Glick D. Novel roles for cholinesterases in stress and inhibitor responses. In: Giacobini E, ed. *Cholinesterases and Cholinesterase Inhibitors*. London: Martin Dunitz, 2000:47-61.
- Soreq H, Ben-Aziz R, Prody CA, Seidman S, Gnatt A, Neville L, Lieman-Hurwitz J, Lev-Lehman E, Ginzberg D, Lapidot-Lifson Y, et al. Molecular cloning and construction of the coding region for human acetylcholinesterase reveals a G + C-rich attenuating structure. *Proc Natl Acad Sci USA* 1990;87:9688-92.
- Loewenstein Lichtenstein Y, Schwarz M, Glick D, Norgaard Pedersen B, Zakut H, Soreq H. Genetic predisposition to adverse consequences of anti-cholinesterases in 'atypical' BCHE carriers. *Nat Med* 1995;1:1082-5.
- Bryson HM, Benfield P. Donepezil. *Drugs Aging* 1997;10:234-9; discussion 240-1.
- Ben Aziz Aloya R, Sternfeld M, Soreq H. Promoter elements and alternative splicing in the human ACHE gene. *Prog Brain Res* 1993;98:147-53.
- Li Y, Camp S, Rachinsky TL, Getman D, Taylor P. Gene structure of mammalian acetylcholinesterase. Alternative exons dictate tissue-specific expression. *J Biol Chem* 1991;266:23083-90.
- Salmon AY, Goren Z, Avissar Y, Soreq H. Human erythrocyte but not brain acetylcholinesterase hydrolyses heroin to morphine. *Clin Exp Pharmacol Physiol* 1999;26:596-600.
- Friedman A, Kaufer D, Shemer J, Hendler I, Soreq H, Tur Kaspas I. Pyridostigmine brain penetration under stress enhances neuronal excitability and induces early immediate transcriptional response. *Nat Med* 1996;2:1382-5.
- Shohami E, Kaufer D, Chen Y, Seidman S, Cohen O, Ginzberg D, Melamed-Book N, Yirmiya R, Soreq H. Antisense prevention of neuronal damages following head injury in mice. *J Mol Med* 2000. In press.
- Kaufer D, Soreq H. Tracking cholinergic pathways from psychological and chemical stressors to variable neurodegeneration paradigms. *Curr Opin Neurol* 1999;12:739-43.
- Kaufer D, Friedman A, Soreq H. The vicious circle: long-lasting transcriptional modulation of cholinergic neurotransmission following stress and anticholinesterase exposure. *The Neuroscientist* 1999;5:173-83.
- Beeri R, Le Novere N, Mervis R, Huberman T, Grauer E, Changeux JP, Soreq H. Enhanced hemicholinium binding and attenuated dendrite branching in cognitively impaired acetylcholinesterase-transgenic mice. *J Neurochem* 1997;69:2441-51.
- Beeri R, Andres C, Lev-Lehman E, Timberg R, Huberman T, Shani M, Soreq H. Transgenic expression of human acetylcholinesterase induces progressive cognitive deterioration in mice. *Curr Biol* 1995;5:1063-71.
- Andres C, Beeri R, Friedman A, Lev-Lehman E, Henis S, Timberg R, Shani M, Soreq H. Acetylcholinesterase-transgenic mice display embryonic modulations in spinal cord choline acetyltransferase and neurexin Ibeta gene expression followed by late-onset neuromotor deterioration. *Proc Natl Acad Sci USA* 1997;94:8173-8.
- Sternfeld M, Shoham S, Klein O, Flores-Flores C, Eylon T, Idelson GH, Katsberg D, Patel JW, Soreq H. Excess "readthrough" acetylcholinesterase attenuates but the "synaptic" variant intensifies neurodegeneration correlates. *Proc Natl Acad Sci USA* 2000; (in press).
- Shapira M, Tur-Kaspas I, Bosgraaf L, Livni N, Grant AD, Grisaru D, Korner M, Elstein RP, Soreq H. A transcription-activating polymorphism in the ACHE promoter associated with acute sensitivity to anti-acetylcholinesterases. *Hum Mol Genet* 2000;9:1273-81.
- Grifman M, Soreq H. Differentiation intensifies the susceptibility of pheochromocytoma cells to antisense oligodeoxynucleotide-dependent suppression of acetylcholinesterase activity. *Antisense Nucleic Acid Drug Dev* 1997;7:351-9.

24. Grisaru D, Sternfeld M, Eldor A, Glick D, Soreq H. Structural roles of acetylcholinesterase variants in biology and pathology. *Eur J Biochem* 1999;264:672-86.
25. Sternfeld M, Ming G, Song H, Sela K, Timberg R, Poo M, Soreq H. Acetylcholinesterase enhances neurite growth and synapse development through alternative contributions of its hydrolytic capacity, core protein, and variable C termini. *J Neurosci* 1998;18:1240-9.
26. Darboux I, Barthalay Y, Pivoant M, Hipeau Jacquotte R. The structure-function relationships in *Drosophila* neurotactin show that cholinesterase domains may have adhesive properties. *EMBO J* 1996;15:4835-43.
27. Ichtchenko K, Nguyen T, Sudhof TC. Structures, alternative splicing, and neurexin binding of multiple neuroligins. *J Biol Chem* 1996;271:2676-82.
28. Grifman M, Galyan N, Seidman S, Soreq H. Functional redundancy of acetylcholinesterase and neuroligin in mammalian neurogenesis. *Proc Natl Acad Sci USA* 1998;95:13935-40.
29. Soreq H, Patinkin D, Lev-Lehman E, Grifman M, Ginzberg D, Eckstein F, Zakut H. Antisense oligonucleotide inhibition of acetylcholinesterase gene expression induces progenitor cell expansion and suppresses hematopoietic apoptosis ex vivo. *Proc Natl Acad Sci USA* 1994;91:7907-11.
30. Lev-Lehman E, Ginzberg D, Hornreich G, Ehrlich G, Meshorer A, Eckstein F, Soreq H, Zakut H. Antisense inhibition of acetylcholinesterase gene expression causes transient hematopoietic alterations in vivo. *Gene Ther* 1994;1:127-35.
31. Lev-Lehman E, Deutsch V, Eldor A, Soreq H. Immature human megakaryocytes produce nuclear-associated acetylcholinesterase. *Blood* 1997;89:3644-53.
32. Patinkin D, Seidman S, Eckstein F, Benseler F, Zakut H, Soreq H. Manipulations of cholinesterase gene expression modulate murine megakaryocytopoiesis in vitro. *Mol Cell Biol* 1990;10:6046-50.
33. Ehrlich G, Patinkin D, Ginzberg D, Zakut H, Eckstein F, Soreq H. Use of partially phosphorothioated "antisense" oligodeoxynucleotides for sequence-dependent modulation of hematopoiesis in culture. *Antisense Res Dev* 1994;4:173-83.
34. Grisaru D, Lev-Lehman E, Shapira M, Chaikin E, Lessing JB, Eldor A, Eckstein F, Soreq H. Human osteogenesis involves differentiation-dependent increases in the morphogenetically active 3' alternative splicing variant of acetylcholinesterase. *Mol Cell Biol* 1999;19:788-95.
35. Glick D, Shapira M, Soreq H. Molecular neurotoxicity implications of acetylcholinesterase inhibition. In: Lazarovici P, Lester D, eds. Site-Specific Neurotoxicology. New York: Plenum Press. In press.
36. Haley RW, Kurt TL, Hom J. Is there a Gulf War Syndrome? Searching for syndromes by factor analysis of symptoms. *JAMA* 1997;277:215-22.
37. Lev-Lehman E, Evron T, Broide RS, Meshorer E, Ariel I, Seidman S, Soreq H. Synaptogenesis and Myopathy under Acetylcholinesterase Overexpression. *J Molec Neurosci* 2000;14:93-105.
38. Schonbeck S, Chrestel S, Hohlfeld R. Myasthenia gravis: prototype of the antireceptor autoimmune diseases. *Int Rev Neurobiol* 1990;32:175-206.
39. Evoli A, Batoocchi AP, Tonali P. A practical guide to the recognition and management of myasthenia gravis. *Drugs* 1996;52:662-70.
40. Swash M. Motor innervation of myasthenic muscles [Letter]. *Lancet* 1975;ii:663.
41. Siesjö BK. Basic mechanisms of traumatic brain damage. *Ann Emerg Med* 1993;22:959-69.
42. Yakovlev AG, Faden AI. Molecular biology of CNS injury. *J Neurotrauma* 1995;12:767-77.
43. Giennarelli TA, Graham DI. Neuropathology of the Head Injuries. *Yeman Clin Neuropsychiatry* 1998;3:160-75.
44. Coyle JT, Price DL, DeLong MR. Alzheimer's disease: a disorder of cortical cholinergic innervation. *Science* 1983;219:1184-90.
45. Giacobini E. Cholinesterase inhibitors for Alzheimer's disease therapy: from tacrine to future applications [Invited review]. *Neurochem Int* 1998;32:413-19.
46. Inestrosa NC, Alvarez A, Perez CA, Moreno RD, Vicente M, Linker C, Casanueva OI, Soto C, Garrido J. Acetylcholinesterase accelerates assembly of amyloid-beta-peptides into Alzheimer's fibrils: possible role of the peripheral site of the enzyme. *Neuron* 1996;16:881-91.
47. Campos EO, Alvarez A, Inestrosa NC. Brain acetylcholinesterase promotes amyloid-beta-peptide aggregation but does not hydrolyze amyloid precursor protein peptides. *Neurochem Res* 1998;23:135-40.

**Correspondence:** Dr. S. Soreq, Dept. of Biological Chemistry, Life Sciences Institute, The Hebrew University, Jerusalem 91904, Israel. Tel: (972-2) 658 5109; Fax: (972-2) 652 0258; email: soreq@cc.huji.ac.il.

---

# 4 Blood-Brain Barrier Modulations and Low-Level Exposure to Xenobiotics

*Hermona Soreq, Daniela Kaufer, Alon Friedman,  
and David Glick*

## CONTENTS

I. Introduction .....	122
II. The Physical Basis of Blood-Brain Barrier Properties.....	122
A. Endothelial Cells in Brain Vasculature .....	123
B. Adherens and Tight Junctions.....	124
C. Potential Involvement of Acetylcholinesterase.....	124
D. Signal-Transducing Elements .....	126
E. Astrocyte Contributions to Blood-Brain Barrier Properties .....	128
III. Functional Characteristics of the Blood-Brain Barrier.....	128
A. Inward and Outward Movement across the Blood-Brain Barrier: Physiological Considerations .....	128
B. Cholinergic Involvement in Blood-Brain Barrier Functioning .....	129
C. Pericellular Passage across Blood-Brain Barrier Structures.....	129
D. Cell Culture, Organ Systems, and Imaging Approaches in Blood-Brain Barrier Research.....	130
E. Transgenic Engineering Models for Blood-Brain Barrier Studies .....	131
IV. Modulators of Blood-Brain Barrier Functions and Their Interrelationships .....	132
A. Nitric Oxide and Vasoactive Agents Involvement.....	133
B. Immunomodulators and Multi-Drug Transporters .....	133
V. Conditions Inducing Blood-Brain Barrier Distruption.....	134
A. Pathophysiological Induction of Blood-Brain Barrier Penetrance .....	134
B. Blood-Brain Barrier Disruption Following Acute Insults.....	135
C. Psychological and Physical Stressors Impair Blood-Brain Barrier Functioning.....	135

D. Blood-Brain Barrier as a Complex Trait with Genetic and Physiological Components: Prospects . . . . .	136
VI. Summary . . . . .	137
Acknowledgments . . . . .	138
References . . . . .	138

## I. INTRODUCTION

Separation of the brain from the peripheral blood is crucial for protecting this most delicate and important organ from various insidious agents that circulate in the blood. Conversely, the separation must allow for the nutrition of the brain and the removal from it of waste products. The existence of a physical barrier that separates the brain tissue from the general circulation was first proposed 100 years ago, by Ehrlich, who discovered that injection of a series of dyes into laboratory animals resulted in uncolored brains, as opposed to highly stained visceral organs.<sup>1</sup> The blood-brain barrier (BBB) is formed during the late embryonic and early postnatal period. It is an endothelial barrier present in the capillaries throughout the brain, contact-influenced by neighboring astrocytes.<sup>2</sup> Electron microscopic studies reveal two major factors that distinguish brain endothelial cells from their peripheral relatives: first, they contain lower amounts of endocytic vesicles, and second, the space between adjacent cells is sealed by tight junctions; both factors restrict intercellular flux. These features enable the formation of a barrier that hinders the entry of most xenobiotics into the brain, and is actively involved in exporting such substances from the brain when they do enter it. Small lipophilic molecules enter the brain fairly freely, but hydrophilic molecules enter via active transport, and specific transporters exist for required nutrients such as glucose, L-DOPA, and certain amino acids.<sup>3</sup>

The physical and functional complexity of the BBB has hampered research efforts to delineate its components and fully understand its mode of action. Numerous experimental approaches were developed for evaluating BBB integrity; these include *in vitro* and *in vivo* systems as well as transgenic engineering approaches. The use of these methods has revealed several modulators of BBB functioning and has demonstrated intricate relationships between these modulators in their effects on BBB integrity. Impairments of any element of these chains of factors can disrupt BBB functioning, but the extent and duration of such disruptions apparently depend on the genetics, health, and wellbeing of the involved organism. In the following, we discuss these considerations as they relate to the issue of low-level exposure to xenobiotics.

## II. THE PHYSICAL BASIS OF BLOOD-BRAIN BARRIER PROPERTIES

Low-level exposure to xenobiotics would first affect the circulation; to affect the brain, the xenobiotic must traverse the BBB. In certain cases, e.g., under exposure to anticholinesterases, these agents interact with and inhibit the catalytic activity of their target enzymes, cholinesterases, in peripheral and brain systems alike. The cellular

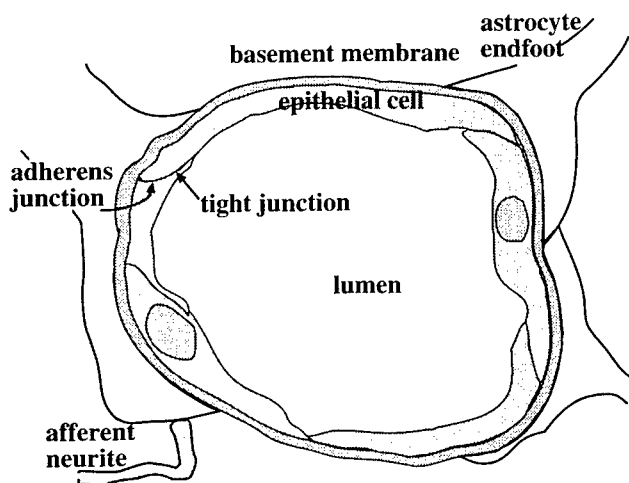


**FIGURE 4.1** The physical components of the blood-brain barrier (BBB): Within the mammalian brain, blood vessels and microvessels transverse the brain tissue, bringing in essential compounds and removing metabolic end products. The three layers surrounding the microvessel lumen comprise the BBB, including endothelial cells lining the blood vessels, a basement membrane surrounding them, and astrocyte endfeet separating these structures from adjacent neurons, some of which interact with these astrocytes through contacting neurites. Two types of junctions connect endothelial cells to each other, tight and adherens junctions.

components of the BBB include the endothelial cells that line the inside of brain capillaries, the basement membrane surrounding them, and brain astrocytes, which constitute a third layer separating these blood vessels from the surrounding brain tissue. Intercellular BBB structures include adherens junctions, which attach endothelial cells to each other, as well as the tight junctions that seal them. Within these cells, surface membrane proteins transduce signals by activation of specific kinases, and the flow of information among the several cell types is affected by neuronal and astrocytic activities in the brain as well as by peripheral metabolic changes and external forces. Figure 4.1 presents a schematic view of these elements.

#### A. ENDOTHELIAL CELLS IN BRAIN VASCULATURE

Many have reported the special properties of endothelial cells in brain vasculature.<sup>4</sup> Small hydrophobic molecules diffuse across the BBB; large and/or hydrophilic molecules may be transported only if a specific receptor or transporter exists. Thus, small hydrophobic molecules penetrate the brain by diffusion; nutrients such as glucose and certain amino acids are transported into the brain by specific transporters; and several large proteins like transferrin are transcytosed into the brain via specific receptors.

To enable these special properties, tight junctions connect brain endothelial cells, so that intercellular transport is extremely limited.<sup>5</sup> The expression of P glycoprotein

(the multi-drug resistance *mdr* protein) on their surface membrane controls both penetration of small molecule drugs into the brain and their export from the brain. Genomic disruption of the *mdr1a* (a.k.a. *mdr3*) gene causes extreme drug sensitivity, for example, to ivermectin.<sup>6</sup> This finding highlights the importance of active transport mechanisms for the integrity of BBB functioning and may imply that cumulative exposure can modulate BBB properties.

## B. ADHERENS AND TIGHT JUNCTIONS

A primary difference between endothelial cells of brain vasculature and the very similar cells that line peripheral blood cells relates to the composition and properties of the tight junctions between these cells.<sup>7-10</sup>

Adherens junctions are similar to the attachment structures of other cells in which their functions may be more easily studied on the molecular level. Yeast, for example, can express an analogue of the adherens junction, and its assembly was shown to depend upon the  $\text{Ca}^{++}$ -dependent protein kinase pathway.<sup>11</sup> Genetic studies in yeast are easy to perform, and since yeast has a well-described genome, the discovery of the genes that regulate junction formation is possible, and once the yeast gene is known, it is a relatively simple matter to discover its homologues in a mammalian genome.

Unlike adherens junctions, which form homophilic intercellular adhesion sites, tight junctions are complex structures recognized as being the molecular site of pericellular transport and its regulation.<sup>12</sup> In addition to adherens and tight junctions, brain capillary endothelial cells have transmembrane receptors for matrix proteins (e.g., integrins).<sup>9</sup> Impairment of either cell-cell or cell-matrix interactions can disrupt the BBB, in processes that parallel those of the peripheral endothelium. However, such impairments occur much less frequently in the brain.

Several proteins, including *ingulin* and *occludin*, were shown to be essential for the function of tight junctions.<sup>13,14</sup> More recently, junction-associated proteins such as *Rho* were reported to regulate tight junctions and perijunctional actin organization in polarized epithelia.<sup>15</sup> Junction proteins are physically linked to cytoskeletal elements such as actin or linking proteins like  $\beta$ -catenin in a manner subject to modulation by phosphorylation or dephosphorylation of specific kinases and phosphatases. This suggests a potential opening of tight junctions by kinase regulation, however, no experimental evidence is yet available to demonstrate such opening *in vivo*. Table 4.1 catalogs key proteins assumed to be associated with BBB junctions.

## C. POTENTIAL INVOLVEMENT OF ACETYLCHOLINESTERASE

Like yeast, for nearly a century the fruit fly *Drosophila melanogaster* has served as a model for genetics studies. With the introduction of genetic engineering and genomic databases, this has also become a powerful tool for the discovery of genes and gene products that participate in physiological functions. The identification of a physiological defect in the insect can be quickly traced to a specific gene, and the homologous sequence in the mammalian genome can then be identified, where it then serves as a candidate gene for the similar function in the mammal. For instance, a defect in

**TABLE 4.1**  
**Protein Components and Candidate Components of the Blood-Brain Barrier**

Component	Intra/Extra Cellular <sup>a</sup>	Interaction Partners <sup>b</sup>	Reviewed in
7H6 antigen	Intra and extra	Tight junction	10
Acetylcholinesterase	Extra	Neurexin	16
Actin	Intra	Catenin	10
Band 4.1 protein	Intra	Cytoskeleton	16
Cadherin	Extra	Catenin, p120	10; 17
CASK <sup>c</sup>	Intra	Neurexin II $\beta$	16
$\beta$ -catenin	Intra	Cadherin, actin	10
Cingulin	Intra	Tight junction	10
Glialactin	Intra and extra	Neurexin IV	16
ICAM-1	Extra	ICAM	18
Neuoligin	Intra and extra	Neurexin II $\beta$	16
Neurexin	Intra and extra	Neuroigin 1, CASK	16
Nitzin	Intra	Cytoskeleton	16
Occludin	Extra	ZO-1/ZO-2/p130	10
p100	Intra	Cadherin	10; 19
p120	Intra	Cadherin/catenin	10; 17; 19
p130	Intra	Tight junction, ZO-1	10
PSD-95 <sup>d</sup>	Intra	Neuroigin 1, NMDA receptor	20
RPTP <sup>d</sup>	Intra	Cadherin/catenin	10
Selectin	Extra		21
src	Intra	Adherens junction	10
Tyrosine kinase	Intra	ZO-1, $\beta$ -catenin	10
ZO-1	Intra	Tight junction, p130, tyrosine kinase	10
ZO-2	Intra	Tight junction	10

<sup>a</sup>BBB components may function in extracellular locations (extra), convey signals within intracellular locations (intra), or do both.

<sup>b</sup>Independent factors to which attachment has been shown are separated by commas; aggregates of factors to which attachment has been shown are indicated by slashes.

<sup>c</sup>Post-synaptic density.

<sup>d</sup>Calmodulin-dependent protein kinase.

<sup>d</sup>Receptor-type protein tyrosine phosphatase.

the hemolymph-neuron barrier, which serves a function analogous to the BBB in mammals, was shown to depend on the structural and functional integrity of the special septate junctions, which seal this barrier in insect larva.<sup>22,23</sup> Disruption of these structures by genomic destruction of either of two different genes, neurexin IV and gliotactin, causes severe neuronal sensitivity to the high concentrations of  $K^+$  in the hemolymph. This leads to paralysis and death of the developing insect larva. Such genomic disruption also impaired the subcellular targeting of coracle, a band 4.1 homologue that transduces signals from the cell membrane to the cytoskeleton.

Gliotactin is one of several structural homologues of the acetylcholine-hydrolyzing enzyme acetylcholinesterase (AChE) that were discovered in the past decade. Gliotactin, however, like the other AChE homologues, has no capacity for acetylcholine (ACh) hydrolysis. Intriguingly, AChE may compete with its structural homologues for their cell-cell interactions.<sup>16,24</sup> This potential involvement of AChE has raised the question of which of the three variants, formed by alternative splicing of the human AChE pre-mRNA, may be involved in these interactions. These variants are: AChE-S, the synaptic form, AChE-E, the erythrocyte form, and AChE-R, a soluble monomeric form which, perhaps significantly for BBB physiology, has been shown to be over-expressed under stress.<sup>25</sup>

Gliotactin, like several other AChE homologues, is equipped with an extracellular domain, a transmembrane peptide and C-terminal peptide that protrudes into the cytoplasm and can transduce signals into cells. In particular, it interacts with proteins, which modulate the cytoskeleton. Therefore, these discoveries present the entire series of AChE homologues and their yet unidentified binding partners as promising candidates to participate in control of the integrity of the BBB and transduction of signals that regulate its functioning. The impressive conservation of these inter- and intracellular factors, and the chain of interactions by which they may affect cytoskeletal properties, suggest a mechanism by which AChE levels, and/or the specific chemical properties of its variants, affect the integrity of the BBB. Kaufer et al.<sup>26</sup> have recently discovered a feedback process that leads to AChE-R accumulation under exposure to anticholinesterases. This points to the AChE protein as a modulator that may be intimately involved in BBB disruption under exposure to such agents. That no embryonic impairment in BBB functioning is known in mammals most likely attests to the essential role played by the BBB in mammalian embryonic development, as early lethality of such a mutant would preclude its discovery. Figure 4.2 summarizes the evolutionary conservation of the structural properties of AChE as these may be involved in BBB integrity.

#### D. SIGNAL-TRANSDUCING ELEMENTS

Appropriate functioning of the BBB and its capacity to respond to environmental insults evidently depend on fast, accurate, and sensitive transduction of appropriate signals from the periphery into the brain and vice versa. Over the past few years, several molecular components were discovered which ascertain such a flow of information and ensure its reliability. The role of guanine nucleotides in regulating BBB properties is of special interest. Endothelial capillary cells are polarized, being long and flat structures linked by tight junctions. GTP-Binding Rho proteins are responsible, in these cells, for the particular organization of the filamentous actin fibers that ensure their polarization.<sup>15</sup> Further, transduction of intracellular signals is based, in most polarized epithelial cells, primarily on PDZ domain proteins. Named for three members of this family, PDZ proteins include the post-synaptic density protein, PSD-95, the *Drosophila* tumor-suppressor protein, discs-large (DlgA), and the tight-junction protein, ZO-1; they are often found at the plasma membrane and transduce signals into the cell, affecting cytoskeletal organization.<sup>27,28</sup> That this is also the case

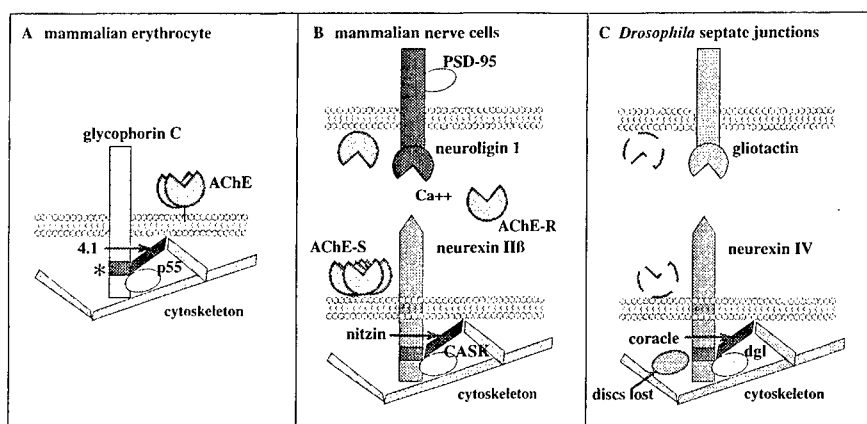


**FIGURE 4.2** AChE and its structural homologues are potentially involved in BBB functioning. Shown are schematic drawings of membrane signaling and cytoskeletal components which involve AChE and its structural homologues. (A) In the mammalian erythrocyte, glycophorin C is located on the surface membrane, with one domain protruding into the cytoplasm. A conserved element within this domain (starred) interacts with the band 4.1 protein that serves as an anchor to the cytoskeleton. Another region in the cytoplasmic domain of glycophorin C binds p55, a PDZ protein. It is not yet known whether the AChE-E dimers, which are anchored by a glycoposphoinositol moiety to the outer surface of the erythrocyte membrane, are involved in glycophorin's role of modulating the erythrocyte structure. (B) In mammalian nerve cells, the major AChE isoform is AChE-S tetramers. The AChE-homologous neuronal membrane proteins, neuroligins, are expressed in the developing brain and in excitatory synapses. At least one of the neuroligins, neuroligin 1, interacts with at least one of the neurexins, neurexin II  $\beta$ , in a  $Ca^{++}$ -dependent manner. Both neuroligin and neurexin protrude into the cytoplasm, and both interact with PDZ proteins such as PSD-95 and CASK. Neurexins further associate with neuronal band 4.1 homologues, like nitzin,<sup>16</sup> creating a link with the cytoskeleton. Modulation of AChE properties under low-level exposure to an anti-cholinesterase (e.g., accumulation of AChE-R monomers) may therefore alter neuroligin-neurexin interactions, transducing signals to the neuronal cytoskeleton. (C) In *Drosophila* septate junctions, the AChE-homologous protein, gliotactin, protrudes into the cytoplasm. Another transmembrane protein, neurexin IV, shares with other neurexins an extracellular domain that may interact with the core domain module that is common to AChE and neuroligins. Neurexin IV also includes cytoplasmic glycophorin C elements; these regions interact with the insect band 4.1 homologue, coracle, as well as with the PDZ protein dgl and the multi-PDZ domain protein, disc lost. Therefore, neurexin IV interactions with either gliotactin or the cytoskeleton are essential for maintaining septate junction integrity. It is not yet known whether AChE itself (broken-line structure) is expressed in these junctions.

for BBB components has recently been demonstrated in *Drosophila* embryos by Bellen and co-workers, who found a third protein that is essential for the integrity of septate junctions formation.<sup>29</sup> This protein, discs-lost, uses multiple PDZ domains to interact with intracellular components in a manner dependent on septate junction interactions. In general, PDZ domains interact with the carboxy terminal end of their

target proteins.<sup>27</sup> Therefore a multi-PDZ protein can aggregate a series of target proteins within the cell, simultaneously transducing multiple signals.<sup>29</sup> This enables an extremely sensitive biosensor activity, as is expected from a system designed to protect the brain from low-level exposures.

#### **E. ASTROCYTE CONTRIBUTIONS TO BLOOD-BRAIN BARRIER PROPERTIES**

Janzer and Raff recognized the key function of astrocytes that surround brain capillaries in the dynamic properties of the BBB.<sup>30</sup> Specific interactions between astrocyte endfeet, which surround brain capillaries, are essential to ensure BBB integrity. The discovery of astrocytic responses to altered ion (e.g.,  $\text{Ca}^{++}$ ) concentrations in their environment sheds new light on the specificity of astrocyte interactions and their importance for ensuring BBB integrity.<sup>31</sup> In a tissue co-culture model, astrocytes were shown to affect the integrity of the tight junctions between adjacent endothelial cells.<sup>32</sup> More recently, astrocytes were demonstrated to enhance the defense of capillary endothelial cells against reactive oxygen species.<sup>33</sup> Thus, astrocytes both signal higher centers of the brain that the BBB has been disrupted and themselves receive signals from higher centers that cause them to modulate the BBB.

### **III. FUNCTIONAL CHARACTERISTICS OF THE BLOOD-BRAIN BARRIER**

Designed to protect the brain from penetration and accumulation of unwanted molecules and cells, the BBB has distinct properties at central and peripheral structures. To properly control the inward and outward flow of constituents to and from the brain, it must sense the needs of both the brain and the peripheral system. Therefore, both the electrophysiological activity in the brain and peripheral properties such as blood pressure must affect BBB properties. Similarly, changes in BBB integrity inevitably affect brain functioning; for example, BBB disruption will allow the passage into the brain of serum constituents, which are known to affect neuronal electric activity (e.g., amino acids). The relative contribution of such agents to brain function under BBB disruption awaits further investigation.

#### **A. INWARD AND OUTWARD MOVEMENT ACROSS THE BLOOD-BRAIN BARRIER: PHYSIOLOGICAL CONSIDERATIONS**

Blood-brain barrier properties largely depend on the surrounding brain tissue. This is evident from a recent study that demonstrated the development of an intact BBB in brain tissue transplants in a manner dependent on the site of transplantation.<sup>34</sup> The integrity of BBB functioning is affected by cellular glutathione and is sensitive to oxidative stress.<sup>35</sup> Neuronal activity is another important factor in BBB functioning, perhaps through the activation of afferent axons innervating brain microvasculature. Indeed, both psychotropic drugs and nicotine impair dopamine transport across the BBB,<sup>36</sup> suggesting that BBB functioning is affected by the state of cholinergic or

dopaminergic neuronal activity, and that BBB integrity is imperative for preventing neurotoxicity under exposure to dopamine analogs (e.g., MPTP).<sup>37</sup> Thus, human cerebrovascular endothelium was shown to possess dopaminergic receptors linked to adenylyl cyclase, suggesting signal transduction activities. Adrenergic influences on BBB control were reported by Sarmiento et al.,<sup>38</sup> who also demonstrated the influence of electrical stimulation of locus coeruleus on the rat BBB permeability to sodium fluorescein. Similar effects in a cell culture model were shown by Borges.<sup>39</sup>

## **B. CHOLINERGIC INVOLVEMENT IN BLOOD-BRAIN BARRIER FUNCTIONING**

The importance of ACh innervation to cortical capillaries has been suggested on the basis of a body of biochemical and morphological data, and indicates the underlying mechanism. Purified capillaries are capable of releasing ACh in a  $Ca^{++}$ -dependent mechanism, in response to  $K^+$  depolarization or electrical stimulation.<sup>40</sup> Moreover, specific cholinergic machinery was identified in isolated microvessels from goat cerebral cortex, as demonstrated by measuring AChE and choline acetyl transferase (ChAT) activities.<sup>41</sup> ChAT activity in bovine cerebral cortex capillaries does not originate from the endothelial cells, nor do they release ACh in response to electrical stimulation. Rather, cerebrovascular ACh apparently has a neuronal origin.<sup>40</sup> The origin of the perivascular cholinergic terminals was examined in rat brains in which the nucleus basalis of Meynert, accounting for 70% of cortical ChAT activity, was lesioned. No change was observed in the microvessel-associated ChAT activity in the lesioned animals, ruling out the basal forebrain as the origin of this pathway.<sup>40</sup> The existence of released ACh hints at the presence of receptors that respond to the signal, and, indeed, muscarinic ACh receptors were identified in rat brain cortical capillaries.<sup>42,43</sup> Taken together, all this points to the involvement of cholinergic innervation of cerebral microvessels in cerebral blood flow and BBB permeability, which is an essential requirement under various physiological and pathological insults. The cholinergic involvement in BBB functioning is particularly important under exposure to cholinesterase inhibitors such as organophosphates or carbamates, since these induce a feedback response of AChE accumulation, which would lead to cholinergic hypo-functioning.<sup>26,44</sup> Therefore, AChE may affect BBB disruption through two inter-related mechanisms, which involve its catalytic capacity for ACh hydrolysis or its structural resemblance to gliotactin, neuroligins, or related proteins.<sup>20,29</sup>

## **C. PERICELLULAR CELL PASSAGE ACROSS BLOOD-BRAIN BARRIER STRUCTURES**

One of the roles of the BBB likely involves protection of the brain from invasive bacteria, viruses, and fungi. However, when under BBB disruption any of these parasites invades the brain, the immune system must respond. This implies that under certain conditions, lymphocytes cross the BBB and reach those sites in the brain where their protective functions are needed. The existence of tight junctions between endothelial

cells in brain vasculature complicates this process and requires specific signaling to ensure the specificity of the pericellular transport. Also, the endothelial monolayer needs to be re-sealed once this transport has been completed. A recent study demonstrates that lymphocyte migration through brain endothelial cell monolayers involves signaling through endothelial I-CAM-1 via a Rho-dependent pathway, thus expanding the list of BBB-involved molecules.<sup>18</sup>

Mast cells represent another cell type that might penetrate the brain through BBB structures. This is of considerable importance because of the key role of mast cells in autoimmune demyelinating diseases.<sup>45-47</sup> When interacting with myelin basic protein, mast cells degranulate to induce by exocytosis immediate demyelination.<sup>48,49</sup> Under normal circumstances mast cells are located in leptomeninges and are concentrated along blood vessels, especially in dorsal thalamic nuclei.<sup>50</sup> Exposure to steroid hormones induces in mast cells massive secretion of, for example, histamine.<sup>51</sup> Several of the other neuromodulators, neurotransmitters, and growth factors secreted by mast cells can alter BBB properties.<sup>52</sup> Using confocal microscopy and vital dyes, Silverman et al.<sup>53</sup> very recently demonstrated rapid penetrance of mast cells through BBB structures into nests of glial processes. This transport may account for the rapid increases in mast cell populations after physiological manipulations.

#### D. CELL CULTURE, ORGAN SYSTEMS, AND IMAGING APPROACHES IN BLOOD-BRAIN BARRIER RESEARCH

The complexity and plasticity of BBB properties called for experimental dissection of the disruption process in both *in vitro* and *in vivo* conditions. Multiple cell and organ cultures, animal models, and measurement techniques have been developed, each of which addresses some of the issues involved. The development of research into BBB characteristics was initially approached in avian embryos, where transplanted endothelial quail cells invaded a developing chick chimera.<sup>54</sup> A simpler cell culture model of the BBB was developed by Rubin and co-workers.<sup>55</sup> More recently, an immortalized cell line created from vascular endothelial cells was used to develop another model of the BBB in co-cultures with glioma cells and was used to demonstrate nitric oxide-induced perturbations of these cells.<sup>56</sup> In another cell culture model, hypoxia was shown to increase the susceptibility to oxidative stress and intercellular permeability.<sup>57</sup>

Measurements of Evans blue penetrance proved useful in analyzing BBB properties in animal models.<sup>58</sup> Recent technological breakthroughs in brain imaging now offer a previously impossible view into the integrity of human BBB under various conditions. Imaging the human brain is widely used in the clinical and research settings by two major methods: (1) computerized tomography (CT) and (2) magnetic resonance imaging (MRI). In both methods, standard techniques use contrast agents to enhance signals and unmask brain pathologies. Both approaches are therefore aimed at delineation of the site, duration, and extent of potential BBB disruption in CNS pathologies.

Iodine is the only heavy atom that possesses the chemical properties suitable for intravascular use in CT analyses. The currently available iodinated contrast agents are

nonionic, are highly hydrophilic, and have low osmolarity and minimal toxicity. The paramagnetic atom gadolinium (Gd), with seven unpaired electrons, forms a stable complex with diethylenetriamine pentaacetic acid (DTPA) and is the contrast material used in MRI. The DTPA complex is well tolerated and even minimal concentrations lead to marked shortening of its observed relaxation times and increase in signal intensity.

Both contrast agents normally do not cross the BBB. When injected intravenously, neither Gd nor DTPA affects BBB integrity. In contrast, intra-arterial injection of iodinated contrast agents was shown to disrupt normal BBB functioning due to both osmotic and chemotoxic effects (reviewed by Sage et al.).<sup>59</sup> This study, performed to determine the safety of currently used contrast agents, is of considerable significance for predicting the risks involved in low-level exposure to xenobiotics, as it indicates that even minor arterial elevation of the concentration of potentially harmful agents may by itself disrupt BBB functions.

In healthy individuals with normally functioning BBB, CT and MRI contrast agents cannot accumulate in the extracellular fluid of the brain parenchyma. Therefore, brain structures are not enhanced and remain relatively transparent in the imaging scans. In cases when the permeability of the BBB is increased because of a pathological process, the passage of iodinated agents (in CT) or paramagnetic DTPA complex (in MRI) leads to enhancement of signals. This occurs through X-ray attenuation, creating enhanced brain images in CT scans, or shortening of relaxation times, which results in sharper images in MRI. Such alterations in BBB penetrance may be local or massive, reflecting brain tumors, infectious disease, or cerebrovascular impairments. Figure 4.3 demonstrates examples for such imaging analyses of human BBB disruption.

## **E. TRANSGENIC ENGINEERING MODELS FOR BLOOD-BRAIN BARRIER STUDIES**

Genetic manipulations of the molecular mechanisms controlling BBB functioning yield new insights into the corresponding physiological or pathological circumstances and the dissection of their effects on BBB integrity. Several transgenic and knockout models have unraveled key elements involved in BBB functioning. These included several intentional as well as serendipitous studies. Mice with a genetic disruption in the *mdr1a* gene (multiple drug resistance), encoding the drug-transporting P-glycoprotein, which resides in the BBB, display up to 10-fold increases in their dexamethasone uptake into the brain.<sup>60</sup> The effect of cytokine overproduction on BBB functioning was checked in transgenic mice that overexpress interleukin 3 (IL3) or interleukin 6 (IL6). The IL3 transgenics develop progressive demyelination and infiltrated CNS lesions associated with BBB defects.<sup>61</sup> The effects observed in IL6 transgenics were even more dramatic: extensive breakdown of the BBB was evident in the cerebellum of IL6-overproducing mice, followed by subsequent inflammation, reactive gliosis, axonal degeneration, and macrophage accumulation.<sup>62</sup> CuZn-superoxide dismutase (SOD) was discovered to have protective effects against trauma-induced BBB disruption, in a model of mice that overexpress human SOD.<sup>63</sup> These

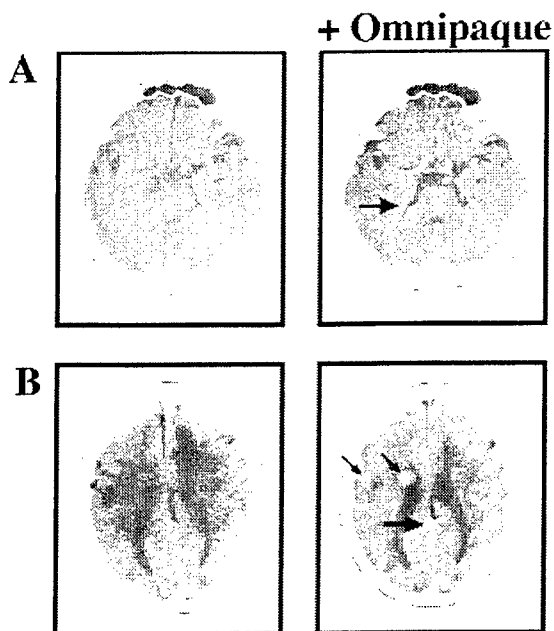


**FIGURE 4.3** Blood-brain barrier disruption as revealed by computerized tomography: A. Normal CT scan, before and after injection of the enhancement material, Omnipaque™. Note the enhancement (hyperdense white) in brain arteries and vein sinuses (wide arrows) without penetration into the brain parenchyma. B. A case of multiple brain metastases in a 41-year-old female with a history of breast cancer. Following injection of Omnipaque™, several round white regions appear, reflecting focal BBB disruption in the regions harboring tumors (thin arrows).

mice were further found to display improved neurological recovery following traumatic brain injury,<sup>64</sup> which emphasizes the importance of oxidative stress in BBB disruption.

#### IV. MODULATORS OF BLOOD-BRAIN BARRIER FUNCTIONS AND THEIR INTERRELATIONSHIPS

Several considerations point to specific natural compounds and therapeutic agents as potential modulators of BBB functions. The rapid kinetics of BBB transport implicates post-translational control mechanisms in this process, simply because there is insufficient time to allow the slow transcription and translation processes to take place. The intimate relationship with vasculature properties points to vasoactive agents as potential modulators, and the necessity for penetrance of cells from the

immune system suggests the involvement of immunomodulators. These, and drug transporters, should all communicate with the complex array of molecules and cellular structures that together compose the BBB.

Kinase cascades, universal pathways for rapid signal transduction in numerous biological processes, were naturally investigated for their potential relevance to BBB functioning. To regulate BBB properties, such kinase cascades should be induced in the various cell types that comprise the BBB. This prediction is verified by the finding that a pituitary adenylyl cyclase-activating polypeptide is successfully transported across the BBB, preventing the ischemia-induced death of hippocampal neurons.<sup>65</sup> The next logical step in this kinase cascade is tyrosine phosphorylation, which may increase tight junction permeability.<sup>66</sup> That such phosphorylation is actively involved in regulating BBB transport processes is evident from findings of phosphorylation of endothelial Na-K-Cl co-transport protein under changes in tonicity and hormones.<sup>67</sup>

#### A. NITRIC OXIDE AND VASOACTIVE AGENTS INVOLVEMENT

A primary mediator that was demonstrated to participate in meningitis-induced BBB disruption is nitric oxide (NO). NO is produced in response to exposure to bacterial endotoxins by the host endothelial cells. In an animal model of lipopolysaccharide-induced meningitis, BBB disruption and NO production sites in the brain co-localized,<sup>68</sup> and NO-synthase inhibitors reduced the meningeal-associated alterations in BBB permeability.<sup>69</sup> NO is likely produced by astrocytes, and it decreases endothelin-1 secretion by brain microvessel endothelial cells.<sup>70,71</sup>

Agents that regulate vasoactive processes, such as bradykinin and angiotensin, were shown to effect biochemical opening of the BBB.<sup>72</sup> In tissue culture experiments, such agents were further demonstrated to modulate tight junction structures in BBB endothelial cells co-cultured with astrocytes.<sup>32</sup> In cultured A431 cells, the signaling cascade induced by these agents was shown to involve tyrosine phosphorylation and reorganization of the tight junction protein ZO-1, processes that are also mediated by epidermal growth factor-1 (EGF1).<sup>73</sup>

#### B. IMMUNOMODULATORS AND MULTI-DRUG TRANSPORTERS

The passage of immunomodulators across the BBB has been the subject of much research activity, especially because of the known impairment in BBB functioning in autoimmune diseases such as multiple sclerosis (MS).<sup>74</sup> It is generally considered that basic mechanisms of brain inflammation involve massive, yet transient, disruption of BBB functioning that plays an important role in the acute episodes of several autoimmune diseases.<sup>75</sup> This may indicate that individuals with an inherited susceptibility to autoimmune responses are a high-risk group for low-level exposure to xenobiotics.

The mdral genomic disruption studies noted above have pointed to this multi-drug transporter protein as a rate-limiting factor in the bidirectional transport of drugs across the BBB. This finding explained the drug-induced neurotoxicity under chemotherapy and opens interesting options for developing BBB-regulating drugs.

Interestingly, the mouse *mdr1a* gene is also the earliest known endothelial cell differentiation marker during BBB development.<sup>76</sup>

## V. CONDITIONS INDUCING BLOOD-BRAIN BARRIER DISRUPTION

The pathophysiological origin of BBB impairments is of major clinical interest for several reasons. Impairment is dangerous, as it may cause extreme susceptibility to adverse drug responses, which would necessitate individualized drug dosage; however, breaching the barrier is sometimes useful to enable delivery of needed drugs to the brain (for example, under bacterial, fungal, or viral brain infection, or in cases of malignant brain tumors).

### A. PATHOPHYSIOLOGICAL INDUCTION OF BLOOD-BRAIN BARRIER PENETRANCE

Several diseases are known which are associated with BBB disruption. These include brain tumor metastases; epilepsy and the more severe condition of status epilepticus; cerebrovascular disorders; autoimmune diseases such as multiple sclerosis; acute cerebral infarcts; meningeal carcinomatosis; and ischemic white matter lesions.<sup>77-84</sup> Several genetic polymorphisms are known which increase the susceptibility to BBB disruption. These include polymorphisms in glutathione transferase, important for protection against oxidative stress,<sup>85</sup> and malfunctioning variants of serum BChE (e.g., "atypical" *BCHE*).<sup>86</sup> In particular, such mutations increase the risk of BBB disruption that is involved with exposure to anticholinesterases or to lead sulfate batteries, with subsequent increased risk for Parkinson's disease.<sup>87,88</sup>

Disruption of the BBB was reported in MS patients examined by contrast-enhanced MRI.<sup>89</sup> Blood-brain barrier disruption in MS patients was suggested to be the initial event in the development of the brain lesions that are characteristic of the advanced stages of this disease.<sup>90</sup> It correlates with the severity of symptoms, and an earlier age of the disease onset.<sup>91</sup> Another pathological condition in which BBB breakdown was demonstrated is epilepsy. Disruption was demonstrated by computerized tomography (CT) in a patient following generalized seizure and by Evans blue penetration in a rat model of pentylentetrazol-induced seizures.<sup>92,93</sup>

Cerebrovascular pathologies are abundant in Alzheimer's disease (AD) and are demonstrated by changes in the endothelium, amyloid depositions in the cerebral blood vessels, and disruption of the BBB.<sup>94</sup> A possible mechanism that underlies this phenomenon may be drawn from *in vitro* studies using a BBB model of a monolayer of vascular endothelial cells. Amyloid  $\beta$ -peptide, which deposits in plaques of AD patients, induced in these cells permeability to albumin and apoptotic cell death.<sup>95</sup> The potential clinical relevance of this finding was emphasized by intracarotid infusion of amyloid  $\beta$ -peptide, which resulted in BBB damage.<sup>96</sup>

BBB disruption has also been reported for CNS infections, primarily in meningitis, where it is used as a differential diagnostic tool. In an acute cytokine-induced mouse model of meningitis, endothelial selectins (glycoproteins involved in cell adhesion) were demonstrated to contribute toward the disruption of the BBB.<sup>21</sup>

HIV-1 infection of the CNS was also suggested to involve a component of chronic brain tissue inflammation and BBB disruption, resulting in neuronal injury and death, which lead to cognitive, motor, and behavioral impairments.<sup>97</sup>

## **B. BLOOD-BRAIN BARRIER DISRUPTION FOLLOWING ACUTE INSULTS**

Blood-brain barrier disruption following ischemia is well documented. Carotid artery occlusion, followed by reperfusion resulted in transendothelial leakage of a marker horseradish peroxidase in the hippocampus.<sup>98</sup> Unilateral BBB permeabilization in the cortex and striatum subregions was demonstrated in a rabbit model of ischemic hemisphere using contrast-enhanced MRI.<sup>99</sup> Extreme temperature changes appear to be an additional factor influencing BBB integrity, as both cold and heat stress impair it. Cold injury in mice induced the penetrance of Evans blue, immediately following the injury, with reversal to the normal situation of intact BBB only 24 h post-injury.<sup>100</sup> In a milder model, infusion of hypothermic saline into the left carotid artery of rats resulted in disruption of the BBB in the left hemisphere, which did not occur with a normothermic solution.<sup>93</sup> The effects of hyperthermia, on the other hand, were checked in a model of local heating of a rat's head. BBB opening was observed from 6 h to 3 days post-injury.<sup>101</sup> Similar results were noted in rats that were exposed to general heat stress (38°C) for 4 hours.<sup>102</sup> The involvement of the NO pathway in this phenomenon<sup>103</sup> was indicated by the up-regulation of neuronal NO synthase activity, which coincided with BBB breakdown in distinct brain regions.<sup>104</sup>

Traumatic brain injury, simulated by a model of closed head injury to mice, had also been shown to result in disruption of the BBB.<sup>105</sup> The temporal resolution of this disruption was monitored by MRI in rats subjected to closed head injury. Blood-brain barrier disruption appeared immediately after the impact, and declined gradually, until full reversal to control levels 30 min post-injury.<sup>106</sup> Opening of the BBB was similarly demonstrated in response to acute anticholinesterase exposure, however, low-level exposure has not yet been tested. BBB disruption under anticholinesterase exposure was proven to be seizure-dependent, as it could be blocked by the use of anticonvulsant agents.<sup>107</sup> The anticholinesterase effect on BBB ultrastructure did not impair endothelial tight junctions. Yet, an increased number of endothelial vesicles were observed, suggesting increased transcytosis as the mechanism involved.<sup>108</sup>

## **C. PSYCHOLOGICAL AND PHYSICAL STRESSORS IMPAIR BLOOD-BRAIN BARRIER FUNCTIONING**

Friedman et al.<sup>58</sup> have demonstrated enhanced brain penetrance under psychological stress of relatively small molecules such as anticholinesterases, as well as larger dye-protein complexes and DNA plasmids. This stress-induced process putatively explains some of the nervous system-associated sequelae reported by Gulf War veterans, who were exposed to unknown doses and combinations of potentially harmful xenobiotics, particularly anticholinesterases. The anticipated chemical warfare agents would have irreversibly blocked AChE. For prophylactic protection from these agents, Gulf War soldiers were administered pyridostigmine, a reversible carbamate

cholinesterase inhibitor which has a quaternary ammonium group that under normal circumstances prevents its transport across the BBB. Pyridostigmine is routinely used to treat peripheral neuromuscular junction deficiencies in myasthenia gravis patients,<sup>109</sup> and was shown to cause mild, primarily peripheral side effects during peacetime clinical tests in healthy volunteers.<sup>110</sup> However, pyridostigmine use during the Gulf War caused a significant increase in reported CNS symptoms. Similarly, in animal experiments the dose of pyridostigmine required to block 50% of brain AChE in stressed mice was found to be 100-fold lower than that required in non-stressed mice, indicating a breakdown of the BBB.<sup>58</sup> More recently, heat stress, even extreme, reportedly failed to induce penetration of pyridostigmine into the brain of guinea pigs.<sup>111</sup> That BBB disruption depends on the status of neuronal activity in a brain-region specific manner was demonstrated in a study that compared stress-induced increase in BBB permeability in control and monosodium glutamate-treated rats, which reported increased BBB disruption in the hypothalamus and decreased in the brain stem, as compared with control animals.<sup>112</sup> Other reports demonstrate AChE overproduction in response to anticholinesterase exposure and to increases in interleukin 1.<sup>26,113,114</sup> Therefore, a long-term outcome of low-level exposure to an anticholinesterase may be a hypocholinergic state, due to entry of the agent into the brain, and the induction of AChE expression and excessive AChE-R accumulation.

#### D. BLOOD-BRAIN BARRIER AS A COMPLEX TRAIT WITH GENETIC AND PHYSIOLOGICAL COMPONENTS: PROSPECTS

Blood-brain barrier properties are probably a complex genetic trait, in which the correlation of genotype to phenotype is difficult to dissect. Such a trait is termed complex or, if the phenotype is measured through a continuous variable, a quantitative trait. In certain cases, complex traits induce a susceptibility to a disease that depends upon environmental conditions. One example is the extreme adverse response to pyridostigmine treatment during the Gulf War that was found in a homozygous carrier of the "atypical" *BCHE* variant. The *BCHE*, with minor expression in the brain, gene encodes the butyrylcholinesterase (BChE, a.k.a. serum cholinesterase), that sequesters anticholinesterases such as pyridostigmine and prevents their reaction with AChE.<sup>86</sup> However, "atypical" BChE is incapable of binding pyridostigmine. Hence, homozygous carriers of this variant are at risk for extremely adverse responses, especially under the stress associated with war, to pyridostigmine doses in the circulation that would not affect individuals with normal *BCHE*. Therefore, the indirectly related *BCHE* gene becomes an important consideration for BBB disruption under the combination of stress and anticholinesterase exposure.

Loci in the genome that affect traits that may be quantified are called quantitative trait loci (QTL). Since many complex traits can be measured through a continuous variable (e.g., anxiety through cortisol measurements, Alzheimer's disease through cognition tests), QTL may serve as a general term for complex traits. Although the identification of QTL in humans and in model organisms is in its infancy, the QTL paradigm fits BBB properties from many points of view. Thanks to the human genome project and the development of related technologies, the detection of BBB genes will soon be aided by high-density single nucleotide polymorphism

(SNP) marker maps, which will allow population-based studies of greater significance than the current family-based studies. The human genome project, soon to be completed, will further provide important information on the sequence of all of the relevant genes and the homologies of their protein products. However, even with all the genome sequenced, significant additional work to assess functionality will be required. Expression analysis of endothelial cell genes through high-density microchip arrays will provide an independent dimension to increase the efficiency and efficacy of the QTL aspects of BBB research. Comparative genetics will also bring essential insights for functional determination. Finally bioinformatics and theoretical developments emerging from it will allow integration of all the various aspects of this multidisciplinary field to achieve the appropriate results. All of these efforts together will be needed to shed more light on the issue of BBB properties.

## VI. SUMMARY

A comprehensive survey of the recent literature reveals an increasingly complex collection of BBB constituents and functions. For example, under low-level exposure to anticholinesterases, BBB integrity may be compromised because of four interrelated processes:

1. Anticholinesterase blockade of the ACh hydrolytic capacity of AChE induces a short-term hypercholinergic activation in the brain, leading by a rapid yet long-term feedback process to accumulation of an excess of AChE-R and modification of the cholinergic status in a manner affecting BBB properties at a later phase.
2. Anticholinesterase-AChE interactions may modify the flexible 3-dimensional structure of the AChE protein and change its capacity to compete in protein-protein interactions with its non-neuronal signal transducing homologues (e.g., gliotactin), or its neuronal homologues, like neuregulin. This could alter astrocyte or neuron properties that control BBB functioning.<sup>115</sup>
3. Anticholinesterase-induced AChE-R may differ from the normally present AChE-S in its ability to affect BBB integrity. Therefore, the combination of AChE's catalytic and structural properties with the anticholinesterase-induced feedback response would have a more dramatic effect on BBB properties than would any of these processes alone.
4. In individuals prone to adverse responses to stress stimuli, all of the above processes may be exacerbated in a complex manner, combining genetic and physiological mechanisms.

Blood-brain barrier disruption would affect brain functioning because of penetration of the brain by peripheral compounds that may modulate the properties of glia and neurons. Therefore, the consequences of breaching the BBB, even for a short duration and in a limited area, may persist for long periods and involve larger brain areas. In an era when breakthroughs in molecular genetics that allow a previously unimagined dissection of biological processes, and with technological developments

that provide a dynamic real-time view of brain functions, the BBB represents a medical and scientific frontier awaiting exploration.

## ACKNOWLEDGMENTS

The authors acknowledge with thanks Profs. E. Reichenthal (Beersheva), A. Miller (Haifa), and C. Minini (Paris) for reviewing a draft of this manuscript. Additionally, HS and AF thank the U.S. Army Medical Research and Materiel Command (DAMD 17-99-1975) and The Israel Science Foundation and Ester Neuroscience for research support.

## REFERENCES

1. Pardridge, W.M., Connor, J.D., and Crawford, I.L., Permeability changes in the blood-brain barrier: Causes and consequences, *CRC Crit. Rev. Toxicol.*, 3(2), 159, 1975.
2. Rubin, L.L. and Staddon, J.M., The cell biology of the blood-brain barrier, *Ann. Rev. Neurosci.*, 22, 11, 1999.
3. Pardridge, W.M., CNS drug design based on principles of blood-brain barrier transport, *J. Neurochem.*, 70(5), 1781, 1998.
4. Gross, P.M., Circumventricular organ capillaries, *Prog. Brain. Res.*, 91, 219, 1992.
5. Risau, W., Differentiation of endothelium, *FASEB J.*, 9(10), 926, 1995.
6. Schinkel, A.H., Smit, J.J., van Tellingen, O., Beijnen, J.H., Wagenaar, E., van Deemter, L., Mol, C.A., van der Valk, M.A., Robanus-Maandag, E.C., te Riele, H.P., et al., Disruption of the mouse *mdr1a* P-glycoprotein gene leads to a deficiency in the blood-brain barrier and to increased sensitivity to drugs, *Cell*, 77(4), 491, 1994.
7. Dejana, E., Corada, M., and Lampugnani, M.G., Endothelial cell-to-cell junctions, *FASEB J.*, 9(10), 910, 1995.
8. Gumbiner, B.M., Cell adhesion: The molecular basis of tissue architecture and morphogenesis, *Cell*, 84(3), 345, 1996.
9. Lum, H. and Malik, A.B., Regulation of vascular endothelial barrier function, *Am. J. Physiol.*, 267(3 Pt 1), L223, 1994.
10. Staddon, J.M. and Rubin, L.L., Cell adhesion, cell junctions and the blood-brain barrier, *Curr. Opin. Neurobiol.*, 6(5), 622, 1996.
11. Balda, M.S., Gonzalez-Mariscal, L., Matter, K., Cerejido, M., and Anderson, J.M., Assembly of the tight junction: The role of diacylglycerol, *J. Cell Biol.*, 123(2), 293, 1993.
12. Anderson, J.M. and Van Itallie, C.M., Tight junctions and the molecular basis for regulation of paracellular permeability, *Am. J. Physiol.*, 269(4 Pt 1), G467, 1995.
13. Citi, S., Sabanay, H., Jakes, R., Geiger, B., and Kendrick-Jones, J., Cingulin, a new peripheral component of tight junctions, *Nature*, 333(6170), 272, 1988.
14. Furuse, M., Hirase, T., Itoh, M., Nagafuchi, A., Yonemura, S., and Tsukita, S., Occludin: A novel integral membrane protein localizing at tight junctions, *J. Cell Biol.*, 123(6 Pt 2), 1777, 1993.
15. Nusrat, A., Giry, M., Turner, J.R., Colgan, S.P., Parkos, C.A., Carnes, D., Lemichez, E., Boquet, P., and Madara, J.L., Rho protein regulates tight junctions and perijunctional actin organization in polarized epithelia, *Proc. Natl. Acad. Sci. U.S.A.*, 92(23), 10629, 1995.

16. Grifman, M., Galyam, N., Seidman, S., and Soreq, H., Functional redundancy of acetylcholinesterase and neuroligin in mammalian neurogenesis, *Proc. Natl. Acad. Sci. U.S.A.*, 95(23), 13935, 1998.
17. Thoreson, M.A., Anastasiadis, P.Z., Daniel, J.M., Ireton, R.C., Whellock, M.J., Johnson, K.R., Hummingbird, D.K., and Reynolds, A.B., Selective uncoupling of p120ctn from E-cadherin disrupts strong adhesion, *J. Cell Biol.*, 148(1), 189, 2000.
18. Adamson, P., Etienne, S., Couraud, P.O., Calder, V., and Greenwood, J., Lymphocyte migration through brain endothelial cell monolayers involves signaling through endothelial ICAM-1 via a rho-dependent pathway, *J. Immunol.*, 162(5), 2964, 1999.
19. Ratcliffe, M.J., Rubin, L.L., and Staddon, J.M., Dephosphorylation of the cadherin-associated p100/p120 proteins in response to activation of protein kinase C in epithelial cells, *J. Biol. Chem.*, 272(50), 31894, 1997.
20. Irie, M., Hata, Y., Takeuchi, M., Ichtchenko, K., Toyoda, A., Hirao, K., Takai, Y., Rosahl, T.W., and Sudhof, T.C., Binding of neuroligins to PSD-95, *Science*, 277(5331), 1511, 1997.
21. Tang, T., Frenette, P.S., Hynes, R.O., Wagner, D.D., and Mayadas, T.N., Cytokine-induced meningitis is dramatically attenuated in mice deficient in endothelial selectins, *J. Clin. Invest.*, 97(11), 2485, 1996.
22. Auld, V.J., Fetter, R.D., Broadie, K., and Goodman, C.S., Gliotactin, a novel transmembrane protein on peripheral glia, is required to form the blood-nerve barrier in *Drosophila*, *Cell*, 81(5), 757, 1995.
23. Baumgartner, S., Littleton, J.T., Broadie, K., Bhat, M.A., Harbecke, R., Lengyel, J.A., Chiquet-Ehrismann, R., Prokop, A., and Bellen, H.J., A *Drosophila* neurexin is required for septate junction and blood-nerve barrier formation and function, *Cell*, 87(6), 1059, 1996.
24. Darboux, I., Barthalay, Y., Piovant, M., and Hipeau-Jacquotte, R., The structure-function relationships in *Drosophila* neurotactin show that cholinesterasic domains may have adhesive properties, *EMBO J.*, 15(18), 4835, 1996.
25. Grisaru, D., Sternfeld, M., Eldor, A., Glick, D., and Soreq, H., Structural roles of acetylcholinesterase variants in biology and pathology, *Eur. J. Biochem.*, 264(3), 672, 1999.
26. Kaufer, D., Friedman, A., Seidman, S., and Soreq, H., Acute stress facilitates long-lasting changes in cholinergic gene expression, *Nature*, 393(6683), 373, 1998.
27. Fanning, A.S. and Anderson, J.M., Protein-protein interactions: PDZ domain networks, *Curr. Biol.*, 6(11), 1385, 1996.
28. Saras, J. and Heldin, C.H., PDZ domains bind carboxy-terminal sequences of target proteins, *Trends Biochem. Sci.*, 21(12), 455, 1996.
29. Bhat, M.A., Izaddoost, S., Lu, Y., Cho, K.O., Choi, K.W., and Bellen, H.J., Discs lost, a novel multi-PDZ domain protein, establishes and maintains epithelial polarity, *Cell*, 96(6), 833, 1999.
30. Janzer, R.C. and Raff, M.C., Astrocytes induce blood-brain barrier properties in endothelial cells, *Nature*, 325(6101), 253, 1987.
31. Bellen, H.J., Lu, Y., Beckstead, R., and Bhat, M.A., Neurexin IV, caspr and paranodin—novel members of the neurexin family: Encounters of axons and glia, *Trends Neurosci.*, 21(10), 444, 1998.
32. Wolburg, H., Neuhaus, J., Kniessel, U., Krauss, B., Schmid, E.M., Ocalan, M., Farrell, C., and Risau, W., Modulation of tight junction structure in blood-brain barrier endothelial cells. Effects of tissue culture, second messengers and cocultured astrocytes, *J. Cell Sci.*, 107(Pt 5), 1347, 1994.

33. Schroeter, M.L., Mertsch, K., Giese, H., Muller, S., Sporbert, A., Hickel, B., and Blasig, I.E., Astrocytes enhance radical defence in capillary endothelial cells constituting the blood-brain barrier, *FEBS Lett.*, 449(2-3), 241, 1999.
34. Granholm, A.C., Curtis, M., Diamond, D.M., Branch, B.J., Heman, K.L., and Rose, G.M., Development of an intact blood-brain barrier in brain tissue transplants is dependent on the site of transplantation, *Cell Transplant*, 5(2), 305, 1996.
35. Hurst, R.D., Heales, S.J., Dobbie, M.S., Barker, J.E., and Clark, J.B., Decreased endothelial cell glutathione and increased sensitivity to oxidative stress in an *in vitro* blood-brain barrier model system, *Brain Res.*, 802(1-2), 232, 1998.
36. Martel, C.L., Mackic, J.B., Adams, J.D., Jr., McComb, J.G., Weiss, M.H., and Zlokovic, B.V., Transport of dopamine at the blood-brain barrier of the guinea pig: Inhibition by psychotropic drugs and nicotine, *Pharm. Res.*, 13(2), 290, 1996.
37. Harik, S.I., MPTP toxicity and the "biochemical" blood-brain barrier, *NIDA Res. Monogr.*, 120, 43, 1992.
38. Sarmiento, A., Borges, N., and Lima, D., Influence of electrical stimulation of locus coeruleus on the rat blood-brain barrier permeability to sodium fluorescein, *Acta Neurochir.*, 127(3-4), 215, 1994.
39. Borges, N., Shi, F., Azevedo, I., and Audus, K.L., Changes in brain microvessel endothelial cell monolayer permeability induced by adrenergic drugs, *Eur. J. Pharmacol.*, 269(2), 243, 1994.
40. Galea, E. and Estrada, C., Periendothelial acetylcholine synthesis and release in bovine cerebral cortex capillaries, *J. Cereb. Blood Flow Metab.*, 11(5), 868, 1991.
41. Estrada, C., Triguero, D., Munoz, J., and Sureda, A., Acetylcholinesterase-containing fibers and choline acetyltransferase activity in isolated cerebral microvessels from goats, *Brain Res.*, 453(1-2), 275, 1988.
42. Luiten, P.G., de Jong, G.I., Van der Zee, E.A., and van Dijken, H., Ultrastructural localization of cholinergic muscarinic receptors in rat brain cortical capillaries, *Brain Res.*, 720(1-2), 225, 1996.
43. Mohr, E., Subcellular RNA compartmentalization, *Prog. Neurobiol.*, 57(5), 507, 1999.
44. Kaufer, D., Friedman, A., Seidman, S., and Soreq, H., Anticholinesterases induce multi-genic transcriptional feedback response suppressing cholinergic neurotransmission, *Chem. Biol. Interact.*, 119-120, 1999.
45. Powell, H.C., Braheny, S.L., Myers, R.R., Rodriguez, M., and Lampert, P.W., Early changes in experimental allergic neuritis, *Lab. Invest.*, 48(3), 332, 1983.
46. Seeldrayers, P.A., Yasui, D., Weiner, H.L., and Johnson, D., Treatment of experimental allergic neuritis with nedocromil sodium, *J. Neuroimmunol.*, 25(2-3), 221, 1989.
47. Brosnan, C.F., Claudio, L., Tansey, F.A., and Martiney, J., Mechanisms of autoimmune neuropathies, *Ann. Neurol.*, 27(Suppl), S75, 1990.
48. Theoharides, T.C., Spanos, C., Pang, X., Alferes, L., Ligris, K., Letourneau, R., Rozniecki, J.J., Webster, E., and Chrousos, G.P., Stress-induced intracranial mast cell degranulation: A corticotropin-releasing hormone-mediated effect, *Endocrinology*, 136(12), 5745, 1995.
49. Guo, Z., Turner, C., and Castle, D., Relocation of the t-SNARE SNAP-23 from lamellipodia-like cell surface projections regulates compound exocytosis in mast cells, *Cell*, 94(4), 537, 1998.
50. Goldschmidt, R.C., Hough, L.B., and Glick, S.D., Rat brain mast cells: Contribution to brain histamine levels, *J. Neurochem.*, 44(6), 1943, 1985.
51. Silver, R., Silverman, A.J., Vitkovic, L., and Lederhendler, I., Mast cells in the brain: Evidence and functional significance, *Trends Neurosci.*, 19(1), 25, 1996.

52. Zhuang, X., Silverman, A.J., and Silver, R., Distribution and local differentiation of mast cells in the parenchyma of the forebrain, *J. Comp. Neurol.*, 408(4), 477, 1999.
53. Silverman, A.-J., Sutherland, A.K., Wilhelm, M., and Silver, R., Mast cells migrate from blood to brain, *J. Neurosci.*, 20(1), 401, 2000.
54. Stewart, P.A. and Wiley, M.J., Developing nervous tissue induces formation of blood-brain barrier characteristics in invading endothelial cells: A study using quail—chick transplantation chimeras, *Dev. Biol.*, 84(1), 183, 1981.
55. Rubin, L.L., Hall, D.E., Porter, S., Barbu, K., Cannon, C., Horner, H.C., Janatpour, M., Liaw, C.W., Manning, K., Morales, J., et al., A cell culture model of the blood-brain barrier, *J. Cell. Biol.*, 115(6), 1725, 1991.
56. Hurst, R.D. and Fritz, I.B., Properties of an immortalised vascular endothelial/glioma cell co-culture model of the blood-brain barrier, *J. Cell Physiol.*, 167(1), 81, 1996.
57. Plateel, M., Dehouck, M.P., Torpier, G., Cecchelli, R., and Teissier, E., Hypoxia increases the susceptibility to oxidant stress and the permeability of the blood-brain barrier endothelial cell monolayer, *J. Neurochem.*, 65(5), 2138, 1995.
58. Friedman, A., Kaufer, D., Shemer, J., Hendler, I., Soreq, H., and Tur-Kaspa, I., Pyridostigmine brain penetration under stress enhances neuronal excitability and induces early immediate transcriptional response, *Nat. Med.*, 2(12), 1382, 1996.
59. Sage, M.R., Wilson, A.J., and Scroop, R., Contrast media and the brain. The basis of CT and MR imaging enhancement, *Neuroimaging Clin. N. Am.*, 8(3), 695, 1998.
60. Meijer, O.C., de Lange, E.C., Breimer, D.D., de Boer, A.G., Workel, J.O., and de Kloet, E.R., Penetration of dexamethasone into brain glucocorticoid targets is enhanced in mdrlA P-glycoprotein knockout mice, *Endocrinology*, 139(4), 1789, 1998.
61. Powell, H.C., Garrett, R.S., Brett, F.M., Chiang, C.S., Chen, E., Masliah, E., and Campbell, I.L., Response of glia, mast cells and the blood-brain barrier, in transgenic mice expressing interleukin-3 in astrocytes, an experimental model for CNS demyelination, *Brain Pathol.*, 9(2), 219, 1999.
62. Brett, F.M., Mizisin, A.P., Powell, H.C., and Campbell, I.L., Evolution of neuropathologic abnormalities associated with blood-brain barrier breakdown in transgenic mice expressing interleukin-6 in astrocytes, *J. Neuropathol. Exp. Neurol.*, 54(6), 766, 1995.
63. Chan, P.H., Epstein, C.J., Li, Y., Huang, T.T., Carlson, E., Kinouchi, H., Yang, G., Kamii, H., Mikawa, S., Kondo, T., et al., Transgenic mice and knockout mutants in the study of oxidative stress in brain injury, *J. Neurotrauma*, 12(5), 815, 1995.
64. Mikawa, S., Kinouchi, H., Kamii, H., Gobbel, G.T., Chen, S.F., Carlson, E., Epstein, C.J., and Chan, P. H., Attenuation of acute and chronic damage following traumatic brain injury in copper, zinc-superoxide dismutase transgenic mice, *J. Neurosurg.*, 85(5), 885, 1996.
65. Banks, W.A., Uchida, D., Arimura, A., Somogyvari-Vigh, A., and Shioda, S., Transport of pituitary adenylate cyclase-activating polypeptide across the blood-brain barrier and the prevention of ischemia-induced death of hippocampal neurons, *Ann. NY Acad. Sci.*, 805, 270, 1996.
66. Staddon, J.M., Smales, C., Schulze, C., Esch, F.S., and Rubin, L.L., p120, a p120-related protein (p100), and the cadherin/catenin complex, *J. Cell Biol.*, 130(2), 369, 1995.
67. O'Donnell, M.E., Martinez, A., and Sun, D., Endothelial Na-K-Cl cotransport regulation by tonicity and hormones: Phosphorylation of cotransport protein, *Am. J. Physiol.*, 269(6 Pt 1), C1513, 1995.
68. Jaworowicz, D.J., Jr., Korytko, P.J., Singh Lakhman, S., and Boje, K.M., Nitric oxide and prostaglandin E2 formation parallels blood-brain barrier disruption in an experimental rat model of bacterial meningitis, *Brain Res. Bull.*, 46(6), 541, 1998.

69. Boje, K.M., Inhibition of nitric oxide synthase attenuates blood-brain barrier disruption during experimental meningitis, *Brain Res.*, 720(1-2), 75, 1996.
70. Federici, C., Camoin, L., Creminon, C., Chaverot, N., Strosberg, A.D, and Couraud, P.O., Cultured astrocytes release a factor that decreases endothelin-1 secretion by brain microvessel endothelial cells, *J. Neurochem.*, 64(3), 1008, 1995.
71. O'Donnell, M.E., Martinez, A., and Sun, D., Cerebral microvascular endothelial cell Na-K-Cl cotransport: Regulation by astrocyte-conditioned medium, *Am. J. Physiol.*, 268(3 Pt 1), C747, 1995.
72. Black, K.L., Biochemical opening of the blood-brain barrier, *Adv. Drug Deliv. Rev.*, 15, 37, 1995.
73. Van Itallie, C.M., Balda, M.S., and Anderson, J.M., Epidermal growth factor induces tyrosine phosphorylation and reorganization of the tight junction protein ZO-1 in A431 cells, *J. Cell Sci.*, 108(Pt 4), 1735, 1995.
74. Stitt, J.T., Passage of immunomodulators across the blood-brain barrier, *Yale J. Biol. Med.*, 63(2), 121, 1990.
75. Lassmann, H., Basic mechanisms of brain inflammation, *J. Neural Transm. Suppl.*, 50, 183, 1997.
76. Qin, Y. and Sato, T.N., Mouse multidrug resistance 1a/3 gene is the earliest known endothelial cell differentiation marker during blood-brain barrier development, *Dev. Dyn.*, 202(2), 172, 1995.
77. Akeson, P., Larsson, E.M., Kristoffersen, D.T., Jonsson, E., and Holtas, S., Brain metastases—comparison of gadodiamide injection-enhanced MR imaging at standard and high dose, contrast-enhanced CT and non-contrast-enhanced MR imaging, *Acta Radiol.*, 36(3), 300, 1995.
78. Cornford, E.M. and Oldendorf, W.H., Epilepsy and the blood-brain barrier, *Adv. Neurol.*, 44, 787, 1986.
79. Correale, J., Rabinowicz, A.L., Heck, C.N., Smith, T.D., Loskota, W.J., and DeGiorgio, C.M., Status epilepticus increases CSF levels of neuron-specific enolase and alters the blood-brain barrier, *Neurology*, 50(5), 1388, 1998.
80. Klatzo, I., Disturbances of the blood-brain barrier in cerebrovascular disorders, *Acta Neuropathol. Suppl.*, 8, 81, 1983.
81. Larsson, H.B., Stubgaard, M., Frederiksen, J.L., Jensen, M., Henriksen, O., and Paulson, O.B., Quantitation of blood-brain barrier defect by magnetic resonance imaging and gadolinium-DTPA in patients with multiple sclerosis and brain tumors, *Magn. Reson. Med.*, 16(1), 117, 1990.
82. Merten, C.L., Knitelius, H.O., Assheuer, J., Bergmann-Kurz, B., Hedde, J.P., and Bewermeyer, H., MRI of acute cerebral infarcts, increased contrast enhancement with continuous infusion of gadolinium, *Neuroradiology*, 41(4), 242, 1999.
83. Siegal, T., Sandbank, U., Gabizon, A., Mizrachi, R., Ben-David, E., and Catane, R., Alteration of blood-brain-CSF barrier in experimental meningeal carcinomatosis. A morphologic and adriamycin-penetration study, *J. Neurooncol.*, 4(3), 233, 1987.
84. Skoog, I., A review on blood pressure and ischaemic white matter lesions, *Dement. Geriatr. Cogn. Disord.*, 9, Suppl 1, 13, 1998.
85. Menegon, A., Board, P.G., Blackburn, A.C., Mellick, G.D., and Le Couteur, D.G., Parkinson's disease, pesticides, and glutathione transferase polymorphisms [see Comments], *Lancet*, 352(9137), 1344, 1998.
86. Loewenstein-Lichtenstein, Y., Schwarz, M., Glick, D., Norgaard-Pedersen, B., Zakut, H., and Soreq, H., Genetic predisposition to adverse consequences of anti-cholinesterases in 'atypical' BCHE carriers, *Nat. Med.*, 1(10), 1082, 1995.

87. Soreq, H. and Glick, D., Novel roles for cholinesterases in stress and inhibitor responses, in *Cholinesterases and Cholinesterase Inhibitors: Basic, Preclinical and Clinical Aspects*, Giacobini, E., ed., Martin Dunitz, Ltd., London, 47-61, 2000.
88. Kuhn, W., Winkel, R., Weitalla, D., Meves, S., Przuntek, H., and Muller, T., High prevalence of Parkinsonism after occupational exposure to lead-sulfate batteries, *Neurology*, 50(6), 1885, 1998.
89. Rosenberg, G.A., Dencoff, J.E., Correa, N., Jr., Reiners, M., and Ford, C.C., Effect of steroids on CSF matrix metalloproteinases in multiple sclerosis: Relation to blood-brain barrier injury, *Neurology*, 46(6), 1626, 1996.
90. McFarland, H.F., The lesion in multiple sclerosis: Clinical, pathological, and magnetic resonance imaging considerations, *J. Neurol. Neurosurg. Psychiatry*, 64, Suppl 1, S26, 1998.
91. Stone, L.A., Smith, M.E., Albert, P.S., Bash, C.N., Maloni, H., Frank, J.A., and McFarland, H.F., Blood-brain barrier disruption on contrast-enhanced MRI in patients with mild relapsing-remitting multiple sclerosis: Relationship to course, gender, and age, *Neurology*, 45(6), 1122, 1995.
92. Clarke, H.B. and Gabrielsen, T.O., Seizure induced disruption of blood-brain barrier demonstrated by CT, *J. Comput. Assist. Tomogr.*, 13(5), 889, 1989.
93. Oztas, B. and Kucuk, M., Intracarotid hypothermic saline infusion: A new method for reversible blood-brain barrier disruption in anesthetized rats, *Neurosci. Lett.*, 190(3), 203, 1995.
94. Hachinski, V. and Munoz, D.G., Cerebrovascular pathology in Alzheimer's disease: Cause, effect or epiphenomenon?, *Ann. N.Y. Acad. Sci.*, 826, 1, 1997.
95. Blanc, E.M., Toborek, M., Mark, R.J., Hennig, B., and Mattson, M.P., Amyloid beta-peptide induces cell monolayer albumin permeability, impairs glucose transport, and induces apoptosis in vascular endothelial cells, *J. Neurochem.*, 68(5), 1870, 1997.
96. Jancso, G., Domoki, F., Santha, P., Varga, J., Fischer, J., Orosz, K., Penke, B., Becskei, A., Dux, M., and Toth, L., Beta-amyloid (1-42) peptide impairs blood-brain barrier function after intracarotid infusion in rats, *Neurosci. Lett.*, 253, 139, 1998.
97. Epstein, L.G. and Gelbard, H.A., HIV-1-induced neuronal injury in the developing brain, *J. Leukoc. Biol.*, 65(4), 453, 1999.
98. Shinnou, M., Ueno, M., Sakamoto, H., and Ide, M., Blood-brain barrier damage in reperfusion following ischemia in the hippocampus of the Mongolian gerbil brain, *Acta Neurol. Scand.*, 98(6), 406, 1998.
99. Lo, E.H., Pan, Y., Matsumoto, K., and Kowall, N.W., Blood-brain barrier disruption in experimental focal ischemia: Comparison between in vivo MRI and immunocytochemistry, *Magn. Reson. Imaging*, 12(3), 403, 1994.
100. Murakami, K., Kondo, T., Yang, G., Chen, S.F., Morita-Fujimura, Y., and Chan, P.H., Cold injury in mice: A model to study mechanisms of brain edema and neuronal apoptosis, *Prog. Neurobiol.*, 57(3), 289, 1999.
101. Urakawa, M., Yamaguchi, K., Tsuchida, E., Kashiwagi, S., Ito, H., and Matsuda, T., Blood-brain barrier disturbance following localized hyperthermia in rats, *Int. J. Hypertherm.*, 11(5), 709, 1995.
102. Sharma, H.S., Westman, J., Cervos-Navarro, J., and Nyberg, F., Role of neurochemicals in brain edema and cell changes following hyperthermic brain injury in the rat, *Acta Neurochir. Suppl.*, 70, 269, 1997.
103. Carpentier, P., Delamanche, I.S., Le Bert, M., Blanchet, G., and Bouchaud, C., Seizure-related opening of the blood-brain barrier induced by soman: possible correlation with the acute neuropathology observed in poisoned rats, *Neurotoxicology*, 11(3), 493, 1990.

104. Alm, P., Sharma, H.S., Hedlund, S., Sjoquist, P.O., and Westman, J., Nitric oxide in the pathophysiology of hyperthermic brain injury. Influence of a new anti-oxidant compound H-290/51. A pharmacological study using immunohistochemistry in the rat, *Amino Acids*, 14(1-3), 95, 1998.
105. Chen, Y., Constantini, S., Trembovler, V., Weinstock, M., and Shohami, E., An experimental model of closed head injury in mice: Pathophysiology, histopathology, and cognitive deficits, *J. Neurotrauma*, 13(10), 557, 1996.
106. Barzo, P., Marmarou, A., Fatouros, P., Corwin, F., and Dunbar, J., Magnetic resonance imaging-monitored acute blood-brain barrier changes in experimental traumatic brain injury, *J. Neurosurg.*, 85(6), 1113, 1996.
107. Petrali, J.P., Maxwell, D.M., Lenz, D.E., and Mills, K.R., Effect of an anticholinesterase compound on the ultrastructure and function of the rat blood-brain barrier: A review and experiment, *J. Submicrosc. Cytol. Pathol.*, 23(2), 331, 1991.
108. Grange-Messent, V., Bouchaud, C., Jamme, M., Lallement, G., Foquin, A., and Carpentier, P., Seizure-related opening of the blood-brain barrier produced by the anticholinesterase compound, soman: New ultrastructural observations, *Cell. Mol. Biol. (Noisy-le-grand)*, 45(1), 1, 1999.
109. Soreq, H. and Zakut, H., *Human Cholinesterases and Anticholinesterases*, Academic Press, San Diego, 1993.
110. Glikson, M., Achiron, A., Ram, Z., Ayalon, A., Karni, A., Sarova-Pinchas, I., Glovinski, J., and Revah, M., The influence of pyridostigmine administration on human neuromuscular functions—studies in healthy human subjects, *Fundam. Appl. Toxicol.*, 16(2), 288, 1991.
111. Lallement, G., Foquin, A., Baubichon, D., Burckhart, M.F., Carpentier, P., and Canini, F., Heat stress, even extreme, does not induce penetration of pyridostigmine into the brain of guinea pigs, *Neurotoxicology*, 19(6), 759, 1998.
112. Skultetyova, I., Tokarev, D., and Jezova, D., Stress-induced increase in blood-brain barrier permeability in control and monosodium glutamate-treated rats, *Brain Res. Bull.*, 45(2), 175, 1998.
113. Kaufer, D., Friedman, A., and Soreq, H., The vicious circle: Long-lasting transcriptional modulation of cholinergic neurotransmission following stress and anticholinesterase exposure, *The Neuroscientist*, 5, 173, 1999.
114. Yuekui, L., Li, Y., Liu, L., Kang, J., Sheng, J.G., Barger, S.W., Mrak, R.E., and Griffin, W.S.T., Neuronal-glia interactions mediated by interleukin-1 enhance neuronal acetylcholinesterase activity and mRNA expression, *J. Neurosci.*, 20(1), 149, 2000.
115. Bourne, Y., Grassi, J., Bougis, P.E., and Marchot, P., Conformational flexibility of the acetylcholinesterase tetramer suggested by x-ray crystallography, *J. Biol. Chem.*, 274(43), 30370, 1999.